BIOTECHNOLOGICAL PRODUCTION AND CONVERSION OF AROMATIC COMPOUNDS AND NATURAL PRODUCTS

EDITED BY: Nils Jonathan Helmuth Averesch and Oliver Kayser
PUBLISHED IN: Frontiers in Bioengineering and Biotechnology

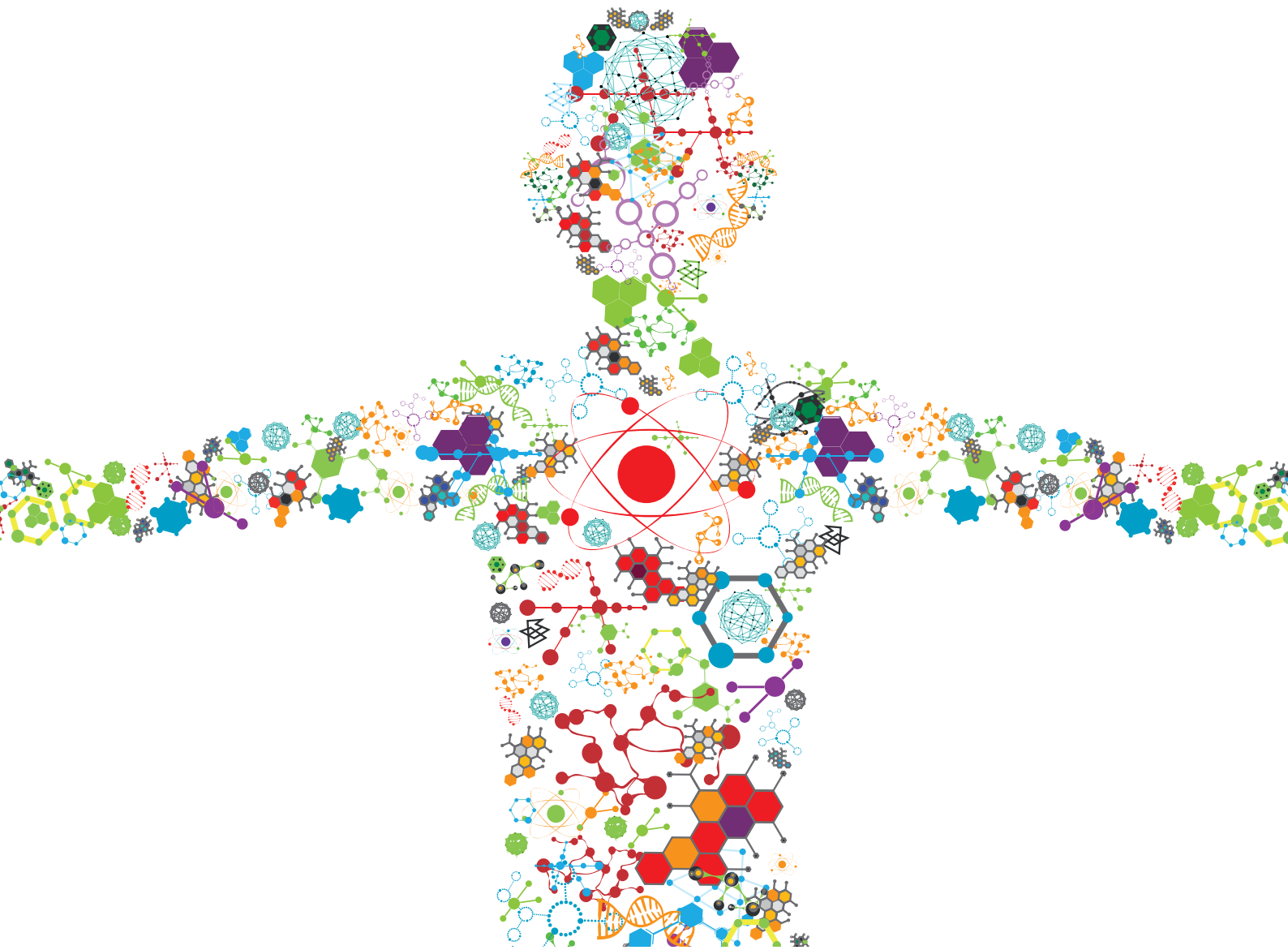

frontiers Research Topics

frontiers

ISSN 1664-8714
ISBN 978-2-88963-913-7
DOI 10.3389/978-2-88963-913-7

About Frontiers

Frontiers is more than just an open-access publisher of scholarly articles: it is a pioneering approach to the world of academia, radically improving the way scholarly research is managed. The grand vision of Frontiers is a world where all people have an equal opportunity to seek, share and generate knowledge. Frontiers provides immediate and permanent online open access to all its publications, but this alone is not enough to realize our grand goals.

Frontiers Journal Series

The Frontiers Journal Series is a multi-tier and interdisciplinary set of open-access, online journals, promising a paradigm shift from the current review, selection and dissemination processes in academic publishing. All Frontiers journals are driven by researchers for researchers; therefore, they constitute a service to the scholarly community. At the same time, the Frontiers Journal Series operates on a revolutionary invention, the tiered publishing system, initially addressing specific communities of scholars, and gradually climbing up to broader public understanding, thus serving the interests of the lay society, too.

Dedication to Quality

Each Frontiers article is a landmark of the highest quality, thanks to genuinely collaborative interactions between authors and review editors, who include some of the world's best academicians. Research must be certified by peers before entering a stream of knowledge that may eventually reach the public - and shape society; therefore, Frontiers only applies the most rigorous and unbiased reviews.
Frontiers revolutionizes research publishing by freely delivering the most outstanding research, evaluated with no bias from both the academic and social point of view. By applying the most advanced information technologies, Frontiers is catapulting scholarly publishing into a new generation.

What are Frontiers Research Topics?

Frontiers Research Topics are very popular trademarks of the Frontiers Journals Series: they are collections of at least ten articles, all centered on a particular subject. With their unique mix of varied contributions from Original Research to Review Articles, Frontiers Research Topics unify the most influential researchers, the latest key findings and historical advances in a hot research area! Find out more on how to host your own Frontiers Research Topic or contribute to one as an author by contacting the Frontiers Editorial Office: researchtopics@frontiersin.org

BIOTECHNOLOGICAL PRODUCTION AND CONVERSION OF AROMATIC COMPOUNDS AND NATURAL PRODUCTS

Topic Editors:
Nils Jonathan Helmuth Averesch, Stanford University, United States
Oliver Kayser, Technical University Dortmund, Germany

Citation: Averesch, N. J. H., Kayser, O., eds. (2020). Biotechnological Production and Conversion of Aromatic Compounds and Natural Products. Lausanne: Frontiers Media SA. doi: 10.3389/978-2-88963-913-7

Table of Contents

frontiers in Bioengineering and Biotechnology

EDITORIAL
published: 19 June 2020
doi: 10.3389/fbioe.2020.00646

Editorial: Biotechnological Production and Conversion of Aromatic Compounds and Natural Products

Nils J. H. Averesch[1,2]* *and Oliver Kayser*[3]

[1] Department of Civil and Environmental Engineering, Stanford University, Stanford, CA, United States, [2] Universities Space Research Association, NASA Ames Research Center, Moffett Field, CA, United States, [3] Department of Technical Biochemistry, Technical University of Dortmund, Dortmund, Germany

Keywords: aromatics, shikimate pathway, natural products, metabolic engineering, degradation

Editorial on the Research Topic

Biotechnological Production and Conversion of Aromatic Compounds and Natural Products

Building blocks of aromatic nature are among the most important bulk-feedstocks in the chemical industry, the majority (by volume) serving as precursors for polymeric materials. As these compounds are commonly derived from petrochemistry, obtaining them is increasingly becoming a matter of costs and sustainability. Biochemistry gives rise to a wealth of compounds that can potentially substitute or replace current petroleum-based chemicals or be used for novel applications. This includes bio-replacements for commonly fossil fuel-derived aromatics, as well as naturally produced secondary metabolites. Also, a great number of natural products and secondary metabolites, which are valuable in food- and pharma-industry, are aromatics. Furthermore, for fine chemicals and pharmaceuticals, which need to be produced with high purity or selectivity, cost-competitiveness is much less of a critical factor. This is a particular chance for biotechnology, especially for compounds, which are impossible or infeasible to produce via chemical synthesis.

Aromatics have great potential for bio-based production, as biochemical pathways like the polyketide biosynthesis or the shikimate pathway give rise to a wealth of aromatics and aromatics-derived compounds, with diverse applications in the chemical-, pharma-, cosmetic-, and food-industry. To achieve commercial viability, processes need to be competitive, as determined by the three factors: titer, yield, and rate (Averesch and Krömer, 2018). Therefore, in addition to metabolic engineering, optimization of the process is also imperative, comprised of reactor-design and -operation and has been included as subject in this Research Topic.

Aromatic compounds of interest may be produced microbially outgoing from sugar-based carbon-sources, while many pharmaceutically utilized natural products are still plant-derived. To supply the growing demand of many of these products while ensuring affordability, as well as to uphold a constant supply chain (tolerant to environmental factors such as weather and climate), heterologous production of natural products in microbes is sought after. For sustainability reasons, as well as a potential cost advantage, biotechnology is also increasingly adapting non-edible carbon-sources for production. This can be lignocellulosic biomass, of which the lignin part is especially attractive for production of aromatics, as it can be de-polymerized to directly obtain aromatic compounds. In this context, the degradation and recycling of spend materials, like polyethylene terephthalate, is also of interest, not only to achieve sustainability but also for environmental protection.

Edited and reviewed by:
Manfred Zinn,
HES-SO Valais-Wallis, Switzerland

***Correspondence:**
Nils J. H. Averesch
nils.averesch@uq.net.au

Specialty section:
This article was submitted to Bioprocess Engineering, a section of the journal Frontiers in Bioengineering and Biotechnology

Received: *09 April 2020*
Accepted: *26 May 2020*
Published: *19 June 2020*

Citation:
Averesch NJH and Kayser O (2020) Editorial: Biotechnological Production and Conversion of Aromatic Compounds and Natural Products. Front. Bioeng. Biotechnol. 8:646. doi: 10.3389/fbioe.2020.00646

This Research Topic was initiated to expand upon a review on biotechnological aromatics production, which ranks metabolic engineering strategies by establishing thresholds of yields, titers and rates for commercial viability (Averesch and Krömer, 2018). Collecting contributions from leaders in the field, we strived to spotlight recent concepts and current trends that shape the future for biotechnological production of aromatic compounds. Deliberately also including research from more peripheral areas, we intended to expand the horizon and show where the field may be headed. Calls for papers resulted in 10 accepted manuscripts, of which eight are original research and two review articles. Topics cover a broad research spectrum, from metabolic engineering for production of compounds valuable in chemical-, food-, and pharmaceutical-industry, including process development and optimization, to studies on mechanisms of degradation, conversion and valorization of aromatic bio-products. Especially the diversity of approaches and deployed organisms, shows that a paradigm shift beyond the established model organisms is taking place.

Two articles review recent advances in microbial production of aromatic compounds: one with a special emphasis on metabolic engineering strategies, as well as bioprocess optimization (Braga and Faria); the other putting special emphasis on melanins (which have applications in the pharmaceutical, cosmetic, optical, and electronic industries) and strategies for their recombinant production (Martínez et al.).

Metabolic Engineering studies utilizing rational strain design are most prominently featured in this Research Topic, three of which are targeting chemical building-blocks for polyesters: through genetic modification of *Pseudomonas taiwanensis*, 4-hydroxybenzoic acid is derived via tyrosine (Lenzen et al.)—an interesting alternative to the more conspicuous pathway where 4-hydroxybenzoic acid is obtained directly from chorismate. In a study more focused on optimization of physiological parameters and process design, conversion of ferulic acid to vanillin is investigated deploying whole-cell biocatalysts with growth arrested *E. coli* (Luziatelli et al.). In another *E. coli* study, deep strain engineering leads to significantly enhanced production of the central shikimate-pathway intermediate 3-dehydroshikimate; in combination with process design this allows downstream conversion into significant amounts of muconic acid (Choi et al.).

Microbial biotechnology has relevance beyond the common carbon-biochemistry, as shown by the fermentative production of natural product 7-bromo-L-tryptophan, a precursor for the proteasome inhibitor and potential anti-cancer agent TMC-95A, which is explored through engineering of *Corynebacterium glutamicum* for the bromination of tryptophan (Veldmann et al.).

Besides bacteria, also fungi have their advantages for production of aromatics: performing Metabolic Engineering on the yeast *Saccharomyces cerevisiae* for production of ergothioneine, an antioxidant, nutraceutical, non-proteinogenic amino acid and not-so-usual aromatic compound (aromatic heterocycle), highlights the diversity of interesting aromatics and the emerging ability to produce these biotechnologically (van der Hoek et al.).

Complementary to the *de-novo* production of aromatics from sugars, two studies evolve around lignin as alternate substrate and biochemically more direct source of aromatic compounds: one study investigates the transcriptional response of the white-rot fungus *Dichomitus squalens* expressing extracellular enzymes during lignin degradation (Kowalczyk et al.). Another study looks at the regulation of degradation of the lignin building-block cinnamic acid in the filamentous fungus *Aspergillus niger* (Lubbers et al.).

Finally, an economic evaluation of a process-model for production of aromatic compounds, sheds light on potential commercial competitiveness and environmental impact, with unexpected and therefore likely often overlooked outcomes (Krömer et al.).

Further reading includes another recent review on "Metabolic engineering of microorganisms for production of aromatic compounds" (Huccetogullari et al., 2019), as well as related Research Topics:

1. Aromatic Amino Acid Metabolism
2. From Biomass-to-Advanced Bio-based Chemicals and Materials.

AUTHOR CONTRIBUTIONS

NA conceived of the idea for the Research Topic and served as editor. OK served as co-editors for the Research Topic. NA wrote the editorial, with editing help from OK. Both authors contributed to the article and approved the submitted version.

REFERENCES

Averesch, N. J. H., and Krömer, J. O. (2018). Metabolic engineering of the shikimate pathway for production of aromatics and derived compounds-present and future strain construction strategies. *Front. Bioeng. Biotechnol.* 6:32. doi: 10.3389/fbioe.2018.00032

Huccetogullari, D., Luo, Z. W., and Lee, S. Y. (2019). Metabolic engineering of microorganisms for production of aromatic compounds. *Microb. Cell Fact.* 18:41. doi: 10.1186/s12934-019-1090-4

Conflict of Interest: The authors declare that the research was conducted in the absence of any commercial or financial relationships that could be construed as a potential conflict of interest.

frontiers in Bioengineering and Biotechnology

ORIGINAL RESEARCH
published: 12 June 2019
doi: 10.3389/fbioe.2019.00130

High-Yield Production of 4-Hydroxybenzoate From Glucose or Glycerol by an Engineered *Pseudomonas taiwanensis* VLB120

Christoph Lenzen[1], *Benedikt Wynands*[1,2], *Maike Otto*[1,2], *Johanna Bolzenius*[1], *Philip Mennicken*[1], *Lars M. Blank*[1] *and Nick Wierckx*[1,2]*

[1] *Institute of Applied Microbiology iAMB, RWTH Aachen University, Aachen, Germany,* [2] *Forschungszentrum Jülich, Institute of Bio- and Geosciences IBG-1: Biotechnology, Jülich, Germany*

Aromatic compounds such as 4-hydroxybenzoic acid are broadly applied in industry for a myriad of applications used in everyday life. However, their industrial production currently relies heavily on fossil resources and involves environmentally unfriendly production conditions, thus creating the need for more sustainable biotechnological alternatives. In this study, synthetic biology was applied to metabolically engineer *Pseudomonas taiwanensis* VLB120 to produce 4-hydroxybenzoate from glucose, xylose, or glycerol as sole carbon sources. Genes encoding a 4-hydroxybenzoate production pathway were integrated into the host genome and the flux toward the central precursor tyrosine was enhanced by overexpressing genes encoding key enzymes of the shikimate pathway. The flux toward tryptophan biosynthesis was decreased by introducing a P290S point mutation in the *trpE* gene, and degradation pathways for 4-hydroxybenzoate, 4-hydroxyphenylpyruvate and 3-dehydroshikimate were knocked out. The resulting production strains were tailored for the utilization of glucose and glycerol through the rational modification of central carbon metabolism. In batch cultivations with a completely mineral medium, the best strain produced 1.37 mM 4-hydroxybenzoate from xylose with a C-mol yield of 8% and 3.3 mM from glucose with a C-mol yield of 19.0%. Using glycerol as a sole carbon source, the C-mol yield increased to 29.6%. To our knowledge, this is the highest yield achieved by any species in a fully mineral medium. In all, the efficient conversion of bio-based substrates into 4-hydroxybenzoate by these deeply engineered *P. taiwanensis* strains brings the renewable production of aromatics one step closer.

Keywords: 4-hydroxybenzoate, aromatics, metabolic engineering, *Pseudomonas taiwanensis* VLB120, shikimate pathway, glycerol, synthetic biology

OPEN ACCESS

Edited by:
Nils Jonathan Helmuth Averesch, Stanford University, United States

Reviewed by:
Jin-ho Lee, Kyungsung University, South Korea
Yaping Yang, University of Georgia, United States

***Correspondence:**
Nick Wierckx
n.wierckx@fz-juelich.de

Specialty section:
This article was submitted to Bioprocess Engineering, a section of the journal Frontiers in Bioengineering and Biotechnology

Received: *19 January 2019*
Accepted: *14 May 2019*
Published: *12 June 2019*

Citation:
Lenzen C, Wynands B, Otto M, Bolzenius J, Mennicken P, Blank LM and Wierckx N (2019) High-Yield Production of 4-Hydroxybenzoate From Glucose or Glycerol by an Engineered Pseudomonas taiwanensis VLB120. Front. Bioeng. Biotechnol. 7:130. doi: 10.3389/fbioe.2019.00130

INTRODUCTION

Aromatic compounds are broadly applied in every-day life. Being the basic substance of the paraben group, 4-hydroxybenzoate and its derivatives mainly serve as a preservative in cosmetic as well pharmaceutical products, and beyond that, it is used for the manufacturing of Vectran fibers (Beers and Ramirez, 1990; Menczel et al., 1997). Currently, 4-hydroxybenzoate is produced commercially via the Kolbe-Schmitt-reaction from potassium phenoxide and carbon dioxide (Lindsey and Jeskey, 1957). This way of production, however, harbors major drawbacks in that fossil resources are used

as substrates and that the reaction takes place under harsh conditions. Due to relatively low and isomerically poor product yields (Lindsey and Jeskey, 1957), improved production strategies using toxic ionic liquids have been developed (Zhao et al., 2007; Benaskar et al., 2009; Stark et al., 2009). In total, these routes render the overall process non-sustainable and the production conditions hazardous and environmentally unfavorable. Biotechnological production of 4-hydroxybenzoate using microbial cell factories, however, would overcome these issues, since renewable substrates such as glucose, xylose, or glycerol are converted under far milder conditions. Nature offers a variety of candidates for the production of aromatics and other bulk and fine chemicals. Among those, Pseudomonads recently have gained great biotechnological interest (Sun et al., 2006; Elbahloul and Steinbüchel, 2009; Loeschcke and Thies, 2015; Tiso et al., 2016; Nikel and de Lorenzo, 2018). In comparison to other bacteria, these Gram-negative soil bacteria exhibit a high tolerance toward organic solvents (Kieboom et al., 1998), and due to their versatile metabolism, they accept a great variety of substrates (Dos Santos et al., 2004; Wierckx et al., 2015). Furthermore, sophisticated tools for genetic manipulation are available (Martínez-García and de Lorenzo, 2011; Silva-Rocha et al., 2013; Martínez-García et al., 2014; Nikel et al., 2014b; Belda et al., 2016) and cultivation conditions are undemanding. Different *Pseudomonas* strains have been used for the production of a range of bio-based aromatics including anthranilate, phenylalanine and derivatives, 4-coumarate, phenazines, 4-hydroxystyrene, and phenol (Wierckx et al., 2005; Nijkamp et al., 2007; Verhoef et al., 2009; Kuepper et al., 2015; Schmitz et al., 2015; Molina-Santiago et al., 2016; Wynands et al., 2018).

In microbes, 4-hydroxybenzoate can be produced in two ways. On the one hand, chorismate, which is formed via the shikimate pathway, can be converted into 4-hydroxybenzoate and pyruvate by the chorismate-pyruvate-lyase (EC 4.1.3.40, UbiC). This reaction was already exploited in *Escherichia coli*, *Corynebacterium glutamicum*, *Klebsiella pneumoniae*, and *Pseudomonas putida* KT2440 (Müller et al., 1995; Barker and Frost, 2001; Yu et al., 2016; Kallscheuer and Marienhagen, 2018; Kitade et al., 2018; Syukur Purwanto et al., 2018). However, in order to assure sufficient flux toward product formation, shutting down competing chorismate consuming pathways is often required. This often results in auxotrophic production strains which require co-feeding of aromatic amino acids or complex medium components such as yeast extract. By overexpression of an *ubiC* gene from *E. coli*, Müller et al. (1995) produced 0.12 g l^{-1} 4-hydroxybenzoate from 18 g l^{-1} glucose with a strain of *K. pneumoniae* which was auxotrophic for all aromatic amino acids. Likewise, Barker and Frost (2001) developed an *E. coli* production strain deficient in biosynthesis of tyrosine, phenylalanine and tryptophan and were able to accumulate 4-hydroxybenzoate with a C-mol yield of 15.2% during fed-batch fermentation. A *P. putida* KT2440 biocatalyst engineered by Yu et al. (2016) achieved a 4-hydroxybenzoate titer of 1.7 g l^{-1} corresponding to a C-mol yield of 18.1%. However, this strain lacked the ability to natively produce tryptophan as well as phenylpyruvate, so that, as in the case for the aforementioned hosts, additional supplementation of intermediates was necessary. Recently, Kallscheuer and Marienhagen (2018) metabolically engineered a *C. glutamicum* strain and produced 3.3 g l^{-1} 4-hydroxybenzoate in shake flasks, which corresponds to a C-mol yield of 12.6%. Using the same species as a platform, Kitade et al. (2018) conducted growth-arrested fermentations by which a 4-hydroxybenzoate titer of 36.6 g l^{-1} and a C-mol yield of 47.8% could be reached. Remarkably, this was achieved without the introduction of auxotrophies by employing a novel UbiC variant from *Providencia rustigianii* which is insensitive to product inhibition. However, this very high yield was achieved in a 2-step process where biomass was first grown on a rich medium, followed by 4-hydroxybenzoate production in a mineral medium using a high density (5% wet weight) of biomass from the rich medium culture. The 1st-stage culture in rich medium, and thus all biomass formation, was not accounted for in the yield calculation. Syukur Purwanto et al. (2018) produced 137.6 mM 4-hydroxybenzoate with a C-mol yield of 9.65% during fed-batch cultivations using an engineered *C. glutamicum* strain. Due to the deletion of the *trpE* gene, however, supplementation of tryptophan was required, and high 4-hydroxybenzoate titers were not reached in a fully mineral medium.

On the other hand, 4-hydroxybenzoate biosynthesis can also be accomplished via tyrosine. The first step of this pathway is deamination of tyrosine into 4-coumarate through a tyrosine ammonia-lyase (EC 4.3.1.23, TAL). Subsequently, 4-coumarate is further processed by moonlight activities of feruloyl-CoA synthetase (EC 6.2.1.34, Fcs), enoyl-CoA hydratase (EC 4.2.1.17, Ech), and vanillin dehydrogenase (EC 1.2.1.67, Vdh) to yield 4-hydroxybenzoate (Harwood and Parales, 1996; Jiménez et al., 2002). Although this approach has a lower maximum theoretical yield due to the loss of one C-atom as CO_2 in the conversion of chorismate to tyrosine, it has the benefit of not requiring auxotrophies since tyrosine is the endpoint of the metabolic pathway rather than a central intermediate as in the case of chorismate. Also, chorismate was shown to be non-enzymatically rearranged to phenylpyruvate in engineered phenylalanine/tyrosine auxotrophic *Saccharomyces cerevisiae* strains, thus lowering its availability as a substrate for production (Winter et al., 2014). Further, both chorismate and tyrosine are key precursors for the production of many other aromatics, thus making it useful to have platform strains that efficiently channel carbon flux toward both of these metabolites. Following the route via tyrosine, Verhoef et al. (2007) accomplished 4-hydroxybenzoate formation with a C-mol yield of 19.3% during shake flask cultivations using glycerol as a sole carbon source and 11.0% with glucose with a modified strain of *P. putida* S12, whereas fed-batch cultivations using glycerol as a sole carbon source lead to a C-mol yield of 8.5%. Further improvement was achieved through the deletion of the *hpd* gene coding for the 4-hydroxyphenylpyruvate dioxygenase, resulting in a C-mol yield of 13.4% on glucose (Verhoef et al., 2010). Implementation of a xylose-degrading pathway and subsequent laboratory evolution resulted in a strain that was able to form 4-hydroxybenzoate with C-mol yield of 12.4% on xylose, 17.5% on glucose, and 19.3% on glycerol in shake flask experiments, whereas cultivation in fed-batch mode using a mixed-substrate

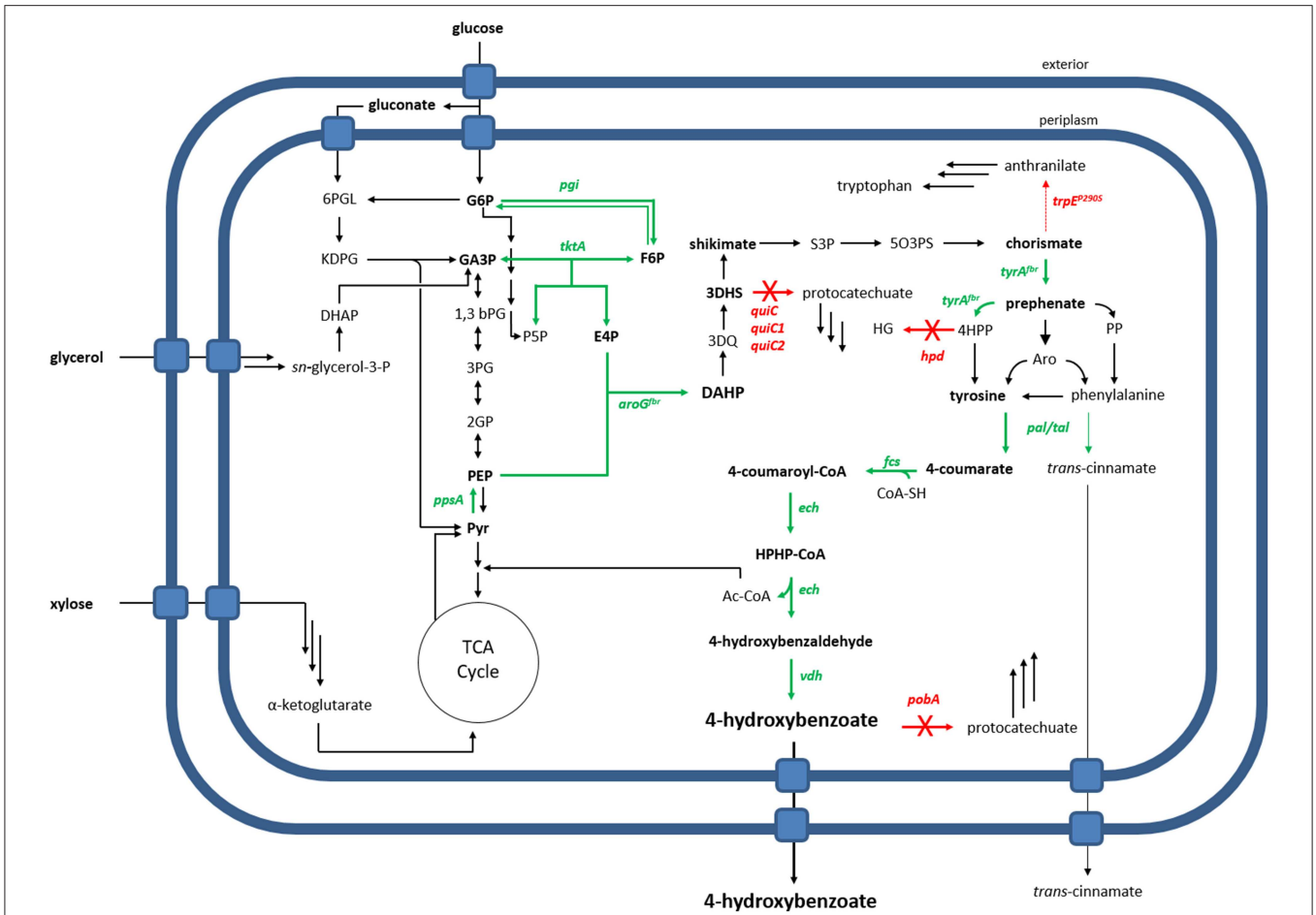

FIGURE 1 | Metabolic overview of 4-hydroxybenzoate production by an engineered *P. taiwanensis* VLB120. Overexpressed genes are shown as green arrows, deleted genes as red arrows with a cross. The dashed red arrow symbolizes a point mutation resulting in a flux decrease. 6PGL, 6-phosphogluconate; G6P, glucose-6-phosphate; KDPG, 2-keto-3-deoxy-6-phosphogluconate; GA3P, glyceraldehyde-3-phosphate; F6P, fructose-6-phosphate; S7P, sedoheptulose-7-phosphate; E4P, erythrose-4-phosphate; P5P, pentose-5-phosphate; 1,3bPG, 1,3-bisphosphoglycerate; 3PG, 3-phosphoglycerate; 2PG, 2-phosphoglycerate; PEP, phosphoenolpyruvate; Pyr, pyruvate; DAHP, 3-Deoxy-D-arabinoheptulosonate 7-phosphate; 3DQ, 3-dehydroquinate; 3DHS, 3-dehydroshikimate; S3P, shikimate-3-phosphate; 5O3PS, 5-O-(1-carboxyvinyl)-3-phosphoshikimate; 4HPP, 4-hydroxyphenylpyruvate; PP, phenylpyruvate; Aro, arogenate; HG, homogentisate; HPHP-CoA, 4-Hydroxyphenyl-β-hydroxypropionyl-CoA; Genes: *pgi*, glucose-6-phosphate isomerase; *ppsA*, phosphoenolpyruvate synthase; *tktA*, transketolase; *aroG*, DAHP synthase; *tyrA*, prephenate dehydrogenase; *quiC*, 3-dehydroshikimate dehydratase; *trpE*, anthranilate synthase; *hpd*, 4-hydroxyphenylpyruvate dioxygenase; *tal*, tyrosine ammonia-lyase; *pal*, phenylalanine ammonia-lyase; *fcs*, feruloyl-CoA synthetase; *ech*, enoyl-CoA dehydratase; *vdh*, vanillin dehydrogenase; *pobA*, *p*-hydroxybenzoic acid hydroxylase.

feeding strategy with glycerol and xylose achieved a C-mol yield of 16.3% 4-hydroxybenzoate (Meijnen et al., 2011).

In this study, *Pseudomonas taiwanensis* VLB120 was subject to metabolic engineering in order to generate a whole-cell biocatalyst for the production of 4-hydroxybenzoate via tyrosine (**Figure 1**). This species is naturally capable of using xylose as a sole carbon source (Köhler et al., 2015), rendering it a superior candidate for conversion of lignocellulosic feedstock compared to other Pseudomonads. For the generation of an efficient 4-hydroxybenzoate production host, we downregulated and disrupted competing pathways, and we overexpressed key precursor-supplying genes through stable genomic integration. Primary metabolic genes were also overexpressed, tailored for the use of glucose or glycerol as sole carbon source, and the intrinsic use of xylose as a substrate for 4-hydroxybenzoate production was demonstrated.

MATERIALS AND METHODS

Chemicals

Unless indicated otherwise, all chemicals were purchased from Sigma Aldrich (Taufkirchen, Germany) or Carl Roth (Karlsruhe, Germany).

Bacterial Strains and Culture Conditions

All strains used in this work are listed in **Table 1**. *E. coli* strains were cultivated in Lysogeny Broth (LB) medium (10 g l^{-1} N-Z-Amine, 5 g l^{-1} yeast extract, 5 g l^{-1} NaCl). When

TABLE 1 | Strains used or engineered in this study.

Strain	Characteristics	References
E. coli PIR1	F$^-$ Δ*lac169 rpoS(Am) robA1 creC510 hsdR514 endA recA1uidA(*Δ*MluI)::pir-116*; host for oriV(R6K) vectors in high copy number	Thermo Fisher Scientific
E. coli DH5α λpir	λpir lysogeny of DH5α	Glover and Hames, 1985
E. coli DH5α pTNS1	*supE44* Δ*lacU169 (φ80 lacZ*Δ*M15) hsdR17 (rk- mk+) recA1 endA1 gyrA96 thi-1 relA1*	de Lorenzo lab
E. coli HB101 pRK2013	Helper strain carrying plasmid pRK2013; F$^-$ λ$^-$ *hsdS20(rB$^-$ mB$^-$) recA13 leuB6(Am) araC14* Δ*(gpt-proA)62 lacY1 galK2(Oc) xyl-5 mtl-1 thiE1 rpsL20(SmR) glnX44(AS)*	Figurski and Helinski, 1979
E. coli DH5α pBBFLP	Strain used for excision of kanamycin resistance cassette F$^-$ *endA1 glnV44 thi-1 recA1 relA1 gyrA96 deoR nupG purB20 φ*80d*lacZ*ΔM15 Δ(*lacZYA-argF*)U169, hsdR17(r_K^- m_K^+), λ$^-$	de las Heras et al., 2008
P. taiwanensis VLB120	Wild type	Panke et al., 1998
P. taiwanensis VLB120 CL1	Derived from *P. taiwanensis* VLB120; Deficient for *pobA*, *hpd*; carrying genes *ech*, *vdh* and *fcs* randomly integrated via Tn5 transposon.	This study
P. taiwanensis VLB120 CL1 *Rt*PAL	*P. taiwanensis* VLB120 CL1 carrying plasmid pJT'*Rt*PAL	This study
P. taiwanensis VLB120 CL1 *Fj*TAL	*P. taiwanensis* VLB120 CL1 carrying plasmid pJT'*Fj*TAL	This study
P. taiwanensis VLB120 CL1 *Tc*XAL	*P. taiwanensis* VLB120 CL1 carrying plasmid pJT'*Tc*XAL	This study
P. taiwanensis VLB120 CL1 *Rs*TAL	*P. taiwanensis* VLB120 CL1 carrying plasmid pJT'*Rs*TAL	This study
P. taiwanensis VLB120 CL1.1 *Rt*PAL	Derived from *P. taiwanensis* VLB120 CL1; Deficient for *quiC*, *quiC1*, *quiC2*; carrying plasmid pJT'*Rt*PAL	This study
P. taiwanensis VLB120 CL2	Derived from *P. taiwanensis* VLB120 CL1.1; Point mutation in *trpE* resulting in P290S substitution	This study
P. taiwanensis VLB120 CL2 *Rt*PAL	*P. taiwanensis* VLB120 CL2 carrying plasmid pJT'*Rt*PAL	This study
P. taiwanensis VLB120 CL2 *Rt*PALa	*P. taiwanensis* VLB120 CL2 carrying plasmid pJT'*Rt*PALa	This study
P. taiwanensis VLB120 CL2 *Rt*PALat	*P. taiwanensis* VLB120 CL2 carrying plasmid pJT'*Rt*PALat	This study
P. taiwanensis VLB120 CL2 *Rt*PALatt	*P. taiwanensis* VLB120 CL2 carrying plasmid pJT'*Rt*PALatt	This study
P. taiwanensis VLB120 CL2 BG14a *Rt*PALat	*P. taiwanensis* VLB120 CL2 carrying genes *RtPAL, aroG^{fbr}*, *tyrA^{fbr}* at *attTn7* site under control of 14a promoter	This study
P. taiwanensis VLB120 CL2 BG14d *Rt*PALat	*P. taiwanensis* VLB120 CL2 carrying genes *RtPAL, aroG^{fbr}*, *tyrA^{fbr}* at *attTn7* site under control of 14d promoter	This study
P. taiwanensis VLB120 CL2 BG14e *Rt*PALat	*P. taiwanensis* VLB120 CL2 carrying genes *RtPAL, aroG^{fbr}*, *tyrA^{fbr}* at *attTn7* site under control of 14e promoter	This study
P. taiwanensis VLB120 CL3	*P. taiwanensis* VLB120 CL2 carrying genes *RtPAL, aroG^{fbr}*, *tyrA^{fbr}* at *attTn7* site under control of 14g promoter	This study
P. taiwanensis VLB120 CL2 BG14fg *Rt*PALat	*P. taiwanensis* VLB120 CL2 carrying genes *RtPAL, aroG^{fbr}*, *tyrA^{fbr}* at *attTn7* site under control of 14fg promoter	This study
P. taiwanensis VLB120 CL2 BG14ffg *Rt*PALat	*P. taiwanensis* VLB120 CL2 carrying genes *RtPAL, aroG^{fbr}*, *tyrA^{fbr}* at *attTn7* site under control of 14ffg promoter	This study
P. taiwanensis VLB120 CL3.1	*P. taiwanensis* VLB120 CL3 carrying plasmid pBNT'*ppsA*	This study
P. taiwanensis VLB120 CL3.2	*P. taiwanensis* VLB120 CL3 carrying plasmid pBNT'*pgi*	This study
P. taiwanensis VLB120 CL3.3	*P. taiwanensis* VLB120 CL3 carrying plasmid pBNT'*ppsA-pgi*	This study
P. taiwanensis VLB120 CL4	Derived from *P. taiwanensis* VLB120 CL4; Carrying genes *RsTAL*, *aroG^{fbr}*, *tyrA^{fbr}* at *attTn7* site under control of 14f promoter	This study
P. taiwanensis VLB120 CL4.3	*P. taiwanensis* VLB120 CL4 carrying plasmid pBNT'*ppsA-pgi*	This study

grown on plates, agar was added to a final concentration of 1.5% before autoclaving. When selection was necessary, the medium was supplemented with the respective antibiotics: 50 mg l^{-1} kanamycin, 10 mg l^{-1} gentamicin, 100 mg l^{-1} ampicillin, 10 mg l^{-1} tetracycline. Gentamicin concentration was raised to 30 mg l^{-1} during selection on agar plates. Shake flasks were filled with 10% of the flask volume and incubated at 37°C and 300 rpm. All *Pseudomonas* strains were grown on LB plates or cetrimide agar plates and selected with the respective antibiotics as described for *E. coli*, at a temperature of 30°C.

For production experiments in batch mode, two liquid precultures were prepared. At first, 500 ml flasks containing 50 ml LB medium were inoculated with cells from a freshly grown LB agar plate or glycerol stock and incubated overnight at 30°C and 300 rpm. The second preculture was conducted in 500 ml flasks containing 50 ml mineral salts medium (MSM) (Hartmans et al., 1989) (buffer: 11.64 g l^{-1} K_2HPO_4, 4.89 g l^{-1} NaH_2PO_4. Nitrogen source: 2 g l^{-1} $(NH_4)_2SO_4$. Trace elements: 10 mg l^{-1} EDTA, 100 mg l^{-1} $MgCl_2 \cdot 6\ H_2O$, 2 mg l^{-1} $ZnSO_4 \cdot 7\ H_2O$, 1 mg l^{-1} $CaCl_2 \cdot 2\ H_2O$, 5 mg l^{-1} $FeSO_4 \cdot 7\ H_2O$, 0.2 mg l^{-1} $Na_2MoO_4 \cdot 2\ H_2O$, 0.2 mg l^{-1} $CuSO_4 \cdot 5\ H_2O$, 0.4 mg l^{-1} $CoCl_2 \cdot 6\ H_2O$, 1 mg l^{-1}, $MnCl_2 \cdot 2\ H_2O$. The medium contained either 20 mM glucose, 40 mM glycerol, or 24 mM xylose as sole carbon source, unless stated otherwise. When using glycerol as a sole carbon source in the main culture, the preculture contained 40 mM glycerol and 5 mM glucose to decrease the lag phase on glycerol. All MSM precultures were incubated for 16–20 h at 300 rpm and 30°C and inoculated into the main culture to a final OD_{600} of 0.1. For the main culture, cells from the MSM preculture were harvested via centrifugation at 5,000 rpm and 4°C for 10 min and washed twice with 0.9% NaCl. Subsequently, 24-well System Duetz plates (Duetz et al., 2000) containing 1.5 ml fresh MSM per well and 0.2 mM IPTG for induction of expression of the ferulic genes (*ech*, *vdh,* and *fcs*) and, if necessary, 0.1 mM salicylate for induction of pBNT plasmids, were inoculated to a final OD_{600} of 0.1 and incubated at 30°C and 300 rpm. Unless indicated otherwise, all strains were cultivated in biological triplicates, and the standard error of the mean was used for indication of error bars. Pulsed fed-batch cultivations using MSM with glycerol as a sole carbon source were conducted with a Biostat® A Plus system (Sartorius Stedim, Göttingen, Germany) with a maximum volume of 2 l. Initial batch phase took place in 1 l MSM containing 120 mM glycerol and twice the amount of mineral salts. Initial stirrer speed was set to 480 rpm and aeration to 1 vvm. Dissolved oxygen tension was regulated at >30% through a stirrer cascade and continuously monitored using an InPro 6800 amperometric oxygen sensor (Mettler Toledo, Columbus, USA). During the course of cultivation, this value was maintained by mixing in pure oxygen using manual control. Monitoring of the pH was carried out with a 405-DPAS-SC-K8S/225 pH electrode (Mettler Toledo, Columbus, USA) and maintained at pH 7 by titration of 4 M HCl and 2 M NH_4OH. During fed-batch phase, glycerol was pulsed through a syringe to a final concentration of 200 mM each time dissolved oxygen tension increased and glycerol in the fermenter was consumed.

DNA Techniques

All primers (see **Table S1**) were designed either with Clone Manager Professional (Sci-Ed, Denver, USA) or NEBuilder® Assembly Tool (New England Biolabs, Ipswich, USA) and purchased from eurofins Genomics (Ebersberg, Germany). Codon-optimization for genes *RsTAL* (*Rhodobacter sphaeroides* ATCC 17025), *FjTAL* (*Flavobacterium johnsoniae* ATCC 17061), and *TcXAL* (*Trichosporon cutaneum* ATCC 90039) for *P. taiwanensis* VLB120 was carried out using the OPTIMIZER online tool (Puigbò et al., 2007), whereas preferences were set as follows: genetic code: eubacterial; method: guided random; manual exclusion of undesired restriction sites and rare codons exhibiting a usage of <6%. Optimized DNA fragments were ordered and purchased from Thermo Fisher Scientific (Thermo Fisher Scientific, Waltham, USA) or Integrated DNA Technologies (Coralville, USA). Inserts for all plasmids were amplified via PCR using Q5® High-Fidelity DNA polymerase (New England Biolabs, Ipswich, USA). Likewise, this was done for backbone plasmids, when cloning took place using the NEBuilder® HiFi DNA Assembly Master Mix (New England Biolabs, Ipswich, USA). When vectors were assembled using T4 DNA Ligase (Thermo Fisher Scientific, Waltham, USA), backbone DNA was isolated from an *E. coli* overnight culture using Monarch® Plasmid Miniprep Kit (New England Biolabs, Ipswich, USA). Subsequently, all DNA fragments were digested with the respective restriction enzymes (New England Biolabs, Ipswich, USA) and purified with the Monarch® PCR & DNA Cleanup Kit (New England Biolabs, Ipswich, USA). Assembled and purified plasmids (**Table 2**) were transferred into *E. coli* and *Pseudomonas* via transformation, whereas conjugation was used for *Pseudomonas* as well. For *E. coli*, heat-shock transformation was done according to a protocol by Sambrook et al. (1989) Conjugation was performed through triparental mating using a streamlined method as outlined by Wynands et al. (2018). Selection of *Pseudomonas* took place on cetrimide agar plates. When pEMG and pBELK plasmids were transferred, helper strain *E. coli* HB101 pRK2013 was used, whereas this strain as well as DH5α pTNS1 were taken for conjugation of pBG14-based constructs.

Gene knockouts were carried out according to a protocol developed by Martínez-García and de Lorenzo (2011). The pEMG suicide vectors containing TS1 and TS2 flanking regions of the gene to be eliminated were conjugated into the respective recipient strain, whereas successful integration was verified via colony PCR. Due to high ampicillin resistance of *P. taiwanensis* VLB120, plasmid pSW-2 encoding enzyme I-SceI was used instead of pSW-I. Induction of expression by addition of 3-methylbenzoate was not required. Knockouts were confirmed by colony PCR and DNA sequencing. Genes *ech*, *vdh,* and *fcs*, were amplified from the genome of *P. putida* S12 (Hartmans et al., 1989) and randomly integrated into the genome of *P. taiwanensis* VLB120 via the pBELK Tn5 mini-transposon system developed by Nikel and de Lorenzo (2013). Integration sites were identified through arbitrary-primed PCR as described by Martínez-García et al. (2014) using the Q5® DNA polymerase and subsequent DNA sequencing and BLAST analysis against the genome of *P. taiwanensis* VLB120. In order to excise the

TABLE 2 | Plasmids used and constructed in this work.

Plasmid	Characteristics	References
pJT'mcs	Amp^R Gm^R, expression vector, under control of P_{tac} promoter	Nijkamp et al., 2007
pTacPAL	Amp^R Gm^R, expression vector, harboring *Rt*PAL under control of P_{tac} promoter	Nijkamp et al., 2007
pBELK	Mini-Tn5 delivery vector; tnpA oriV(R6Kγ) oriT(RK2) $lacI^Q$ P_{trc} bla *FRT*-aphA-*FRT*, Amp^R Km^R	Nikel and de Lorenzo, 2013
pBELK ferulic s	Mini-Tn5 delivery vector harboring genes *ech*, *vdh* and *fcs* from *P. putida* S12	This study
pJT'*Rs*TAL	pJT expression vector harboring *RsTAL*	This study
pJT'*Fj*TAL	pJT expression vector harboring *FjTAL*	This study
pJT'*Tc*XAL	pJT expression vector harboring *TcXAL*	This study
pJT *Rt*PAL	pJT expression vector harboring *RtPAL*	This study
pBWatt	pSEVA234 expression vector harboring genes $aroG^{fbr}$, $tyrA^{fbr}$, *tktA*; Km^R, ori pBBR1, $laqI^q$-P_{trc}	This study
pJT'*Rt*PALa	pJT expression vector harboring gene $aroG^{fbr}$	This study
pJT'*Rt*PALat	pJT expression vector harboring gene $aroG^{fbr}$, $tyrA^{fbr}$	This study
pJT'*Rt*PALatt	pJT expression vector harboring gene $aroG^{fbr}$, $tyrA^{fbr}$, *tktA*	This study
pBG14a	Tn7 delivery vector; KmR GmR, ori *R6K*, *Tn7L,* and *Tn7R* flanks, BCD2–*msfgfp* fusion, promoter no. 28	Zobel et al., 2015
pBG14d	Tn7 delivery vector; KmR GmR, ori *R6K*, *Tn7L,* and *Tn7R* flanks, BCD2–*msfgfp* fusion, promoter no. 51	Zobel et al., 2015
pBG14e	Tn7 delivery vector; KmR GmR, ori *R6K*, *Tn7L,* and *Tn7R* flanks, BCD2–*msfgfp* fusion, promoter no. 17	Zobel et al., 2015
pBG14f	Tn7 delivery vector; KmR GmR, ori *R6K*, *Tn7L,* and *Tn7R* flanks, BCD2–*msfgfp* fusion, promoter no. 25	Zobel et al., 2015
pBG14g	Tn7 delivery vector; KmR GmR, ori *R6K*, *Tn7L,* and *Tn7R* flanks, BCD2–*msfgfp* fusion, promoter no. 42	Zobel et al., 2015
pBG14fg	Tn7 delivery vector; KmR GmR, ori *R6K*, *Tn7L,* and *Tn7R* flanks, BCD2–*msfgfp* fusion, hybrid promoter composed of No. 25 & No. 42	Köbbing et al. in preparation
pBG14ffg	Tn7 delivery vector; KmR GmR, ori *R6K*, *Tn7L,* and *Tn7R* flanks, BCD2–*msfgfp* fusion, hybrid promoter 2 x No. 25 & No. 42	Köbbing et al. in preparation
pBG14a *Rt*PALat	Tn7 delivery vector harboring genes *RtPAL*, $aroG^{fbr}$, $tyrA^{fbr}$, promoter no. 28	This study
pBG14d *Rt*PALat	Tn7 delivery vector harboring genes *RtPAL*, $aroG^{fbr}$, $tyrA^{fbr}$, promoter no. 51	This study
pBG14e *Rt*PALat	Tn7 delivery vector harboring genes *RtPAL*, $aroG^{fbr}$, $tyrA^{fbr}$, promoter no. 17	This study
pBG14g *Rt*PALat	Tn7 delivery vector harboring genes *RtPAL*, $aroG^{fbr}$, $tyrA^{fbr}$, promoter no. 42	This study
pBG14fg *Rt*PALat	Tn7 delivery vector harboring genes *RtPAL*, $aroG^{fbr}$, $tyrA^{fbr}$, hybrid promoter no. 25 & no. 42	This study
pBG14ffg *Rt*PALat	Tn7 delivery vector harboring genes *RtPAL*, $aroG^{fbr}$, $tyrA^{fbr}$, hybrid promoter 2 × no. 25 & no. 42	This study
pBG14f *Rs*TALat	Tn7 delivery vector harboring genes *RsTAL*, $aroG^{fbr}$, $tyrA^{fbr}$, promoter no. 25	This study
pRK2013	Helper plasmid for conjugational transfer; Km^R, *oriV*(RK2/ColE1), mob^+ tra^+	Figurski and Helinski, 1979
pTNS1	Helper plasmid; Amp^R, *ori* R6K, *TnSABC+D* operon	Choi et al., 2005
pSW-2	Gm^R, *ori*RK2, *xylS, Pm*→ I-*sce*I (transcriptional fusion of I-*sce*I to *Pm*)	Martínez-García and de Lorenzo, 2011
pBBFLP	Helper plasmid for excision of antibiotic markers, *oriV*(pBBR1), *oriT*(RK2) RK2 mob^+ λP_R::*FLP* λ(*cI*857) *sacB tet*, Tet^R	de las Heras et al., 2008
pEMG *pobA*	Knockout vector carrying TS1 and TS2 flanking regions of *p*-hydroxybenzoic acid hydroxylase (*pobA*)	Wynands et al., 2018
pEMG *hpd*	Knockout vector carrying TS1 and TS2 flanking regions of 4-hydroxyphenylpyruvate dioxygenase (*hpd*)	Wynands et al., 2018
pEMG *quiC*	Knockout vector carrying TS1 and TS2 flanking regions of dehydroshikimate dehydratase (*quiC*)	Wynands et al., 2018
pEMG *quiC1*	Knockout vector carrying TS1 and TS2 flanking regions of dehydroshikimate dehydratase (*quiC1*)	Wynands et al., 2018
pEMGu *quiC2*	Knockout vector carrying TS1 and TS2 flanking regions dehydroshikimate dehydratase (*quiC2*)	Wynands et al., 2018
pEMGu $trpE^{P290S}$	Knockout vector carrying TS1 and TS2 flanking regions of the codon for the P290S substitution of *trpE* gene	Wynands et al., 2018
pBNT'mcs	Expression vector harboring salicylate-inducible nagR/P_{NagAa} promoter, Km^R	Verhoef et al., 2010
pBNT'*ppsA*	pBNT expression vector harboring gene encoding phosphoenolpyruvate synthase (*ppsA*)	This study
pBNT'*pgi*	pBNT expression vector harboring gene encoding glucose-6-phosphate isomerase (*pgi*)	This study
pBNT'*ppsA-pgi*	pBNT expression vector harboring gene encoding phosphoenolpyruvate synthase (*ppsA*), and glucose-6-phosphate isomerase (*pgi*)	This study

kanamycin resistance cassette, plasmid pBBFLP harboring a flippase gene was transformed into selected clones and loss of resistance was confirmed via selection of Km^s clones on LB agar plates. Stable integration of key genes and modulated expression was achieved by using the Tn7-based calibrated promoter system developed by Zobel et al. (2015).

Cloning procedures were routinely verified via colony PCR using *OneTaq*® DNA polymerase (New England Biolabs,

Ipswich, USA). Colonies were picked from transformation plates and lysed in 30 µl PEG200 (pH 12) for 5–10 min (Chomczynski and Rymaszewski, 2006).

Analytical Methods

Optical densities of cell cultures were measured at a wavelength of 600 nm using an Ultrospec 10 spectrophotometer (GE Healthcare, Chicago, USA). Cell dry weight was determined by multiplying OD_{600} values by the empirical factor 0.505. Aromatics were analyzed by HPLC. Samples taken during cultivations were centrifuged at 17,000 *g* for 2 min and the supernatant was filtered using syringe filters with a pore size of 0.2 µm. After addition of methanol (Th. Geyer, Renningen, Germany) in a 1:1 ratio, samples were stored at 4°C overnight in order to precipitate any salts or proteins. After another centrifugation at 13,000 rpm for 2 min, the supernatant was taken for analysis. HPLC was performed using a System Gold 168 diode array detector (Beckman Coulter, Brea, USA) and an ISAspher 100-5 C18 BDS reversed phase HPLC column (ISERA, Düren, Germany) at 30°C and a flow rate of 0.8 ml min. Elution took place with a gradient starting at 95% of 0.1% (v/v) TFA and 5% methanol for 2 min, followed by gradual increase to 100% methanol over 18 min. After 2 min at 100% methanol, initial ratios were reached again within 2 min. UV detection of aromatics was conducted at a wavelength of 260 nm. Glycerol concentrations were determined using the Glycerol GK Assay Kit (Megazyme, Bray, Ireland). Glucose concentrations were determined via HPLC using an Aminex Ion Exclusion HPX-87H column (Bio-Rad, Hercules, USA) and a Smartline RI detector 2300 (Knauer, Berlin, Germany), whereas isocratic elution took place in 5 M H_2SO_4 at 1.2 ml/min and 70°C. For calculation of production rates, CDW was estimated by multiplying OD values with the empirical factor 0.505. The increase of 4-hydroxybenzoate concentration between two time points was then divided by average biomass of those time points and the period of time. Growth data of the 4-hydroxybenzoate pulse experiment carried out in the Growth Profiler® (Enzyscreen, Heemstede, Netherlands) were normalized by subtracting the initial offset values of each curve compared to that of the cultivation with no 4-hydroxybenzoate pulse, thereby setting all initial points to the same value.

RESULTS AND DISCUSSION

Establishing 4-Hydroxybenzoate Production in *P. taiwanensis*

One important requirement for an efficient biocatalyst to be functional is that degradation of the product itself, as well as that of potential precursors, is prevented. Wierckx et al. (2008) and Verhoef et al. (2010) showed that producers of aromatic compounds had upregulated metabolic pathways for the degradation of 4-hydroxybenzoate, protocatechuate, and tyrosine. Therefore, the *pobA* gene (PVLB_11545) responsible for the conversion of 4-hydroxybenzoate into protocatechuate, and the *hpd* gene (PVLB_11760), encoding the 4-hydroxyphenylpyruvate dioxygenase, were knocked out, rendering the cells unable to use 4-hydroxybenzoate and tyrosine as a sole carbon sources (Wynands et al., 2018). In doing so, the strain *P. taiwanensis* VLB120 Δ*pobA*Δ*hpd* was constructed. Unlike many Pseudomonads, the genome of *P. taiwanensis* VLB120 does not contain genes encoding a ferulic acid degradation pathway, and indeed this strain is unable to grow on ferulate. Since this pathway is necessary to convert 4-coumarate into 4-hydroxybenzoate, the operon containing ferulic genes *fcs*, *ech,* and *vdh* was amplified from the genome of *P. putida* S12 and cloned into the pBELK transposon vector (Nikel and de Lorenzo, 2013) under the control of the IPTG-inducible P_{trc} promoter. Subsequently, this operon was randomly integrated into the genome of *P. taiwanensis* VLB120 Δ*pobA*Δ*hpd*. Three clones were randomly picked and cultivated in MSM containing 20 mM glucose and 3 mM 4-coumarate. Under these conditions, all three strains produced 4-hydroxybenzoate at a rate of 0.45 mmol g_{CDW}^{-1} h^{-1}, proving the functionality of the pathway encoded by the ferulic operon. Another variant of the ferulic operon containing the additional genes encoding feruloyl-CoA dehydrogenase (*fcd*) and β-ketothiolase (*aat*) was also tested, but the addition of these two genes did not affect 4-hydroxybenzoate production rates from 4-coumarate, and they were therefore omitted in further strain engineering (data not shown). The integration sites of the operon were identified by arbitrary PCR and DNA sequencing as described in Martínez-García et al. (2014). The transposons had integrated 1,049 bp downstream from the start codon of the gene encoding the plug domain of a TonB-dependent receptor (PVLB_16205, clone 1), 242 bp downstream from the start codon of a radical SAM protein (PVLB_20680, clone 2), and 1,696 bp downstream from the start codon of a gene encoding a sensory box protein (PVLB_25350, clone 3). A map depicting the integration sites can be found in **Figure S1**. Since no detectable differences regarding growth or production could be observed among the different clones, a negative effect of disruption of these genes on production performance can be excluded. All further experiments were carried out with clone 1**,** which hereafter is named *P. taiwanensis* VLB120 CL1.

This strain was subsequently equipped with different ammonia-lyases which catalyze the conversion of tyrosine into 4-coumarate, including a native *pal* from *Rhodosporidium toruloides* (*Rt*PAL; Verhoef et al., 2007) and codon-optimized versions of a *tal* from *Rhodobacter sphaeroides* (*Rs*TAL; Xue et al., 2007), from *Flavobacterium johnsoniae* (*Fj*TAL), and a *xal* from *Trichosporon cutaneum* (*Tc*XAL) (Jendresen et al., 2015), cloned into plasmid pJT'mcs (Nijkamp et al., 2007) under the control of the constitutive P_{tac} promoter. This setup of genomic integration of the ferulic operon and plasmid-based expression of PAL/TAL-encoding genes was chosen because the ammonia-lyase is generally the rate-limiting step (Verhoef et al., 2007; Jendresen et al., 2015), and expression from a multicopy plasmid was expected to increase its activity. Co-feeding experiments with 20 mM glucose and 3 mM tyrosine confirmed the ammonia-lyase reaction as the rate-limiting step of the pathway. Among the four tested lyases, *Rt*PAL enabled the highest 4-hydroxybenzoate production rate (0.20 mmol g_{CDW}^{-1} h^{-1}), reaching 44% of the

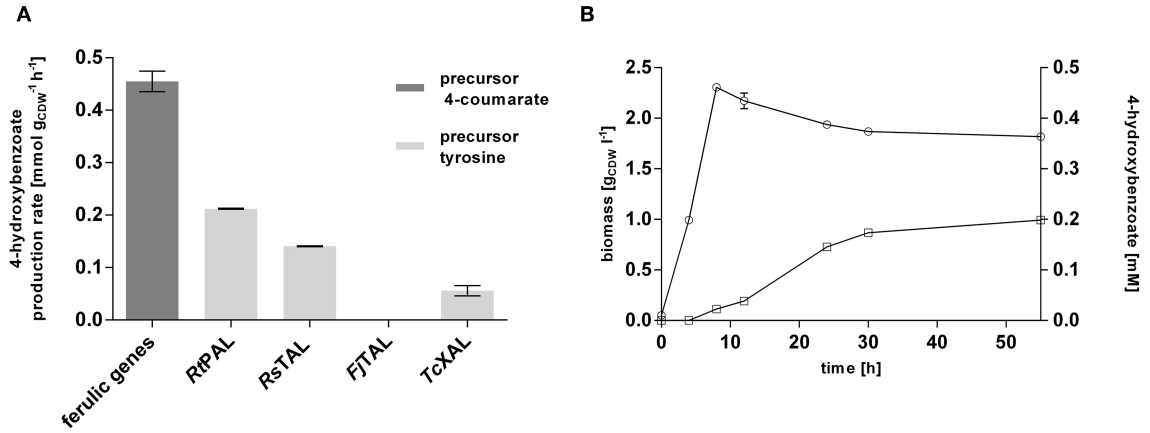

FIGURE 2 | Evaluation of the 4-hydroxybenzoate production pathway in *P. taiwanensis* VLB120 CL1 in co-feeding experiments. **(A)** Comparison of the conversion rates of the two different pathway components (encoded by the ferulic operon and the ammonia-lyase genes). Cells were grown in biological triplicates in MSM with 5 mM glucose in System Duetz plates at 30°C and 300 rpm. After ∼6 h, 3 mM 4-coumarate (ferulic operon) or tyrosine (PAL and TAL genes), and another 20 mM glucose were added. Highest measured rates are indicated. **(B)** 4-hydroxybenzoate production (squares) and growth (circles) of *P. taiwanensis* VLB120 CL1 (containing *Rt*PAL). Cells were cultivated in triplicates in MSM supplemented with 20 mM glucose as a sole carbon source at 30°C and 300 rpm in System Duetz plates. Expression of ferulic genes was induced with 0.2 mM IPTG. Error bars indicate standard error of the mean.

conversion velocity of the downstream pathway encoded by the ferulic operon (**Figure 2A**). The second best performance was exhibited by the strain harboring the *Rs*TAL construct with a rate of 0.14 mmol g_{CDW}^{-1} h^{-1}. When cultivated with 20 mM glucose in mineral medium without precursor supplementation (**Figure 2B**), the strain harboring the ferulic operon and the *Rt*PAL construct produced 0.20 mM 4-hydroxybenzoate, corresponding to a C-mol yield of 1.2% with a maximum production rate of 0.004 mmol g_{CDW}^{-1} h^{-1}, which is only 2% of the rate achieved with additional feed of tyrosine. However, considerable accumulation of 4-hydroxybenzoate could only be detected after cells had reached stationary phase, suggesting that at least some of the pathway genes are catabolite-repressed. Indeed, the recognition sequence motif (5′-AANAANAA-3′) characteristic for catabolite-repressed expression (Moreno et al., 2009b, 2015) could be found 37 base pairs downstream from the start codon of *fcs*, encoding the first enzymatic step in 4-coumarate conversion, and 20 bp upstream from the start codon of *ech*, which is the first gene downstream from the promoter. These findings are in accordance to those described by Verhoef et al. (2010). However, the latter site was deleted during the cloning into the pBELK vector. Upon binding of the Crc global regulator protein in conjunction with the Hfq chaperone to this motif on the mRNA level, translation is prevented (Wolff et al., 1991; MacGregor et al., 1996; Hester et al., 2000a,b; Morales et al., 2004; Ruiz-Manzano et al., 2005; Moreno et al., 2009a; Hernández-Arranz et al., 2016). Knockout of *crc* or *hfq* in order to override catabolite-repression, however, did not beneficially influence 4-hydroxybenzoate production (**Figure S2**). In summary, an efficient 4-hydroxybenzoate production pathway from tyrosine could be implemented in *P. taiwanensis* VLB120 CL1, in which the selection of an efficient ammonia-lyase was a key enabling factor. The fact that feeding of precursors such as tyrosine results in a greatly increased 4-hydroxybenzoate production rate suggests that, as expected, the *de novo* formation of tyrosine is a bottleneck for efficient 4-hydroxybenzoate production from glucose or glycerol.

Enhancing Supply of Tyrosine

As in the case of *pobA* and *hpd*, upregulation of 3-dehydroshikimate (3DHS) dehydratase (*quiC1*) (Peek et al., 2017) was observed in the phenol producing strain *P. putida* S12 TPL3 (Wierckx et al., 2008), converting 3DHS, one of the upper metabolites of the shikimate pathway, into protocatechuate. Recently, investigations on quinate metabolism in *P. taiwanensis* VLB120 revealed the presence of a total of three genes encoding 3DHS dehydratase (Wynands et al., 2018). Therefore, genes *quiC* (PVLB_18200), *quiC1* (PVLB_10935), and *quiC2* (PVLB_13075) were knocked out in *P. taiwanensis* VLB120 CL1 in order to prevent the degradation of aromatic pathway intermediates, thus generating VLB120 CL1.1. Besides tyrosine, tryptophan is also formed via the shikimate pathway. In *P. putida* S12 TPL3, genome analysis revealed a mutation in the gene encoding the anthranilate synthase (*trpE*), resulting in a P290S amino acid exchange (Wierckx et al., 2008). This mutation substantially increased the carbon flux toward tyrosine in a *P. taiwanensis*-based phenol overproducer (Wynands et al., 2018). Therefore, the same point mutation as described in Wynands et al. (2018) resulting in a P290S substitution was introduced in *P. taiwanensis* VLB120 CL1.1, thereby generating *P. taiwanensis* VLB120 CL2. These genetic modifications together with the pJT'*Rt*PAL construct lead to an almost 2-fold increase in 4-hydroxybenzoate titer for *P. taiwanensis* VLB120 CL1.1 and 6.9-fold for *P. taiwanensis* VLB120 CL2 compared to *P. taiwanensis* VLB120 CL1, corresponding to C-mol yields of

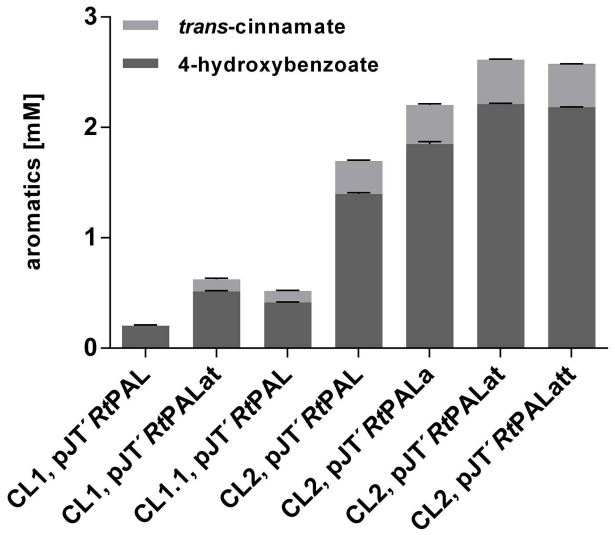

FIGURE 3 | Comparison of aromatics titers of *P. taiwanensis* VLB120 CL1, *P. taiwanensis* CL1.1, and *P. taiwanensis* CL2 with overexpression of different bottleneck genes. All strains were cultivated for 96 h in biological triplicates in MSM containing 20 mM glucose as a sole carbon source in System Duetz plates at 30°C and 300 rpm, expression of ferulic genes was induced with 0.2 mM IPTG. Error bars indicate standard error of the mean.

2.4 and 8.1%, respectively (**Figure 3**). The large increase in production obtained with CL2 confirms the importance of the $trpE^{P290S}$ mutation. The difference between CL1 and CL1.1 indicates that indeed a substantial portion of the carbon flux into the shikimate pathway is diverted into the 3DHS degradation pathway, thereby creating a futile cycle. These strains also produced 0.10 ± 0.01 mM (CL1.1) and 0.30 ± 0.01 mM (CL2) of *trans*-cinnamate due to loose substrate specificity of the used *Rt*PAL enzyme which is capable of converting both tyrosine and phenylalanine.

Former studies in *E. coli* revealed genes *aroG*, *tyrA,* and *tktA* as key steps in increasing tyrosine supply (Kikuchi et al., 1997; Li et al., 1999; Lütke-Eversloh and Stephanopoulos, 2007; Kim et al., 2014). Therefore, along with the gene encoding *Rt*PAL, feedback-resistant versions of *aroG* and *tyrA* ($aroG^{fbr}$, with a D146N substitution, and $tyrA^{fbr}$, with A354V and M53I substitutions) as well as *tktA*, from *E. coli*, were codon-optimized and cloned into the pJT'mcs vector. In the experiment shown in **Figure 3**, synergistic effects of these genes on 4-hydroxybenzoate production were investigated in MSM with 20 mM glucose as sole carbon source. When using the pJT'*Rt*PALat construct (overexpression of *Rt*PAL, $aroG^{fbr}$, and $tyrA^{fbr}$) in VLB120 CL1, the 4-hydroxybenzoate titer was raised to 0.51mM with a C-mol yield of 3%. Strain *P. taiwanensis* VLB120 CL2 harboring the same pJT'*Rt*PALat plasmid produced 2.21 ± 0.01 mM 4-hydroxybenzoate with a C-mol yield of 12.9%, confirming that a major contribution to enhanced production is made by downregulation and elimination of competing pathways (*quiC*, *quiC1*, *quiC2,* and $trpE^{P290S}$), but also showing that the additional expression of both $aroG^{fbr}$ and $tyrA^{fbr}$ significantly enhances production. Compared to these strains, the inclusion of $aroG^{fbr}$ alone shows an intermediate phenotype. The additional overexpression of the *tktA* gene (pJT'*Rt*PALatt) did not further increase the product concentration. The highest *trans*-cinnamate concentration of 0.40 ± 0.01 mM was found for *P. taiwanensis* VLB120 CL2 harboring pJT'*Rt*PALat, making up 15.9% of the total aromatics produced.

Stable Genomic Integration of 4-Hydroxybenzoate Production Modules

The use of plasmid-based expression systems in a bioprocess has the disadvantage that selective pressure has to be maintained throughout the entire cultivation, thus leading to increased burden (Mi et al., 2016). Furthermore, plasmids inherently vary in their copy number from cell to cell, which results in greater variability and instability (Gao et al., 2014; Jahn et al., 2014). To address these issues, a Tn7 transposon system with a calibrated promoter library (Zobel et al., 2015) was used in order to stably integrate one copy of *RtPAL*, $aroG^{fbr}$, and $tyrA^{fbr}$ into the genome of *P. taiwanensis* VLB120 CL2. Different promoter strengths were tested in order to investigate optimal constitutive expression levels (**Figure 4**). In addition, the 14fg and 14ffg variants were included, which are stacked promoters with activities higher than 14g (Sebastian Köbbing, RWTH Aachen University, personal communication). The highest final 4-hydroxybenzoate concentration was achieved with the 14g construct, which reached a titer equal to that of the plasmid-based system. Unexpectedly, the strongest investigated promoter 14ffg resulted in a tyrosine titer of 2.4 mM, but no accumulation of 4-hydroxybenzoate or *trans*-cinnamate. Since this promoter exhibits 80% more activity than the BG14g promoter, one explanation for this may be that expression levels of *Rt*PAL were too high, leading to the selection of mutated constructs. The strain harboring the P_{14g} *Rt*PALat construct exhibited the best performance and is hereafter designated *P. taiwanensis* VLB120 CL3.

Although the *Rt*PAL enzyme enabled the highest production rate of 4-hydroxybenzoate in co-feeding experiments, one major disadvantage of this enzyme is its relaxed substrate specificity, causing it to also convert phenylalanine into *trans*-cinnamate. Thus, not only is a fraction of valuable precursor converted into a byproduct, it also hampers the downstream purification of 4-hydroxybenzoate. In an attempt to circumvent this issue, *Rt*PAL was replaced by a codon-optimized gene encoding the tyrosine ammonia-lyase from *Rhodobacter sphaeroides* (*Rs*TAL) (Xue et al., 2007). Although this TAL supports a lower 4-hydroxybenzoate production rate (**Figure 2**), it has a much higher relative affinity for tyrosine, thus potentially generating less byproduct. The gene was cloned along with $aroG^{fbr}$ and $tyrA^{fbr}$ into the pBG14f transposon vector and integrated at the *att*Tn7 site into the genome of *P. taiwanensis* VLB120 CL2, thereby generating *P. taiwanensis* VLB120 CL4. The construct containing the 14f promoter was chosen because cloning attempts using stronger promoters failed. After 96 h of cultivation in MSM containing 20 mM glucose, a 4-hydroxybenzoate titer of 2.62 ± 0.03 mM was reached, with

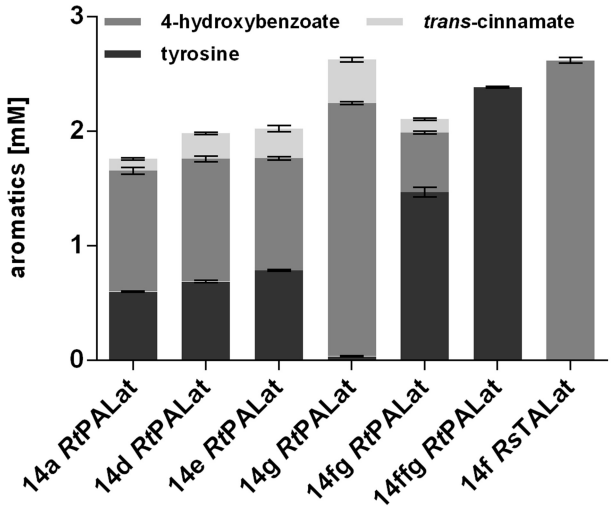

FIGURE 4 | Modulation of expression of genomically integrated *RtPAL, RsTAL, aroG*^{fbr}, and *tyrA*^{fbr}. Increasing promoter strengths are listed from left to right. Cells were cultivated in biological triplicates in MSM containing 20 mM glucose as a sole carbon source at 30°C and 300 rpm in System Duetz plates, expression of ferulic genes was induced with 0.2 mM IPTG. Titers of final samples (96 h) are shown. Error bars indicate standard error of the mean.

no detectable formation of *trans*-cinnamate. The increase of 4-hydroxybenzoate corresponds to the amount of *trans*-cinnamate produced by the same strain using *Rt*PAL, indicating that in this case the *Rs*TAL enzyme efficiently redirected the flux toward the main product, likely aided by the phenylalanine hydroxylase PhhAB which converts phenylalanine into tyrosine (Arias-Barrau et al., 2004).

Enhanced 4-Hydroxybenzoate Production Through Overexpression of *ppsA* and *pgi*

Overall, the biosynthesis of one mole of tyrosine requires one mole of erythrose-4-phosphate (E4P) and two moles of phosphoenolpyruvate (PEP). In *E. coli*, glucose is taken up through a phosphotransferase system which converts PEP into pyruvate. This system poses a severe drain on PEP, and enhanced production of tyrosine could be achieved by overexpression of the *ppsA* gene encoding phosphoenolpyruvate synthase A, which re-converts pyruvate into PEP (Yi et al., 2002; Lütke-Eversloh and Stephanopoulos, 2007; Juminaga et al., 2012). Although Pseudomonads do not take up glucose via a phosphotransferase system (Romano et al., 1970), they mainly metabolize glucose via the Entner-Doudoroff pathway (Nikel et al., 2015), which yields one PEP and one pyruvate per glucose molecule. The Embden-Meyerhof-Parnas pathway employed by *E. coli* yields two PEP per mole of glucose, and thus both organisms theoretically yield the same net production of one PEP and one pyruvate per mole of transported glucose through their major metabolic pathway. In order to increase the PEP precursor supply, we overexpressed *ppsA* in the 4-hydroxybenzoate producing strains. The gene was amplified from the genome of *P. taiwanensis* VLB120 and cloned into the pBNT'mcs expression vector (Verhoef et al., 2010) under the control of the salicylate-inducible NagR/P_{nagAa}-promoter system. The second precursor E4P is formed by transketolase (*tktA*), the overexpression of which did not increase 4-hydroxybenzoate production (**Figure 3**). In Pseudomonads, the flux through the pentose phosphate pathway (PPP) is generally low (Fuhrer et al., 2005; Wierckx et al., 2009; Nikel et al., 2015), and enhancement of the flux through the PPP through evolution on xylose also increased 4-hydroxybenzoate production in an engineered *P. putida* S12 (Meijnen et al., 2011), making it likely that this pathway poses a bottleneck in the engineered *P. taiwanensis* strains as well. Given that overexpression of *tktA* did not improve production, phosphoglucose isomerase (*pgi*) was chosen as upstream target, converting glucose-6-phosphate into fructose-6-phosphate.

To investigate whether the overexpression of these two genes has a beneficial effect on 4-hydroxybenzoate formation, they were cloned separately and together into the pBNT'mcs plasmid and transformed into *P. taiwanensis* VLB120 CL3, thereby generating *P. taiwanensis* VLB120 CL3.1 overexpressing *ppsA*, *P. taiwanensis* VLB120 CL3.2 overexpressing *pgi* and *P. taiwanensis* VLB120 CL3.3 overexpressing both genes. The strains were cultivated in mineral medium containing 20 mM glucose as a sole carbon source (**Figure 5**). Overexpression of the individual genes did not result in an increase of 4-hydroxybenzoate titer. However, a synergistic effect of both genes could be observed, by which a 4-hydroxybenzoate concentration of 2.62 ± 0.07 mM was produced from 20 mM glucose, corresponding to a C-mol yield of 15.3%, which is an increase of 18.6% compared to the equivalent strain without *ppsA-pgi* overexpression. As the best performance of 4-hydroxybenzoate production was achieved upon combined overexpression of both *ppsA* and *pgi*, the *Rs*TAL-harboring strain *P. taiwanensis* VLB120 CL4 was equipped with plasmid pBNT'*ppsA-pgi* and hereafter named *P. taiwanensis* VLB120 CL4.3. Under the same conditions as strain *P. taiwanensis* VLB120 CL3.3, this strain produced 3.26 ± 0.05 mM 4-hydroxybenzoate with a C-mol yield of 19.0%. Compared to the reference strain, overexpression of *ppsA* and/or *pgi* had a negative effect on growth. On the one hand, this may be due to the additional plasmid-borne metabolic load. However, since lowest biomass values can be observed in strains harboring *ppsA-pgi* constructs, it can be assumed that poorer growth may be due to reduced availability of PEP and E4P which is now channeled into the shikimate pathway and toward 4-hydroxybenzoate. In addition, PpsA phosphorylates pyruvate through the conversion of ATP into AMP (Berman and Cohn, 1970), and may thus constitute an ATP-wasting futile cycle in conjunction with the reverse pyruvate kinase reaction (Hädicke et al., 2015).

Production of 4-Hydroxybenzoate Is Enhanced on Glycerol, but Not on Xylose

Former studies showed that glycerol represents a promising alternative to glucose as a renewable biotechnological feedstock (Murarka et al., 2008; Yang et al., 2012; West, 2013; Zambanini et al., 2017; Wynands et al., 2018). Being a byproduct formed

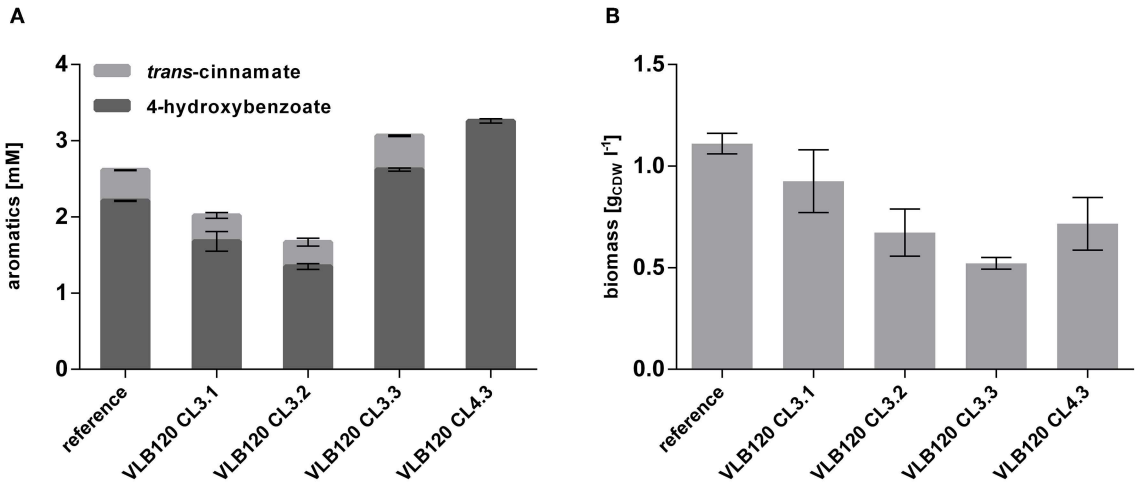

FIGURE 5 | Overexpression of *ppsA* and *pgi* in *P. taiwanensis* VLB120 CL3 and CL4. Cells were cultivated in biological triplicates in MSM with 20 mM glucose as a sole carbon source at 30°C and 300 rpm in System Duetz plates. Expression of *ppsA* and *pgi* was induced with 0.1 mM salicylate and expression of the ferulic genes with 0.2 mM IPTG. Concentrations of aromatics **(A)** and biomass **(B)** measured after 96 h. Error bars indicate standard error of the mean.

during biodiesel production, it is a cheap substrate, and another advantage over glucose is that it can be applied in higher concentrations for *Pseudomonas* batch cultivations, since no gluconate is formed which acidifies the medium. To evaluate the performance of *P. taiwanensis* VLB120 CL3 and *P. taiwanensis* VLB120 CL3.3 on this substrate, they were cultivated in MSM containing glycerol as sole carbon source. When grown on 40 mM glycerol (**Figure 6A**), a final titer of 4.72 ± 0.01 mM 4-hydroxybenzoate was achieved, corresponding to a C-mol yield of 27.5%. A maximum production rate of 0.57 mmol g_{CDW}^{-1} h^{-1} was reached after 16 h, which is a 1.8-fold increase compared to the same strains on glucose, and a 2.6-fold increase compared to the *P. putida* S12 strain of Verhoef et al. (2007) under similar conditions. The overexpression of *ppsA-pgi* in *P. taiwanensis* VLB120 CL3.3 further increased the titer to 5.1 ± 0.1 mM of 4-hydroxybenzoate with a C-mol yield of 29.6% (**Figure 6B**). Considering formation of *trans*-cinnamate as a byproduct of *Rt*PAL, *P. taiwanensis* VLB120 CL3 and *P. taiwanensis* VLB120 CL3.3 reached a total aromatics C-mol yield of 32.3% and 35.1%, respectively.

Increasing the initial glycerol concentration also increased product titers. This did, however, affect production efficiency, as C-mol yields of 23.9, 20.0, and 16.0% were reached using 80, 120, and 200 mM glycerol, respectively (**Figure 6C**). The relatively low yield achieved with 200 mM glycerol is likely, at least in part, caused by the fact that such a substrate concentration will lead to a nitrogen limitation under the conditions tested. Still, it is remarkable that 4-hydroxybenzoate production is more than twice as efficient from glycerol as from an equivalent concentration of glucose. For *P. putida* KT2440, it was shown that growth on glycerol leads to metabolic and regulatory rearrangements within the cell (Nikel et al., 2014a). Genes belonging to the Entner-Doudoroff pathway as well as stress-related genes are downregulated and enhanced expression of genes of the glyoxylate shunt as well as *pgi* was detected. In concert, these actions may result in increased availability of PEP and E4P which, together with the lower growth rate, could lead to a more efficient channeling of these central metabolites into the shikimate pathway.

Production of 4-hydroxybenzoate from glycerol was also investigated for strain *P. taiwanensis* VLB120 CL4 and *P. taiwanensis* VLB120 CL4.3. Unexpectedly, these strains only reached a final 4-hydroxybenzoate concentration of 0.44 ± 0.01 mM without and 0.43 ± 0.03 mM with *ppsA-pgi* overexpression, which is only 9.4% of the 4-hydroxybenzoate concentrations produced by *P. taiwanensis* VLB120 CL3. Additionally, for the strain *P. taiwanensis* VLB120 CL4, a residual concentration of 0.81 ± 0.01 mM tyrosine and 0.78 ± 0.01 mM for strain *P. taiwanensis* VLB120 CL4.3 was measured in the supernatant. These low titers may be caused by the lack of conversion of phenylalanine into *trans*-cinnamate, which could lead to an increased intracellular phenylalanine concentration, triggering feedback-inhibition mechanisms in the upstream pathway. This may be exacerbated by a reduced expression of *phhAB*, which is 20–30-fold less strongly induced on glycerol than on glucose in the 4-hydroxybenzoate producing *P. putida* S12palB1 (Verhoef et al., 2010). Indeed, the culture supernatant of the *Rs*TAL strains turned brownish during cultivation, hinting toward the accumulation of shikimate pathway intermediates, as described by Wynands et al. (2018).

Lignocellulosic biomass contains up to 25% pentose sugars such as xylose (Lee, 1997), making it a relevant alternative substrate especially on lignocellulosic hydrolysates. In contrast to e.g., *C. glutamicum* and *P. putida*, *P. taiwanensis* VLB120 is natively capable of assimilating xylose via the Weimberg pathway (Köhler et al., 2015). To exploit this trait for 4-hydroxybenzoate biosynthesis, production performance of strains *P. taiwanensis*

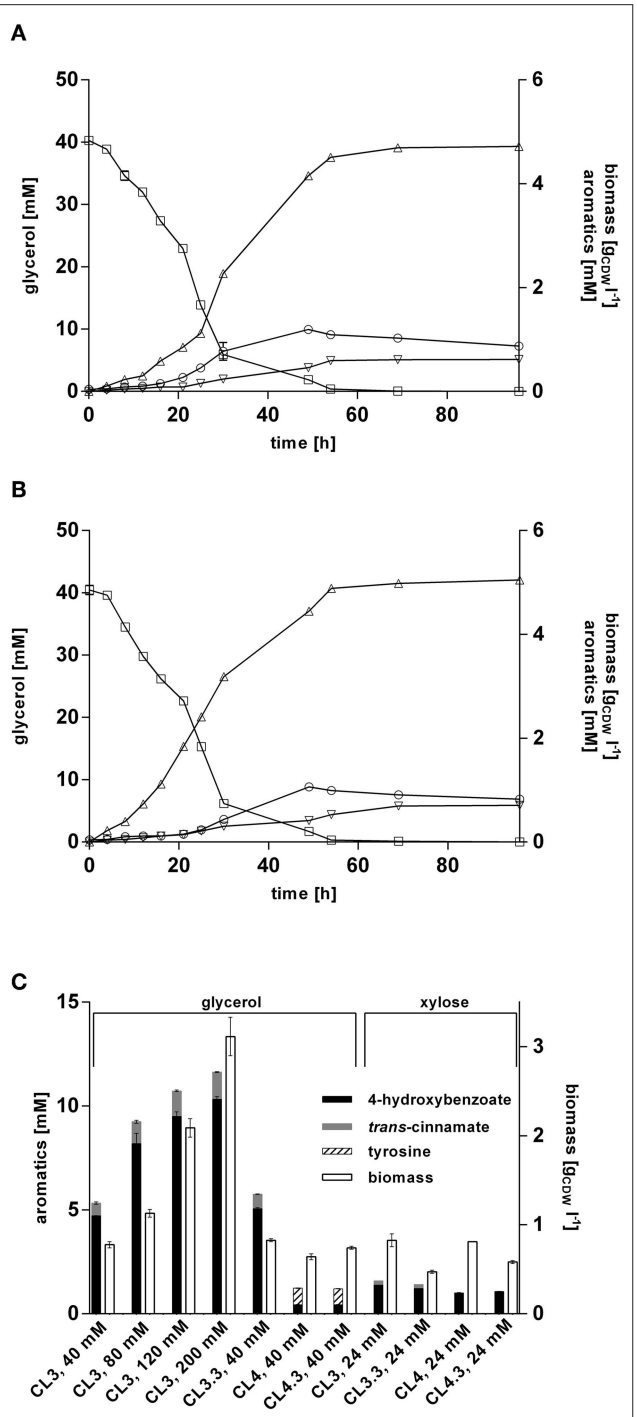

FIGURE 6 | 4-hydroxybenzoate production from glycerol and xylose by engineered *P. taiwanensis* VLB120 strains. Cells were grown in biological triplicates in MSM containing glycerol or 24 mM xylose as a sole carbon source in 24-well System Duetz plates at 30°C and 300 rpm. Expression of ferulic genes was induced with 0.2 mM IPTG. Cultivations of **(A)** strain CL3 and **(B)** CL3.3 Values of biomass (circles), glycerol (squares), 4-hydroxybenzoate (triangles), and *trans*-cinnamate (inverted triangles) are shown. **(C)** Aromatics concentrations and biomass after 96 h. The used substrate concentrations are indicated on the X-axis. For *P. taiwanensis* VLB120 CL3.3 and CL4.3, expression of *ppsA-pgi* was induced with 0.1 mM salicylate. Error bars indicate standard error of the mean.

VLB120 CL3 harboring *Rt*PAL and the *ppsA-pgi* overexpressing variant CL3.3, as well as their *Rs*TAL-harboring equivalents *P. taiwanensis* VLB120 CL 4 and CL4.3, was investigated in MSM containing 24 mM of xylose (**Figure 6C**). Strain CL3 produced 1.37 mM and strain CL3.3 (*ppsA-pgi* overexpression) 1.21 mM 4-hydroxybenzoate, which is 38% and 54%, respectively, less than on the equivalent amount of glucose. The counterparts CL4 and CL4.3. containing *Rs*TAL. reached similar titers of 1.0 mM and 1.1 mM. During its multi-step assimilation, xylose is converted to α-ketoglutarate and thus enters the primary metabolism at the level of the TCA cycle (Weimberg, 1961). This sets it apart from glucose and glycerol in that PEP and E4P as precursors for 4-hydroxybenzoate formation are formed by gluconeogenic reactions at a higher energetic expense compared to glycolysis. This is likely one explanation for the lower production performance. In accordance with Köhler et al. (2015), growth on xylose also resulted in decreased formation of biomass compared to glucose, with 0.83 g_{CDW} l^{-1} for strain CL3, 0.47 g_{CDW} l^{-1} for CL3.3, 0.8 g_{CDW} l^{-1} for CL4, and 0.58 g_{CDW} l^{-1} for strain CL4.3. In summary, the feasibility of 4-hydroxybenzoate production upon intrinsic use of xylose as sustainable carbon source could be demonstrated. However, the fact that neither the avoidance of *trans*-cinnamate formation through the use of *Rs*TAL, nor *ppsA-pgi* overexpression could considerably enhance 4-hydroxybenzoate titers, underlines that, as in the case of glucose and glycerol, production has to be tailored to the respective substrate. To this end, the insertion of a non-oxidative xylose metabolic pathway, likely coupled to adaptive laboratory evolution, may be a promising strategy (Meijnen et al., 2008, 2011).

Production of 4-Hydroxybenzoate From Glycerol Via Pulsed Fed-Batch Cultivation

In order to increase final product titers beyond those enabled by simple shake-flask cultivations, strain *P. taiwanensis* VLB120 CL3.3 was cultivated in 1 l MSM with glycerol as sole carbon source in controlled bioreactors under pulsed fed-batch conditions (**Figure 7**). After an initial batch phase on 120 mM glycerol, the cultures were pulsed multiple times with 200 mM glycerol when an increase in the dissolved oxygen tension was observed, indicating a depletion of the carbon source. The reactors were titrated with ammonium hydroxide to maintain a neutral pH and to avoid a nitrogen limitation at higher cell densities. With this system, a final 4-hydroxybenzoate titer of 72.0 ± 0.96 mM (9.9 g l^{-1}) was reached, and 11.2 ± 0.37 mM (1.7 g l^{-1}) *trans*-cinnamate was produced, whereas no tyrosine was detected in the culture supernatant. After 85 h of cultivation, both growth and production ceased immediately, so that the last pulse of glycerol had no more effect on biomass and product formation and appeared to be only consumed for homeostasis. Excluding this final pulse, a 4-hydroxybenzoate C-mol yield of 19.2% and total aromatics C-mol yield of 23.0% were reached, with maximum production rate of 0.49 mmol g_{CDW}^{-1} h^{-1}.

The rather abrupt cessation of growth and product formation is likely due to product toxicity, product inhibition, or both. In order to test this, batch cultures of *P. taiwanensis* VLB120

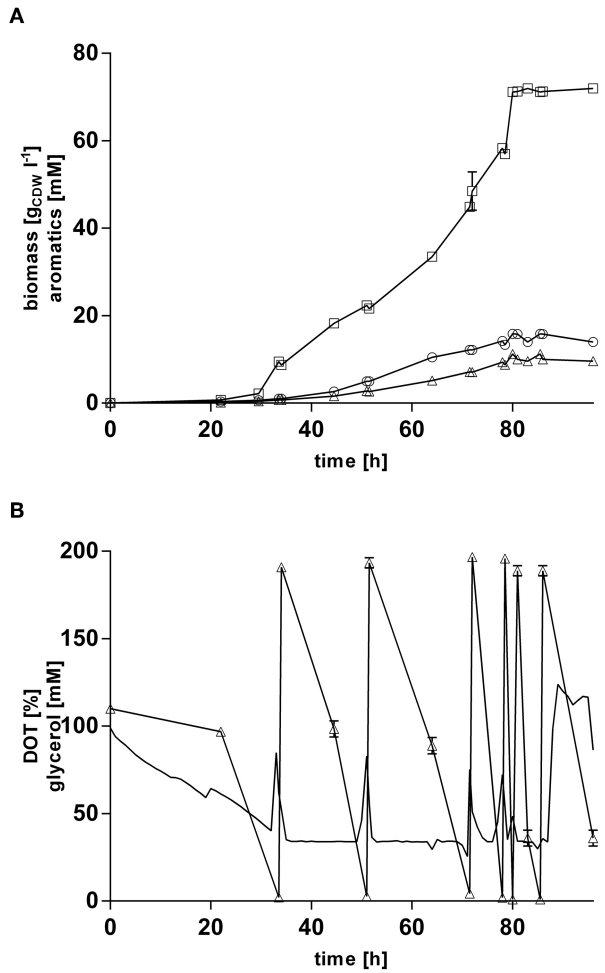

FIGURE 7 | Glycerol pulsed fed-batch cultivation of *P. taiwanensis* VLB120 CL3.3. Cultivation took place in MSM containing an initial glycerol concentration of 120 mM as a sole carbon source. Expression of the ferulic operon and *ppsA-pgi* was induced by addition of 0.2 mM IPTG and 0.1 mM salicylate. Two biological replicates were cultivated. **(A)** Mean values of biomass (circles), 4-hydroxybenzoate (squares), *trans*-cinnamate (triangles) are shown. **(B)** Dissolved oxygen tension (no symbols) and glycerol (triangles). Dissolved oxygen tension values from one replicate are shown. Error bars indicate the deviation from the mean.

CL3.3 on MSM with 120 mM glycerol were pulsed with different concentrations of 4-hydroxybenzoate in the exponential growth phase after 23 h (**Figure 8**). At this point, the culture had already produced 3.7 ± 0.11 mM 4-hydroxybenzoate. Growth was monitored using a Growth Profiler® and 4-hydroxybenzoate concentrations were measured immediately after the pulse and at the end of the experiment. Compared to the control (no addition) which continued growing as expected and produced 14.4 ± 0.04 mM 4-hydroxybenzoate, a strong inhibition of growth was already observed at the lowest added concentration of 50 mM 4-hydroxybenzoate. Upon addition of 50 and 60 mM 4-hydroxybenzoate, a significant additional 2.2 ± 0.08 mM, respectively, 1.5 ± 0.33 mM 4-hydroxybenzoate were produced, which amounts to total titers of 5.9 ± 0.19 mM and 5.2 ± 0.33 mM, respectively. No significant increase in concentration was measured after a pulse of 70 mM 4-hydroxybenzoate and higher concentrations. These results are in good accordance with the final titer of 72 mM reached in the pulsed fed-batch cultivation, and indicate that both product toxicity and product inhibition are severe at this concentration of 4-hydroxybenzoate, and that product toxicity likely is the predominant factor. In comparison, an impressive tolerance of *C. glutamicum* toward up to 300 mM 4-hydroxybenzoate was shown by Kitade et al. (2018). During growth-arrested production, the engineered *C. glutamicum* strains produced 4-hydroxybenzoate with a remarkable titer of 37 g l^{-1} and a yield of 41% (mol/mol). This was achieved in a two-step-process comprising formation of biomass in a rich medium and subsequent high-cell density production in minimal medium. The *P. taiwanensis* VLB120 strains developed in this study, however, were subject to 4-hydroxybenzoate production using a fully mineral medium combined with cell growth, which hence was included in all yield calculations. The two-stage process reported by Kitade et al. (2018) could provide a promising approach to reduce product toxicity for *Pseudomonas*, given that the cells only need to survive, rather than grow. Alternatively, *in situ* product removal could be applied to circumvent the accumulation of inhibiting concentrations of 4-hydroxybenzoate, and thereby increase production performance of *P. taiwanensis* VLB120 hosts. Regarding this approach, strategies such as Calcium salt precipitation (Zambanini et al., 2016), co-crystallization (Urbanus et al., 2010) as well as reactive extraction (Schügerl and Hubbuch, 2005; Kreyenschulte et al., 2018) have been proven to be applicable for organic acids.

CONCLUSION

This study describes the rational metabolic engineering of a *P. taiwanensis* VLB120 strain for high-yield microbial catalysis of glucose or glycerol into 4-hydroxybenzoate via the central metabolite L-tyrosine. This was achieved in a completely minimal medium, without the use of auxotrophies to force metabolic flux toward the product of interest. The formation of *trans*-cinnamate as a byproduct could be avoided through the use of the tyrosine-specific *Rs*TAL, but this only enabled efficient 4-hydroxybenzoate production from glucose, and not from glycerol. Large differences in product to substrate yields were achieved on these two carbon sources, with glycerol being the preferred substrate with C-mol yields up to 29.6% (= 0.19 g/g) as long as the less specific *Rt*PAL was used. To the best of our knowledge, this is the highest reported 4-hydroxybenzoate yield on a fully mineral medium. The unexpected interplay between the up- and downstream pathways of tyrosine should be further investigated, which would likely yield valuable insights into the underlying mechanisms of the fundamental synthetic

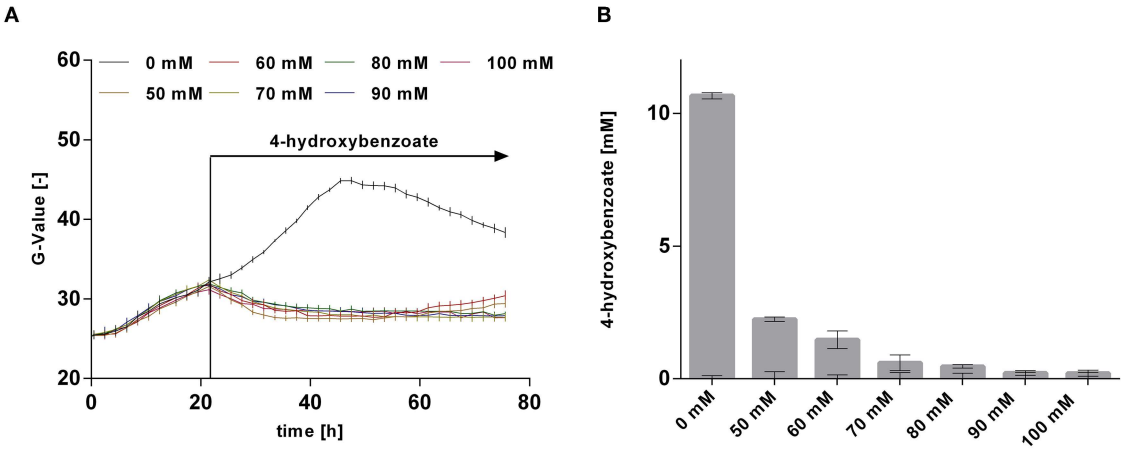

FIGURE 8 | Growth and production upon a 4-hydroxybenzoate pulse. *P. taiwanensis* VLB120 CL3.3 was cultivated in 24-well System Duetz plates in a Growth Profiler in MSM containing 120 mM glycerol as sole carbon source. Each well was filled with a culture volume of 1,350 µl. At an OD_{600} of ∼1, different concentrations of 4-hydroxybenzoate were applied as indicated, using 150 µl of a 10x stock solution for each concentration adjusted to pH 7, whereas water was added to the wells with no 4-hydroxybenzoate pulse. Growth **(A)** was monitored by image analysis and concentrations were measured immediately after addition and at the end of experiment. **(B)** Difference between 4-hydroxybenzoate concentrations just after the pulse and after 96 h. Values of triplicate samples are shown, error bars indicate standard error of the mean.

biology concept of chassis and modules. Production of 4-hydroxybenzoate from xylose was also demonstrated, although in this case the relatively low performance compared to glucose or glycerol indicates that further improvement of central precursor supply is needed. In all, this work provides a significant advance in the efficiency of aromatics production in non-pathogenic Pseudomonads, the fundamentals of which can be applied to enable the sustainable production of 4-hydroxybenzoate. In addition, the development of the solvent-tolerant *P. taiwanensis* as aromatics platform can be further exploited for the biosynthesis of a wide range of other more toxic chemicals.

AUTHOR CONTRIBUTIONS

All authors saw and approved the manuscript. All authors contributed significantly to the work. NW conceived the project. NW, CL, and LB designed experiments and analyzed results. CL and NW wrote the manuscript with the help of LB, BW, and MO. CL performed experiments, supported by BW, MO, JB, and PM.

FUNDING

This project was funded by the German Research Foundation through the Emmy Noether program (WI 4255/1-1). LB also acknowledges funding by the Cluster of Excellence The Fuel Science Center–Adaptive Conversion Systems for Renewable Energy and Carbon Sources, which is funded by the Excellence Initiative of the German federal and state governments to promote science and research at German universities.

ACKNOWLEDGMENTS

We thank Sebastian Köbbing for providing plasmids pBG14fg and pBG14ffg.

SUPPLEMENTARY MATERIAL

The Supplementary Material for this article can be found online at: https://www.frontiersin.org/articles/10.3389/fbioe.2019.00130/full#supplementary-material

REFERENCES

Arias-Barrau, E., Olivera, E. R., Luengo, J. M., Fernández, C., Galán, B., García, J. L., et al. (2004). The homogentisate pathway: a central catabolic pathway involved in the degradation of L-phenylalanine, L-tyrosine, and 3-hydroxyphenylacetate in *Pseudomonas putida*. *J. Bacteriol.* 186, 5062–5077. doi: 10.1128/JB.186.15.5062-5077.2004

Barker, J. L., and Frost, J. W. (2001). Microbial synthesis of *p*-hydroxybenzoic acid from glucose. *Biotechnol. Bioeng.* 76, 376–390. doi: 10.1002/bit.10160

Beers, D. E., and Ramirez, J. E. (1990). Vectran high-performance fibre. *J. Text. Inst.* 81, 561–574. doi: 10.1080/00405009008658729

Belda, E., van Heck, R. G., José Lopez-Sanchez, M., Cruveiller, S., Barbe, V., Fraser, C., et al. (2016). The revisited genome of *Pseudomonas putida* KT2440 enlightens its value as a robust metabolic chassis. *Environ. Microbiol.* 18, 3403–3424. doi: 10.1111/1462-2920.13230

Benaskar, F., Hessel, V., Krtschil, U., and Lo, P. (2009). Intensification of the capillary-based Kolbe-Schmitt synthesis from resorcinol by reactive ionic liquids, microwave heating, or a combination thereof. *Org. Process Res. Dev.* 13, 970–982. doi: 10.1021/op9000803

Berman, K. M., and Cohn, M. (1970). Phosphoenolpyruvate synthetase Partial reactions studied with adenosine triphosphate analogues and the inorganic phosphate-h2 18O exchange reaction. *J. Biol. Chem.* 245, 5319–5325.

Choi, K. H., Gaynor, J. B., White, K. G., Lopez, C., Bosio, C. M., Karkhoff-Schweizer, R. R., et al. (2005). A Tn7-based broad-range bacterial cloning and expression system. *Nat. Methods* 2, 443–448. doi: 10.1038/nmeth765

Chomczynski, P., and Rymaszewski, M. (2006). Alkaline polyethylene glycol-based method for direct PCR from bacteria, eukaryotic tissue samples, and whole blood. *Biotechniques* 40, 454–458. doi: 10.2144/000112149

de las Heras, A., Carreño, C. A., and de Lorenzo, V. (2008). Stable implantation of orthogonal sensor circuits in Gram-negative bacteria for environmental release. *Environ. Microbiol.* 10, 3305–3316. doi: 10.1111/j.1462-2920.2008.01722.x

Dos Santos, V. A., Heim, S., Moore, E. R., Strätz, M., and Timmis, K. N. (2004). Insights into the genomic basis of niche specificity of *Pseudomonas putida* KT2440. *Environ. Microbiol.* 6, 1264–1286. doi: 10.1111/j.1462-2920.2004.00734.x

Duetz, W. A., Rüedi, L., Hermann, R., O'Connor, K., Büchs, J., and Witholt, B. (2000). Methods for intense aeration, growth, storage, and replication of bacterial strains in microtiter plates. *Appl. Environ. Microbiol.* 66, 2641–2646. doi: 10.1128/AEM.66.6.2641-2646.2000

Elbahloul, Y., and Steinbüchel, A. (2009). Large-scale production of poly(3-hydroxyoctanoic acid) by *Pseudomonas putida* GPo1 and a simplified downstream process. *Appl. Environ. Microbiol.* 75, 643–651. doi: 10.1128/AEM.01869-08

Figurski, D. H., and Helinski, D. R. (1979). Replication of an origin-containing derivative of plasmid RK2 dependent on a plasmid function provided in trans. *Proc. Natl. Acad. Sci. U.S.A.* 76, 1648–1652. doi: 10.1073/pnas.76.4.1648

Fuhrer, T., Fischer, E., and Sauer, U. (2005). Experimental identification and quantification of glucose metabolism in seven bacterial species. *J. Bacteriol.* 187, 1581–1590. doi: 10.1128/JB.187.5.1581-1590.2005

Gao, Y., Liu, C., Ding, Y., Sun, C., Zhang, R., and Xian, M. (2014). Development of genetically stable *Escherichia coli* strains for poly (3-hydroxypropionate) production. *PLoS ONE* 9:e97845. doi: 10.1371/journal.pone.0097845

Glover, D. M., and Hames, B. D. (1985). DNA *Cloning: A Practical Approach*. Oxford; Washington, DC: IRL press Oxford.

Hädicke, O., Bettenbrock, K., and Klamt, S. (2015). Enforced ATP futile cycling increases specific productivity and yield of anaerobic lactate production in *Escherichia coli*. *Biotechnol. Bioeng.* 112, 2195–2199. doi: 10.1002/bit.25623

Hartmans, S., Smits, J. P., van der Werf, M. J., Volkering, F., and de Bont, J. A. (1989). Metabolism of styrene oxide and 2-phenylethanol in the styrene-degrading *Xanthobacter* strain 124X. *Appl. Environ. Microbiol.* 55, 2850–2855.

Harwood, C. S., and Parales, R. E. (1996). The β-ketoadipate pathway and the biology of self-identity. *Annu. Rev. Microbiol.* 50, 553–590. doi: 10.1146/annurev.micro.50.1.553

Hernández-Arranz, S., Sánchez-Hevia, D., Rojo, F., and Moreno, R. (2016). Effect of Crc and Hfq proteins on the transcription, processing, and stability of the *Pseudomonas putida* CrcZ sRNA. *RNA* 22, 1–16. doi: 10.1261/rna.058313.116

Hester, K. L., Lehman, J., Najar, F., Song, L., Roe, B. A., Macgregor, C. H., et al. (2000a). Crc is involved in catabolite repression control of the *bkd* operons of *Pseudomonas putida* and *Pseudomonas aeruginosa*. *J. Bacteriol.* 182, 1144–1149. doi: 10.1128/JB.182.4.1144-1149.2000

Hester, K. L., Madhusudhan, K. T., and Sokatch, J. R. (2000b). Catabolite repression control by Crc in 2xYT medium is mediated by posttranscriptional regulation of *bkdR* expression in *Pseudomonas putida*. *J. Bacteriol.* 182, 1150–1153. doi: 10.1128/JB.182.4.1150-1153.2000

Jahn, M., Vorpahl, C., Türkowsky, D., Lindmeyer, M., Bühler, B., Harms, H., et al. (2014). Accurate determination of plasmid copy number of flow-sorted cells using droplet digital PCR. *Anal. Chem.* 86, 5969–5976. doi: 10.1021/ac501118v

Jendresen, C. B., Stahlhut, S. G., Li, M., Gaspar, P., Siedler, S., Förster, J., et al. (2015). Highly active and specific tyrosine ammonia-lyases from diverse origins enable enhanced production of aromatic compounds in bacteria and *Saccharomyces cerevisiae*. *Appl. Environ. Microbiol.* 81, 4458–4476. doi: 10.1128/AEM.00405-15

Jiménez, J. I., Miñambres, B., García, J. L., and Díaz, E. (2002). Genomic analysis of the aromatic catabolic pathways from *Pseudomonas putida* KT2440. *Environ. Microbiol.* 4, 824–841. doi: 10.1046/j.1462-2920.2002.00370.x

Juminaga, D., Baidoo, E. E., Redding-Johanson, A. M., Batth, T. S., Burd, H., Mukhopadhyay, A., et al. (2012). Modular engineering of L-tyrosine production in *Escherichia coli*. *Appl. Environ. Microbiol.* 78, 89–98. doi: 10.1128/AEM.06017-11

Kallscheuer, N., and Marienhagen, J. (2018). *Corynebacterium glutamicum* as platform for the production of hydroxybenzoic acids. *Microb. Cell Fact.* 17, 1–13. doi: 10.1186/s12934-018-0923-x

Kieboom, J., Dennis, J. J., de Bont, J. A. M., and Zylstra, G. J. (1998). Identification and molecular characterization of an efflux pump involved in *Pseudomonas putida* S12 solvent tolerance. *J. Biol. Chem.* 273, 85–91. doi: 10.1074/jbc.273.1.85

Kikuchi, Y., Tsujimoto, K., and Kurahashi, O. (1997). Mutational analysis of the feedback sites of phenylalanine-sensitive 3- deoxy-d-arabino-heptulosonate-7-phosphate synthase of *Escherichia coli*. *Appl. Environ. Microbiol.* 63, 761–762.

Kim, B., Park, H., Na, D., and Lee, S. Y. (2014). Metabolic engineering of *Escherichia coli* for the production of phenol from glucose. *Biotechnol. J.* 9, 621–629. doi: 10.1002/biot.201300263

Kitade, Y., Hashimoto, R., Suda, M., Hiraga, K., and Inui, M. (2018). Production of 4-hydroxybenzoic acid by an aerobic growth-arrested bioprocess using metabolically engineered *Corynebacterium glutamicum*. *Appl. Environ. Microbiol.* 84:e02587-17. doi: 10.1128/AEM.02587-17

Köhler, K. A. K., Blank, L. M., Frick, O., and Schmid, A. (2015). D-Xylose assimilation via the Weimberg pathway by solvent-tolerant *Pseudomonas taiwanensis* VLB120. *Environ. Microbiol.* 17, 156–170. doi: 10.1111/1462-2920.12537

Kreyenschulte, D., Heyman, B., Eggert, A., Maßmann, T., Kalvelage, C., Kossack, R., et al. (2018). *In situ* reactive extraction of itaconic acid during fermentation of *Aspergillus terreus*. *Biochem. Eng. J.* 135, 133–141. doi: 10.1016/j.bej.2018.04.014

Kuepper, J., Dickler, J., Biggel, M., Behnken, S., Jäger, G., Wierckx, N., et al. (2015). Metabolic engineering of *Pseudomonas putida* KT2440 to produce anthranilate from glucose. *Front. Microbiol.* 6:1310. doi: 10.3389/fmicb.2015.01310

Lee, J. (1997). Biological conversion of lignocellulosic biomass to ethanol. *J. Biotechnol.* 56, 1–24. doi: 10.1016/S0168-1656(97)00073-4

Li, K., Mikola, M. R., Draths, K. M., Worden, R. M., and Frost, J. W. (1999). Fed-batch fermentor synthesis of 3-dehydroshikimic acid using recombinant *Escherichia coli*. *Biotechnol. Bioeng.* 64, 61–73. doi: 10.1002/(SICI)1097-0290(19990705)64:1<61::AID-BIT7>3.0.CO;2-G

Lindsey, A. S., and Jeskey, H. (1957). The Kolbe-Schmitt reaction. *Chem. Rev.* 57, 583–620. doi: 10.1021/cr50016a001

Loeschcke, A., and Thies, S. (2015). *Pseudomonas putida*—a versatile host for the production of natural products. *Appl. Microbiol. Biotechnol.* 99, 6197–6214. doi: 10.1007/s00253-015-6745-4

Lütke-Eversloh, T., and Stephanopoulos, G. (2007). L-tyrosine production by deregulated strains of *Escherichia coli*. *Appl. Microbiol. Biotechnol.* 75, 103–110. doi: 10.1007/s00253-006-0792-9

MacGregor, C. H., Arora, S. K., Hager, P. W., Dail, M. B., and Phibbs, P. V. (1996). The nucleotide sequence of the *Pseudomonas aeruginosa pyrE-crc-rph* region and the purification of the *crc* gene product. *J. Bacteriol.* 178, 5627–5635. doi: 10.1128/jb.178.19.5627-5635.1996

Martínez-García, E., Aparicio, T., de Lorenzo, V., and Nikel, P. I. (2014). New transposon tools tailored for metabolic engineering of Gram-negative microbial cell factories. *Front. Bioeng. Biotechnol.* 2, 1–13. doi: 10.3389/fbioe.2014.00046

Martínez-García, E., and de Lorenzo, V. (2011). Engineering multiple genomic deletions in Gram-negative bacteria: Analysis of the multi-resistant antibiotic profile of *Pseudomonas putida* KT2440. *Environ. Microbiol.* 13, 2702–2716. doi: 10.1111/j.1462-2920.2011.02538.x

Meijnen, J. P., de Winde, J. H., and Ruijssenaars, H. J. (2008). Engineering *Pseudomonas putida* S12 for efficient utilization of D-xylose and L-arabinose. *Appl. Environ. Microbiol.* 74, 5031–5037. doi: 10.1128/AEM.00924-08

Meijnen, J. P., Verhoef, S., Briedjlal, A. A., de Winde, J. H., and Ruijssenaars, H. J. (2011). Improved *p*-hydroxybenzoate production by engineered *Pseudomonas putida* S12 by using a mixed-substrate feeding strategy. *Appl. Microbiol. Biotechnol.* 90, 885–893. doi: 10.1007/s00253-011-3089-6

Menczel, J. D., Collins, G. L., and Saw, S. K. (1997). Thermal analysis of Vectran fibers and films. *J. Therm. Anal.* 49, 201–208. doi: 10.1007/BF01987440

Mi, J., Sydow, A., Schempp, F., Becher, D., Schewe, H., Schrader, J., et al. (2016). Investigation of plasmid-induced growth defect in *Pseudomonas putida*. *J. Biotechnol.* 231, 167–173. doi: 10.1016/j.jbiotec.2016.06.001

Molina-Santiago, C., Cordero, B. F., Daddaoua, A., Udaondo, Z., Manzano, J., Valdivia, M., et al. (2016). *Pseudomonas putida* as a platform for the synthesis of aromatic compounds. *Biotechnol. Bioeng.* 162, 1535–1543. doi: 10.1099/mic.0.000333

Morales, G., Linares, J. F., Beloso, A., Albar, J. P., Martínez, J. L., and Rojo, F. (2004). The *Pseudomonas putida* Crc global regulator controls the expression of genes from several chromosomal catabolic pathways for aromatic compounds. *J. Bacteriol.* 186, 1337–1344. doi: 10.1128/JB.186.5.1337-1344.2004

Moreno, R., Hernández-Arranz, S., La Rosa, R., Yuste, L., Madhushani, A., Shingler, V., et al. (2015). The Crc and Hfq proteins of *Pseudomonas putida* cooperate in catabolite repression and formation of ribonucleic acid complexes with specific target motifs. *Environ. Microbiol.* 17, 105–118. doi: 10.1111/1462-2920.12499

Moreno, R., Martínez-Gomariz, M., Yuste, L., Gil, C., and Rojo, F. (2009a). The *Pseudomonas putida* Crc global regulator controls the hierarchical assimilation of amino acids in a complete medium: evidence from proteomic and genomic analyses. *Proteomics* 9, 2910–2928. doi: 10.1002/pmic.200800918

Moreno, R., Marzi, S., Romby, P., and Rojo, F. (2009b). The Crc global regulator binds to an unpaired A-rich motif at the *Pseudomonas putida alkS* mRNA coding sequence and inhibits translation initiation. *Nucleic Acids Res.* 37, 7678–7690. doi: 10.1093/nar/gkp825

Müller, R., Wagener, A., Schmidt, K., and Leistner, E. (1995). Microbial production of specifically ring-13C-labelled 4-hydroxybenzoic acid. *Appl. Microbiol. Biotechnol.* 43, 985–988. doi: 10.1007/BF00166913

Murarka, A., Dharmadi, Y., Yazdani, S. S., and Gonzalez, R. (2008). Fermentative utilization of glycerol by *Escherichia coli* and its implications for the production of fuels and chemicals. *Appl. Environ. Microbiol.* 74, 1124–1135. doi: 10.1128/AEM.02192-07

Nijkamp, K., Westerhof, R. G., Ballerstedt, H., de Bont, J. A., and Wery, J. (2007). Optimization of the solvent-tolerant *Pseudomonas putida* S12 as host for the production of *p*-coumarate from glucose. *Appl. Microbiol. Biotechnol.* 74, 617–624. doi: 10.1007/s00253-006-0703-0

Nikel, P. I., Chavarría, M., Fuhrer, T., Sauer, U., and de Lorenzo, V. (2015). *Pseudomonas putida* KT2440 strain metabolizes glucose through a cycle formed by enzymes of the Entner-Doudoroff, Embden-Meyerhof-Parnas, and pentose phosphate pathways. *J. Biol. Chem.* 290, 25920–25932. doi: 10.1074/jbc.M115.687749

Nikel, P. I., and de Lorenzo, V. (2013). Implantation of unmarked regulatory and metabolic modules in Gram-negative bacteria with specialised mini-transposon delivery vectors. *J. Biotechnol.* 163, 143–154. doi: 10.1016/j.jbiotec.2012.05.002

Nikel, P. I., and de Lorenzo, V. (2018). *Pseudomonas putida* as a functional chassis for industrial biocatalysis: from native biochemistry to trans-metabolism. *Metab. Eng.* 50, 142–155. doi: 10.1016/j.ymben.2018.05.005

Nikel, P. I., Kim, J., and de Lorenzo, V. (2014a). Metabolic and regulatory rearrangements underlying glycerol metabolism in *Pseudomonas putida* KT2440. *Environ. Microbiol.* 16, 239–254. doi: 10.1111/1462-2920.12224

Nikel, P. I., Martínez-García, E., and de Lorenzo, V. (2014b). Biotechnological domestication of Pseudomonads using synthetic biology. *Nat. Rev. Microbiol.* 12, 368–379. doi: 10.1038/nrmicro3253

Panke, S., Witholt, B., Schmid, A., and Wubbolts, M. G. (1998). Towards a biocatalyst for (*S*)-styrene oxide production: characterization of the styrene degradation pathway of *Pseudomonas* sp. strain VLB120. *Appl. Environ. Microbiol* 64, 2032–2043.

Peek, J., Roman, J., Moran, G. R., and Christendat, D. (2017). Structurally diverse dehydroshikimate dehydratase variants participate in microbial quinate catabolism. *Mol. Microbiol.* 103, 39–54. doi: 10.1111/mmi.13542

Puigbò, P., Guzmán, E., Romeu, A., and Garcia-Vallvé, S. (2007). OPTIMIZER: A web server for optimizing the codon usage of DNA sequences. *Nucleic Acids Res.* 35, 126–131. doi: 10.1093/nar/gkm219

Romano, A. H., Eberhard, S. J., Dingle, S. L., and Mcdowell, T. D. (1970). Distribution of the phosphoenolpyruvate: glucose phosphotransferase system in bacteria. *J. Bacteriol.* 104, 808–813.

Ruiz-Manzano, A., Yuste, L., and Rojo, F. (2005). Levels and activity of the *Pseudomonas putida* global regulatory protein Crc vary according to growth conditions. *J. Bacteriol.* 187, 3678–3686. doi: 10.1128/JB.187.11.3678-3686.2005

Sambrook, J., Fritsch, E. F., and Maniatis, T. (1989). *Molecular Cloning: A Laboratory Manual, 2nd Edn*. New York, NY: Cold Spring Harbor Laboratory.

Schmitz, S., Nies, S., Wierckx, N., Blank, L. M., and Rosenbaum, M. A. (2015). Engineering mediator-based electroactivity in the obligate aerobic bacterium *Pseudomonas putida* KT2440. *Front. Microbiol.* 6:284. doi: 10.3389/fmicb.2015.00284

Schügerl, K., and Hubbuch, J. (2005). Integrated bioprocesses. *Curr. Opin. Microbiol.* 8, 294–300. doi: 10.1016/j.mib.2005.01.002

Silva-Rocha, R., Martínez-García, E., Calles, B., Chavarría, M., Arce-Rodríguez, A., de las Heras, A., et al. (2013). The Standard European Vector Architecture (SEVA): a coherent platform for the analysis and deployment of complex prokaryotic phenotypes. *Nucleic Acids Res.* 41, D666–D675. doi: 10.1093/nar/gks1119

Stark, A., Huebschmann, S., Sellin, M., Kralisch, D., Trotzki, R., and Ondruschka, B. (2009). Microwave-assisted Kolbe-Schmitt synthesis using ionic liquids or dimcarb as reactive solvents. *Chem. Eng. Technol.* 32, 1730–1738. doi: 10.1002/ceat.200900331

Sun, Z., Ramsay, J. A., Guay, M., and Ramsay, B. A. (2006). Automated feeding strategies for high-cell-density fed-batch cultivation of *Pseudomonas putida* KT2440. *Appl. Microbiol. Biotechnol.* 71, 423–431. doi: 10.1007/s00253-005-0191-7

Syukur Purwanto, H., Kang, M.-S., Ferrer, L., Han, S.-S., Lee, J.-Y., Kim, H.-S., et al. (2018). Rational engineering of the shikimate and related pathways in *Corynebacterium glutamicum* for 4-hydroxybenzoate production. *J. Biotechnol.* 282, 92–100. doi: 10.1016/j.jbiotec.2018.07.016

Tiso, T., Sabelhaus, P., Behrens, B., Wittgens, A., Rosenau, F., Hayen, H., et al. (2016). Creating metabolic demand as an engineering strategy in *Pseudomonas putida* – rhamnolipid synthesis as an example. *Metab. Eng. Commun.* 3, 234–244. doi: 10.1016/j.meteno.2016.08.002

Urbanus, J., Roelands, C. P. M., Verdoes, D., Jansens, P. J., and ter Horst, J. H. (2010). Co-crystallization as a separation technology: controlling product concentrations by co-crystals. *Cryst. Growth Des.* 10, 1171–1179. doi: 10.1021/cg9010778

Verhoef, S., Ballerstedt, H., Volkers, R. J. M., de Winde, J. H., and Ruijssenaars, H. J. (2010). Comparative transcriptomics and proteomics of *p*-hydroxybenzoate producing *Pseudomonas putida* S12: novel responses and implications for strain improvement. *Appl. Microbiol. Biotechnol.* 87, 679–690. doi: 10.1007/s00253-010-2626-z

Verhoef, S., Ruijssenaars, H. J., de Bont, J. A., and Wery, J. (2007). Bioproduction of *p*-hydroxybenzoate from renewable feedstock by solvent-tolerant *Pseudomonas putida* S12. *J. Biotechnol.* 132, 49–56. doi: 10.1016/j.jbiotec.2007.08.031

Verhoef, S., Wierckx, N., Westerhof, R. G., de Winde, J. H., and Ruijssenaars, H. J. (2009). Bioproduction of *p*-hydroxystyrene from glucose by the solvent-tolerant bacterium *Pseudomonas putida* S12 in a two-phase water-decanol fermentation. *Appl. Environ. Microbiol.* 75, 931–936. doi: 10.1128/AEM.02186-08

Weimberg, R. (1961). Pentose oxidation by *Pseudomonas fragi*. *J. Biol. Chem* 236, 629–635.

West, T. P. (2013). Citric acid production by *Candida* species grown on a soy-based crude glycerol. *Prep. Biochem. Biotechnol.* 43, 601–611. doi: 10.1080/10826068.2012.762929

Wierckx, N., Prieto, M. A., Pomposiello, P., de Lorenzo, V., O'Connor, K., and Blank, L. M. (2015). Plastic waste as a novel substrate for industrial biotechnology. *Microb. Biotechnol.* 8, 900–903. doi: 10.1111/1751-7915.12312

Wierckx, N., Ruijssenaars, H. J., de Winde, J. H., Schmid, A., and Blank, L. M. (2009). Metabolic flux analysis of a phenol producing mutant of *Pseudomonas putida* S12: verification and complementation of hypotheses derived from transcriptomics. *J. Biotechnol.* 143, 124–129. doi: 10.1016/j.jbiotec.2009.06.023

Wierckx, N. J., Ballerstedt, H., de Bont, J. A., de Winde, J. H., Ruijssenaars, H. J., and Wery, J. (2008). Transcriptome analysis of a phenol-producing *Pseudomonas putida* S12 construct: genetic and physiological basis for improved production. *J. Bacteriol.* 190, 2822–2830. doi: 10.1128/JB.01379-07

Wierckx, N. J., Ballerstedt, H., de Bont, J. A., and Wery, J. (2005). Engineering of solvent-tolerant *Pseudomonas putida* S12 for bioproduction of phenol from glucose. *Appl. Environ. Microbiol.* 71, 8221–8227. doi: 10.1128/AEM.71.12.8221-8227.2005

Winter, G., Averesch, N. J., Nunez-Bernal, D., and Krömer, J. O. (2014). *In vivo* instability of chorismate causes substrate loss during fermentative production of aromatics. *Yeast* 31, 333–341. doi: 10.1002/yea.3025

Wolff, J. A., MacGregor, C. H., Eisenberg, R. C., and Phibbs, P. V. (1991). Isolation and characterization of catabolite repression control mutants of *Pseudomonas aeruginosa* PAO. *J. Bacteriol.* 173, 4700–4706. doi: 10.1128/jb.173.15.4700-4706.1991

Wynands, B., Lenzen, C., Otto, M., Koch, F., Blank, L. M., and Wierckx, N. (2018). Metabolic engineering of *Pseudomonas taiwanensis* VLB120 with minimal genomic modifications for high-yield phenol production. *Metab. Eng.* 47, 121–133. doi: 10.1016/j.ymben.2018.03.011

Xue, Z., McCluskey, M., Cantera, K., Sariaslani, F. S., and Huang, L. (2007). Identification, characterization and functional expression of a tyrosine ammonia-lyase and its mutants from the photosynthetic bacterium *Rhodobacter sphaeroides*. *J. Ind. Microbiol. Biotechnol.* 34, 599–604. doi: 10.1007/s10295-007-0229-1

Yang, F., Hanna, M. A., and Sun, R. (2012). Value-added uses for crude glycerol–a byproduct of biodiesel production. *Biotechnol. Biofuels* 5, 1–10. doi: 10.1186/1754-6834-5-13

Yi, J., Li, K., Draths, K. M., and Frost, J. W. (2002). Modulation of phosphoenolpyruvate synthase expression increases shikimate pathway product yields in *E. coli*. *Biotechnol. Prog.* 18, 1141–1148. doi: 10.1021/bp020101w

Yu, S., Plan, M. R., Winter, G., and Krömer, J. O. (2016). Metabolic engineering of *Pseudomonas putida* KT2440 for the production of *para*-hydroxybenzoic acid. *Front. Bioeng. Biotechnol.* 4:90. doi: 10.3389/fbioe.2016.00090

Zambanini, T., Hosseinpour Tehrani, H., Geiser, E., Sonntag, C. K., Buescher, J. M., Meurer, G., et al. (2017). Metabolic engineering of *Ustilago trichophora* TZ1 for improved malic acid production. *Metab. Eng. Commun.* 4, 12–21. doi: 10.1016/j.meteno.2017.01.002

Zambanini, T., Kleineberg, W., Sarikaya, E., Buescher, J. M., Meurer, G., Wierckx, N., et al. (2016). Enhanced malic acid production from glycerol with high-cell density *Ustilago trichophora* TZ1 cultivations. *Biotechnol. Biofuels* 9:135. doi: 10.1186/s13068-016-0553-7

Zhao, D., Liao, Y., and Zhang, Z. (2007). Toxicity of ionic liquids. *Clean* 35, 42–48. doi: 10.1002/clen.200600015

Zobel, S., Benedetti, I., Eisenbach, L., de Lorenzo, V., Wierckx, N., and Blank, L. M. (2015). Tn7-based device for calibrated heterologous gene expression in *Pseudomonas putida*. *ACS Synth. Biol.* 4, 1341–1351. doi: 10.1021/acssynbio.5b00058

Conflict of Interest Statement: NW is employed by the Institute for Bio-und Geosciences (IBG-1): Biotechnology, Forschungszentrum Jülich GmbH.

The remaining authors declare that the research was conducted in the absence of any commercial or financial relationships that could be construed as a potential conflict of interest.

frontiers in Bioengineering and Biotechnology

ORIGINAL RESEARCH
published: 18 September 2019
doi: 10.3389/fbioe.2019.00219

Bromination of L-tryptophan in a Fermentative Process With *Corynebacterium glutamicum*

*Kareen H. Veldmann[1], Steffen Dachwitz[2], Joe Max Risse[3], Jin-Ho Lee[4], Norbert Sewald[2] and Volker F. Wendisch[1]**

[1] Genetics of Prokaryotes, Faculty of Biology & Center for Biotechnology (CeBiTec), Bielefeld University, Bielefeld, Germany, [2] Organic and Bioorganic Chemistry, Faculty of Chemistry & Center for Biotechnology (CeBiTec), Bielefeld University, Bielefeld, Germany, [3] Fermentation Technology, Technical Faculty & Center for Biotechnology (CeBiTec), Bielefeld University, Bielefeld, Germany, [4] Major in Food Science and Biotechnology, School of Food Biotechnology and Nutrition, BB21+, Kyungsung University, Busan, South Korea

Brominated compounds such as 7-bromo-L-tryptophan (7-Br-Trp) occur in Nature. Many synthetic and natural brominated compounds have applications in the agriculture, food, and pharmaceutical industries, for example, the 20S-proteasome inhibitor TMC-95A that may be derived from 7-Br-Trp. Mild halogenation by cross-linked enzyme aggregates containing FAD-dependent halogenase, NADH-dependent flavin reductase, and alcohol dehydrogenase as well as by fermentation with recombinant *Corynebacterium glutamicum* expressing the genes for the FAD-dependent halogenase RebH and the NADH-dependent flavin reductase RebF from *Lechevalieria aerocolonigenes* have recently been developed as green alternatives to more hazardous chemical routes. In this study, the fermentative production of 7-Br-Trp was established. The fermentative process employs an L-tryptophan producing *C. glutamicum* strain expressing *rebH* and *rebF* from *L. aerocolonigenes* for halogenation and is based on glucose, ammonium and sodium bromide. *C. glutamicum* tolerated high sodium bromide concentrations, but its growth rate was reduced to half-maximal at 0.09 g L^{-1} 7-bromo-L-tryptophan. This may be, at least in part, due to inhibition of anthranilate phosphoribosyltransferase by 7-Br-Trp since anthranilate phosphoribosyltransferase activity in crude extracts was half-maximal at about 0.03 g L^{-1} 7-Br-Trp. Fermentative production of 7-Br-Trp by recombinant *C. glutamicum* was scaled up to a working volume of 2 L and operated in batch and fed-batch mode. The titers were increased from batch fermentation in CGXII minimal medium with 0.3 g L^{-1} 7-Br-Trp to fed-batch fermentation in HSG complex medium, where up to 1.2 g L^{-1} 7-Br-Trp were obtained. The product isolated from the culture broth was characterized by NMR and LC-MS and shown to be 7-Br-Trp.

Keywords: *Corynebacterium*, fermentation, halogenation, amino acids, 7-bromo-L-tryptophan

OPEN ACCESS

Edited by:
Nils Jonathan Helmuth Averesch, Stanford University, United States

Reviewed by:
Si Jae Park, Ewha Womans University, South Korea
Zhen Chen, Tsinghua University, China

***Correspondence:**
Volker F. Wendisch
volker.wendisch@uni-bielefeld.de

Specialty section:
This article was submitted to Bioprocess Engineering, a section of the journal Frontiers in Bioengineering and Biotechnology

Received: *28 April 2019*
Accepted: *27 August 2019*
Published: *18 September 2019*

Citation:
Veldmann KH, Dachwitz S, Risse JM, Lee J-H, Sewald N and Wendisch VF (2019) Bromination of L-tryptophan in a Fermentative Process With Corynebacterium glutamicum. Front. Bioeng. Biotechnol. 7:219. doi: 10.3389/fbioe.2019.00219

INTRODUCTION

Brominated tryptophan is typically not found in free form in Nature, but as a biosynthetic precursor in complex structures that for example occur in sponges and lower marine invertebrates (Bittner et al., 2007). The brominated molecules often exhibit pharmaceutical and biological activities. For example, TMC-95A which derives from 7-bromo-L-tryptophan (7-Br-Trp) is biologically active

against the chymotrypsin-like, trypsin-like, and peptidyl-glutamyl-peptide-hydrolyzing activities of the 20S proteasome of eukaryotic cells (Koguchi et al., 2000). Protease inhibitors may be promising candidates for tumor and inflammation therapies (Adams, 2004; Vergnolle, 2016). Free unprotected halotryptophans including 7-Br-Trp and 7-chloro-L-tryptophan (7-Cl-Trp) can serve as substrates for Pd-catalyzed cross-coupling reactions (Willemse et al., 2017) for example in the Suzuki-Miyaura cross-coupling in order to attach an aryl, heteroaryl, or alkenyl substituent to the indole ring (Roy et al., 2008). For this reaction, 7-Br-Trp is preferred because it is more reactive than 7-Cl-Trp (Corr et al., 2017). In addition, 7-Br-Trp can also be used in other transition metal-catalyzed cross couplings such as the Mizoroki-Heck reaction (Gruß et al., 2019) giving fluorescent styryl-tryptophans or the Sonogashira cross-coupling reaction (Sonogashira, 2002) to generate compounds such as the new-to-nature bromo-cystargamide or to selectively modify bromo-tryptophan residues as a component of a tripeptide (Corr et al., 2017). 7-Cl-Trp is not useful for the Sonogashira cross coupling reaction since it is too unreactive (Corr et al., 2017). Furthermore, 7-Br-Trp can easily be converted to 7-bromoindole, which may give rise to many indole derivates including the MOM-protected 7-bromoisatin, which is the precursor of the antimitotic agent diazonamide A (Nicolaou et al., 2002; Wang et al., 2007; Bartoli et al., 2014). Halogenation of L-tryptophan (Trp) involves two enzymes of the *reb* operon of *Lechevalieria aerocolonigenes*, the FAD-dependent halogenase RebH and the NADH-dependent flavin reductase RebF required for NADH-dependent redox cofactor regeneration (Nishizawa et al., 2005). The halogenase RebH from *L. aerocolonigenes* chlorinates Trp to 7-Cl-Trp, the precursor of rebeccamycin. While this enzyme also accepts bromide, it prefers chloride over bromide (Yeh et al., 2005). Purified cross-linked enzyme aggregates comprising RebH, RebF, and an alcohol dehydrogenase to regenerate NADH by oxidation of isopropanol have successfully been applied to the enzymatic bromination of Trp at the gram-scale (Frese and Sewald, 2015; Schnepel and Sewald, 2017). Fermentative production of 7-Cl-Trp has recently been established using recombinant *Corynebacterium glutamicum* (Veldmann et al., 2019).

Fermentation processes with *C. glutamicum* that serves as a work horse for the biotechnological production of different amino acids are scalable and in the case of L-lysine and L-glutamate applied at the million-ton scale (Wendisch, 2019). Fermentative processes unlike chemical synthesis routes do not require environmentally hazardous compounds (e.g., elemental chlorine or bromine) or protecting/activating groups because of the high stereo-and regioselectivities of the enzymes involved. Biotransformations using purified enzymes may suffer from low stability and low activity (e.g., of halogenases), especially under non-native reaction conditions in the presence of high substrate concentrations (Latham et al., 2017). Fermentative processes start from sugars and the biocatalyst is (re)generated during growth. Fermentative processes are excellent for synthesis if export of the product out of the cell is efficient and neither substrates nor products nor intermediates inhibit cellular metabolism.

C. glutamicum typically shows higher tolerance to many substances including organic acids, furan, and phenolic inhibitors present in lignocellulose hydrolysates (Sakai et al., 2007). Adaptive laboratory evolution led to increased tolerance to methanol (Leßmeier and Wendisch, 2015) or lignocellulose derived inhibitors (Wang et al., 2018). Thus, *C. glutamicum* was engineered for production of carboxylic acids such as pyruvate (Wieschalka et al., 2012) and succinate (Litsanov et al., 2012), oxoacids such as 2-ketoisovalerate (Krause et al., 2010) and 2-ketoisocaproate (Bückle-Vallant et al., 2014), alcohols such as ethanol (Inui et al., 2004a), isobutanol (Blombach et al., 2011), and *n*-propanol (Siebert and Wendisch, 2015), polymers such as polyhydroxyalkanoate (Ma et al., 2018). As industrial amino acid producer *C. glutamicum* is ideal for fermentative production of various other nitrogenous compounds such as the cyclic amino acid pipecolic acid (Pérez-García et al., 2016), the ω-amino acids γ-aminobutyrate (Kim et al., 2013; Jorge et al., 2016; Pérez-García et al., 2016) and 5-aminovalerate (Rohles et al., 2016; Jorge et al., 2017), the diamines putrescine (Schneider and Wendisch, 2010) and cadaverine (Tateno et al., 2009; Kim et al., 2018) and alkylated and hydroxylated amino acids such as *N*-methylalanine (Mindt et al., 2018) and 5-hydroxy-isoleucine (Wendisch, 2019). Noteworthy, several excellent *C. glutamicum* producer strains have been developed for production of muconic acid (Becker et al., 2018), phenylpropanoids (Kallscheuer and Marienhagen, 2018), *para*-hydroxybenzoic acid (Purwanto et al., 2018), and protocatechuate (Wendisch et al., 2016; Lee and Wendisch, 2017).

Accordingly, the Trp overproducing strain Tp679 (Purwanto et al., 2018) served as excellent base strain for halogenation of Trp (Veldmann et al., 2019). In *C. glutamicum* wildtype mutant *trpE* encoding a feedback resistant anthranilate synthase component 1 from *C. glutamicum* and *trpD* encoding an anthranilate phosphoribosyltransferase from *E. coli* were overexpressed to channel the flux from chorismate to Trp. The chorismate mutase *csm* was deleted to prevent the formation of the by-products L-phenylalanine and L-tyrosine. The precursor supply was optimized with the overexpression of *aroG* encoding a feedback resistant 3-deoxy-D-arabinoheptulosonate-7-phosphate synthase from *E. coli* (**Figure 1**). The production of 7-Cl-Trp had already been established with the Trp producing *C. glutamicum* strain overexpressing *rebH* and *rebF*. The strain produced about 0.1 g L^{-1} of 7-Cl-Trp (Veldmann et al., 2019). However, bromination of Trp *in vivo* has not yet been described as basis of a fermentative process leading 7-Br-Trp or other brominated tryptophans. Here, we describe the production of 7-Br-Trp with the above described Trp overproducing *C. glutamicum* strain expressing *rebH* and *rebF* in media with low chloride, but high bromide concentrations. The process was upscaled in bioreactors with a volume of 2 L and 7-Br-Trp was isolated and characterized by NMR and MS.

MATERIALS AND METHODS

Bacterial Strains and Growth Conditions

Bacterial strains and plasmids used in this study are listed in **Table 1**. *Escherichia coli* DH5α (Hanahan, 1983) was used for

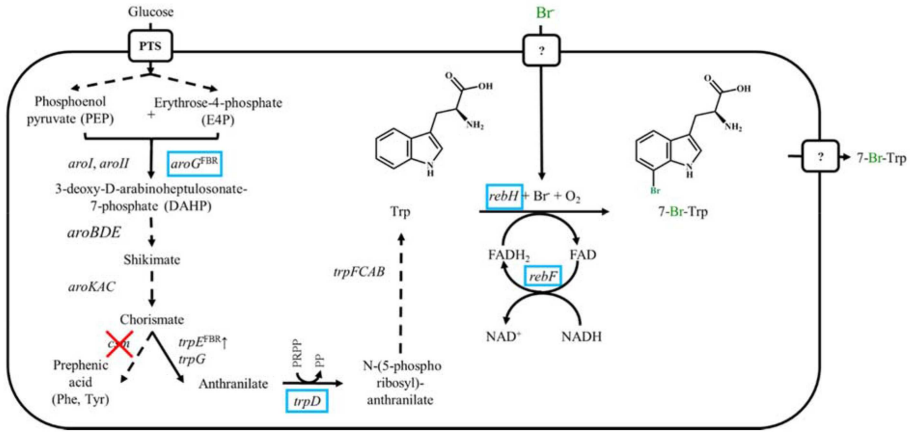

FIGURE 1 | Schematic representation of metabolic engineered *C. glutamicum* overproducing Trp and 7-Br-Trp. Genes names are shown next to reaction represented by the arrows. Dashed arrows show several reactions. Heterologously expressed genes are marked by blue boxes, endogenously overexpressed genes are marked by ↑ and deleted genes are showed by red crosses. FBR, feedback resistant.

TABLE 1 | Strains and plasmids used in this work.

Strains and plasmids	Description	Source
Strains		
WT	*C. glutamicum* wild type, ATCC 13032	ATCC
Tp679 (pCES208-*trpD*)	Δ*csm* Δ*trpL*::P_{ilvCM1}-$trpE^{FBR}$ Δ*vdh*::P_{ilvCM1}-$aroG^{FBR}$ with pCES208-*trpD*	Purwanto et al., 2018
HalT2	Tp679 (pCES208-*trpD*)(pEKEx3-optimRBS-*rebH-rebF*)	Veldmann et al., 2019
Plasmids		
(pCES208-*trpD*)	Kan^R, pCES208 overexpressing *trpD* from *E. coli* with P_{ilvCM1}	Purwanto et al., 2018
(pEKEx3-optimRBS-*rebH-rebF*)	$Spec^R$, pEKEx3 overexpressing *rebH*, *rebF* from *L. aerocolonigenes* with optimized RBS for *rebH*	Veldmann et al., 2019

cloning the plasmid constructs. *E. coli* and *C. glutamicum* were regularly grown in lysogeny broth medium (LB medium) in 500 mL baffled flasks at 120 rpm at 37°C or 30°C, respectively. For growth and production experiments *C. glutamicum* was inoculated in CGXII minimal medium (Eggeling and Bott, 2005) in 500 or 100 mL baffled flasks (filling volume 10%) to an optical density (OD_{600}) of 1 and incubated at 120 rpm. Growth was monitored by measuring the optical density at 600 nm using a V-1200 spectrophotometer (VWR, Radnor, PA, USA). For toxicity test *C. glutamicum* was grown in the BioLector® (M2P Labs) in CGXII medium supplemented with the substance to be tested. To produce 7-Br-Trp, CGXII minimal medium or HSG rich medium (40.0 g L^{-1} glucose, 13.5 g L^{-1} soy peptone, 7 g L^{-1} yeast extract, 0.01 g L^{-1} NaCl, 2.3 g L^{-1} K_2HPO_4, 1.5 g L^{-1} KH_2PO_4, 0.249 g L^{-1} $MgSO_4 \times H_2O$) were used and supplemented with 50 mM NaBr. Strains derived from Tp679 were supplemented additionally with 1.37 mM L-tyrosine and 1.5 mM L-phenylalanine in minimal medium. If necessary, the growth medium was supplemented with kanamycin (25 μg mL^{-1}) and/or spectinomycin (100 μg mL^{-1}). Isopropyl-β-D-1-thiogalactopyranoside (IPTG) (1 mM) was added to induce the gene expression from the vector pEKEx3 (Stansen et al., 2005).

Determination of the Specific Activity of the Anthranilate Phosphoribosyltransferase TrpD

The anthranilate phosphoribosyltransferase overproducing strain Tp679 (pCES208-*trpD*) was inoculated from an overnight culture and was cultivated for 24 h in LB medium at 30°C with 120 rpm before cells were centrifuged for 10 min at 4°C and 4,000 rpm and stored at −20°C. After resuspension in 100 mM Tricine buffer (pH 7.0), the cells were sonicated for 9 min at 55% amplitude and 0.5 cycles on ice in the UP200S Ultrasonic Processor from Hielscher Ultrasound Technology. The supernatant obtained after centrifugation (60 min, 4°C, 16,400 rpm) was used as crude extract for the enzyme assay. The activity was assayed fluorometrically by monitoring the decrease of anthranilate (Ant) at room temperature. The reaction mixture with a final volume of 1 mL contained 100 mM Tricine buffer (pH 7.0), 15 μM Ant, 0.3 mM PRPP, 10 mM $MgCl_2$, and the crude extract and was filled in a quartz glass cuvette (Hellma Analytics, High Precision cell, Light Path 10 × 4 mm). Ant was detected by fluorescence at 325 nm excitation and 400 nm emission wavelength with the Shimadzu Spectrofluorophotometer RF-5301PC. Protein concentrations were determined by the Bradford method (Bradford, 1976) with bovine serum albumin as reference. Means and errors from triplicates were calculated.

Bioreactor Cultures Operated in Batch and Fed-Batch Mode

A 3.7 L KLF Bioengineering AG stirred tank reactor was used for the production of 7-Br-Trp. The fermentation was performed at pH 7.0, 30°C, and an aeration rate of 2 norm liter (NL) min^{-1}. pH was controlled by automatic addition of phosphoric acid [10% (w/w)] and ammonium hydroxide [25% (w/w)]. Struktol®J647 (Schill and Seilenbacher, Boeblingen, Germany) serves as antifoam agent and was also added automatically. Samples were taken automatically every 2 h and cooled to 4°C until analysis.

For the batch fermentations the relative dissolved oxygen saturation (rDOS) of 15, 30, and 60%, respectively, was controlled by enhancing the stirrer speed gradually in steps of 2%. Two liter CGXII without MOPS but with 50 mM NaBr, 1.37 mM L-tyrosine, 1.5 mM L-phenylalanine, and 1 mM IPTG (added at timepoint 0 h) was used as culture medium.

For the fed-batch fermentation the initial volume was 2 L and a constant overpressure of 0.2 bar was adjusted. Due to the new findings (see **Figure 6**), the culture medium was changed to HSG rich medium supplemented with 50 mM NaBr and 1 mM IPTG (added at timepoint 0 h). The feeding medium contained 150 g L^{-1} ammonium sulfate, 400 g L^{-1} glucose, 5.14 g L^{-1} NaBr, 0.25 g L^{-1} L-tyrosine, and 0.25 g L^{-1} L-phenylalanine. Automatic control of the stirrer speed kept the rDOS at 30%. The feeding started automatically when rDOS exceeds 60% and stops when rDOS felt again under the set-point. Here, a pH of 7.0 was established and controlled by automatic addition of phosphoric acid [10% (w/w)] and potassium hydroxide (4 M). Instead of using ammonium hydroxide as alkali to avoid nitrogen limitation in batch cultures, potassium hydroxide was used in the fed-batch fermentation, since the HSG complex medium is nitrogen rich and, hence, a nitrogen limitation was excluded.

The titer and yield were calculated to the initial volume.

Analytical Procedures

For the quantification of the extracellular Trp, 7-Br-Trp and anthranilate (Ant) a high-pressure liquid chromatography (HPLC) system was used (1200 series, Agilent Technologies Deutschland GmbH, Böblingen, Germany). The supernatants of the cell culture were collected by centrifugation (14,680 rpm, 20 min, RT) and further used for analysis. For detection of Ant, Trp, and the derivatives, samples were reacted with *ortho*-phthaldialdehyde (OPA) (Schneider and Wendisch, 2010). The amino acid separation was performed by a precolumn (LiChrospher 100 RP18 EC-5 µ (40 × 4 mm), CS-Chromatographie Service GmbH, Langerwehe, Germany) and a column (Li-Chrospher 100 RP18 EC-5 µ (125 × 4 mm), CS Chromatographie Service GmbH). The detection was carried out with a fluorescence detector (FLD G1321 A, 1200 series, Agilent Technologies) with the excitation and emission wavelengths of 230 and 450 nm, respectively. The quantification of carbohydrates and organic acids was done using a column for organic acids (300 × 8 mm, 10 mm particle size, 25 Å pore diameter, CS Chromatographie Service GmbH) and detected by a refractive index detector (RID G1362A, 1200 series, Agilent Technologies) and a diode array detector (DAD G1315B, 1200 series, Agilent Technologies) (Schneider et al., 2011).

Analytical RP-HPLC and RP-HPLC-MS

Analytical HPLC was performed on a Shimadzu NexeraXR 20A System with autosampler, degasser, column oven, diode array detector, and a Phenomex Luna C18 column (2.9 µm, 50 × 2.1 mm) with a gradient (in 5.5 min from 5% B to 95% B, 0.5 min 95% B and back to 5% B in 3 min, total run time 9 min) at a flow rate of 650 µL/min and column oven temperature of 40°C. HPLC solvent A consists of 99.9% water and 0.1% TFA, solvent B of 99.9% acetonitrile and 0.1% TFA.

Analytical LC-MS was performed on an Agilent 6220 TOF-MS with a Dual ESI-source, 1200 HPLC system with autosampler, degasser, binary pump, column oven, diode array detector, and a Hypersil Gold C18 column (1.9 µm, 50 × 2.1 mm) with a gradient (in 11 min from 0% B to 98% B, back to 0% B in 0.5 min, total run time 15 min) at a flow rate of 300 µL/min and column oven temperature of 40°C. HPLC solvent A consisted of 94.9% water, 5% acetonitrile, and 0.1% formic acid, solvent B of 5%

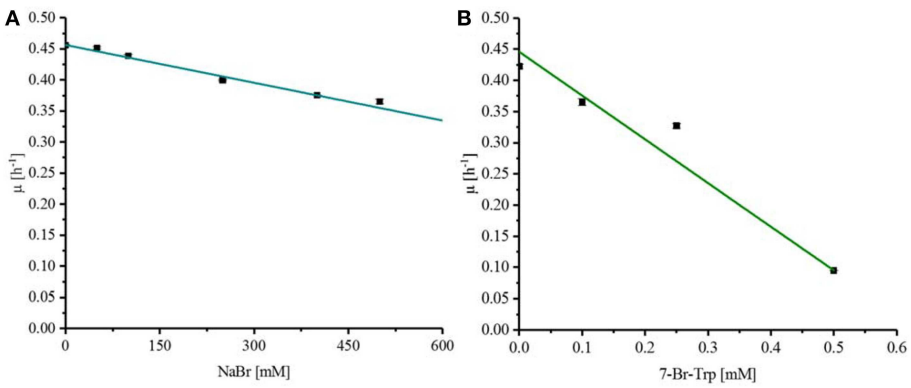

FIGURE 2 | Response of *C. glutamicum* wild type to externally added NaBr **(A)** and 7-Br-Trp **(B)**. To determine the K_i for NaBr and 7-Br-Trp *C. glutamicum* wildtype was grown in CGXII minimal medium with 40 g L^{-1} glucose and different concentration of the substances to be tested. A linear regression was done to determine the half maximal specific growth rate with the substances to be tested. **(A)** NaBr concentrations between 0 and 500 mM were tested with *C. glutamicum*. **(B)** 7-Br-Trp concentrations between 0 and 0.5 mM were tested.

water, 94.9% acetonitrile and 0.1% formic acid. ESI mass spectra were recorded after sample injection via 1200 HPLC system in extended dynamic range mode equipped with a Dual-ESI source, operating with a spray voltage of 2.5 kV.

NMR Spectroscopy

NMR spectra were recorded on a Bruker Avance III 500 HD (^{1}H: 500 MHz, ^{13}C: 126 MHz, ^{19}F: 471 MHz). Chemical shifts δ [ppm] are reported relative to residual solvent signal (DMSO-d_6, ^{1}H: 2.50 ppm, ^{13}C: 39.5 ppm). 2D spectra (COSY, HMQC, HMBC) spectra were used for signal assignment.

High-Resolution MS

ESI mass spectra were recorded using an Agilent 6220 time-of-flight mass spectrometer (Agilent Technologies, Santa Clara, CA, USA) in extended dynamic range mode equipped with a Dual-ESI source, operating with a spray voltage of 2.5 kV. Nitrogen served both as the nebulizer gas and the dry gas. Nitrogen was generated by a nitrogen generator NGM 11. Samples are introduced with a 1200 HPLC system consisting of an autosampler, degasser, binary pump, column oven, and diode array detector (Agilent Technologies, Santa Clara, CA, USA) using a C18 Hypersil Gold column (length: 50 mm, diameter: 2.1 mm, particle size: 1.9 µm) with a short isocratic flow (60% B for 5 min) at a flow rate of 250 µL/min and column oven temperature of 40°C. HPLC solvent A consisted of 94.9% water, 5% acetonitrile, and 0.1% formic acid, solvent B of 5% water, 94.9% acetonitrile, and 0.1% formic acid. The mass axis was externally calibrated with ESI-L Tuning Mix (Agilent Technologies, Santa Clara, CA, USA) as calibration standard. The mass spectra were recorded in both profile and centroid mode with the MassHunter Workstation Acquisition B.04.00 software (Agilent Technologies, Santa Clara, CA, USA). MassHunter Qualitative Analysis B.07.00 software (Agilent Technologies, Santa Clara, CA, USA) was used for processing and averaging of several single spectra.

Reversed-Phase Column Chromatography (GP1)

Automated column chromatography was performed on a Büchi Reveleris X2 with a binary pump and ELSD Detector using a Biotage Snap Ultra C18 column with a gradient (4 min at 5% B, up to 25% B in 14 min, in 1 min up to 100% B for 2 min and flushing with 80% B for 5 min, total run time 27 min) at a flow rate of 30 mL/min. Solvent A consisted of 99.9% water and 0.1% TFA, solvent B of 99.9% acetonitrile and 0.1% TFA.

Isolation and Purification of 7-Bromo-L-tryptophan From HSG Rich Medium

7-Br-Trp was isolated from 30 mL HSG rich medium (3 × 10 mL) (see chapter growth conditions) by an automated reversed phase column chromatography. The crude medium was centrifuged (10,000 rpm, 4°C, 30 min) and filtrated over a short plug of celite. The crude filtrate was loaded on a 12 g C18-column and purified according to GP1. The TFA salt of 7-Br-Trp was isolated as a colorless solid (14.3 mg, 36 µmol). RP-column chromatography: t_R = 11.5 min; Anal. RP-HPLC: t_R = 3.3 min; LC-MS: t_R = 5.1 min; ^{1}H NMR (500 MHz, DMSO-d_6) δ [ppm] = 11.28 (d, ^3J = 2.7 Hz, 1H, indole-N**H**), 8.16 (brs, 3H, N**H**$_3^+$), 7.58 (d, ^3J = 7.9 Hz, 1H, C4-**H**), 7.32 (d, ^3J = 7.5 Hz, 1H, C6-**H**), 7.30 (d, ^3J = 2.7 Hz, 1H, C2-**H**), 6.97 (dd, ^3J = 7.8 Hz, ^3J = 7.8 Hz, 1H, C5-**H**), 4.15 (dd, ^3J = 7.1 Hz, ^3J = 6.2 Hz, 1H, Cα-**H**), 3.27 (dd, ^2J = 15.0 Hz, ^3J = 5.7 Hz, 1H, Cβ-**H**), 3.22 (dd, ^2J = 14.8 Hz, ^3J = 6.9 Hz, 1H, Cβ-**H**); low res. MS (ESI): found [m/z] = 265.9 [M(^{79}Br)-NH$_2$]$^+$, 267.9 [M(^{81}Br)-NH$_2$]$^+$, 283.0 [M(^{79}Br)+H]$^+$, 285.0 [M(^{81}Br)+H]$^+$; calcd. [m/z] = 265.9 [M(^{79}Br)-NH$_2$]$^+$, 267.9 [M(^{81}Br)-NH$_2$]$^+$, 283.0 [M(^{79}Br)+H]$^+$, 285.0 [M(^{81}Br)+H]$^+$.

RESULTS

Production of 7-Bromo-L-tryptophan in Flasks Culture

Fermentative processes are ideal if substrates, intermediates, and products do not inhibit growth and production. The effect of the substrate NaBr and the product 7-Br-Trp on growth of *C. glutamicum* was assessed when various concentrations of these compounds were added upon inoculation of *C. glutamicum* wild type to CGXII minimal medium with 40 g L^{-1} glucose. NaBr concentrations (0–500 mM) had a negligible effect on growth and it was estimated by extrapolation that the growth rate would be reduced to 50% at about 1.2 M NaBr (**Figure 2A**). Therefore, the use of NaBr as a substrate was presumed to be possible. By contrast, already low concentrations of the target product 7-Br-Trp inhibited growth in the BioLector® (M2P Labs). The half maximal specific growth rate of *C. glutamicum* was reached already at a concentration of about 0.32 mM or 0.091 g L^{-1}

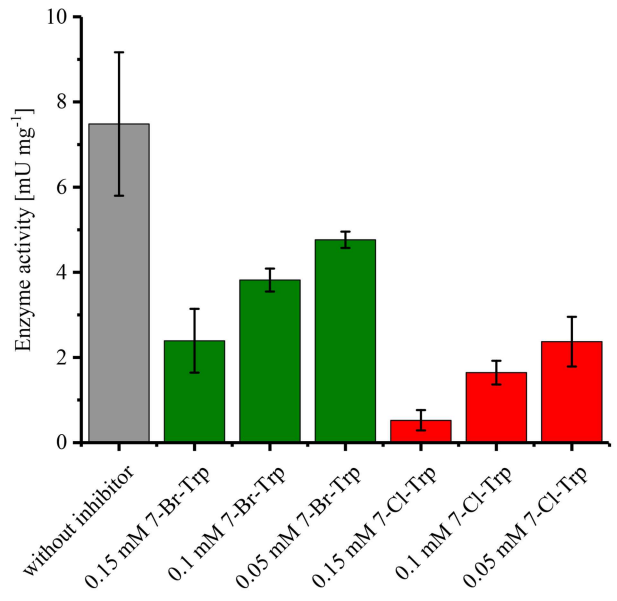

FIGURE 3 | Specific activities of anthranilate phosphoribosyltransferase TrpD in the presence or absence of either 7-Br-Trp or 7-Cl-Trp. Crude extracts of *C. glutamicum* Tp679 (pCES208-*trpD*) grown in LB rich media were assayed for TrpD activity in the presence of different concentrations of either 7-Br-Trp or 7-Cl-Trp. Means and standard deviations of triplicates are shown.

7-Br-Trp (**Figure 2B**). This inhibition is threefold lower than previously observed with 7-Cl-Trp (K_i of about 0.1 mM or 0.024 g L^{-1} (Veldmann et al., 2019). We hypothesize that the difference is due to the hydration shell of chlorine substituents being smaller than that of a bromo substituent. Accordingly, we speculate that due to its smaller size 7-Cl-Trp can enter catalytic active centers and/or allosteric sites of enzymes easier than 7-Br-Trp and, thus, inhibitory effects are expected to be more pronounced. This may explain why the inhibitory effect of 7-Cl-Trp exceeds that of 7-Br-Trp.

Since it is known that halogenated Ant competitively inhibits Ant converting anthranilate phosphoribosyltransferase TrpD (Lesic et al., 2007), it was tested whether 7-Br-Trp inhibits anthranilate phosphoribosyltransferase in crude extracts of *C. glutamicum* Tp679 (pCES208-*trpD*). This strain possesses endogenous *trpD* on its chromosome and expresses *E. coli trpD* from a plasmid. Crude extracts of *C. glutamicum* Tp679 (pCES208-*trpD*) grown in LB rich medium were assayed for TrpD activity in the presence of different concentrations of either 7-Br-Trp or 7-Cl-Trp (**Figure 3**). The specific activity of anthranilate phosphoribosyltransferase was reduced to about one third by either 0.15 mM 7-Br-Trp or by 0.05 mM 7-Cl-Trp (**Figure 3**). Thus, inhibition by 7-Cl-Trp was more pronounced than inhibition by 7-Br-Trp, which showed a K_i value of about 0.03 g L^{-1}. At least in part, the growth inhibition by 7-Br-Trp (**Figure 2B**) may be due to inhibition of anthranilate phosphoribosyltransferase by 7-Br-Trp (**Figure 3**). Since 7-Br-Trp exerts a lower inhibitory effect than 7-Cl-Trp and since the latter could be produced to a titer of 0.108 g L^{-1}, i.e., five times as high as K_i (Veldmann et al., 2019), it is expected that *C. glutamicum* likely produces 7-Br-Trp only to relatively low concentrations as well.

For the fermentative production of 7-Br-Trp, the *C. glutamicum* strain HalT2 was used. This strain was derived from the Trp overproducing strain Tp679 (pCES208-*trpD*), which overexpresses additionally genes encoding FAD-dependent halogenase RebH and NADH-dependent flavin reductase RebF from the expression vector pEKEx3 (Veldmann et al., 2019). In our previous study, we tried to optimize RebF and RebH gene expression. On the one hand, a more active promoter helped increase RebH and RebF activities, on the other hand, production could be improved as consequence of optimizing the ribosome binding site [and thus, translation initiation efficiency; (Veldmann et al., 2019)]. Bioinformatics analysis revealed that the codon usage of RebH fits to the codon usage of *C. glutamicum* and hence was not further optimized. For RebF the codon usage fits to *C. glutamicum* except one triplet. The ribosome binding site was not optimized for RebF. HalT2 was inoculated in CGXII minimal medium with 40 g L^{-1} glucose and 50 mM NaBr in 500 mL baffled flasks (50 mL culture) to an OD_{600} of 1. At inoculation, 1 mM IPTG was added. The culture showed a specific growth rate 0.12 ± 0.01 h^{-1}. After 72 h 0.25 ± 0.01 g L^{-1} 7-Br-Trp, 0.81 ± 0.02 g L^{-1} Trp and 1.69 ± 0.03 g L^{-1} Ant were measured (**Figure 4**). When the same strain was inoculated in 500 mL without baffles the specific growth rate was 0.11 ± 0.01 h^{-1} and the production of 7-Br-Trp increased by 38% to a titer of 0.34 ± 0.02 g L^{-1}. Production of Trp was decreased by 34% to 0.54 ± 0.02 g L^{-1}, but production of Ant increased to

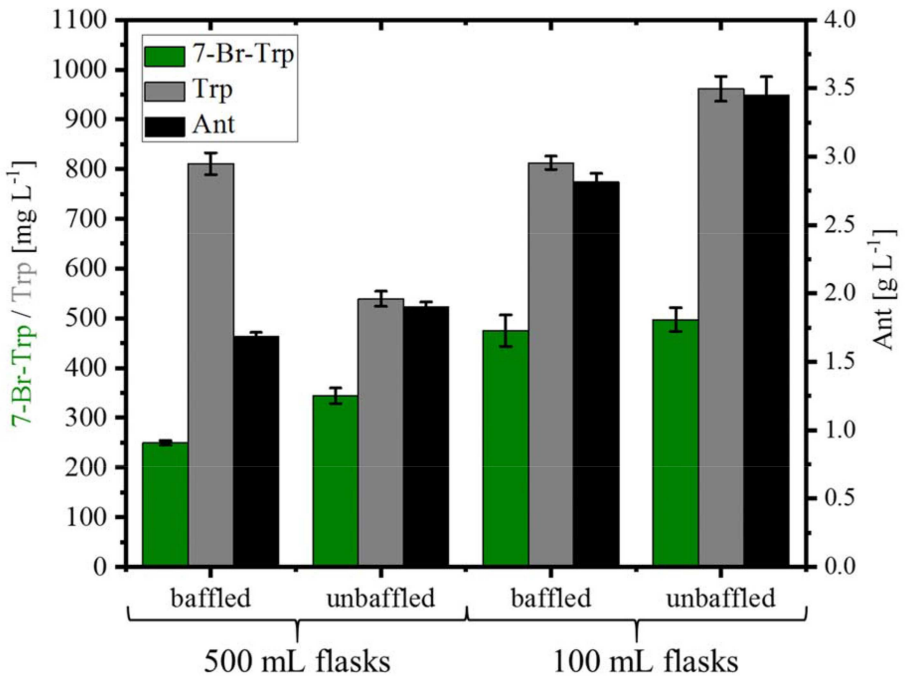

FIGURE 4 | Production of 7-Br-Trp, Trp, and Ant by *C. glutamicum* HalT2 under different shake flask conditions. HalT2 was grown in CGXII with 40 g L^{-1} glucose after 72 h were measured the titers of 7-Br-Trp, Trp, and Ant. The filling volume was 10% of the flask volume. Means and standard deviations of three replicate cultivations are shown.

1.91 ± 0.03 g L^{-1}. Using 100 mL flasks with 10 mL culture was beneficial for production of 7-Br-Trp by *C. glutamicum* HalT2 as in baffled flasks 0.48 ± 0.03 g L^{-1} 7-Br-Trp were produced after 72 h and 0.81 ± 0.01 g L^{-1} Trp and 2.82 ± 0.06 g L^{-1} Ant accumulated. In 100 mL flasks without baffles 0.49 ± 0.02 g L^{-1} 7-Br-Trp were produced after 72 h and 0.96 ± 0.03 g L^{-1} Trp and 3.45 ± 0.13 g L^{-1} Ant accumulated (**Figure 4**). With the assumption that the oxygen supply is lower in the 100 ml than in the 500 ml flasks, the production was increased with less oxygen supply. The specific growth rate was lower in 100 mL flasks with baffles (0.09 ± 0.01 h^{-1} as compared to 0.13 ± 0.01 h^{-1}). These results were unexpected since oxygen supply in 500 mL baffled flasks is considered higher than in 100 mL unbaffled flasks we expected higher 7-Br-Trp in 500 ml baffled flasks. Halogenase RebH requires $FADH_2$ as cofactor, L-Trp, molecular oxygen and a halide salt as substrates. RebH regioselectively chlorinates or brominates L-Trp at the 7-position. $FADH_2$ is regenerated by RebF, which reduces FAD to $FADH_2$ in an NADH-dependent manner. NADH is provided by cellular metabolism (oxidation of glucose). RebH and RebF derive from the host organism *Lechevalieria aerocolonigenes* which has a growth optimum at 28°C (Parte, 2012), which fits well with the optimal growth temperature of *C. glutamicum* of 30°C. Nonetheless, the highest 7-Br-Trp titer observed (about 0.49 g L^{-1}; **Figure 4**) exceeded the K_i value (about 0.09 g L^{-1}; **Figure 2B**) about five-fold.

Batch Production of 7-Bromo-L-tryptophan in a Bioreactor

To scale up the fermentation process and to test the influence of pH control, optimal stirring and controlled oxygen supply, strain HalT2 was cultivated in a 3.7 L baffled bioreactor with a working volume of 2 L with three different rDOSs (rDOS = 15, 30, and 60%). Whereas, the maximal specific growth rate was comparable and in a range between 0.07 and 0.08 h^{-1}, *C. glutamicum* HalT2 grew to a higher biomass concentration at rDOS of 15% (OD_{600} of 27; **Figure 5C**) than with rDOS at either 30 or 60% (OD_{600} of 11 and 12, respectively; **Figures 5A,B**). Glucose was utilized completely (with the exception of 3.6 g L^{-1} glucose remaining in the rDOS 60% bioreactor condition). Lactate accumulated transiently peaking at 32 h, 28 and 16 h with maximal concentrations of 3.8, 3.8, and 0.5 g L^{-1} lactate for the bioreactors operated at 15, 30, and 60%, respectively (**Figure 5**). The byproducts Trp and Ant accumulated to higher concentrations than 7-Br-Trp. Maximal 7-Br-Trp titers increased slightly with decreasing rDOS, i.e., 0.26, 0.26, and 0.30 g L^{-1} 7-Br-Trp for the bioreactors operated at 15, 30, and 60%, respectively (**Figure 5**). The corresponding yields on glucose were 6.6, 6.6, and 7.5 mg g^{-1}. The yields on biomass differed to a larger extent since higher biomass concentrations were observed at low rDOS. At 15% rDOS, for example, an OD_{600} 21 (corresponding to 7.4 gCDW L^{-1}) and a 7-Br-Trp titer of 0.26 g L^{-1} were observed at 56 h, which is equivalent to a 7-Br-Trp yield on biomass of 36 mg $(gCDW)^{-1}$. At 30% rDOS, the 7-Br-Trp yield on biomass was almost two-fold higher [74 mg $(gCDW)^{-1}$] and it was almost three-fold higher at 60% rDOS [95 mg $(gCDW)^{-1}$]. This may indicate that less cells are required for 7-Br-Trp production at high rDOS and/or that growth proceeds to higher biomass concentrations at low rDOS.

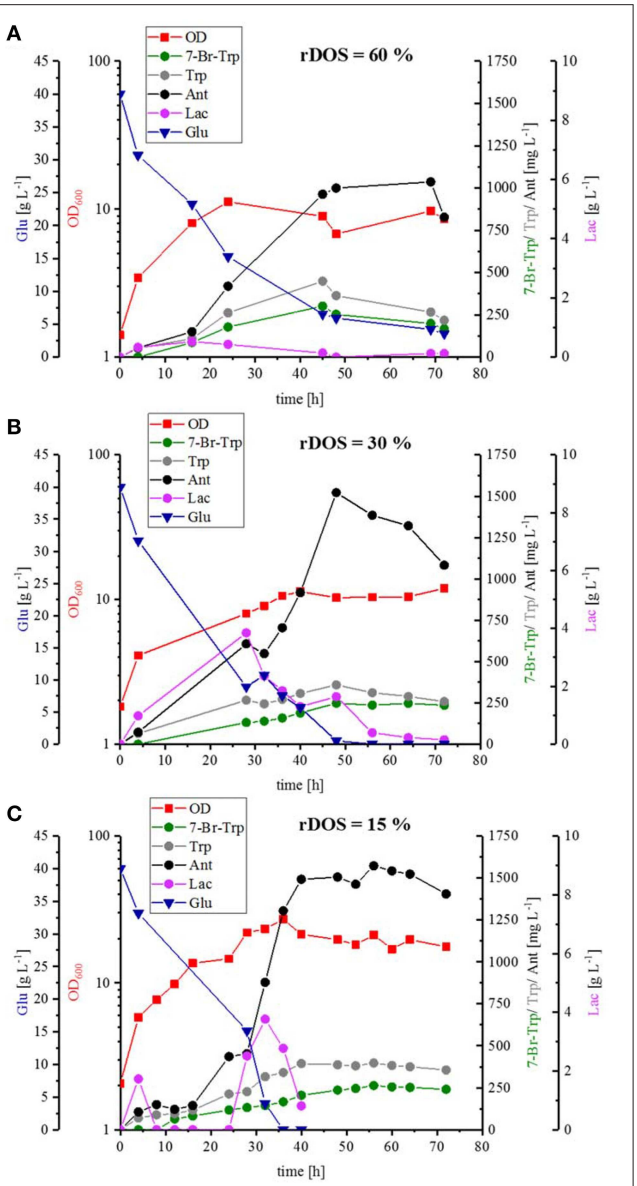

FIGURE 5 | Batch fermentation of 7-Br-Trp by *C. glutamicum* HalT2 with three different rDOS. The data given include the glucose consumption [blue triangle], the OD_{600} [red squares], the production of 7-Br-Trp [green circles], Trp [gray circles], Ant [black circles], and Lac [light purple circles]. The initial culture volume was 2 L. **(A)** Batch fermentation with a rDOS set-point of 60%. **(B)** Batch fermentation with a rDOS set-point of 30%. **(C)** Batch fermentation with a rDOS set-point of 15%.

Fed-Batch Production of 7-Bromo-L-tryptophan in a Bioreactor

Stirred tank bioreactor cultivations operated in batch mode yielded lower titers (0.26–0.30 g L^{-1}; **Figure 5**) than shake flask cultivation (up to about 0.49 g L^{-1}; **Figure 4**). Under both conditions CGXII glucose minimal medium was used. Since

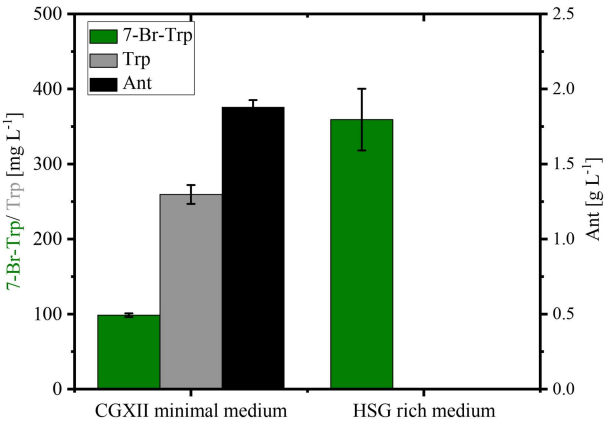

FIGURE 6 | Production of 7-Br-Trp by *C. glutamicum* HalT2 in different media. HalT2 was grown in CGXII minimal medium and HSG rich medium with 40 g L^{-1} glucose. The strain was cultivated in 100 mL flasks with 10% filling volume. After 24 h were determined the production of 7-Br-Trp, Trp, and Ant. Means and standard deviations of three replicate cultivations are shown.

fermentations are often performed in media containing complex sources such as yeast extract and/or protein hydrolysates, production of 7-Br-Trp by *C. glutamicum* HalT2 was compared in 100 mL baffled flasks with either CGXII glucose minimal medium or HSG rich medium containing yeast extract and soy peptone. Growth in the HSG rich medium was faster (a specific growth rate of 0.39 ± 0.02 h^{-1} as compared to 0.19 ± 0.01 h^{-1} in CGXII minimal medium). Within 24 h 0.36 ± 0.04 g L^{-1} 7-Br-Trp were produced in HSG rich medium, but only 0.10 ± 0.01 g L^{-1} 7-Br-Trp in the minimal medium (**Figure 6**). Moreover, the 7-Br-Trp yield on biomass in HSG rich medium [39 ± 5 mg $g(CDW)^{-1}$] was higher than in CGXII minimal medium [6 ± 1 mg $g(CDW)^{-1}$]. Notably, neither Trp nor Ant accumulated as byproducts in HSG rich medium, whereas 0.26 ± 0.01 g L^{-1} Trp and 1.88 ± 0.05 g L^{-1} Ant were produced in CGXII minimal medium (**Figure 6**).

The product formed by *C. glutamicum* HalT2 in 30 mL HSG rich medium (3 × 10 mL) was isolated and purified in a single step by an automated reversed phase column chromatography. In total 14.3 mg (36 μmol) of 7-Br-Trp as a TFA salt were isolated. The product was identified as 7-Br-Trp by NMR studies. The purity (>95%) was verified by both NMR (**Figure 7A**) and LC-MS (**Figure 7B**) experiments.

Taken together, HSG rich medium was chosen for fed-batch fermentation because the production occurred faster and the precursors Trp and Ant did not accumulate as byproducts and the specific growth rate in rich medium was two-fold higher than in CGXII medium as mentioned above (0.39 h^{-1} for HSG medium vs. 0.19 h^{-1} for CGXII medium). In **Figure 6**, the concentrations of Trp, Ant, and 7-Br-Trp after 24 h of cultivation in shake flasks are given. Most likely, in contrast to CGXII medium product formation was finished at this time point using rich medium. This was also confirmed by **Figure 5**, because 7-Br-Trp formation was not finished after 24 h of cultivation, irrespective of whether rDOS level was used. At 30% rDOS, the highest 7-Br-Trp yield on biomass of 74 mg $(gCDW)^{-1}$ was reached as mentioned above. Therefore, the same set point was used for fed-batch fermentation. *C. glutamicum* HalT2 was used for the fed-batch fermentation to inoculate 2 L HSG rich medium containing 40 g L^{-1} glucose to an initial OD_{600} of 1.8 (**Figure 8**). The maximal specific growth rate was 0.32 h^{-1}. A total feed of 975 mL was added in the whole process. Four major phases of the fed-batch fermentation could be distinguished. In the first (batch) phase *C. glutamicum* HalT2 grew to an OD_{600} of 37.3 within 18 h. Lactate accumulated transiently peaking at 7.0 g L^{-1} after 10 h. At 18 h, titers of 0.19 g L^{-1} 7-Br-Trp and 0.1 g L^{-1} Trp were observed. In the next phase (until 30 h when exponential feeding started), 7-Br-Trp was produced to a titer of 0.30 g L^{-1} with a yield on biomass of 0.7 mg $(gCDW)^{-1}$ and a volumetric productivity of 10 mg L^{-1} h^{-1}. Neither Trp nor Ant accumulated during this phase. The third phase is characterized by an exponential increase of the feed volume (at 50 h about 293 mL feed had been added and the OD_{600} reached 62), while the 7-Br-Trp concentration increased linearly to 0.66 g L^{-1}. During this phase the volumetric productivity was 18 mg g^{-1} h^{-1} and the specific productivity was 1 mg $gCDW^{-1}$ h^{-1}. While Trp accumulated to a titer of 0.17 g L^{-1}, Ant was not produced in the third phase. In the last phase that started at 50 h, the residual feed (682 mL) was added until 55 h. The 7-Br-Trp and Trp titers increased in parallel to 1.2 g L^{-1} and about 0.25 g L^{-1}. Only in this last phase, Ant accumulated with Ant titers fluctuating around 0.5 g L^{-1} from 57 h to 72 h (**Figure 8**).

DISCUSSION

Heterologous expression of the genes *rebH* for FAD-dependent halogenase and *rebF* for NADH-dependent flavin reductase from the *reb* cluster of *L. aerocolonigenes* to enable regioselective chlorination of Trp at the 7 position (Nishizawa et al., 2005) in a Trp overproducing *C. glutamicum* strain (Purwanto et al., 2018) provided the basis for the development of fermentative processes for chlorination (Veldmann et al., 2019) and bromination of Trp (this study). Production of 7-Br-Trp by the engineered *C. glutamicum* strain was possible in glucose minimal media supplemented with sodium bromide.

C. glutamicum belongs to the group of bacteria that require chloride for growth at high (sodium) salt concentrations since growth was inhibited in the presence of high concentrations of sodium sulfate and sodium gluconate, but not of sodium chloride (Roeßler et al., 2003). It was postulated that chloride may enhance excretion of cytotoxic sodium ions by salt-induced Na^+/H^+ antiporters and/or simultaneous export of these anions via the ClC-type sodium channels as observed for *E. coli* (Iyer et al., 2002). The finding reported here that *C. glutamicum* can withstand high sodium bromide concentrations (K_i of about 1.2 M; **Figure 2A**) indicates that bromide may substitute for chloride to sustain growth of *C. glutamicum* at high sodium salt concentrations.

The engineered *C. glutamicum* strain produced 7-Br-Trp to higher titers (1.2 g L^{-1}, **Figure 8**) than 7-Cl-Trp [0.1 g L^{-1}; (Veldmann et al., 2019)]. This was surprising since pure

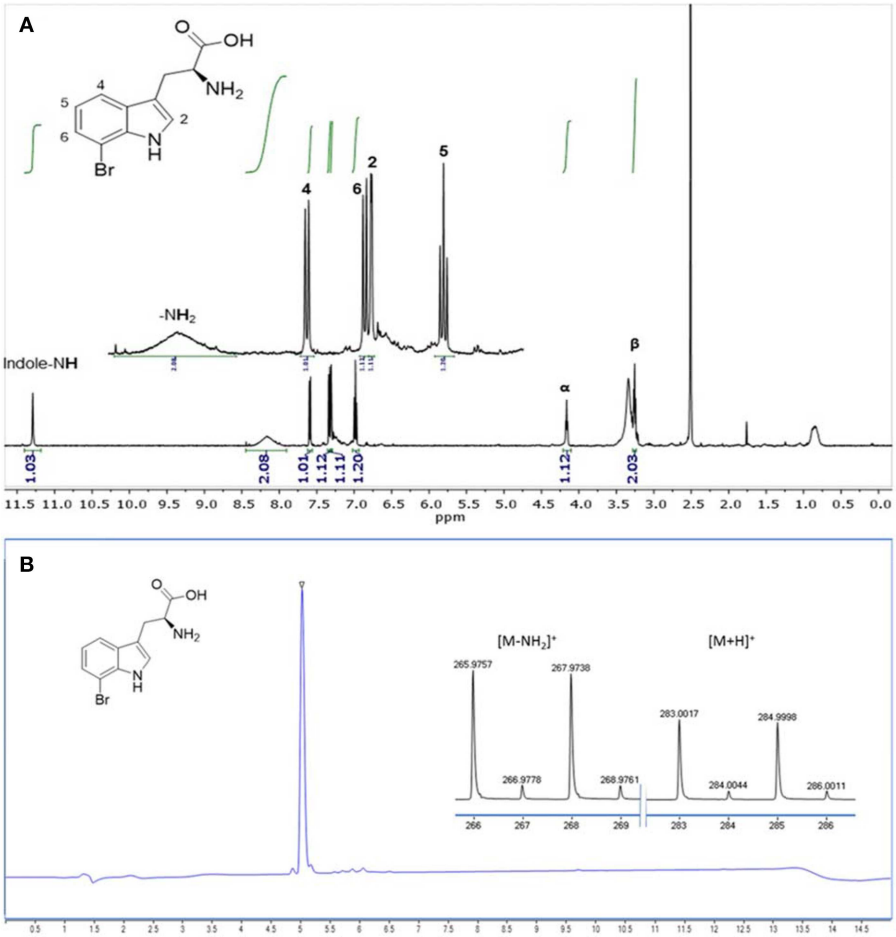

FIGURE 7 | Analysis of 7-Br-Trp isolated from HSG medium by **(A)** ^{1}H NMR (500 MHz, 298 K, DMSO-d_6) and by **(B)** RP-HPLC-MS analysis. The ionization was performed with a Dual-ESI with a voltage of 2.5 kV leading to an expected deamination during the ionization process. The characteristic isotopic pattern of a single brominated species is clearly observable.

RebH prefers chlorination (k_{cat} of 1.4 min^{-1}) over bromination (k_{cat} of 0.4 min^{-1}) (Yeh et al., 2005). Unlike in enzyme catalysis with pure RebH (Yeh et al., 2005; Payne et al., 2013), chloride could not be completely replaced by bromide since chloride is required for growth of *C. glutamicum* (s. above). However, at a low chloride concentration in the growth medium a high bromide salt supply (277-fold excess) allowed for bromination by the engineered *C. glutamicum* strain *in vivo*. The purified product of this fermentative process was shown to be 7-Br-Trp without detectable contamination by 7-Cl-Trp (**Figure 7**). Brominated natural products and intermediates are found predominantly in marine environments as ocean water contains a relatively high bromide ion concentration (Gribble, 1996). Moreover, halogenases which prefer bromination are more abundant in marine habitats, those preferring chlorination are encountered more often in terrestrial habitats (Van Peè, 2001). Thus, future process improvement may make use of halogenases preferring bromination over chlorination such as BrvH from *Brevundimonas* BAL3 (Neubauer et al., 2018) or three halogenases from *Xanthomonas campestris* pv. campestris strain B10046 (Ismail et al., 2019).

FAD-dependent halogenases require molecular oxygen (Bitto et al., 2008). In the reaction catalyzed by RebH, $FADH_2$ binds to the FAD binding pocket of the RebH and reacts with molecular oxygen to flavin hydroperoxide (Andorfer et al., 2016). Flavin peroxide in turn oxidizes the halide anion (X^-, X = Cl, Br) to hypohalous acid (HOX), which is channeled to the active tryptophan binding pocket. The role of the conserved lysine residue K79 in giving a haloamine intermediate (Yeh et al., 2007) is still under debate (Flecks et al., 2008). The hypohalous acid effects the regioselective electrophilic aromatic substitution of Trp resulting in halogenation at the C7 position (Andorfer et al., 2016). Thus, the supply of molecular oxygen to RebH within the *C. glutamicum* cell may be a bottleneck for halogenation of Trp. Since, of course, *C. glutamicum* requires oxygen for respiration, the response to increased molecular oxygen supply during growth-coupled fermentative production of 7-Br-Trp may be complex. Production of 7-Br-Trp was found to be higher under

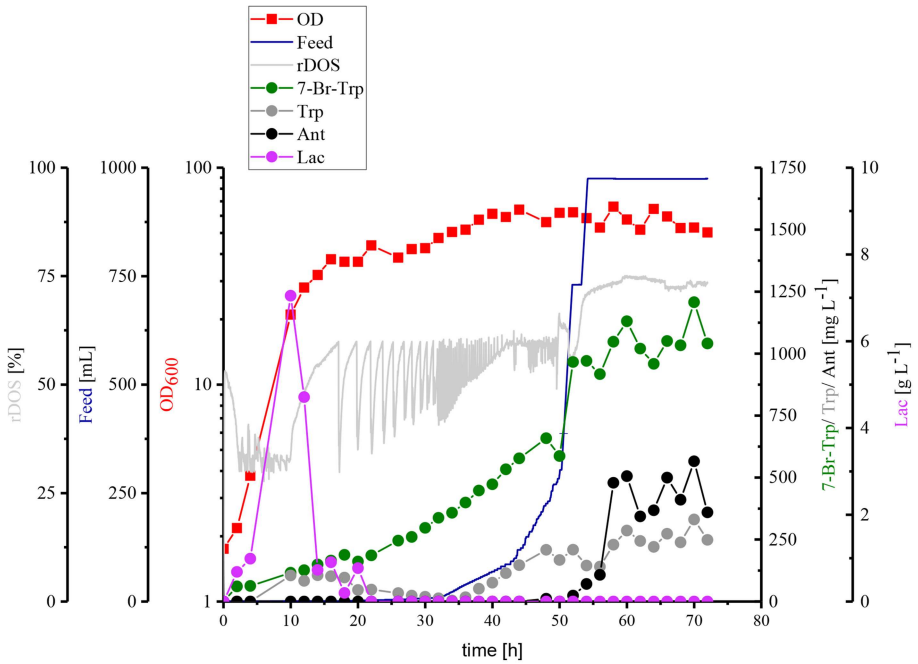

FIGURE 8 | Fed-batch fermentation of 7-Br-Trp by *C. glutamicum* HalT2. The data given include rDOS [%] [light gray], the feed [blue], OD_{600} [red squares], 7-Br-Trp [green circles], Trp [gray circles], Ant [black circles], and Lac [light purple circles]. The initial volume was 2 L and 975 mL feed was added. The titer was calculated to the initial volume.

low oxygen supply in shake flask (although these are relatively ill-defined) or comparable under controlled conditions in bioreactor fermentations with rDOS of 15, 30, and 60% (**Figures 4**, **5**). For different microorganisms the Monod constants for oxygen are in a range between $3.0 \cdot 10^{-4}$ mg L^{-1} and 0.1 mg L^{-1} (Longmuir, 1954) Therefore, cell growth was not notably affected by oxygen supply even at a rDOS level of 15%. Surprisingly, biomass formation was declined with increasing rDOS set points as shown by the courses of OD_{600} and glucose in **Figure 5**. While glucose was depleted after 35 h for rDOS of 15% and 48 h for rDOS of 30%, respectively, nearly 4 g L^{-1} glucose remained at the end of cultivation (73 h) at a rDOS level of 60% also indicating a reduced biomass formation. However, halogenation by RebH-RebF requires molecular oxygen. Obviously, a better oxygen supply improves RebH-RebF activity, which counteracts biomass formation (see also max. OD_{600} mit tiefer gesetzten 600 values as given in line 719–722). This conclusion is supported by lower specific growth rates during stirred tank reactor cultivation (line 719) in contrast to shake flask cultivation (line 649–653, 694), despite a poorer oxygen input in the latter case. In addition, halogenation by RebH-RebF requires both molecular oxygen and NADH at the same time. This is difficult to achieve in fast growing cells as NADH is oxidized by the respiratory chain using molecular oxygen to generate a trans-membrane pH gradient and subsequently ATP. Moreover, if the oxygen supply is too high, the flavin-hydroperoxide formed upon reaction of $FADH_2$ with molecular oxygen is hydrolyzed to yield H_2O_2. This is commonly observed for flavin-dependent enzymes like monooxygenases and halogenases ("oxygen dilemma"; Ismail et al., 2019). Thus, all reactions in *C. glutamicum* requiring $FADH_2$ [e.g., *p*-hydroxybenzoate hydroxylase (Kwon et al., 2007) or flavin-dependent thymidylate synthase; (Kan et al., 2010)] or containing this flavin bound to the enzyme [e.g., membrane-associated malate dehydrogenase (acceptor) (EC 1.1.99.16); (Molenaar et al., 1998)] may be compromised at high oxygen levels in the presence of flavin reductase RebF. Thus, an aeration protocol ensuring optimal supply of oxygen for growth on the one hand and for RebH catalyzed bromination on the other hand remains to be developed.

Another optimization step for the fermentative production of 7-Br-Trp, would be the reduction of by-products, like L-lactate. *C. glutamicum* produces L-lactate from pyruvate via the NAD-dependent L-lactate dehydrogenase (encoded by *ldhA*) (Inui et al., 2004b) and is able to utilize the L-lactate as carbon source via the lactate dehydrogenase (encoded by *lldD*) (Stansen et al., 2005). Transient L-lactate accumulation (formed by LdhA and subsequently utilize by LldD) is often observed when glucose uptake is higher than oxygen uptake. Once the glucose uptake rate ceases, L-lactate is re-utilized. Transcription of *ldhA* is regulated by transcriptional regulator SugR (Engels et al., 2008; Toyoda et al., 2009). Under oxygen limitation glucose uptake exceeds oxygen uptake and L-lactate is produced by LdhA to regenerate NAD^+ (Engels et al., 2008). Accordingly, transient L-lactate was more pronounced with low (rDOS of 15%, 30%, and fed-batch) as compared to high oxygen supply (rDOS of 60%). We have discussed these facts along with a strategy to avoid transient lactate formation, i.e., by deletion of *ldhA* as has been shown before (Inui et al., 2004b).

Inhibition by halogenated Trp appeared to be the major bottleneck to achieve high product titers. Growth as well as anthranilate phosphoribosyltransferase activity in crude extracts from *C. glutamicum* Tp679 (pCES208-*trpD*) were inhibited by 7-Br-Trp and 7-Cl-Trp (**Figure 3** and Veldmann et al., 2019). When comparing growth and 7-Br-Trp production in CGXII and HSG media, the latter of which is a complex medium and contains about 0.5 mM Trp (data not shown), the specific growth rate in rich medium was two-fold higher than in CGXII medium (0.39 h^{-1} for HSG medium vs. 0.19 h^{-1} for CGXII medium, s. results section). Thus, addition of Trp may alleviate the growth inhibition as consequence of TrpD inhibition.

Previously, O'Gara and Dunican (1995) have shown that purified anthranilate phosphoribosyltransferase TrpD from *C. glutamicum* is inhibited by Trp (K_i of 0.83 mM) and by 5-methyl-L-tryptophan (K_i of 0.32 mM). In this study, anthranilate phosphoribosyltransferase activity in crude extracts was shown to be inhibited by 7-Br-Trp (K_i of about 0.1 mM) and by 7-Cl-Trp (K_i of about 0.06 mM). It should be noted that besides endogenous *trpD* on the *C. glutamicum* chromosome *E. coli trpD* was expressed from a plasmid. TrpD from *E. coli* is insensitive to Trp in the absence of *E. coli* TrpE (Ito and Yanofsky, 1969). Feedback resistant TrpD has been isolated from *C. glutamicum,* which was isolated from a tyrosine and phenylalanine double auxotrophic strain due to its resistance to analogs of Trp, tyrosine, phenylalanine, and 5-methyl-L-tryptophan. Feedback resistant TrpD from this *C. glutamicum* strain was shown to confer resistance to 5-methyl-L-tryptophan and 6-fluoro-L-tryptophan on *E. coli* (Herry and Dunican, 1993). Resistance to Trp derivatives with modifications at the 7 position of Trp such as 7-Br-Trp or 7-Cl-Trp has not been determined, thus, it cannot be inferred that the feedback resistant TrpD from *C. glutamicum* ATCC 21850 would alleviate the inhibition of *C. glutamicum* growth and/or TrpD activity by 7-Br-Trp and 7-Cl-Trp. Likely, other TrpD variants either from *C. glutamicum* or from *E. coli* have to be isolated after mutation and screening or by rational enzyme engineering. Alternatively, process intensification may involve fermentation strategies including *in situ* product removal (ISPR) to maintain sub-threshold concentrations of 7-Br-Trp as has been shown for L-phenylalanine separation and concentration by reactive-extraction with liquid-liquid centrifuges in a fed-batch fermentation process with recombinant *E. coli* (Rüffer et al., 2004).

Halogenated amino acids such as 7-Br-Trp are relevant for peptide synthesis, since they can be converted further by Pd-catalyzed cross coupling and nucleophilic substitution reactions (Diederich and Stang, 2008). Various halogenated forms of tryptophan and its derivatives may have potential in the synthesis of serotonin and melatonin agonists or antagonists (Frese et al., 2014). As shown here, based on the insight from enzyme catalysis using pure RebH, crude RebH preparations or CLEAs containing RebH, a fermentative process based on RebH was developed and adjusted to yield either 7-Cl-Trp or 7-Br-Trp by *C. glutamicum in vivo*. Since halogenases such as RebH, PrnA, or BrvH differ in their substrate spectra and regioselectivities, the fermentative approach holds the potential to be extended for various halogenation processes starting from glucose and halide salts *in vivo* provided that the halogenated products do not interfere with vital cellular functions and can be exported out of the cell efficiently.

DATA AVAILABILITY

This manuscript contains previously unpublished data. All data sets generated for this study are included in the manuscript and the supplementary files.

AUTHOR CONTRIBUTIONS

KV and SD carried out experimental procedures of the present study. KV, SD, JR, J-HL, NS, and VW analyzed data. KV prepared a draft of the manuscript. KV, J-HL, and VW finalized the manuscript. VW coordinated the study. All authors read and approved the final version of the manuscript.

FUNDING

We acknowledge the support for the article processing charge from the Deutsche Forschungsgemeinschaft and the Open Access Publication Fund of Bielefeld University.

ACKNOWLEDGMENTS

VW wishes to dedicate this paper to Prof. Dr. Michael Bott on the occasion of his 60th birthday. The authors thank Thomas Schäffer from the Department of Fermentation Technology at Bielefeld University for his support during the batch and fed-batch fermentations.

REFERENCES

Adams, J. (2004). "Proteasome inhibitors in cancer therapy," in *Cancer Chemoprevention (Cancer Drug Discovery and Development)*, eds G. J. Kelloff, E. T. Hawk, and C. C. Sigman (Totowa, NJ: Humana Press).

Andorfer, M. C., Park, H. J., Vergara-Coll, J., and Lewis, J. C. (2016). Directed evolution of RebH for catalyst-controlled halogenation of indole C–H bonds. *Chem. Sci.* 7, 3720–3729. doi: 10.1039/C5SC04680G

Bartoli, G., Dalpozzo, R., and Nardi, M. (2014). Applications of Bartoli indole synthesis. *Chem. Soc. Rev.* 43, 4728–4750. doi: 10.1039/C4CS00045E

Becker, J., Kuhl, M., Kohlstedt, M., Starck, S., and Wittmann, C. (2018). Metabolic engineering of *Corynebacterium glutamicum* for the production of *cis*, *cis*-muconic acid from lignin. *Microb. Cell. Fact.* 17:115. doi: 10.1186/s12934-018-0963-2

Bittner, S., Scherzer, R., and Harlev, E. (2007). The five bromotryptophans. *Amino Acids* 33, 19–42. doi: 10.1007/s00726-006-0441-8

Bitto, E., Huang, Y., Bingman, C. A., Singh, S., Thorson, J. S., and Phillips, G. N. (2008). The structure of flavin-dependent tryptophan 7-halogenase RebH. *Proteins Struct. Funct. Bioinf.* 70, 289–293. doi: 10.1002/prot.21627

Blombach, B., Riester, T., Wieschalka, S., Ziert, C., Youn, J.-W., Wendisch, V. F., et al. (2011). *Corynebacterium glutamicum* tailored for efficient isobutanol production. *Appl. Environ. Microbiol.* 77, 3300–3310. doi: 10.1128/AEM.02972-10

Bradford, M. M. (1976). A rapid and sensitive method for the quantitation of microgram quantities of protein utilizing the principle of protein-dye binding. *Anal. Biochem.* 72, 248–254. doi: 10.1016/0003-2697(76)90527-3

Bückle-Vallant, V., Krause, F. S., Messerschmidt, S., and Eikmanns, B. J. (2014). Metabolic engineering of *Corynebacterium glutamicum* for 2-ketoisocaproate production. *Appl. Microbiol. Biotechnol.* 98, 297–311. doi: 10.1007/s00253-013-5310-2

Corr, M. J., Sharma, S. V., Pubill-Ulldemolins, C., Bown, R. T., Poirot, P., Smith, D. R. M., et al. (2017). Sonogashira diversification of unprotected halotryptophans, halotryptophan containing tripeptides; and generation of a new to nature bromo-natural product and its diversification in water. *Chem. Sci.* 8, 2039–2046. doi: 10.1039/C6SC04423A

Diederich, F., and Stang, P. J. (Eds.). (2008). *Metal-Catalyzed Cross-Coupling Reactions*. Weinheim: Wiley-VCH.

Eggeling, L., and Bott, M. (2005). *Handbook of Corynebacterium glutamicum*. Boca Raton, FL: CRC Press.

Engels, V., Lindner, S. N., and Wendisch, V. F. (2008). The global repressor SugR controls expression of genes of glycolysis and of the L-lactate dehydrogenase LdhA in *Corynebacterium glutamicum*. *J. Bacteriol.* 190, 8033–8044. doi: 10.1128/JB.00705-08

Flecks, S., Patallo, E. P., Zhu, X., Ernyei, A. J., Seifert, G., Schneider, A., et al. (2008). New insights into the mechanism of enzymatic chlorination of tryptophan. *Angew. Chem. Int. Ed. Engl.* 47, 9533–9536. doi: 10.1002/anie.200802466

Frese, M., Guzowska, P. H., Voss, H., and Sewald, N. (2014). Regioselective enzymatic halogenation of substituted tryptophan derivatives using the FAD-dependent halogenase RebH. *ChemCatChem* 6, 1270–1276. doi: 10.1002/cctc.201301090

Frese, M., and Sewald, N. (2015). Enzymatic halogenation of tryptophan on a gram scale. *Angew. Chem. Int. Ed.* 54, 298–301. doi: 10.1002/anie.201408561

Gribble, G. W. (1996). "Naturally occuring organohalogen compounds—a comprehensive survery," in *Progress in the Chemistry of Organic Natural Products. Fortschritte der Chemie organischer Naturstoffe/Progress in the Chemistry of Organic Natural Products, Vol. 68*, eds W. Herz, G. W. Kirby, R. E. Moore, W. Steglich, and C. Tamm (Vienna: Springer).

Gruß, H., Belu, C., Bernhard, L. M., Merschel, A., and Sewald, N. (2019). Fluorogenic diversification of unprotected bromotryptophan by aqueous Mizoroki–Heck cross-coupling. *Chem. Eur. J.* 25, 5880–5883. doi: 10.1002/chem.201900437

Hanahan, D. (1983). Studies on transformation of *Escherichia coli* with plasmids. *J. Mol. Biol.* 166, 557–580. doi: 10.1016/S0022-2836(83)80284-8

Herry, D. M., and Dunican, L. K. (1993). Cloning of the *trp* gene cluster from a tryptophan-hyperproducing strain of *Corynebacterium glutamicum*: identification of a mutation in the *trp* leader sequence. *Appl. Environ. Microbiol.* 59, 791–799.

Inui, M., Kawaguchi, H., Murakami, S., Vertès, A. A., and Yukawa, H. (2004a). Metabolic engineering of *Corynebacterium glutamicum* for fuel ethanol production under oxygen-deprivation conditions. *J. Mol. Microbiol. Biotechnol.* 8, 243–254. doi: 10.1159/000086705

Inui, M., Murakami, S., Okino, S., Kawaguchi, H., Vertès, A. A., and Yukawa, H. (2004b). Metabolic analysis of *Corynebacterium glutamicum* during lactate and succinate productions under oxygen deprivation conditions. *J. Mol. Microbiol. Biotechnol.* 7, 182–196. doi: 10.1159/000079827

Ismail, M., Frese, M., Patschkowski, T., Ortseifen, V., Niehaus, K., and Sewald, N. (2019). Flavin-dependent halogenases from *Xanthomonas campestris* pv. campestris B100 prefer bromination over chlorination. *Adv. Synth. Catal.* 361, 2475–2486. doi: 10.1002/adsc.201801591

Ito, J., and Yanofsky, C. (1969). Anthranilate synthetase, an enzyme specified by the tryptophan operon of *Escherichia coli*: comparative studies on the complex and the subunits. *J. Bacteriol.* 97, 734–742.

Iyer, R., Iverson, T. M., Accardi, A., and Miller, C. (2002). A biological role for prokaryotic ClC chloride channels. *Nature* 419, 715–718. doi: 10.1038/nature01000

Jorge, J. M. P., Leggewie, C., and Wendisch, V. F. (2016). A new metabolic route for the production of gamma-aminobutyric acid by *Corynebacterium glutamicum* from glucose. *Amino Acids* 48, 2519–2531. doi: 10.1007/s00726-016-2272-6

Jorge, J. M. P., Pérez-García, F., and Wendisch, V. F. (2017). A new metabolic route for the fermentative production of 5-aminovalerate from glucose and alternative carbon sources. *Bioresour. Technol.* 245, 1701–1709. doi: 10.1016/j.biortech.2017.04.108

Kallscheuer, N., and Marienhagen, J. (2018). *Corynebacterium glutamicum* as platform for the production of hydroxybenzoic acids. *Microb. Cell. Fact.* 17:70. doi: 10.1186/s12934-018-0923-x

Kan, S.-C., Liu, J.-S., Hu, H.-Y., Chang, C.-M., Lin, W.-D., Wang, W.-C., et al. (2010). Biochemical characterization of two thymidylate synthases in *Corynebacterium glutamicum* NCHU 87078. *Biochim. Biophys. Acta* 1804, 1751–1759. doi: 10.1016/j.bbapap.2010.05.006

Kim, H. T., Baritugo, K.-A., Oh, Y. H., Hyun, S. M., Khang, T. U., Kang, K. H., et al. (2018). Metabolic engineering of *Corynebacterium glutamicum* for the high-level production of cadaverine that can be used for the synthesis of biopolyamide 510. *ACS Sustain. Chem. Eng.* 6, 5296–5305. doi: 10.1021/acssuschemeng.8b00009

Kim, J. Y., Lee, Y. A., Wittmann, C., and Park, J. B. (2013). Production of non-proteinogenic amino acids from α-keto acid precursors with recombinant *Corynebacterium glutamicum*. *Biotechnol. Bioeng.* 110, 2846–2855. doi: 10.1002/bit.24962

Koguchi, Y., Kohno, J., Nishio, M., Takahashi, K., Okuda, T., Ohnuki, T., et al. (2000). TMC-95A, B, C, and D, novel proteasome inhibitors produced by *Apiospora montagnei* Sacc. TC 1093. *J. Antibiot.* 53, 105–109. doi: 10.7164/antibiotics.53.105

Krause, F. S., Blombach, B., and Eikmanns, B. J. (2010). Metabolic engineering of *Corynebacterium glutamicum* for 2-ketoisovalerate production. *Appl. Environ. Microbiol.* 76, 8053–8061. doi: 10.1128/AEM.01710-10

Kwon, S. Y., Kang, B. S., Kim, G. H., and Kim, K. J. (2007). Expression, purification, crystallization and initial crystallographic characterization of the p-hydroxybenzoate hydroxylase from *Corynebacterium glutamicum*. *Acta Crystallogr. Sect. F Struct. Biol. Cryst. Commun.* 63, 944–946. doi: 10.1107/S1744309107046386

Latham, J., Brandenburger, E., Shepherd, S. A., Menon, B. R. K., and Micklefield, J. (2017). Development of halogenase enzymes for use in synthesis. *Chem. Rev.* 118, 232–269. doi: 10.1021/acs.chemrev.7b00032

Lee, J.-H., and Wendisch, V. F. (2017). Biotechnological production of aromatic compounds of the extended shikimate pathway from renewable biomass. *J. Biotechnol.* 257, 211–221. doi: 10.1016/j.jbiotec.2016.11.016

Lesic, B., Lépine, F., Déziel, E., Zhang, J., Zhang, Q., Padfield, K., et al. (2007). Inhibitors of pathogen intercellular signals as selective anti-infective compounds. *PLoS Pathog.* 3:e126. doi: 10.1371/journal.ppat.0030126

Leßmeier, L., and Wendisch, V. F. (2015). Identification of two mutations increasing the methanol tolerance of *Corynebacterium glutamicum*. *BMC Microbiol.* 15:216. doi: 10.1186/s12866-015-0558-6

Litsanov, B., Kabus, A., Brocker, M., and Bott, M. (2012). Efficient aerobic succinate production from glucose in minimal medium with *Corynebacterium glutamicum*. *Microb. Biotechnol.* 5, 116–128. doi: 10.1111/j.1751-7915.2011.00310.x

Longmuir, I. S. (1954). Respiration rate of bacteria as a function of oxygen concentration. *Biochem. J.* 57:81. doi: 10.1042/bj0570081

Ma, W., Wang, J., Li, Y., Yin, L., and Wang, X. (2018). Poly (3-hydroxybutyrate-co-3-hydroxyvalerate) co-produced with L-isoleucine in *Corynebacterium glutamicum* WM001. *Microb. Cell. Fact.* 17:93. doi: 10.1186/s12934-018-0942-7

Mindt, M., Risse, J. M., Gruß, H., Sewald, N., Eikmanns, B. J., and Wendisch, V. F. (2018). One-step process for production of *N*-methylated amino acids from sugars and methylamine using recombinant *Corynebacterium glutamicum* as biocatalyst. *Sci. Rep.* 8:12895. doi: 10.1038/s41598-018-31309-5

Molenaar, D., van der Rest, M. E., and Petrović, S. (1998). Biochemical and genetic characterization of the membrane-associated malate dehydrogenase (acceptor) from *Corynebacterium glutamicum*. *Eur. J. Biochem.* 254, 395–403. doi: 10.1046/j.1432-1327.1998.2540395.x

Neubauer, P. R., Widmann, C., Wibberg, D., Schröder, L., Frese, M., Kottke, T., et al. (2018). A flavin-dependent halogenase from metagenomic analysis prefers bromination over chlorination. *PLoS ONE* 13:e0196797. doi: 10.1371/journal.pone.0196797

Nicolaou, K. C., Bella, M., Chen, D. Y. K., Huang, X., Ling, T., and Snyder, S. A. (2002). Total synthesis of diazonamide A. *Angew. Chem. Int. Ed.* 41, 3495–3499. doi: 10.1002/1521-3773(20020916)41:18<3495::AID-ANIE3495>3.0.CO;2-7

Nishizawa, T., Aldrich, C. C., and Sherman, D. H. (2005). Molecular analysis of the rebeccamycin L-amino acid oxidase from *Lechevalieria aerocolonigenes*

ATCC 39243. *J. Bacteriol.* 187, 2084–2092. doi: 10.1128/JB.187.6.2084-2092.2005

O'Gara, J. P., and Dunican, L. K. (1995). Mutations in the *trpD* gene of *Corynebacterium glutamicum* confer 5-methyltryptophan resistance by encoding a feedback-resistant anthranilate phosphoribosyltransferase. *Appl. Environ. Microbiol.* 61, 4477–4479.

Parte, A. (2012). *Bergey's Manual of Systematic Bacteriology, Vol. 5: The Actinobacteria*. Heidelberg: Springer Science and Business Media.

Payne, J. T., Andorfer, M. C., and Lewis, J. C. (2013). Regioselective arene halogenation using the FAD-dependent halogenase RebH. *Angew. Chem. Int. Ed. Engl.* 125, 5379–5382. doi: 10.1002/ange.201300762

Pérez-García, F., Peters-Wendisch, P., and Wendisch, V. F. (2016). Engineering *Corynebacterium glutamicum* for fast production of L-lysine and L-pipecolic acid. *Appl. Microbiol. Biotechnol.* 100, 8075–8090. doi: 10.1007/s00253-016-7682-6

Purwanto, H. S., Kang, M.-S., Ferrer, L., Han, S.-S., Lee, J.-Y., Kim, H.-S., et al. (2018). Rational engineering of the shikimate and related pathways in *Corynebacterium glutamicum* for 4-hydroxybenzoate production. *J. Biotechnol.* 282, 92–100. doi: 10.1016/j.jbiotec.2018.07.016

Roeßler, M., Sewald, X., and Müller, V. (2003). Chloride dependence of growth in bacteria. *FEMS Microbiol. Lett.* 225, 161–165. doi: 10.1016/S0378-1097(03)00509-3

Rohles, C. M., Gießelmann, G., Kohlstedt, M., Wittmann, C., and Becker, J. (2016). Systems metabolic engineering of *Corynebacterium glutamicum* for the production of the carbon-5 platform chemicals 5-aminovalerate and glutarate. *Microb. Cell. Fact.* 15:154. doi: 10.1186/s12934-016-0553-0

Roy, A. D., Goss, R. J. M., Wagner, G. K., and Winn, M. (2008). Development of fluorescent aryltryptophans by Pd mediated cross-coupling of unprotected halotryptophans in water. *Chem. Commun.* 39, 4831–4833. doi: 10.1039/B807512C

Rüffer, N., Heidersdorf, U., Kretzers, I., Sprenger, G. A., Raeven, L., and Takors, R. (2004). Fully integrated L-phenylalanine separation and concentration using reactive-extraction with liquid-liquid centrifuges in a fed-batch process with *E. coli*. *Bioprocess Biosyst. Eng.* 26, 239–248. doi: 10.1007/s00449-004-0354-4

Sakai, S., Tsuchida, Y., Okino, S., Ichihashi, O., Kawaguchi, H., Watanabe, T., et al. (2007). Effect of lignocellulose-derived inhibitors on growth of and ethanol production by growth-arrested *Corynebacterium glutamicum* R. *Appl. Environ. Microbiol.* 73, 2349–2353. doi: 10.1128/AEM.02880-06

Schneider, J., Niermann, K., and Wendisch, V. F. (2011). Production of the amino acids L-glutamate, L-lysine, L-ornithine and L-arginine from arabinose by recombinant *Corynebacterium glutamicum*. *J. Biotechnol.* 154, 191–198. doi: 10.1016/j.jbiotec.2010.07.009

Schneider, J., and Wendisch, V. F. (2010). Putrescine production by engineered *Corynebacterium glutamicum*. *Appl. Microbiol. Biotechnol.* 88, 859–868. doi: 10.1007/s00253-010-2778-x

Schnepel, C., and Sewald, N. (2017). Enzymatic halogenation: a timely strategy for regioselective C– H activation. *Chem. Eur. J.* 23, 12064–12086. doi: 10.1002/chem.201701209

Siebert, D., and Wendisch, V. F. (2015). Metabolic pathway engineering for production of 1, 2-propanediol and 1-propanol by *Corynebacterium glutamicum*. *Biotechnol. Biofuels* 8:91. doi: 10.1186/s13068-015-0269-0

Sonogashira, K. (2002). Development of Pd–Cu catalyzed cross-coupling of terminal acetylenes with sp^2-carbon halides. *J. Organometal. Chem.* 653, 46–49. doi: 10.1016/S0022-328X(02)01158-0

Stansen, C., Uy, D., Delaunay, S., Eggeling, L., Goergen, J.-L., and Wendisch, V. F. (2005). Characterization of a *Corynebacterium glutamicum* lactate utilization operon induced during temperature-triggered glutamate production. *Appl. Environ. Microbiol.* 71, 5920–5928. doi: 10.1128/AEM.71.10.5920-5928.2005

Tateno, T., Okada, Y., Tsuchidate, T., Tanaka, T., Fukuda, H., and Kondo, A. (2009). Direct production of cadaverine from soluble starch using *Corynebacterium glutamicum* coexpressing α-amylase and lysine decarboxylase. *Appl. Microbiol. Biotechnol.* 82, 115–121. doi: 10.1007/s00253-008-1751-4

Toyoda, K., Teramoto, H., Inui, M., and Yukawa, H. (2009). The *ldhA* gene, encoding fermentative L-lactate dehydrogenase of *Corynebacterium glutamicum*, is under the control of positive feedback regulation mediated by LldR. *J. Bacteriol.* 191, 4251–4258. doi: 10.1128/JB.00303-09

Van Peè, K.-H. (2001). Microbial biosynthesis of halometabolites. *Arch. Microbiol.* 175, 250–258. doi: 10.1007/s002030100263

Veldmann, K. H., Minges, H., Sewald, N., Lee, J.-H., and Wendisch, V. F. (2019). Metabolic engineering of *Corynebacterium glutamicum* for the fermentative production of halogenated tryptophan. *J. Biotechnol.* 291, 7–16. doi: 10.1016/j.jbiotec.2018.12.008

Vergnolle, N. (2016). Protease inhibition as new therapeutic strategy for GI diseases. *Gut* 65, 1215–1224. doi: 10.1136/gutjnl-2015-309147

Wang, G., Shang, L., Burgett, A. W. G., Harran, P. G., and Wang, X. (2007). Diazonamide toxins reveal an unexpected function for ornithine δ-amino transferase in mitotic cell division. *Proc. Natl. Acad. Sci. U.S.A.* 104, 2068–2073. doi: 10.1073/pnas.0610832104

Wang, X., Khushk, I., Xiao, Y., Gao, Q., and Bao, J. (2018). Tolerance improvement of *Corynebacterium glutamicum* on lignocellulose derived inhibitors by adaptive evolution. *Appl. Microbiol. Biotechnol.* 102, 377–388. doi: 10.1007/s00253-017-8627-4

Wendisch, V. F. (2019). Metabolic engineering advances and prospects for amino acid production. *Metab. Eng.* doi: 10.1016/j.ymben.2019.03.008

Wendisch, V. F., Jorge, J. M. P., Pérez-García, F., and Sgobba, E. (2016). Updates on industrial production of amino acids using *Corynebacterium glutamicum*. *World J. Microbiol. Biotechnol.* 32:105. doi: 10.1007/s11274-016-2060-1

Wieschalka, S., Blombach, B., and Eikmanns, B. J. (2012). Engineering *Corynebacterium glutamicum* for the production of pyruvate. *Appl. Microbiol. Biotechnol.* 94, 449–459. doi: 10.1007/s00253-011-3843-9

Willemse, T., Schepens, W., Vlijmen, H., Maes, B., and Ballet, S. (2017). The suzuki–miyaura cross-coupling as a versatile tool for peptide diversification and cyclization. *Catalysts* 7:74. doi: 10.3390/catal7030074

Yeh, E., Blasiak, L. C., Koglin, A., Drennan, C. L., and Walsh, C. T. (2007). Chlorination by a long-lived intermediate in the mechanism of flavin-dependent halogenases. *Biochemistry* 46, 1284–1292. doi: 10.1021/bi0621213

Yeh, E., Garneau, S., and Walsh, C. T. (2005). Robust *in vitro* activity of RebF and RebH, a two-component reductase/halogenase, generating 7-chlorotryptophan during rebeccamycin biosynthesis. *Proc. Natl. Acad. Sci. U.S.A.* 102, 3960–3965. doi: 10.1073/pnas.0500755102

Conflict of Interest Statement: The authors declare that the research was conducted in the absence of any commercial or financial relationships that could be construed as a potential conflict of interest.

frontiers in Bioengineering and Biotechnology

ORIGINAL RESEARCH
published: 20 September 2019
doi: 10.3389/fbioe.2019.00229

The White-Rot Basidiomycete *Dichomitus squalens* Shows Highly Specific Transcriptional Response to Lignocellulose-Related Aromatic Compounds

*Joanna E. Kowalczyk[1], Mao Peng[2], Megan Pawlowski[3], Anna Lipzen[3], Vivian Ng[3], Vasanth Singan[3], Mei Wang[3], Igor V. Grigoriev[3] and Miia R. Mäkelä[1]**

[1] Department of Microbiology, University of Helsinki, Helsinki, Finland, [2] Fungal Physiology, Westerdijk Fungal Biodiversity Institute and Fungal Molecular Physiology, Utrecht University, Utrecht, Netherlands, [3] U.S. Department of Energy Joint Genome Institute, Walnut Creek, CA, United States

OPEN ACCESS

Edited by:
Nils Jonathan Helmuth Averesch, Stanford University, United States

Reviewed by:
Victor C. Ujor, The Ohio State University, United States
Xu Fang, State Key Laboratory of Microbial Technology, Shandong University, China

***Correspondence:**
Miia R. Mäkelä
miia.r.makela@helsinki.fi

Specialty section:
This article was submitted to Bioprocess Engineering, a section of the journal Frontiers in Bioengineering and Biotechnology

Received: 27 June 2019
Accepted: 05 September 2019
Published: 20 September 2019

Citation:
Kowalczyk JE, Peng M, Pawlowski M, Lipzen A, Ng V, Singan V, Wang M, Grigoriev IV and Mäkelä MR (2019) The White-Rot Basidiomycete Dichomitus squalens Shows Highly Specific Transcriptional Response to Lignocellulose-Related Aromatic Compounds. Front. Bioeng. Biotechnol. 7:229. doi: 10.3389/fbioe.2019.00229

Lignocellulosic plant biomass is an important feedstock for bio-based economy. In particular, it is an abundant renewable source of aromatic compounds, which are present as part of lignin, as side-groups of xylan and pectin, and in other forms, such as tannins. As filamentous fungi are the main organisms that modify and degrade lignocellulose, they have developed a versatile metabolism to convert the aromatic compounds that are toxic at relatively low concentrations to less toxic ones. During this process, fungi form metabolites some of which represent high-value platform chemicals or important chemical building blocks, such as benzoic, vanillic, and protocatechuic acid. Especially basidiomycete white-rot fungi with unique ability to degrade the recalcitrant lignin polymer are expected to perform highly efficient enzymatic conversions of aromatic compounds, thus having huge potential for biotechnological exploitation. However, the aromatic metabolism of basidiomycete fungi is poorly studied and knowledge on them is based on the combined results of studies in variety of species, leaving the overall picture in each organism unclear. *Dichomitus squalens* is an efficiently wood-degrading white-rot basidiomycete that produces a diverse set of extracellular enzymes targeted for lignocellulose degradation, including oxidative enzymes that act on lignin. Our recent study showed that several intra- and extracellular aromatic compounds were produced when *D. squalens* was cultivated on spruce wood, indicating also versatile aromatic metabolic abilities for this species. In order to provide the first molecular level systematic insight into the conversion of plant biomass derived aromatic compounds by basidiomycete fungi, we analyzed the transcriptomes of *D. squalens* when grown with 10 different lignocellulose-related aromatic monomers. Significant differences for example with respect to the expression of lignocellulose degradation related genes, but also putative genes encoding transporters and catabolic pathway genes were observed between the cultivations supplemented with the different aromatic compounds. The

results demonstrate that the transcriptional response of *D. squalens* is highly dependent on the specific aromatic compounds present suggesting that instead of a common regulatory system, fine-tuned regulation is needed for aromatic metabolism.

Keywords: transcriptome, gene expression, basidiomycete, *Dichomitus squalens*, aromatic compounds, lignocellulose, lignin, platform chemicals

INTRODUCTION

Non-edible lignocellulosic biomass is increasingly researched as a sustainable alternative to fossil fuel-based energy sources, biomaterials, and chemicals. Majority of lignocellulose waste originates from forestry (e.g., bark, logging debris, and sawdust) or agriculture (e.g., rice and wheat straw, corn stover and sugar cane bagasse) and is mainly composed of cellulose, hemicelluloses, and lignin. Lignin is an aromatic polymer and the most recalcitrant constituent present in woody plant cell walls, where it e.g., provides rigidity, resistance against microbial invasion and facilitates water transportation (Tolbert et al., 2014). In softwoods, the amount of lignin can be up to 32% of plant dry weight (Sjöström, 1993), and it is the most abundant renewable source of aromatic compounds on earth. Lower amounts of aromatic compounds are also present in plant biomass as side-groups of polysaccharides xylan and pectin, as well as in tannins (McLeod, 1974; Mäkelä et al., 2015). Aromatics derived from plant biomass have applications in various industrial sectors, e.g., as precursors for synthesis of biopolymers (Kawaguchi et al., 2017; Feghali et al., 2018; Kohlstedt et al., 2018). Therefore, lignocellulose holds a great potential as a source of chemical building blocks for the sustainable production of valuable compounds in biorefineries.

Despite huge prospects, lignin remains the least utilized polymer in lignocellulose (Rinaldi et al., 2016). Degradation of lignin is difficult due to its insolubility and complex, random structure with various non-hydrolysable intramolecular C-C, C-O, and β-aryl ether bonds (Hatakka and Hammel, 2011). Therefore, the vast majority of lignin, which is formed as major byproduct of the wood-related biorefineries as well as pulp and paper industry, is currently being used for low-value production of heat and electricity (Calvo-Flores and Dobado, 2010). However, fragmentation of lignin can be achieved by physical and/or chemical methods, and several phenolic compounds, such as *p*-coumaric acid, *p*-hydroxybenzoic acid, ferulic acid, vanillin, and vanillic acid, are already produced from lignin via chemical oxidation or pyrolysis (Otto and Simpson, 2006; Li et al., 2015). Nowadays, with the global move toward the bio-based economy, great attention is given to development of environmentally friendly modification methods of lignocellulose, such as enzymatic conversion (Den et al., 2018).

Basidiomycete white-rot fungi are the only organisms that are able to degrade all polymers present in lignocellulose, including high molecular weight native lignin molecules (Hatakka and Hammel, 2011). During this process, fungi form metabolites some of which represent high-value platform chemicals or industrially important chemical building blocks, such as benzoic and protocatechuic acid (Lubbers et al., 2019). While, the extracellular plant biomass degrading enzyme systems of the white-rot fungi have been extensively studied (Mäkelä et al., 2014; Rytioja et al., 2014; Manavalan et al., 2015; An et al., 2019), the knowledge on their metabolism converting the resulting small aromatic compounds is still far from complete. For example, instead of systematic characterization of full metabolic pathways, mainly single conversions of specific compounds have been studied (Mäkelä et al., 2015; Lubbers et al., 2019). It should also be noted that many wood-degrading basidiomycetes have been reported to synthesize aromatic compounds such as vanillin and veratryl alcohol (Harper et al., 1990; Lomascolo et al., 1999).

Dichomitus squalens is an efficient wood-degrading white-rot fungus that predominantly degrades softwood (Andrews and Gill, 1943; Renvall et al., 1991), but can also grow on hardwoods (Blanchette et al., 1987) in nature. *D. squalens* is a promising reference species to investigate white-rot fungal plant biomass degradation, as it has a flexible physiology to utilize different types of biomass as sources of carbon and energy (Rytioja et al., 2017; Daly et al., 2018). We recently showed that *D. squalens* produces several intra- and extracellular aromatic compounds during cultivation of on wood (Daly et al., 2018) and characterized the first functional β-*O*-4 bond cleaving fungal β-etherase (GST1) from this species (Marinović et al., 2018). All these aspects higlight the suitability of *D. squalens* for studies on fungal metabolism of lignocellulose-related aromatic compounds.

In this study, we aimed to provide the first systematic, molecular level insight into the white-rot fungal response to plant biomass related aromatic monomers. For this, we used RNA sequencing (RNA-seq) to identify all differentially expressed transcripts in *D. squalens* when the fungus was exposed to 10 different monomeric aromatic compounds in comparison with control conditions without aromatic compounds. The aromatic compounds included cinnamic acid, which in lignin biosynthesis can be converted to the three monolignol building blocks of lignin, i.e., coniferyl, sinapyl, and *p*-coumaryl alcohol (Humphreys and Chapple, 2002), coniferyl alcohol, which is one of the monolignols (Vanholme et al., 2010), and eight putative metabolic conversion products of lignin (ferulic acid, vanillin, vanillyl alcohol, vanillic acid, protocatechuic acid, veratryl alcohol, *p*-coumaric acid, *p*-hydroxybenzoic acid). Regulons for each aromatic compound were defined as the number of genes with differential expression when compared to control conditions. Significant differences were observed between the studied cultivations, i.e., with respect to the expression of

genes with predicted intracellular oxidative activity including oxidoreductases, alcohol dehydrogenases, and cytochrome P450 monooxygenases, showing that the transcriptional response of *D. squalens* is highly dependent on the specific aromatic compounds present.

MATERIALS AND METHODS

Fungal Strain and Growth Conditions

Dichomitus squalens dikaryotic strain FBCC312 was obtained from the FBCC-HAMBI culture collection (www.helsinki.fi/hambi/) and maintained on 2% (w/v) malt extract 2% (w/v) agar (MEA) plates. All other cultivations were inoculated with single mycelium-covered agar plug (0.5 cm in diameter) from a freshly growing MEA plate. Stocks of ferulic acid (Sigma), vanillyl alcohol (Fluka), vanillin (Merck), vanillic acid (Fluka), *p*-coumaric acid (Sigma), protocatechuic acid (Sigma), *p*-hydroxybenzoic acid (Fluka), cinnamic acid (Merck), veratryl alcohol (Fluka), or coniferyl alcohol (gift from the Department of Chemistry, University of Helsinki) were prepared by dissolving in 40% (v/v) dimethyl sulfoxide (DMSO; VWR Chemicals) to the final concentration of 40 mM. The inhibiting effect of the tested aromatics and/or DMSO on *D. squalens* was assessed by growing the fungus on low-nitrogen asparagine-succinate (LN-AS, pH 4.5) 1.5% (w/v) agar plates with 0.05% (v/v) glycerol (Hatakka and Uusi-Rauva, 1983) and supplemented with 0.2, 0.5, or 1 mM aromatic compounds, which contained 0.2, 0.5, or 1% DMSO, respectively. The duplicate plates were inoculated with a centrally placed agar plug and incubated at 28°C in the dark for 4 days. The toxicity was assessed by measuring the diameter of the radial growth of fungal colony in comparison to the plates without aromatic compounds.

For the gene expression analyses, the fungus was grown on LN-AS agar plates containing 0.05% (v/v) glycerol and 0.5% (v/v) DMSO (no aromatics control) or 0.05% (v/v) glycerol and 0.5 mM of one of the mentioned aromatic compounds as the only carbon sources. Before inoculation with an agar plug, each plate was covered with a sterile polycarbonate membrane (GVS Life Sciences) to facilitate the harvesting of the mycelia. After 4 days of growth at 28°C, mycelium from the outer ring (1.5 cm wide) of the fungal colony was carefully scraped with an RNase-free spatula and flash frozen in liquid nitrogen. For each condition, three biological replicate cultures were performed.

Preparation and Sequencing of RNA

Dichomitus squalens RNA was extracted from the cultivations supplemented with the 10 different aromatic compounds and analyzed by RNA sequencing (RNA-seq). First, frozen mycelia were transferred to a pre-chilled 2 mL lysing matrix tube (MP Biomedicals) with 1 mL of TRIzol (Sigma) and ground in a tissue homogenizer (FastPrep-24™, MP Biomedicals) for 2 × 10 s at maximum speed, with a cooling on ice between the grinding. After 5 min incubation at RT, 0.2 mL chloroform was added, the tubes were shaken vigorously and incubated for additional 3 min at RT. Then, the samples were centrifuged for 10 min, 13,000 × g, at 4°C and the aqueous phase containing RNA was carefully collected and processed using the NucleoSpin RNA II purification kit (Macherey-Nagel) according to manufacturer's instructions. The quantity and integrity of RNA were measured with NanoDrop One Microvolume UV-Vis Spectrophotometer (Thermo Scientific) and RNA600 Nano Assay using the Agilent 2100 Bioanalyzer (Agilent Technologies, USA).

Purification of mRNA, synthesis of cDNA library and sequencing on the Illumina HiSeq2500 platform were performed at the Joint Genome Institute (JGI, Walnut Creek, USA) as described previously (Daly et al., 2018). One sample from veratryl alcohol cultivation did not pass the quality control and was removed from the sequencing queue.

The monokaryotic *D. squalens* CBS464.89 strain derived from the FBCC312 dikaryon (Pham et al., 1990; Casado López et al., 2017) is currently the best *D. squalens* reference genome available (Casado López et al., 2019), and was therefore used to map the filtered reads from each library. The reads from each of the RNA-seq samples were deposited in the Sequence Read Archive at NCBI with individual sample BioProject Accession numbers (PRJNA500193 to PRJNA500234).

RNA-Seq Data Analysis

Gene expression levels were measured as Fragments Per Kilobase of transcript per Million mapped reads or FPKM (Trapnell et al., 2010). Genes with FPKM > 70 and FPKM < 10 were considered highly and lowly expressed, respectively, and genes with 10–70 FPKM moderately expressed. The correlation matrix and principal component analysis (PCA) were performed using the corrplot and FactoMineR package (Lê et al., 2008), respectively, in R version 3.5.0.

Transcript levels of the samples cultivated with glycerol and aromatic compounds (ferulic acid, vanillyl alcohol, vanillin, vanillic acid, *p*-coumaric acid, protocatechuic acid, *p*-hydroxybenzoic acid, cinnamic acid, veratryl alcohol, or coniferyl alcohol) were compared to the control cultures without aromatics using DESeq2 version 1.10.0 (Love et al., 2014). Between each pair of conditions, differentially expressed genes with fold change > 2, adjusted $p < 0.01$, and FPKM > 10 in at least one condition were identified. Functional annotation of differentially expressed genes was based on combined information from EuKaryotic Orthologous Groups (KOG), Kyoto Encyclopedia of Genes and Genomes (KEGG) pathway mapping, InterPro protein sequence analysis & classification, and Carbohydrate-Active enZymes (CAZy) classifications for *D. squalens* CBS464.89 (Dicsqu464_1) retrieved from JGI MycoCosm database (https://genome.jgi.doe.gov/cgi-bin/kogBrowser?db=Dicsqu464_1) and updated with information from Daly et al. (2018). Genes with annotation in more than one database were manually assigned into one of the four main functional groups created based on KOG system: "Carbohydrate-Active enzyme (CAZyme)," "Metabolism," "Cellular processes and signaling," or "Information storage and processing." Genes lacking well-defined annotation or present in only one database were collected in "General function prediction only" and genes without any available annotation in "Not annotated" groups, respectively.

The statistically overrepresented Gene Ontology (GO) terms were analyzed using the Biological Networks Gene Ontology (BiNGO) plugin in the Cytoscape v 3.6.0 software (Maere et al.,

2005), with custom input Dicsqu464_1 GO annotation retrieved from JGI MycoCosm database (https://genome.jgi.doe.gov/cgi-bin/kogBrowser?db=Dicsqu464_1). Hierarchical clustering heatmaps were made using gplots package in R, with the complete-linkage clustering method and Euclidean distance. Intersection groups, representing unique sets of gene identified only between intersected elements, were visualized using UpSetR package v1.3.3 in R. Protein sequences of previously identified bacterial and fungal aromatic metabolic genes were retrieved from National Center for Biotechnology Information (NCBI, https://www.ncbi.nlm.nih.gov/) based on information collected in Lubbers et al. (2019) and used as a query for homology search in Dicsqu464_1 genome.

RESULTS

Growth of *D. squalens* on Different Aromatic Monomers

In this study, we aimed to provide the first molecular level systematic insight into the conversion of lignocellulose-related aromatic monomers by the basidiomycete fungus *D. squalens*. Ten compounds were chosen for the comparative analysis: coniferyl alcohol, ferulic acid, vanillin, vanillyl alcohol, vanillic acid, veratryl alcohol, protocatechuic acid, *p*-coumaric acid, *p*-hydroxybenzoic acid, and cinnamic acid. Cinnamic acid is a plant L-phenylalanine-derived compound that can be converted via several biosynthetic steps into three different phenylpropanoid precursors of lignin (monolignols), including coniferyl alcohol (Leisola et al., 2012; Wang et al., 2013). The remaining monomeric aromatic compounds are predicted to be intermediate products of aromatic metabolism in filamentous fungi (Mäkelä et al., 2015). Vanillin and *p*-coumaric acid were previously reported to be formed during lignin degradation by several bacterial species (Lubbers et al., 2019), and ferulic acid was chosen because it is commonly present in biomass as e.g., substituent of xylans. Additionally, *p*-hydroxybenzoic acid, protocatechuic acid and vanillic acid were identified in the metabolome of *D. squalens* grown on spruce wood for two and four weeks (Daly et al., 2018), while *p*-hydroxybenzoic acid and vanillic acid have also been formed during spruce degradation by the white-rot fungus *Phanerochaete chrysosporium* (Chen et al., 1982).

Many aromatic compounds have inhibitory effect on fungal growth even at low concentrations (Adeboye et al., 2014; Lima et al., 2018). Therefore, the influence of the selected aromatics on the growth of *D. squalens* was tested in final concentrations of 0.2, 0.5, and 1 mM. The growth medium was additionally supplemented with 0.05% glycerol due to previous reports showing that many white-rot fungi metabolize lignin-related aromatic compounds only in the presence of an alternate carbon and energy source (Kirk and Farrel, 1987). None of the tested aromatic compounds had inhibitory effect of the growth of *D. squalens* determined as the diameter of the colony at final concentration 0.2 mM, while at 0.5 mM small growth reduction was observed on vanillin and cinnamic acid (**Figure 1**). In final concentration of 1 mM, all aromatics, except *p*-hydroxybenzoic acid, inhibited the growth of *D. squalens*. Vanillin and cinnamic acid restricted the growth most. All aromatic compounds were dissolved in 40% DMSO, since DMSO was previously reported as an optimal solvent for Kraft lignin without affecting activity of the main lignin-degrading enzymes in the white-rot fungus *Coriolus (Trametes) versicolor* (Brzonova et al., 2017). The radial growth of *D. squalens* was not reduced by the presence of 0.2–0.5% DMSO as observed from the control cultivations without addition of aromatic compound (**Figure 1**). However, a small reduction in the growth of the fungal colony was observed with 1% DMSO. Based on these results, an intermediate concentration of aromatics, 0.5 mM with 0.5% DMSO, was chosen for the transcriptome induction in *D. squalens*.

D. squalens Showed Specific Transcriptional Response to Lignin-Related Aromatic Compounds

Gene expression in *D. squalens* exposed to the monomeric aromatic compounds was analyzed by RNA-seq. Genes with FPKM < 10 in all tested conditions were considered not expressed and excluded from the analysis. Correlation matrix and PCA analysis of the remaining set of 8,733 expressed genes showed high correlation between the biological triplicate cultivations, but also close similarity between different aromatic compounds (correlation coefficient 0.95–1; **Supplementary Table 1**), suggesting that the most differences are in the subsets of genes. Regulons, i.e., the sets of the regulated genes, were defined as the number of the differentially expressed genes in *D. squalens* cultures supplemented with aromatic compounds when compared to the control conditions using the cutoff values described in Material and Methods. Control cultivations were performed with 0.05% glycerol and 0.5% DMSO without addition of aromatics. It is worth mentioning that the sum of the genes identified in each aromatic regulon was higher than the total number of the regulated genes due to the fact that some genes were co-regulated by two or more aromatic compounds. Expression of all genes identified as up- and downregulated in *D. squalens* in the presence of aromatic compounds can be found in the **Supplementary Tables 1**, **2**. Regulons for each aromatic compound were compared to identify sets of commonly and uniquely affected genes (**Figures 2**, **3** and **Table 1**).

Among the upregulated genes, 268 (46.9%) were affected by a single aromatic compound. Notably lower number of upregulated genes was affected by more than one of the tested aromatic compounds (**Table 1**). Vanillin upregulated the largest set of genes (303) and also the largest number of uniquely upregulated genes (74; **Figure 2**). Large number of these genes was functionally associated with metabolism, although genes with only general prediction available were also abundant. Cinnamic acid upregulated the second largest regulon (230 genes) and the second largest unique intersection (60 genes). The third largest group of uniquely upregulated genes (42) responded to both vanillin and cinnamic acid. Similarly, aromatics that upregulated large regulons (coniferyl alcohol, 140 genes; *p*-coumaric acid, 148 genes) are among the

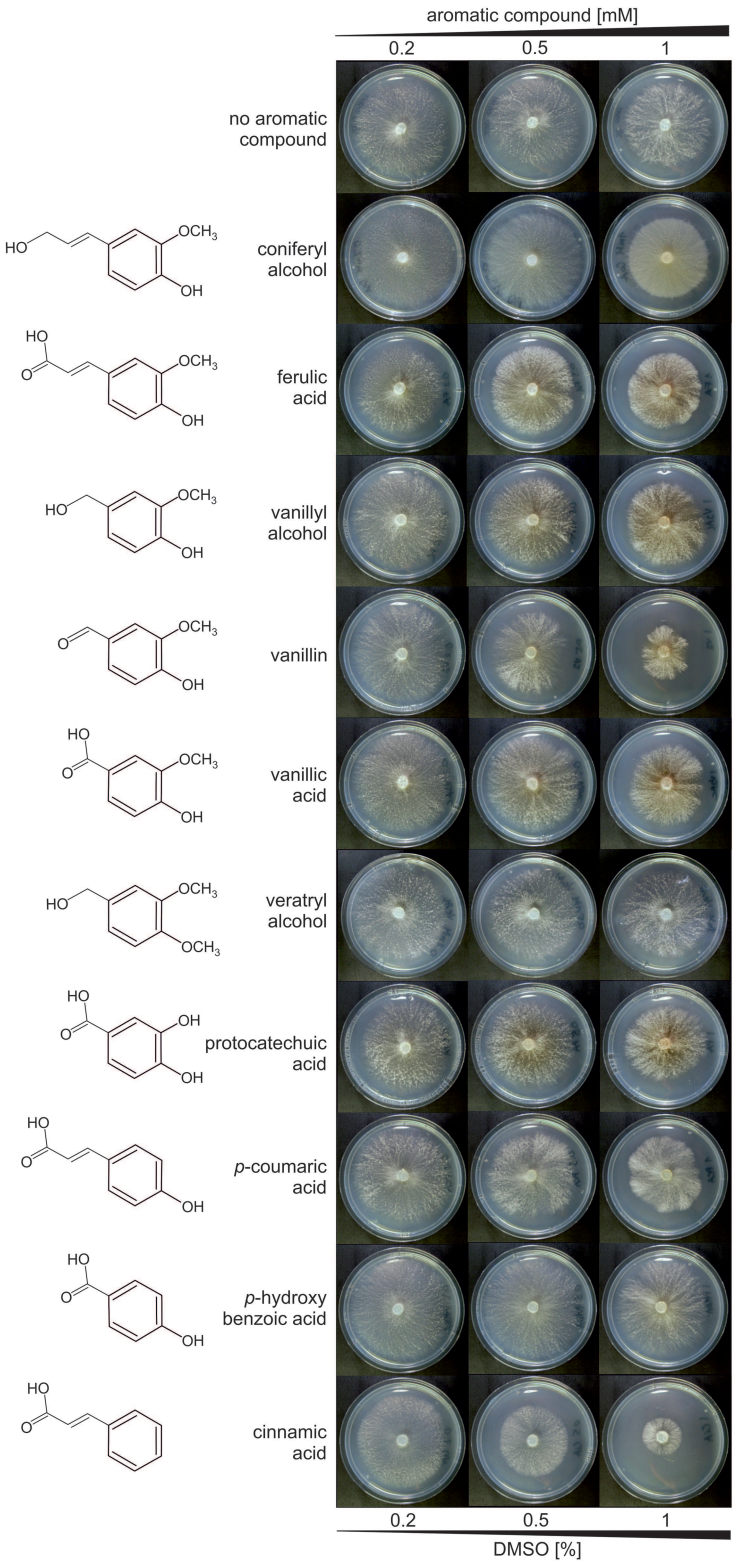

FIGURE 1 | *D. squalens* FBCC312 grown on LN-AS agar medium supplemented with 0.05% glycerol and increasing concentrations (0.2, 0.5, 1 mM) of selected aromatic compounds. Several tested aromatics had inhibitory effect on fungal growth at 1 mM, and therefore the final concentration of 0.5 mM was used for transcriptome induction. Low concentrations of DMSO (0.2–0.5%) used as a solvent for the aromatic compounds did not affect fungal growth. Plates were incubated for 4 days at 28°C.

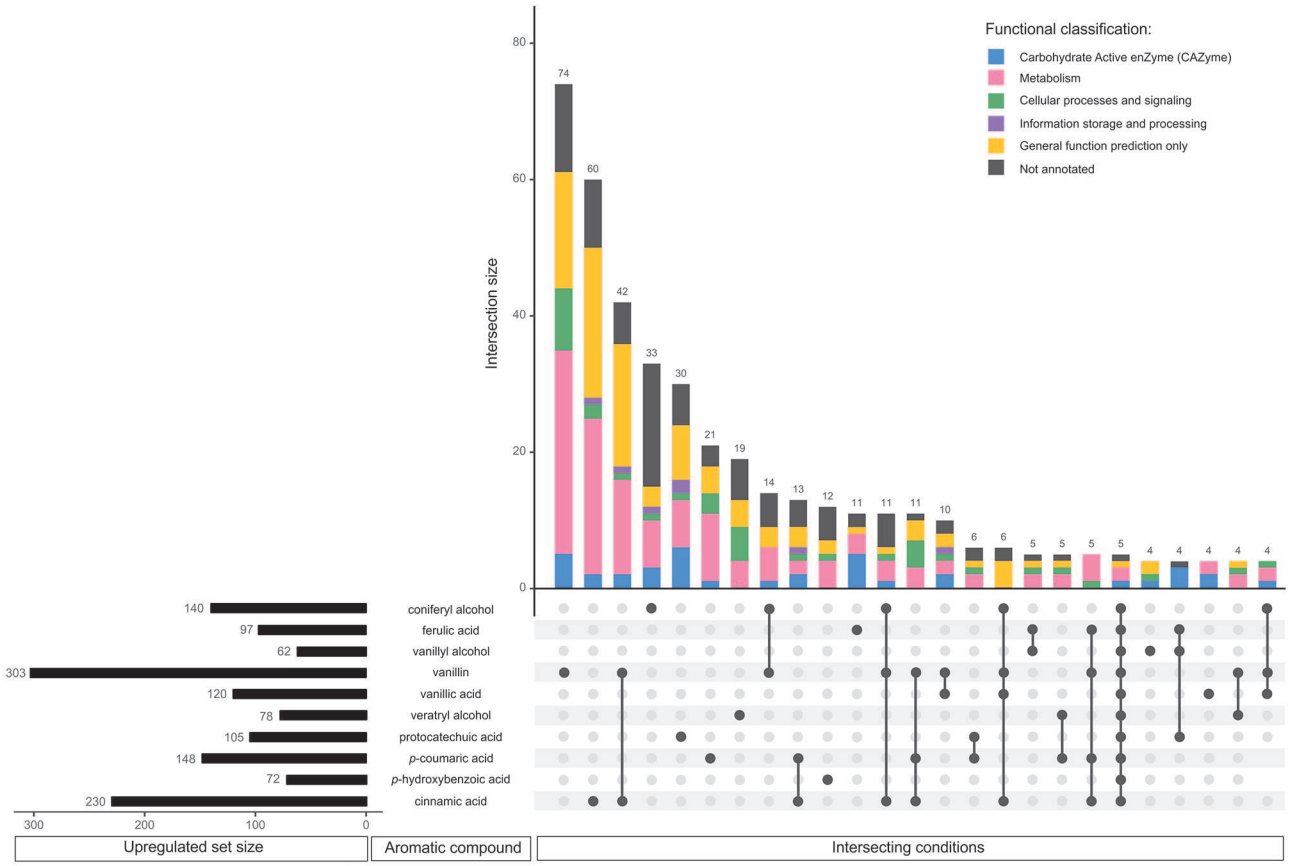

FIGURE 2 | Comparative analysis of all upregulated genes in *D. squalens* grown in the presence of aromatic compounds. The horizontal bars represent the total number of genes identified as upregulated on the individual aromatic compounds using criteria specified in the Materials and Methods. The vertical bars or intersections represent the number of genes that were regulated by one or more aromatic compounds (intersecting conditions). The intersections were organized by size and top 25 sets with the highest number of genes were presented. The genes in each intersection were color-coded according to their predicted functional classification.

conditions with the highest uniquely upregulated intersections (>20 genes). However, protocatechuic acid upregulated more specific genes (30) than *p*-coumaric acid (21), despite much smaller regulon (105). On vanillic acid, which upregulated one of the largest sets of genes (120), only four genes were specifically affected. It is also worth mentioning that out of the 10 largest intersections, seven are upregulated specifically by a single aromatic compound (**Figure 2**).

In total 197 (40.9%) of all, downregulated genes were affected by a single aromatic compound (**Table 1**). Accordingly with the upregulated genes, much lower number of the genes were affected by two or more aromatic compounds. None of the genes was downregulated in response to all 10 aromatic compounds. Similarly to the upregulated regulons, vanillin downregulated the largest set of genes (297) including 71 specifically affected genes (**Figure 3**). In addition, the downregulated genes included much lower number of putative metabolic genes and large set of genes with poor or not existing annotation. Remarkably, out of 14 intersections containing two or more conditions, vanillin was involved in co-regulation of 11 intersections of genes (**Figure 3**). Coniferyl alcohol and cinnamic acid downregulated 46 and 28 unique genes, respectively, followed by another 28 genes, which were downregulated by both vanillin and cinnamic acid.

Aromatic Monomers Induce Expression of Genes Relevant for the Utilization of Lignocellulose

Gene Ontology Enrichment Analysis

To identify cellular processes that are activated and repressed in response to each aromatic compound, all functionally annotated genes were subjected to the Gene Ontology (GO) enrichment analysis. Many GO terms linked to aromatic metabolism (oxidative activities) and lignocellulose utilization (hydrolytic activities, carbohydrate binding and metabolism, and lignin-modifying activities) were over-represented among upregulated genes (**Figure 4** and **Supplementary Table 3**). Several broad GO terms related to oxidative activity were commonly enriched among genes upregulated by tested aromatic compounds. These included e.g., dioxygenase activity (GO:0051213) that was enriched on ferulic acid, vanillyl alcohol, vanillin, vanillic acid, protocatechuic acid, *p*-coumaric acid, *p*-hydroxybenzoic

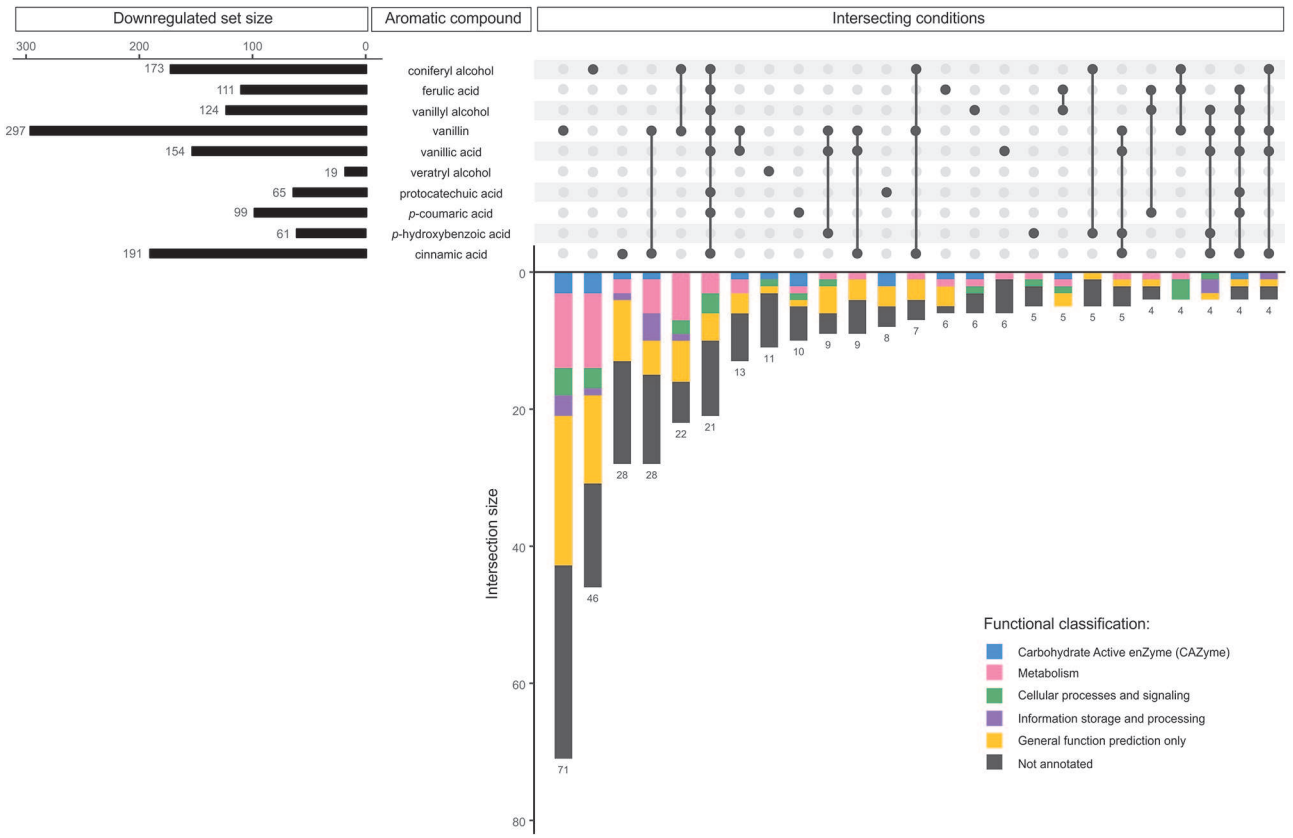

FIGURE 3 | Comparative analysis of all downregulated genes in *D. squalens* grown in the presence of aromatic compounds. The horizontal bars represent the total number of genes identified as downregulated on the individual aromatic compounds. The vertical bars or intersections represent the number of genes that were regulated by one or more aromatic compounds (intersecting conditions). The intersections were organized by size and top 25 sets with the highest number of genes were presented. The genes in each intersection were color-coded according to their functional classification.

TABLE 1 | Number of genes differentially expressed by *D. squalens* in response to one or more aromatic compounds (intersecting conditions).

No. of intersecting conditions	1	2	3	4	5	6	7	8	9	All
Upregulated genes	268 (46.9%)	127 (22.2%)	60 (10.5%)	44 (7.7%)	24 (4.2%)	18 (3.2%)	10 (1.8%)	6 (1.1%)	9 (1.6%)	5 (0.9%)
Downregulated genes	197 (40.9%)	97 (20.1%)	66 (13.7%)	39 (8.1%)	22 (4.6%)	19 (3.9%)	15 (3.1%)	23 (4.8%)	4 (0.8%)	0 (0%)

Genes that were up- or downregulated in response to unique aromatic compound were considered to be part of specific transcriptional response in D. squalens. Total of 1,053 genes were differentially expressed in response to aromatic compounds, of which 571 were upregulated and 482 downregulated.

acid and cinnamic acid, and oxidoreductase activity acting on the CH-OH group of donors, NAD or NADP as acceptor (GO:0016616) that was enriched on ferulic acid, vanillin, vanillic acid, *p*-coumaric acid, and cinnamic acid (**Figure 4**). Nonetheless, differences between aromatics were found at the higher specificity level, for example direct descendants (child terms) of GO:0016616, such as epoxide dehydrogenase activity and phenylcoumaran benzylic ether reductase activity were only enriched on vanillin and cinnamic acid, while 3-oxoacyl-[acyl-carrier-protein] reductase activity was specifically enriched on vanillic acid (**Supplementary Table 3**).

GO terms related to hydrolytic activity acting on glycosyl bonds (GO:0004553) were commonly enriched among upregulated genes, including mannosidase, fucosidase, and amylase activities on coniferyl alcohol, ferulic acid, vanillyl alcohol, vanillin and vanillic acid, and polygalacturonase activity on ferulic acid and vanillyl alcohol (**Figure 4** and **Supplementary Table 3**). GO terms associated with lignin oxidation, including laccase activity and copper ion binding, were over-represented among genes upregulated by coniferyl alcohol, veratryl alcohol, and *p*-coumaric acid. GO terms linked to other metabolic processes were less abundant, such as lipase activity uniquely enriched on veratryl alcohol and peptidase activity on coniferyl alcohol. Interestingly, two GO terms related to transcriptional regulation, i.e., regulation of nitrogen utilization and transcription repressor

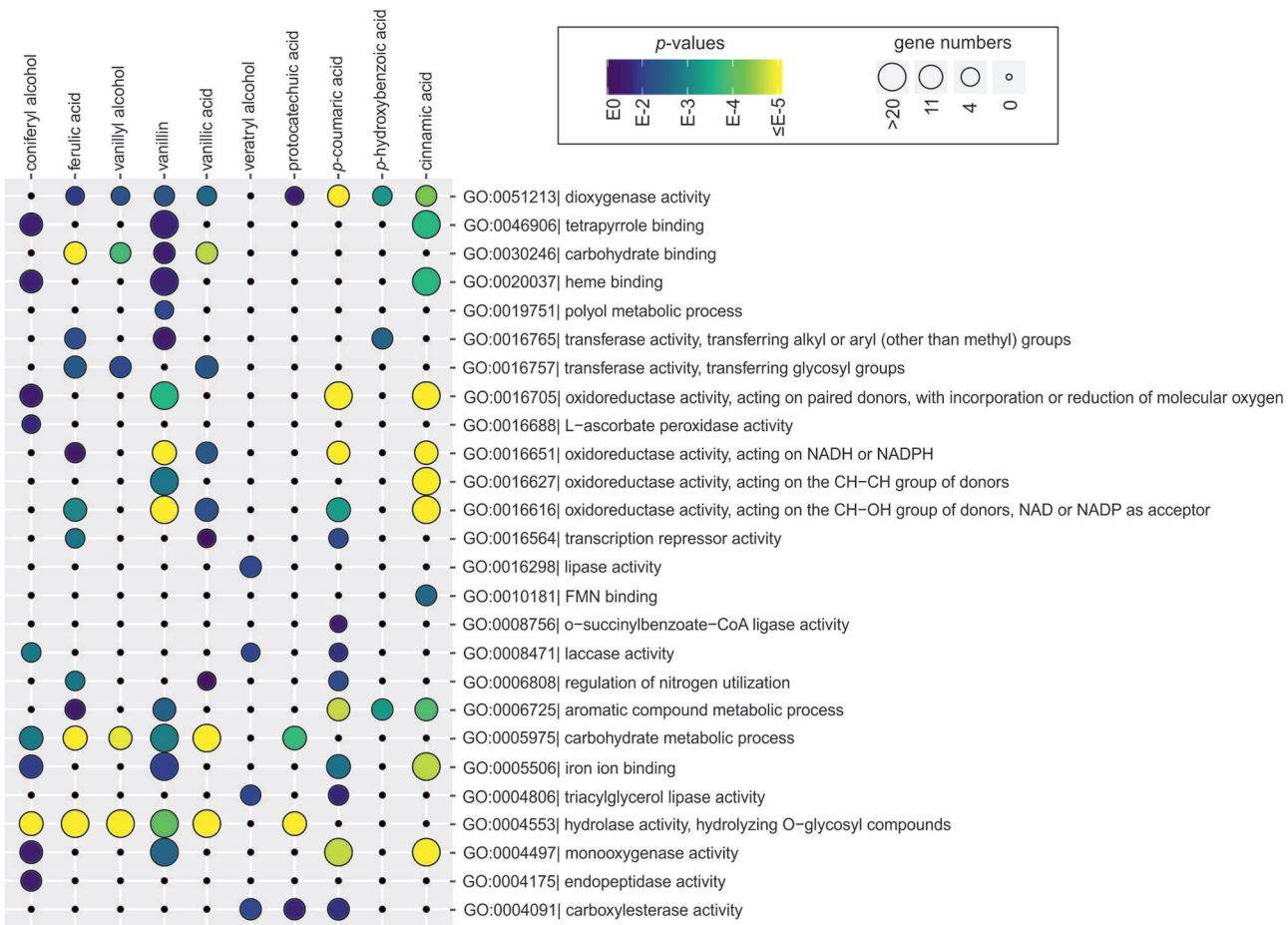

FIGURE 4 | Gene Ontology (GO) terms associated with the function of genes upregulated in the presence of aromatic compounds in *D. squalens*. The size and color of the circles represent the number of genes and statistical significance of enriched GO terms, respectively. The GO terms with redundant biological role were manually removed on the figure. The full list of enriched GO terms can be found in **Supplementary Table 3**.

activity, were enriched on ferulic acid, vanillic acid, and *p*-coumaric acid.

Among the downregulated genes, notably lower number of enriched GO terms was found. Several GO terms related to structural elements of cell wall (GO:0005199) were overrepresented among genes downregulated by coniferyl alcohol, ferulic acid, vanillyl alcohol, and vanillin (**Supplementary Table 3**). Vanillin, vanillic acid, and cinnamic acid also downregulated genes enriched in metal ion binding (iron, heme). Additionally, few GO terms related to oxidoreductase activity (e.g., GO:0016491, GO:0016705) with lower enrichment score were identified among genes downregulated in the presence of cinnamic acid, vanillic acid, vanillin, and ferulic acid.

Metabolic Genes Important for Conversion of Aromatics

To facilitate the functional analysis, all differentially expressed genes were tentatively assigned to groups using the above-mentioned KOG-based classification system (**Supplementary Table 1**; columns: assigned functional group and class). The presence of lignocellulose-related aromatic compounds, induced expression of 192 putative metabolic genes (43% of all upregulated genes) in *D. squalens*, including large set of putative cytochrome P450 (cytP450) and aldehyde dehydrogenase encoding genes that may be involved in aromatic metabolism (**Supplementary Table 1**). Additionally, several differentially expressed genes were identified as best hits in protein sequence homology search using previously characterized bacterial and fungal aromatic enzymes as query (**Table 2**, **Supplementary Table 4**). Expression-based hierarchical clustering of 147 metabolic genes that were considered relevant to lignin utilization led to the identification of eight clusters of upregulated genes (**Figure 5**, Clusters A–H). Upregulated metabolic genes associated with amino acid (29), lipid (14), and nucleotide (2) transport and metabolism (**Supplementary Table 1**) were omitted when drawing **Figure 5**, as they are less likely to be related to aromatic metabolism and lignin utilization. Cluster A contains genes with high expression levels (>70 FPKM) only in the presence of aromatic compounds,

TABLE 2 | Differentially expressed *D. squalens* genes with low to medium level of sequence homology to previously identified bacterial (Atu1415, BadA, BagX, BclA, BenD, CalA, CalB, CouL, Fcs, HapB, HbaA, PobA, XlnD, SdgC, NahG) and fungal (BphA, CprA, Phhy, PcCYP1f, CYP53A15) aromatic enzymes.

Protein ID	Best hit for (% hit coverage/ % hit identity)	Control	Coniferyl alcohol	Ferulic acid	Vanillyl alcohol	Vanillin	Vanillic acid	Veratryl alcohol	Protocatechuic acid	*p*-coumaric acid	*p*-hydroxy-benzoic acid	Cinnamic acid
416914	*p*-Hydroxyphenoxy-β-hydroxyacyl-CoA dehydrogenae Atu1415 (31.56%/40.86%), Benzoate 1,2-dioxygenase BenD (39.92%/40.28%)	38.80	35.12	49.66	49.84	32.28	26.44	59.61	35.56	38.69	22.33	77.62
974457	Benzoate-CoA ligase BadA (16.84%/30.46%), Feruloyl-CoA synthase Fcs (15.39%/43.4%), 4-Hydroxybenzoate-CoA ligase HbaA (16.36%/33.73%), Salicylyl-AMP ligase SdgA (15.2%/32.48%)	17.41	15.81	33.66	29.65	27.99	32.58	23.09	20.25	20.64	17.75	20.97
937941	3-Hydroxybenzoate 6-hydroxylase BagX (38.8%/35.43%) and XlnD (38.14%/40.12%), Salicylate hydroxylase NahG (37.25%/40.48%)	6.20	5.64	5.92	3.96	65.26	8.88	6.12	6.44	14.87	5.82	36.33
941829	Benzoate 1,2-dioxygenase BenD (54.98%/44.2%)	5.85	3.47	4.32	5.21	52.44	5.58	6.32	6.18	4.80	5.55	5.44
814004	Benzoate 4-monooxygenase BphA (78.89%/56.57%) and BzuA (82.78%/53.02%), high homology to PcCYP1f and CYP53A15	120.15	105.00	93.75	84.17	172.24	127.83	112.43	172.44	293.26	215.09	672.43
933407	Coniferyl alcohol dehydrogenase CalA (62.97%/32.41%)	6.47	18.94	10.42	3.18	21.72	26.00	3.56	4.29	8.10	32.53	33.80
944663	Coniferyl alcohol dehydrogenase CalA (15.83%/40%)	254.71	293.32	403.89	401.00	395.35	377.30	499.35	476.23	373.26	271.77	252.50
931033	Coniferyl aldehyde dehydrogenase CalB (68.48%/36.65%)	49.05	72.69	60.61	62.57	81.69	55.57	92.79	63.18	175.47	52.98	94.27
95238	Cytochrome P450 reductase CprA (76.89%/50.27%)	255.90	276.98	263.57	257.70	399.19	270.07	241.24	225.57	295.19	271.23	490.25
826556	4-Hydroxyphenylacetate esterase HapB (49.48%/40.14%)	36.04	41.89	52.28	52.36	65.83	54.86	73.38	44.51	59.65	48.04	50.72
485773	4-Hydroxyphenylacetate esterase HapB (42.6%/36.81%)	57.59	94.48	137.58	113.06	259.10	89.72	128.15	71.71	165.76	70.93	228.08
919857	Phenol hydroxylase PhhY (77.48%/50.3%)	28.90	17.98	25.56	24.53	20.76	25.18	28.04	30.73	72.59	73.58	58.87
919904	Phenol hydroxylase PhhY (75.12%/46.49%)	4.20	9.98	5.03	4.14	14.94	10.37	5.67	5.65	46.25	17.25	38.02
351556	*p*-Hydroxybenzoate-*m*-hydroxylase PobA (17.75%/45.07%)	1.92	4.08	2.33	1.64	30.34	2.66	2.80	2.95	4.98	3.75	2.53
834942	Salicylyl-CoA 5-hydroxylase SdgC (57.87%/40.59%)	100.15	104.67	110.27	107.04	139.98	112.45	110.58	157.76	140.45	113.81	248.15

(Continued)

TABLE 2 | Continued

Protein ID	Best hit for (% hit coverage/ % hit identity)	Control	Coniferyl alcohol	Ferulic acid	Vanillyl alcohol	Vanillin	Vanillic acid	Veratryl alcohol	Protocatechuic acid	*p*-coumaric acid	*p*-hydroxy-benzoic acid	Cinnamic acid
813648	Salicylyl-CoA 5-hydroxylase SdgC (26.33%/52.53%)	4.86	5.62	23.96	4.09	15.07	5.07	5.41	4.75	6.85	5.16	3.91
816083	Salicylyl-CoA 5-hydroxylase SdgC (26.03%/48.51%)	35.98	63.37	47.78	51.56	63.56	40.63	60.82	56.43	82.57	44.58	62.69
812913	Salicylyl-CoA 5-hydroxylase SdgC (36.73%/39.42%)	22.97	22.65	60.33	109.77	1071.38	473.08	47.31	58.65	50.88	36.22	57.09
923090	3-Hydroxybenzoate 6-hydroxylase XlnD (39.16%/37.85%)	8.02	11.03	17.45	10.85	175.42	11.63	9.47	11.45	36.57	12.33	29.14

For comprehensive review of characterized bacterial and fungal aromatic metabolic enzymes see Lubbers et al. (2019). Genes with fold change > 2 and adjusted p-value < 0.01 in the presence of aromatics when compared to the control conditions without aromatics were highlighted in gray.

including four genes encoding putative cytP450 oxidoreductases (Dicsqu464_1_PID_810755, Dicsqu464_1_PID_43835, Dicsqu 464_1_PID_953386, Dicsqu464_1_PID_808449) and seven genes encoding other oxidoreductases (Dicsqu464_1_PID_ 816083, Dicsqu464_1_PID_930248, Dicsqu464_1_PID_80 2628, Dicsqu464_1_PID_131091, Dicsqu464_1_PID_966 453, Dicsqu464_1_PID_934340, Dicsqu464_1_PID_812913). Interestingly, Dicsqu464_1_PID_816083 and Dicsqu464_1 _PID_812913 had low sequence homology to salicylyl-CoA 5-hydroxylase SdgC, which is involved in salicylic acid pathway in *Streptomyces* sp. (Ishiyama et al., 2004). Majority of genes in cluster A, 20 out of 29, were co-regulated by more than one aromatic compound. These include two genes (Dicsqu464_1 _PID_914361 encoding putative UDP-glucosyl transferase and Dicsqu464_1_PID_953386 encoding cytP450) that were induced by all 10 compounds and another two genes (Dicsqu464_1 _PID_131091 encoding putative zinc-binding oxidoreductase and Dicsqu464_1_PID_845669 encoding putative glutathione S-transferase) that were affected by nine aromatics. Vanillin, *p*-coumaric acid, and cinnamic acid had the strongest effect and upregulated 22, 18, and 17 genes from cluster A, respectively. Genes in clusters B, C, and E were moderately expressed in the presence of the studied aromatic compounds. Vanillin and cinnamic acid upregulated the highest number of genes: 19 and 18 in cluster B, 24 and 15 in cluster C, and 5 and 4 in cluster E, respectively. Genes in cluster D were strongly upregulated in the presence of cinnamic acid and contained six putative NADP-dependent oxidoreductases (Dicsqu464_1_PID_9 10000, Dicsqu464_1_PID_1041364, Dicsqu464_1_PID_90 7982, Dicsqu464_1_PID_932020, Dicsqu464_1_PID_93513, Dicsqu464_1_PID_914731) and two cytP450 encoding genes (Dicsqu464_1_PID_821434, Dicsqu464_1_PID_978088). Cluster F contains a single gene encoding zinc-binding oxidoreductase that was very strongly upregulated in the presence of *p*-coumaric acid (928-fold change when compared to control). Clusters G and H contain genes, which were highly expressed in the control samples. However, their expression showed significant increase with some of the aromatic compounds. Interestingly, 10 out of 19 genes in cluster G were uniquely upregulated by a single aromatic compound.

Genes Encoding Plant Cell Wall Modifying Enzymes

In total 74 (13%) of all upregulated genes encoded putative Carbohydrate-Active enZymes (CAZymes), including 53 and 13 that were related to plant polysaccharide and lignin degradation, respectively. Vanillic acid, vanillin and ferulic acid upregulated the largest sets of polysaccharide-related genes (> 22 each), while veratryl alcohol, *p*-coumaric acid and *p*-hydroxybenzoic acid induced the smallest sets (< five genes each). Majority of induced genes related to lignin-degradation responded to coniferyl alcohol (nine out of 13), while vanillyl alcohol did not induce any lignin-degradation related genes. Induced CAZyme encoding genes clustered based on their expression into seven groups (**Figure 6**). Cluster I include four putative lignin-, eight (hemi)cellulose-, and five pectin-related CAZyme encoding genes. One laccase encoding gene (Dicsqu464_1_PID_928381) was induced 3.5-fold by coniferyl alcohol, 2.8-fold by veratryl

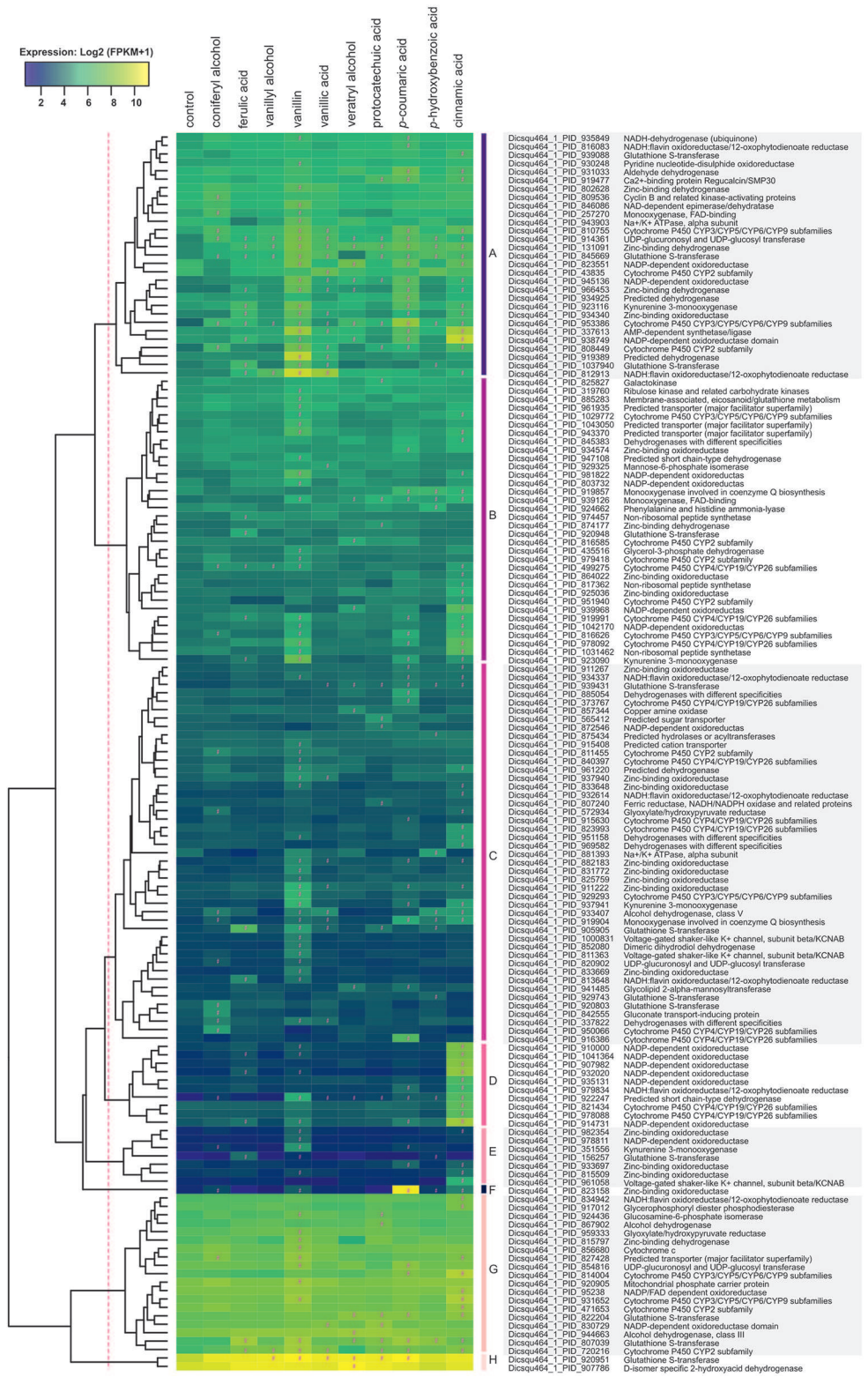

FIGURE 5 | Hierarchical clustering of metabolic genes that were upregulated in the presence of aromatic compounds in *D. squalens*. The color code represents average and $\log_2$ expression values (FPKM+1) from biological triplicate cultures. Significantly upregulated genes are marked with a hashtag sign (#). The protein ID and (putative) function are shown on the right. Genes that belong to "Amino acid transport and metabolism" (29), "Lipid transport and metabolism" (14), and "Nucleotide transport and metabolism" (2) classes were omitted.

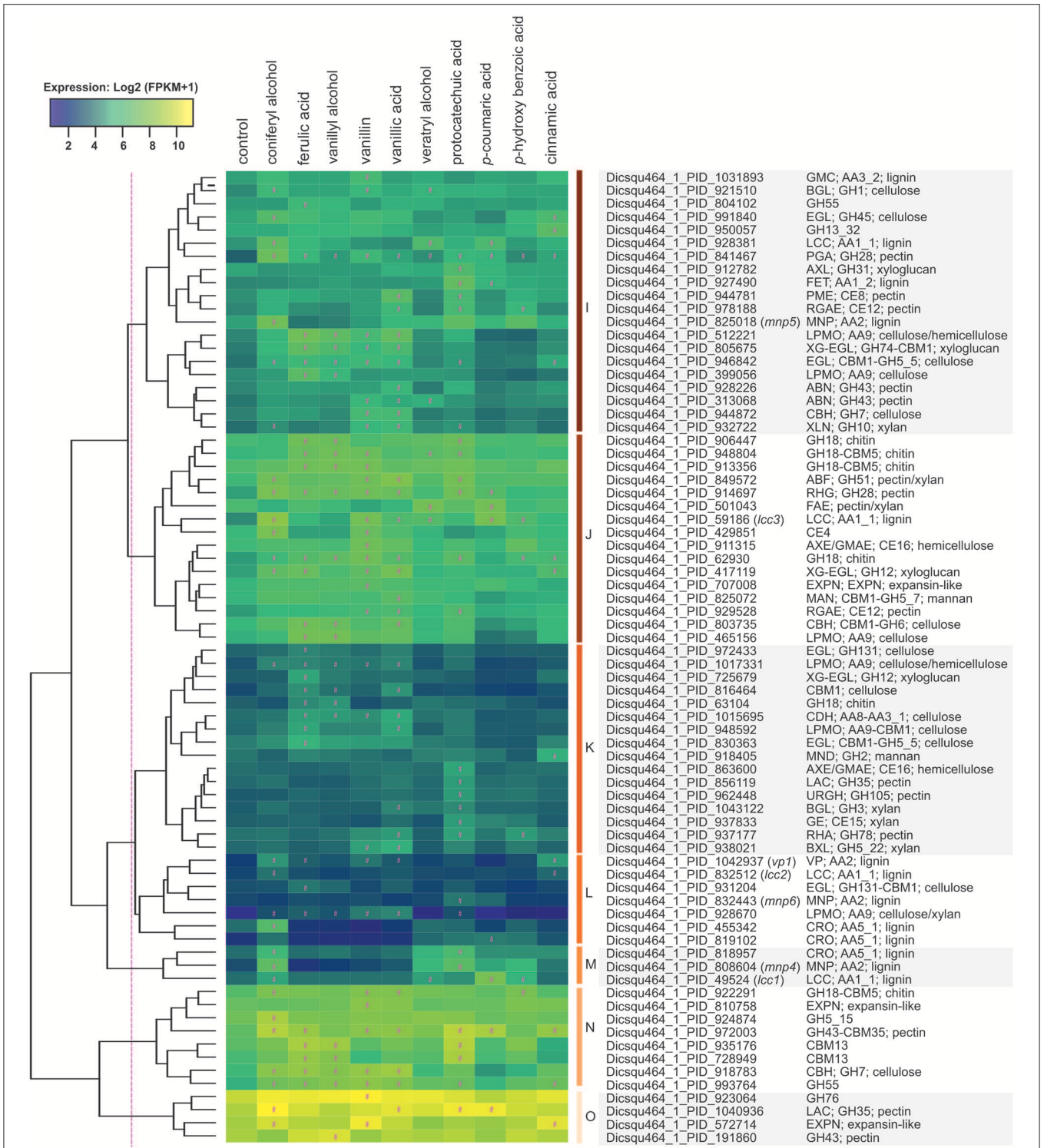

FIGURE 6 | Hierarchical clustering of CAZy genes that were upregulated in the presence of aromatic compounds in *D. squalens*. The color code represents average and $\log_2$ expression values (FPKM+1) from biological triplicate cultures. Significantly upregulated genes are marked with a hashtag sign (#). The protein ID and (putative) function are shown on the right.

alcohol, and 2.5-fold by *p*-coumaric acid, while one manganese peroxidase (MnP) encoding gene (Dicsqu464_1_PID_825018) was 4.2-fold upregulated only in the presence of the monolignol coniferyl alcohol. Cluster K includes lower expressed genes and

genes putatively encoding enzymes involved in (hemi)cellulose and pectin degradation, whereas majority of genes in clusters L and M are predicted to be involved in lignin-degradation (eight out of ten). Coniferyl alcohol induced the highest number of genes (seven out of ten) in clusters L and M when compared to other aromatic compounds. Despite low expression in control conditions, cluster L contains interesting expression patterns including one versatile peroxidase (VP) encoding gene (Dicsqu464_1_PID_1042937), which was 6.7-fold up-regulated by coniferyl alcohol, 7.6-fold by cinnamic acid, and 4.0-fold by vanillin. Cluster M contains one *mnp* gene (Dicsqu464_1_PID_808604) strongly up-regulated (>14-fold increase) by coniferyl alcohol and protocatechuic acid, and one laccase gene (Dicsqu464_1_PID_49524) strongly upregulated (12.4-fold increase) by *p*-coumaric acid among others.

Clusters J and N included genes that were highly expressed (>70 FPKM) only in the presence of aromatic compounds. Vanillin induced the highest number of genes (11) in cluster J, followed by ferulic and vanillic acid (8 genes both). One laccase encoding gene (Dicsqu464_1_PID_59186) was strongly upregulated in the presence of coniferyl alcohol showing 10.5-fold increase, while vanillin caused 6.3-fold and *p*-coumaric acid 6.9-fold induction, and 3.3-, 3.5-, and 3.3-fold increase was caused by vanillic acid, veratryl alcohol, and *p*-hydroxybenzoic acid, respectively. The genes encoding putative pectin-acting enzymes in cluster J were generally upregulated in the presence of vanillin, vanillic acid and protocatechuic acid, with exception of a feruloyl esterase encoding gene (Dicsqu464_1_PID_501043) that was induced only by veratryl alcohol and *p*-coumaric acid. Cluster O contain genes with the highest expression among all CAZymes. These genes encoded mainly putative glycoside hydrolase (GH) enzymes related to pectin degradation.

Other Differentially Expressed Genes

Beside metabolic enzymes and CAZymes encoding genes, aromatic compounds induced expression of several other genes that could be relevant for lignocellulose degradation in *D. squalens*. Upregulated genes included 17 putative transporters (three ABC and 14 Major Facilitator Superfamily transporters), 14 genes involved in defense mechanisms/metabolism (mainly NAD-dependent epimerase/dehydratases), and four putative hydrophobin encoding genes tentatively assigned to "cellular processes and signaling" group (**Supplementary Table 1**). Additionally, hierarchical clustering analysis of genes with only partial annotation or not included in the traditional KOG classification (here tentatively assigned to a group with "general function prediction only"), showed interesting expression patterns (**Supplementary Figure 2**). Genes from cluster P and R were especially highly expressed in the presence of aromatic compounds, and at least 20 had putative metabolic function related to oxidoreductase activity and therefore could be related to aromatic metabolism. Interestingly, one putative intradiol ring-cleaving dioxygenase encoding gene, Dicsqu464_1_PID_972012, clustered together with the highest expressed genes in this group and was additionally upregulated on vanillin, *p*-coumaric acid, *p*-hydroxybenzoic acid, and cinnamic acid (**Supplementary Figure 2**, Cluster R). There are two types of aromatic ring-cleaving enzymes, intradiol dioxygenases, which cleave aromatic ring between the OH groups and extradiol dioxygenases, which cut next to the OH group (Lubbers et al., 2019). Besides Dicsqu464_1_PID_972012, *D. squalens* expressed second putative intradiol dioxygenase, Dicsqu464_1_PID_819116, and one putative extradiol dioxygenase, Dicsqu464_1_PID_963638. While both genes were not highly expressed, their expression was upregulated by nearly all tested aromatic compounds (nine out of ten, **Supplementary Table 1**). Another important group of genes included three upregulated putative transcription factor encoding genes ("information storage and processing"), while additional three putative transcription factor candidates were found in the group of genes with general function prediction only (**Supplementary Figure 2**). Moreover, large part of the transcriptome upregulated in *D. squalens* in the presence of aromatic compounds was very poorly annotated, including many gene models without any annotation available (**Figures 2**, **3** and **Supplementary Table 1**). Expression of these genes was analyzed using hierarchical clustering and several highly expressed clusters strongly affected by the aromatic compounds were identified (**Supplementary Figure 3**).

DISCUSSION

Aromatic components present in lignocellulose, especially in the aromatic lignin polymer hold a great potential for production of renewable high-value products, e.g., multifunctional aromatic compounds that could be used as alternative to fossil fuel-derived chemicals or their precursors (Li et al., 2015; Feghali et al., 2018). While many microbes can degrade lignocellulose, white-rot basidiomycete fungi are the only organisms in nature that break down all the polymeric components of lignocellulose, including recalcitrant lignin (Rytioja et al., 2014; Manavalan et al., 2015; Sista Kameshwar and Qin, 2018). Moreover, these fungi have developed a complex metabolic system for conversion of lignocellulose-related aromatic compounds (Mäkelä et al., 2015), which makes them interesting candidates to study especially with relation to lignin valorization.

In this study, we used genome-wide transcriptomic analysis to provide the first systematic insight into conversion of various lignocellulose-related aromatic compounds by the well-studied white-rot fungus *D. squalens* (Dong et al., 2014; Rytioja et al., 2015, 2017; Casado López et al., 2017; Daly et al., 2018). While previous works have applied high-throughput RNA sequencing (RNA-seq) to identify upregulated transcripts from *D. squalens* cultivated on various lignocellulosic substrates (Rytioja et al., 2017; Daly et al., 2018) and lignocellulose-derived monomeric sugars (Casado López et al., 2018), providing novel insights into plant biomass degrading machinery and transcriptional response in this fungus, its molecular response to lignocellulose-derived aromatic compounds has not been studied so far. However, the potential of *D. squalens* for diverse aromatic conversions has been indicated (Daly et al., 2018; Marinović et al., 2018), but more detailed studies are needed to advance our

understanding of these processes before assessing their potential in biotechnological applications.

We selected 10 aromatic compounds, which were used as inducing compounds in the *D. squalens* cultures, possibly originating from fungal lignin degradation process (cinnamic acid, coniferyl alcohol) and/or aromatic metabolism (ferulic acid, vanillin, vanillyl alcohol, vanillic acid, veratryl alcohol, protocatechuic acid, *p*-coumaric acid, *p*-hydroxybenzoic acid) (Bugg et al., 2011; Mäkelä et al., 2015). Although, cinnamic acid is an amino acid derived precursor for synthesis of monolignols (Maeda and Dudareva, 2012), it has previously been identified as one of the products of technical Kraft lignin degradation by the bacteria *Bacillus* sp. and *Cupriavidus basilensis* B-8 (Raj et al., 2007; Shi et al., 2013). Some of the tested aromatics, i.e., coniferyl alcohol, ferulic acid and *p*-coumaric acid, also represent naturally occurring *p*-hydroxyphenyl and guaiacyl units of lignin.

Generally, low molecular weight phenolic compounds are toxic to fungi at relatively low concentrations, but differences between compounds and fungal species have been reported (Buswell and Eriksson, 1994; Guiraud et al., 1995; Neves et al., 2005). None of the 10 aromatics tested in this study inhibited growth of *D. squalens* at 0.2 mM concentration. However, higher concentrations (0.5 and 1 mM) of cinnamic acid and vanillin had clearly higher inhibitory effect than the other tested compounds (**Figure 1**). This is in agreement with a previous study, which showed that 1 mM vanillin inhibited growth by 5–39% in eight white-rot fungi, while 1 mM cinnamic acid abolished growth of six out of the eight species (Buswell and Eriksson, 1994). In the yeast *Saccharomyces cerevisiae*, degree of toxicity was shown to be related to the functional groups on the aromatic compounds, with aldehydes being the most toxic (Ando et al., 1986; Klinke et al., 2003). However, other studies have indicated that additional functional groups also affect the overall toxicity (Adeboye et al., 2014). In *D. squalens*, the particularly strong effect of vanillin (phenolic aldehyde) and cinnamic acid (containing alkene and carboxylic acid groups) when compared to the other aromatic compounds (phenolic acids and alcohols) could be explained by their chemical character and/or presence of functional groups. Nevertheless, higher concentration (1 mM) of all aromatic compounds, except for *p*-hydroxybenzoic acid, inhibited the radial growth of *D. squalens* when compared to lower concentrations of aromatics (**Figure 1**). Although the amount of these aromatic compounds under natural wood degrading conditions are not known, this suggests that *D. squalens* has not been adapted to encounter very high concentrations of the aromatic monomers in its biotope. The fungus together with other microbes present in the natural community may efficiently convert these compounds already at lower concentrations, thus preventing accumulation of toxic levels of aromatics. Interestingly, brown discoloration of the media was observed in the presence of coniferyl alcohol, ferulic acid, vanillyl alcohol, vanillin, vanillic acid, and protocatechuic acid, suggesting a possible production of an unknown dark-colored metabolite in those cultures (**Figure 1**). We hypothesize that this phenomenon could be related to the formation of quinones (e.g., methoxyhydroquinone, hydroxyquinol, benzoquinone). Polymerized quinones, which are produced from aromatic compounds naturally present in some fruits have been linked to brown discoloration known as fruit browning (Schieber, 2018). Conversion of vanillic acid, and thus also vanillin, vanillyl alcohol, ferulic acid, and coniferyl alcohol, to methoxyhydroquinone by decarboxylating vanillate hydroxylase and further to hydroxyquinol has been reported in several white-rot fungi, including *Phanerochaete chrysosporium* (Yajima et al., 1979) and its anamorph *Sporotrichum pulverulentum* (Buswell et al., 1981), suggesting it is a common pathway among wood-degrading basidiomycetes. However, conversion of protocatechuic acid to hydroxyquinone have been so far only reported in the yeast *Candida parapsilosis* (Eppink et al., 1997; Holesova et al., 2011).

The molecular responses of *D. squalens* to lignin-related aromatic compounds were analyzed at transcriptome level after induction with 0.5 mM concentration of the selected aromatics. While previous reports investigated the inducing effect of various aromatic compounds on expression of several laccase-encoding genes (Terrón et al., 2004; Piscitelli et al., 2011; Yang et al., 2013, 2016; Moiseenko et al., 2018) in basidiomycete fungi, this is, to the best of our knowledge, the first study that addresses the genome-wide transcriptional response to aromatics and therefore provides a new level of width and depth. The Pearson correlation matrix of all expressed genes (8,733 genes with FPKM >10 in at least one condition) demonstrated high correlation between the biological triplicates, but also between several different aromatics (**Supplementary Figure 1**), suggesting that the genome-wide response toward different aromatic compounds in *D. squalens* is relatively similar. This may be due to the chemical character of the tested compounds that are all small molecular weight phenylpropane derivatives. However, the two-dimensional PCA highlighted differences between the cultivations induced with the aromatics and the control without aromatics (**Supplementary Figure 1**). Identification of differentially expressed genes showed that the main differences in mRNA levels were restricted to subsets of genes, and ∼6.5 and 5.5% of all expressed genes were identified as up- and downregulated, respectively (**Table 1**). Moreover, comparative analyses demonstrated that nearly half of these genes were specifically triggered in response to a single aromatic compound (46.9 and 40.9% of up- and downregulated genes, respectively; **Table 1**) in *D. squalens*. Expression of much lower number of genes was affected by two or more aromatics, and expression of $<1\%$ of genes was affected by all the 10 tested compounds. This was further visualized by plotting the top 25 intersections with the highest number of differentially expressed genes and analysing their respective regulating conditions (**Figures 2**, **3**). Respectively, seven and five out of 10 of the biggest intersections were up- and downregulated by a single aromatic compound, indicating very specific transcriptional response of *D. squalens* to lignocellulose-related aromatics. Although, single aromatic compounds affected the highest intersections of both up- and downregulated genes, the specificity seems to be stronger among upregulated genes.

Specifically regulated genes in *D. squalens* were tentatively assigned to six main KOG-related groups based on their functional annotation (**Figures 2**, **3**), which highlighted

functional distribution among intersecting conditions. Unfortunately, it also pointed out that KOG categorization is rather outdated in this species and the information between KOG and other available databases has not been integrated. While *D. squalens* is certainly not the poorest annotated basidiomycete fungal genome (Casado López et al., 2019), comparison of the available annotations (KOG, InterPro, KEGG, CAZy) revealed large amount of gaps and a need for careful manual curation and functional data integration, which, however, was out of the scope of this study. It should be noted that various functional categorisations may generate minor mistakes, especially when based on partial gene annotation. We focused our analyses on upregulated genes, as these could be directly involved in aromatic metabolism and thus have potential from the biotechnological point of view. Among annotated genes, a large subset was functionally assigned to metabolism (**Figure 2**) and many enriched GO terms related to oxidative and hydrolytic activities were detected (**Figure 4** and **Supplementary Table 3**), indicating that at least part of the regulon induced in the presence of aromatic compounds in *D. squalens* is involved in aromatic metabolism and lignocellulose utilization. Additionally, genes upregulated in the presence of aromatics were enriched in GO terms related to lipase and endopeptidase activity (**Figure 4**). Upregulation of genes linked to lipid and amino acid metabolism (**Supplementary Table 1**) could indicate that the fungus is dealing with an increased lipid and protein turnover e.g., due to aromatics-inflicted injuries on cellular membranes (Fitzgerald et al., 2004; Gu et al., 2015; Wu et al., 2016; Wang et al., 2017).

Fungal aromatic metabolism is not well-understood yet. However, a schema of aromatic metabolism, based on combined information from many bacterial and fungal species, have been proposed including various known conversions of aromatic compounds (Mäkelä et al., 2015; Lubbers et al., 2019). While many enzymes involved in aromatic metabolism have been characterized in bacteria, only a few of these are known in fungi. A large sequence homology search in *D. squalens* CBS464.89 genome sequence using known bacterial and fungal aromatic enzymes as query identified 145 putative proteins. However, due to low or medium homology, these should not be directly treated as orthologs. Additionally, some *D. squalens* genes had sequence homology to several characterized proteins. Nonetheless, 33 of the corresponding genes were upregulated in the presence of tested aromatic compounds (**Table 2**), making those interesting candidates for further studies. Dicsqu464_1_PID_814004 was identified with high homology to ascomycete fungal cytP450 monooxygenases (PcCYT1f in *Penicillium chrysogenum* and CYP53A15 in *Cochliobolus lunatus*) and benzoate 4-monooxygenases (BphA in *Aspergillus niger* and BzuA in *Aspergillus nidulands*) involved in benzoic acid pathway e.g., hydroxylation of benzoic acid to *p*-hydroxybenzoic acid (van Gorcom et al., 1990; Fraser et al., 2002; Matsuzaki and Wariishi, 2005; Lah et al., 2011). Interestingly, Dicsqu464_1_PID_814004 was upregulated by 6.1-, 2.5-, and 1.9-fold in the presence of cinnamic acid, *p*-coumaric acid, and *p*-hydroxybenzoic acid, respectively (**Table 2**). According to the aromatic metabolism schema, cinnamic acid can converted to benzoic acid in three steps while *p*-coumaric acid cam be converted to *p*-hydroxybenzoic acid in four steps, which suggest that upregulation of Dicsqu464_1_PID_814004 could indeed be related to benzoic acid metabolism in *D. squalens*. Another cytP450 encoding gene, Dicsqu464_1_PID_95238, which was identified by sequence homology to CprA involved in benzoic acid pathway in *A. niger*, was 2.1-fold upregulated on cinnamic acid. Two genes, Dicsqu464_1_PID_919857 and Dicsqu464_1_PID_919904, with homology to phenol hydroxylase Phhy that catalyzes conversion of phenol to catechol in yeast *Trichosporon cutaneum*, were upregulated on *p*-coumaric acid, *p*-hydroxybenzoic acid and cinnamic acid suggesting a possible link to (*p*-hydroxy) benzoic pathways. Production of phenol by decarboxylation of *p*-hydroxybenzoic acid have been observed in bacteria but not yet in fungi or yeast (Lubbers et al., 2019). While the sequence homology was certainly higher when comparing *D. squalens* with enzymes characterized in ascomycete fungi, such as Aspergilli, it should be remembered that basidiomycete and ascomycete fungi differ in their abilities to degrade lignin and thus could have very different aromatic metabolism. For example, the white-rot fungus *Lentinula edodes* has been described to hydroxylate ferulic acid to 2-hydroxyferulic acid and then to 2,3,4-trihydroxycinnamic acid (Crestini and Sermanni, 1994). This is one example of many basidiomycete-specific metabolic pathways that have not been observed in ascomycetes.

Out of all differentially expressed genes, vanillin and cinnamic acid upregulated the highest number of genes as well as the highest specifically affected intersections (**Figure 2**), including the largest subset of metabolic genes enriched in several GO terms related to oxidoreductase activity acting on the CH-CH and CH-OH group of donors with NAD or NADP as an acceptor (**Figure 4**). These genes, annotated as e.g., putative NADP-dependent oxidoreductases or short-chain dehydrogenase/reductases (SDRs), catalyze electron transfer and are involved in extremely vast range of reactions (Sellés Vidal et al., 2018). Accordingly, GO analysis showed that the genes upregulated by both vanillin and cinnamic acid have diverse activities, such as epoxide dehydrogenase and mevaldate reductase, and thus could be involved in several processes (**Supplementary Table 3**). Other highly enriched GO terms, oxidoreductase activity acting on paired donors with incorporation or reduction of molecular oxygen and monooxidase activities, included genes annotated as e.g., FAD-binding monooxygenases and cytP450 monooxygenases. CytP450 monooxygenases together with gluthatione S-transferases (GSTs) are especially interesting since their encoding genes are very abundant in the genomes of the white-rot fungi and these enzymes are considered to be involved in conversion of toxic aromatic compounds released from wood degradation (Morel et al., 2013; An et al., 2019) and thus have potential for biotechnological applications (Girvan and Munro, 2016). Interestingly, 22 cytP450 and 17 GST encoding genes were induced in the presence of tested aromatic compounds (**Figure 5**, **Supplementary Table 1** and **Supplementary Figure 2**). Vanillin upregulated the highest number of GSTs (11) on average by 6-fold change, while cinnamic acid upregulated the highest

number of cytP450s (15) on average by 5.8-fold. Three of the induced cytP450 encoding genes (Dicsqu464_1_PID_810755, Dicsqu464_1_PID_808449 and Dicsqu464_1_PID_471653) were previously shown to be upregulated in *D. squalens* when grown on birch and spruce wood (Daly et al., 2018) Additionally, vanillin and cinnamic acid were shown to have the most inhibitory effect on *D. squalens* colony growth diameter (**Figure 1**), thus suggesting that upregulated genes could catalyze conversion of these specific compounds into less toxic ones.

White-rot fungi secrete an array of CAZymes to break large lignocellulose polymers to smaller units that can be taken into the fungal cells, where they are metabolized as sources of carbon and energy or, in the case of aromatics, converted to less toxic compounds. Several CAZyme encoding genes involved in extracellular plant biomass degradation were upregulated in *D. squalens* in response to aromatic compounds (**Figures 2**, **6**). Vanillic acid, vanillin, and ferulic acid upregulated the largest sets of polysaccharide-related genes, including those encoding cellulose and hemicellulose-active enzymes, while veratryl alcohol, *p*-coumaric acid, and *p*-hydroxybenzoic acid induced the smallest sets. Interestingly, ferulic acid induced 22 genes involved in polysaccharide degradation. However, none of these genes encode putative enzymes that cleave the bonds between hemicellulose and lignin. Nonetheless, upregulation of hydrolytic activities by ferulic acid could be linked to the presence of this compound in plant cell wall polysaccharides. All aromatic compounds induced expression of some pectinolytic genes (**Figure 6**). Pectin, which is present in high concentrations in the bordered pits in plant cell walls, has been suggested to be degraded first in order of the fungus to be able to enter in the plant cell. Previous transcriptome analysis from *D. squalens* mono- and disaccharide cultures demonstrated that cellobiose and L-rhamnose trigger expression of enzymes involved in polysaccharide degradation in *D. squalens* (Casado López et al., 2018), while induction of ligninolytic genes in *D. squalens* has been shown to be specifically triggered in the presence of lignin-rich substrates (Rytioja et al., 2017). However, our study indicated that lignin-degrading enzymatic machinery of *D. squalens* was only partially induced in the presence of the monomeric aromatic compounds. In total 13 lignin-degradation related enzymes encoding genes were upregulated in *D. squalens* exposed to aromatic monomers, majority of which (nine) were induced by coniferyl alcohol alone (two out of nine) or in combination with other aromatics (seven out of nine). Partial induction of laccase encoding genes by aromatic compounds was also shown in other white-rot fungus, *Trametes hirsuta* (Moiseenko et al., 2018). This suggests that lignin-degrading enzymes in the white-rot fungi may not be similarly induced as the polysaccharide degrading ones, i.e., by the monomeric building blocks of the lignin polymer. However, differences between species are also expected. For example, two laccase encoding genes, *lcc3* and *lcc1*, were highly expressed (>70 FPKM) in *D. squalens* grown with *p*-coumaric acid when compared to the control conditions, while in *T. hirsuta* the expression of homologous genes was strongly repressed by *p*-coumaric acid (Moiseenko et al., 2018).

In summary, *D. squalens* showed a prominent ability for conversion of aromatic compounds as indicated by the number of upregulated genes under the studied conditions, indicating a potential of this fungus for bio-based valorization of lignocellulosic biomass. We showed that regulons induced in the presence of aromatic compounds differ with respect to both the number and function of the genes. For example, cinnamic acid, vanillin, and *p*-coumaric acid upregulated the most diverse array of GO terms associated with oxidoreductase activities, while coniferyl alcohol, ferulic acid, and vanillyl alcohol upregulated the highest number of GO terms associated with lignocellulolytic activities. Additionally, we showed that transcriptional response of *D. squalens* to aromatics is largely compound-specific and indicated the set of highly induced oxidative enzymes that are potentially involved in aromatic metabolism.

DATA AVAILABILITY STATEMENT

The datasets generated for this study can be found in the NCBI with individual sample Accession Numbers from PRJNA500193 to PRJNA500234.

AUTHOR CONTRIBUTIONS

JK performed the experiments, analyzed the data, and wrote the paper. MPe contributed to the bioinformatics analysis and data visualization. MPa, AL, VN, VS, MW, and IG performed the RNA sequencing and analysis. MM conceived the study and revised the paper.

FUNDING

JK was supported by the Academy of Finland research Grant No. 308284. The work conducted by the U.S. Department of Energy Joint Genome Institute, a DOE Office of Science User Facility, was supported by the Office of Science of the U.S. Department of Energy under Contract No. DE-AC02-05CH11231.

ACKNOWLEDGMENTS

The authors would like to thank Dr. Paul Daly for his assistance during the GO ontology analysis.

SUPPLEMENTARY MATERIAL

The Supplementary Material for this article can be found online at: https://www.frontiersin.org/articles/10.3389/fbioe.2019.00229/full#supplementary-material

REFERENCES

Adeboye, P. T., Bettiga, M., and Olsson, L. (2014). The chemical nature of phenolic compounds determines their toxicity and induces distinct physiological responses in *Saccharomyces cerevisiae* in lignocellulose hydrolysates. *AMB Express* 4:46. doi: 10.1186/s13568-014-0046-7

An, Q., Wu, X.-J., and Dai, Y.-C. (2019). Comparative genomics of 40 edible and medicinal mushrooms provide an insight into the evolution of lignocellulose decomposition mechanisms. *3 Biotech* 9:157. doi: 10.1007/s13205-019-1689-5

Ando, S., Arai, I., Kiyoto, K., and Hanai, S. (1986). Identification of aromatic monomers in steam-exploded poplar and their influences on ethanol fermentation by *Saccharomyces cerevisiae*. *J. Ferment. Technol.* 64, 567–570. doi: 10.1016/0385-6380(86)90084-1

Andrews, S. R., and Gill, L. S. (1943). Western red rot in immature ponderosa pine in the southwest. *J. Forest.* 41, 565–573.

Blanchette, R., Otjen, L., and Carlson, M. (1987). Lignin distribution in cell walls of birch wood decayed by white rot basidiomycetes. *Phytopathology* 77, 684–690. doi: 10.1094/Phyto-77-684

Brzonova, I., Asina, F., Andrianova, A. A., Kubátová, A., Smoliakova, I. P., Kozliak, E. I., et al. (2017). Fungal biotransformation of insoluble kraft lignin into a water soluble polymer. *J. Biosci. Bioeng.* 56, 6103–6113. doi: 10.1021/acs.iecr.6b04822

Bugg, T. D. H., Ahmad, M., Hardiman, E. M., and Rahmanpour, R. (2011). Pathways for degradation of lignin in bacteria and fungi. *Nat. Prod. Rep.* 28, 1883–1896. doi: 10.1039/c1np00042j

Buswell, J. A., Eriksson, K.-E., and Pettersson, B. (1981). Purification and partial characterization of vanillate hydroxylase (decarboxylating) from *Sporotrichum pulverulentum*. *J. Chromatogr. A* 215, 99–108. doi: 10.1016/S0021-9673(00)81390-4

Buswell, J. A., and Eriksson, K.-E. L. (1994). Effect of lignin-related phenols and their methylated derivatives on the growth of eight white-rot fungi. *World J. Microbiol. Biotechnol.* 10, 169–174. doi: 10.1007/BF00360880

Calvo-Flores, F. G., and Dobado, J. A. (2010). Lignin as renewable raw material. *ChemSusChem* 3, 1227–1235. doi: 10.1002/cssc.201000157

Casado López, S., Peng, M., Daly, P., Andreopoulos, B., Pangilinan, J., Lipzen, A., et al. (2019). Draft genome sequences of three monokaryotic isolates of the white-rot basidiomycete fungus *Dichomitus squalens*. *Microbiol. Res. Announc.* 8, e00264–e00219. doi: 10.1128/MRA.00264-19

Casado López, S., Peng, M., Issak, T., Daly, P., de Vries, R. P., and Mäkelä, M. R. (2018). Induction of plant cell wall degrading CAZyme encoding genes by lignocellulose-derived monosaccharides and cellobiose in the white-rot fungus *Dichomitus squalens*. *Appl. Environ. Microbiol.* 84, e00403–e00418. doi: 10.1128/AEM.00403-18

Casado López, S., Theelen, B., Manserra, S., Issak, T. Y., Rytioja, J., Mäkelä, M. R., et al. (2017). Functional diversity in *Dichomitus squalens* monokaryons. *IMA Fungus* 8, 17–25. doi: 10.5598/imafungus.2017.08.01.02

Chen, C.-L., Chang, H.-M., and Kirk, T. K. (1982). Aromatic acids produces during degradation of lignin in spruce wood by *Phanerochaete chrysosporium*. *Holzforschung* 36, 3–9. doi: 10.1515/hfsg.1982.36.1.3

Crestini, C., and Sermanni, G. G. (1994). Oxidation and aromatic ring cleavage of 4-methoxy and 3,4-dimethoxycennamic acid by *Lentinus edodes*. *Biotechnol. Lett.* 16, 995–1000. doi: 10.1007/BF00128640

Daly, P., Casado López, S., Peng, M., Lancefield, C. S., Purvine, S. O., Kim, Y., et al. (2018). *Dichomitus squalens* partially tailors its molecular responses to the composition of solid wood. *Environ. Microbiol.* 20, 4141–4156. doi: 10.1111/1462-2920.14416

Den, W., Sharma, V. K., Lee, M., Nadadur, G., and Varma, R. S. (2018). Lignocellulosic biomass transformations via greener oxidative pretreatment processes: access to energy and value-added chemicals. *Front. Chem.* 6:141. doi: 10.3389/fchem.2018.00141

Dong, Y.-C., Dai, Y.-N., Xu, T.-Y., Cai, J., and Chen, Q.-H. (2014). Biodegradation of chestnut shell and lignin-modifying enzymes production by the white-rot fungi *Dichomitus squalens, Phlebia radiata*. *Bioprocess Biosyst. Eng.* 37, 755–764. doi: 10.1007/s00449-013-1045-9

Eppink, M. H., Boeren, S. A., Vervoort, J., and van Berkel, W. J. (1997). Purification and properties of 4-hydroxybenzoate 1-hydroxylase (decarboxylating), a novel flavin adenine dinucleotide-dependent monooxygenase from *Candida parapsilosis* CBS604. *J. Bacteriol.* 179, 6680–6687. doi: 10.1128/jb.179.21.6680-6687.1997

Feghali, E., Torr, K. M., van de Pas, D. J., Ortiz, P., Vanbroekhoven, K., Eevers, W., et al. (2018). Thermosetting polymers from lignin model compounds and depolymerized lignins. *Topics Curr. Chem.* 376:32. doi: 10.1007/s41061-018-0211-6

Fitzgerald, D. J., Stratford, M., Gasson, M. J., Ueckert, J., Bos, A., and Narbad, A. (2004). Mode of antimicrobial action of vanillin against *Escherichia coli*, *Lactobacillus plantarum* and *Listeria innocua*. *J. Appl. Microbiol.* 97, 104–113. doi: 10.1111/j.1365-2672.2004.02275.x

Fraser, J. A., Davis, M. A., and Hynes, M. J. (2002). The genes *gmdA*, encoding an amidase, and *bzuA*, encoding a cytochrome P450, are required for benzamide utilization in *Aspergillus nidulans*. *Fungal Genet. Biol.* 35, 135–146. doi: 10.1006/fgbi.2001.1307

Girvan, H. M., and Munro, A. W. (2016). Applications of microbial cytochrome P450 enzymes in biotechnology and synthetic biology. *Curr. Opin. Chem. Biol.* 31, 136–145. doi: 10.1016/j.cbpa.2016.02.018

Gu, H., Zhang, J., and Bao, J. (2015). High tolerance and physiological mechanism of *Zymomonas mobilis* to phenolic inhibitors in ethanol fermentation of corncob residue. *Biotechnol. Bioeng.* 112, 1770–1782. doi: 10.1002/bit.25603

Guiraud, P., Steiman, R., Seiglemurandi, F., and Benoitguyod, J. L. (1995). Comparison of the toxicity of various lignin-related phenolic compounds toward selected fungi perfecti and fungi imperfecti. *Ecotoxicol. Environ. Saf.* 32, 29–33. doi: 10.1006/eesa.1995.1081

Harper, D. B., Buswell, J. A., Kennedy, J. T., and Hamilton, J. T. (1990). Chloromethane, methyl donor in veratryl alcohol biosynthesis in *Phanerochaete chrysosporium* and other lignin-degrading fungi. *Appl. Environ. Microbiol.* 56, 3450–3457.

Hatakka, A., and Hammel, K. E. (2011). "Fungal Biodegradation of Lignocelluloses," in *Industrial Applications,* ed M. Hofrichter (Berlin; Heidelberg: Springer), 319–340. doi: 10.1007/978-3-642-11458-8_15

Hatakka, A. I., and Uusi-Rauva, A. K. (1983). Degradation of 14C-labelled poplar wood lignin by selected white-rot fungi. *Eur. J. Appl. Microbiol. Biotechnol.* 17, 235–242. doi: 10.1007/BF00510422

Holesova, Z., Jakubkova, M., Zavadiakova, I., Zeman, I., Tomaska, L., and Nosek, J. (2011). Gentisate and 3-oxoadipate pathways in the yeast *Candida parapsilosis*: identification and functional analysis of the genes coding for 3-hydroxybenzoate 6-hydroxylase and 4-hydroxybenzoate 1-hydroxylase. *Microbiology* 157, 2152–2163. doi: 10.1099/mic.0.048215-0

Humphreys, J. M., and Chapple, C. (2002). Rewriting the lignin roadmap. *Curr. Opin. Plant Biol.* 5, 224–229. doi: 10.1016/S1369-5266(02)00257-1

Ishiyama, D., Vujaklija, D., and Davies, J. (2004). Novel pathway of salicylate degradation by *Streptomyces* sp. strain WA46. *Appl. Environ. Microbiol.* 70, 1297–1306. doi: 10.1128/AEM.70.3.1297-1306.2004

Kawaguchi, H., Ogino, C., and Kondo, A. (2017). Microbial conversion of biomass into bio-based polymers. *Biores. Technol.* 245, 1664–1673. doi: 10.1016/j.biortech.2017.06.135

Kirk, T. K., and Farrel, R. L. (1987). Enzymatic "combustion": the microbial degradation of lignin. *Annu. Rev. Microbiol.* 41, 465–505. doi: 10.1146/annurev.mi.41.100187.002341

Klinke, H. B., Olsson, L., Thomsen, A. B., and Ahring, B. K. (2003). Potential inhibitors from wet oxidation of wheat straw and their effect on ethanol production of *Saccharomyces cerevisiae*: wet oxidation and fermentation by yeast. *Biotechnol. Bioeng.* 81, 738–747. doi: 10.1002/bit.10523

Kohlstedt, M., Starck, S., Barton, N., Stolzenberger, J., Selzer, M., Mehlmann, K., et al. (2018). From lignin to nylon: cascaded chemical and biochemical conversion using metabolically engineered *Pseudomonas putida*. *Metab. Eng.* 47, 279–293. doi: 10.1016/j.ymben.2018.03.003

Lê, S., Josse, J., and Husson, F. (2008). FactoMineR: an R package for multivariate analysis. *J. Stat. Softw.* 25, 1–18. doi: 10.18637/jss.v025.i01

Lah, L., Podobnik, B., Novak, M., Korošec, B., Berne, S., Vogelsang, M., et al. (2011). The versatility of the fungal cytochrome P450 monooxygenase system

is instrumental in xenobiotic detoxification. *Mol. Microbiol.* 81, 1374–1389. doi: 10.1111/j.1365-2958.2011.07772.x,

Leisola, M., Pastinen, O., and Axe, D. D. (2012). Lignin - designed randomness. *Biocomplexity* 2012, 1–11. doi: 10.5048/BIO-C.2012.3

Li, C., Zhao, X., Wang, A., Huber, G. W., and Zhang, T. (2015). Catalytic transformation of lignin for the production of chemicals and fuels. *Chem. Rev.* 115, 11559–11164. doi: 10.1021/acs.chemrev.5b00155

Lima, T. C., Ferreira, A. R., Silva, D. F., Lima, E. O., and de Sousa, D. P. (2018). Antifungal activity of cinnamic acid and benzoic acid esters against *Candida albicans* strains. *Nat. Prod. Res.* 32, 572–575. doi: 10.1080/14786419.2017.1317776

Lomascolo, A., Lesage-Meessen, L., Labat, M., Navarro, D., Delattre, M., and Asther, M. (1999). Enhanced benzaldehyde formation by a monokaryotic strain of *Pycnoporus cinnabarinus* using a selective solid adsorbent in the culture medium. *Can. J. Microbiol.* 45, 653–657. doi: 10.1139/w99-056

Love, M. I., Huber, W., and Anders, S. (2014). Moderated estimation of fold change and dispersion for RNA-seq data with DESeq2. *Genome Biol.* 15:550. doi: 10.1186/s13059-014-0550-8

Lubbers, R. J. M., Dilokpimol, A., Visser, J., Mäkelä, M. R., Hildén, K. S., and de Vries, R. P. (2019). A comparison between the homocyclic aromatic metabolic pathways from plant-derived compounds by bacteria and fungi. *Biotechnol. Adv.* S0734-9750, 30077–30071. doi: 10.1016/j.biotechadv.2019.05.002

Maeda, H., and Dudareva, N. (2012). The shikimate pathway and aromatic amino acid biosynthesis in plants. *Annu. Rev. Plant Biol.* 63, 73–105. doi: 10.1146/annurev-arplant-042811-105439

Maere, S., Kuiper, M., and Heymans, K. (2005). BiNGO: a cytoscape plugin to assess overrepresentation of gene ontology categories in biological networks. *Bioinformatics* 21, 3448–3449. doi: 10.1093/bioinformatics/bti551

Mäkelä, M. R., Hilden, K. S., and de Vries, R. P. (2014). "8 degradation and modification of plant biomass by fungi," in *The Mycota: A Comprehensive Treatise on Fungi as Experimental Systems for Basic and Applied Research, 2nd Edn.* ed M. Nowrousian (Berlin; Heidelberg: Springer). 175–208. doi: 10.1007/978-3-642-45218-5_8

Mäkelä, M. R., Marinovic, M., Nousiainen, P., Liwanag, A. J. M., Benoit, I., Sipila, J., et al. (2015). Aromatic metabolism of filamentous fungi in relation to the presence of aromatic compounds in plant biomass. *Adv. Appl. Microbiol.* 91, 63–137. doi: 10.1016/bs.aambs.2014.12.001

Manavalan, T., Manavalan, A., and Heese, K. (2015). Characterization of lignocellulolytic enzymes from white-rot fungi. *Curr. Microbiol.* 70, 485–498. doi: 10.1007/s00284-014-0743-0

Marinović, M., Nousiainen, P., Dilokpimol, A., Kontro, J., Moore, R., Sipilä, J., et al. (2018). Selective cleavage of lignin β-O-4 aryl ether bond by β-etherase of the white-rot fungus *Dichomitus squalens*. *ACS Sustain. Chem. Eng.* 6, 2878–2882. doi: 10.1021/acssuschemeng.7b03619

Matsuzaki, F., and Wariishi, H. (2005). Molecular characterization of cytochrome P450 catalyzing hydroxylation of benzoates from the white-rot fungus *Phanerochaete chrysosporium*. *Biochem. Biophys. Res. Commun.* 334, 1184–1190. doi: 10.1016/j.bbrc.2005.07.013

McLeod, M. N. (1974). Plant tannins-their role in forage quality. *Nutr. Abstr. Rev.* 44, 803–815.

Moiseenko, K. V., Vasina, D. V., Farukshina, K. T., Savinova, O. S., Glazunova, O. A., Fedorova, T. V., et al. (2018). Orchestration of the expression of the laccase multigene family in white-rot basidiomycete *Trametes hirsuta* 072: evidences of transcription level subfunctionalization. *Fungal Biol.* 122, 353–362. doi: 10.1016/j.funbio.2018.02.006

Morel, M., Meux, E., Mathieu, Y., Thuillier, A., Chibani, K., Harvengt, L., et al. (2013). Xenomic networks variability and adaptation traits in wood decaying fungi. *Microb. Biotechnol.* 6, 248–263. doi: 10.1111/1751-7915.12015

Neves, F. M., Kawano, C. Y., and Said, S. (2005). Effect of benzene compounds from plants on the growth and hyphal morphology in *Neurospora crassa*. *Braz. J. Microbiol.* 36, 190–195. doi: 10.1590/S1517-83822005000200016

Otto, A., and Simpson, M. J. (2006). Evaluation of CuO oxidation parameters for determining the source and stage of lignin degradation in soil. *Biogeochemistry* 80, 121–142. doi: 10.1007/s10533-006-9014-x

Pham, T. T. T., Maaroufi, A., and Odier, E. (1990). Inheritance of cellulose- and lignin-degrading ability as well as endoglucanase isozyme pattern in *Dichomitus squalens*. *Appl. Microbiol. Biotechnol.* 33, 99–104. doi: 10.1007/BF00170579

Piscitelli, A., Giardina, P., Lettera, V., Pezzella, C., Sannia, G., and Faraco, V. (2011). Induction and transcriptional regulation of laccases in fungi. *Curr. Genom.* 12, 104–112. doi: 10.2174/138920211795564331

Raj, A., Krishna Reddy, M. M., and Chandra, R. (2007). Identification of low molecular weight aromatic compounds by gas chromatography–mass spectrometry (GC–MS) from kraft lignin degradation by three *Bacillus* sp. *Int. Biodeter. Biodegr.* 59, 292–296. doi: 10.1016/j.ibiod.2006.09.006

Renvall, P., Renvall, T., and Niemelä, T. (1991). Basidiomycetes at the timberline in Lapland 2. An annotated checklist of the polypores of northeastern Finland. *Karstenia* 31, 13–28. doi: 10.29203/ka.1991.282

Rinaldi, R., Jastrzebski, R., Clough, M. T., Ralph, J., Kennema, M., Bruijnincx, P. C. A., et al. (2016). Paving the way for lignin valorisation: recent advances in bioengineering, biorefining and catalysis. *Angew. Chem. Int. Ed. Engl.* 55, 8164–8215. doi: 10.1002/anie.201510351

Rytioja, J., Hildén, K., Di Falco, M., Zhou, M., Aguilar-Pontes, M. V., Sietiö, O. M., et al. (2017). The molecular response of the white-rot fungus *Dichomitus squalens* to wood and non-woody biomass as examined by transcriptome and exoproteome analyses. *Environ. Microbiol.* 19, 1237–1250. doi: 10.1111/1462-2920.13652

Rytioja, J., Hildén, K. S., Mäkinen, S., Vehmaanperä, J., Hatakka, A., and Mäkelä, M. R. (2015). Saccharification of lignocelluloses by carbohydrate active enzymes of the white rot fungus *Dichomitus squalens*. *PLoS ONE* 10:e0145166. doi: 10.1371/journal.pone.0145166

Rytioja, J., Hildén, K. S., Yuzon, J., Hatakka, A., de Vries, R. P., and Mäkelä, M. R. (2014). Plant-polysaccharide-degrading enzymes from basidiomycetes. *Microbiol. Mol. Biol. Rev.* 78, 614–649. doi: 10.1128/MMBR.00035-14

Schieber, A. (2018). Reactions of quinones - mechanisms, structures, and prospects for food research. *J. Agric. Food Chem.* 66, 13051–13055. doi: 10.1021/acs.jafc.8b05215

Sellés Vidal, L., Kelly, C. L., Mordaka, P. M., and Heap, J. T. (2018). Review of NAD(P)H-dependent oxidoreductases: properties, engineering and application. *Biochim. Biophys. Acta* 1866, 327–347. doi: 10.1016/j.bbapap.2017.11.005

Shi, Y., Chai, L., Tang, C., Yang, Z., Zhang, H., Chen, R., et al. (2013). Characterization and genomic analysis of kraft lignin biodegradation by the beta-proteobacterium *Cupriavidus basilensis* B-8. *Biotechnol. Biofuels* 6:1. doi: 10.1186/1754-6834-6-1

Sista Kameshwar, A. K., and Qin, W. (2018). Comparative study of genome-wide plant biomass-degrading CAZymes in white rot, brown rot and soft rot fungi. *Mycology* 9, 93–105. doi: 10.1080/21501203.2017.1419296

Sjöström, E. (1993). *Wood Chemistry: Fundamentals and Applications*. San Diego, CA: Elsevier.

Terrón, M. C., González, T., Carbajo, J. M., Yagüe, S., Arana-Cuenca, A., Téllez, A., et al. (2004). Structural close-related aromatic compounds have different effects on laccase activity and on lcc gene expression in the ligninolytic fungus *Trametes* sp. I-62. *Fungal Genet. Biol.* 41, 954–962. doi: 10.1016/j.fgb.2004.07.002

Tolbert, A., Akinosho, H., Khunsupat, R., Naskar, A. K., and Ragauskas, A. J. (2014). Characterization and analysis of the molecular weight of lignin for biorefining studies. *Biofuels Bioprod. Bioref.* 8, 836–856. doi: 10.1002/bbb.1500

Trapnell, C., Williams, B. A., Pertea, G., Mortazavi, A., Kwan, G., van Baren, M. J., et al. (2010). Transcript assembly and quantification by RNA-Seq reveals unannotated transcripts and isoform switching during cell differentiation. *Nat. Biotechnol.* 28, 511–555. doi: 10.1038/nbt.1621

van Gorcom, R. F., Boschloo, J. G., Kuijvenhoven, A., Lange, J., van Vark, A. J., Bos, C. J., et al. (1990). Isolation and molecular characterization of the benzoate-para-hydroxylase gene (bphA) of Aspergillus niger: a member of a new gene family of the cytochrome P450 superfamily. *Mol. Gen. Genet.* 223, 192–197. doi: 10.1007/BF00265053

Vanholme, R., Demedts, B., Morreel, K., Ralph, J., and Boerjan, W. (2010). Lignin biosynthesis and structure. *Plant Physiol.* 153, 895–905. doi: 10.1104/pp.110.155119

Wang, X., Tsang, Y. F., Li, Y., Ma, X., Cui, S., Zhang, T.-A., et al. (2017). Inhibitory effects of phenolic compounds of rice straw formed by saccharification

during ethanol fermentation by *Pichia stipitis*. *Biores. Technol.* 244, 1059–1067. doi: 10.1016/j.biortech.2017.08.096

Wang, Y., Chantreau, M., Sibout, R., and Hawkins, S. (2013). Plant cell wall lignification and monolignol metabolism. *Front. Plant Sci.* 4:220. doi: 10.3389/fpls.2013.00220

Wu, Y., Bai, J., Zhong, K., Huang, Y., Qi, H., Jiang, Y., et al. (2016). Antibacterial activity and membrane-disruptive mechanism of 3-p-trans-coumaroyl-2-hydroxyquinic acid, a novel phenolic compound from pine needles of *Cedrus deodara*, against *Staphylococcus aureus*. *Molecules* 21:1084. doi: 10.3390/molecules21081084

Yajima, Y., Enoki, A., Mayfield, M. B., and Gold, M. H. (1979). Vanillate hydroxylase from the white rot basidiomycete *Phanerochaete chrysosporium*. *Arch. Microbiol.* 123, 319–321. doi: 10.1007/BF00406669

Yang, J., Wang, G., Ng, T. B., Lin, J., and Ye, X. (2016). Laccase production and differential transcription of laccase genes in *Cerrena* sp. in response to metal ions, aromatic compounds, and nutrients. *Front. Microbiol.* 6:1558. doi: 10.3389/fmicb.2015.01558

Yang, Y., Wei, F., Zhuo, R., Fan, F., Liu, H., Zhang, C., et al. (2013). Enhancing the laccase production and laccase gene expression in the white-rot fungus Trametes velutina 5930 with great potential for biotechnological applications by different metal ions and aromatic compounds. *PLoS ONE* 8:e79307. doi: 10.1371/journal.pone.0079307

Conflict of Interest: The authors declare that the research was conducted in the absence of any commercial or financial relationships that could be construed as a potential conflict of interest.

frontiers in Bioengineering and Biotechnology

ORIGINAL RESEARCH
published: 27 September 2019
doi: 10.3389/fbioe.2019.00249

Cinnamic Acid and Sorbic acid Conversion Are Mediated by the Same Transcriptional Regulator in *Aspergillus niger*

Ronnie J. M. Lubbers[1], Adiphol Dilokpimol[1], Jorge Navarro[2], Mao Peng[1], Mei Wang[3], Anna Lipzen[3], Vivian Ng[3], Igor V. Grigoriev[3], Jaap Visser[1], Kristiina S. Hildén[4] and Ronald P. de Vries[1]*

[1] Fungal Physiology, Westerdijk Fungal Biodiversity Institute and Fungal Molecular Physiology, Utrecht University, Utrecht, Netherlands, [2] Fungal Natural Products, Westerdijk Fungal Biodiversity Institute, Utrecht, Netherlands, [3] US Department of Energy Joint Genome Institute, Walnut Creek, CA, United States, [4] Department of Microbiology, University of Helsinki, Helsinki, Finland

OPEN ACCESS

Edited by:
Nils Jonathan Helmuth Averesch, Stanford University, United States

Reviewed by:
Dirk Tischler, Ruhr University Bochum, Germany
Miguel Cacho Teixeira, University of Lisbon, Portugal

***Correspondence:**
Ronald P. de Vries
r.devries@wi.knaw.nl

Specialty section:
This article was submitted to Bioprocess Engineering, a section of the journal Frontiers in Bioengineering and Biotechnology

Received: 13 May 2019
Accepted: 16 September 2019
Published: 27 September 2019

Citation:
Lubbers RJM, Dilokpimol A, Navarro J, Peng M, Wang M, Lipzen A, Ng V, Grigoriev IV, Visser J, Hildén KS and de Vries RP (2019) Cinnamic Acid and Sorbic acid Conversion Are Mediated by the Same Transcriptional Regulator in Aspergillus niger. Front. Bioeng. Biotechnol. 7:249. doi: 10.3389/fbioe.2019.00249

Cinnamic acid is an aromatic compound commonly found in plants and functions as a central intermediate in lignin synthesis. Filamentous fungi are able to degrade cinnamic acid through multiple metabolic pathways. One of the best studied pathways is the non-oxidative decarboxylation of cinnamic acid to styrene. In *Aspergillus niger*, the enzymes cinnamic acid decarboxylase (CdcA, formally ferulic acid decarboxylase) and the flavin prenyltransferase (PadA) catalyze together the non-oxidative decarboxylation of cinnamic acid and sorbic acid. The corresponding genes, *cdcA* and *padA*, are clustered in the genome together with a putative transcription factor previously named sorbic acid decarboxylase regulator (SdrA). While SdrA was predicted to be involved in the regulation of the non-oxidative decarboxylation of cinnamic acid and sorbic acid, this was never functionally analyzed. In this study, *A. niger* deletion mutants of *sdrA*, *cdcA*, and *padA* were made to further investigate the role of SdrA in cinnamic acid metabolism. Phenotypic analysis revealed that *cdcA*, *sdrA* and *padA* are exclusively involved in the degradation of cinnamic acid and sorbic acid and not required for other related aromatic compounds. Whole genome transcriptome analysis of Δ*sdrA* grown on different cinnamic acid related compounds, revealed additional target genes, which were also clustered with *cdcA*, *sdrA*, and *padA* in the *A. niger* genome. Synteny analysis using 30 *Aspergillus* genomes demonstrated a conserved cinnamic acid decarboxylation gene cluster in most Aspergilli of the Nigri clade. Aspergilli lacking certain genes in the cluster were unable to grow on cinnamic acid, but could still grow on related aromatic compounds, confirming the specific role of these three genes for cinnamic acid metabolism of *A. niger*.

Keywords: fungal aromatic metabolism, Aspergilli, synteny analysis, transcription factor, flavoprotein, cinnamic acid decarboxylase

INTRODUCTION

Cinnamic acid, an aromatic compound with a distinct aroma, is naturally found as a free compound in several plants, such as *Cinnamomum verum, C. cassia*, and *C. zeylanicum* (He et al., 2005; Gruenwald et al., 2010). Cinnamic acid is also one of the central intermediates for the biosynthesis of lignin, flavonoids and coumarins in plants (Hoskins, 1984; Chemler and Koffas, 2008; Vargas-Tah and Gosset, 2015) and it is synthesized through the deamination of phenylalanine (Yamada et al., 1981). High concentrations of cinnamic acid can accumulate in soil, especially in those soils that are continuously used for crop cultivation, where it is released by root exudation and decaying plant tissue (Xie and Dai, 2015; Latif et al., 2017). Cinnamic acid has antioxidant and antimicrobial properties, it can be used as a precursor for the synthesis of thermoplastics and flavoring agents, and it is also widely used in cosmetic and health products (Chemler and Koffas, 2008; Vargas-Tah and Gosset, 2015). Hence, recent studies have focused on metabolic engineering of the microbial shikimate pathway to produce cinnamic acid from simple sugars and complex substrates (Thompson et al., 2015; Vargas-Tah and Gosset, 2015; Averesch and Krömer, 2018).

A recent review summarized the various metabolic pathways used by microorganisms to degrade cinnamic acid, and its role as a carbon source (**Figure 1**) (Lubbers et al., 2019). One of the most studied pathways of cinnamic acid metabolism is the non-oxidative decarboxylation of cinnamic acid to styrene, which was reported to occur in several fungi, such as *Aspergillus, Penicillium*, *Saccharomyces,* and *Trichoderma* (Marth et al., 1966; Clifford et al., 1969; Milstein et al., 1983; Pinches and Apps, 2007; Lafeuille et al., 2009; Plumridge et al., 2010; Richard et al., 2015; Liewen and Marth, 2016). Two genes were identified in *Aspergillus niger* and *Saccharomyces cerevisiae*, that are involved in the non-oxidative decarboxylation of cinnamic acid using prenylated flavin mononucleotide (FMN) as a cofactor to convert cinnamic acid to styrene (Plumridge et al., 2010; Payne et al., 2015). These genes are clustered in the genome and encode a putative 3-octaprenyl-4-hydroxybenzoate carboxy-lyase, referred to as cinnamic acid decarboxylase (*cdcA*, formerly ferulic acid decarboxylase (*fdcA*), see Discussion), and a flavin prenyltransferase (*padA*) (**Figure 1**) (Plumridge et al., 2010; Payne et al., 2015). In addition, CdcA and PadA also catalyze the decarboxylation of the food preservative sorbic acid to 1,3-pentadiene. An additional pathway was suggested in *A. niger* in which cinnamic acid is *para*-hydroxylated to *p*-coumaric acid (Bocks, 1966), but this seems to play a minor role in *A. niger* since only small amounts of *p*-coumaric acid were detected. In *Aspergillus japonicus,* cinnamic acid was suggested to be reduced to cinnamaldehyde and cinnamyl alcohol (Milstein et al., 1983). Better understanding of the cinnamic acid metabolic pathway in *A. niger* can aid in the creation of cell factories or unlock new strategies to make valuable aromatic building blocks.

Transcriptional regulation is important in controlling the metabolic flux and energy usage in metabolic processes in microorganisms. Many transcription regulators involved in carbohydrate metabolism of filamentous fungi have been identified (Benocci et al., 2017), but less is known about the transcriptional regulation of aromatic metabolic pathways. It has been shown that a Zn_2Cys_6-finger transcription factor named sorbic acid decarboxylase regulator (SdrA), is involved in the regulation of *cdcA* and *padA* (Plumridge et al., 2010). The corresponding gene (*sdrA*) is located between *cdcA* and *padA* in a gene cluster. While deletion of *sdrA* revealed that it is essential for the non-oxidative decarboxylation of cinnamic acid, until now its regulatory targets are still unknown. In *S. cerevisiae,* orthologs of *cdcA* and *padA* are also clustered, but no transcription factor has been found between these genes (Mukai et al., 2010; Plumridge et al., 2010).

In this paper, we studied SdrA in more detail in order to identify its regulatory targets using transcriptomic data of the *A. niger* deletion strain Δ*sdrA* cultivated in cinnamic acid and sorbic acid. We used whole genome transcriptome analysis of Δ*sdrA* to identify new regulatory targets and performed a phenotypic analysis of *cdcA*, *padA* and *sdrA* deletion strains to determine the role of CdcA, PadA, and SdrA in other aromatic metabolic pathways. Finally, synteny analysis of the cinnamic acid decarboxylation gene cluster using the genomes of 30 Aspergilli was performed to analyze the conservation of the gene cluster. Growth tests on cinnamic acid were performed on a subset of these species to confirm predictions made on the basis of the synteny analysis.

MATERIALS AND METHODS

Strains, Media, and Culture Conditions

All strains used in this study are shown in **Tables 1**, **2**, and were grown on complete medium for *Aspergillus* (CM, de Vries et al., 2004) containing 1.5% (w/v) agar supplemented with 1% fructose and 1.22 g L^{-1} uridine at 30°C for 4 days. Spores were harvested with 10 mL *N*-(2-acetamido)-2-aminoethanesulfonic acid buffer. Phenotypic experiments were performed using minimal medium for *Aspergillus* (MM, de Vries et al., 2004) containing aromatic compounds as sole carbon source, supplemented with 1.22 g L^{-1} uridine and inoculated with 10^3 spores in 2 μl. Due to variable toxicity of the aromatic compounds different concentrations were used for the growth profile, i.e., 2 mM for ferulic acid, 3 mM for benzoic acid, benzaldehyde, styrene and 5 mM for the remaining compounds. All aromatic compounds were purchased from Sigma Aldrich.

Construction of Gene Deletion Cassettes and Transformation of *A. niger*

The gene deletion cassettes were constructed using 1,000 bp upstream and downstream DNA fragment of the gene containing an overlap of the selection marker hygromycin B (*hph*) from *Escherichia coli*. The *hph* selection marker was amplified from plasmid pAN7.1 (Punt et al., 1987). These three fragments were fused in a PCR reaction using the GoTaq Long PCR Master Mix (Promega, Madison, WI, USA). The fusion PCR mixture contained 0.4 μl of each amplified product, 0.6 μl of 10 μM upstream and downstream primers (**Supplementary Table 1**), 12.5 μl GoTaq Long PCR Master Mix in a total volume of 25 μl. The following PCR conditions were used: 94°C for 2 min, 35 cycles of 94°C for 30 s, 60°C for 30 s, 72°C for 5 min, and

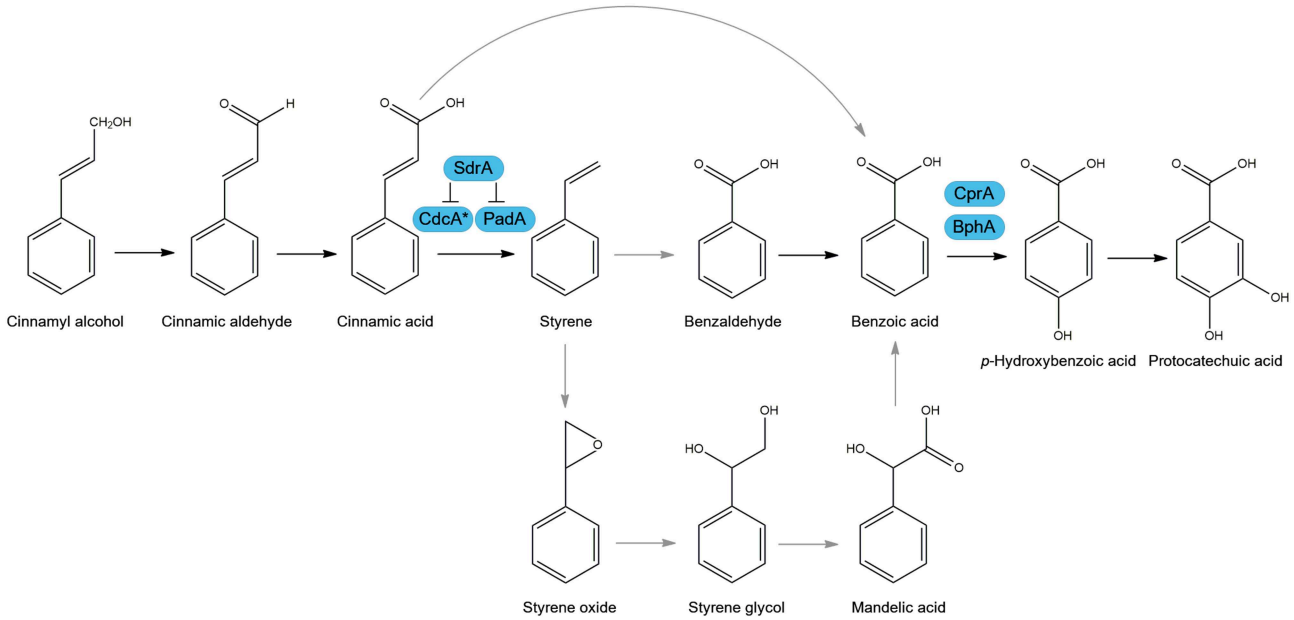

FIGURE 1 | Suggested cinnamic acid metabolic pathways in *Aspergillus niger*. Arrows in black are observed metabolic conversions in literature and in gray are suggested conversions. Boxed in blue are characterized enzymes of *A. niger* involved in this metabolic pathway. Cinnamic acid decarboxylase (CdcA), Flavin prenyltransferase (PadA), sorbic acid decarboxylase regulator (SdrA), benzoate 4-monooxygenase (BphA), cytochrome P450 reductase (CprA). *FdcA is renamed to CdcA, see Discussion.

TABLE 1 | *A. niger* strains used in this study.

Strain	CBS number	Genotype	References
N402	141247	*cspA1*	Bos et al., 1988
N593 Δ*kusA*	138852	*cspA1, pyrG, kusA::amdS*	Meyer et al., 2007
Δ*cdcA*	145475	*cspA1, pyrG, kusA::amdS, ΔcdcA::hph*	This study
Δ*sdrA*	145476	*cspA1, pyrG, kusA::amdS, ΔsdrA::hph*	This study
Δ*padA*	145477	*cspA1, pyrG, kusA::amdS, ΔpadA::hph*	This study

TABLE 2 | Aspergilli used in this study.

Aspergilli	Strain	Section	Growth temperature (°C)	References
A. aculeatus	CBS 106.47	*Nigri*	25	de Vries et al., 2017
A. brasiliensis	CBS 101740	*Nigri*	30	de Vries et al., 2017
A. carbonarius	CBS 141172	*Nigri*	30	de Vries et al., 2017
A. clavatus	NRRL 1	*Clavati*	25	Fedorova et al., 2008
A. flavus	NRRL 3357	*Flavi*	37	Payne et al., 2006
A. fumigatus	Af293	*Fumigati*	25	Nierman et al., 2005
A. nidulans	FGSCA4	*Nidulantes*	37	Galagan et al., 2005
A. niger	NRRL 3	*Nigri*	30	Aguilar-Pontes et al., 2018
A. oryzae	Rib40	*Flavi*	37	Machida et al., 2005
A. sydowii	CBS 141172	*Versicolores*	30	de Vries et al., 2017
A. terreus	NIH2624	*Terrei*	37	Arnaud et al., 2012
A. tubingensis	CBS 134.48	*Nigri*	30	de Vries et al., 2017
A. wentii	CBS 141173	*Cremei*	25	de Vries et al., 2017

a final extension at 72°C for 10 min. *A. niger* N593 Δ*kusA* was transformed through protoplast-mediated transformation as described in Kowalczyk et al. (2017).

Transfer Conditions, RNA Extraction, and Transcriptome Analysis

The transcriptomes of the reference strain *A. niger* N593 and Δ*sdrA* induced for 2 h in cinnamic acid and sorbic acid were analyzed with RNAseq by DOE Joint Genome Institute (JGI, Walnut Creek, CA, USA). Transfer experiments and subsequent RNA-sequencing were performed in biological triplicates. *A. niger* strains were pre-grown in 200 mL CM with 2% fructose inoculated with 1 x 10^6 spores/mL and incubated overnight on rotary shakers at 30°C, 250 rpm. Freshly germinated mycelia were harvested on Miracloth and washed with MM. Equal portions of mycelia were transferred to 250 mL flasks containing 50 mL MM and 0.02% (w/v) cinnamic acid, sorbic acid, benzoic acid, cinnamyl alcohol and salicylic acid. The cultures were incubated on rotary shakers for 2 h at 30°C, 250 rpm. Mycelia were harvested, dried between tissue paper to remove excess liquid and frozen in liquid nitrogen. Frozen mycelia were ground using the tissue lyser

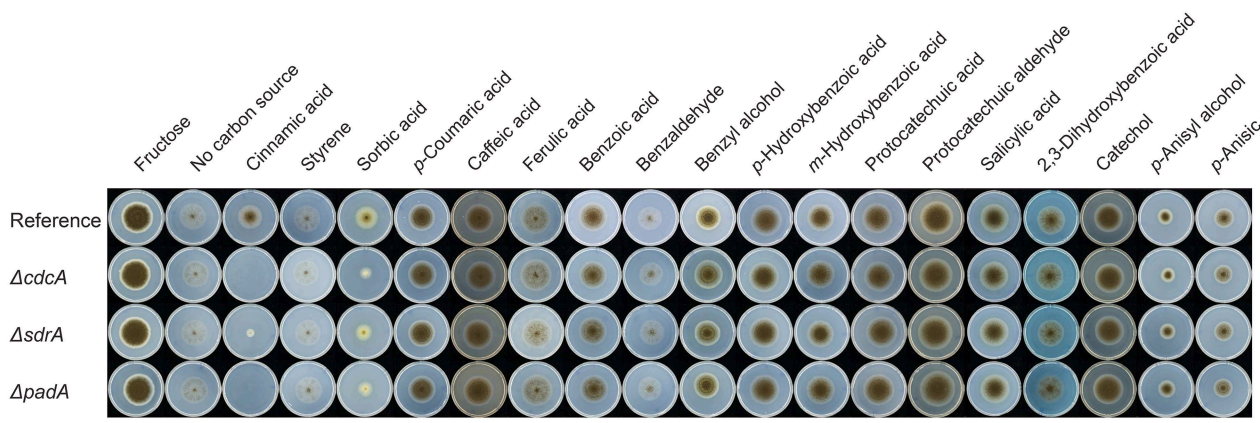

FIGURE 2 | Phenotypic analysis of the cinnamic acid decarboxylase mutants. Strains were grown for 10 days at 30°C. The reference strain is *A. niger* N593 Δ*kusA*. Due to variable toxicity of the aromatic compounds different concentrations were used for the growth profile, i.e., 2 mM for ferulic acid, 3 mM for benzoic acid, benzaldehyde, styrene and 5 mM for the remaining compounds. Fructose and the no carbon source were used as growth controls.

(QIAGEN, Hilden, Germany) and total RNA was extracted using TRIzol reagent (Invitrogen, Life Technologies, Carlsbad, CA, USA) and RNA isolation kit (NucleoSpin RNA, MACHEREY-NAGEL GmbH & Co. KG, Düren, Germany) according the manufacturer's recommendation. The quality and quantity of RNA was determined by gel electrophoresis and RNA6000 Nano Assay using the Agilent 2100 Bioanalyzer (Agilent Technologies, Santa Clara, CA, USA). Purification of mRNA, synthesis of cDNA library and sequencing were conducted at the JGI. Data was processed as described in Kowalczyk et al. (2017). The transcriptome data was stored at the NCBI Sequence Read Archive (SRA) (**Supplementary Table 2**).

Synteny Analysis

BLAST analyses were performed using the amino acid sequence of *cdcA*, *sdrA*, *padA*, NRRL3_8293, NRRL3_8294, NRRL3_8295, NRRL3_8299, NRRL3_8300, and NRRL3_8301 as a query on 30 *Aspergillus* genomes. All genomes used in this analysis were downloaded from JGI Mycocosm (Grigoriev et al., 2014). Synteny analysis was performed on the cinnamic acid decarboxylation core cluster (*cdcA*, *sdrA*, *padA*) with 20.000 bp on each side. BLAST hits and protein IDs used for the synteny analysis are mentioned in **Supplementary Table 3**.

RESULTS

CdcA, SdrA, and PadA Are Essential for Cinnamic Acid and Sorbic Acid Utilization

To understand the role of CdcA (NRRL3_8296), SdrA (NRRL3_8297), and PadA (NRRL3_8298) for aromatic metabolism in *A. niger*, deletion mutants (Δ*cdcA*, Δ*sdrA*, and Δ*padA*) were made and tested on a set of related aromatic compounds as a sole carbon source. Δ*cdcA* and Δ*padA* resulted in abolished growth on cinnamic acid and reduced growth on sorbic acid, while deletion of Δ*sdrA* resulted in reduced growth on both cinnamic acid and sorbic acid. This demonstrated that all three genes, *cdcA*, *sdrA*, and *padA,* are important for the metabolism of cinnamic acid and sorbic acid. No growth reduction was observed on other tested aromatic compounds (**Figure 2**), indicating that *cdcA* and *padA* are not essential for the conversion of these related compounds (**Figure 2**).

Cinnamic Acid and Sorbic Acid Both Induce the Cinnamic Acid and Sorbic Acid Decarboxylation Cluster and Neighboring Genes

A. niger N593 was pre-grown in CM with fructose and transferred to MM containing cinnamic acid, sorbic acid, cinnamyl alcohol, benzoic acid, 2-hydroxybenzoic acid (salicylic acid), or a no carbon source condition and were incubated for 2 h. Cinnamyl alcohol and benzoic acid are both related to cinnamic acid as they are among conversion products of cinnamic acid (**Figure 1**). The cultivation without any carbon source was used as a reference control to remove background noise between the conditions. Salicylic acid has not been observed to have any connection with cinnamic acid metabolic pathways (Martins et al., 2015). Therefore, it was used as a control representing an aromatic compound, which does not induce the expression of the cinnamic acid decarboxylase cluster.

Genome-wide gene expression analysis of the samples was performed using RNA-seq. A total of 3,921 genes were upregulated in all five conditions by *A. niger* N593 compared to the no carbon source control (**Figure 3**). Two thousand four hundred and ninety and two thousand one hundred and fourty eight genes were upregulated on cinnamic acid and sorbic acid, respectively, compared to the no carbon source control, while 211 of these genes were upregulated in both conditions (**Figure 3**). Upregulation of *cdcA, sdrA,* and *padA* was observed on cinnamic acid, cinnamyl alcohol, sorbic acid, and benzoic acid (**Table 3**). The three genes (NRRL3_8293, NRRL3_8294, and NRRL3_8295) located next to *cdcA* and one gene (NRRL3_8299) located next to *padA* were induced by both cinnamic acid and sorbic acid (**Table 3**). On cinnamyl

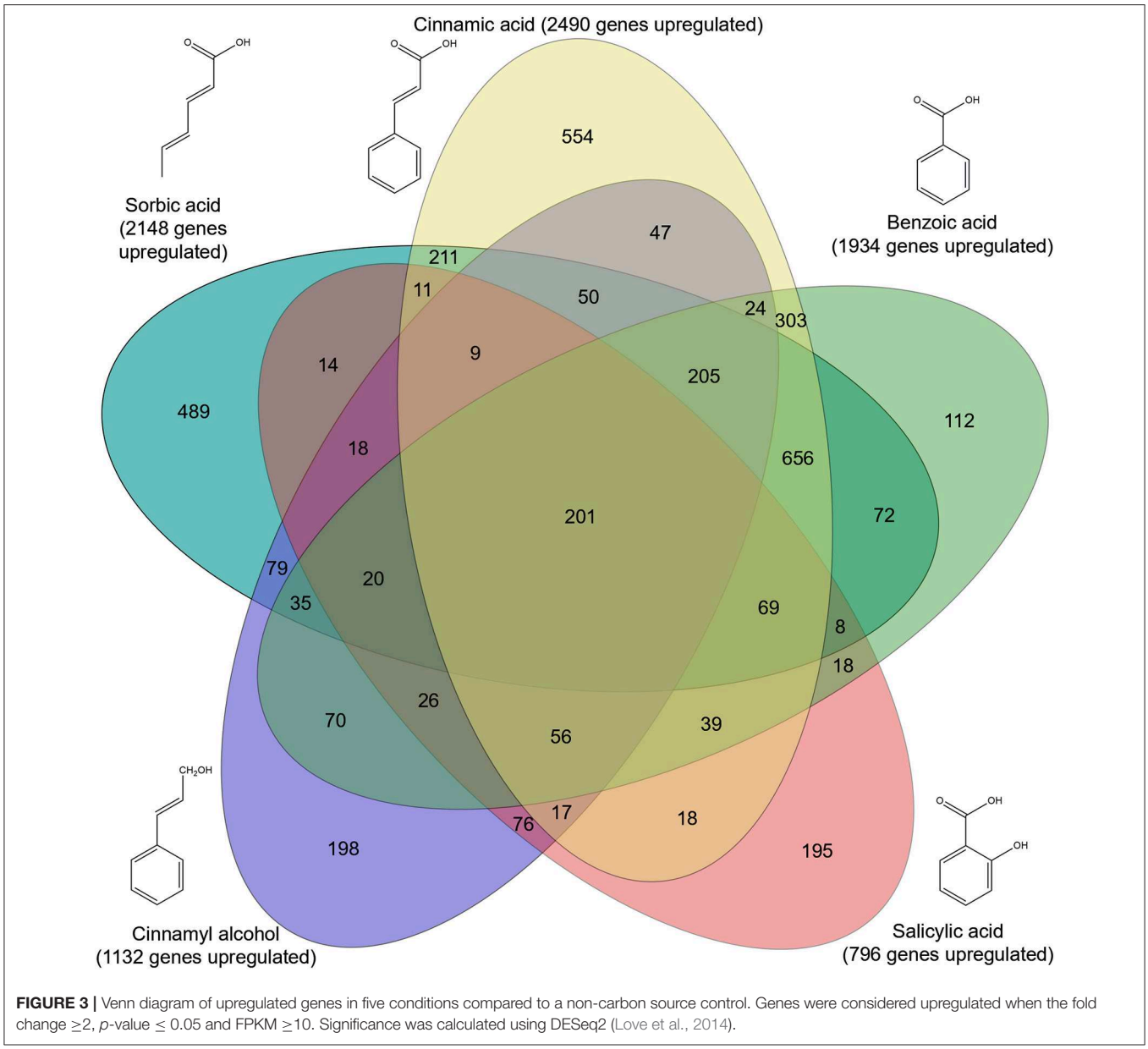

FIGURE 3 | Venn diagram of upregulated genes in five conditions compared to a non-carbon source control. Genes were considered upregulated when the fold change ≥2, *p*-value ≤ 0.05 and FPKM ≥10. Significance was calculated using DESeq2 (Love et al., 2014).

alcohol, *cdcA*, *padA*, NRRL3_8293, and NRRL3_8295 were also upregulated, but this was not the case for *sdrA*, NRRL3_8294, and NRRL3_8299. Two other genes, NRRL3_8300 and NRRL3_8301 were specifically induced by cinnamic acid. The lowest overlap in upregulated transcripts was found between salicylic acid and cinnamic acid/sorbic acid suggesting that the genes involved in the cinnamic acid/sorbic acid pathway are not involved in the conversion of salicylic acid. This was also supported by the fact that *cdcA*, *sdrA* and *padA* and their neighboring genes were not induced on salicylic acid (**Table 3**). The eukaryotic protein subcellular localization predictor software DeepLoc-1.0 was used to predict the cellular localization of the cinnamic acid and sorbic acid decarboxylation cluster genes (**Table 3**).

Deletion of *sdrA* Reveals Tight Regulation of the Cinnamic Acid and Sorbic Acid Decarboxylation Cluster

To further study the regulatory targets of SdrA, genome-wide transcriptome profiles of Δ*sdrA* was performed. The expression of 420 genes was reduced in Δ*sdrA* compared to *A. niger* N593 on cinnamic acid and 362 genes were reduced on sorbic acid, with only 50 genes that were reduced in both conditions (**Supplementary Table 4**). Transcript levels of *cdcA* and *padA* were significantly reduced in Δ*sdrA* confirming that *cdcA* and *padA* are both regulated by SdrA (**Table 4**). Interestingly, the transcript levels of *cdcA* were less affected by the deletion of *sdrA* on cinnamic acid than those of *padA*, which could indicate involvement of an additional regulator. The transcript

TABLE 3 | Fold change and schematic presentation[a] of the cinnamic acid and sorbic acid decarboxylation gene cluster and neighboring genes.

Gene ID NRRL3	Prediction according to JGI	Deeploc localization prediction[c]	Fold change[b]				
			Cinnamic acid	Sorbic acid	Cinnamyl alcohol	Benzoic acid	Salicylic acid
8293	Flavin reductase-like domain-containing protein	Cytoplasm	**17.8**	**38.1**	**72.5**	**5.2**	1.2
8294	Hypothetical protein	Cell membrane	**645.8**	**1014.7**	126.8	**35.8**	0.6
8295	BTB/POZ domain-containing protein	Cytoplasm	**102.1**	**195.3**	**34.5**	1.7	0.3
8296 (*cdcA*)	3-octaprenyl-4-hydroxybenzoate carboxy-lyase	Cytoplasm	**311.4**	**525.9**	**465.3**	**10.4**	0.1
8297 (*sdrA*)	Fungal-specific transcription factor	Nucleus	**123.0**	**88.2**	16.8	27.4	3.0
8298 (*padA*)	Flavin prenyltransferase	Mitochondrion	**330.6**	**230.8**	**203.0**	**4.0**	0.6
8299	Carboxylesterase	Extracellular	**5.1**	**3.7**	1.2	0.1	0.1
8300	Glucoamylase Gla15A	Extracellular	**2.8**	0.7	0.3	0.4	0.5
8301	Sulphatase	Extracellular	**5.7**	1.5	1.0	0.7	0.6

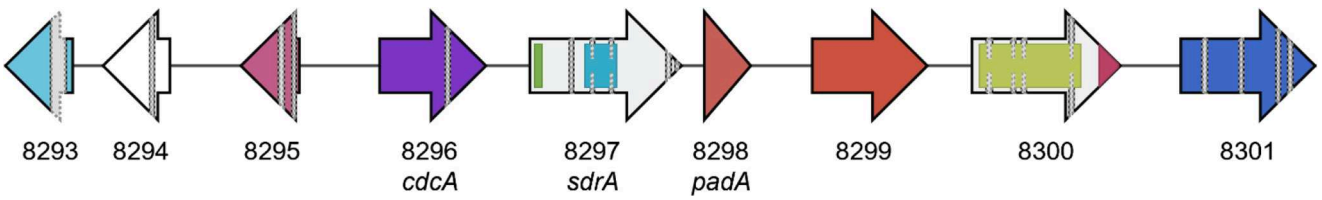

[a] *For schematic representation, the arrow indicates the transcription direction, gaps in the arrow represent introns, and colors represent domains corresponding with Pfam 32.0 domain signatures. NRRL3_8293, FMN-split barrel domain (light blue), NRRL3_8294, no predicted domains (no color), NRRL3_8295, BTB/POZ domain (pink), cdcA, 3-octaprenyl-4-hydroxybenzoate carboxy-lyase domain (purple), sdrA, Zn-finger (green) and fungal specific transcription factor (light blue) domains, padA, flavoprotein domain (red), NRRL3_8299, carboxylesterase family domain (red), NRRL3_8300, glycosyl hydrolases family 15 (green) and starch binding (pink) domains, NRRL3_8301, sulphatase domain (dark blue).*

[b] *Numbers in bold are significantly upregulated genes compared to the no carbon source control (fold change ≥ 2, P-value ≤ 0.05, FPKM ≥ 10).*

[c] *Cellular locations of the genes were predicted using DeepLoc-1.0: Eukaryotic protein subcellular localization predictor (Almagro Armenteros et al., 2017).*

levels of the four clustered genes (NRRL3_8293, NRRL3_8294, NRRL3_8295, and NRRL3_8299) were also reduced in Δ*sdrA* and therefore likely regulated by SdrA (**Table 4**). Transcription levels of NRRL3_8300 and NRRL3_8301 were reduced in Δ*sdrA* on cinnamic acid compared to *A. niger* N593, but not on sorbic acid. Therefore, we speculate that these genes are not part of the cinnamic acid and sorbic acid decarboxylation cluster. Similar expression profiles were observed in cinnamyl alcohol with high fold changes, but on this compound the FPKM values of NRRL3_8294 and *sdrA* were below 10 (**Table 4**) which makes it difficult to draw conclusions.

The Cinnamic Acid and Sorbic Acid Decarboxylation Cluster Is Conserved in Aspergilli From the Nigri-Biseriates Clade

To study whether the cinnamic acid and sorbic acid decarboxylation cluster is conserved in Aspergilli, a synteny study using 30 *Aspergillus* genomes was performed (**Supplementary Figure 1**). In *A. niger*, two homologs of *cdcA* (NRRL3_3 and NRRL3_3023, 51.5 and 47.7% identity, respectively) and two homologs of *padA* (NRRL3_2 and NRRL3_3024, 74.6 and 55.8% identity, respectively) were observed and both of these are also clustered but in a different genomic location. However, they are not separated by a transcription factor. In addition, the expression of these genes was not induced by any of the tested compounds. BLAST analyses with the amino acid sequence of *cdcA* and *padA* revealed that most Aspergilli had on average two homologs of *cdcA* and *padA* in their genomes (**Table 5**). To identify the true orthologs of the cinnamic acid decarboxylation cluster we used the following criteria. First, either *cdcA* or *padA* is located next to a transcription factor. If no transcription factor is found next to one of the orthologs, the *cdcA* or *padA* ortholog with the highest E-value is used. From the 30 Aspergilli genomes, 27 genomes had a transcription factor next to the homolog of *padA* while the remaining three genomes did not have *cdcA, sdrA,* and *padA* orthologs in their genome (**Table 5**).

Most Aspergilli from the Nigri-Biserates clade had a conserved cinnamic/sorbic acid gene cluster, except *A. ibericus, A. sclerotiicarbonarius* (no ortholog of NRRL3_8293), and *A. carbonarius* and *A. sclerotioniger* (no ortholog of *cdcA* and NRRL3_8293) (**Figure 3**, **Table 5**). However, orthologs of NRRL3_8293 and *cdcA* that were located elsewhere in their

TABLE 4 | Transcriptome data of the cinnamic acid and sorbic acid decarboxylation cluster genes of *A. niger* N593 compared to Δ*sdrA* in both cinnamic acid, sorbic acid, cinnamyl alcohol, benzoic acid, and sorbic acid.

Gene ID NRRL3	Gene name	Fold change (N593/Δ*sdrA*)[a]				
		Cinnamic acid	Sorbic acid	Cinnamyl alcohol	Benzoic acid	Salicylic acid
8293	–	**3.4**	**15.6**	**21.1**	0.7	**2.6**
8294	–	**5.7**	**6.7**	11.5	0.2	0.8
8295	–	**12.8**	**8.0**	**6.1**	0.2	0.2
8296	*cdcA*	**4.3**	**17.0**	**131.6**	0.2	0.4
8297	*sdrA*	**51.2**	**33.8**	71.8	27.9	73.7
8298	*padA*	**18.5**	**9.0**	**72.5**	0.7	0.5
8299	–	**15.4**	**6.0**	1.1	0.2	0.7
8300	–	**2.3**	1.6	0.7	0.8	0.6
8301	–	**5.7**	0.8	0.6	0.5	0.5

The fold changes and significance calculated using DESeq2 (Love et al., 2014).

[a]*Numbers in bold are significantly upregulated genes compared to Δ*sdrA *(fold change ≥2, P-value ≤ 0.05, FPKM ≥ 10).*

genomes were found for these species. NRRL3_8294 is only present in Aspergilli that are closely related to *A. niger* (**Supplementary Figure 1**). Species from the Nigri-Uniseriates clade do not have *cdcA* homolog ortholog in their cluster or were missing *cdcA* and NRRL3_8300 orthologs in their cluster. The cinnamic/sorbic acid cluster of *A. japonicus* and *A. sydowii* only contained orthologs of NRRL3_8293, *cdcA*, *sdrA*, and *padA*, while orthologs of the remaining genes were scattered over different chromosomes. Similar observations were found for *A. nidulans*, however the *padA* homolog appears to be truncated (**Figure 3**). Two species from the section Flavi, *A. flavus* and *A. oryzea*, had orthologs of *cdcA*, *sdrA*, and *padA*, while NRRL3_8293 was separated by multiple genes from the core cluster (**Figure 4**). The orthologs of NRRL3_8299, NRRL3_8300, and NRRL3_8301 were clustered, but located on a different scaffold. It appeared that the *sdrA* and *padA* orthologs of *A. terreus* are fused and the zinc finger domain of *sdrA* is missing (**Figure 4**). *A. fumigatus, A. clavatus, and A. campestris* do not have an ortholog of *cdcA, sdrA*, and *padA*. In addition, only low e-value BLAST hits of *sdrA* were found in these Aspergilli.

Correlation Between the Ability to Grow on Cinnamic Acid and the Occurrence of an Intact Cinnamic Acid and Sorbic Acid Decarboxylation Gene Cluster

To confirm our findings and the correlation between the cinnamic acid and sorbic acid decarboxylation gene cluster and the ability to convert cinnamic acid, a growth test was performed with selected Aspergillus species based on the following criteria:

1. Species having an intact cinnamic acid and sorbic acid decarboxylation gene cluster containing *cdcA*, *sdrA* and *padA* homologs (*A. brasiliensis, A. niger*, and *A. tubengensis*).
2. Species containing a gene cluster without a *cdcA* homolog, but the homolog is present on a different scaffold (*A. aculeatus* and *A. carbonarius*).
3. Species containing no *cdcA* homolog (*A. clavatus* and *A. fumigatus*).
4. Species with miscellaneous gene clusters. *A. oryzae* and *A. flavus* were chosen since the location of *cdcA* and *sdrA* are swapped. *A. terreus* was selected because of the fused *sdrA* and *padA* genes. *A. nidulans* has a truncated *padA*. *A. sydowii* lacks an ortholog of NRRL3_8293 in its cluster. *A. wentii* lacks NRRL3_8295 and NRRL3_8301 orthologs in its cluster.

The Aspergilli of criteria one (*A. niger A. brasiliensis, A. tubengensis,* and *A. wentii*) and two (*A. carbonarius* and *A. aculeatus*) were all able to grow on cinnamic acid and the distinct smell of styrene was present. This indicates that *A. carbonarius* and *A. aculeatus* both have a functional *cdcA* despite its different genomic location. The Aspergilli of criteria three (*A. fumigatus* and *A. clavatus*) were not able to grow on cinnamic acid, which corresponds to the absence of *cdcA*, *sdrA* and *padA* homologs. Three Aspergilli of criteria four, *A. flavus, A. oryzae,* and *A. wentii*, were able to grow on cinnamic acid, while *A. nidulans, A. sydowii,* and *A. terreus* were not. In addition, all strains tested were able to grow on ferulic acid, *p*-coumaric acid and caffeic acid indicating that the cinnamic acid decarboxylation cluster in not required for ferulic acid, *p*-coumaric acid and caffeic acid utilization.

DISCUSSION

This paper provides new insights into the regulation by the transcription factor SdrA of the cinnamic acid and sorbic acid decarboxylation cluster in Aspergilli and its regulatory targets, which also determines their ability to grow on cinnamic acid. Based on phenotypic screening of the deletion mutants of *cdcA*, *sdrA*, and *padA*, it is clear that the decarboxylation of cinnamic acid and sorbic acid represents a relevant step in the metabolic pathway for *A. niger* to utilize these compounds since the deletion of *cdcA* or *padA* resulted in abolished or reduced growth on cinnamic acid and sorbic acid (**Figure 2**). This also indicates that the suggested alternative cinnamic acid pathway toward *p*-coumaric acid is not sufficient to counteract the toxicity of cinnamic acid. Growth was not completely abolished on

TABLE 5 | Number of BLAST hits of the cinnamic acid decarboxylation cluster.

Aspergilli	Section	Gene ID NRRL3_								
					cdcA	*sdrA*	*padA*			
		8293	8294	8295	8296	8297[a]	8298	8299[a]	8300	8301
A. niger	NB	5	1	3	3	1	3	1	2	7
A. luchuensis	NB	3	1	8	3	1	2	2	2	6
A. kawachii	NB	3	1	4	2	1	2	2	2	6
A. tubingensis	NB	4	1	2	3	1	2	2	2	7
A. neoniger	NB	3	1	2	3	1	2	2	2	6
A. vadensis	NB	3	1	6	3	1	2	1	2	6
A. piperis	NB	3	1	4	2	1	2	2	2	6
A. brasiliensis	NB	3	0	7	3	1	3	1	2	9
A. sclerotiicarbonarius	NB	4	1	3	2	1	2	2	2	7
A. ibericus	NB	3	0	7	1	1	2	2	2	7
A. carbonarius	NB	3	0	6	2	1	2	2	2	7
A. sclerotioniger	NB	3	0	4	1	1	1	2	2	4
A. ellipticus	NB	3	0	1	7	1	5	1	4	6
A. heteromorphus	NB	3	0	1	2	1	2	1	3	7
A. aculeatus	NU	4	0	2	3	1	2	1	4	5
A. japonicus	NU	4	0	3	3	1	2	1	4	6
A. violaceofuscus	NU	4	0	2	2	1	2	1	4	7
A. nidulans	*Nidulantes*	2	0	1	1	1	1	0	4	6
A. sydowii	*Versicolores*	3	0	4	3	1	3	2	4	9
A. versicolor	*Versicolores*	4	0	6	1	1	1	4	4	11
A. steynii	*Circumdati*	3	0	3	3	1	3	1	4	3
A. wentii	*Cremei*	3	0	6	2	1	2	1	4	8
A. terreus	*Terrei*	3	0	2	2	1	2	2	5	5
A. glaucus	*Aspergillus*	4	0	5	3	1	2	1	1	3
A. flavus	*Flavi*	3	0	2	2	1	2	1	2	9
A. oryzea	*Flavi*	3	0	0	2	1	2	1	2	9
A. campestris	*Candidi*	1	0	3	0	0	0	1	2	4
A. novofumigatus	*Fumigati*	2	0	3	2	1	2	2	5	6
A. fumigatus	*Fumigati*	1	0	1	0	0	0	1	4	3
A. clavatus	*Clavati*	1	0	3	0	0	0	1	7	3

The amino acid sequence of the A. niger genes were used as queries against Aspergillus genomes downloaded from JGI Mycocosm. Numbers represent the number of BLAST hits. Highlighted in green are genes clustered with cdcA or padA and with sdrA. Highlighted in white are genes not clustered with cdcA, sdrA, or padA and in yellow are genes that are clustered but not together with cdcA, sdrA, or padA.

[a]*Amino acid sequence BLASTS resulted in ≥15 hits, therefore an E-value cut-off of 10^{-60} was used.*

NB, Nigri-Biseriates; NU, Nigri-Uniseriates.

cinnamic acid when *sdrA* was deleted, which could be explained by the fact that *cdcA* and *padA* were still lowly expressed (**Table 3**). Deletion of either *cdcA*, *sdrA*, or *padA* did not affect the growth on ferulic and *p*-coumaric acid, which supports the outcome of a previous study showing that *cdcA* and *padA* were not induced by ferulic acid or *p*-coumaric acid (Stratford et al., 2012). This indicates that *cdcA*, *sdrA*, and *padA* are exclusively involved in cinnamic acid and sorbic acid metabolism.

Transcriptome analysis of *A. niger* revealed that *sdrA* was lowly expressed by cinnamic acid, cinnamyl alcohol and sorbic acid (**Supplementary Table 4**), which is in agreement with a previous study which showed this by qRT-PCR (Plumridge et al., 2010). However, its expression was significantly upregulated during growth on cinnamic acid and sorbic acid (**Table 3**), which indicates that low levels of SdrA are sufficient for the regulation of the cinnamic acid and sorbic acid decarboxylation cluster. Deletion of *sdrA* revealed a significant reduction of the expression of 50 genes in both cinnamic acid and sorbic acid. These 50 genes included *cdcA* and *padA*, revealing that SdrA regulates these two genes either directly or indirectly (**Supplementary Table 4**). It was reported earlier that the genes, flanking either side of the cluster, are not induced by sorbic acid (Plumridge et al., 2010). However, our transcriptome data revealed that SdrA tightly regulates six of these genes. It remains unknown which function the corresponding enzymes have in the cinnamic/sorbic acid decarboxylation pathway. NRRL3_8293 encode a flavin reductase and could be involved in the reduction of prenylated FMN. NRRL3_8295 contains a BTB/POZ domain

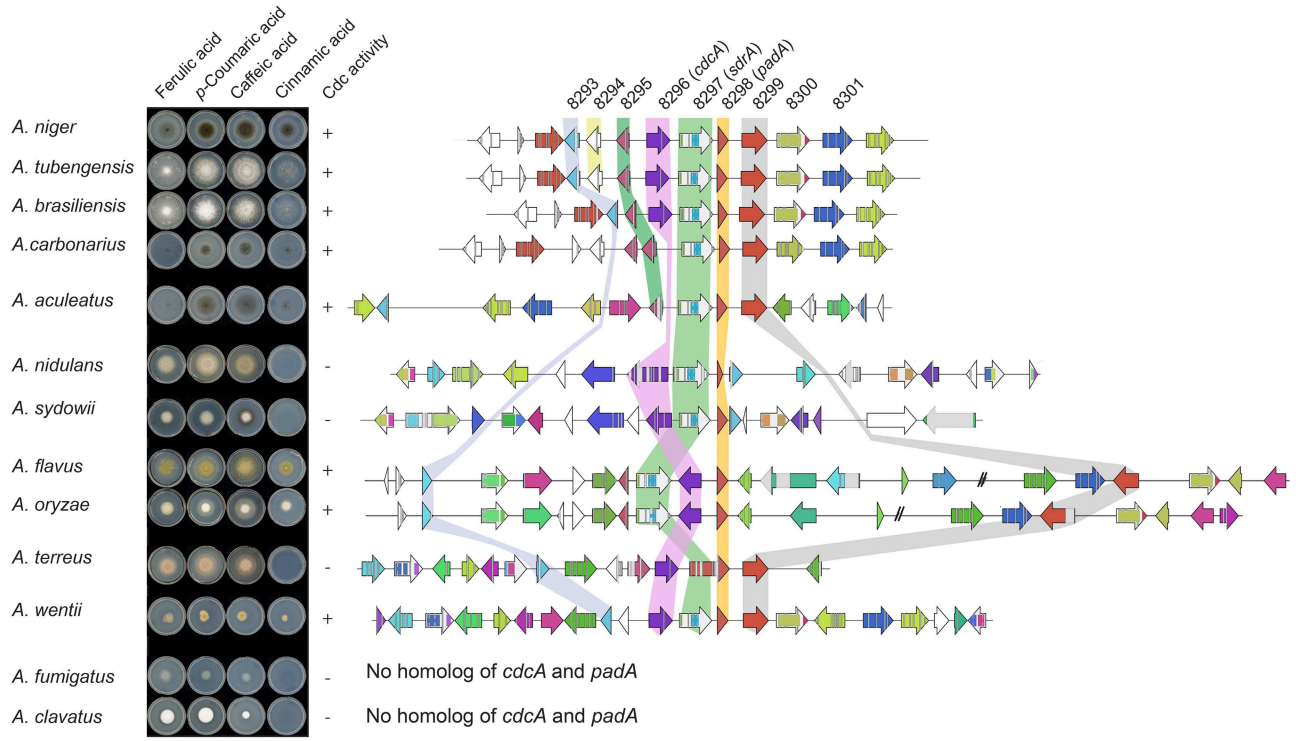

FIGURE 4 | Synteny analysis and growth test of 13 Aspergilli. No orthologs of *cdcA* or *padA* were found in *A. fumigatus* and *A. clavatus*, therefore no cluster was added. Genes clustered on another scaffold are marked with a double dash.

which are known to be involved in transcriptional regulation (Zollman et al., 1994; Daniel and Reynolds, 1999; Li et al., 1999). NRRL3_8299 encode a carboxylesterase which could be involved in the hydrolysis of cinnamyl esters. Several genes of the cinnamic acid and sorbic acid decarboxylation cluster were also affected by cinnamyl alcohol with the exception of *sdrA*, NRRL3_8294, and NRRL3_8299. Both *sdrA* and NRRL3_8294 have a high fold change and were significantly different but the FPKM value were below 10 and therefore we cannot state with certainty that these genes are affected (**Tables 3**, **4**). The deletion of *sdrA* resulted in reduced expression of *cdcA*, *padA*, NRRL3_8293, and NRRL3_8295 on cinnamyl alcohol, indicating that cinnamyl alcohol is part of the cinnamic acid metabolic pathway. The remaining 43 down-regulated genes are currently not connected to the cinnamic acid metabolic pathway. However, the expression of three putative transporters was reduced, which could be important for cinnamic acid or styrene transport (**Supplementary Table 4**).

Deletion of *sdrA* did not result in abolished growth on cinnamic acid or sorbic acid. In addition, *cdcA* and *padA* were still expressed in Δ*sdrA* indicating that a second transcription factor is likely involved. One candidate for regulation of *cdcA* and *padA* is NRRL3_8295, present in the cluster, but also three putative fungal-specific transcription factors (NRRL3_7314, NRRL3_9846, and NRRL3_7351) were upregulated by cinnamic acid, sorbic acid and cinnamyl alcohol in N593 and were not affected by the deletion of *sdrA* (data not shown). Fungal specific transcription factors containing Zinc fingers are known to bind directly to regulatory motifs in promoters. Such regulatory motifs have been suggested in the promoters of *cdcA* and *padA* (Plumridge et al., 2010), but these did not occur in the neighboring genes.

Synteny analysis of the cinnamic acid and sorbic acid decarboxylation cluster in 30 *Aspergillus* genomes revealed that the cluster is highly conserved in Aspergilli of the Nigri-Biseriates clade. Other Aspergilli, such as *A. fumigatus* and *A. clavatus* that lack orthologs of *cdcA* and *padA* were unable to grow on cinnamic acid (**Figure 4**, **Table 5**). It has been reported that *A. nidulans* is unable to decarboxylate cinnamic acid, which could be caused by the truncated PadA protein (Plumridge et al., 2010). In addition, analysis of RNAseq data of *A. nidulans* revealed that the predicted intron and exon boundaries of *A. nidulans cdcA* were incorrect (**Supplementary Figure 1**). Ahen comparing the corrected gene model to *A. niger cdcA*, two internal deletions, one insertion and one substitution were identified in the sequence of *A. nidulans cdcA*. The second deletion results in a premature stop codon. This could be an alternative explanation why *A. nidulans* is unable to grow on cinnamic acid. *A. flavus, A. oryzae,* and *A. wentii* were able to grow on cinnamic acid and all had orthologs of *cdcA*, *sdrA, padA,* and NRRL3_8293 in their genome. In agreement with this, two *A. oryzae* strains were able to grow on cinnamic acid in a previous study (Plumridge et al., 2010).

Transcriptome analysis also revealed that an enzyme converting benzoic acid to *p*-hydroxybenzoic acid (**Figure 1**), benzoate 4-monooxygenase A (BphA, Van Gorcom et al., 1990), is highly upregulated (170.6 fold) by benzoic acid compared

to no carbon source control. In addition, *bphA* is 24.7- and 59.6-fold upregulated by cinnamic acid and cinnamyl alcohol, respectively, while it was not induced by sorbic acid and salicylic acid, confirming that cinnamic acid and cinnamyl alcohol are converted toward benzoic acid. Our results suggest that SdrA is specifically involved in cinnamic acid conversion and not in the downstream regulation of this pathway since no phenotypic effect was observed on styrene, benzoic acid or *p*-hydroxybenzoic acid (**Figure 2**). In addition, there is strong induction of *bphA* by benzoic acid, cinnamic acid and cinnamyl alcohol in both *A. niger* N593 and Δ*sdrA*, supporting the finding that SdrA is not involved in the expression of genes of the downstream pathway. This induction of *bphA* by cinnamic acid and benzoic acid corresponds with a previous study (de Vries et al., 2002). It is clear that the decarboxylation of cinnamic acid to styrene is the main pathway in *A. niger*. Styrene, styrene glycol and two unidentified compounds have been detected from *A. niger* grown on cinnamic acid (Clifford et al., 1969). In the basidiomycete *Pleurotus ostreatus,* styrene is converted to phenyl-1,2-ethanediol (styrene glycol) and benzoic acid and it has been suggested that styrene oxide and mandelic acid are intermediates in this metabolic pathway (Braun-Lüllemann et al., 1997). Another pathway has been observed in the ascomycete *Phomopsis liquidambari*, where cinnamic acid is decarboxylated to styrene after which it is oxidized to benzaldehyde followed by the oxidation to benzoic acid (Xie and Dai, 2015).

Recently, an extensive substrate analysis of CdcA from *A. niger* showed that the main substrates for CdcA are cinnamic acid and sorbic acid since ≥99% was decarboxylated, while ≤70% of the ferulic acid or *p*-coumaric acid was decarboxylated (Aleku et al., 2018). No phenotypic difference on ferulic acid, *p*-coumaric acid and caffeic acid were observed (**Figure 1**). In addition, Aspergilli that were unable to grow on cinnamic acid could grow on ferulic acid, *p*-coumaric acid and caffeic acid. This indicates that the biological function of CdcA is not the decarboxylation of ferulic acid since no induction or phenotype was observed by ferulic acid (**Figure 4**). We propose, based on the substrate preference, the induction pattern and the phenotypic and transcriptomic analysis, to change the name of ferulic acid decarboxylase (FdcA) to cinnamic acid decarboxylase (CdcA) which fits with its biological function. In addition, CdcA also corresponds better with its enzymatic function since ferulic acid (3-methoxy-4-hydroxycinnamic acid) and *p*-coumaric acid (4-hydroxycinnamic acid) both have a cinnamic acid-based chemical structure. In *Aspergillus luchuensis*, which is closely related to *A. niger*, a phenolic acid decarboxylase (AlPad) has been characterized which is able to decarboxylate ferulic acid, *p*-coumaric acid and caffeic acid (Maeda et al., 2018). In *A. niger*, a 99% identical ortholog of this gene is present and therefore it is more likely that this enzyme is the ferulic acid decarboxylase.

CONCLUSION

In summary, we identified new regulatory targets of SdrA through the whole genome transcriptome analysis. These genes are clustered in the *A. niger* genome and highly conserved in Aspergilli closely related to *A. niger*. In addition, phenotypic analysis revealed that CdcA (formerly FdcA) and PadA are required exclusively for the decarboxylation of cinnamic acid and sorbic acid, but not for the decarboxylation of other aromatic compounds. Our results provide a better understanding of the aromatic metabolic pathways and their regulation in filamentous fungi. This can unlock strategies to design new fungal cell factories, e.g., to obtain higher yields of cinnamic acid by blocking the degradation pathway, or to increase the synthesis of styrene by overexpressing *cdcA*.

DATA AVAILABILITY STATEMENT

The datasets generated for this study can be found in the Gene Expression Omnibus (GEO) under accession numbers SRR8275478, SRR8275427, SRR8275426, SRR8275534, SRR8275532, SRR8275533, SRR8275539, SRR8275424, SRR8275535, SRR8275425, SRR8275431, SRR8275436, SRR8275434, SRR8275437, SRR8275435, SRR8275432, SRR8275406, SRR8275433, SRR8275414, SRR8275470, SRR8275471, SRR8275472, SRR8275446, SRR8275447, SRR8275468, SRR8275469, SRR8275467, SRR8275449, SRR8275448, SRR8275450, SRR8275439, SRR8275523, SRR8275522, SRR8275404, SRR8275498, and SRR8275413.

AUTHOR CONTRIBUTIONS

RL conducted the experiments, analyzed the data, and wrote the manuscript. JN contributed to the synteny analysis and visualization. MP processed and analyzed the RNA sequencing data. MW, AL, VN, and IG performed the RNA sequencing. AD, JV, and KH contributed to data interpretation and commented on the manuscript. RV conceived and supervised the overall project. All authors commented on the manuscript.

FUNDING

This project was supported through FALCON by the European Union's Horizon 2020 research and innovation programme under grant agreement No. 720918. The work conducted by the U.S. Department of Energy Joint Genome Institute, a DOE Office of Science User Facility, was supported by the Office of Science of the U.S. Department of Energy under Contract No. DE-AC02-05CH11231.

ACKNOWLEDGMENTS

We want to thank DOE Joint Genome Institute for their RNAseq service and David B. Archer, Jos Houbraken and Willem J. H. van Berkel for helpful discussion.

SUPPLEMENTARY MATERIAL

The Supplementary Material for this article can be found online at: https://www.frontiersin.org/articles/10.3389/fbioe.2019.00249/full#supplementary-material

REFERENCES

Aguilar-Pontes, M. V., Brandl, J., McDonnell, E., Strasser, K., Nguyen, T. T. M., Riley, R., et al. (2018). The gold-standard genome of *Aspergillus niger* NRRL 3 enables a detailed view of the diversity of sugar catabolism in fungi. *Stud. Mycol.* 91, 61–78. doi: 10.1016/j.simyco.2018.10.001

Aleku, G. A., Prause, C., Bradshaw-allen, R. T., and Plasch, K. (2018). Terminal alkenes from acrylic acid derivatives via non-oxidative enzymatic decarboxylation by ferulic acid decarboxylases. *ChemCatChem* 10, 4043–4052. doi: 10.1002/cctc.201800643

Almagro Armenteros, J. J., Sønderby, C. K., Sønderby, S. K., Nielsen, H., and Winther, O. (2017). DeepLoc: prediction of protein subcellular localization using deep learning. *Bioinformatics* 33, 3387–3395. doi: 10.1093/bioinformatics/btx431

Arnaud, M. B., Cerqueira, G. C., Inglis, D. O., Skrzypek, M. S., Binkley, J., Chibucos, M. C., et al. (2012). The Aspergillus Genome Database (AspGD): recent developments in comprehensive multispecies curation, comparative genomics and community resources. *Nucleic Acids Res.* 40, 653–659. doi: 10.1093/nar/gkr875

Averesch, N. J. H., and Krömer, J. O. (2018). Metabolic engineering of the shikimate pathway for production of aromatics and derived compounds—present and future strain construction strategies. *Front. Bioeng. Biotechnol.* 6:32. doi: 10.3389/fbioe.2018.00032

Benocci, T., Aguilar-Pontes, M. V., Zhou, M., Seiboth, B., and De Vries, R. P. (2017). Regulators of plant biomass degradation in ascomycetous fungi. *Biotechnol. Biofuels* 10, 1–25. doi: 10.1186/s13068-017-0841-x

Bocks, S. M. (1966). Fungal metabolism I the transformation of coumarin, o-coumaric acid and trans-cinnamic acid by *Aspergillus niger*. *Phytochemistry* 398, 127–130. doi: 10.1016/0031-9422(67)85017-9

Bos, C. J., Debets, A. J. M., Swart, K., Huybers, A., Kobus, G., and Slakhorst, S. M. (1988). Genetic analysis and the construction of master strains for assignment of genes to six linkage groups in *Aspergillus niger*. *Curr. Genet*. 14, 437–443. doi: 10.1007/BF00521266

Braun-Lüllemann, A., Majcherczyk, A., and Hüttermann, A. (1997). Degradation of styrene by white-rot fungi. *Appl. Microbiol. Biotechnol.* 47, 150–155. doi: 10.1007/s002530050904

Chemler, J. A., and Koffas, M. A. (2008). Metabolic engineering for plant natural product biosynthesis in microbes. *Curr. Opin. Biotechnol.* 19, 597–605. doi: 10.1016/j.copbio.2008.10.011

Clifford, D. R., Faulkner, J. K., Walker, J. R. L., and Woodcock, D. (1969). Metabolism of cinnamic acid by *Aspergillus niger*. *Phytochemistry* 8, 549–552. doi: 10.1016/S0031-9422(00)85398-4

Daniel, J. M., and Reynolds, A. B. (1999). The catenin p120 ctn interacts with Kaiso, a novel BTB/POZ domain zinc finger transcription factor. *Mol. Cell. Biol.* 19, 3614–3623. doi: 10.1128/MCB.19.5.3614

de Vries, R. P., Burgers, K., Samson, R. A., and Visser, J. (2004). A new black *Aspergillus* species, *A.* vadensis*, is a promising host for homologous and heterologous protein production. Appl. Environ. Microbiol.* 70, 3954–3959. doi: 10.1128/AEM.70.7.3954-3959.2004

de Vries, R. P., Riley, R., Wiebenga, A., Aguilar-Osorio, G., Amillis, S., Uchima, C. A., et al. (2017). Comparative genomics reveals high biological diversity and specific adaptations in the industrially and medically important fungal genus *Aspergillus*. *Genome Biol.* 18:28. doi: 10.1186/s13059-017-1151-0

de Vries, R. P., Van Kuyk, P. A., Kester, H. C. M., and Visser, J. (2002). The *Aspergillus niger faeB* gene encodes a second feruloyl esterase involved in pectin and xylan degradation and is specifically induced in the presence of aromatic compounds. *Biochem. J.* 363, 377–386. doi: 10.1042/bj3630377

Fedorova, N. D., Khaldi, N., Joardar, V. S., Maiti, R., Amedeo, P., Anderson, M. J., et al. (2008). Genomic islands in the pathogenic filamentous fungus *Aspergillus fumigatus*. *PLoS Genet.* 4:e1000046. doi: 10.1371/journal.pgen.1000046

Galagan, J. E., Calvo, S. E., Cuomo, C., Ma, L. J., Wortman, J. R., Batzoglou, S., et al. (2005). Sequencing of *Aspergillus nidulans* and comparative analysis with *A. fumigatus* and *A. oryzae*. *Nature* 438, 1105–1115. doi: 10.1038/nature04341

Grigoriev, I. V., Nikitin, R., Haridas, S., Kuo, A., Ohm, R., Otillar, R., et al. (2014). MycoCosm portal: gearing up for 1000 fungal genomes. *Nucleic Acids Res.* 42, 699–704. doi: 10.1093/nar/gkt1183

Gruenwald, J., Freder, J., and Armbruester, N. (2010). Cinnamon and health. *Crit. Rev. Food Sci. Nutr.* 50, 822–834. doi: 10.1080/10408390902773052

He, Z. D., Qiao, C. F., Han, Q. B., Cheng, C. L., Xu, H. X., Jiang, R. W., et al. (2005). Authentication and quantitative analysis on the chemical profile of Cassia Bark (*Cortex Cinnamomi*) by high-pressure liquid chromatography. *J. Agric. Food Chem.* 53, 2424–2428. doi: 10.1021/jf048116s

Hoskins, J. A. (1984). The occurrence, metabolism and toxicity of cinnamic acid and related compounds. *J. Appl. Toxicol.* 4, 283–292. doi: 10.1002/jat.2550040602

Kowalczyk, J. E., Lubbers, R. J. M., Peng, M., Battaglia, E., Visser, J., and De Vries, R. P. (2017). Combinatorial control of gene expression in *Aspergillus niger* grown on sugar beet pectin. *Sci. Rep.* 7, 1–12. doi: 10.1038/s41598-017-12362-y

Lafeuille, J. L., Buniak, M. L., Vioujas, M. C., and Lefevre, S. (2009). Natural formation of styrene by cinnamon mold flora. *J. Food Sci.* 74:M276–M283. doi: 10.1111/j.1750-3841.2009.01206.x

Latif, S., Chiapusio, G., and Weston, L. A. (2017). *Allelopathy and the Role of Allelochemicals in Plant Defence*. Oxford: Elsevier Ltd.

Li, X., Peng, H., Schultz, D. C., Lopez-Guisa, J. M., Rauscher, F. J., and Marmorstein, R. (1999). Structure-function studies of the BTB/POZ transcriptional repression domain from the promyelocytic leukemia zinc finger oncoprotein. *Cancer Res.* 59, 5275–5282. doi: 10.2210/pdb1cs3/pdb

Liewen, M. B., and Marth, E. H. (2016). Growth and inhibition of microorganisms in the presence of sorbic acid: a review. *J. Food Prot.* 48, 364–375. doi: 10.4315/0362-028X-48.4.364

Love, M. I., Huber, W., and Anders, S. (2014). Moderated estimation of fold change and dispersion for RNA-seq data with DESeq2. *Genome Biol.* 15, 1–21. doi: 10.1186/s13059-014-0550-8

Lubbers, R. J. M., Dilokpimol, A., Visser, J., Mäkelä, M. R., Hildén, K. S., and de Vries, R. P. (2019). A comparison between the homocyclic aromatic metabolic pathways from plant-derived compounds by bacteria and fungi. *Biotechnol. Adv*. doi: 10.1016/j.biotechadv.2019.05.002

Machida, M., Asai, K., Sano, M., Tanaka, T., Kumagai, T., Terai, G., et al. (2005). Genome sequencing and analysis of *Aspergillus oryzae*. *Nature* 438, 1157–1161. doi: 10.1038/nature04300

Maeda, M., Tokashiki, M., Tokashiki, M., Uechi, K., Ito, S., and Taira, T. (2018). Characterization and induction of phenolic acid decarboxylase from *Aspergillus luchuensis*. *J. Biosci. Bioeng.* 126, 162–168. doi: 10.1016/j.jbiosc.2018.02.009

Marth, E. H., Capp, C. M., Hasenzahl, L., Jackson, H. W., and Hussong, R. V. (1966). Degradation of potassium sorbate by *Penicillium* species. *J. Dairy Sci.* 49, 1197–1205. doi: 10.3168/jds.S0022-0302(66)88053-0

Martins, T. M., Hartmann, D. O., Planchon, S., Martins, I., Renaut, J., and Silva Pereira, C. (2015). The old 3-oxoadipate pathway revisited: new insights in the catabolism of aromatics in the saprophytic fungus *Aspergillus nidulans*. *Fungal Genet. Biol.* 74, 32–44. doi: 10.1016/j.fgb.2014.11.002

Meyer, V., Arentshorst, M., El-Ghezal, A., Drews, A. C., Kooistra, R., van den Hondel, C. A. M. J. J., et al. (2007). Highly efficient gene targeting in the *Aspergillus niger kusA* mutant. *J. Biotechnol.* 128, 770–775. doi: 10.1016/j.jbiotec.2006.12.021

Milstein, O., Vered, Y., Shragina, L., Gressel, J., Flowers, H. M., and Hüttermann, A. (1983). Metabolism of lignin related aromatic compounds by *Aspergillus japonicus*. *Arch. Microbiol.* 135, 147–154. doi: 10.1007/BF00408025

Mukai, N., Masaki, K., Fujii, T., Kawamukai, M., and Iefuji, H. (2010). PAD1 and FDC1 are essential for the decarboxylation of phenylacrylic acids in *Saccharomyces cerevisiae*. *J. Biosci. Bioeng.* 109, 564–569. doi: 10.1016/j.jbiosc.2009.11.011

Nierman, W. C., Pain, A., Anderson, M. J., Wortman, J. R., Kim, H. S., Arroyo, J., et al. (2005). Genomic sequence of the pathogenic and allergenic filamentous fungus *Aspergillus fumigatus*. *Nature* 438, 1151–1156. doi: 10.1038/nature04332

Payne, G. A., Nierman, W. C., Wortman, J. R., Pritchard, B. L., Brown, D., Dean, R. A., et al. (2006). Whole genome comparison of *Aspergillus flavus* and *A. oryzae*. *Med. Mycol.* 44, 9–11. doi: 10.1080/13693780600835716

Payne, K. A. P., White, M. D., Fisher, K., Khara, B., Bailey, S. S., Parker, D., et al. (2015). New cofactor supports α,β-unsaturated acid decarboxylation via 1,3-dipolar cycloaddition. *Nature* 522, 497–501. doi: 10.1038/nature14560

Pinches, S. E., and Apps, P. (2007). Production in food of 1,3-pentadiene and styrene by *Trichoderma* species. *Int. J. Food Microbiol.* 116, 182–185. doi: 10.1016/j.ijfoodmicro.2006.12.001

Plumridge, A., Melin, P., Stratford, M., Novodvorska, M., Shunburne, L., Dyer, P. S., et al. (2010). The decarboxylation of the weak-acid preservative, sorbic acid,

is encoded by linked genes in *Aspergillus* spp. *Fungal Genet. Biol.* 47, 683–692. doi: 10.1016/j.fgb.2010.04.011

Punt, P. J., Oliver, R. P., Dingemanse, M. A., Pouwels, P. H., and van den Hondel, C. A. (1987). Transformation of *Aspergillus* based on the hygromycin B resistance marker from *Escherichia coli*. *Gene* 56, 117–124. doi: 10.1016/0378-1119(87)90164-8

Richard, P., Viljanen, K., and Penttilä, M. (2015). Overexpression of PAD1 and FDC1 results in significant cinnamic acid decarboxylase activity in *Saccharomyces cerevisiae*. *AMB Express* 5, 1–5. doi: 10.1186/s13568-015-0103-x

Stratford, M., Plumridge, A., Pleasants, M. W., Novodvorska, M., Baker-Glenn, C. A. G., Pattenden, G., et al. (2012). Mapping the structural requirements of inducers and substrates for decarboxylation of weak acid preservatives by the food spoilage mould *Aspergillus niger*. *Int. J. Food Microbiol.* 157, 375–383. doi: 10.1016/j.ijfoodmicro.2012.06.007

Thompson, B., Machas, M., and Nielsen, D. R. (2015). Creating pathways towards aromatic building blocks and fine chemicals. *Curr. Opin. Biotechnol.* 36, 1–7. doi: 10.1016/j.copbio.2015.07.004

Van Gorcom, R. F. M., Boschloo, J. G., Kuijvenhoven, A., Lange, J., Vanvark, A. J., Bos, C. J., et al. (1990). Isolation and molecular characterization of the benzoate-*para*-hydroxylase gene (*Bpha*) of *Aspergillus-niger* - a member of a new gene family of the cytochrome-P450 superfamily. *Mol. Gen. Genet.* 223, 192–197. doi: 10.1007/BF00265053

Vargas-Tah, A., and Gosset, G. (2015). Production of cinnamic and *p*-hydroxycinnamic acids in engineered microbes. *Front. Bioeng. Biotechnol.* 3, 1–10. doi: 10.3389/fbioe.2015.00116

Xie, X. G., and Dai, C. C. (2015). Biodegradation of a model allelochemical cinnamic acid by a novel endophytic fungus *Phomopsis liquidambari*. *Int. Biodeterior. Biodegrad.* 104, 498–507. doi: 10.1016/j.ibiod.2015.08.004

Yamada, S., Nabe, K., and Izuo, N. (1981). Production of L-phenylalanine from trans-cinnamic acid with *Rhodotorula glutinis* containing L-phenylalanine ammonia-lyase activity. *Appl. Environ. Microbiol.* 42, 773–778.

Zollman, S., Godt, D., Privé, G. G., Couderc, J. L., and Laski, F. A. (1994). The BTB domain, found primarily in zinc finger proteins, defines an evolutionarily conserved family that includes several developmentally regulated genes in *Drosophila*. *Proc. Natl. Acad. Sci. U.S.A.* 91, 10717–10721. doi: 10.1073/pnas.91.22.10717

Conflict of Interest: The authors declare that the research was conducted in the absence of any commercial or financial relationships that could be construed as a potential conflict of interest.

frontiers in Bioengineering and Biotechnology

ORIGINAL RESEARCH
published: 09 October 2019
doi: 10.3389/fbioe.2019.00241

Cell Factory Design and Culture Process Optimization for Dehydroshikimate Biosynthesis in *Escherichia coli*

Si-Sun Choi[1†], *Seung-Yeul Seo*[2,3†], *Sun-Ok Park*[2], *Han-Na Lee*[1,2], *Ji-soo Song*[1], *Ji-yeon Kim*[1], *Ji-Hoon Park*[1], *Sangyong Kim*[4,5], *Sang Joung Lee*[2], *Gie-Taek Chun*[3*] and *Eung-Soo Kim*[1*]

[1] Department of Biological Engineering, Inha University, Incheon, South Korea, [2] STR Biotech Co., Ltd., Chuncheon-si, South Korea, [3] Department of Molecular Bio-Science, Kangwon National University, Chuncheon-si, South Korea, [4] Green Chemistry and Materials Group, Korea Institute of Industrial Technology, Cheonan-si, South Korea, [5] Green Process and System Engineering Major, Korea University of Science and Technology (UST), Daejeon, South Korea

3-Dehydroshikimate (DHS) is a useful starting metabolite for the biosynthesis of muconic acid (MA) and shikimic acid (SA), which are precursors of various valuable polymers and drugs. Although DHS biosynthesis has been previously reported in several bacteria, the engineered strains were far from satisfactory, due to their low DHS titers. Here, we created an engineered *Escherichia coli* cell factory to produce a high titer of DHS as well as an efficient system for the conversion DHS into MA. First, the genes showing negative effects on DHS accumulation in *E. coli*, such as *tyrR* (tyrosine dependent transcriptional regulator), *ptsG* (glucose specific sugar: phosphoenolpyruvate phosphotransferase), and *pykA* (pyruvate kinase 2), were disrupted. In addition, the genes involved in DHS biosynthesis, such as *aroB* (DHQ synthase), *aroD* (DHQ dehydratase), *ppsA* (phosphoenolpyruvate synthase), *galP* (D-galactose transporter), *aroG* (DAHP synthase), and *aroF* (DAHP synthase), were overexpressed to increase the glucose uptake and flux of intermediates. The redesigned DHS-overproducing *E. coli* strain grown in an optimized medium produced ∼117 g/L DHS in 7-L fed-batch fermentation, which is the highest level of DHS production demonstrated in *E. coli*. To accomplish the DHS-to-MA conversion, which is originally absent in *E. coli*, a codon-optimized heterologous gene cassette containing *asbF, aroY*, and *catA* was expressed as a single operon under a strong promoter in a DHS-overproducing *E. coli* strain. This redesigned *E. coli* grown in an optimized medium produced about 64.5 g/L MA in 7-L fed-batch fermentation, suggesting that the rational cell factory design of DHS and MA biosynthesis could be a feasible way to complement petrochemical-based chemical processes.

Keywords: dehydroshikimate, cell factory design, *Escherichia coli*, culture process, production optimization

OPEN ACCESS

Edited by:
Nils Jonathan Helmuth Averesch, Stanford University, United States

Reviewed by:
Zhen Chen, Tsinghua University, China
Zhi-Gang Jeff Qian, Shanghai Jiao Tong University, China

***Correspondence:**
Gie-Taek Chun
gtchun8547@gmail.com
Eung-Soo Kim
eungsoo@inha.ac.kr

†These authors have contributed equally to this work

Specialty section:
This article was submitted to Bioprocess Engineering, a section of the journal Frontiers in Bioengineering and Biotechnology

Received: *29 June 2019*
Accepted: *11 September 2019*
Published: *09 October 2019*

Citation:
Choi S-S, Seo S-Y, Park S-O, Lee H-N, Song J, Kim J, Park J-H, Kim S, Lee SJ, Chun G-T and Kim E-S (2019) Cell Factory Design and Culture Process Optimization for Dehydroshikimate Biosynthesis in Escherichia coli. Front. Bioeng. Biotechnol. 7:241. doi: 10.3389/fbioe.2019.00241

INTRODUCTION

Aromatic amino acid biosynthetic pathways have long been a potential source for commercially relevant chemicals with diverse industrial applications (Tzin and Galili, 2010). One of the core metabolites that facilitate the production of useful intermediates in aromatic amino acid biosynthetic pathways is 3-dehydroshikimate (DHS), a key intermediate in the biosynthesis of shikimic acid (SA), muconic acid (MA), vanillin, and protocatechuate (PCA) (Li et al., 2019). This group of chemicals has drawn much attention for the major feedstock for food, drugs and commodity chemicals (Chen and Nielsen, 2013; Becker and Wittmann, 2015). Bio-based production of these compounds is a promising alternative to the current petrochemical-based production routes that are a cause of environment and energy concerns (Jan and Cavallaro, 2015). MA is easily converted into adipic acid and terephthalic acid, which find universal application in the synthesized nylons and polymer polyethylene terephthalate (PET) industries (Draths and Frost, 1994; Kruyer and Peralta-Yahya, 2017). In addition, SA is an initial precursor for the production of a well-known anti-virial compound named oseltamivir phosphate, also known as Tamiflu®.

DHS has a six-member carbon ring with two asymmetric carbons, which is difficult and costly to synthesize chemically (Richman et al., 1996; Nishikura-Imamura et al., 2014). On the other hand, DHS is a natural metabolite found in the shikimate pathway in plants, fungi, and bacteria, making its production feasible through microbial fermentation (Li et al., 1999). DHS biosynthesis in *E. coli* starts from glucose, via the glycolysis pathway, a central carbon metabolism (**Figure 1**). Two intermediates, phosphoenolpyruvate (PEP) and erythrose-4-phosphate (E4P), are converted to DHS via 3-deoxy-D-arabino-heptulosonate-7-phosphate (DAHP) and dehydroquinate (DHQ) by DAHP synthase (*aroG, aroF,* and *aroH*), DHQ synthase (*aroB*), and DHQ dehydratase (*aroD*).

For several decades, many approaches have been applied to increase the carbon flux toward shikimate biosynthetic pathway for the production of several aromatic compounds. For example, there was an attempt to solve the feedback inhibition issue of DAHP synthase to improve the production of aromatic compounds (Pittard and Yang, 2008; Wang et al., 2013). Another strategy involved the inactivation of the PEP-consuming PTS system and use of another PEP-independent glucose uptake pathway, as PEP is an important precursor of an

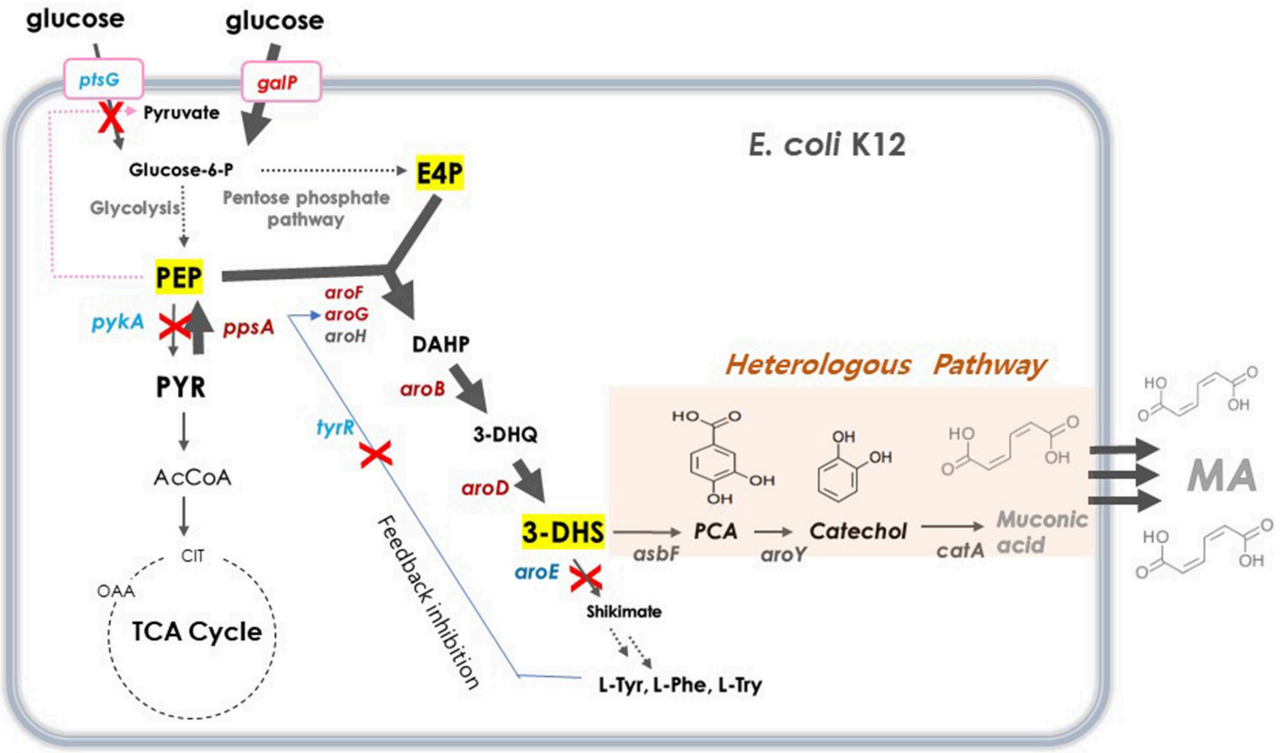

FIGURE 1 | Schematic overview of metabolic pathway for DHS biosynthesis in *E. coli*. Red crosses denote disrupted genes and bold blue arrows denote steps that are overexpressed. Dashed arrows represent two or more steps. G6P, glucose-6-phosphate; PEP, phosphoenolpyruvate; PYR, pyruvate; AcCoA, acetyl-coenzyme A; OAA, oxaloacetate; CIT, citrate; E4P, erythrose4-phosphate; DAHP, 3-deoxy-D-arabinoheptulosonate-7-phosphate; DHQ, 3-de-hydroquinate; DHS, 3-dehydroshikimate; SA, shikimic acid; PCA, protocatechuate; CA, catechol, MA, muconic acid. *ptsG*, glucose specific sugar: phosphoenolpyruvate phosphotransferase; *galP*, D-galactose transporter; *zwf*, glucose-6-phosphate 1-dehydrogenase; *tktA*, transketolase; *tyrR*, tyrosine dependent transcriptional regulator; *pykF*, pyruvate kinase 1; *pykA*, pyruvate kinase 2; *ppsA*, phosphoenolpyruvate synthase; *pckA*, phosphoenolpyruvate carboxykinase; *aroG*, DAHP synthase; *aroF*, DAHP synthase; *aroB*, DHQ synthase; *aroD*, DHQ dehydratase; *aroE*, shikimate dehydrogenase: $asbF^{Eopt}$, 3-dehydroshikimate(DHS) dehydratase; *pcaG/H*, codon-optimized PCA deoxygenase; $aroY^{Eopt}$, codon-optimized PCA decarboxylase; $catA^{Eopt}$, codon-optimized CA 1,2 -dioxygenase.

aromatic compound (Patnaik et al., 1995; Chandran et al., 2003; Johansson et al., 2005). Yet another approach was to eliminate the pyruvate kinases involved in PEP conversion to pyruvate, thereby enhancing the pathway that converts pyruvate to PEP (Patnaik et al., 1995; Chandran et al., 2003; Johansson et al., 2005; Meza et al., 2012; Rodriguez et al., 2013). Combinations of these strategies are typically used to improve the productivity of aromatic compounds (Yi et al., 2002; Wang et al., 2013; Rodriguez et al., 2014; Martínez et al., 2015; Lee et al., 2018).

Recently, we engineered a *Corynebacterum glutamicum* strain to overproduce MA from glucose, through redesign of the aromatic amino acid biosynthetic pathway (Lee et al., 2018). Through heterologous expression of a codon-optimized PCA decarboxylase gene cluster under a strong promoter, and deletions of several key genes involved in MA intermediate bypass routes, an optimized pathway for DHS-PCA-CA-MA was successfully constructed in *C. glutamicum*. Optimization of culture media and processes using the MA-producing *C. glutamicum* strain were performed to achieve a significantly increased titer of MA (Lee et al., 2018).

In this study, we generated engineered *E. coli* strains to overproduce both DHS and MA, through manipulation of several key genes involved in DHS biosynthesis and heterologous expression of codon-optimized foreign genes involved in DHS-to-MA conversion. These redesigned DHS-overproducing and MA-overproducing *E. coli* strains, grown in optimized media, produced the highest levels of both DHS and MA production in 7L fed-batch fermentations, indicating that the rational microbial cell factory design of DHS and MA biosynthesis could be an alternative way to complement petrochemical-based chemical processes.

MATERIALS AND METHODS

Bacterial Strains, Media, and Culture Conditions

The bacterial strains and plasmids used in this study are listed in **Table 1**. *E. coli* DH5a was used as the cloning host, and *E. coli* K12 & AB2834 were used as parent strains. *E. coli* strains for genetic manipulations were grown in Luria-Bertani (LB) medium at 37 or 30°C. For DHS production in small-scale culture, a single colony was inoculated in LB medium at 30°C for 15 h, and secondary culture was inoculated with 1% (v/v) in the same medium at 30°C for 6 h. The miniature culture was grown using 1.3 mL of *E. coli* production medium (EPM) in a 24-well cell culture plate, at 220 rpm under 30°C, for 4 days. The composition of the EPM for DHS and MA production was: glucose (5 g/L), glycerol (10 g/L), yeast extract (2.5 g/L), tryptone (2.5 g/L), KH_2PO_4 (7.5 g/L), $MgSO_4$ (0.5 g/L), $(NH_4)_2SO_4$ (3.5 g/L), NH_4Cl (2.7 g/L), Na_2SO_4 (0.7 g/L), $Na_2HPO_4 \bullet 12H_2O$ (9 g/L), and a trace metal solution (1 mL/L). The trace metal solution contained $FeSO_4 \bullet 7H_2O$ (10 g/L), $CaCl_2 \bullet 2H_2O$ (2 g/L), $ZnSO_4 \bullet 7H_2O$ (2.2 g/L), $MnSO_4 \bullet 4H_2O$ (0.5 g/L), $CuSO_4 \bullet 5H_2O$ (1 g/L), $(NH_4)_6Mo_7O_{24} \bullet 4H_2O$ (0.1 g/L), and $Na_2B_4O_7 \bullet 10H_2O$ (0.02 g/L).

Construction of Plasmids and Strains

All constructed plasmids for integration and disruption are listed in **Table 1**. Plasmid DNA extraction and purification were performed using a commercial kit (TIANGEN). For PCR, the Pfu DNA polymerase and HIFI DNA polymerase (TransGen) were used. For disruption and substitution of chromosomal genes, suicide vector pKOV (Addgene, USA) was used, which has the *sacB* gene for providing a markerless system. The constructed plasmids were transformed into *E. coli* AB2834 by electroporation.

For disruption of *tyrR, ptsG, pykA*, and *lacI* genes, homologous DNA fragments were PCR-amplified with primer sets R1-R4, G1-G4, A1-A4, and I1-I4, respectively, which were then inserted into the pKOV vector, generating pKOV-R, pKOV-G, pKOV-A, and pKOV-I, respectively. For overexpression of several genes, T-lac was generated by inserting the lac promoter and RBS into T-vector. The lac promoter and RBS were amplified with primer sets Plac1-Plac2 and RBS1-RBS2 from pUC18 and the pET-21b(+) vector. DNA fragments containing *E. coli aroB, aroD, galP, ppsA, aroG,* and *aroF* genes were amplified with primer sets B1-B2, D1-D2, P1-P2, A3-A4, G3-G4, and F1-F2, respectively, and the amplified DNA fragments were inserted into the T-lac vector, generating T-BD, T-PA, and T-GF. Subsequently, Plac*_aroB_aroD* cassette was amplified with primer sets BD1-BD2 and T-BD as a template, and the amplified cassette was inserted into pKOV-I, generating pKOV-BD. The Plac*_aroB_aroD* and Plac*_galP_ppsA* cassettes were amplified with primer sets BD1-BD3 and PA1-PA2, using T-BD and T-PA as a template, respectively, and the amplified cassettes were inserted into pKOV-I, generating pKOV-PABD. The Plac*_aroG_aroF* cassette was amplified with primer sets GF1-GF2, using T-GF as a template, and the amplified cassette was inserted into pKOV-PABD, generating pKOV-PAGFBD (**Supplementary Table 1**).

A series of *E. coli* DHS-producing strains were constructed using the host strain AB2834, which was constructed by the markerless disruption of the *aroE* gene. The *tyrR* gene in AB2834 was disrupted using plasmid pKOV-R, generating the Inha 24 strain. Subsequently, the *ptsG* and *pykA* genes were disrupted from Inha 24 using plasmids pKOV-G and pKOV-A, generating strains Inha 29 and Inha 52, respectively. Markerless integration of *aroB* and *aroD* genes, under the control of the *lac* promoter, were integrated at *LacI* gene locus into strain Inha 52 using plasmid pKOV-BD, generating the strain Inha 99 (**Figure 2A**). Using the plasmid pKOV-PABD, the *aroB, aroD, ppsA,* and *galP* genes, under the control of the lac promoter, were integrated into strain Inha 52, generating strain Inha 95. The *aroB, aroD, ppsA, galP, aroG,* and *aroF* genes, under the control of the lac promoter, were chromosome-integrated using plasmid pKOV-PAGFBD in Inha 52 strain, generating strain Inha 103.

RNA Sequencing

For RNA sequencing, *E. coli* strains AB2834 and Inha52 were cultured in LB media for seeding, and in 500 mL of EPM media for the main production. Growth curves were generated,

TABLE 1 | Plasmids and strains used in the study.

Strains	Relevant characteristics	References
E. coli AB2834	K12 *ΔaroE*	YALE univ.
E. coli Inha24	*E. coli ΔtyrR*	This study
E. coli Inha29	*E. coli* Inha24 *ΔptsG*	This study
E. coli Inha52	*E. coli* Inha29 *ΔpykA*	This study
E. coli Inha95	*E. coli* Inha52 *ΔlacI*:: P*lac_aroB_aroD*_P*lac_ppsA_galP*	This study
E. coli Inha99	*E. coli* Inha52 *ΔlacI*:: P*lac_aroB_ aroD*	This study
E. coli Inha103	*E. coli* Inha52 *ΔlacI*:: P*lac_aroB_aroD*_P*lac_aroG_aroF*P*lac_ppsA_galP*	This study
E. coli InhaM101	*E. coli* Inha103/pMESK1	This study
E. coli InhaM104	*E. coli* Inha103/pMESK4	This study
E. coli InhaM105	*E. coli* Inha103/pMESK5	This study
E. coli InhaM106	*E. coli* Inha103/pMESK6	This study
E. coli InhaM107	*E. coli* Inha103/pMESK7	This study
E. coli InhaM108	*E. coli* 4 Inha103/pMESK8	This study
Plasmids		
T-vector	T&A cloning vector	RBC Real biotech.
pUC18	Standard backborn vector for MA expression	Clontech
pET21b(+)	Protein expression vector for *E. coli*	Novagen
pKOV	The suicide vector containing the *Bacillus subtilis sacB* gene and temperature sensitive pSC101 replication origin	Addgene
pKOV_*tyrR*	pKOV containing a PCR fragment for the markerless disruption of the *tyrR* gene	This study
pKOV_*ptsG*	pKOV containing a PCR fragment for the markerless disruption of the *ptsG* gene	This study
pKOV_*pykA*	pKOV containing a PCR fragment for the markerless disruption of the *pykA* gene	This study
pKOV_*lacI*	pKOV containing a PCR fragment for the markerless disruption of the *lacI* gene	This study
pKOV_BD	pKOV_*lacI* derivative for P*lac_aroB_aroD* integration into *lacI* region	This study
pKOV_PABD	pKOV_*lacI* derivative for P*lac_ppsA_galP*_P*lac_aroB_aroD* integration into *lacI* region	This study
pKOV_PAGFBD	pKOV_*lacI* derivative for P*lac_ppsA_galP*_P*lac_aroG_aroF*_P*lac_aroB_aroD* integration into *lacI* region	This study
pMESK1	pUC18 modification vector including Lac promoter $asbF^{Eopt}$- $aroY^{Eopt}$- $catA^{Eopt}$	This study
pMESK4	pUC18 modification vector including *oppA* promoter $asbF^{Eopt}$- $aroY^{Eopt}$- $catA^{Eopt}$	This study
pMESK5	pUC18 modification vector including *dps* promoter $asbF^{Eopt}$- $aroY^{Eopt}$- $catA^{Eopt}$	This study
pMESK6	pUC18 modification vector including *rmf* promoter $asbF^{Eopt}$- $aroY^{Eopt}$- $catA^{Eopt}$	This study
pMESK7	pUC18 modification vector including *fusA* promoter $asbF^{Eopt}$- $aroY^{Eopt}$- $catA^{Eopt}$	This study
pMESK8	pUC18 modification vector including *rnpB* promoter $asbF^{Eopt}$- $aroY^{Eopt}$- $catA^{Eopt}$	This study

and each strain was sampled at the early stage of exponential phase (AB2834, 4 h; Inha52, 7 h) as well as the early stage of stationary phase (AB2834, 9 h; Inha52, 12 h). RNeasy mini prep kit (Qiagen, CA) was used for total RNA isolation, according to the manufacturer's instructions. DNaseI (TaKaRa, Japan) was used to eliminate any potential chromosomal DNA contamination. RNA-Seq was performed by ChunLab Inc., Korea.

Metabolite Analysis

The *E. coli* cells were removed from cultures by centrifugation and culture supernatant was filtered using a membrane filter. The metabolites were separated by HPLC using an Aminex HPX-87H column (Bio-rad, Japan). The mobile phase was 2.5 mM H_2SO_4, and a flow rate of 0.6 mL/min was used for metabolites. The column had to be heated at a temperature of 65°C for detection of metabolites. MA and DHS were analyzed at wavelengths of 262 and 236 nm, respectively. Organic acids, including succinic acid, acetic acid, formic acid, and lactic acid, were detected at wavelengths of 210 nm.

Fed-Batch Fermentation

The first growth culture was carried out in a conical tube containing 5 mL of LBG medium (30°C and 200 rpm). After 12 h of culture, 0.2 mL of the culture broth was inoculated in a 250-mL baffled flask containing 20 mL of culture medium, and cultured at 30°C and 200 rpm in an incubator. After 6 h, the second culture broth was inoculated into a 7-L fermenter (1% v/v inoculum). Production culture was carried out using the PB4-md5 medium in a 7-L fermenter (working volume: 2 L). The PB4-md5 medium includes: 30 g/L glucose, 10 g/L glycerol, 15.75 g/L yeast extract, 21.375 g/L tryptone, 5.25 g/L KH_2PO_4, 1 g/L $MgSO_4 \cdot 7H_2O$, 0.8 g/L citric acid, 1 mL/L trace metals, and 200 μg/L thiamine hydrochloride. The feeding medium includes: 600 g/L glucose, 100 g/L yeast extract, 20 g/L $MgSO_4 \cdot 7H_2O$, and 5 mL/L trace metal. Phosphate was not added to the feeding medium, to allow for the regulation of cell growth. The pH levels were 7.0 in each

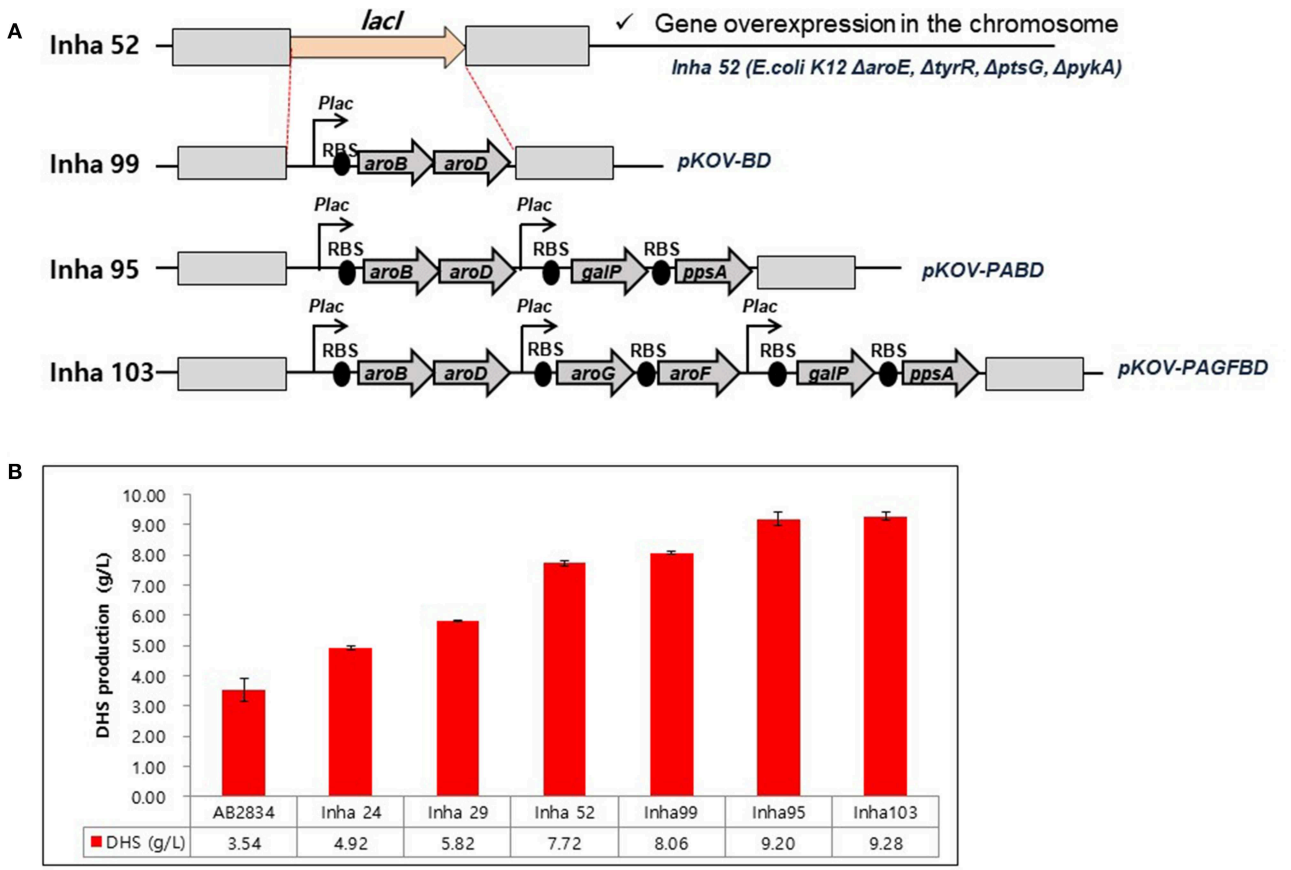

FIGURE 2 | (A) Construction of *E. coli* mutants for overproduction of DHS. **(B)** HPLC analysis of DHS production yields in DHS-producing *E. coli* strains. *E. coli* cells were cultured in 1.3 mL of EPM at 30°C for 96 h. Data represent averages and standard deviations from two independent experiments.

culture (10N NaOH, 3M HCl), and the DO level was maintained above at 30% by controlling the agitation, aeration, and feeding rates. The configuration of the fermenter was as follows: two impellers with turbine and marine impeller, ring-type sparger with 12 holes, top-driven, and 160 mm tank diameter. The feeding medium was supplied when glucose was depleted, using a peristaltic pump.

Construction of a Gene Cassette Involved in DHS-to-MA Conversion

E. coli Inha M101 was prepared by transformation of a plasmid pMESK1 into Inha M103. pMESK1 was prepared by ligation of an $AsbF^{Eopt}$ -$aroY^{Eopt}$ -$catA^{Eopt}$ cassette to pUC18. Codon-optimized gene versions for increased protein expression in *E. coli* were synthesized from Cosmo Genetech, Korea. Digestion of pUC57_M1 with *Xba*I and *Hind*III liberated a 3.3-kb $asbF^{Eopt}$ -$aroY^{Eopt}$ -$catA^{Eopt}$ fragment. Plasmid pUC18 was digested at the same restriction site. Subsequent ligation of $asbF^{Eopt}$ -$aroY^{Eopt}$ -$catA^{Eopt}$ to pUC18 resulted in pMESK1. The ligation of *the* $asbF^{Eopt}$ -$aroY^{Eopt}$ -$catA^{Eopt}$ cassette was verified by restriction enzyme digestion analysis. To select the promoter for expression of heterologous gene cluster, the intergenic region of *rnpB, fusA, oppA, dps,* and *rmf* genes (upstream region of the start codon) was amplified by PCR and cloned into pMESK1 digested by *Eco*RI and *Xba*I.

RESULTS

Redesign of 3-Dehydroshikimate Biosynthetic Pathway in *Escherichia coli*

We used the *E. coli* AB2834 strain as a parental host for DHS accumulation, which is an *aroE* mutant strain lacking shikimate dehydrogenase (Draths and Frost, 1994). To further improve DHS accumulation, we first disrupted the key genes involved in DHS accumulation in *E. coli* AB2834. The *tyrR* repressor, which exerts negative control on the transcription of *aroG* and *aroF* genes with two aromatic amino acids (L-phenylalanine and L-tyrosine), was disrupted (Bongaerts et al., 2001). The *tyrR*-disruption mutant strain (named Inha 24) accumulated 4.92 g/L of DHS in the culture medium after 96 h, whereas the parental strain produced 3.54 g/L of DHS under the same culture condition. Next, the *ptsG* gene, one of the phosphotransferase system genes that consume PEP for glucose uptake, was disrupted in the Inha 24 strain (named Inha 29) to increase the availability of PEP, a DHS precursor. The Inha 29 strain produced 5.82 g/L of

DHS under the same culture condition. Finally, the *pykA* gene, encoding a pyruvate kinase, was also disrupted in the Inha 29 strain (named Inha 52), leading to a production of 7.72 g/L of DHS, signifying a more than 2-fold improvement in production yield relative to the parental strain (**Figure 2B**).

RNA sequencing-based comparative transcriptome analysis between the parental strain and Inha52 revealed that the transcription levels of the DHS biosynthetic pathway genes such as *aroB* (encoding DHQ synthease) and *aroD* (encoding DHQ dehydratase) were significantly reduced in the Inha52 strain (data not shown). To overcome this limitation, both *aroB* and *aroD* genes were overexpressed under the control of the *lac* promoter via an integration plasmid pKOV-BD, generating the strain Inha 99 (**Figure 2A**). The Inha 99 strain, harboring an extra copy of *aroB* and *aroD* genes, produced 8.06 g/L of DHS (**Figure 2B**). In addition, Inha 95 was constructed using pKOV-PABD to overexpress the *galP* and *ppsA* genes as well as *aroB* and *aroD* genes in the Inha 52 strain (**Figure 2A**). The *galP* gene, encoding D-galactose transporter, was overexpressed to improve the level of glucose uptake. The *ppsA* gene, encoding a phosphoenolpyruvate synthase, was also overexpressed to increase the availability of PEP. Inha 95, overexpressing the *aroB, aroD, galP,* and *ppsA* genes, produced 9.20 g/L of DHS (**Figure 2B**). Subsequently, *aroG* and *aroF* genes, encoding DAHP synthase, were additionally overexpressed in strain Inha 95, generating the Inha 103 strain (**Figure 2A**). The Inha 103 strain, harboring extra copies of *aroB, aroD, galP, ppsA, aroG,* and *aroF* genes under the control of the *lac* promoter, produced 9.28 g/L of DHS, which is 20% higher DHS yield than that of strain Inha 52, and 2.6-fold higher than that of the parental strain (**Figure 2B**; **Supplementary Table 2**). Thus, the DHS production yield of our recombinant strains increased gradually through serial disruptions and overexpression of the genes involved in DHS synthesis.

Fed-Batch Fermentation for DHS Production

During the statistical medium optimization process in shake-flask cultures using the metabolically engineered *E. coli* cells, composition of the production medium was found to be a very important factor for enhanced DHS production. Sufficient supply of dissolved oxygen during the entire fermentation period was also observed to be crucial, as revealed by higher DHS production yield according to increase in oxygen mass transfer rate (kLa) through increment of agitation speed (rpm). Therefore, we intended to develop a fed-batch operation process that could efficiently control the producers' fermentation physiology, simultaneously overcoming the oxygen-limited culture conditions caused by high cell density in bioreactor fermentations. The fed-batch culture was carried out using the abovementioned four strains, i.e., Inha 24, Inha 29, Inha 52, and Inha 103. The optimized medium from flask culture was again optimized for the C/N ratio in the fermenter. The DHS production yield was confirmed by fed-batch culture based on this medium. Scaled-up operations from shake flasks to fermenters are largely affected by the operating conditions such as gas-liquid mass transfer, shear stress, mixing time, antifoam, pH regulation, and power input. A phosphate-limited fed-batch culture was performed to regulate cell growth. After the glucose level were almost depleted in the fermentation broth, feeding medium was continuously injected using a peristaltic pump to maintain below 10 g/L to prevent the production of organic acids by residual glucose. As shown in **Figure 3**, DO levels could be successfully maintained above 30% during the whole fermentation time in the respective fed-batch fermentation, thereby leading to overcoming the undesirable oxygen-limited conditions due to relatively high cell density. It is well-known that when *E. coli* cells become oxygen-limited, cellular metabolism rapidly changes, producing proteases that can degrade foreign proteins, thus lowering the production ability of the transformed *E. coli* cells.

All four strains consumed glucose for 17 h and started feeding from this time onwards. As a result, in the Inha 24 strain, the cells showed steady growth, and the DCW (Dry cell weight) and production yield declined 48 h after the incubation; the DCW was about 42 g/L and the DHS was about 45 g/L. In the same culture condition, the Inha 29 strain exhibited the maximum cell dry weight of about 37 g/L and a DHS level of 74 g/L. In the Inha 52 strain, DCW was lower than that of the Inha 29 strain, but DHS production yield was as high as 81 g/L, implying that there is a competitive relationship between cell growth and DHS production. Although DHS is a primary metabolite, its production in the engineered strains exhibited typical secondary metabolite patterns (**Figure 3**). In aromatic amino acid processes, *E. coli* and *C. glutamicum* have characteristic metabolites that suppress cell density at certain concentrations (Cheng et al., 2012; Rodriguez et al., 2014; Lee et al., 2018). Finally, in the Inha 103 strain with enhanced flux to DHS, the DCW was about 35 g/L, slightly lower than that of Inha 52, while the production yield of DHS had increased by 44% to 117 g/L. The specific production yield (Yp/x) was 1.07 g DHS/g DCW for the Inha 24 strain, 2 g DHS/g DCW for the Inha 29 strain, 2.25 g DHS/g DCW for the Inha 52 strain, and 3.34 g DHS/g DCW for the Inha 103 strain. The specific production yield of the Inha 103 strain was 3.1-times higher than that of Inha 24 (**Table 2**; **Supplementary Figure 3**).

Heterologous Expression of the Genes Involved in DHS-to-MA Conversion

We tried to produce muconic acid, another valuable compound, through heterologous expression of the genes involved in DHS-to-MA conversion in the DHS-overproducing *E. coli* strain. Previously, three foreign genes (*aroZ, aroY,* and *catA*) were reported to be responsible for the DHS-to-MA conversion in *E. coli* (Draths and Frost, 1994, **Figure 1**). Similarly, we generated a codon-optimized single operon construct containing three genes, *asbF* from *Bacillus thuringiensis* (encoding DHS dehydratase for DHS-to-PCA), *aroY* from *Klebsiella pneumoniae* (encoding PCA decarboxylase for PCA-to-CA), and *catA* from *Acinetobacter calcoaceticus* (encoding catechol 1,2-dioxygenase for CA-to-MA). Genes $asbF^{Eopt}$, $aroY^{Eopt}$, and $catA^{Eopt}$ were cloned into modified pUC18 under the control of the lac promoter, thus generating pMESK1. To optimize the heterologous foreign

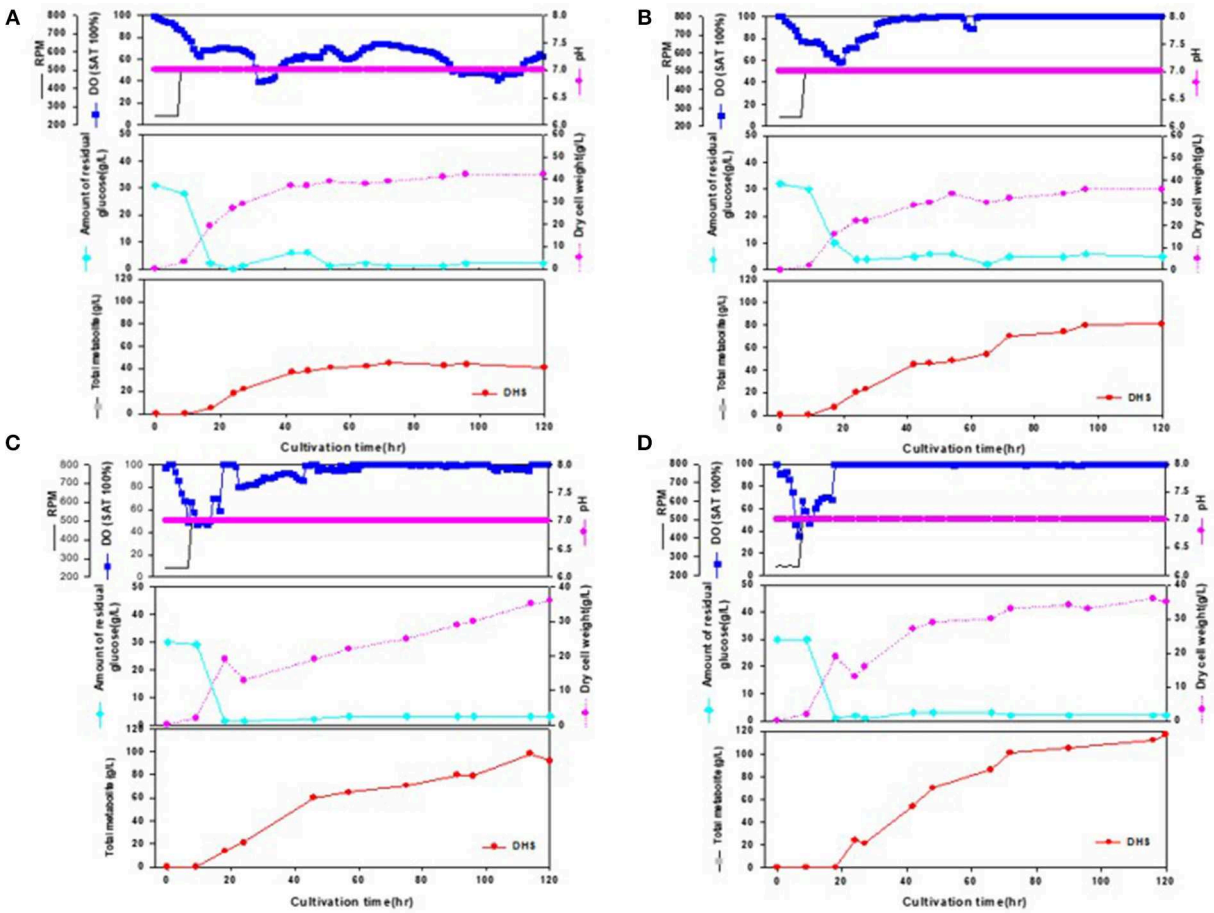

FIGURE 3 | Time-course profiles of cell growth (DCW), glucose, organic acid, and metabolite production by strains in the 7-L fermenter. **(A)** Inha 24: The feeding medium was sequentially injected at culture periods of 17, 19, 24, 27, 42, 47, and 54 h, at a rate of 0.1176, 0.1568, 0.1176, 0.1568, 0.0784, 0.0522, and 0.1176 mL/min, respectively. **(B)** Inha 29: The feeding medium was sequentially injected at culture periods of 17, 19, 24, 42, 47, 54, and 89 h, at a rate of 0.0392, 0.1176, 0.1568, 0.0784, 0.0522, 0.1176, and 0.0784 mL/min, respectively. **(C)** Inha 52: The feeding medium was sequentially injected at culture periods of 17, 19, 42, 47, 54, 65, and 89 h, at a rate of 0.0392, 0.1176, 0.0784, 0.0522, 0.1568, 0.1176, and 0.0522 mL/min, respectively. **(D)** Inha 103: The feeding medium was sequentially injected at culture periods of 18, 24, 42, and 66 h at a rate of 0.1306, 0.1568, 0.1306, and 0.1045 mL/min, respectively.

TABLE 2 | A, 7-L lab-scale fermentation; B, 50-L pilot-scale fermentation; P_f, maximum DHS production (g IA/L); X_f, maximum dry cell weight (g DCW/L); S_f, final residual glucose concentration (g glucose/L); Q_p, average volumetric DHS production rate (g DHS/L/h); q_p, average specific DHS production rate (g DHS/g DCW/h); $Y_{p/x}$, specific DHS production (g DHS/g DCW); $Y_{p/s}$, DHS production yield based on glucose (g DHS/g glucose); $Y_{x/s}$, DCW yield based on glucose (g DCW/g glucose).

	P_f	X_f	S_f	Q_p	q_p	$Y_{p/x}$	$Y_{p/s}$	$Y_{x/s}$
Inha 24	45	42	2	0.375	0.009	1.07	0.21	0.19
Inha 29	74	37	2	0.616	0.017	2.0	0.27	0.14
Inha 52	81	36	5	0.675	0.019	2.25	0.34	0.15
Inha 103	117	35	2	0.975	0.028	3.34	0.39	0.12

genes expression in a DHS-overproducing *E. coli* strain, we searched for a naturally-suitable promoter *via* comparative transcriptome analysis between the parental strain and Inha 52 (**Supplementary Figure 1**). Among the gene expression profiles during the culture duration, five promoters were selected according to their transcription strength, and each selected promoter was cloned to control the foreign gene cassette (**Supplementary Figure 2A**). The *E. coli* strains expressing each promoter from pMESK4 to pMESK8 were named *E. coli* Inha M104–M108, respectively, and were tested to determine whether MA accumulated in their culture broths. The production level of MA varied, depending on the promoter, as shown in **Supplementary Figures 2B** and **4**. The highest MA titer was observed in strain Inha 103, expressing *oppA* gene promoter, which encodes periplasmic oligopeptides-binding protein in *E. coli*. It yielded up to 1,789 mg/L of MA, an 8-fold increase compared with strain Inha M101 (Plac_ $asbF^{Eopt}$ -$aroY^{Eopt}$ -$catA^{Eopt}$), which showed an MA titer of 223 mg/L. DHS was accumulated in relatively large amounts in two strains (P*lac* and P*dps*), and only a small amount of MA was produced in the other two strains (P*rmf* and P*rmpB*). In the 7-L fermenter, the Inha 103 strain containing the $asbF^{Eopt}$ -$aroY^{Eopt}$ -$catA^{Eopt}$ operon cassette

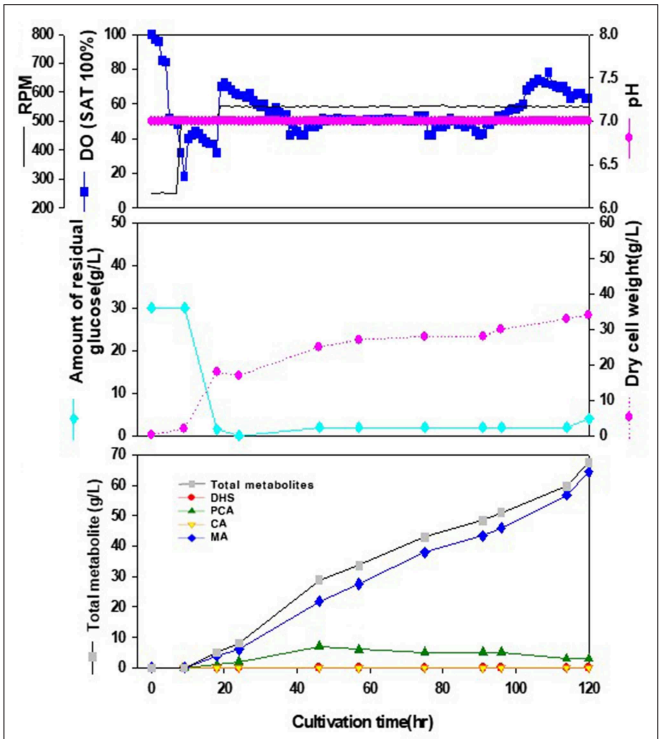

FIGURE 4 | Time-course profiles of cell growth (DCW, pink closed diamond), glucose (cyan closed diamond), organic acid, and metabolite production by the engineered *E. coli* InhaM104 in the 7-L fermenter. The feeding medium was sequentially injected at culture periods of 18, 24, and 46 h, at a rate of 0.0392, 0.0784, and 0.0653 mL/min, respectively. Closed gray square, total metabolite; red closed diamond, DHS (3-dehydroshikimic acid); green closed diamond, PCA (protocatechuate); yellow closed triangle, CA (catechol); blue closed diamond, MA (*cis-cis* muconic acid).

under the control of *oppA* promoter produced 64.5 g/L MA with little accumulation of other intermediates (**Figure 4**).

DISCUSSION

In general, strategies to redesign metabolic pathways constitute the primary goal of metabolic engineering, which is a prerequisite to produce certain valuable compounds. This strategy has been used to engineer the shikimate pathway for producing a number of useful aromatic products in *E. coli*. For example, Chandran et al. reported an engineered *E. coli* strain that achieved 84 g/L of shikimate with a yield of 0.33 mol/mol glucose (Chandran et al., 2003). In addition, Wang et al. reported a 48 g/L yield of L-tryptophan, with a conversion ratio of 21.87% from glucose (Wang et al., 2013). It was previously reported that the introduction of heterologous biosynthetic genes such as *aroZ, aroY,* and *catA* into the *aroE*-deleted *E. coli* led to the accumulation of MA up to 36 g/L via benzene-independent pathway (Niu et al., 2002). In addition, various microbial cell factory strategies were also purposed to enhance production of MA or shikimic acid (**Table 3**) (Noda and Kondo, 2017; Bilal et al., 2018a).

In this study, a phosphate-limited fed-batch fermentation process was successfully developed for enhanced production of DHS using a DHS-overproducing *E. coli* strain constructed by redesigning its biosynthetic pathway. The phosphate-limited fed-batch operation in the 7 L bioreactor level was observed to strictly regulate the specific growth rate (μ) and the glucose consumption rate and suppresses the production of undesirable byproducts by effectively controlling DO levels. Notably, under this culture conditions, DHS was biosynthesized in a non-growth-associated mode during the later stage of the fed-batch operations, efficiently utilizing higher portion of the supplied nutrients into the DHS biosynthesis rather than cellular growth. As a result, the Inha 103 strain showed significantly high level of DHS production amounting to 117 g/L (at a production yield (Yp/s) of 0.39 g/g glucose) in the 7-L fed-batch bioreactor culture, ∼13-fold increase as compared to the parallel flask culture (9 g/L) performed under the identical culture conditions.

It was observed that sufficient amount of dissolved oxygen (DO) should be supplied in the cultivation of the metabolically engineered *E. coli* cells for enhanced production of DHS: Increase in oxygen mass transfer rate (kLa) through increment of agitation speed (rpm), and expansion of the diameter ratio of the impeller to the fermenter vessel up to 0.46 resulted in higher productivity of DHS. In addition, as described in this paper, by installing a turbine impeller just above the ring-type sparger for efficient break-down of the sparged air, and a marine impeller above the turbine impeller for proficient mixing of the dissolved oxygen, DO levels could be successfully maintained above 50% during the whole fermentation period, thereby leading to overcoming the undesirable oxygen-limited conditions due to relatively high cell density. Notably, with almost the same configuration of this fermenter system, higher production levels of MA (muconic acid) had been observed, maintaining DO levels above 40% during the entire fermentation time, leading to facilitated transfer of DO to the producing cells, and thereby improving MA production (**Figure 4**). In addition, by carefully controlling the composition and feeding rate of the supplied medium during the fed-batch operation, it was possible to overcome DO-limited conditions, simultaneously minimizing the production of the byproducts caused by high levels of residual glucose in the fermentation broth. Notably, under the phosphate-limited fed-batch fermentations, DHS was observed to be biosynthesized almost in a growth-associated mode, thus resulting in the remarkable enhancement in DHS productivity (i.e., ∼6-fold increase as compared to the parallel batch bioreactor fermentation performed under the identical environments).

Such a remarkable production yield could be achieved by applying a combination of several metabolic engineering strategies for DHS production to *E. coli* strains. We demonstrated that engineering of key genes for DHS production using the host strain *E. coli* AB2834, in which the *aroE*-encoded shikimate dehydrogenase is inactivated, gradually increased the DHS production. We inactivated the *tyrR*-encoded tyrosine-dependent transcriptional regulator, which is a feedback repressor of *aroG*- and *aroF*-encoding DAHP synthase,

TABLE 3 | Recent overview of engineered microbial strains for enhanced shikimate and MA biosynthesis.

Product	Organism/strain	Feedstock	Culture style	Titer	Fermentation duration (h)	References
Shikimate	*Escherichia coli*	Glycerol + glucose	Batch	1.78 g/L	36	Bilal et al., 2018b
Shikimate	*E. coli*	Glycerol	Batch	5.33 g/L	24	Lee et al., 2017
Shikimate	*E. coli*	Glucose	Batch and fed-batch	1.73 g/L (Batch) 13.15g/L (Fed batch)	54	Gu et al., 2016
Shikimate	*E. coli*	Glycerol + glucose	Fed-batch	4.14 g/L (Batch) 27.41 g/L (Fed-batch)	48	Liu et al., 2016
Shikimate	*E. coli*	Glucose	Batch	3.12 g/L	–	Cui et al., 2014
Shikimate	*E. coli*	Glucose	Batch and fed-batch	1.12 g/L (Batch) 14.6 g/L (Fed-batch)	–	Chen et al., 2014
Shikimate	*E. coli*	Glycerol	Fed-batch	1.85 g/L	44	Chen et al., 2012
Shikimate	*Pichia stipites*	Glucose	Batch	3.11 g/L	120	Gao et al., 2017
Shikimate	*Corynebacterium glutamicum*	Glucose	Fed-batch	141 g/L	48	Kogure et al., 2016
MA	*E. coli*	Glucose, xylose	Fed-batch	4.7 g/L	72	Zhang et al., 2015
MA	*E. coli*	Glucose, glycerol	Batch	390 mg/L	32	Sun et al., 2013
MA	*E. coli*	Glucose, glycerol	Batch	1.5 g/L	48	Lin et al., 2014
MA	*E. coli*	Glucose	Batch	170 mg/L	72	Sengupta et al., 2015
MA	*Saccharomyces cerevisiae*	Glucose	Batch	1.56 mg/L	170	Weber et al., 2012
MA	*S. cerevisiae*	Glucose	Batch	141 mg/L	108	Curran et al., 2013
DHS	*E. coli*	Glucose	Batch	25.48 g/L	62	Yuan et al., 2014
DHS	*E. coli*	Glucose	Fed-batch	69g/L	–	Li et al., 1999

for improving the transcription levels. Among the several approaches to improve PEP availability for promoting DHS production, we generated PTS-inactivated strain by disrupting *ptsG*, which is a PEP-dependent glucose transporter. Instead, we overexpressed *galP*-encoding D-galactose transporter, which is another glucose-uptake route. In addition, *pykA*-encoding pyruvate kinase 2 was removed and *ppsA*-encoded PEP synthase was overexpressed for reconversion of pyruvate to PEP. Furthermore, we overexpressed the genes on the biosynthetic pathway to complete the DHS-overproducing strain. Construction of an MA-producing *E. coli* cell factory was carried out by the introduction of a single operon containing $asbF^{Eopt}$ -$aroY^{Eopt}$ -$catA^{Eopt}$ gene cluster, as well as applying a promoter engineering strategy through the transcriptome analysis. Although the current heterologous gene cluster converts MA to about 50% of DHS, strengthening and optimization of the DHS-PCA-CA-MA route in further studies could result in better performing strains with higher DHS-to-MA bioconversion efficiency.

In summary, we report the construction of *E. coli* strains capable of producing DHS at high concentrations from D-glucose. To accumulate high concentrations of DHS, *tyrR, ptsG,* and *pykA* gene were sequentially deleted from *E. coli* AB2834, in which the *aroE* gene was mutated to prevent the conversion of DHS to SA. Extra copies of *aroB, aroD, galP, ppsA, aroG,* and *aroF* genes involved in DHS biosynthesis were additionally inserted to maximize DHS accumulation. MA was also successfully produced by a heterologous expression pathway for DHS-to-MA bioconversion. A controlled fed-batch operation was performed with a statistically optimized production medium in a 7L bioreactor and the redesigned *E. coli* strain could convert DHS to MA efficiently, thereby producing about 64.5 g/L MA with almost no accumulation of metabolic intermediates such as PCA, CA, and DHS. This study demonstrates the potential value of *E. coli* host to produce high level of an intermediate metabolite of aromatic pathways and the rational cell factory design approach to possibly complement petrochemical-based chemical processes.

DATA AVAILABILITY STATEMENT

The datasets generated for this study are available on request to the corresponding author.

AUTHOR CONTRIBUTIONS

SK, SL, G-TC, and E-SK designed the research and provided the improvement of the manuscript. S-SC, S-YS, S-OP, H-NL, JS, JK and J-HP performed the experiments, as well as data collection and analysis. JS and JK performed RNA-seq analysis. S-SC and H-NL performed genetic engineering. S-YS and S-OP performed medium optimization and fermentation. S-SC and S-YS wrote the article.

ACKNOWLEDGMENTS

This work was carried out with the support of (1) Cooperative Research Program for Agriculture Science and Technology Development (Project No. PJ01318701) Rural Development Administration, (2) Agricultural Microbiome R&D Program,

Ministry of Agriculture, Food and Rural Affairs, Republic of Korea [as part of the (multi-ministerial) Genome Technology to Business Translation Program] No. 918008-04 and (3) partially by the 2015 Research Grant Program (520150308) from Kangwon National University, Republic of Korea.

SUPPLEMENTARY MATERIAL

The Supplementary Material for this article can be found online at: https://www.frontiersin.org/articles/10.3389/fbioe.2019.00241/full#supplementary-material

REFERENCES

Becker, J., and Wittmann, C. (2015). Advanced biotechnology: metabolically engineered cells for the bio-based production of chemicals and fuels, materials, and health-care products. *Angew. Chem. Int. Ed Engl.* 54, 3328–3350. doi: 10.1002/anie.201409033

Bilal, M., Wang, S., Iqbal, H. M. N., Zhao, Y., Hu, H., Wang, W., et al. (2018a). Metabolic engineering strategies for enhanced shikimate biosynthesis: current scenario and future developments. *Appl. Microbiol. Biotechnol.* 102, 7759–7773. doi: 10.1007/s00253-018-9222-z

Bilal, M., Yue, S., Hu, H., Wang, W., and Zhang, X. (2018b). Systematically engineering *Escherichia coli* for enhanced shikimate biosynthesis co-utilizing glycerol and glucose. *Biofuels Bioprod. Biorefin.* 12, 348–361. doi: 10.1002/bbb.1867

Bongaerts, J., Krämer, M., Müller, U., Raeven, L., and Wubbolts, M. (2001). Metabolic engineering for microbial production of aromatic amino acids and derived compounds. *Metab. Eng.* 3, 289–300. doi: 10.1006/mben.2001.0196

Chandran, S. S., Yi, J., Draths, K. M., von Daeniken, R., Weber, W., and Frost, J. W. (2003). Phosphoenolpyruvate availability and the biosynthesis of shikimic acid. *Biotechnol. Prog.* 19, 808–814. doi: 10.1021/bp025769p

Chen, K., Dou, J., Tang, S., Yang, Y., Wang, H., Fang, H., et al. (2012). Deletion of the *aroK* gene is essential for high shikimic acid accumulation through the shikimate pathway in *E. coli*. *Bioresour. Technol.* 119, 141–147. doi: 10.1016/j.biortech.2012.05.100

Chen, X., Li, M., Zhou, L., Shen, W., Algasan, G., Fan, Y., et al. (2014). Metabolic engineering of *Escherichia coli* for improving shikimate synthesis from glucose. *Bioresour. Technol.* 166, 64–71. doi: 10.1016/j.biortech.2014.05.035

Chen, Y., and Nielsen, J. (2013). Advances in metabolic pathway and strain engineering paving the way for sustainable production of chemical building blocks. *Curr. Opin. Biotechnol.* 24, 965–972. doi: 10.1016/j.copbio.2013.03.008

Cheng, L., Wang, J., Xu, Q., Xie, X., Zhang, Y., Zhao, C., et al. (2012). Effect of feeding strategy on L-tryptophan production by recombinant *Escherichia coli*. *Ann. Microbiol.* 62, 1625–1634. doi: 10.1007/s13213-012-0419-6

Cui, Y. Y., Chen, L., Zhang, Y. Y., Jian, H., and Liu, J. Z. (2014). Production of shikimic acid from *Escherichia coli* through chemically inducible chromosomal evolution and cofactor metabolic engineering. *Microb. Cell Fact.* 13:21. doi: 10.1186/1475-2859-13-21

Curran, K. A., Leavitt, J. M., Karim, A. S., and Alper, H. S. (2013). Metabolic engineering of muconic acid production in *Saccharomyces cerevisiae*. *Metab. Eng.* 15, 55–66. doi: 10.1016/j.ymben.2012.10.003

Draths, K. M., and Frost, J. W. (1994). Environmentally compatible synthesis of adipic acid from D-glucose. *J. Am. Chem. Soc.* 116, 399–400. doi: 10.1021/ja00080a057

Gao, M., Cao, M., Suástegui, M., Walker, J., Rodriguez Quiroz, N., Wu, Y., et al. (2017). Innovating a nonconventional yeast platform for producing shikimate as the building block of high-value aromatics. *ACS. Synth. Biol.* 6, 29–38. doi: 10.1021/acssynbio.6b00132

Gu, P., Su, T., Wang, Q., Liang, Q., and Qi, Q. (2016). Tunable switch mediated shikimate biosynthesis in an engineered non-auxotrophic *Escherichia coli*. *Sci. Rep.* 6:29745. doi: 10.1038/srep29745

Jan, C. J. B., and Cavallaro, S. (2015). Transiting from adipic acid to bioadipic acid. 1, Petroleum-based processes. *Ind. Eng. Chem. Res.* 54, 1–46. doi: 10.1021/ie5020734

Johansson, L., Lindskog, A., Silfversparre, G., Cimander, C., Nielsen, K. F., and Lidén, G. (2005). Shikimic acid production by a modified strain of *E. coli* (W3110.shik1) under phosphate-limited and carbon-limited conditions. *Biotechnol. Bioeng.* 92, 541–552. doi: 10.1002/bit.20546

Kogure, T., Kubota, T., Suda, M., Hiraga, K., and Inui, M. (2016). Metabolic engineering of *Corynebacterium glutamicum* for shikimate overproduction by growth-arrested cell reaction. *Metab. Eng.* 38, 204–216. doi: 10.1016/j.ymben.2016.08.005

Kruyer, N. S., and Peralta-Yahya, P. (2017). Metabolic engineering strategies to bio-adipic acid production. *Curr. Opin. Biotechnol.* 45,136–143. doi: 10.1016/j.copbio.2017.03.006

Lee, H. N., Shin, W. S., Seo, S. Y., Choi, S. S., Song, J. S., Kim, J. Y., et al. (2018). *Corynebacterium* cell factory design and culture process optimization for muconic acid biosynthesis. *Sci. Rep.* 8:18041. doi: 10.1038/s41598-018-36320-4

Lee, M. Y., Hung, W. P., and Tsai, S. H. (2017). Improvement of shikimic acid production in *Escherichia coli* with growth phase-dependent regulation in the biosynthetic pathway from glycerol. *World J. Microbiol. Biotechnol.* 33:25. doi: 10.1007/s11274-016-2192-3

Li, K., Mikola, M. R., Draths, K. M., Worden, R. M., and Frost, J. W. (1999). Fed-batch fermentor synthesis of 3-dehydroshikimic acid using recombinant *Escherichia coli*. *Biotechnol. Bioeng.* 64, 61–733. doi: 10.1002/(SICI)1097-0290(19990705)64:1<61::AID-BIT7>3.0.CO;2-G

Li, L., Tu, R., Song, G., Cheng, J., Chen, W., Li, L., et al. (2019). Development of a synthetic 3-dehydroshikimate biosensor in *Escherichia coli* for metabolite monitoring and genetic screening. *ACS Synth. Biol.* 8, 297–306. doi: 10.1021/acssynbio.8b00317

Lin, Y., Sun, X., Yuan, Q., and Yan, Y. (2014). Extending shikimate pathway for the production of muconic acid and its precursor salicylic acid in *Escherichia coli*. *Metab. Eng.* 23, 62–69. doi: 10.1016/j.ymben.2014.02.009

Liu, X., Lin, J., Hu, H., Zhou, B., and Zhu, B. (2016). Site-specific integration and constitutive expression of key genes into *Escherichia coli* chromosome increases shikimic acid yields. *Enzyme Microb. Technol.* 82, 96–104. doi: 10.1016/j.enzmictec.2015.08.018

Martínez, J. A., Bolívar, F., and Escalante, A. (2015). Shikimic acid production in *Escherichia coli*: from classical metabolic engineering strategies to omics applied to improve its production. *Front. Bioeng. Biotechnol.* 3:145. doi: 10.3389/fbioe.2015.00145

Meza, E., Becker, J., Bolivar, F., Gosset, G., and Wittmann, C. (2012). Consequences of phosphoenolpyruvate sugar phosphotranferase system and pyruvate kinase isozymes inactivation in central carbon metabolism flux distribution in *Escherichia coli*. *Microb. Cell Fact.* 11:127. doi: 10.1186/1475-2859-11-127

Nishikura-Imamura, S., Matsutani, M., Insomphun, C., Vangnai, A., Toyama, H., Yakushi, T., et al. (2014). Overexpression of a type II 3-dehydroquinate dehydratase enhances the biotransformation of quinate to 3-dehydroshikimate in *Gluconobacter oxydans*. *Appl. Microbiol. Biotechnol.* 98, 2955–2963. doi: 10.1007/s00253-013-5439-z

Niu, W., Draths, K. M., and Frost, J. W. (2002). Benzene-free synthesis of adipic acid. *Biotechnol. Prog.* 18, 201–211. doi: 10.1021/bp010179x

Noda, S., and Kondo, A. (2017). Recent advances in microbial production of aromatic chemicals and derivatives. *Trends Biotechnol.* 35, 785–796. doi: 10.1016/j.tibtech.2017.05.006

Patnaik, R., Spitzer, R. G., and Liao, J. C. (1995). Pathway engineering for production of aromatics in *Escherichia coli*: confirmation of stoichiometric analysis by independent modulation of *AroG, TktA*, and *Pps* activities. *Biotechnol. Bioeng.* 46, 361–370. doi: 10.1002/bit.260460409

Pittard, J., and Yang, J. (2008). Biosynthesis of the aromatic amino acids. *EcoSal Plus* 3, 1–39. doi: 10.1128/ecosalplus.3.6.1.8

Richman, J. E., Chang, Y., Kambourakis, S., Draths, K. M., Almy, E., Snell, K. D., et al. (1996). Reaction of 3-dehydroshikimic acid with molecular oxygen and hydrogen peroxide: products, mechanism, and associated antioxidant activity. *J. Am. Chem. Soc.* 118, 11587–11591. doi: 10.1021/ja952317i

Rodriguez, A., Martínez, J. A., Báez-Viveros, J. L., Flores, N., Hernández-Chávez, G., Ramírez, O. T., et al. (2013). Constitutive expression of selected genes from the pentose phosphate and aromatic pathways increases the shikimic acid yield in high-glucose batch cultures of an *Escherichia coli* strain lacking PTS and *pykF*. *Microb. Cell Fact.* 12:8. doi: 10.1186/1475-2859-12-86

Rodriguez, A., Martínez, J. A., Flores, N., Escalante, A., Gosset, G., and Bolivar, F. (2014). Engineering *Escherichia coli* to overproduce aromatic amino acids and derived compounds. *Microb. Cell Fact.* 13:126. doi: 10.1186/s12934-014-0126-z

Sengupta, S., Jonnalagadda, S., Goonewardena, L., and Juturu, V. (2015). Metabolic engineering of a novel muconic acid biosynthesis pathway via 4-hydroxybenzoic acid in *Escherichia coli*. *Appl. Environ. Microbiol.* 81, 8037–8043. doi: 10.1128/AEM.01386-15

Sun, X., Lin, Y., Huang, Q., Yuan, Q., and Yan, Y. (2013). A novel muconic acid biosynthesis approach by shunting tryptophan biosynthesis via anthranilate. *Appl. Environ. Microbiol.* 79, 4024–4030. doi: 10.1128/AEM.00859-13

Tzin, V., and Galili, G. (2010). The biosynthetic pathways for shikimate and aromatic amino acids in *Arabidopsis thaliana*. *Arabidopsis Book* 8:e0132. doi: 10.1199/tab.0132

Wang, J., Cheng, L., Wang, J., Liu, Q., Shen, T., and Chen, N. (2013). Genetic engineering of *Escherichia coli* to enhance production of L-tryptophan. *Appl. Microbiol. Biotechnol.* 97, 7587–7596. doi: 10.1007/s00253-013-5026-3

Weber, C., Brückner, C., Weinreb, S., Lehr, C., Essl, C., and Boles, E. (2012). Biosynthesis of *cis,cis*-muconic acid and its aromatic precursors, catechol and protocatechuic acid, from renewable feedstocks by *Saccharomyces cerevisiae*. *Appl. Environ. Microbiol.* 78, 8421–8430. doi: 10.1128/AEM.01983-12

Yi, J., Li, K., Draths, K. M., and Frost, J. W. (2002). Modulation of phosphoenolpyruvate synthase expression increases shikimate pathway product yields in *E. coli*. *Biotechnol. Prog.* 18, 1141–1148. doi: 10.1021/bp020101w

Yuan, F., Chen, W., Jia, S., and Wang, Q. (2014). Improving 3-dehydroshikimate production by metabolically engineered *Escherichia coli*. *Sheng Wu Gong Cheng Xue Bao* 30, 1549–1560. doi: 10.13345/j.cjb.140019

Zhang, H., Pereira, B., Li, Z., and Stephanopoulos, G. (2015). Engineering *Escherichia coli* coculture systems for the production of biochemical products. *Proc. Natl. Acad. Sci. U.S.A.* 112, 8266–8271. doi: 10.1073/pnas.1506781112

Conflict of Interest: S-YS, S-OP, H-NL, and SL were employed by the company STR Biotech Co., Ltd.

The remaining authors declare that the research was conducted in the absence of any commercial or financial relationships that could be construed as a potential conflict of interest.

frontiers in Bioengineering and Biotechnology

ORIGINAL RESEARCH
published: 11 October 2019
doi: 10.3389/fbioe.2019.00262

Engineering the Yeast *Saccharomyces cerevisiae* for the Production of L-(+)-Ergothioneine

Steven A. van der Hoek[1], Behrooz Darbani[1], Karolina E. Zugaj[1], Bala Krishna Prabhala[1†], Mathias Bernfried Biron[1], Milica Randelovic[1], Jacqueline B. Medina[1], Douglas B. Kell[1,2] and Irina Borodina[1*]*

[1] The Novo Nordisk Foundation Center for Biosustainability, Technical University of Denmark, Kongens Lyngby, Denmark,
[2] Department of Biochemistry, Institute of Integrative Biology, University of Liverpool, Liverpool, United Kingdom

OPEN ACCESS

Edited by:
Nils Jonathan Helmuth Averesch,
Stanford University, United States

Reviewed by:
Tsutomu Tanaka,
Kobe University, Japan
Jingwen Zhou,
Jiangnan University, China

***Correspondence:**
Douglas B. Kell
doukel@biosustain.dtu.dk
Irina Borodina
irbo@biosustain.dtu.dk

†Present address:
Bala Krishna Prabhala,
Faculty of Science, Institute of Physics, Chemistry and Pharmacy, University of Southern Denmark, Odense, Denmark

Specialty section:
This article was submitted to Bioprocess Engineering, a section of the journal Frontiers in Bioengineering and Biotechnology

Received: 21 May 2019
Accepted: 26 September 2019
Published: 11 October 2019

Citation:
van der Hoek SA, Darbani B, Zugaj KE, Prabhala BK, Biron MB, Randelovic M, Medina JB, Kell DB and Borodina I (2019) Engineering the Yeast Saccharomyces cerevisiae for the Production of L-(+)-Ergothioneine. Front. Bioeng. Biotechnol. 7:262. doi: 10.3389/fbioe.2019.00262

L-(+)-Ergothioneine (ERG) is an unusual, naturally occurring antioxidant nutraceutical that has been shown to help reduce cellular oxidative damage. Humans do not biosynthesise ERG, but acquire it from their diet; it exploits a specific transporter (SLC22A4) for its uptake. ERG is considered to be a nutraceutical and possible vitamin that is involved in the maintenance of health, and seems to be at too low a concentration in several diseases *in vivo*. Ergothioneine is thus a potentially useful dietary supplement. Present methods of commercial production rely on extraction from natural sources or on chemical synthesis. Here we describe the engineering of the baker's yeast *Saccharomyces cerevisiae* to produce ergothioneine by fermentation in defined media. After integrating combinations of ERG biosynthetic pathways from different organisms, we screened yeast strains for their production of ERG. The highest-producing strain was also engineered with known ergothioneine transporters. The effect of amino acid supplementation of the medium was investigated and the nitrogen metabolism of *S. cerevisiae* was altered by knock-out of *TOR*1 or *YIH*1. We also optimized the media composition using fractional factorial methods. Our optimal strategy led to a titer of 598 ± 18 mg/L ergothioneine in fed-batch culture in 1 L bioreactors. Because *S. cerevisiae* is a GRAS ("generally recognized as safe") organism that is widely used for nutraceutical production, this work provides a promising process for the biosynthetic production of ERG.

Keywords: ergothioneine, metabolic engineering, medium optimization, *Saccharomyces cerevisiae*, yeast, nutraceutical

INTRODUCTION

Ergothioneine (ERG) (2-mercaptohistidine trimethylbetaine, IUPAC name (2S)-3-(2-Thioxo-2,3-dihydro-1H-imidazol-4-yl)-2-(trimethylammonio)propanoate) is a naturally occurring antioxidant that can be found universally in plants and mammals (Melville, 1959); it possesses a tautomeric structure, but is mainly present in the thione form at physiological pH (**Figure 1**). Ergothioneine was discovered in 1909 in the ergot fungus *Claviceps purpurea* (Tanret, 1909), and its structure was determined 2 years later (Barger and Ewins, 1911). Subsequently, several other organisms were found to produce ergothioneine, including the filamentous fungus *Neurospora crassa* (Genghof et al., 1956), the yeast *Schizosaccharomyces pombe* (Pluskal et al., 2014), various actinobacteria (Genghof, 1970) including *Mycobacterum smegmatis* (Seebeck, 2010),

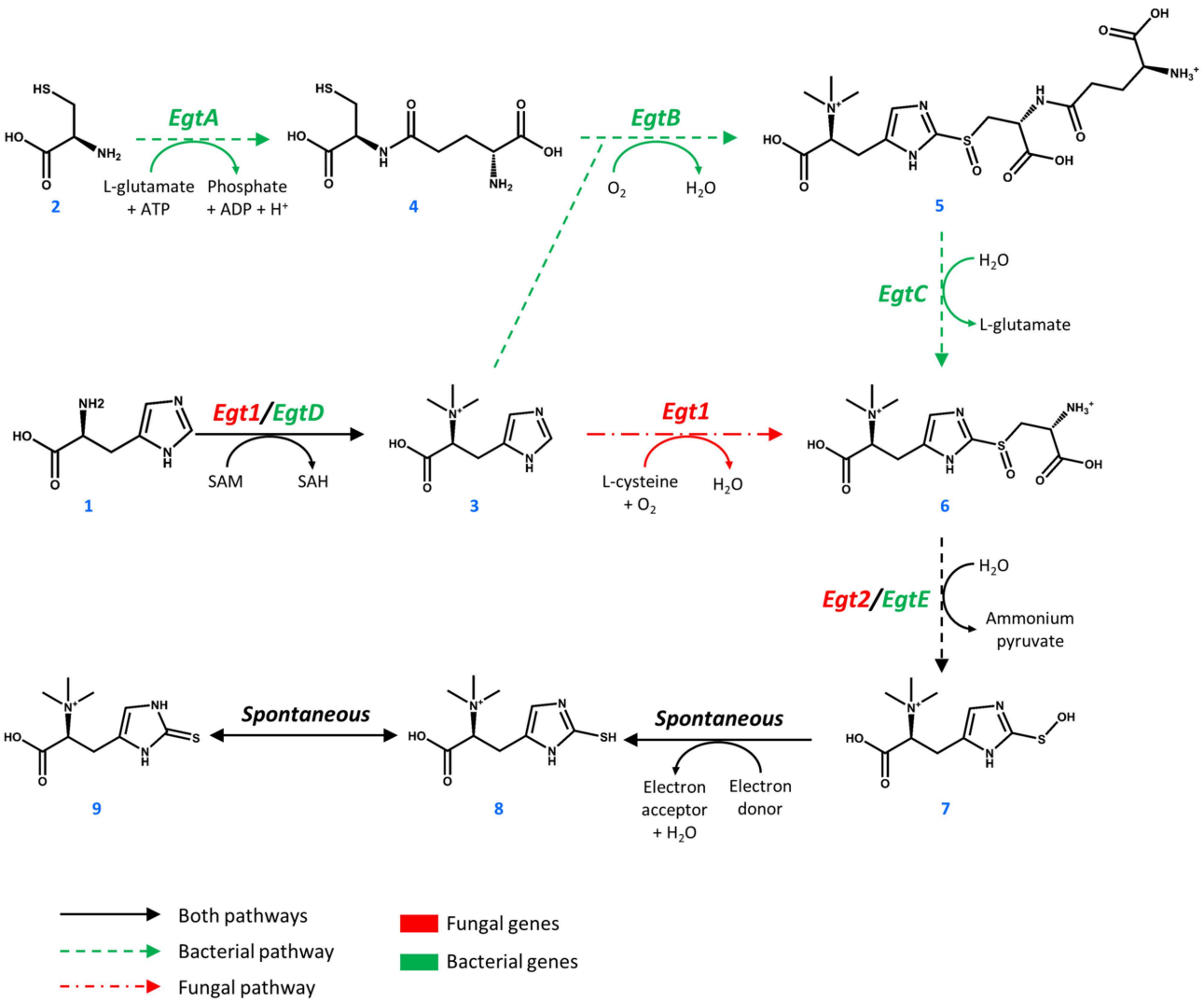

FIGURE 1 | Pathways toward ergothioneine biosynthesis in bacteria and fungi.

and in particular various basidiomycetes (mushrooms) (Genghof, 1970). Higher eukaryotes have been shown to contain ergothioneine (Melville, 1959; Halliwell et al., 2018), but to date no higher eukaryotes have been reported to biosynthesize ergothioneine. Plants are thought to take ergothioneine excreted by fungi up from the soil (Audley and Tan, 1968; Tan and Audley, 1968) or through symbiotic relationships (Park et al., 2010; Guo et al., 2016).

Ergothioneine is synthesized from one molecule of L-histidine (**1**), one molecule of L-cysteine (**2**), and 3 methyl groups donated by S-adenosyl-L-methionine (SAM, **Figure 1**). In *M. smegmatis*, the reaction sequence is catalyzed by five enzymes, encoded by *egtA-E* genes arranged in an operon (Sao Emani et al., 2018).

Four enzymes of the cluster EgtA, EgtB, EgtC, and EgtD catalyze four individual reactions that methylate L-histidine to form hercynine (**3**), convert L-cysteine to γ-L-glutamyl-L-cysteine (**4**), combine hercynine and γ-L-glutamyl-L-cysteine to generate γ-L-glutamyl-S-(hercyn-2-yl)-L-cysteine S-oxide (**5**) and produce the S-(hercyn-2-yl)-L-cysteine S-oxide (**6**, HCO). In fungi, the biosynthetic pathway is different, as a single enzyme Egt1 catalyzes the methylation of L-histidine (**1**) to give hercynine (**3**), which in turn is sulfoxidized with cysteine, producing HCO (**6**). HCO is converted into 2-(hydroxysulfanyl)hercynine (**7**) by a β-lyase, encoded by *egtE* in *M. smegmatis* and by the *EGT2* gene in fungi. This compound is spontaneously reduced to ergothioneine (**8**, thiol form and **9**, thione form). Comparing the bacterial and fungal pathway, it is important to note that the utilization of glutamate in the ergothioneine biosynthesis pathway also requires ATP. Recently, enzymes for the anaerobic production of ergothioneine were found in *Chlorobium limicola*

Abbreviations: ERG, L-(+)-ergothioneine; HCO, S-(hercyn-2-yl)-L-cysteine S-oxide; PBS, phosphate-buffered saline; PI, propidium iodide; PLP, pyridoxal 5′-phosphate; SAM, S-adenosyl-L-methionine.

(Burn et al., 2017), where sulfur is directly transferred to the imidazole ring of hercynine to form ergothioneine (Leisinger et al., 2019). However, it is suggested that the anaerobic C-S bond formation is less efficient than it's aerobic counterpart (Burn et al., 2017).

The antioxidant properties of ERG include the scavenging of free radicals and reactive oxygen species (Akanmu et al., 1991; Park et al., 2010; Ta et al., 2011) and the chelation of divalent metal ions (Hanlon, 1971). ERG has been shown to reduce oxidative damage in a variety of mammals (Deiana et al., 2004; Cheah and Halliwell, 2012). In humans, ERG is mainly accumulated in the liver, the kidneys, in erythrocytes, the eye lens, and in seminal fluid (Leone and Mann, 1951; Melville et al., 1954; Shires et al., 1997). It is transported by a specific transporter SLC22A4 (previously known as OCTN1) (Grundemann et al., 2005; Tschirka et al., 2018). The natural selection of such a transporter implies that ergothioneine is involved in the maintenance of health or the mitigation of disease, and it may even be a vitamin (Paul and Snyder, 2010). ERG has demonstrated effects in *in vivo* models of several neurodegenerative diseases (Link, 1995; Yang et al., 2012; Song et al., 2014), in ischemia reperfusion injury (Bedirli et al., 2004; Sakrak et al., 2008a,b), and in a variety of other diseases (Halliwell et al., 2018). Ergothioneine accumulates at sites of injury through the upregulation of SLC22A4/OCTN1 (Cheah et al., 2016; Tang et al., 2016). It is only slowly metabolized and excreted in humans (Cheah et al., 2017).

Because humans cannot produce ERG, they must obtain it through their diet. Although plants and animals also accumulate it to some degree, the main natural dietary source of ERG is basidiomycete mushrooms, where some species contain up to 7 mg of ERG per gram dry weight (Ey et al., 2007; Pfeiffer et al., 2011; Kalaras et al., 2017; Halliwell et al., 2018). Because of the beneficial effects and possible involvement of ERG in disease, ergothioneine may potentially prove its value in the global dietary supplement market, which was estimated at some $241.1 billion in 2019 (Wang et al., 2016). Currently, commercial ergothioneine is extracted from mushrooms or synthesized chemically.

Production of ergothioneine in microbial cell factories would provide a sustainable low-cost alternative to its current manufacturing processes. So far, fermentative ERG production has been reported in bacteria and filamentous fungi, including *Methylobacterium aquaticum* strain 22A (Alamgir et al., 2015), *Aureobasidium pullulans* (Fujitani et al., 2018), *Rhodotorula mucilaginosa* (Fujitani et al., 2018), *cyanobacteria* (Pfeiffer et al., 2011), *Aspergillus oryzae* (Takusagawa et al., 2019), and *Escherichia coli* (Osawa et al., 2018; Tanaka et al., 2019). Engineering of *M. aquaticum* with an extra copy of *egtBD* and the deletion of *hutH* (histidine-ammonia-lyase gene) lead to a strain that produced 7.0 mg ERG/g dry cell weight and 100 μg ERG/5 mL/7 days (Fujitani et al., 2018). In another study, multiple copies of *EGT1* and *EGT2* genes from *N. crassa* were integrated into the genome of the filamentous fungi *A. oryzae*. The engineered strain produced 231 mg ergothioneine per kg solid media (Takusagawa et al., 2019). In *E. coli*, at first 24 mg/L of secreted ERG was produced by expression of *egtBCDE* genes from *M. smegmatis* and optimization of the medium composition (Osawa et al., 2018). This was followed up by a study, in which the authors also expressed *egtA* and improved the strain by enhancing the cysteine and S-adenosyl methionine biosynthesis, as well as optimizing their medium further, to produce 1.3 g/L of ergothioneine in 216 h by fermentation (Tanaka et al., 2019). To the best of our knowledge, there are no reports on ergothioneine production in baker's yeast, which is the preferred host for the production of nutraceuticals (Huang et al., 2008; Li and Borodina, 2014; Yuan and Alper, 2019). In this study we describe the metabolic engineering of the yeast *Saccharomyces cerevisiae* for the production of ergothioneine, reaching a titer of 0.6 g/L in fed-batch fermentation for 84 h.

MATERIALS AND METHODS

Strains and Chemicals

S. cerevisiae strain CEN.PK113-7D (MATa URA3 HIS3 LEU2 TRP1 MAL2-8^c SUC2) was a gift from Peter Kötter (Goethe University, Frankfurt/Main, Germany). *S. pombe* strain DSM 70572, obtained from Leibniz-Institut DSMZ-Deutsche Sammlung von Mikroorganismen und Zeilkulturen GmbH (Germany) was used for genomic DNA extraction. *E. coli* DH5α was used for cloning. Ergothioneine (catalog #E7521, ≥98% purity) was from Sigma-Aldrich, hercynine (catalog # H288900, ≥95% purity) was from Toronto Research Chemicals Inc. Simulated fed-batch medium components (EnPump 200) were from EnPresso GmbH (Germany). These components consist of a polysaccharide, in powder form, to add to the medium and an enzyme to release glucose from the polysaccharide. The rate of release is dependent on the enzyme concentration and allows for simulated carbon-limited fermentation.

Cloning

CpEgt1, MsEgtA, and MsEgtE were codon-optimized for *S. cerevisiae* using GeneGenie (Swainston et al., 2014), while the other genes were codon-optimized for *S. cerevisiae* using the codon-optimization tool provided by GeneArt. The genes were then ordered as synthetic gene strings from IDT DNA (MsEgtA) or GeneArt (all other synthetic gene strings). The only exceptions were two genes from *S. pombe*, which were isolated from genomic DNA. The DNA sequences of the genes are in **Supplementary Table 1**. All yeast strain construction was done using CRISPR/Cas9 and EasyClone-MarkerFree methods (Stovicek et al., 2015; Jessop-Fabre et al., 2016). Correct cloning was validated by sequencing (Eurofins Genomics). Correct genome modification of yeasts was validated by colony PCR. The details on primers (**Supplementary Tables 2, 3**), biobricks (**Supplementary Table 4**), plasmids (**Supplementary Tables 5, 6**), and strains (**Supplementary Table 7**) are in **Supplementary Materials**.

Media and Small-Scale Cultivation Conditions

For *E. coli* selection, we used Lysogeny Broth (LB) with 100 mg/L ampicillin. For the selection of yeast strains, we used Yeast-Peptone-Dextrose (YPD) agar supplemented with 200 mg/L G418 for selection of Cas9 vector and 100 mg/L nourseothricin

for selection of the gRNA vector. Synthetic Complete (SC) medium was prepared using 6.7 g/L Yeast Nitrogen Base without amino acids from Sigma-Aldrich, 1.92 g/L Synthetic Drop-out supplement without histidine from Sigma-Aldrich and 76 mg/L histidine. For ERG production, yeast strains were cultivated in SC medium with 20 or 40 g/L glucose or with 60 g/L EnPump substrate (and 0.6% enzyme reagent) as carbon source. Precultures for cultivation experiments were prepared by inoculating a single colony of a strain into 5 mL of the medium used in the cultivation experiment and incubating at 30°C and 250 rpm for 24 h. The cultivations were performed in 24-deep-well plates from EnzyScreen, 3 mL of medium was used per well and the starting OD_{600} was 0.5. The plates were incubated at 30°C with 250 rpm agitation.

HPLC Analyses

To determine the extracellular ergothioneine concentration, a 1 mL sample of fermentation broth was centrifuged at 3,000 × g for 5 min, the supernatant was moved into an HPLC vial and stored at −20°C until the analysis. The remaining cell pellet was washed twice with 1 mL MilliQ water and resuspended in 1 mL water. The extraction of intracellular ERG was performed according to Alamgir et al. (2015) as following. The mixture was heated at 94°C for 10 min, vortexed at 1,600 rpm for 30 min using a DVX-2500 Multi-Tube Vortexer from VWR, and centrifuged at 10,000 × g for 5 min. The supernatant was transferred into an HPLC vial and stored at +4°C until analysis. The ERG concentrations were measured using a Dionex Ultimate 3000 HPLC system. Quantification was done based on standard curves using Chromeleon software. Five microliter of sample was injected on a Cortects UPLC T3 reversed-phase column (particle size 1.6 µm, pore size 120 Å, 2.1 × 150 mm). The flow rate was 0.3 mL/min, starting with 2.5 min of 0.1% formic acid, going up to 70% acetonitrile, 30% 0.1% formic acid at 3 min for 0.5 min, after which 100% 0.1% formic acid was run from min 4 to 9. Ergothioneine was detected at a wavelength of 254 nm. For analysis of bioreactor samples, we additionally quantified glucose, ethanol, pyruvate, and acetate concentrations by HPLC as described (Borodina et al., 2015).

Fed-Batch Fermentation in Bioreactors

A single colony from a YPD plate with ST8927 colonies (see below) was used to inoculate 5 mL of minimal media in 14 mL tube. The tube was incubated at 30°C and 250 rpm overnight. This overnight culture was transferred into 95 mL mineral medium in 500 mL baffled shake flask. The shake flask was then incubated overnight at 30°C and 250 rpm. Forty milliliters of this dense culture was used to inoculate 60 mL mineral medium in a new 500 mL baffled shake flask. Two shake flasks were prepared this way. These shake flasks were incubated at 30°C and 250 rpm for 4 h, the content of both shake flasks was combined, then centrifuged at 3,000 × g for 5 min. The supernatant was discarded, the pellet was washed with 25 mL sterile water, resuspended and centrifuged as before. The supernatant was discarded and the pellet resuspended in 10 mL mineral medium. This was then used to inoculate 0.5 L mineral medium in a 1 L Sartorius bioreactor. The starting OD600 was 0.85. The stirring rate was set at 500 rpm, the temperature was kept at 30°C, and pH was maintained at pH 5.0 using 2 M KOH and 2 M H_2SO_4. The feeding was started as soon as CO_2 in the off-gas decreased by 50%. The initial feed rate was set at 0.6 g glucose h^{-1}, linearly increasing to 2.5 g glucose h^{-1} over the span of 25.5 h. After that, the feed was set at a constant 1.4 g glucose h^{-1} and 17.8 h later, the feeding rate was set to a constant 2.9 g glucose h^{-1}. The feed was stopped at 84 h. At 60.5 and 75.5 h, 2 g $(NH_4)_2SO_4$ was added as a sterile 100 g/L solution. At 60.5 and 73.5 h, 0.5 g $MgSO_4$ was added as a sterile 50 g/L solution, while 4 mL sterile trace metals solution and 2 mL sterile vitamin solution were added.

Propidium Iodide Staining and Flow Cytometry Analysis

Precultures were prepared by inoculating a single colony of strain ST7574, ST8461, and ST8654 into separate 14-mL tubes containing 5 ml of SC + 40 g/L glucose + 1 g/L His/Cys/Met and incubating at 30°C and 250 rpm for 24 h. Precultures were used to inoculate 25 mL SC + 40 g/L glucose + 1 g/L His/Cys/Met at a starting OD_{600} of 0.5, which was incubated at 30°C and 250 rpm for 72 h. Every 24 h, a 1 mL sample of cell culture was taken from the yeast cultivation. This sample was washed two times with 1 mL phosphate-buffered saline (PBS), subsequently resuspended in 0.5 µg/mL propidium iodide (PI) in PBS and incubated for 20 min at room temperature in the dark. After incubation, the cells were washed two times with PBS and the percentage of PI stained cells was determined using a MACSQuant VYB system (Miltenyi Biotec). Data analysis was performed using the FlowJo software.

Fluorescent Microscopy

Precultures were prepared by inoculating a single colony into a 14 mL tube containing 5 mL YPD medium and incubating at 30°C and 250 rpm overnight. Overnight precultures of strains containing transporters linked to GFP and the control strain were used to inoculate 5 mL YPD medium in 14 mL tubes at OD_{600} = 2 and were cultured at 30°C and 250 rpm for 5 h. One milliliter of the culture was harvested at 3,000 × g for 5 min. The cells were washed two times with PBS and subsequently pictures of the cells were taken using a Leica DM 400 B system, using Leica Application Suite V4 as image software.

Medium Optimization

A two-level fractional factorial based on the components of SC medium, with the levels high (+1, component 5-folds higher than original SC medium) and low (−1, component 5-folds lower than original SC medium), was used to determine the impact of individual components on the yield of ergothioneine. Two different stocks of all the individual components were prepared, one each for high and low concentrations and these were mixed together for all components to yield 64 different designed media. The design matrix for the fractional factorial grid has been attached (**Supplementary Table 8**). Precultures were prepared by inoculating a single colony of strain ST8461 into a 14 mL tube containing 5 mL SC medium and incubating at 30°C and 250 rpm overnight. Precultures were then used to inoculate 300 µL media in 96-deep-well plates from EnzyScreen at OD_{600} = 0.1 in

duplicate for each different medium and incubated at 30°C and 225 rpm for 48 h. Samples for analysis were taken at 24 and 48 h.

LC-MS Analysis for Medium Optimization

Amounts of total ergothioneine were analyzed my LC-MS in MRM mode. The analysis was performed on a Bruker EVOQ (QqQ) coupled to UPLC. The LC part of the LC-MS/MS system consisted of a CTC autosampler module, a high pressure mixing pump and a column module (Advance, Bruker, Fremont, CA, USA). The injection volume was 1 µL. The chromatography was performed on a ZIC-cHILIC column, 150 × 2.1 mm, 3 µm particle size (SeQuant, Merck Millipore), equipped with a 0.5 µ

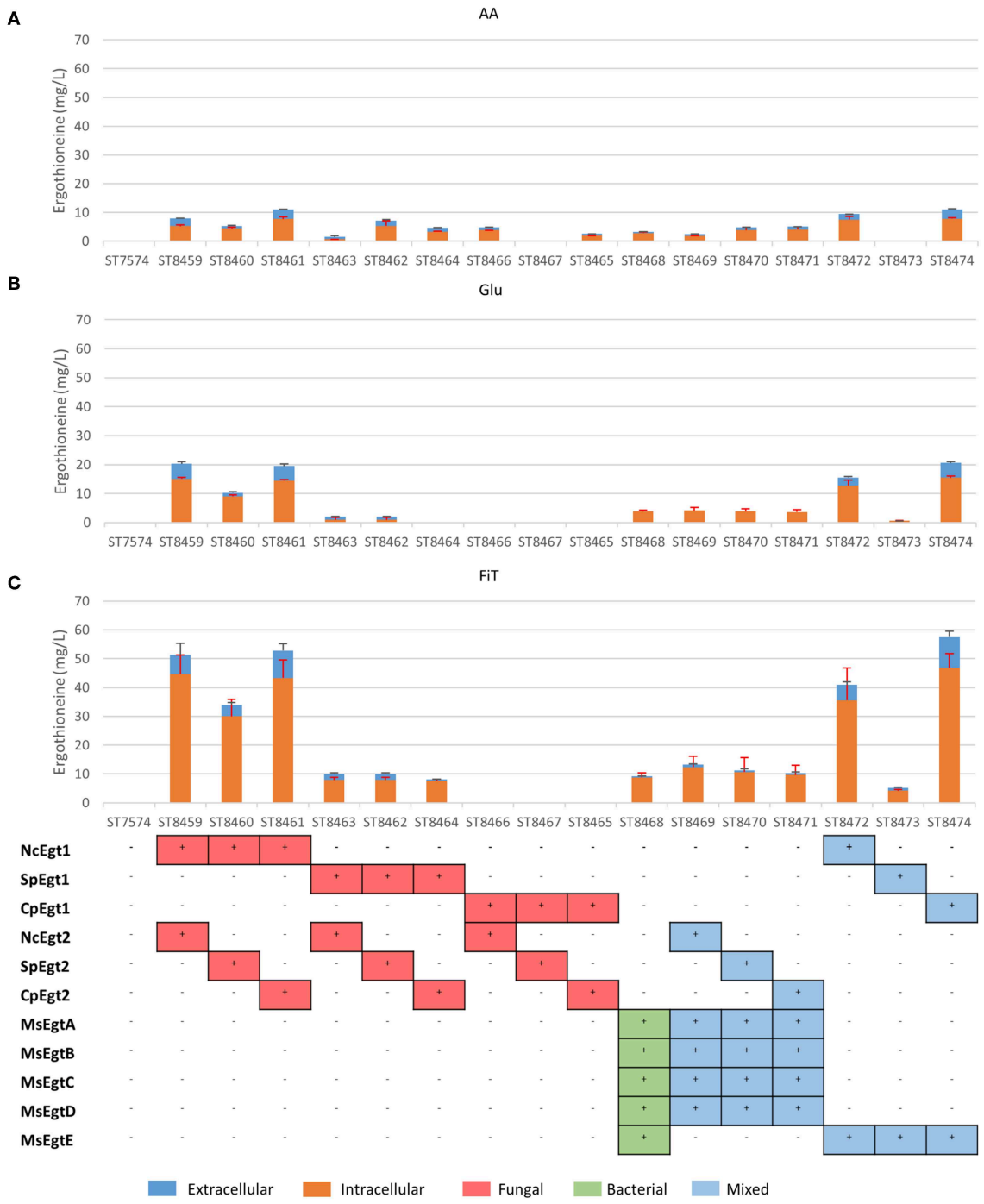

FIGURE 2 | Ergothioneine production in strains with different ERG pathway combinations on three variations of synthetic complete medium: **(A)** AA: 20 g/l glucose and 1 g/l of each L-His, L-Met, and L-Cys, **(B)** Glu: 40 g/l glucose, **(C)** FiT: 60 g/l EnPump substrate for slow glucose release to simulate fed-batch conditions.

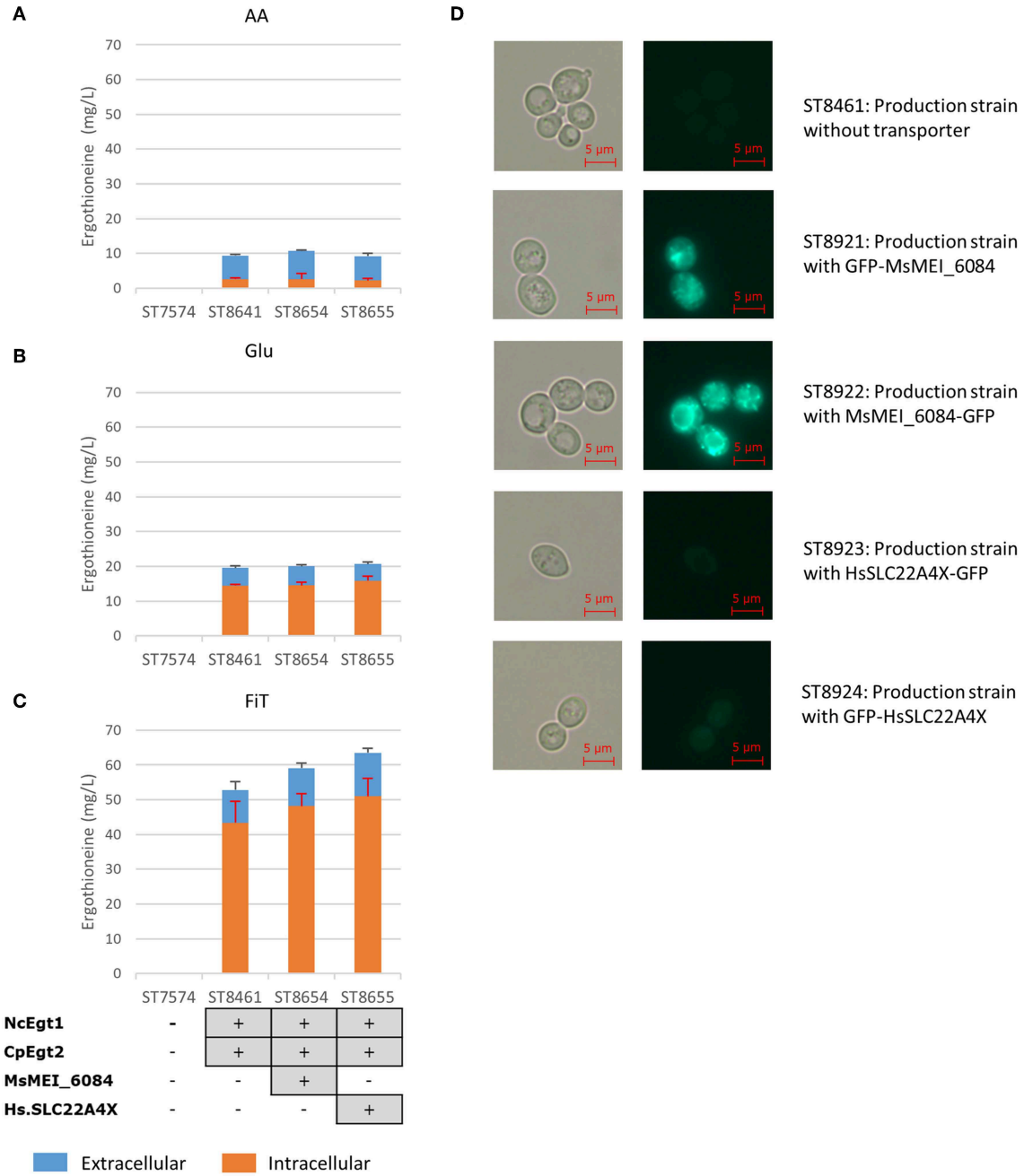

FIGURE 3 | Ergothioneine production by yeast strains expressing human ERG transporter SLC22A4X or a putative ERG transporter from *M. smegmatis* on three variations of synthetic complete medium: **(A)** AA: 20 g/l glucose and 1 g/l of each L-His, L-Met, and L-Cys, **(B)** Glu: 40 g/l glucose, **(C)** FiT: 60 g/l EnPump substrate for slow glucose release to simulate fed-batch conditions, **(D)** Microscope images of yeast cells with ergothioneine transporters linked to GFP. To the left are Brightfield images and to the right GFP images. Top panels; ST8461, ergothioneine producing strain without transporter. Middle-top panels, ST8921, ergothioneine producing strain with a putative transporter from *Mycobacterium smegmatis* linked to GFP at the N-terminus. Middle panels, ST8922, ergothioneine producing strain with a putative transporter from *Mycobacterium smegmatis* linked to GFP at the C-terminus. Middle-bottom panels, ST8923, ergothioneine producing strain with a transporter from *Homo sapiens* linked to GFP at the C-terminus. Bottom panels, ST8924, ergothioneine producing strain with a transporter from *Homo sapiens* linked to GFP at the N-terminus.

depth filter (KrudKatcher Classic, Phenomenex). Eluent A was 20 mM ammonium acetate, pH adjusted to 3.5 with formic acid in MilliQ water. Eluent B was acetonitrile. The total flow rate of eluent A and B was 0.4 mL/min. The isocratic elution was 30% A, and the total run time was 5 min. Retention time was 1.8 min for ergothioneine. The mass spectrometer was operated

with electrospray in the positive ion mode (ESI+). The spray voltage was set to 4,500 V. The cone gas flow was 20 L/h, and the cone temperature was set at 350°C. The heated probe gas flow was set at 50 L/h with a temperature of 350°C. Nebulizer flow was set at 50 L/h, and the exhaust gas was turned on. Argon was used as collision gas at a pressure of 1.5 mTorr. Detection was performed in multiple reacting monitoring (MRM) mode. The quantitative transition was 198 → 95 for ergothioneine and the qualitative transition was 198 → 154. The collision energy was optimized to 15 and 7 eV, respectively. The xms files were converted into cdf files and were analyzed using Mzmine 2.33.

RESULTS

Expression of Bacterial, Fungal, and Chimeric Biosynthetic Pathways Toward Ergothioneine in *S. cerevisiae*

The biosynthetic genes for ERG production were of both bacterial origin (*M. smegmatis*) and of fungal origin (*C. purpurea*, *N. crassa*, *S. pombe)*. The Egt1 homologs in *C. purpurea* and *S. pombe* were identified by BLASTp using the sequence of Egt1 for *N. crassa* (Genbank accession: XP_956324.3). Similarly, Egt2 from *S. pombe* (Genbank accession: NP_595091.1) was used to find the Egt2 homologs in *N. crassa* and *C. purpurea*. Genbank accession numbers are provided in **Supplementary Table 1**. The genes were combined into sixteen pathway variants, where nine pathway variants were made of fungal genes, one pathway variant comprised bacterial genes only, and six variants contained both fungal and bacterial genes. The 16 yeast strains with different pathway variants were cultivated in three different media and the intra- and extracellular concentrations of ergothioneine were measured (**Figure 2**).

ERG titers were the highest in simulated fed-batch medium (up to 60 mg/L as compared to a maximum of 20 mg/L under batch conditions). Of the five best-performing pathway variants, four contained Egt1 from *N. crassa* and any other of the four enzymes catalyzing the 2nd enzymatic step (MsEgtE, NcEgt2, SpEgt2, or CpEgt2). The fifth contained CpEgt1 and MsEgtE. Curiously, CpEgt1 combined with any fungal Egt2 variants only produced ERG on the medium that contained high levels of histidine, cysteine and methionine (**Figure 2A**). We speculate that *C. purpurea* enzyme CpEgt1 has a lower affinity to one or several of the substrate(s) (histidine, SAM, cysteine) than the enzyme from *N. crassa* and hence ERG production was only feasible when the intracellular levels of the substrates was increased through supplementation in the medium. Overall, only 5–30% of the total ERG was secreted, while the rest was retained intracellularly. The strain ST8461, combining Egt1 from *N. crassa* and Egt2 from *C. purpurea,* was selected for further engineering.

Engineering Ergothioneine Transport

The concentration of ERG inside the cells can be estimated to be ∼3.5 mM (for strain ST8461 on simulated fed-batch medium), which is 80-fold higher than in the broth. As *M. smegmatis* is known to secrete ergothioneine to levels up to 4 times the intracellular concentration (Sao Emani et al., 2013), we speculated that it may contain an equilibrative or effluxing ERG transporter. On the *M. smegmatis* genome, adjacent to the *egtA-E* operon, there is an open reading frame MSMEI_6084, encoding a protein annotated as a chloramphenicol exporter (**Supplementary Figure 1**). The protein has 12 transmembrane domains as predicted by Phyre2 (Kelley et al., 2015) (**Supplementary Figure 2**). We expressed codon-optimized variants of this gene and of the (normally concentrative) human ERG transporter SLC22A4 in strain ST8461 (**Figure 3**). However, there was no significant increase of intracellular or extracellular ERG production. To determine why neither transporter had an effect, we investigated their cellular localization by green fluorescent protein (GFP) tagging on the

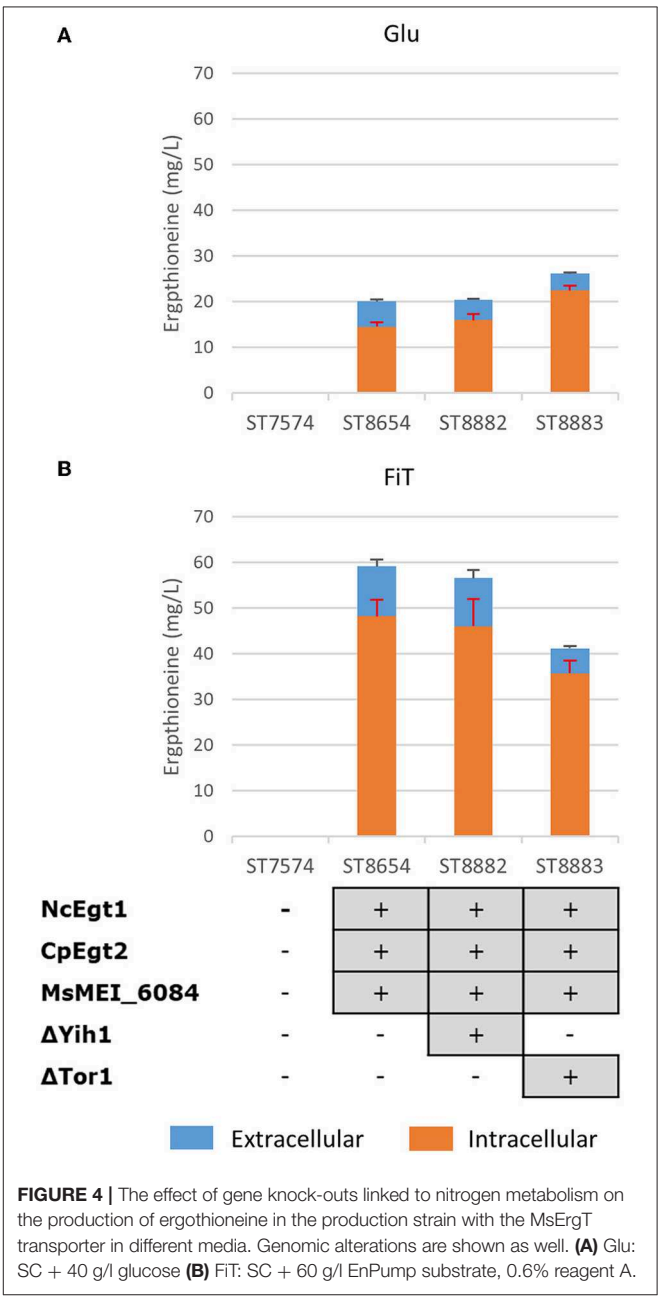

FIGURE 4 | The effect of gene knock-outs linked to nitrogen metabolism on the production of ergothioneine in the production strain with the MsErgT transporter in different media. Genomic alterations are shown as well. **(A)** Glu: SC + 40 g/l glucose **(B)** FiT: SC + 60 g/l EnPump substrate, 0.6% reagent A.

C- or N-termini (**Figure 3**). Interestingly, MsMEI_6084 mainly localized to the vacuolar membrane of *S. cerevisiae*, while human SLC22A4X was only weakly expressed and its localization could not be determined. Since neither of the transporters localized to the plasma membrane specifically, it can explain the lack of effect on ERG secretion.

Engineering of Nitrogen Metabolism

Both Tor1 (Hinnebusch, 2005; Ljungdahl and Daignan-Fornier, 2012) and Yih1 (Hinnebusch, 2005) inhibit Gcn2p, a positive regulator of *GCN4*. Deletion of either of these enzymes could lead to increased ERG production by increasing the amino acid pools in yeast. In **Figure 4**, we show the results of these alterations in the nitrogen metabolism of *S. cerevisiae* in different media. Yih1 deletion does not have an effect on the production of ergothioneine, while Tor1 only seems to lead to an increase in ERG under batch conditions. Since eventual ERG production is likely to be carried out under fed-batch conditions and neither of the deletions gave a positive effect under fed-batch conditions, we decided not to proceed with these genetic modifications.

Supplementation of the Medium With Precursor Amino Acids

To determine whether the supply of the three amino acids (L-histidine, L-cysteine, and L-methionine) that serve as precursors for ERG biosynthesis is limited, we cultivated several yeast strains with supplementation of 1 or 2 g/L of each of L-methionine, L-cysteine, and L-histidine. We chose two producing strains, ST8461 and ST8654, the latter containing the MsMEI_8064 gene.

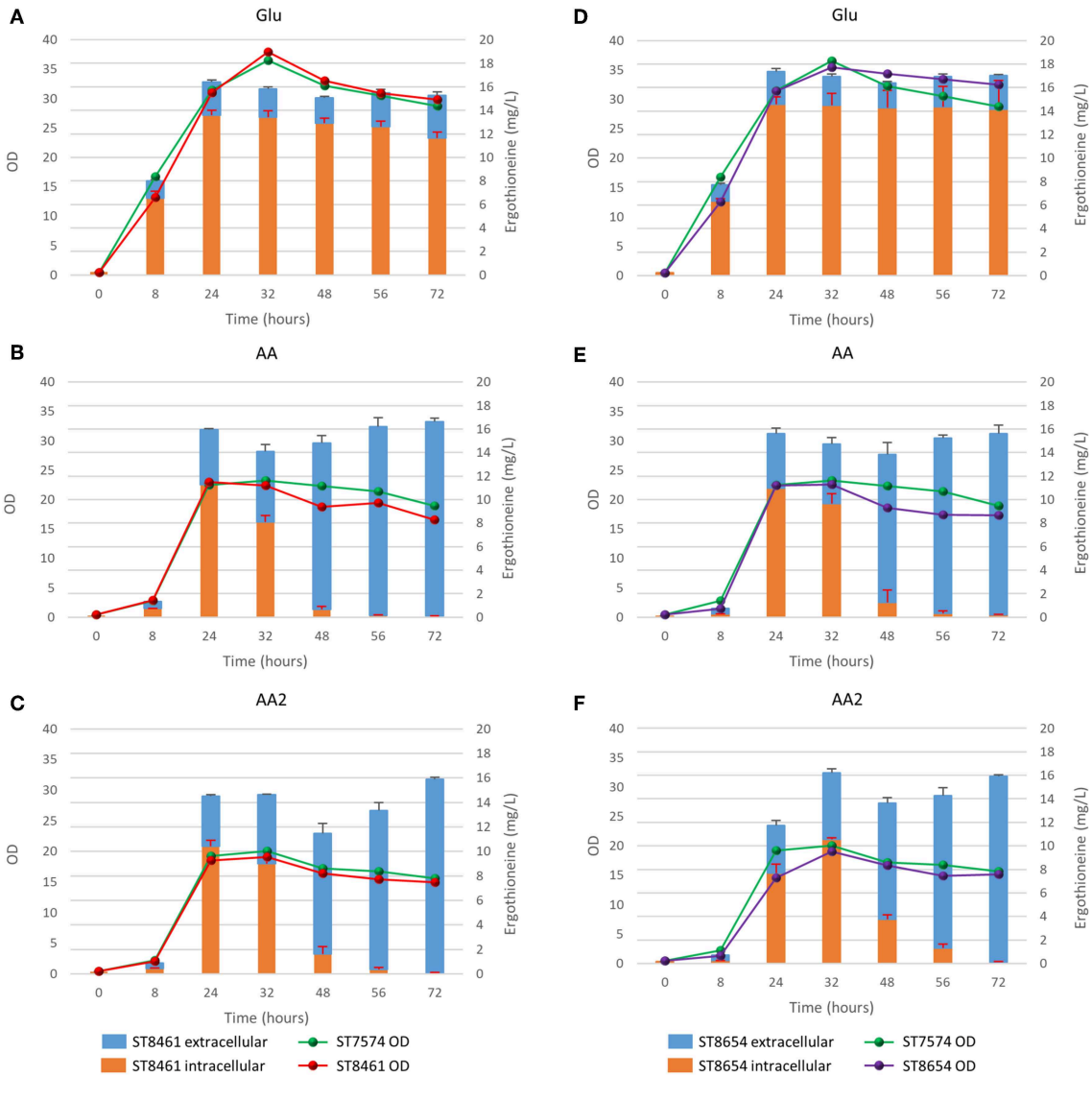

FIGURE 5 | Production of ergothioneine over time in the production strain with or without transporter in different media compositions. **(A,D)** Glu: SC + 40 g/l glucose, **(B,E)** AA: SC + 40 g/l glucoe + 1 g/l His/Met/Cys, **(C,F)** AA2: SC + 40 g/l glucose + 2 g/l His/Cys/Met.

A non-producing strain ST7574 was used as a control. The experiments were performed in shake flasks and growth and ERG production were monitored over the course of 3 days (**Figure 5**). ERG accumulated primarily in the first 24 h of cultivation, which would correspond to the exponential growth on glucose, reaching ca. 16 mg/L in both producing strains, independent of any amino acid supplementation. The supplementation, however, affected the cellular growth, with the final OD being ∼46 and 52% lower when 1 or 2 g/L, respectively, of the amino acids were added. No degradation of ERG was observed; however surprisingly, there was a large variation in the intracellular vs. extracellular distribution of ERG depending on the addition of amino acids. Specifically, the addition of amino acids promoted the excretion of ERG in the stationary phase. We hypothesized that this was due to cell death because of the toxic effects of the added amino acids, in particular histidine (Watanabe et al., 2014) and cysteine (Kumar et al., 2006). Indeed propidium iodide staining of cells sampled every 24 h for 72 h, showed an increase in the fraction of dead cells from 9 to 70%, when amino acids were added at concentrations of 1 g/L (**Supplementary Figure 3**). Clearly, the concentrations of amino acids used were too high and hence we decided to undertake a more systematic medium optimization approach as described in the next section.

Medium Optimization

To perform optimization of medium composition, we chose a two-level fractional factorial design, where the concentrations each of the components of the synthetic complete medium were varied 5-fold (**Figure 6**, **Supplementary Table 8**). Strain ST8461 was cultured in SC medium (medium 65 in **Figure 6**) to provide a baseline for the ergothioneine production during the experiment with which to compare the performance of the other media. After 48 h, 63% of the designed media outperformed SC medium with regard to ERG titers. To be able to identify the best contributing components, the analysis was narrowed down to the eight top-performing media. Higher levels of arginine, histidine, methionine, and pyridoxine were present in these media, while we could find no compound that had its concentration reduced across most or all of these media. Even though cysteine is a precursor for ergothioneine, it is not universally increased across the different media. However, as methionine can be converted into both S-adenosyl methionine and cysteine by yeast, increased levels of methionine in the medium by itself could be enough for increasing ERG titers. Pyridoxine is a precursor for pyridoxal 5′-phosphate (PLP), which binds to EgtE to facilitate the conversion of HCO to 2-(hydroxysulfanyl)hercynine in a PLP-dependent manner (Song et al., 2015). Since CpEgt2 is the fungal equivalent of EgtE, it is likely that pyridoxine has a positive effect on ERG production through CpEgt2. Interestingly, higher concentrations of arginine also increased ergothioneine production. The amino acid metabolism of *S. cerevisiae* contains many degradation and bioconversion pathways for arginine to be converted into other amino acids (Ljungdahl and Daignan-Fornier, 2012), which might contribute to the increased ERG titers.

Enhancing the Expression of Ergothioneine Biosynthetic Genes

We recognized that the ERG-producing strain could be improved by increasing the expression of the ERG biosynthetic genes. We integrated an additional copy of NcEgt1 and/or CpEgt2 expression cosseted into ST8461 (**Figure 7**). An additional copy of NcEgt1 increased the titer by 80 and 20% for batch and

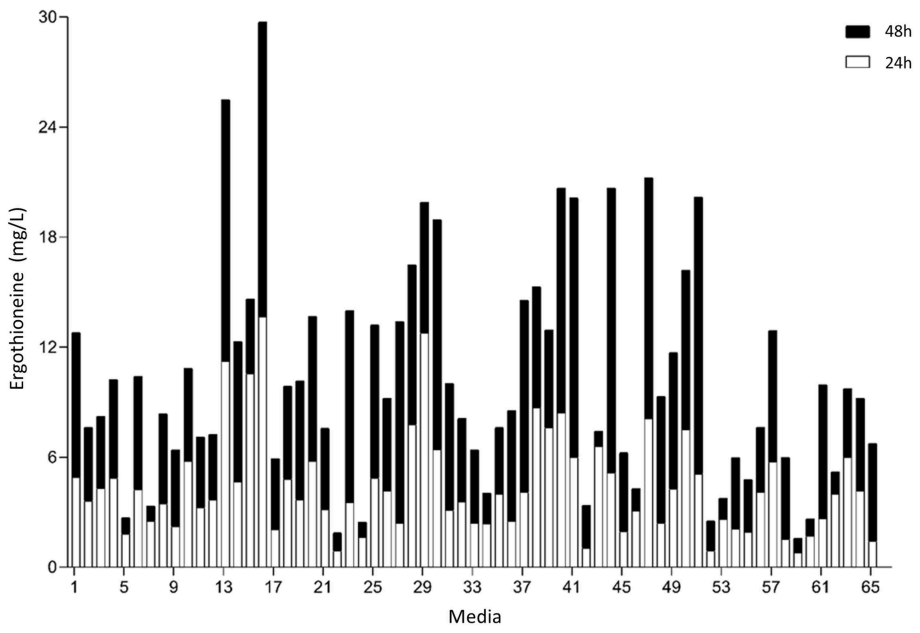

FIGURE 6 | Median concentration of ergothionine produced after 24 and 48 h. The values are additive. Open bars represent values obtained after 24 h while the closed bars represent values obtained after 48 h.

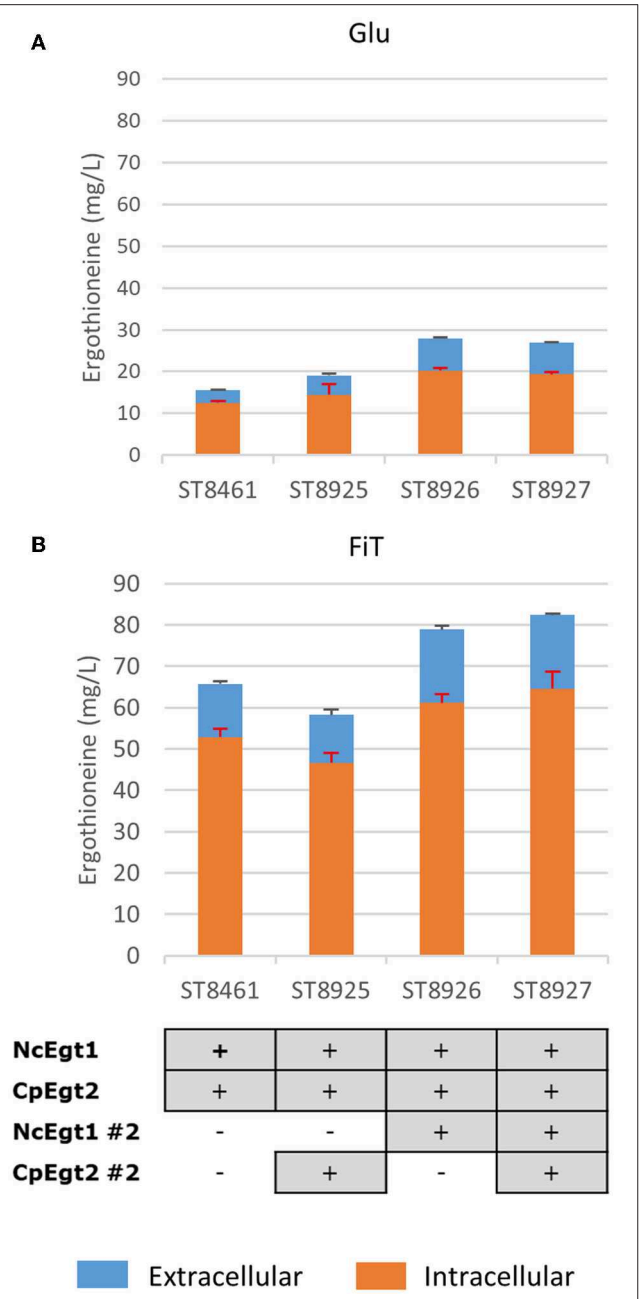

FIGURE 7 | The effect of the integration of a second copy of Egt enzymes on the production of ergothioneine in the high producing strain in different media. Genomic alterations are shown as well. **(A)** Glu: SC + 40 g/l glucose **(B)** FiT: SC + 60 g/l EnPump substrate, 0.6% reagent A.

simulated fed-batch medium, respectively, while an additional copy of Egt2 did not increase the ergothioneine titer and even caused a decrease in simulated fed-batch medium. When additional copies of both genes were integrated, the total titer was increased by 25% on simulated fed-batch medium (ST8927). The marginal increase in titer indicates that the flux control of the pathway mainly resides elsewhere, either with the precursor supply or NcEgt1 and CpEgt2 may experience inhibition from ERG or its intermediates; this needs to be addressed through further strain engineering.

Ergothioneine Production in Controlled Fed-Batch Fermentation

Finally, the engineered ERG-producing ST8927 strain was cultivated in bioreactors under glucose-limited fed-batch conditions. Based on the medium optimization results from section Medium Optimization, we supplemented the fed-batch fermentation medium with arginine, histidine, methionine and pyridoxine. During the 84-h cultivation, 598 ± 18 mg/L erg was produced, of which 59% was extracellular, from 175.0 ± 3.5 g/L glucose (**Figure 8**). Next to that, a total of 3.2 g arginine, histidine, and methionine, as well as 192 mg pyridoxine was added through the starting medium and the feeding medium. The final dry weight of biomass was 55 ± 1 g/L, and as baker's yeast has a cell density of ∼1.103 g/mL (Bryan et al., 2010), this brings the intracellular concentration of ERG to 17.7 mM, which is 11-fold higher than the extracellular concentration of 1.6 mM at the end of the fermentation. During the fermentation, at two points (after 48 and 72 h), the growth of the cells started stagnating. However, when we added extra $(NH_4)_2SO_4$, $MgSO_4$, trace metal solution, and vitamins, the cells began growing again. Most likely, the strain has an extra requirement for one or more of these components that was not found via the medium optimization, as the medium optimization was run under batch conditions, rather than fed-batch conditions in which yeast can reach much higher cell densities. Between 48 and 60 h, biomass concentration declined slightly and the ratio between the extra- and the intra-cellular ERG increased, which could be caused by increased cell death, similar as we observed upon the supplementation of high concentrations of amino acids (section Medium Optimization). The process performance could be improved by optimization of the medium composition, process physical parameters, and the feeding profile.

DISCUSSION

Ergothioneine is an antioxidant with many potential health benefits (Cheah and Halliwell, 2012; Ames, 2018; Halliwell et al., 2018). Furthermore, the interaction of ERG with metal ions (Hanlon, 1971) could conceivably play a role in the intracellular chaperoning of trace elements. Fermentation could provide an alternative and sustainable way for ergothioneine production compared to the current commercial processes. To this end, we have engineered *S. cerevisiae* for the production of ergothioneine, reaching levels of 0.6 g/L. As there are many different organisms that produce ergothioneine (Tanret, 1909; Genghof et al., 1956; Genghof and Vandamme, 1964; Genghof, 1970; Seebeck, 2010; Pfeiffer et al., 2011; Pluskal et al., 2014; Sheridan et al., 2016; Kalaras et al., 2017) (**Supplementary Tables 9**, **10**), we have focused on the organisms in which genes for ergothioneine production were identified. Other heterologous or from different organisms could therefore also be tested in *S. cerevisiae* to potentially find better performing combinations than those described here.

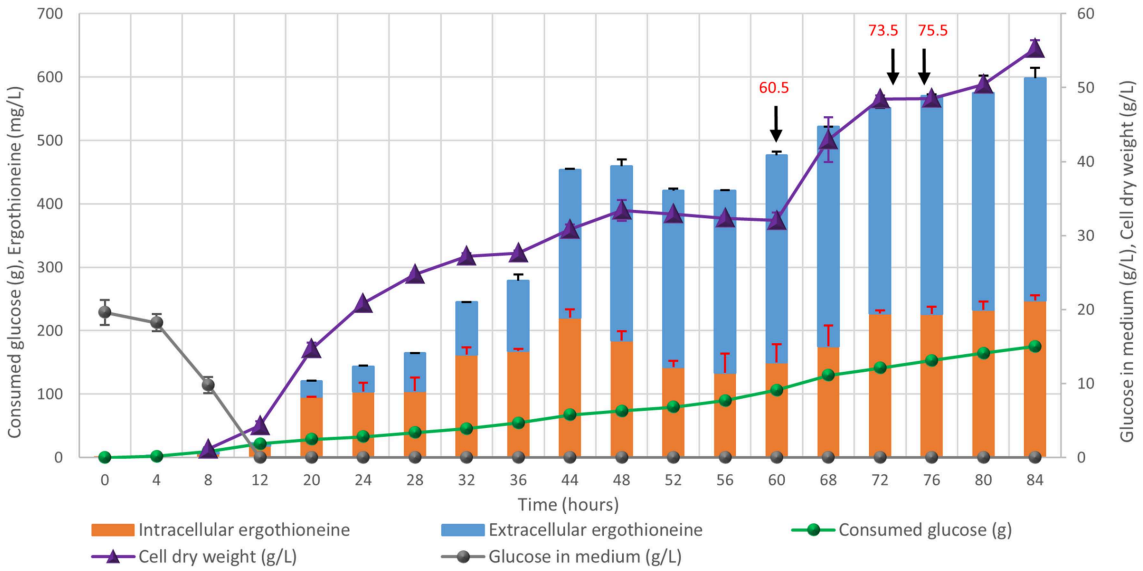

FIGURE 8 | Fed-batch cultivation of ERG-producing strain ST8927. The cultivations were performed in duplicate, the average values are shown. The error bars show standard deviations. The additions of minerals, trace metals, and/or vitamins are indicated by black arrows. At 60.5 h, we added 2 g $(NH_4)_2SO_4$, 0.5 g $MgSO_4$, 4 ml trace metals solution, and 2 ml vitamin solution, at 73.5 h we added 0.5 g $MgSO_4$, 4 ml trace metals solution 2 ml vitamin solution and at 75.5 h we added 2 g $(NH_4)_2SO_4$. At 60.5 and 75.5 h, 2 g $(NH_4)_2SO_4$ was added as a sterile 100 g/l solution. At 60.5 and 73.5 h, 0.5 g $MgSO_4$ was added as a sterile 50 g/l solution, while 4 ml sterile trace metals solution and 2 ml sterile vitamin solution were added.

In our ERG-producing strain, as much as 59% of the ergothioneine was detected extracellularly during fermentation, even though no ERG-specific transporter has been found in yeast so far. High intracellular concentrations of a product may inhibit its own biosynthesis or lead to product degradation (Kell et al., 2015; Borodina, 2019; Kell, 2019). We speculated that expressing an ERG-specific transporter might improve the secretion of ERG from the yeast cells. Expression of heterologous human ergothioneine transporter or a potential ergothioneine transporter from *M. smegmatis* did not improve the secretion, however the transporters were not well-expressed in the plasma membrane of *S. cerevisiae*.

The amino acid metabolism of *S. cerevisiae* is tightly regulated and its networks highly intertwined (Hinnebusch, 1988, 2005; Hinnebusch and Natarajan, 2002; Ljungdahl and Daignan-Fornier, 2012). Therefore, it would be easier to increase the total amino acid pool rather than increasing the individual amino acid pools. The general amino acid control of yeast is mainly regulated by *GCN4* (Hinnebusch, 1988; Ljungdahl and Daignan-Fornier, 2012) and upregulation of *GCN4* leads to transcription of the biosynthetic genes of various amino acids. As knock-out of Tor1 and Yih1 did not yield higher ERG titers, more difficult metabolic engineering of yeast for higher production of individual amino acids pools could lead to higher ERG titers. This is similar to the approach taken in *E. coli*, where use was made of a strain that was already overproducing cysteine (Osawa et al., 2018). In yeast, it is also possible to adopt several strategies that increase the amount of available SAM and/or methionine (Chen et al., 2016) to potentially improve ergothioneine production.

Additional to genetic manipulation, medium optimization has the benefit that it does not require extensive engineering of the strain to increase its production capabilities, while it gives a wealth of information on multiple components in the system that the strain might need for better production (Link and Weuster-Botz, 2011). However, supplementation of certain compounds can be expensive in an industrial setting and therefore the information gained can be used to lead further engineering efforts.

Ergothioneine production was only increased by a small amount following the integration of a second copy of both Egt genes. There are a number of potential explanations for this, such as a lack of precursors or [as is common (Cornishbowden et al., 1995)] possible feedback inhibition by pathway intermediates or products. Interestingly, integrating a second copy of NcEgt1 by itself, but not CpEgt2, did lead to an increase in ERG production. Indeed, in engineering *A. oryzae* (Takusagawa et al., 2019), it has been shown that hercynine accumulated following the integration of multiple copies of Egt1. This suggests that the second reaction catalyzed by the Egt1 enzyme, converting hercynine into HCO, tends to contribute more significantly to flux control.

Recently, another group managed to produce 1.3 g/L ergothioneine in using *E. coli* as a production organism (Tanaka et al., 2019). They used a cysteine hyperproducing strain, which was also engineered for increased methionine production. Additionally, their ERG production genes are on a plasmid which is present in the cells with 15–20 copy numbers. During fermentation, they supplemented the medium with histidine, methionine, thiosulfate, and pyridoxine, supporting the results

found in our medium optimization experiment. While the titer obtained in *E. coli* was higher than in our fed-batch fermentation, the duration of the fermentation with *E. coli* was much longer at 216 h vs. the 84 h-fermentation using *S. cerevisae* presented here.

The fungal pathway for the biosynthesis of ERG only encompasses two enzymes compared to the five of the bacterial pathway, and eliminates the need for the use of glutamate and energy in the form of ATP. While NcEgt1 has been produced in *E. coli* for *in vitro* studies of the enzyme (Hu et al., 2014), to the best of our knowledge, the fungal pathway has to date not been used for ERG production in *E. coli*. As we have shown *S. cerevisiae* is able to produce ergothioneine using the fungal pathway, the more energetically efficient biosynthesis pathway of fungi could lead to better product yield.

In conclusion, we produced ERG with a titer of 598 ± 18 mg/L in *S. cerevisiae* expressing fungal ERG biosynthesis pathway. As the first report of ergothioneine production in *S. cerevisiae,* our investigation into the impact of amino acid supplementation and the flux in the ERG pathway will help further ERG production efforts by yeast fermentation.

DATA AVAILABILITY STATEMENT

All datasets generated for this study are included in the manuscript/**Supplementary Files**.

AUTHOR CONTRIBUTIONS

IB and DK conceived the study. IB, SH, BP, and BD designed the experiments and analyzed the data. SH and KZ performed the strain screening and transporter experiments. MB performed the nitrogen metabolism alteration experiments. SH performed the amino acid supplementation time course. BP performed the medium optimization. The second copy integration experiments were performed by SH. The fed-batch fermentation was performed by SH, MR, and JM. SH, IB, and DK wrote the manuscript. IB and DK secured the funding and supervised the project.

FUNDING

This project has received funding from the European Research Council (ERC) under the European Union's Horizon 2020 research and innovation programme (grant agreement No 757384). The work has also been funded by the Novo Nordisk Foundation (grant number NNF10CC1016517). Furthermore, funding from an Erasmus+ grant (grant agreement no. 2017-1-PL01-KA103-035590, university code PL WROCLAW04) has contributed to this work.

ACKNOWLEDGMENTS

The authors would like to thank Jolanda ter Horst for her help with the fed-batch fermentation experiment.

SUPPLEMENTARY MATERIAL

The Supplementary Material for this article can be found online at: https://www.frontiersin.org/articles/10.3389/fbioe.2019.00262/full#supplementary-material

REFERENCES

Akanmu, D., Cecchini, R., Aruoma, O. I., and Halliwell, B. (1991). The antioxidant action of ergothioneine. *Arch. Biochem. Biophys.* 288, 10–16. doi: 10.1016/0003-9861(91)90158-F

Alamgir, K. M., Masuda, S., Fujitani, Y., Fukuda, F., and Tani, A. (2015). Production of ergothioneine by *Methylobacterium* species. *Front. Microbiol.* 6:1185. doi: 10.3389/fmicb.2015.01185

Ames, B. N. (2018). Prolonging healthy aging: longevity vitamins and proteins. *Proc. Natl. Acad. Sci. U.S.A.* 115, 10836–10844. doi: 10.1073/pnas.1809045115

Audley, B. G., and Tan, C. H. (1968). The uptake of ergothioneine from the soil into the latex of *Hevea brasiliensis*. *Phytochemistry* 7, 1999–2000. doi: 10.1016/S0031-9422(00)90759-3

Barger, G., and Ewins, A. J. (1911). CCLVII.—the constitution of ergothioneine: a betaine related to histidine. *J. Chem. Soc. Trans.* 99, 2336–2341. doi: 10.1039/CT9119902336

Bedirli, A., Sakrak, O., Muhtaroglu, S., Soyuer, I., Guler, I., Riza Erdogan, A., et al. (2004). Ergothioneine pretreatment protects the liver from ischemia-reperfusion injury caused by increasing hepatic heat shock protein 70. *J. Surg. Res.* 122, 96–102. doi: 10.1016/j.jss.2004.06.016

Borodina, I. (2019). Understanding metabolite transport gives an upper hand in strain development. *Microb. Biotechnol.* 12, 69–70. doi: 10.1111/1751-7915.13347

Borodina, I., Kildegaard, K. R., Jensen, N. B., Blicher, T. H., Maury, J., Sherstyk, S., et al. (2015). Establishing a synthetic pathway for high-level production of 3-hydroxypropionic acid in *Saccharomyces cerevisiae* via β-alanine. *Metab. Eng.* 27, 57–64. doi: 10.1016/j.ymben.2014.10.003

Bryan, A. K., Goranov, A., Amon, A., and Manalis, S. R. (2010). Measurement of mass, density, and volume during the cell cycle of yeast. *Proc. Natl. Acad. Sci. U.S.A.* 107, 999–1004. doi: 10.1073/pnas.0901851107

Burn, R., Misson, L., Meury, M., and Seebeck, F. P. (2017). Anaerobic origin of ergothioneine. *Angew. Chem. Int. Ed.* 56, 12508–12511. doi: 10.1002/anie.201705932

Cheah, I. K., and Halliwell, B. (2012). Ergothioneine; antioxidant potential, physiological function and role in disease. *Biochim. Biophys. Acta* 1822, 784–793. doi: 10.1016/j.bbadis.2011.09.017

Cheah, I. K., Tang, R., Ye, P., Yew, T. S. Z., Lim, K. H. C., and Halliwell, B. (2016). Liver ergothioneine accumulation in a guinea pig model of non-alcoholic fatty liver disease. A possible mechanism of defence? *Free Radic. Res.* 50, 14–25. doi: 10.3109/10715762.2015.1099642

Cheah, I. K., Tang, R. M. Y., Yew, T. S. Z., Lim, K. H. C., and Halliwell, B. (2017). Administration of pure ergothioneine to healthy human subjects: uptake, metabolism, and effects on biomarkers of oxidative damage and inflammation. *Antioxid. Redox Signal.* 26, 193–206. doi: 10.1089/ars.2016.6778

Chen, H., Wang, Z., Cai, H., and Zhou, C. (2016). Progress in the microbial production of S-adenosyl-l-methionine. *World J. Microbiol. Biotechnol.* 32:153. doi: 10.1007/s11274-016-2102-8

Cornishbowden, A., Hofmeyr, J. H. S., and Cardenas, M. L. (1995). Strategies for manipulating metabolic fluxes in biotechnology. *Bioorg. Chem.* 23, 439–449. doi: 10.1006/bioo.1995.1030

Deiana, M., Rosa, A., Casu, V., Piga, R., Assunta Desi, M., and Aruoma, O. I. (2004). L-Ergothioneine modulates oxidative damage in the kidney and liver of rats *in vivo*: studies upon the profile of polyunsaturated fatty acids. *Clin. Nutr.* 23, 183–193. doi: 10.1016/S0261-5614(03)00108-0

Ey, J., Schömig, E., and Taubert, D. (2007). Dietary sources and antioxidant effects of ergothioneine. *J. Agric. Food Chem.* 55, 6466–6474. doi: 10.1021/jf071328f

Fujitani, Y., Alamgir, K. M., and Tani, A. (2018). Ergothioneine production using *Methylobacterium* species, yeast, and fungi. *J. Biosci. Bioeng.* 126, 715–722. doi: 10.1016/j.jbiosc.2018.05.021

Genghof, D. S. (1970). Biosynthesis of ergothioneine and hercynine by fungi and *Actinomycetales*. *J. Bacteriol.* 103, 475–478.

Genghof, D. S., Inamine, E., Kovalenko, V., and Melville, D. B. (1956). Ergothioneine in microorganisms. *J. Biol. Chem.* 223, 9–17.

Genghof, D. S., and Vandamme, O. (1964). Biosynthesis of ergothioneine and hercynine by mycobacteria. *J. Bacteriol.* 87, 852–862.

Grundemann, D., Harlfinger, S., Golz, S., Geerts, A., Lazar, A., Berkels, R., et al. (2005). Discovery of the ergothioneine transporter. *Proc. Natl. Acad. Sci. U.S.A.* 102, 5256–5261. doi: 10.1073/pnas.0408624102

Guo, Q.-L., Lin, S., Wang, Y.-N., Zhu, C.-G., Xu, C.-B., and Shi, J.-G. (2016). Gastrolatathioneine, an unusual ergothioneine derivative from an aqueous extract of "tian ma": a natural product co-produced by plant and symbiotic fungus. *Chin. Chem. Lett.* 27, 1577–1581. doi: 10.1016/j.cclet.2016.06.040

Halliwell, B., Cheah, I. K., and Tang, R. M. Y. (2018). Ergothioneine - a diet-derived antioxidant with therapeutic potential. *FEBS Lett.* 592, 3357–3366. doi: 10.1002/1873-3468.13123

Hanlon, D. P. (1971). Interaction of ergothioneine with metal ions and metalloenzymes. *J. Med. Chem.* 14, 1084–1087. doi: 10.1021/jm00293a017

Hinnebusch, A. G. (1988). Mechanisms of gene regulation in the general control of amino acid biosynthesis in *Saccharomyces cerevisiae*. *Microbiol. Rev.* 52, 248–273.

Hinnebusch, A. G. (2005). Translational regulation of GCN4 and the general amino acid control of yeast. *Annu. Rev. Microbiol.* 59, 407–450. doi: 10.1146/annurev.micro.59.031805.133833

Hinnebusch, A. G., and Natarajan, K. (2002). Gcn4p, a master regulator of gene expression, is controlled at multiple levels by diverse signals of starvation and stress. *Eukaryot. Cell* 1, 22–32. doi: 10.1128/EC.01.1.22-32.2002

Hu, W., Song, H., Sae Her, A., Bak, D. W., Naowarojna, N., Elliott, S. J., et al. (2014). Bioinformatic and biochemical characterizations of C–S Bond formation and cleavage enzymes in the fungus *Neurospora crassa* ergothioneine biosynthetic pathway. *Organ. Lett.* 16, 5382–5385. doi: 10.1021/ol502596z

Huang, B., Guo, J., Yi, B., Yu, X., Sun, L., and Chen, W. (2008). Heterologous production of secondary metabolites as pharmaceuticals in *Saccharomyces cerevisiae*. *Biotechnol. Lett.* 30, 1121–1137. doi: 10.1007/s10529-008-9663-z

Jessop-Fabre, M. M., Jakočiunas, T., Stovicek, V., Dai, Z., Jensen, M. K., Keasling, J. D., et al. (2016). EasyClone-MarkerFree: a vector toolkit for marker-less integration of genes into *Saccharomyces cerevisiae* via CRISPR-Cas9. *Biotechnol. J.* 11, 1110–1117. doi: 10.1002/biot.201600147

Kalaras, M. D., Richie, J. P., Calcagnotto, A., and Beelman, R. B. (2017). Mushrooms: a rich source of the antioxidants ergothioneine and glutathione. *Food Chem.* 233, 429–433. doi: 10.1016/j.foodchem.2017.04.109

Kell, D. B. (2019). "Control of metabolite efflux in microbial cell factories: current advances and future prospects," in *Fermentation Microbiology and Biotechnology*, eds E. M. T. El-Mansi, J. Nielsen, D. Mousdale, T. Allman, and P. C. Ross (Boca Raton, FL: CRC Press), 117–138.

Kell, D. B., Swainston, N., Pir, P., and Oliver, S. G. (2015). Membrane transporter engineering in industrial biotechnology and whole cell biocatalysis. *Trends Biotechnol.* 33, 237–246. doi: 10.1016/j.tibtech.2015.02.001

Kelley, L. A., Mezulis, S., Yates, C. M., Wass, M. N., and Sternberg, M. J. E. (2015). The Phyre2 web portal for protein modeling, prediction and analysis. *Nat. Protoc.* 10, 845–858. doi: 10.1038/nprot.2015.053

Kumar, A., John, L., Alam, M. M., Gupta, A., Sharma, G., Pillai, B., et al. (2006). Homocysteine- and cysteine-mediated growth defect is not associated with induction of oxidative stress response genes in yeast. *Biochem. J.* 396, 61–69. doi: 10.1042/BJ20051411

Leisinger, F., Burn, R., Meury, M., Lukat, P., and Seebeck, F. P. (2019). Structural and mechanistic basis for anaerobic ergothioneine biosynthesis. *J. Am. Chem. Soc.* 141, 6906–6914. doi: 10.1021/jacs.8b12596

Leone, E., and Mann, T. (1951). Ergothioneine in the seminal vesicle secretion. *Nature* 168, 205–206. doi: 10.1038/168205b0

Li, M., and Borodina, I. (2014). Application of synthetic biology for production of chemicals in yeast *Saccharomyces cerevisiae*. *FEMS Yeast Res.* 15, 1–12. doi: 10.1111/1567-1364.12213

Link, C. D. (1995). Expression of human beta-amyloid peptide in transgenic *Caenorhabditis elegans*. *Proc. Natl. Acad. Sci. U.S.A.* 92, 9368–9372. doi: 10.1073/pnas.92.20.9368

Link, H., and Weuster-Botz, D. (2011). "Medium formulation and development," in *Comprehensive Biotechnology*, ed M. Moo-Young (Amsterdam: Elsevier), 119–134. doi: 10.1016/B978-0-08-088504-9.00092-1

Ljungdahl, P. O., and Daignan-Fornier, B. (2012). Regulation of amino acid, nucleotide, and phosphate metabolism in *Saccharomyces cerevisiae*. *Genetics* 190, 885–929. doi: 10.1534/genetics.111.133306

Melville, D. B. (1959). Ergothioneine. *Vitam. Horm.* 17, 155–204. doi: 10.1016/S0083-6729(08)60271-X

Melville, D. B., Horner, W. H., and Lubschez, R. (1954). Tissue ergothioneine. *J. Biol. Chem.* 206, 221–228.

Osawa, R., Kamide, T., Satoh, Y., Kawano, Y., Ohtsu, I., and Dairi, T. (2018). Heterologous and high production of ergothioneine in *Escherichia coli*. *J. Agric. Food Chem.* 66, 1191–1196. doi: 10.1021/acs.jafc.7b04924

Park, E. J., Lee, W. Y., Kim, S. T., Ahn, J. K., and Bae, E. K. (2010). Ergothioneine accumulation in a medicinal plant *Gastrodia elata*. *J. Med. Plants Res.* 4, 1141–1147. doi: 10.5897/JMPR10.184

Paul, B. D., and Snyder, S. H. (2010). The unusual amino acid L-ergothioneine is a physiologic cytoprotectant. *Cell Death Differ.* 17, 1134–1140. doi: 10.1038/cdd.2009.163

Pfeiffer, C., Bauer, T., Surek, B., Schömig, E., and Gründemann, D. (2011). Cyanobacteria produce high levels of ergothioneine. *Food Chem.* 129, 1766–1769. doi: 10.1016/j.foodchem.2011.06.047

Pluskal, T., Ueno, M., and Yanagida, M. (2014). Genetic and metabolomic dissection of the ergothioneine and selenoneine biosynthetic pathway in the fission yeast, *S. pombe*, and construction of an overproduction system. *PLoS ONE* 9:e97774. doi: 10.1371/journal.pone.0097774

Sakrak, O., Kerem, M., Bedirli, A., Pasaoglu, H., Akyurek, N., Ofluoglu, E., et al. (2008a). Ergothioneine modulates proinflammatory cytokines and heat shock protein 70 in mesenteric ischemia and reperfusion injury. *J. Surg. Res.* 144, 36–42. doi: 10.1016/j.jss.2007.04.020

Sakrak, Ö., Kerem, M., Bedirli, A., Pasaoglu, H., Alper, M., Ofluoglu, E., et al. (2008b). Ergothioneine prevents acute lung injury in mesenteric ischemia and reperfusion injury in rats. *J. Crit. Care* 23, 268–269. doi: 10.1016/j.jcrc.2008.03.021

Sao Emani, C., Williams, M. J., Van Helden, P. D., Taylor, M. J. C., Wiid, I. J., and Baker, B. (2018). Gamma-glutamylcysteine protects ergothioneine-deficient *Mycobacterium tuberculosis* mutants against oxidative and nitrosative stress. *Biochem. Biophys. Res. Commun.* 495, 174–178. doi: 10.1016/j.bbrc.2017.10.163

Sao Emani, C., Williams, M. J., Wiid, I. J., Hiten, N. F., Viljoen, A. J., Pietersen, R.-D. D., et al. (2013). Ergothioneine is a secreted antioxidant in *Mycobacterium smegmatis*. *Antimicrob. Agents Chemother.* 57, 3202–3207. doi: 10.1128/AAC.02572-12

Seebeck, F. P. (2010). *In vitro* reconstitution of Mycobacterial ergothioneine biosynthesis. *J. Am. Chem. Soc.* 132, 6632–6633. doi: 10.1021/ja101721e

Sheridan, K. J., Lechner, B. E., Keeffe, G. O., Keller, M. A., Werner, E. R., Lindner, H., et al. (2016). Ergothioneine biosynthesis and functionality in the opportunistic fungal pathogen, *Aspergillus fumigatus*. *Sci. Rep.* 6:35306. doi: 10.1038/srep35306

Shires, T. K., Brummel, M. C., Pulido, J. S., and Stegink, L. D. (1997). Ergothioneine distribution in bovine and porcine ocular tissues. *Comp. Biochem. Physiol. C. Pharmacol. Toxicol. Endocrinol.* 117, 117–120. doi: 10.1016/S0742-8413(96)00223-X

Song, H., Hu, W., Naowarojna, N., Her, A. S., Wang, S., Desai, R., et al. (2015). Mechanistic studies of a novel C-S lyase in ergothioneine biosynthesis: the involvement of a sulfenic acid intermediate. *Sci. Rep.* 5:11870. doi: 10.1038/srep11870

Song, T.-Y., Lin, H.-C., Chen, C.-L., Wu, J.-H., Liao, J.-W., and Hu, M.-L. (2014). Ergothioneine and melatonin attenuate oxidative stress and protect against learning and memory deficits in C57BL/6J mice treated with D-galactose. *Free Radic. Res.* 48, 1049–1060. doi: 10.3109/10715762.2014.920954

Stovicek, V., Borodina, I., and Forster, J. (2015). CRISPR–Cas system enables fast and simple genome editing of industrial *Saccharomyces cerevisiae*

strains. *Metab. Eng. Commun.* 2, 13–22. doi: 10.1016/j.meteno.2015.03.001

Swainston, N., Currin, A., Day, P. J., and Kell, D. B. (2014). GeneGenie: optimized oligomer design for directed evolution. *Nucleic Acids Res.* 42, W395–W400. doi: 10.1093/nar/gku336

Ta, P., Buchmeier, N., Newton, G. L., Rawat, M., and Fahey, R. C. (2011). Organic hydroperoxide resistance protein and ergothioneine compensate for loss of mycothiol in *Mycobacterium smegmatis* mutants. *J. Bacteriol.* 193, 1981–1990. doi: 10.1128/JB.01402-10

Takusagawa, S., Satoh, Y., Ohtsu, I., and Dairi, T. (2019). Ergothioneine production with *Aspergillus oryzae*. *Biosci. Biotechnol. Biochem.* 83, 181–184. doi: 10.1080/09168451.2018.1527210

Tan, C., and Audley, B. (1968). Ergothioneine and hercynine in *Hevea brasiliensis* latex. *Phytochemistry* 7, 109–118. doi: 10.1016/S0031-9422(00)88213-8

Tanaka, N., Kawano, Y., Satoh, Y., Dairi, T., and Ohtsu, I. (2019). Gram-scale fermentative production of ergothioneine driven by overproduction of cysteine in *Escherichia coli*. *Sci. Rep.* 9:1895. doi: 10.1038/s41598-018-38382-w

Tang, Y., Masuo, Y., Sakai, Y., Wakayama, T., Sugiura, T., Harada, R., et al. (2016). Localization of xenobiotic transporter OCTN1/SLC22A4 in hepatic stellate cells and its protective role in liver fibrosis. *J. Pharm. Sci.* 105, 1779–1789. doi: 10.1016/j.xphs.2016.02.023

Tanret, C. (1909). The new base drawn from rye ergot, ergothioneine. *C. R. Hebd. Acad. Sci.* 25, 222–224. doi: 10.1080/00369220908733970

Tschirka, J., Kreisor, M., Betz, J., and Gründemann, D. (2018). Substrate selectivity check of the ergothioneine transporter. *Drug Metab. Dispos.* 46, 779–785. doi: 10.1124/dmd.118.080440

Wang, J., Guleria, S., Koffas, M. A., and Yan, Y. (2016). Microbial production of value-added nutraceuticals. *Curr. Opin. Biotechnol.* 37, 97–104. doi: 10.1016/j.copbio.2015.11.003

Watanabe, D., Kikushima, R., Aitoku, M., Nishimura, A., Ohtsu, I., Nasuno, R., et al. (2014). Exogenous addition of histidine reduces copper availability in the yeast *Saccharomyces cerevisiae*. *Microb. Cell* 1, 241–246. doi: 10.15698/mic2014.07.154

Yang, N.-C., Lin, H.-C., Wu, J.-H., Ou, H.-C., Chai, Y.-C., Tseng, C.-Y., et al. (2012). Ergothioneine protects against neuronal injury induced by β-amyloid in mice. *Food Chem. Toxicol.* 50, 3902–3911. doi: 10.1016/j.fct.2012.08.021

Yuan, S.-F., and Alper, H. S. (2019). Metabolic engineering of microbial cell factories for production of nutraceuticals. *Microb. Cell Fact.* 18:46. doi: 10.1186/s12934-019-1096-y

Conflict of Interest: SH, BD, DK, and IB are named inventors on a European Patent application covering parts of the work described above.

The remaining authors declare that the research was conducted in the absence of any commercial or financial relationships that could be construed as a potential conflict of interest.

frontiers in Bioengineering and Biotechnology

ORIGINAL RESEARCH
published: 18 October 2019
doi: 10.3389/fbioe.2019.00279

Maximizing the Efficiency of Vanillin Production by Biocatalyst Enhancement and Process Optimization

*Francesca Luziatelli, Lorenza Brunetti, Anna Grazia Ficca and Maurizio Ruzzi**

Department for Innovation in Biological, Agro-Food and Forest Systems (DIBAF), University of Tuscia, Viterbo, Italy

The rising demand of bio-vanillin and the possibility to use microbial biotransformation to produce this compound from agroindustrial byproducts are economically attractive. However, there are still several bottlenecks, including substrate and product toxicity, formation of undesired products and genetic stability of the recombinant strains, that impede an efficient use of recombinant *Escherichia coli* strains to make the whole process cost effective. To overcome these problems, we developed a new *E. coli* strain, named FR13, carrying the *Pseudomonas* genes encoding feruloyl-CoA synthetase and feruloyl-CoA hydratase/aldolase integrated into the chromosome and, using resting cells, we demonstrated that the vanillin yield and selectivity were strongly affected by the physiological state of the cells, the temperature used for the growth and the recovery of the biomass and the composition and pH of the bioconversion buffer. The substrate consumption rate and the vanillin yield increased using a sodium/potassium phosphate buffer at pH 9.0 as bioconversion medium. Optimization of the bioprocess variables, using response surface methodology, together with the use of a two-phase (solid-liquid) system for the controlled release of ferulic acid allowed us to increase the vanillin yield up to 28.10 ± 0.05 mM. These findings showed that recombinant plasmid-free *E. coli* strains are promising candidates for the production of vanillin at industrial scale and that a reduction of the cost of the bioconversion process requires approaches that minimize the toxicity of both ferulic acid and vanillin.

Keywords: vanillin biosynthesis, ferulic acid, bioconversion, metabolic engineering, *Escherichia coli*, resting cells, alkaline conditions

OPEN ACCESS

Edited by:
Nils Jonathan Helmuth Averesch, Stanford University, United States

Reviewed by:
Ignacio Poblete-Castro, Universidad Andrés Bello, Chile
Jin-Song Gong, Jiangnan University, China

****Correspondence:***
Maurizio Ruzzi
ruzzi@unitus.it

Specialty section:
This article was submitted to Bioprocess Engineering, a section of the journal Frontiers in Bioengineering and Biotechnology

Received: *30 June 2019*
Accepted: *03 October 2019*
Published: *18 October 2019*

Citation:
Luziatelli F, Brunetti L, Ficca AG and Ruzzi M (2019) Maximizing the Efficiency of Vanillin Production by Biocatalyst Enhancement and Process Optimization. Front. Bioeng. Biotechnol. 7:279. doi: 10.3389/fbioe.2019.00279

INTRODUCTION

Vanilla is one of the most used flavors in foods, beverages, sodas, pharmaceutics, cosmetics, tobacco, and traditional crafts industries. Natural vanilla is a complex mixture of more than 200 molecules extracted from the cured pods of plants belonging to selected species of the *Vanilla* genus: *Vanilla planifolia* Jacks ex Andrews and *Vanilla tahitensis* J.W. Moore (Ramachandra Rao and Ravishankar, 2000).

The characteristic flavor of vanilla is mainly due to vanillin (cas n. 121-33-5), a phenolic aldehyde present in cured vanilla pods in a concentration ranging from 1.0 to 2.0% (w/w; Sinha et al., 2008). As the extraction process from cured beans is relatively expensive, vanilla represents about 5% of the global vanilla and vanillin market (IMARC Group, 2019).

Even though synthetic vanillin is available at a very low price, the increasing consumer awareness for natural ingredients, which are considered "healthy," has led many companies to find new strategies for the production of natural flavors such as bio-vanillin. According to recent industry research reports, the global bio-vanillin market is expected to rise with a strong CAGR of 7.4% within the forecast period from 2017 to 2025 (Transparency Market Research, 2017), which is expected to be a great opportunity for the production of bio-vanillin from natural substrates by biotechnological tools (Banerjee and Chattopadhyay, 2019; Galadima et al., 2019).

The Flavoring Regulation (EC) No 1334/2008 (December 16th 2008) established that natural vanillin can be produced combining biotechnology-based approaches, which use lignin, ferulic acid, eugenol or isoeugenol as natural precursors (Gallage and Møller, 2015) and microorganisms as production hosts (Lesage-Meessen et al., 1996; Overhage et al., 1999b; Plaggenborg et al., 2006; Di Gioia et al., 2007, 2011a; Hansen et al., 2009; Tilay et al., 2010; Fleige et al., 2013).

Ferulic acid is a phenylpropanoic acid, naturally occurring in plants, which confers rigidity to the cell wall by cross-linking with polysaccharides and lignin (Ou and Kwok, 2004; Boz, 2015; Oliveira et al., 2015). In a large number of microorganisms, vanillin is a transient intermediate of ferulic acid catabolism (Masai et al., 2007; Kumar and Pruthi, 2014; Brink et al., 2019) and it is either rapidly converted to other products or utilized as a carbon source and energy.

Microorganisms naturally capable of converting ferulic acid to vanillin mainly belong to the genera *Amycolatopsis*, *Streptomyces*, *Pseudomonas,* and *Delftia* (Sutherland et al., 1983; Barghini et al., 1998; Muheim and Lerch, 1999; Oddou et al., 1999; Achterholt et al., 2000; Plaggenborg et al., 2003; Brunati et al., 2004; Hua et al., 2007; Di Gioia et al., 2011a; Fleige et al., 2013; Simon et al., 2014). Moreover, several authors have reported the feasibility to use agroindustrial wastes rich in ferulic acid as valuable renewable sources for bio-vanillin production (Di Gioia et al., 2009, 2011b; Fava et al., 2013; Zamzuri and Abd-Aziz, 2013; Banerjee and Chattopadhyay, 2019; Galadima et al., 2019).

In bacteria, five ferulate catabolic pathways can be distinguished based on the reactions involved in ferulic acid activation (reviewed by Gallage and Møller, 2015). In *Pseudomonas* and related species, the conversion of ferulic acid into vanillin is a two-step process that involves the formation of a high-energy thioester as a key intermediate (Narbad and Gasson, 1998; Overhage et al., 1999a; Calisti et al., 2008). As shown in **Figure 1**, this reaction is catalyzed by a feruloyl-CoA synthetase (EC 6.2.1.34) and requires a carrier of acyl groups (such as acetyl-CoA), $MgCl_2$ and ATP, as cofactors. The feruloyl-CoA is subsequently hydrated and cleaved to vanillin and acetyl-CoA by a lyase, enoyl-CoA hydratase/aldolase (EC 4.2.1.101), that combines hydratase and aldolase activity (Narbad and Gasson, 1998; **Figure 1**).

Due to its toxicity, vanillin is quickly oxidized or reduced to vanillic acid and vanillyl alcohol respectively, using enzymes that are specific for this substrate (i.e., vanillin dehydrogenase; EC 1.2.1.67) or have a broad substrate specificity. In bacterial strains able to grow on ferulic acid as a sole carbon source, inactivation of vanillin dehydrogenase-encoding gene (*vdh*) is a valuable tool to obtain mutants that accumulate vanillin (**Table 1**). However, as reported for *Amycolatopsis* sp. ATCC39116 (Fleige et al., 2016) and *Pseudomonas putida* KT2440 (Graf and Altenbuchner, 2014), inactivation of *vdh* gene is not sufficient to reduce the formation of toxic byproducts (i.e., vanillyl alcohol) when prolonged bioconversion times are required.

Over the last decades, the increase of knowledge about the catabolic genes and the corresponding enzymes involved in the conversion of ferulic acid into vanillin gave new opportunity to bioengineering microorganisms for vanillin biosynthesis and now recombinant strains represent an efficient alternative to the use of wild-type strains (**Table 1**). In fact, recombinant *Escherichia coli* strains harboring heterologous genes for coenzyme A-dependent or coenzyme A-independent conversion of ferulic acid to vanillin have been used as alternative platforms for vanillin production (Yoon et al., 2005; Barghini et al., 2007; Furuya et al., 2014). Nevertheless, the vanillin yield obtained using these biocatalysts was affected by the genetic instability of the recombinant strains and the toxicity of the vanillin that, during the growth, can be converted to less inhibitory compounds, such as vanillyl alcohol, using endogenous aldo-keto reductases and aldehyde dehydrogenases (Pugh et al., 2015).

In this study, we have investigated the possibility to obtain a more stable recombinant *E. coli* strain, integrating the *Pseudomonas* genes encoding feruloyl-CoA synthetase (Fcs) and enoyl-CoA hydratase/aldolase (Ech) into the chromosome, and to establish a bioconversion process with resting cells in which we could apply environmental conditions (notably pH) adverse to *E. coli* growth cells, but favoring the entrance of the substrate in the cell, enhancing the catalytic activity of Fcs, inhibiting endogenous enzymes responsible for the reduction of vanillin to vanillyl alcohol. Finally, to better understand the relationship between the variables (initial ferulic acid concentration and agitation speed) and the response (vanillin yield and selectivity) and obtain the optimum conditions for vanillin production we used response surface methodology and, at the same time, incorporating the substrate in a gel matrix we could evaluate the cellular response to ferulic acid.

MATERIALS AND METHODS

Bacterial Strains, Plasmids, and Growth Conditions

Bacterial strains and plasmids used in this study are listed in **Table 2**. *E. coli* was routinely grown on LB broth Lennox (Acumedia, Baltimore, MD, USA; Miller, 1992). For selection, antibiotics were added at the following concentrations: kanamycin, 50 μg/mL; ampicillin, 100 μg/mL; and chloramphenicol, 30 μg/mL. *E. coli* was routinely grown at 37°C; recombinant strains containing plasmids with a temperature-sensitive origin were grown at 30°C for episomal maintenance of the plasmid and at 44°C (non-permissive temperature) for plasmid curing (integration). Growth was monitored by measuring the turbidity of the cultures at 600 nm (OD_{600}).

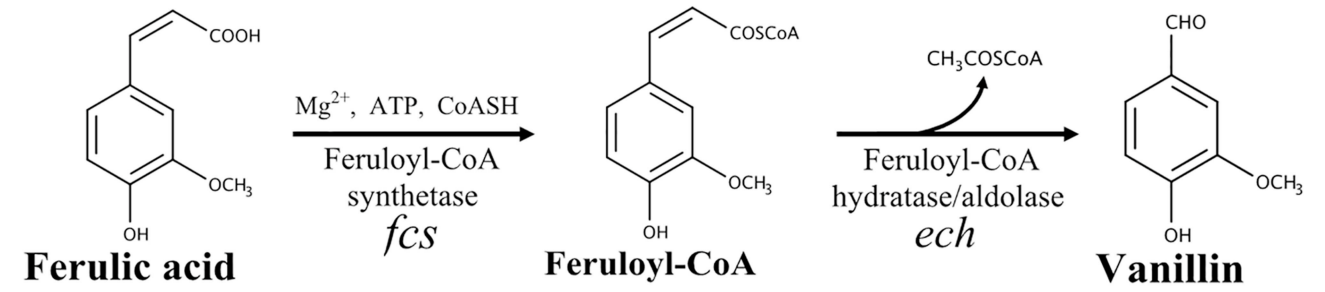

FIGURE 1 | Schematic representation of the non-β-oxidative pathway for conversion of ferulic acid into vanillin.

TABLE 1 | Bacteria capable of producing vanillin from ferulic acid.

Microorganism	Yield (mM)	References
Amycolatopsis sp. HR167	75.58*	Rabenhorst and Hopp, 2002
Amycolatopsis sp. ATCC 39116	146.57*	Fleige et al., 2016
Streptomyces sp. V-1	126.19*	Hua et al., 2007
Streptomyces sannanensis MTCC 6637	4.65	Chattopadhyay et al., 2018
Pseudomonas putida GN442	8.61*	Graf and Altenbuchner, 2014
Pseudomonas fluorescens BF13-1p4(pBB1)	8.41*	Di Gioia et al., 2011a
Recombinant *Escherichia coli* JM109	16.56	Barghini et al., 2007
Recombinant *Escherichia coli* BW25113	33.78	Lee et al., 2009
Recombinant *Escherichia coli* BL21(DE3)	51.26	Furuya et al., 2015

**Data referred to mutants lacking a functional vdh gene.*

DNA Manipulations

Standard protocols were used for DNA manipulations and recombinant DNA techniques (Sambrook et al., 1989). QIAquick Gel Extraction kit (QIAGEN, Germany) was used for recovery of DNA fragments from agarose gels. Plasmids were prepared using a QIAprep spin miniprep kit (QIAGEN, Germany). Restriction enzymes and T4 DNA ligase were purchased from Invitrogen (Carlsbad, CA). Taq Polymerase was from QIAGEN (Germany).

Chemicals

All chemicals were of the highest purity commercially available and were purchased from Sigma-Aldrich (Italy).

Construction of Recombinant Plasmids

Plasmid pFR2 was used for integrating the ferulic acid catabolic genes onto the *E. coli* genome. To construct this plasmid, pBB1 was cut with *Hind*III and *Sst*I to generate a 5036-bp DNA fragment which contains the promoter region (P_{fer}) and the genes encoding feruloyl-CoA synthetase (*fcs*) and enoyl-CoA hydratase/aldolase (*ech*) from *Pseudomonas fluorescens* BF13 (GenBank accession number AJ536325). This fragment was subcloned in the corresponding sites of pPR9TT to obtain pFF0. Then, pFF0 was linearized by *Eco*RI and ligated with a 3016-bp *Eco*RI fragment containing the entire *lacZ* gene and the rrnBT1T2 transcriptional terminator to construct pFR1. Finally, to generate pFR2, a 7715-bp *Sst*I fragment from pFR1, containing *ech* and *fcs* genes under the control of P_{fer} promoter and the 3′-terminal portion of *lac*Z, was subcloned in the corresponding site of pLOI2227, an integration vector with a low-copy temperature-sensitive pSC101 origin of replication. Integration of the ferulic acid catabolic cassette into the *E. coli* genome was confirmed by PCR using a junction site and a donor-specific primer pair:

FFZ_F (5′-CTTCTACTGCTCGGGGGATG-3′)
FFZ_R (5′-AATGGCTTTCGCTACCTGGA-3′).

Determination of Integrants' Stability

Cells were picked from LB plates containing kanamycin and cultivated for 15 generations in order to allow excision of the plasmid and loss of pFR2 from the population. Aliquots of these cultures were diluted and plated on LB plates to form single colonies. After 24 h of incubation at 30°C, colonies were picked on agar plates containing kanamycin and X-Gal to screen for antibiotic resistance and β-galactosidase activity.

Bioconversion Experiments in Shake Flask Using Resting Cells

Experiments were carried out in shake-flasks, each experiment was performed in duplicate or triplicate and results were presented as mean and standard deviation. For bioconversion experiments, cells were cultivated, up to the desired optical density, in LB medium, collected by centrifugation and washed twice in saline-phosphate buffer before use (Barghini et al., 2007). Biotransformation was carried out in saline phosphate buffer (15 mL) containing 4.5–7.5 g of cells (wet weight)/L and 5.0–23.2 mM of ferulic acid, and flasks were shaken 120–180 rpm, at 30°C, for 24 h. Substrate and metabolites occurring in the bioconversion medium were analyzed by liquid chromatography as reported before (Barghini et al., 2007). Compounds were identified and quantified by comparison of retention time and peak area with standard solutions of authentic standards.

TABLE 2 | Strains and plasmids used in this study.

Strain or plasmid	Description	Source or reference
Strains		
P. fluorescens		
BF13	Wild type, ferulate-positive	Ruzzi et al., 1997
E. coli		
B	Wild type	CGCS 5365
JM109	*rec*A1 *end*A1 *gyr*A96 *thi*-1 *hsd*R17 r_K^- m_K^+ *sup*E44 *rel*A1 λ- Δ*lac-pro*AB F' *tra*D36 *pro*AB$^+$ *lac*Iq ZΔM15	Promega
DH5α	F$^-$ ϕ80*lac*ZΔM15 Δ(*lac*ZYA-*arg*F)U169 *rec*A1 *end*A1 *hsd*R17(r_K^-, m_K^+) *pho*A *sup*E44 λ- *thi*-1 *gyr*A96 *rel*A1	
FR12	*E. coli* B derivate carrying plasmid pFR2 integrated into *lac*Z locus	This study
FR13	*E. coli* JM109 derivate carrying plasmid pFR2 integrated into *lac*Z locus	This study
FR14	*E. coli* DH5α derivate carrying plasmid pFR2 integrated into *lac*Z locus	This study
FR13 (pJBA27)	*E. coli* FR13 carrying plasmid pJBA27	Andersen et al., 1998
Plasmids		
pPR9TT	Broad-host range plasmid carrying promoter-less *lac*Z; Ap^r; Cm^r; 9.3 kb	Santos et al., 2001
pLOI2227	Integration vector containing FRT-Km^r-FRT fragment, pSC101 origin, Km^r, 3443 kb	Martinez-Morales et al., 1999
pE0	pPR9TT derivate containing a 423-bp *Kpn*I-*Bam*HI fragment with the *ech* upstream region and the first 36 *ech* codons fused in frame with the *lac*Z gene; Ap^r; Cm^r; 9810 kb	Calisti et al., 2008
pFR0	pPR9TT derivative containing a 5036-bp *Hind*III-*Sst*I fragment from plasmid pBB1; Ap^r; Cm^r; 11290 kb	This study
pFR1	pFR0 derivative containing a 3016 *Eco*RI fragment from plasmid pPR9TT; Ap^r; Cm^r; 14306 kb	This study
pFR2	Integration vector; pFR1 derivative containing a 7715-bp *Sst*I fragment from plasmid pFR1; Km^r; 10034 kb	This study
pJBA27	Ap^r; pUC18Not-$P_{A1/04/03}$-RBSII-*gfpmut3**-T_0-T_1	Andersen et al., 1998

Ap^r, ampicillin resistance; Tc^r, tetracycline resistance; Cm^r, chloramphenicol resistance; Km^r, kanamycin resistance.

Preparation of Cell Extract and Enzyme Assays

Crude extracts of *P. fluorescens* BF13 were prepared from cells grown at 30°C on M9 medium (Sambrook et al., 1989) supplemented with ferulic acid (0.2% wt/vol) as the sole carbon source. Feruloyl-CoA synthetase activity was assayed spectrophotometrically, measuring the increase in absorbance at 345 nm due to the formation of feruloyl-CoA (Calisti et al., 2008). Experiments were carried out at two temperatures (30 and 44°C) using phosphate buffers of different pH (7.0 to 10.0).

Effect of growth temperature and temperature shift (from 44 to 30°C) on P_{fer} promoter-driven expression in *E. coli* cells were evaluated using a recombinant strain carrying a plasmid, named pE0, which contains the *ech* upstream region and the first 36 *ech* codons fused in frame with the *lac*Z gene (Calisti et al., 2008). β-Galactosidase activity in *E. coli* JM109(pE0) cells grown at 30 and 44°C was measured as described by Calisti et al. (2008), using the β-Galactosidase Assay Kit (Stratagene, USA). One unit of β-galactosidase activity was equal to 1 nmol of o-nitrophenyl-ß-D-galactopyranoside hydrolyzed per min per mg of protein under assay conditions.

The amount of soluble protein was determined using the BCA Protein Assay Kit (Pierce, Rockford IL), with bovine serum albumin as a standard.

Fluorescence Spectroscopy

For quantification of green fluorescence, F13 cells carrying pJBA27 (**Table 2**) were cultured under aerobic conditions (at 30°C) on LB medium containing ampicillin and kanamycin until the OD_{600} reached 1.0. Cells were then harvested by centrifugation and resuspended in sterile water at an OD_{600} of 0.5. For cytoplasmic pH measurement, aliquots of FR13(pJBA27) cell suspension were transferred in 96-well plates and emended with an equal volume of saline phosphate buffer (2x) adjusted to pH values in the range of 6.5–9.0. The plate was incubated at 30°C for 2 h, and excitation spectra were recorded using a Beckman Coulter DTX 880 Multimode Detector. GFPmut3* excitation was measured at 485 nm using an emission wavelength of 535 nm. Spectra were measured for three biological replicates at each pH.

Intracellular inorganic polyphosphate (polyP) in LB grown cells and in cells incubated for 2 h in phosphate buffer amended with ferulic acid was measured using the DAPI (4′,6-diamidino-2-phenylindole)-based approach described by Aschar-Sobbi et al. (2008). In this test, fluorescence (in arbitrary units) of the DAPI-polyP complex at 550 nm is used to estimate the intracellular polyP pool. Fluorescence intensities were measured by using a Perkin-Elmer FS-55 spectrofluorometer with excitation at 415 nm and emission between 445 and 650 nm.

Intracellular ATP was quantified using the BacTiter-Glo™ Microbial Cell Viability Assay (Promega, Madison, WI, USA).

Buffer Composition

Reaction conditions for vanillin production were optimized using saline phosphate buffers with different phosphate molarity, sodium-to-potassium ratio and pH. In brief, the following saline phosphate buffers were used: 70 mM sodium-potassium phosphate buffers at different pH values (between 7.0 and 9.0); 40, 100, and 200 mM sodium-potassium phosphate buffer at pH 9.0.

TABLE 3 | Dimensionless, coded independent variable used for optimization of vanillin production.

Variable	Nomenclature	Definition	Variation range
Dimensionless stirring	X_1	Stirring sped 180–120 (rpm)	(−1.1)
Dimensionless ferulic acid concentration	X_2	Ferulic acid 23.1–7.7 (mM)	(−1.1)

Experimental Design for Optimization of Bioconversion Parameters

Central Composite Design (CCD) and Response Surface Methodology (RSM) (Biles, 1975; Bezerra et al., 2008) were used to evaluate the interactive effects of agitation speed and substrate concentration on vanillin and vanillyl alcohol production. All data were treated with the aid of Modde 5.0 (Umetrics AB, Umea, Sweden) as reported elsewhere (Brunetti, 2013).

The design and levels of each variable are shown in **Table 3**. The behavior of the system was explained by the following equation:

$$Y = \beta_0 + \Sigma\beta_i X_i + \Sigma\beta_{ii} X_i^2 + \Sigma\beta_{ij} X_i X_j$$

where Y is the predicted response variable, β_0 is the intercept, β_i and β_{ii} the linear coefficient and quadratic coefficients, respectively, β_{ij} the interaction coefficient and X_i and X_j the coded forms of the input variables.

The impact of single independent variables on the responses (maximum vanillin concentration [Y_1] and minimum vanillyl alcohol production [Y_2]) was calculated by the following equation:

$$Y = \beta_0 + \beta_i X_i + \beta_{ii} X_i^2$$

All bioconversion experiments were carried out in a final bioconversion volume of 15 mL using cells suspended in 70 mM phosphate saline M9 buffer (pH 9.0). Duplicates were performed at all design points in randomized order.

Preparation and Use of Ferulic Acid Loaded Agarose Rods

Ferulic acid (1.5% w/vol) was entrapped into agarose (1.75% w/vol) gel cylinders of 1 ± 0.001 cm height and 0.6 ± 0.001 cm diameter. Each cylinder contained 0.034 ± 0.02 mmoles of ferulic acid. Bioconversions were carried out in shaken flasks, and the ferulic acid-loaded gel cylinders were immersed in 15 mL volume of cell suspension in 70 mM saline phosphate buffer (pH 9.0).

RESULTS

Effects of Incubation Conditions on Feruloyl-CoA Synthetase Activity and Expression of Ferulic Catabolic Genes

Genes and enzymes from *P. fluorescens* BF13, a bacterial strain known for its ability to degrade ferulic acid and produce high levels of feruloyl CoA-synthetase (Fcs) activity (Calisti et al., 2008), were used as a model system to evaluate the effect of pH and temperature on Fcs activity and expression of the ferulic catabolic genes. In standard conditions (buffer at pH 7.0; Overhage et al., 1999a), using crude extracts from ferulic-acid-induced cells, we observed a 97% decrease in Fcs activity, from 0.375 ± 0.009 up to 0.01 ± 0.002U/mg protein, increasing the incubation temperature from 30 to 44°C. At 30°C, the highest Fcs activity (0.69 ± 0.02 U/mg protein) was measured increasing the pH up to 8.0-8.5 (**Figure 2**).

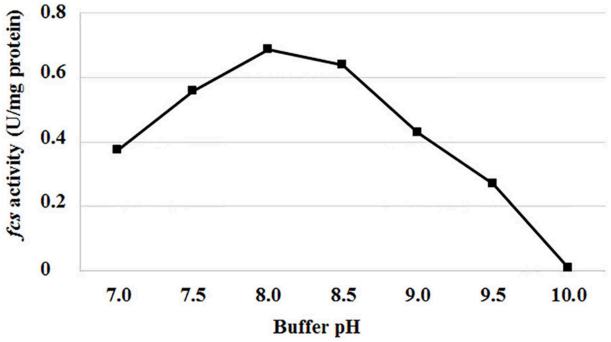

FIGURE 2 | Effect of pH on feruloyl-CoA synthetase activity (*fcs*) from *P. fluorescens* BF13. Fcs activity was measured at 30°C in phosphate buffer at pH range from 7.0 to 10.0. Enzymatic activity was determined on crude extract from cells grown to mid-exponential phase on minimal medium containing ferulic acid as the sole carbon source. Data are representative of three independent experiments and values are expressed in units per milligram of total proteins. Standard deviations were <10% unless noted.

In consideration of the inability of *P. fluorescens* cells to grow at 44°C, the effect of incubation temperature on the expression of ferulic catabolic genes was evaluated using an *E. coli* derivative, JM109(pE0) (**Table 2**), which contains the *lacZ* reporter gene under the control of BF13 P_{fer} promoter. The β-galactosidase assay was performed with cell extracts from stationary phase cultures grown at 30 and 44°C. Results indicated that the production of β-galactosidase activity was not significantly affected by growth temperature and was comprised between 2.23 ± 0.22 (44°C) and 2.74 ± 0.35 U/10^9 CFU (30°C).

Insertion of Ferulic Catabolic Genes From *P. fluorescens* BF13 Into *E. coli* Chromosome

In a previous work, we demonstrated (Barghini et al., 2007) that the ability of recombinant *E. coli* cells to convert ferulic acid to vanillin inversely correlates with the gene copy number and the strength of the promoter used to drive expression of feruloyl-CoA synthetase (*fcs*) and feruloyl-CoA hydratase/aldolase (*ech*) encoding genes. To generate single copy insertions of ferulic catabolic genes into different *E. coli* strains and evaluate the best host strain/gene combination, we constructed a temperature-sensitive suicide plasmid, named pFR2, carrying a 5.098-bp fragment encompassing *ech, fcs* and the P_{fer} promoter region from *P. fluorescens* BF13 and the 3′-terminal part of *E. coli*

lacZ gene. This plasmid enabled targeted integration of the sequences into the *E. coli lacZ* locus and rapid white/blue selection of integrants.

In a typical experiment, pFR2 plasmid DNA was introduced into *E. coli* B-type strain by electroporation, and transformants were selected at 30°C (permissive temperature) on LB plates supplemented with kanamycin and X-Gal (see Materials and Methods). On this medium, cells carrying the plasmid in the episomal form gave blue colonies, and integrants obtained after prolonged cultivation (16–24 h) at non-permissive temperature (44°C) gave white colonies. The genetic stability of the integrants was tested at permissive temperature (30°C) in the presence or absence of kanamycin, as reported in Material and Methods. All clones examined retained the ability to grow in the presence of kanamycin and exhibited a white phenotype on X-gal-containing plate indicating that pFR2 was stably integrated in the *lacZ* locus. One of these integrants, designated FR12, was chosen for further analysis. The same strategy was used to integrate the catabolic genes in the *E. coli* K-12 derivatives JM109 and DH5α strain, and the corresponding integrants were designated FR13 and FR14, respectively. Additional PCR amplification of the integration-junction sequences with specific primer sets for right and left junctions confirmed that integration occurred at the correct site (data not shown). Moreover, to exclude the possibility that *ech* and *fcs* genes have undergone mutational inactivation after stable integration into the *E. coli* chromosome, the coding region of each gene was amplified as PCR product, cloned and sequenced. This analysis allowed us to demonstrate that all reported recombinant strains had no alteration in the ferulic catabolic genes and could produce enzymatic activities required for conversion of ferulic acid to vanillin.

Comparison Between K-12 and B-type *E. coli* Derivatives as Platforms for Vanillin Production

In preliminary experiments, integrants of different *E. coli* cell lines were tested for their ability to convert ferulic acid into vanillin. Experiments were carried out using a resting cell system (with cells grown at 44°C and harvested from early stationary-phase cultures), performing the bioconversion assay at two temperatures: 30 and 44°C. In agreement with our results on the effect of temperature on *fcs* activity, no degradation of ferulic acid was detected when bioconversion experiments were carried out at 44°C. In contrast, vanillin accumulated in the medium, albeit at different levels, when ferulic acid was provided to resting cells incubated at 30°C (**Table 4**). With the integrative vector, higher vanillin production (3.51 ± 0.14 mM) was obtained using *E. coli* K-12 derivatives, in particular with JM109 as a parental strain (FR13; **Table 4**). With the latter strain, the amount of vanillin was 1.45–2.18-fold higher than that obtained with DH5α (FR14 strain; 2.42 ± 0.09 mM) or CGCS (FR12 strain; 1.61 ± 0.04 mM) derivatives. Data reported in **Table 4** also indicated that, with JM109 as recipient strain, the use of a single copy integrative vector allowed us to obtain a 52% increase in the maximum amount of vanillin (from 2.31 ± 0.21 to 3.51 ± 0.14 mM) compared to the low copy pBB1vector.

TABLE 4 | Vanillin yield obtained at 30°C from different *E. coli* cell line and cloning vector.

Wild type	Strain		Vector	Vanillin yield* (mM)
	Parental	Derivate		
E. coli K12	JM109	JM109(pBB1)	Replicative	2.31 ± 0.21[a]
		FR13	Integrative	3.51 ± 0.14[b]
	DH5α	FR14	Integrative	2.42 ± 0.09[a]
E. coli B	CGCS	FR12	Integrative	1.61 ± 0.04[c]

**Values calculated after 24 h of bioconversion. The superscript letters indicate similarities or significant differences between the values. Values with no letter in common significantly differ at $p \leq 0.05$ (Tukey HSD test).*

Optimization of Cultivation Conditions

To evaluate the dependence of vanillin production on incubation temperature and growth phase, bioconversion experiments were carried out using cells collected from exponentially and stationary cultures. Results reported in **Table 5** indicated that vanillin production yield and specific productivity acid were higher when cells, grown up to stationary culture phase at 44°C (condition 1), were transferred to fresh medium and allowed to do one cell duplication (condition 2–4). Better results (4.5/5-fold increase in the vanillin specific productivity) were obtained with cells from cultures shifted from 44 to 30°C (condition 2; **Table 5**). These variations seem to be imputable to different ferulic acid consumption rates that increased from 0.41 to 0.46 mmole/h (condition 3 and 4) up to 2.15 ± 0.02 mmole/h (condition 2).

Optimization of the Bioconversion Buffer

Data presented in **Figure 3** indicated that no bioconversion was observed when cells were incubated in saline phosphate buffer at pH 10. The results also indicated that a pH increase from 7.0 to 9.0 had a positive effect on ferulic acid consumption rate (from 0.40 ± 0.01 to 0.94 ± 0.01 mmoles/h) and determined an increase in vanillin production yield (from 62.8 to 77.9%) and product selectivity (from 67.2 to 83.3%), as well as a decrease in vanillyl alcohol production yield (from 30.7 to 15.6%). Interestingly, the incubation in phosphate buffer at pH 7 and 9 resulted in differences in intracellular ATP concentration which varied from 15 ± 0.02 (pH 7) to 20 ± 0.01 (pH 9) $\mu M/10^{10}$ cells.

Data reported in **Figure 4A** indicated that ferulic acid consumption rate was affected by phosphate concentration. The substrate consumption rate increased from 0.86 ± 0.01 to 0.94 ± 0.01 mmoles/h as phosphate concentration increased from 40 to 70 mM. A further increase in phosphate concentration had minor effects on ferulic acid consumption rate (**Figure 4A**).

Measuring the formation of DAPI-poly-P complex, we observed an increase of fluorescence at 550 nm (from 60,710 ± 1,150 AU to 130,000 ± 900 AU) when exponentially growing cells in LB were transferred in saline phosphate buffer at pH 9 and incubated at 30°C for 15 min. As shown in **Figure 4A** (white bars), this increase was independent from phosphate concentration and no significant difference was observed comparing the fluorescence intensity of all tested samples.

Measuring intracellular poly-P during bioconversion (2 h after the addition of ferulic acid), we observed a significant

TABLE 5 | Effect of physiological state and temperature of growth on vanillin production by FR13 cells.

Condition[1]	Growth recovery[2]	Recovery temperature (°C)	Vanillin yield (mM)	Specific Productivity (mmol vanillin/Kg biomass/h)	Ferulic acid consumption rate (mmol/h)
1	None	-	3.51 ± 0.21^{a}	43.35 ± 1.14^{a}	0.40 ± 0.01^{a}
2	Yes	30	5.62 ± 0.11^{b}	312.35 ± 6.35^{b}	2.15 ± 0.05^{b}
3	Yes	37	5.47 ± 0.09^{b}	67.52 ± 2.29^{c}	0.46 ± 0.01^{a}
4	Yes	44	4.84 ± 0.14^{c}	59.81 ± 3.50^{c}	0.41 ± 0.01^{a}

[1] *Main culture was grown at 44°C until stationary phase.*
[2] *One cell duplication.*
The superscript letters indicate similarities or significant differences between the values. Values with no letter in common significantly differ at $p \leq 0.05$ (Tukey HSD test).

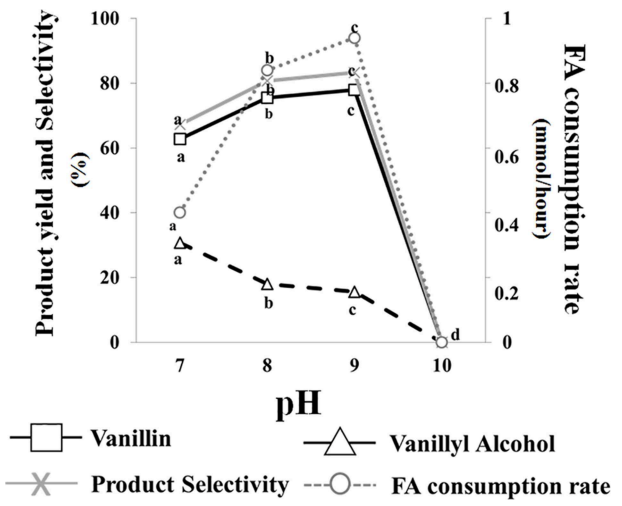

FIGURE 3 | Effect of pH on the bioconversion performance of *E. coli* FR13 cells. All experiments were carried out in triplicate at 30°C. Product yield and selectivity were calculated after 24 h of bioconversion. Average of substrate consumption rates was calculated measuring the amount of ferulic acid that was consumed between the second and the fifth hour. Values in each series with no letter in common significantly differ at $p \leq 0.05$ (Tukey HSD test).

reduction in DAPI-poly-P associated fluorescence at phosphate concentrations ≥70 mM (black bars). Interestingly, this reduction, indicating hydrolysis of intracellular poly-P, was enhanced in samples in which the ferulic consumption rate was higher (**Figure 4A**). At pH 9, independently from the phosphate concentration and the ferulic acid consumption rate, ATP concentration within the cells remained constant (20 ± 0.01 $\mu M/10^{10}$ cells) during the first 2 h of bioconversion.

Results reported in **Figure 4B**, indicated that changes in phosphate concentration affected the bioconversion process. The increase from 40 to 70 mM determined an increase in vanillin yield (from 70.4 to 77.9%) and product selectivity (from 79 to 83.3%) and a 1.2-fold reduction in vanillyl alcohol production (from 18.7 to 15.6%). A further increase of phosphate concentration, from 70 to 200 mM, had an opposite effect on both vanillin yield and product selectivity, which decreased up to 61.1 and 70.1%, respectively. Differences in product selectivity were correlated with vanillyl alcohol production, whose yield increased from 15.6 to 26% (**Figure 4B**).

Interaction Between Extracellular and Intracellular pH

In vitro spectral properties of Green Fluorescent Protein (GFP) may be influenced by several parameters, including pH (Campbell and Choy, 2001). The latter characteristic has led to the developments of different GFP variants with different pH sensitivities that can be used, as a pH indicator, to study processes in either alkaline or acidic environments (Kneen et al., 1998; Bizzarri et al., 2009).

In order to measure the effect of the bioconversion buffer on the intracellular pH, FR13 cells were tagged using a pH-sensitive GFP-derivative, named GFPmut3* (Andersen et al., 1998), and incubated in a saline phosphate buffer adjusted to pH values in the range of 6.5–9.0. The excitation spectra at 485 nm showed a two-fold increase in the fluorescence signal when cells were incubated in buffer at pH 9.0 rather than 6.5 (**Figure 5**). These results clearly indicated that the intracellular pH significantly increased when FR13 cells were incubated in buffered medium in alkaline conditions.

Optimization of Bioconversion Conditions Using the RSM Methodology

Optimization of the bioconversion parameters was analyzed by RSM. **Table 6** represents the design matrix of the variables (stirring speed [X_1] and initial substrate concentration [X_2]) in coded units along with vanillin (Y_1) and vanillyl alcohol (Y_2) yield in mM. The equations with the best fit coefficients are given below:

$$Y_1 = 7.7956 - 0.9302X_1^2 - 0.8095\,X_2^2$$
$$Y_2 = 0.8952 - 0.1900X_1 - 0.2383X_2 + 0.1519\,X^2$$

The 3D response surface graphs (**Figures 6A,B**) that fit to the following equations were plotted to better visualize the significant interaction effects of independent variables on the production of vanillin (Y_1) and vanillyl alcohol (Y_2) after 24 h of incubation. The highest vanillin production was 8.11 ± 0.25 mM (with 15.4 mM ferulic acid and 150 rpm), whereas the lowest vanillyl alcohol yield was 0.68 ± 0.03 mM (with 23.1 mM ferulic acid and 180 rpm). **Table 7** shows the analysis of variance (ANOVA) for the quadratic model of vanillin (Panel A) and vanillyl alcohol (Panel B) production. The regression analysis demonstrates that the quadratic parameters for these compounds were significant

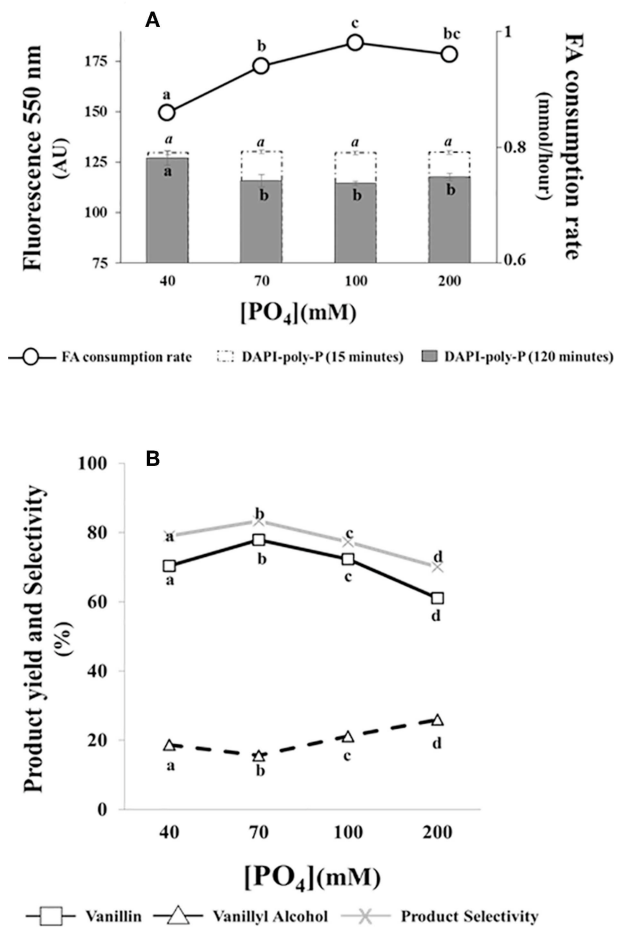

FIGURE 4 | Effect of phosphate concentration on the bioconversion performance and intracellular poly-P level of *E. coli* FR13 cells. All experiments were carried out at 30°C with phosphate solutions buffered at pH 9. Data are representative of three independent experiments. **(A)** Average of substrate consumption rates was calculated measuring the amount of ferulic acid that was consumed between the second and the fifth hour; DAPI-poly-P fluorescence was measured in cells incubated for 15 min in buffered solution without ferulic acid (white bars) and after 2 h of bioconversion (black bars). **(B)** Product yield and selectivity were calculated after 24 h of bioconversion. Values in each series with no letter in common significantly differ at $p \leq 0.05$ (Tukey HSD test).

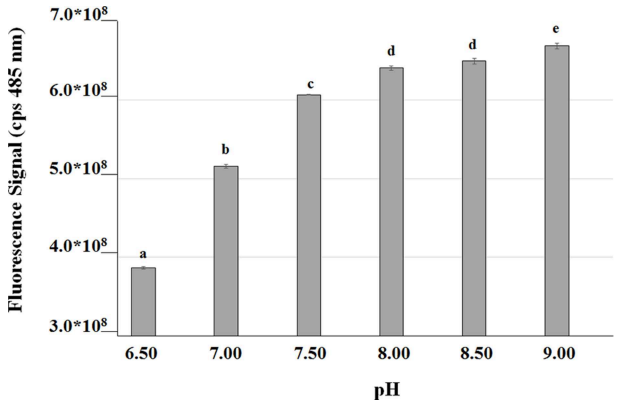

FIGURE 5 | Fluorescence of GFPmut3* as a function of medium pH. GFP was used as an indicator to evaluate the effect of saline phosphate solutions with different pH values on the intracellular pH of FR13 cells. Fluorescence was measured at 485 nm on cells incubated in buffered solution for 2 h at 30°C. The error bars represent standard errors of the means ($n = 3$). Values with no letter in common significantly differ at $p \leq 0.05$ (Tukey HSD test).

at the level of $p < 0.0001$ and that linear and interaction terms were insignificant at the level of $p > 0.1$ (**Table 7**). *F*-test and probability value for the model and the lack of fit showed that both models were statistically significant and fitted well the experimental data (**Table 7**).

Experiments carried out in triplicate in the conditions favoring higher vanillin yield and lower vanillyl alcohol accumulation (ferulic acid concentration of 14.94 mM and stirring speed of 151 rpm) allowed us to obtain vanillin and vanillyl alcohol concentration of 8.51 ± 0.02 mM and 1.15 ± 0.02 mM, respectively (in agreement with the model predicted concentration values of 8.24 mM for vanillin and 0.90 mM for vanillyl alcohol). Under the same conditions, using a 70 mM phosphate buffer (pH 9.0) with low Na/K ratio (0.013; sodium and potassium ion concentration of 1.75 and 140 mM, respectively), we observed an increase in vanillin yield (from 8.51 ± 0.02 to 11.63 ± 0.10 mM) and a 9% decrease in product selectivity due to a concurrent increase in vanillyl alcohol concentration (from 1.15 ± 0.01 to 1.73 ± 0.08 mM).

Comparison Between Batch and Fed-Batch Experiments

To evaluate, in more detail, the effect of the initial substrate concentration on vanillin production, we carried out time course experiments at ferulic acid concentrations of 14 and 20 mM (batch mode) or using a fixed volume fed-batch approach in which ferulic acid was entrapped and released from an agarose-gel matrix.

Results reported in **Figure 7** showed that, during the first 6 h of incubation, the increase in the initial ferulic acid concentration (from 14 to 20 mM) had no significant effect on ferulic acid consumption and vanillin accumulation rate in batch mode, whereas, in agreement with RSM data presented before, a significant difference in the vanillin concentration was detected after 24 h incubation. Increasing the initial ferulic acid concentration from 14 to 20 mM, the maximal level of vanillin decreased from 8.15 ± 0.04 to 6.24 ± 0.06 mM. In contrast, significant differences in the bioconversion rates and vanillin accumulation profile were observed comparing experiments carried out in batch and fed-batch mode. The use of the sol-gel technology to encapsulate ferulic acid and modulate its release in the liquid phase delayed the exposure of the cells to high substrate concentrations and allowed their adaptation to ferulic acid burden. The diffusion kinetics of ferulic acid in agarose gels revealed that, in the absence of cells, 60–70% of the compound was released during the first hour, 80% at the third hour, and almost 100% at the sixth hour of incubation (data not shown). Interestingly, using ferulic acid-adapted cells in fed-batch operation mode, ferulic acid consumption and vanillin production rate increased between 2 and 6 h of incubation and

TABLE 6 | 3^2 full factorial design matrix and responses of the two independent variables showing observed vanillin and vanillyl alcohol yield.

Run n°	x_1	x_2	Stirring speed (rpm)	Ferulic acid (mM)	Vanillin (Y_1)		Vanillyl alcohol (Y_2)	
					Exp.	Pred.	Exp.	Pred.
1	−1	−1	120	7.7	4.34	4.48	1.56	1.58
2	0	−1	150	7.7	6.51	6.44	1.36	1.29
3	1	−1	180	7.7	4.73	4.84	1.10	1.12
4	−1	0	120	15.4	5.72	5.84	1.23	1.15
5	0	0	150	15.4	7.00	7.80	1.04	0.90
6	1	0	180	15.4	5.90	6.19	0.84	0.77
7	−1	1	120	23.1	4.30	4.09	0.97	1.02
8	0	1	150	23.1	5.98	6.05	0.91	0.81
9	1	1	180	23.1	4.60	4.44	0.65	0.73
10	0	0	150	15.4	7.82	7.80	0.78	0.90
11	0	0	150	15.4	8.54	7.80	0.84	0.90
12	0	0	150	15.4	8.22	7.80	0.78	0.90
13	−1	−1	120	7.7	4.50	4.48	1.56	1.58
14	0	−1	150	7.7	6.51	6.44	1.30	1.29
15	1	−1	180	7.7	4.93	4.84	1.10	1.12
16	−1	0	120	15.4	5.85	5.84	1.23	1.15
17	0	0	150	15.4	7.20	7.80	0.97	0.90
18	1	0	180	15.4	6.10	6.19	0.84	0.77
19	−1	1	120	23.1	4.10	4.09	0.97	1.02
20	0	1	150	23.1	5.63	6.05	0.91	0.81
21	1	1	180	23.1	4.60	4.44	0.71	0.73
22	0	0	150	15.4	7.80	7.80	0.84	0.90
23	0	0	150	15.4	8.15	7.80	0.84	0.90
24	0	0	150	15.4	8.10	7.80	0.78	0.90

Bioconversions were carried out in phosphate saline M9 buffer (pH 9.0) using E. coli FR13 as biocatalyst. Experimental values are average of duplicate within ± 5% standard error. x_1 = coded value of stirring speed (X_1); x_2 = coded value for ferulic acid initial concentration (X_2).

the total amount of vanillin that accumulated in the medium after 24 h increased 2.5–3.3 fold (up to 20.6 ± 0.11 mM) compared to the batch mode of operation (**Figure 7**). Using the 70 mM phosphate buffer (pH 9.0) with low Na/K ratio (0.013), the vanillin yield increased up to 28.10 ± 0.05 mM.

DISCUSSION

Although feruloyl-CoA synthetase (Fcs) is a key enzyme for the coenzyme-A-dependent conversion of ferulic acid into vanillin, the effect of temperature and pH on this enzyme activity has not been described before. Analyzing the catalytic activity profile of the enzyme produced by the ferulic acid-degrader *P. fluorescens* strain BF13, we showed that Fcs activity is affected by both temperature and pH, and almost 97% of its initial activity is lost, increasing the temperature from 30 to 44°C or pH from 7 to 10 (**Figure 2**). In parallel, gene expression experiments carried out using the β-galactosidase reporter gene under the control of P_{fer}, the promoter that allows inducible expression of ferulic catabolic genes in strain BF13 (Calisti et al., 2008), revealed that incubation temperature and culture broth initial pH had no effect on the transcriptional activity of this promoter in *E. coli* JM109 cells. *E. coli* is a non-native vanillin producer that can grow over a wide range of temperatures (up to 44°C; Van Derlinden et al., 2008) and external pH values (from 4.5 to 9.0; de Jonge et al., 2003) and it is widely used in industrial fermentation processes (Lee and Kim, 2015). *Pseudomonas* genes responsible for the conversion of ferulic acid to vanillin can be constitutively expressed in *E. coli* under the control of their native P_{fer} promoter, but the biocatalytic activity of the recombinant cells is negatively affected by overexpression of these genes (Barghini et al., 2007) and by accumulation of vanillin, whose toxicity against *E. coli* is well documented (Fitzgerald et al., 2004). Fcs activity is dependent on the size and composition of the intracellular CoA pool and might compete with the major *E. coli* metabolic pathways for unbound acyl-CoA esters (de la Peña Mattozzi et al., 2010). In this regard, the growth of recombinant *E. coli* cells at 44°C, which allows the production of feruloyl-CoA synthetase in an almost inactive form, can be a valuable strategy to relieve the stress induced by over-production of this enzyme. An alternative strategy that could be pursued to reduce problems associated to accumulation of this enzyme activity is the modulation of *fcs* transcript levels by decreasing the copy number of the ferulic catabolic operon. Single-copy integration of *ech-fcs* gene cassette into *E. coli* JM109 chromosome allowed us to obtain an increase of about 52% in vanillin production yield (from 2.31 ± 0.21 to

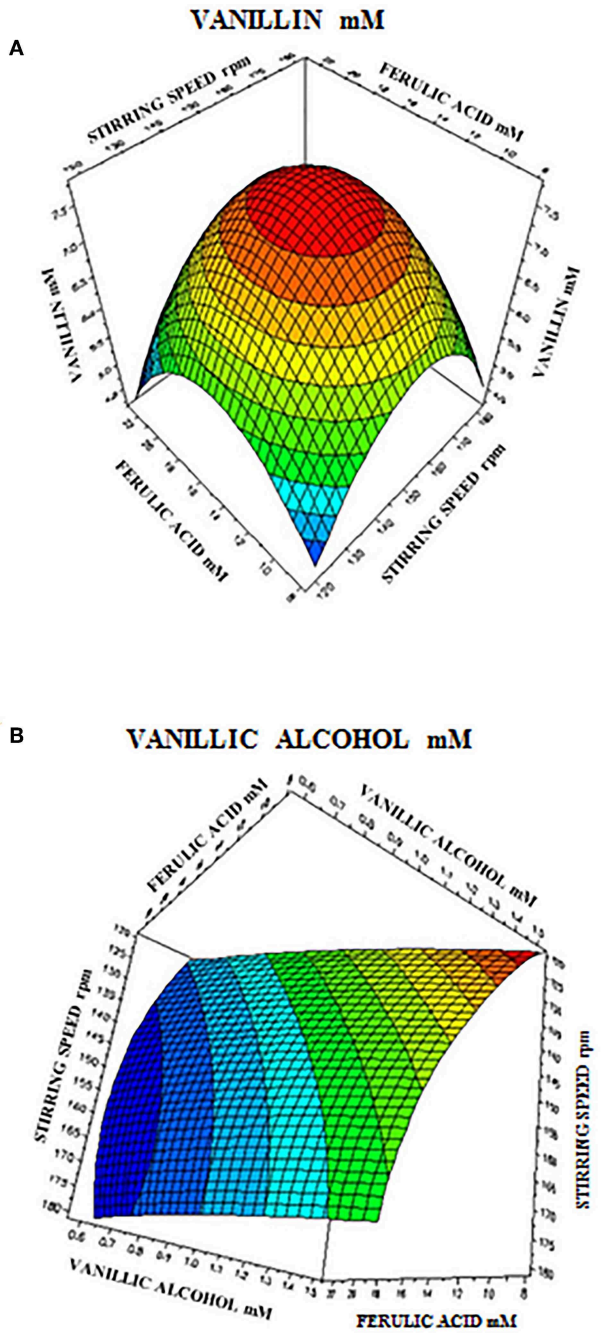

FIGURE 6 | Response surface plot showing the effect of stirring speed and initial ferulic acid concentration on vanillin **(A)** and vanillyl alcohol **(B)** yield.

TABLE 7 | ANOVA table for the quadratic model for vanillin **(A)** and vanillyl alcohol production **(B)**.

Source	Sum of square	Degree of freedom	Mean square	*F*-value	*p*-value
(A)					
Model	45.42	5	9.08	69.88	<0.0001
Residual	2.34	18	0.13		
Lack of fit	0.31	3	0.10	0.76	0.53
Pure error	2.03	15	0.13		
Total	949.13	24			
(B)					
Model	1.33	5	0.27	35.02	<0.0001
Residual	0.14	18	0.01		
Lack of fit	0.07	3	0.02	5.02	0.01
Pure error	0.07	15	0.01		
Total	25.69	24	1.071		

3.51 ± 0.14 mM) compared to the isogenic strain in which the genes were placed on a low-copy plasmid (**Table 4**). The same strategy was successfully applied to integrate the ferulic catabolic operon in different *E. coli* strains, and a comparative analysis of their biocatalytic performances allowed us to demonstrate that B-type derivatives were less suitable than K12-type strains for conversion of ferulic acid into vanillin (**Table 4**). These results may reflect differences in cellular metabolism and physiology between *E. coli* B and K12 strains (Yoon et al., 2012; Marisch et al., 2013), including the ability of B-type strains to produce higher amounts of recombinant proteins compared to K-12 derivatives (Shiloach et al., 1996), which may lead to an undesired accumulation of Fcs in the host cell.

Results reported in **Table 5** indicated that the use of *E. coli* cells from actively growing rather than stationary cultures had a significant positive effect on product yield and specific productivity. In contrast, an increase in the ferulic acid consumption rate was observed only in cells grown at 30°C. The latter result is in agreement with our previous observations that vanillin production in *E. coli* JM109 (pBB1) could be enhanced growing cells at sub-optimal temperature (Barghini et al., 2007). The shift in the growth recovery temperature from 44 to 30°C determined a five-fold increase in ferulic acid consumption rate and vanillin productivity compared to overnight growth at 44°C (**Table 5**, condition 1 and 2). This result is consistent with the negative correlation between Fcs activity and temperature and supports the hypothesis that a temperature-mediated reactivation of Fcs during the cell recovery at 30°C can enhance the catalytic performances of FR12 cells under non-proliferating conditions. Interestingly, the same observations were obtained shifting the growth temperature from 44 to 30°C with a JM109 derivative carrying ferulic catabolic genes on RK2-based low-copy or ColE1-based high-copy plasmids (data not shown), which indicated that temperature-dependent modulation of the intracellular activity of Fcs can be a valuable strategy to increase vanillin productivity in recombinant *E. coli*.

Another remarkable result that was achieved through the use of non-proliferating cells was the demonstration that bioconversion of ferulic acid to vanillin is strongly affected by extracellular and intracellular pH. Mitra et al. (1999) reported that the highest activity for 4-hydroxycinnamoyl-CoA hydratase/aldolase, the enzyme responsible for the conversion of feruloyl-CoA to vanillin, is obtained at pH 8.5–9.5 and that the activity of this enzyme declines to ca. 50% of its maximum value when the pH is decreased up to 6.5. Combining this information

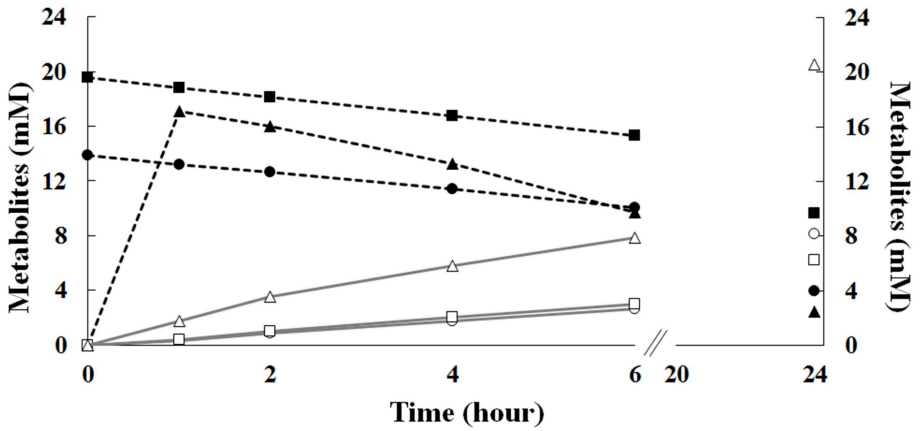

FIGURE 7 | Effect of the initial ferulic acid concentration on the production of vanillin. Experiments were carried out in triplicate in saline phosphate buffer at pH 9.0 (15 mL), using *E. coli* FR13 cells. Bioconversions were carried out in batch mode, in the presence of 14 (circle) or 20 mM (square) ferulic acid, or in fed-batch mode (triangle), using 12 agarose-ferulic acid cylinders (0.0348 mmoles of ferulic acid per cylinder). Ferulic acid: filled symbols; vanillin: empty symbols.

with our evidence that Fcs activity can be enhanced, about 1.8-fold, by increasing the pH from 7.0 to 9.0, it was predictable that the coenzyme-A-dependent conversion of ferulic acid to vanillin could be favored under moderate alkaline conditions. Using resting cells of recombinant *E. coli* F12 strain expressing GFPmut3*, we showed that incubation in a phosphate buffer at pH values from 8.0 to 9.0, determined an increase in the intracellular pH of *E. coli* cells (**Figure 5**). It can be predicted that extracellular acid-base disturbance of intracellular pH can influence transport and reactivity of specific compounds such as phenolic acids. At pH 9.0, due to its pK_a values, ferulic acid occurs in its anionic phenolate form, which is expected to be transported more easily inside the cell (Biała and Jasinski, 2018), increasing its availability for the bioconversion process, and determine a lower damage on cell membrane (Borges et al., 2013). At the same time, as reported for ketosteroid isomerase, the model system used for enzymatic proton-transfer chemistry (Kraut et al., 2006), an increase in the pH determines an increase in the negative charge density at the phenolate oxygen that can favor substrate-enzyme binding as well as positively affect catalytic activity. An additional factor that can positively impact vanillin production is ATP availability. ATP is an essential cofactor for the activation of ferulic acid to the corresponding CoA thioester (**Figure 1**) and, as demonstrated by Padan et al. (2005), ATP availability increases in *E. coli* cells exposed to alkaline pH. In agreement with this hypothesis, we observed that the pH-dependent increase in ferulic acid consumption rate (**Figure 3**) was consistent with changes in the level of intracellular ATP, which increased 1.33-fold changing the pH value from 7 to 9.

It can also be postulated that deprotonation of vanillin could negatively affect its reduction to the corresponding alcohol by *E. coli* reductases, which could result in an increase in product selectivity. Combining the information on the effect of pH on enzymatic activities involved in the conversion of ferulic acid to vanillin, on protonation of the substrate and the final product and on intracellular pH of *E. coli* resting cells, we demonstrated that modifying operating conditions and increasing the pH of the bioconversion buffer from 7.0 to 9.0, we could achieve simultaneous improvement in ferulic acid consumption rate, vanillin yield and product selectivity (**Figure 3**). Similar results were reported by Gunnarsson and Palmqvist (2006), which demonstrated that conversion of vanillin to vanillic acid and vanillyl alcohol in *Streptomyces setonii* ATCC 39116 is strongly influenced by the intracellular pH and that this effect is related to the protonation/deprotonation ratio of these compounds.

Therefore, incubation temperature and pH affect the efficacy of the whole ferulic acid to vanillin biotransformation process through different mechanisms, which include modulation of Fcs activity, availability of the substrate (ferulic acid), impact of the protonation state of the substrate on the enzyme-substrate interaction and inhibitory effects on enzymes involved in byproduct (vanillyl alcohol) formation.

Bioconversion experiments carried out at pH 9.0 also demonstrated a significant effect of phosphate on product yield and selectivity, with the highest vanillin yield and vanillin-to-vanillyl alcohol ratio achieved at a phosphate concentration of 70 mM. In agreement with Gray and Jakob (2015), which demonstrated that, in *E. coli*, intracellular Poly-P level is influenced by extracellular phosphate, we observed that incubation at pH 9, in a buffer with a phosphate concentration higher than 40 mM, resulted in a 2-fold increase in intracellular Poly-P compared to LB-grown cells. Interestingly, the partial hydrolysis of Poly-P pool, which occurred in actively vanillin producing cells, was enhanced when the rate of ferulic acid consumption was higher (at a phosphate concentration $\geq$ of 70 mM; **Figure 4A**). As reviewed by Korneberg (1995), inorganic polyphosphate can act as a substitute for ATP, which is required for the activity of feruloyl-CoA synthetase (**Figure 1**) and can be a buffer against alkali ions. In our experiments with resting cells, these properties of polyphosphates can explain the direct correlation that was observed between Poly-P hydrolysis and consumption rates of the substrate. Schurig-Briccio et al.

(2009) demonstrated that the intracellular Poly-P level is also important in cell fitness and in the regulation of several stress response pathways in *E. coli* cells. Vanillin is toxic to microorganisms (Fitzgerald et al., 2004), and to withstand to its deleterious effects *S. cerevisiae* and *E. coli* convert it in less toxic compounds, such as vanillic alcohol (Liu, 2011; Kunjapur et al., 2014). It should be noted that, under our experimental conditions, vanillin yield and product selectivity decreased independently by Poly-P level (**Figures 4A,B**). Based on these observations we can conclude that Poly-P level can have a positive effect on Fcs activity and, probably, as a buffer against alkali ions, but the response elicited by Poly-P is not sufficient to alleviate vanillin-induced stress and stimulation of detoxifying enzymes responsible for the conversion of vanillin to vanillyl alcohol.

In order to determine the optimal operating conditions of the bioconversion process, maximization of the vanillin yield and product selectivity is required. By using response surface methodology, we demonstrated that the catalytic activity of *E. coli* FR13 is affected by both stirring speed and initial substrate concentration. The elliptical contour of the response surface (**Figure 6A**) indicated that there was a perfect interaction between both independent variables. At the extreme values of stirring speed and initial ferulic acid concentration, vanillin yield was low. These observations indicated that bioconversion of ferulic acid into vanillin is affected by several parameters: dissolved oxygen (DO) level that regulates the oxidation-reduction potential (ORP) and activity of enzymes involved in conversion of vanillin to vanillyl alcohol (stirring speed); substrate toxicity (ferulic acid concentration); shortage of acetyl-CoA and ATP (both variables). The highest predicted vanillin concentration (7.8 mM) was obtained decreasing the stirring speed from 180 to 150 rpm and increasing the initial ferulic acid concentration from 7.7 to 15.5 mM (**Table 6**). A further decrease in the stirring speed from 150 to 120 rpm, which resulted in a reduction of ORP and DO levels, had a negative effect on vanillin yield and led to an increase in vanillyl alcohol concentration, determining a reduction in the product selectivity (**Table 6**). The experimental results indicated a minimum vanillyl alcohol concentration of 0.71 mM, which is in good agreement with the model prediction (0.73 mM; **Table 6**, run 21) and a negative effect of the increase of both independent variables on the production of this unwanted compound (**Figure 6B**). The verification experiments carried out under the optimum conditions obtained from RSM studies (ferulic acid concentration of 14.94 mM and stirring speed of 151 rpm) confirmed a good agreement between experimental (8.51 $\pm$ 0.02 mM) and predicted data (8.21 $\pm$ 0.01 mM) for vanillin production. Moreover, these results clearly indicated that in the bioconversion process of ferulic acid into vanillin with *E. coli* cells, there is a dependency among ORP, substrate toxicity, vanillin yield and product selectivity.

Interestingly, the sol-gel technology allowed us to demonstrate that the catalytic activity of *E. coli* FR13 can be enhanced adapting cells to a low concentration of ferulic acid during the first hour of incubation (**Figure 7**). In the fed-batch operation mode, the vanillin production rate referred to the first 6 h, increased significantly and remained high up to 24 h (2.5–3.3-fold increase). Interestingly, the use of saline phosphate buffer with a high concentration of potassium ions (140 m), which reduces the alkaline stress on *E. coli* cells, allowed us to obtain a 36% increase in vanillin yield, up to 28.10 $\pm$ 0.05 mM.

CONCLUSION

To the best of our knowledge, this is the first report in which vanillin is produced from ferulic acid using a plasmid-free *E. coli* strain. The use of this strain under resting cell conditions allowed us to improve the vanillin yield and selectivity minimize the toxic effect of ferulic acid and vanillin.

By using the two-phase system, it was possible to increase the productivity of 68% compared to the isogenic strain containing the genes responsible for conversion of ferulic acid into vanillin on a plasmid, reduce the bioconversion time from 4 to 1 day, and increase the final vanillin concentration in the liquid phase sevenfold. The maximum amount of vanillin that accumulated in the liquid phase under optimized conditions was 28.02 $\pm$ 0.05 mM, one of the highest found in the literature for recombinant *E. coli* strains. FR13 can be used as a platform strain to test metabolic engineering strategies to further improve vanillin production in *E. coli*.

DATA AVAILABILITY STATEMENT

All datasets generated for this study are included in the manuscript/supplementary files.

AUTHOR CONTRIBUTIONS

MR and FL conceived the project and wrote the manuscript. FL performed the experiment supported by AF and LB. All authors contributed to the analysis of results, read and approved the manuscript and significantly to the work.

REFERENCES

Achterholt, S., Priefert, H., and Steinbüchel, A. (2000). Identification of *Amycolatopsys* sp. Strain HR167 genes, involved in the bioconversion of ferulic acid to vanillin. *Appl. Microbiol. Biotecnol.* 54, 799–807. doi: 10.1007/s002530000431

Andersen, J. B., Sternberg, C., Poulsen, L. K., Bjorn, S. P., Givskov, M., and Molin, S. (1998). New unstable variants of green fluorescent protein for studies of transient gene expression in bacteria. *Appl. Environ. Microbiol.* 64, 2240–2246.

Aschar-Sobbi, R., Abramov, A. Y., Diao, C., Kargacin, M. E., Kargacin, G. J., French, R. J., et al. (2008). High sensitivity, quantitative measurements of polyphosphate using a new DAPI-based approach. *J. Fluoresc.* 18, 859–866. doi: 10.1007/s10895-008-0315-4

Banerjee, G., and Chattopadhyay, P. (2019). Vanillin biotechnology: the perspectives and future. *J. Sci. Food Agric.* 99, 499–506. doi: 10.1002/jsfa.9303

Barghini, P., Di Gioia, D., Fava, F., and Ruzzi, M. (2007). Vanillin production using metabolically engineered *Escherichia coli* under non-growing conditions. *Microb. Cell Fact.* 6, 13–24. doi: 10.1186/1475-2859-6-13

Barghini, P., Montebove, F., Ruzzi, M., and Schiesser, A. (1998). Optimal conditions for bioconversion of ferulic acid into vanillic acid by *Pseudomonas fluorescens* BF13 cells. *Appl. Microbiol. Biotechnol.* 49:309. doi: 10.1007/s002530051174

Bezerra, M. A., Santelli, R. E., Oliveira, E. P., Villar, L. S., and Escaleira, L. A. (2008). Response surface methodology (RSM) as a tool for optimization in analytical chemistry. *Talanta* 76, 965–977. doi: 10.1016/j.talanta.2008.05.019

Biała, W., and Jasinski, M. (2018). The phenylpropanoid case - it is transport that matters. *Front. Plant Sci.* 9:1610. doi: 10.3389/fpls.2018.01610

Biles, W. E. (1975). A response surface method for experimental optimization of multi-response processes. *Ind. Eng. Chem. Process Des. Dev.* 14, 152–158. doi: 10.1021/i260054a010

Bizzarri, R., Serres, M., Luin, S., and Beltram, F. (2009). Green fluorescent protein-based pH indicators for *in vivo* use: a review. *Anal. Bioanal. Chem.* 393, 1107–1122. doi: 10.1007/s00216-008-2515-9

Borges, A., Ferreira, C., Saavedra, M. J., and Simões, M. (2013). Antibacterial activity and mode of action of ferulic and gallic acids against pathogenic bacteria. *Microb. Drug Res.* 19, 256–265. doi: 10.1089/mdr.2012.0244

Boz, H. (2015). Ferulic acid in cereals – a review. *Czech J. Food Sci.* 33, 1–7. doi: 10.17221/401/2014-CJFS

Brink, D. P., Ravi, K., Lidén, G., and Gorwa-Grauslund, M. F. (2019). Mapping the diversity of microbial lignin catabolism: experiences from the eLignin database. *Appl. Microbiol. Biotechnol.* 103, 3979–4002. doi: 10.1007/s00253-019-09692-4

Brunati, M., Marinelli, F., Bertolini, C., Gandolfi, R., Daffonchio, D., and Molinari, F. (2004). Biotransformations of cinnamic and ferulic acid with actinomycetes. *Enz. Microb. Technol.* 34, 3–9. doi: 10.1016/j.enzmictec.2003.04.001

Brunetti, L. (2013). *Biotechnological production of vanillin using microbial cells* (Ph.D. thesis). University of Tuscia. Available online at: http://dspace.unitus.it/bitstream/2067/2703/1/lbrunetti_tesid.pdf (accessed September 25, 2019).

Calisti, C., Ficca, A. G., Barghini, P., and Ruzzi, M. (2008). Regulation of ferulic catabolic genes in *Pseudomonas fluorescens* BF13: involvement of a MarR family regulator. *Appl. Microbiol. Biotechnol.* 80, 475–483. doi: 10.1007/s00253-008-1557-4

Campbell, T. N., and Choy, F. Y. M. (2001). The effect of pH on green fluorescent protein: a brief review. *Mol. Biol. Today* 2, 1–4. Available online at: https://www.caister.com/backlist/mbt/v/v2/01.pdf

Chattopadhyay, P., Banerjee, G., and Sen, S. K. (2018). Cleaner production of vanillin through biotransformation of ferulic acid esters from agroresidue by *Streptomyces sannanensis*. *J. Clean. Prod.* 182, 272–279. doi: 10.1016/j.jclepro.2018.02.043

de Jonge, R., Takumi, K., Ritmeester, W. S., and van Leusden, F. M. (2003). The adaptive response of *Escherichia coli* O157 in an environment with changing pH. *J. Appl. Microbiol.* 94, 555–560. doi: 10.1046/j.1365-2672.2003.01865.x

de la Peña Mattozzi, M., Kang, Y., and Keasling, J. D. (2010). "Feast: choking on Acetyl-CoA, the Glyoxylate Shunt, and Acetyl-CoA-Driven Metabolism," in *Handbook of Hydrocarbon and Lipid Microbiology,* ed K. N. Timmis (Berlin: Springer Verlag), 1–12.

Di Gioia, D., Fava, F., Luziatelli, F., and Ruzzi, M. (2011b). "Vanillin production from agro-industrial wastes," in *Comprehensive Biotechnology 2nd Edn,* ed M. Y. Murray (Burlington, VT: Academic Press), 661–667. doi: 10.1016/B978-0-08-088504-9.00397-4

Di Gioia, D., Luziatelli, F., Negroni, A., Ficca, A. G., Fava, F., and Ruzzi, M. (2011a). Metabolic engineering of *Pseudomonas fluorescens* for the production of vanillin from ferulic acid. *J. Biotechnol.* 156, 309–316. doi: 10.1016/j.jbiotec.2011.08.014

Di Gioia, D., Sciubba, L., Ruzzi, M., Setti, L., and Fava, F. (2009). Production of vanillin from wheat bran hydrolyzates via microbial bioconversion. *J. Chem. Technol. Biotechnol.* 84, 1441–1448. doi: 10.1002/jctb.2196

Di Gioia, D., Sciubba, L., Setti, L., Luziatelli, F., Ruzzi, M., Zanichelli, D., et al. (2007). Production of biovanillin from wheat bran. *Enz. Microb. Technol.* 41, 498–505. doi: 10.1016/j.enzmictec.2007.04.003

Fava, F., Zanaroli, G., Vannini, L., Guerzoni, E., Bordoni, A., et al. (2013). New advances in the integrated management of food processing by-products in Europe: sustainable exploitation of fruit and cereal processing by-products with the production of new food products (NAMASTE EU). *New Biotechnol.* 30, 647–655. doi: 10.1016/j.nbt.2013.05.001

Fitzgerald, D. J., Stratford, M., Gasson, M. J., Ueckert, J., Bos, A., and Narbad, A. (2004). Mode of antimicrobial action of vanillin against *Escherichia coli*, *Lactobacillus plantarum* and *Listeria innocua*. *J. Appl. Microbiol.* 97, 104–113. doi: 10.1111/j.1365-2672.2004.02275.x

Fleige, C., Hansen, G., Kroll, J., and Steinbüchel, A. (2013). Investigation of the *Amycolatopsis* sp. strain ATCC 39116 vanillin dehydrogenase and its impact on the biotechnical production of vanillin. *Appl. Environ. Microbiol.* 79, 81–90. doi: 10.1128/AEM.02358-12

Fleige, C., Meyer, F., and Steinbüchel, A. (2016). Metabolic engineering of the actinomycete *Amycolatopsis* sp. strain ATCC 39116 towards enhanced production of natural vanillin. *Appl. Environ. Microbiol.* 82, 3410–3419. doi: 10.1128/AEM.00802-16

Furuya, T., Miura, M., and Kino, K. (2014). A coenzyme-independent decarboxylase/oxygenase cascade for the efficient synthesis of vanillin. *ChemBioChem* 15, 2248–2254. doi: 10.1002/cbic.201402215

Furuya, T., Miura, M., Kuroiwa, M., and Kino, K. (2015). High-yield production of vanillin from ferulic acid by a coenzyme-independent decarboxylase/oxygenase two-stage process. *N. Biotechnol.* 32, 335–339. doi: 10.1016/j.nbt.2015.03.002

Galadima, A. I., Salleh, M. M., Hussin, H., et al. (2019). Biovanillin: production concepts and prevention of side product formation. *Biomass Conv. Bioref.* 1–21. doi: 10.1007/s13399-019-00418-0

Gallage, N. J., and Møller, B. L. (2015). Vanillin–bioconversion and bioengineering of the most popular plant flavor and its *de novo* biosynthesis in the vanilla orchid. *Mol. Plant* 8, 40–57. doi: 10.1016/j.molp.2014.11.008

Graf, N., and Altenbuchner, J. (2014). Genetic engineering of *Pseudomonas putida* KT2440 for rapid and high-yield production of vanillin from ferulic acid. *Appl. Microbiol. Biotechnol.* 98, 137–149. doi: 10.1007/s00253-013-5303-1

Gray, M. J., and Jakob, U. (2015). Oxidative stress protection by polyphosphate–new roles for an old player. *Curr. Opin. Microbiol.* 24, 1–6. doi: 10.1016/j.mib.2014.12.004

Gunnarsson, N., and Palmqvist, E. A. (2006). Influence of pH and carbon source on the production of vanillin from ferulic acid by *Streptomyces setonii* ATCC 39116. *Develop. Food Sci.* 43, 73–76. doi: 10.1016/S0167-4501(06)80018-X

Hansen, E. H., Møller, B. L., Kock, G. R., Bünner, C. M., Kristensen, C., Jensen, O. R., et al. (2009). *De novo* biosynthesis of vanillin in fission yeast (*Schizosaccharomyces pombe*) and baker's yeast (*Saccharomyces cerevisiae*). *Appl. Environ. Microbiol.* 75, 2765–2774. doi: 10.1128/AEM.02681-08

Hua, D., Ma, C., Song, L., Lin, S., Zhang, Z., Deng, Z., et al. (2007). Enhanced vanillin production from ferulic acid using adsorbent resin. *Appl. Microbiol. Biotechnol.* 74, 783–790. doi: 10.1007/s00253-006-0735-5

IMARC Group (2019). *Vanilla and Vanillin Market: Global Industry Trends, Share, Size, Growth, Opportunity and Forecast 2019-2024*. IMARC Services Private Limited.

Kneen, M., Farinas, J., Li, Y., and Verkman, A. S. (1998). Green fluorescent protein as a noninvasive intracellular pH indicator. *Biophys. J.* 74, 1591–1599. doi: 10.1016/S0006-3495(98)77870-1

Korneberg, A. (1995). Inorganic polyphosphate: toward making a forgotten polymer unforgettable. *J. Bacteriol.* 177, 491–496. doi: 10.1128/jb.177.3.491-496.1995

Kraut, D. A., Sigala, P. A., Pybus, B., Liu, C. W., Ringe, D., Petsko, G. A., et al. (2006). Testingelectrostatic complementarity in enzyme catalysis: hydrogen bonding in the ketosteroid isomeraseoxyanion hole. *PLoS Biol.* 4:e99. doi: 10.1371/journal.pbio.0040099

Kumar, N., and Pruthi, V. (2014). Potential applications of ferulic acid from natural sources. *Biotechnol. Rep.* 4, 86–93. doi: 10.1016/j.btre.2014.09.002

Kunjapur, A. M., Tarasova, Y., and Prather, K. L. J. (2014). Synthesis and accumulation of aromatic aldehydes in an engineered strain of *Escherichia coli*. *J. Am. Chem. Soc.* 136, 11644–11654. doi: 10.1021/ja506664a

Lee, E. G., Yoon, S. H., Das, A., Lee, S. H., Li, C., Kim, J. Y., et al. (2009). Directing vanillin production from ferulic acid by increased acetyl-CoA consumption in recombinant *Escherichia coli*. *Biotechnol. Bioeng.* 102, 200–208. doi: 10.1002/bit.22040

Lee, S. Y., and Kim, H. U. (2015). Systems strategies for developing industrial microbial strains. *Nat. Biotechnol.* 33, 1061–1072. doi: 10.1038/nbt.3365

Lesage-Meessen, L., Delattre, M., Haon, M., Thibault, J. F., Ceccaldi, B. C., Brunerie, P., et al. (1996). A two-step bioconversion process for vanillin production from ferulic acid combining *Aspergillus niger* and *Pycnoporus cinnabarinus*. *J. Biotechnol.* 50, 107–113. doi: 10.1016/0168-1656(96)01552-0

Liu, Z. L. (2011). Molecular mechanisms of yeast tolerance and *in situ* detoxification of lignocellulose hydrolysates. *Appl. Microbiol. Biotechnol.* 90, 809–825. doi: 10.1007/s00253-011-3167-9

Marisch, K., Bayer, K., Scharl, T., Mairhofer, J., Krempl, P. M., Hummel, K., et al. (2013). A comparative analysis of industrial *Escherichia coli* K-12 and B strains in high-glucose batch cultivations on process-, transcriptome- and proteome level. *PLoS ONE* 8: e70516. doi: 10.1371/journal.pone.0070516

Martinez-Morales, F., Borges, A. C., Martinez, A., Shanmugam, K. T., and Ingram, L. O. (1999). Chromosomal integration of heterologous DNA in *Escherichia coli* with precise removal of markers and replicons used during construction. J. *Bacteriol.* 181, 7143–7148.

Masai, E., Katayama, Y., and Fukuda, M. (2007). Genetic and biochemical investigations on bacterial catabolic pathways for lignin-derived aromatic compounds. *Biosci. Biotechnol. Biochem.* 71, 1–15. doi: 10.1271/bbb.60437

Miller, J. H. (1992). *A Short Course in Bacterial Genetics. A Laboratory 847 Manual and Handbook for Escherichia coli and Related Bacteria*. New York, NY: Cold Spring Harbor Laboratory Press.

Mitra, A., Kitamura, Y., Gasson, M. J., Narbad, A., Parr, J., Payne, J., et al. (1999). 4-hydroxycinnamoyl-CoA hydratase/lyase (HCHL), an enzyme of phenylpropanoid chain cleavage from *Pseudomonas*. *Arch. Biochem. Biophys.* 365, 10–16. doi: 10.1006/abbi.1999.1140

Muheim, A., and Lerch, K. (1999). Towards a high-yield bioconversion of ferulic acid to vanillin. *Appl. Microbiol. Biotechnol.* 51, 456–461. doi: 10.1007/s002530051416

Narbad, A., and Gasson, M. J. (1998). Metabolism of ferulic acid via vanillin using a novel CoA-dependent pathway in a newly-isolated strain of *Pseudomonas fluorescens*. *Microbiology* 194, 1397–1405. doi: 10.1099/00221287-144-5-1397

Oddou, J., Stentelaire, C., Lesage-Meessen, L., Asther, M., and Colonna Ceccaldi, B. (1999). Improvement of ferulic acid bioconversion into vanillin by use of high-density cultures of *Pycnoporus cinnabarinus*. *Appl. Microbiol. Biotechnol.* 53, 1–6. doi: 10.1007/s002530051605

Oliveira, D. M., Finger-Teixeira, A., Rodrigues Mota, T., Salvador, V. H., Moreira-Vilar, F. C., et al. (2015). Ferulic acid: a key component in grass lignocellulose recalcitrance to hydrolysis. *Plant Biotechnol. J.* 13, 1224–1232. doi: 10.1111/pbi.12292

Ou, S., and Kwok, K. (2004). Ferulic acid: pharmaceutical functions, preparation and applications in foods. *J. Sci. Food Agric.* 8, 1261–1269. doi: 10.1002/jsfa.1873

Overhage, J., Priefert, H., Rabenhorst, J., and Steinbüchel, A. (1999b). Biotransformation of eugenol to vanillin by a mutant of *Pseudomonas* sp. strain HR199 constructed by disruption of the vanillin dehydrogenase (*vdh*) gene. *Appl. Microbiol. Biotechnol.* 52, 820–828. doi: 10.1007/s002530051598

Overhage, J., Priefert, H., and Steinbüchel, A. (1999a). Biochemical and genetic analyses of ferulic acid catabolism in *Pseudomonas* sp. strain HR199. *Appl. Environ. Microbiol.* 65, 4837–4847.

Padan, E., Bibi, E., Ito, M., and Krulwich, T. A. (2005). Alkaline pH homeostasis in bacteria: new insights. *Biochim. Biophys. Acta* 1717, 67–88. doi: 10.1016/j.bbamem.2005.09.010

Plaggenborg, R., Overhage, J., Loos, A., Archer, J. A., Lessard, P., Sinskey, A. J., et al. (2006). Potential of *Rhodococcus* strains for biotechnological vanillin production from ferulic acid and eugenol. *Appl. Microbiol. Biotechnol.* 72, 745–755. doi: 10.1007/s00253-005-0302-5

Plaggenborg, R., Overhage, J., Steinbüchel, A., and Priefert, H. (2003). Functional analyses of genes involved in the metabolism of ferulic acid in *Pseudomonas putida* KT2440. *Appl. Microbiol. Biotechnol.* 61, 528–535. doi: 10.1007/s00253-003-1260-4

Pugh, S., McKenna, R., Halloum, I., and Nielsen, D. R. (2015). Engineering *Escherichia coli* for renewable benzyl alcohol production. *Metab. Eng. Commun.* 2, 39–45. doi: 10.1016/j.meteno.2015.06.002

Rabenhorst, J., and Hopp, R. (2002). *Process for the Preparation of Vanillin and Suitable Microorganisms*. Munich: European Union Patent EP0761817.

Ramachandra Rao, S., and Ravishankar, G. (2000). Vanilla flavour: production by conventional and biotechnological routes. *J. Sci. Food Agric.* 80, 289–304. doi: 10.1002/1097-0010(200002)80:3and<289::AID-JSFA543and>3.0.CO;2-2

Ruzzi, M., Barghini, P., Montebove, F., and Schiesser, A. (1997). Effect of the carbon source on the utilization of ferulic, *m* and *p*-coumaric acids by a *Pseudomonas fluorescens* strain. *Ann. Microbiol.* 47, 87–96.

Sambrook, J., Fritsch, E. F., and Maniatis, T. (1989). *Molecular Cloning: A Laboratory Manual, 2nd Edn*. New York, NY: Cold Spring Harbor Laboratory Press.

Santos, P. M., Di Bartolo, I., Blatny, J. M., Zennaro, E., and Valla, S. (2001). New broad-host-range promoter probe vectors based on the plasmid RK2 replicon. *FEMS Microbiol. Lett.* 195, 91–96. doi: 10.1111/j.1574-6968.2001.tb10503.x

Schurig-Briccio, L. A., Farias, R. N., Rintoul, M. R., and Rapisarda, V. A. (2009). Phosphate-enhanced stationary-phase fitness of *Escherichia coli* is related to inorganic polyphosphate level. *J. Bacteriol.* 191, 4478–4481. doi: 10.1128/JB.00082-09

Shiloach, J., Kaufman, J., and Guillard, A. S. (1996). Effect of glucose supply strategy on acetate accumulation, growth, and recombinant protein production by *Escherichia coli* BL21 (lambda DE3) and *Escherichia coli* JM109. *Biotechnol. Bioeng.* 49, 421–428.

Simon, O., Klaiber, I., Huber, A., and Pfannstiel, J. (2014). Comprehensive proteome analysis of the response of *Pseudomonas putida* KT2440 to the flavor compound vanillin. *J. Proteomics.* 109, 212–227. doi: 10.1016/j.jprot.2014.07.006

Sinha, A. K., Sharma, U. K., and Sharma, N. (2008). A comprehensive review on vanilla flavor: extraction, isolation and quantification of vanillin and other constituents. *Int. J. Food Sci. Nutr.* 59, 299–326. doi: 10.1080/09687630701539350

Sutherland, J. B., Crawford, D. L., and Pometto, A. L. III. (1983). Metabolism of cinnamic, *p*-coumaric, and ferulic acids by *Streptomyces setonii*. *Can. J. Microbiol.* 29, 1253–1257. doi: 10.1139/m83-195

Tilay, A., Bule, M., and Annapure, U. (2010). Production of biovanillin by one-step biotransformation using fungus *Pycnoporous cinnabarinus*. *J. Agric. Food Chem.* 58, 4401–4405. doi: 10.1021/jf904141u

Transparency Market Research (2017). *Bio Vanillin Market (Application - Food, Beverages, Pharmaceuticals, and Fragrances) - Global Industry Analysis, Size, Share, Growth, Trends and Forecast 2017 – 2025*. Albany NY: Transparency Market Research Pvt. Ltd.

Van Derlinden, E., Bernaerts, K., and Van Impe, J. F. (2008). Dynamics of *Escherichia coli* at elevated temperatures: effect of temperature history and medium. *J. Appl. Microbiol.* 104, 438–453. doi: 10.1111/j.1365-2672.2007.03592.x

Yoon, S. H., Han, M. J., Jeong, H., Lee, C. H., Xia, X. X., Lee, D. H., et al. (2012). Comparative multi-omics systems analysis of *Escherichia coli* strains B and K-12. *Genome Biol.* 13:R37. doi: 10.1186/gb-2012-13-5-r37

Yoon, S. H., Li, C., Kim, J. E., Lee, S. H., Yoon, J. Y., Choi, M. S., et al. (2005). Production of vanillin by metabolically engineered *Escherichia coli*. *Biotechnol. Lett.* 27, 1829–1832. doi: 10.1007/s10529-005-3561-4

Zamzuri, N. A., and Abd-Aziz, S. (2013). Biovanillin from agro wastes as an alternative food flavour. *J. Sci. Food Agric.* 93, 429–438. doi: 10.1002/jsfa.5962

Conflict of Interest: The authors declare that the research was conducted in the absence of any commercial or financial relationships that could be construed as a potential conflict of interest.

frontiers in Bioengineering and Biotechnology

REVIEW
published: 24 October 2019
doi: 10.3389/fbioe.2019.00285

Production of Melanins With Recombinant Microorganisms

*Luz María Martínez, Alfredo Martinez and Guillermo Gosset**

Departamento de Ingeniería Celular y Biocatálisis, Instituto de Biotecnología, Universidad Nacional Autónoma de México, Cuernavaca, Mexico

The melanins constitute a diverse group of natural products found in most organisms, having functions related to protection against chemical and physical stresses. These products originate from the enzyme-catalyzed oxidation of phenolic and indolic substrates that polymerize to yield melanins, which include eumelanin, pheomelanin, pyomelanin, and the allomelanins. The enzymes involved in melanin formation belong mainly to the tyrosinase and laccase protein families. The melanins are polymeric materials having applications in the pharmaceutical, cosmetic, optical, and electronic industries. The biotechnological production of these polymers is an attractive alternative to obtaining them by extraction from plant or animal material, where they are present at low concentrations. Several species of microorganisms have been identified as having a natural melanogenic capacity. The development and optimization of culture conditions with these organisms has resulted in processes for generating melanins. These processes are based on the conversion of melanin precursors present in the culture medium to the corresponding polymers. With the application of genetic engineering techniques, it has become possible to overexpress genes encoding enzymes involved in melanin formation, mostly tyrosinases, leading to an improvement in the productivity of melanogenic organisms, as well as allowing the generation of novel recombinant microbial strains that can produce diverse types of melanins. Furthermore, the metabolic engineering of microbial hosts by modifying pathways related to the supply of melanogenic precursors has resulted in strains with the capacity of performing the total synthesis of melanins from simple carbon sources in the scale of grams. In this review, the latest advances toward the generation of recombinant melanin production strains and production processes are summarized and discussed.

Keywords: melanin, metabolic engineering, aromatics, tyrosinase, process engineering

OPEN ACCESS

Edited by:
Nils Jonathan Helmuth Averesch, Stanford University, United States

Reviewed by:
Zhen Chen, Tsinghua University, China
Thomas Carl Williams, Macquarie University, Australia

****Correspondence:***
Guillermo Gosset
gosset@ibt.unam.mx

Specialty section:
This article was submitted to Bioprocess Engineering, a section of the journal Frontiers in Bioengineering and Biotechnology

Received: *17 April 2019*
Accepted: *07 October 2019*
Published: *24 October 2019*

Citation:
Martínez LM, Martinez A and Gosset G (2019) Production of Melanins With Recombinant Microorganisms. Front. Bioeng. Biotechnol. 7:285. doi: 10.3389/fbioe.2019.00285

INTRODUCTION

The melanins comprise a group of polymeric pigments that are widely found in nature (d'Ischia et al., 2015). These are the result of the enzyme-catalyzed oxidation of phenolic or indolic substrates. The melanins are considered one of the most ancient pigments found in nature. These pigments have been detected in fossils of birds and dinosaurs (Zhang et al., 2010). Remarkably, preserved melanin was found in cephalopod ink sacs from the Jurassic period (Glass et al., 2012). Thus, melanin is proposed as a biomarker to study evolution (Wogelius et al., 2011).

The main types of melanin are eumelanin, pheomelanin, the allomelanins and pyomelanin. Eumelanin is the product of the oxidation of the amino acid L-tyrosine and/or L-dihydroxyphenylalanine (L-DOPA). The resulting polymer displays a brown or black color. Pheomelanin is produced when L-tyrosine and/or L-DOPA are oxidized in the presence of L-cysteine, resulting in pigment with a red-yellow color. The allomelanins are the result of oxidation of either one of the following compounds: 4-hydroxyphenylacetic acid, catechols, dihydroxynaphthalene (DHN), γ-glutaminyl-4-hydroxybenzene or tetrahydroxynaphthalene, protocatechualdehyde, and caffeic acid. Pyomelanin is a type of melanin resulting from the oxidation of homogentisic acid (HGA) (**Figure 1**) (Lindgren et al., 2015).

In humans and many mammals, eumelanin and pheomelanin are the prevalent skin pigment. Skin pigmentation has been a subject of interest since ancient times. There are references to diseases affecting skin color, such as vitiligo, dating back to the year 2200 BC. It was until the year 1819 that pigment cells, called chromatophores, were described in studies with the squid. A few years later, similar structures were recognized in human skin and eyes. The term melanin was used for the first time by C. P. Robin in 1873 and later, the specialized cells responsible for melanin synthesis in the skin, the melanocytes, were identified. Further studies in the following years established the existence of melanin grains in the melanocytes and the process for the transfer of these structures to the epithelial cells (Westerhof, 2006).

As a result of their chemical composition, the melanins display distinct physicochemical properties. Thus, these polymers can act as ultraviolet light, X-ray and γ-ray absorbers, cation exchangers and amorphous semiconductors (Sarna et al., 1976; della-Cioppa et al., 1990; Krol and Liebler, 1998; Rózanowska et al., 1999; Ambrico et al., 2014). Melanins have also been shown to have antioxidant and antiviral activities (Montefiori and Zhou, 1991; Nofsinger et al., 2002). Diverse applications and products derived from melanins are dependent on obtaining these polymers at a relatively low cost and in a large quantity. Melanins can be extracted from plant and animal tissues, or generated by chemical synthesis. However, these processes are relatively expensive and in some cases, not sustainable (Saini and Melo, 2015). A potentially viable alternative to obtain melanins is based on the culture of melanogenic microorganisms. This method has the advantage of being scalable and providing a good yield of melanins. This approach can be improved by applying genetic engineering techniques to increase the natural melanogenic capacity of some organisms or generating novel melanin-producing strains. The most common genetic modification to enhance/generate a production strain involves the expression of genes encoding the enzymes involved in the oxidation of melanin precursors.

ENZYMES INVOLVED IN MELANIN FORMATION

The enzyme-dependent oxidation of phenolic or indolic compounds is the first step leading to the generation of the melanins. Melanogenic enzymes belong mainly to the tyrosinase and laccase protein families. The tyrosinases are the most common type of enzyme associated with melanogenesis. These enzymes can employ both mono and diphenolic compounds as substrates. Examples of these substrates are L-tyrosine, L-DOPA, and catechols. The tyrosinases are mono-oxygenases having a dinuclear copper catalytic center. These enzymes catalyze the ortho-hydroxylation of monophenols (cresolase activity) and also the oxidation of catechols (catecholase activity), generating ortho-quinone products (Garcia-Molina et al., 2007) (**Figure 1**). The enzyme tyrosinase catalyzes the hydroxylation of L-tyrosine to L-DOPA using molecular oxygen and then oxidizes this compound to dopachrome, which non-enzymatically polymerizes to yield melanin (Ito, 2003). Based on their amino acid sequence and functional features, microbial tyrosinases can be divided into five main groups (Fairhead and Thöny-Meyer, 2012). The tyrosinase from *Streptomyces* sp. is included in one of these groups. They have in common the requirement of a chaperone protein that inserts copper atoms into the active site of the tyrosinase. In contrast, the tyrosinases from bacteria, such as *Rhizobium etli*, *Bacillus megaterium*, and *Bacillus thuringiensis*, do not require a chaperone for copper insertion into the active site. The lacasses are another group of enzymes involved in melanogenesis. These enzymes are not related to the tyrosinases but are also copper-dependent oxidoreductases. The laccases have been found in bacteria, fungi, and plants (Valderrama et al., 2003). The enzyme 4-hydroxyphenylacetic acid (4-HPA) hydroxylase is involved in the catabolism of 4-HPA in bacteria. This group of enzymes displays a broad substrate range, they can hydroxylate various monohydric and dihydric phenols (Prieto et al., 1993). 4-HPA hydroxylase is a two-component flavin adenine dinucleotide (FAD)-dependent monooxygenase (Gibello et al., 1995).

BIOLOGICAL FUNCTIONS OF MELANINS

The melanins are found in species of the three domains of life: Archaea, Bacteria, and Eukarya. These pigments have diverse functions related to the survival of many species in their natural environment (**Figure 2**). In humans, eumelanin and pheomelanin are involved in protection against UV radiation (Coelho et al., 2009). Another important protective activity of these pigments includes their functions as free radical scavengers. This activity reduces the production of reactive oxygen species (Meredith and Sarna, 2006). Melanin is also found in the eyes and brain of humans and other vertebrates. However, the role of the pigment in these organs is not completely understood. In birds, melanin is involved in feather coloring. This function is related to signaling, having an impact on reproductive fitness (McGraw, 2008). The dark color imparted by melanin serves a function in thermoregulation by absorbing radiant energy in organisms, such as amphibians and reptiles (Clusella-Trullas et al., 2007). In some species of the molluscs octopus and squid, the production and secretion of ink is a distinctive defense mechanism. The main constituent of this product is eumelanin, which is synthesized by an ink gland in these organisms

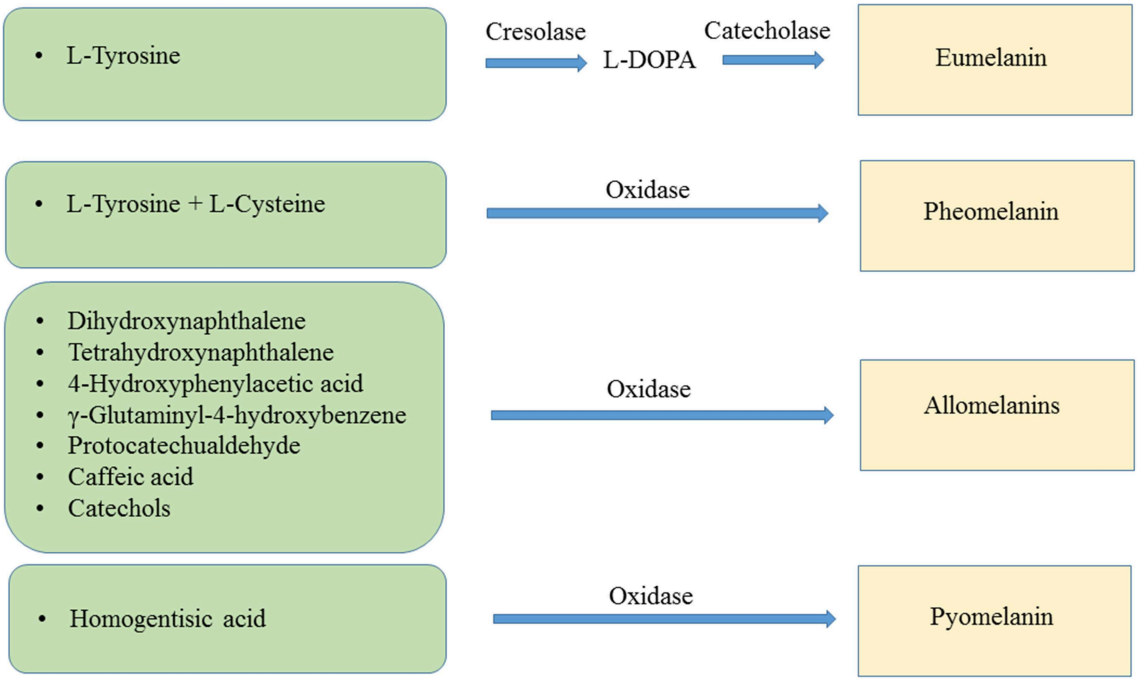

FIGURE 1 | Biochemical reactions leading to the synthesis of eumelanin, pheomelanin, allomelanins, and pyomelanin.

(Palumbo, 2003). In insects, melanin formation is related to cuticle sclerotization. The cuticle is the outer component of the exoskeleton of insects. Melanogenesis leads to the hardening of the cuticle, providing protection against physical damage. In addition, melanization functions as a defense mechanism against pathogens in insects. Upon infection, melanin formation around a pathogen blocks its proliferation (Vavricka et al., 2014). In fungi, melanization is a common trait that is related to pathogenesis. In these organisms, melanin precursors include DHN, HGA, γ-glutaminyl-4-hydroxybenzene, catechol and tyrosine. In addition to photoprotection and antioxidant activities, in fungi, melanins are also involved in providing resistance against chemical and mechanical stresses (Cordero and Casadevall, 2017). Furthermore, melanin has been proposed as an energy harvesting pigment in fungi. In has been determined that sub-lethal doses of gamma rays cause an enhanced increase in NADPH levels and rate of growth in several fungi species (Dadachova et al., 2007). Melanin production by bacteria has been identified in species from *Rhizobium*, *Streptomyces*, *Marinomonas*, *Pseudomonas*, *Serratia*, and *Bacillus*. In these organisms, melanin is involved in virulence, as well as protection against ultraviolet light and oxidation agents (Trias et al., 1989; Patel et al., 1996; López-Serrano et al., 2004; Piñero et al., 2007; Manivasagan et al., 2013).

APPLICATIONS OF MELANINS

The melanins have a very complex polymeric structure, resulting in diverse chemical and physical properties. In addition to blocking UV light, they can also absorb X and γ-rays (Hill, 1992). These polymers also have the capacity of scavenging reactive oxygen species and free radicals, as well as exhibiting redox behavior (Liu et al., 2015). Melanin is an amorphous semiconductor, as such, it is being evaluated as a component of electronic circuits, batteries as well as solar cells (Bothma et al., 2008; Kim et al., 2013; Ambrico et al., 2014). Inorganic semiconductors are currently being employed for these applications. However, they have a high environmental impact and relatively high cost. In contrast, organic semiconductors, such as melanins, do not have the same drawbacks and are easier to process. An additional advantage of melanin over traditional semiconductors is its biocompatibility, making it suitable to be used in implantable devices.

In another type of application, melanin has been employed as a template to synthesize silver or gold nanostructures and nanoparticles, having potential uses in the food and health industries (Apte et al., 2013; Patil et al., 2018). Melanin has also been evaluated as an additive of a synthetic polymer. The addition of eumelanin to poly(methyl methacrylate) (PMMA) was observed to cause a significant increase in thermal stabilization (Shanmuganathan et al., 2011). Further studies will be required to show if melanins can be employed to enhance the properties of other synthetic polymers. In a related study, it was demonstrated that allomelanin could be incorporated as a dye to hydrogel of soft contact lenses (Ahn et al., 2019). As compared to synthetic dyes, the use of allomelanin offers the advantage of antibacterial and antioxidant activity. In the medical field, it has been reported that *Escherichia coli* cells expressing the *melA* gene encoding tyrosinase from *Rhizobium etli* can be employed

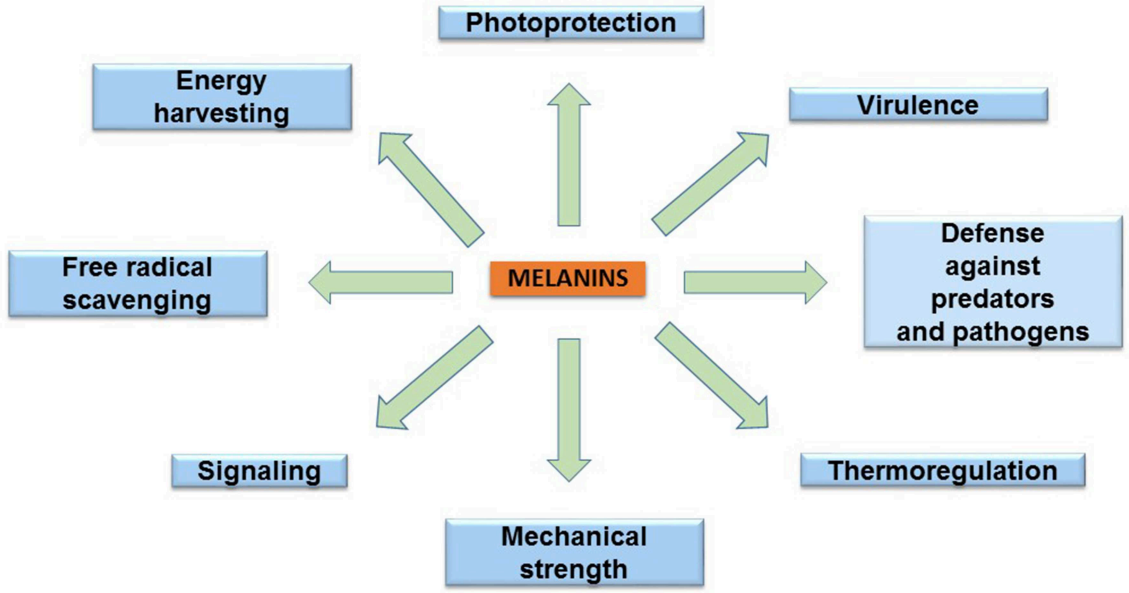

FIGURE 2 | The main biological functions of melanins.

for photoacoustic imaging, a method with improved depth-to-resolution ratio when compared to optical imaging (Paproski et al., 2015). This approach holds the potential of improving the understanding of bacterial pathogenic processes. In another imaging application, melanin has been employed as a contrast agent in magnetic resonance imaging probes (Williams, 1994). Dermal and cosmetic applications of melanin include its use for hair dyeing. The widely used synthetic oxidative dyes cause hair damage and are not easy to handle. In contrast, a process based on the use of melanin precursors that can bind to hair after air oxidation has the advantage of not causing damage and being safer (Koike and Ebato, 2013).

The melanins can act as metal chelators and this capacity can be employed in environmental applications. The binding of metals to melanin involves multiple coordination bonds between the hydroxyl, amine and carboxyl functional groups in this polymer. In a soil bioremediation study, melanin from fungi has been shown to efficiently bind heavy metals, such as zinc and lead (Fogarty and Tobin, 1996). In another study, melanin was synthesized by employing a tyrosinase extracted from the plant *Amorphophallus campanulatus* and L-DOPA as substrate. It was determined that melanin could efficiently remove uranium from an aqueous solution (Saini and Melo, 2013).

It should be noted that the previous cases are still in the development stage and have not yet been commercialized. However, there are a few examples of melanin-containing products that are commercially available. At present, the main commercial application of melanin is as a dye in lenses of sunglasses. In this case, it is not known which are the chemical dyes replaced by melanin, but the natural origin of the pigment and the capacity to reduce high energy visible light are highlighted as an advantage (https://espeyewear.com/). A commercial product related to dermatology is a sunscreen for dry skin containing squid ink as an antioxidant. An advantage of this product over competing sunscreens is the expected reduced irritation on the skin when compared to synthetic dyes (https://chicet.com/product/melanin-sunscreen-for-dry-skin/).

PRODUCTION OF MELANINS WITH NATURAL MELANOGENIC ORGANISMS

The current and potential applications with melanins are dependent on the possibility of obtaining these pigments from abundant and relatively inexpensive sources. These products can be extracted from natural sources, such as animal or plant tissues by following relatively inexpensive methods. However, these sources usually contain a mixture of different types of melanins and related substances, which complicate purification procedures and might yield a product of variable composition. These polymers can also be obtained by either the chemical or enzymatic oxidation of phenolic or indolic substrates (Saini and Melo, 2015). These methodologies can generate melanins with a high degree of purity but at a relatively high cost. Another option for obtaining these polymers is based on the culture of natural melanin-producing microbes or microbes that have been genetically engineered to produce melanins. This approach has the potential for generating this class of products with a relatively low cost and high yield.

Although this review focuses mainly on engineered microorganisms, a brief description of efforts toward the development of melanin production processes with natural melanogenic organisms is included. The production of melanin has been observed in several species of microorganisms and fungi both in their natural environment an under laboratory growth conditions. Species of organisms with melanogenic capacity that have been employed for developing production processes include

Pseudomonas stutzeri, *Gliocephalotrichum simplex*, *Rhizobium* sp., *Brevundimonas* sp., *Aspergillus fumigatus*, *Bacillus safensis*, *Streptomyces lusitanus*, and *Streptomyces kathirae* (Jalmi et al., 2012; Zhao and Tong-Suo, 2012; Ganesh Kumar et al., 2013; Surwase et al., 2013; Guo et al., 2014; Madhusudhan et al., 2014; Tarangini and Mishra, 2014; Raman et al., 2015). Processes for obtaining melanin with these organisms usually involves statistical experimental methods aimed at identifying culture conditions and media components that positively impact the productivity (Zhao and Tong-Suo, 2012; Tarangini and Mishra, 2014). Culture parameters, such as temperature, pH, oxygen, and melanin precursors concentrations have been found to contribute to productivity. The developed processes have enabled the production of melanin at titers that span 0.01–13.7 g/L (Guo et al., 2014; Raman et al., 2015). In most of these processes, a positive correlation with polymer production was observed by increasing in culture media the amount of L-tyrosine or components that contain it. Thus, the polymer produced is likely eumelanin. However, in most cases, culture media includes yeast extract or protein hydrolysates. Therefore, during the melanin formation process, some media components in addition to L-tyrosine can be incorporated into the polymer, yielding a pigment that is not pure eumelanin. This is an important drawback of most processes developed with melanogenic organisms that require complex media for growth and production.

PRODUCTION OF MELANINS WITH GENETICALLY ENGINEERED MICROORGANISMS

The experimental methodologies collectively known as genetic engineering techniques allow the modification of the genetic material of microbes with the purpose of enhancing or generating the capacity to produce specific molecules. It is possible currently to genetically engineering diverse microorganisms and this number is continuously growing. The application of DNA sequencing technology combined with biochemical analyses has permitted the elucidation of pathways and specific genes related to the production of melanins. This knowledge and technologies are the basis for generating recombinant microbes for enhanced melanin production and for transferring this capacity to non-melanogenic microorganisms.

GENERATION OF MELANOGENIC MICROORGANISMS BY EXPRESSION OF GENES ENCODING TYROSINASES

What follows is a review and analysis of advances related to the generation of recombinant microbial strains and production processes for the synthesis of melanins. The first example of a recombinant melanogenic microbe was reported with the bacterium *E. coli*. This organism was modified to express genes from the actinomycete *Streptomyces antibioticus*. In *S. antibioticus*, the *mel* locus includes two genes, *mel*, and ORF438, that are required for melanin production. The recombinant *E. coli* strain was shown to produce eumelanin from L-tyrosine in agar plates and liquid cultures but the titers were not reported. Interestingly, it was also demonstrated that synthetic non-natural amino acids, such as N-acetyl-L-tyrosine and L-tyrosine ethyl ester could be taken as substrates by the *S. antibioticus* tyrosinase, yielding synthetic melanins (della-Cioppa et al., 1990). In another report, the *mel* locus from *S. antibioticus* was also employed to generate a recombinant *E. coli* strain derived from JM109. The gene *mel* was placed under transcriptional control of the phage T5 promoter and two *lac* operators. Culturing this recombinant strain in LB medium resulted in the recovery of 0.4 g/L of eumelanin (**Table 1**). The recovery of eumelanin from the culture medium was based on precipitation by adjusting pH to 3.0, followed by dissolving it in distilled water at pH 8.0. This procedure was followed by liquid chromatography on Sephadex LH-20. The purified eumelanin was employed to study the effect of the presence of this polymer on the antimicrobial activity of several antibiotics. It was determined that eumelanin reduced the antibiotic effect on *E. coli* of ampicillin, kanamycin, polymyxin B, and tetracycline in a dose-dependent manner (Lin et al., 2005). In addition to the clinical importance of such results, the observed response could be employed to select higher melanin-producing recombinant strains, based on antibiotic resistance.

In another early example, the *Bacillus thuringiensis* strain 4D11 was shown to produce melanin when cultured for several hours with L-tyrosine at 42°C (Ruan et al., 2004). These results indicated that this organism should contain a gene encoding a tyrosinase in its genome. Since the sequence of the genome of *B. thuringiensis* 4D11 was not known, a cloning strategy was devised based on expected sequence similarity with a tyrosinase gene from *Bacillus cereus* 10987. A pair of PCR primers were designed based on the tyrosinase gene sequence from *B. cereus* 10987 and employed to amplify an 1,179 bp DNA fragment from *B. thuringiensis* 4D11 purified DNA. Sequence analysis showed this DNA fragment displayed 99% amino acid sequence similarity with the tyrosinase from *B. cereus* 10987. The PCR product was cloned in plasmid pGEM-7zf under the control of the *lac* promoter. Strain *E. coli* DH5α was transformed with this plasmid and the recombinant strain was shown to produce eumelanin at a titer of 5.6 g/L when grown in casein liquid medium (**Table 1**). Interestingly, it was also determined that this recombinant strain displayed a significantly higher survival rate when compared to DH5α, in experiments of exposure to UV-radiation (Ruan et al., 2005). These results show how in addition to conferring the capacity of producing melanin as a biotechnological product, the heterologous expression of a gene encoding a tyrosinase can increase the host's capacity to resist UV-radiation. This is the consequence of melanin production, a trait that can be beneficial in the case of microorganisms that are employed in the field, such as *B. thuringiensis*. The possibility of engineering microbes to survive in high-UV environments is also relevant for future space applications. Microbes are considered essential for helping to support human life by providing food, useful chemicals and recycling waste in long-range space missions and planet-colonization projects (Horneck et al., 2010; https://blogs.scientificamerican.com/observations/

TABLE 1 | Engineered microbial strains for the production of melanins.

Promoter	Inducer	Expressed gene(s)	Expression vectors	Genes origin	Production organism	Melanin precursor	Carbon source	Process temperature	Volumetric productivity (mg/L/h)	Titer (g/L)	References
lac	Not reported	*mel*	pGEM-7Zf	*Bacillus thuringiensis 4D11*	*Escherichia coli*	Casein	Casein	Not reported	155.5	5.6	Ruan et al., 2005
T5	IPTG 0.36 mM	*mel*	pQE32	*Streptomyces antibioticus*	*Escherichia coli*	L-tyrosine	LB medium	37°C	8.3	0.4	Lin et al., 2005
trc	IPTG 0.1 mM	*MutmelA*	pTrc99A	*Rhizobium etli*	*Escherichia coli*	L-tyrosine	Glucose	30°C	75	6	Lagunas-Muñoz et al., 2006
None	None	None	None	*Pseudomonas putida* strain F6	*Pseudomonas putida* strain F6-HDO	L-tyrosine	Citrate	30°C	17.5	0.35	Nikodinovic-Runic et al., 2009
P_{skmel}	Constitutive	*melC*	pIJ86	*Streptomyces kathirae*	*Streptomyces kathirae*	L-tyrosine	Amylodextrine, yeast extract	28°C	225	28.8	Guo et al., 2015
None	None	Not identified	None	*Escherichia coli*	*Escherichia coli*	Caffeic acid	Glucose	30°C	16.7	0.15	Jang et al., 2018
T7	IPTG 1 mM	*fcs*	pRSF duet-1 pET duet-1	*Burkholderia glumae* BGR1	*Escherichia coli*	Caffeic acid	Glucose	30°C		0.20	Jang et al., 2018
T7	IPTG 1 mM	*ech*		*Burkholderia glumae* BGR1							Jang et al., 2018
lac	IPTG 0.1 mM	$aroG^{fbr}$	pTrc99A	*Escherichia coli*	*Escherichia coli*	None	Glucose	30°C	26.8	3.2	Chávez-Béjar et al., 2013
trc	IPTG 0.1 mM	*tyrC*		*Zymomonas mobilis*							Chávez-Béjar et al., 2013
trc	IPTG 0.1 mM	$pheA_{CM}$		*Escherichia coli*							Chávez-Béjar et al., 2013
trc	IPTG 0.1 mM	*MutmelA*		*Rhizobium etli*							Chávez-Béjar et al., 2013
lac	IPTG 0.1 mM	$aroG^{fbr}$	pTrc99A	*Escherichia coli*	*Escherichia coli*	None	Glycerol	30°C	16.8	1.21	Mejía-Caballero et al., 2016
PtktA	None	*tktA*		*Escherichia coli*							Mejía-Caballero et al., 2016
trc	IPTG 0.1 mM	*antABC*		*Pseudomonas aeruginosa PAO1*							Mejía-Caballero et al., 2016
trc	IPTG 0.1 mM	*MutmelA*		*Rhizobium etli*							Mejía-Caballero et al., 2016

microbes-might-be-key-to-a-mars-mission/). Melanin can also absorb X and γ-rays, a characteristic that could increase the survival of engineered microbes in environments outside our planet.

Among soil bacteria, *Rhizobium etli* is especially important for agriculture since it can fix nitrogen when it forms nodules in the root of the plant *Phaseolus vulgaris*. It has been determined that this bacterium can produce melanin in the symbiotic nodules and a gene encoding a tyrosinase has been identified in a symbiotic plasmid (*melA*) (González et al., 2003; Piñero et al., 2007). The gene *melA* was cloned in the expression vector pTrc99A under control of the strong *trc* promoter and the resulting plasmid pTrc*melA* was transformed in *E. coli*. The recombinant *E. coli* strain produced eumelanin when L-tyrosine was provided as a substrate at 30°C and at a much lower quantity at 37°C (Cabrera-Valladares et al., 2006). It was also noted that melanin synthesis occurred only during the stationary culture phase. During cloning of the *melA* gene, a colony of recombinant *E. coli* in medium containing L-tyrosine was found to display a darker color when compared to the rest of the colonies. After DNA sequencing of the *melA* gene in this clone, it was determined that it had a spontaneous mutation of a single nucleotide change where the Asp535 residue was changed to a Gly residue in the MelA tyrosinase enzyme. This mutant version of MelA was named MutMelA. Further characterization revealed that eumelanin production in liquid cultures starts earlier in cultures of *E. coli* expressing MutmelA when compared to a strain expressing the wild type version of this enzyme. To develop and optimize a process for eumelanin production, a study was conducted to determine optimal condition for pigment synthesis in liquid cultures with a recombinant *E. coli* strain expressing MutmelA. The effect of the concentration of antibiotic for plasmid selection pressure, isopropyl-d-thio-galactopyranoside (IPTG) as gene inducer, culture temperature and pH on eumelanin concentration were determined. The best conditions for production in bioreactor consisted on the use of 0.1 mmol/L of IPTG, a culture temperature of 30°C and changing the pH of the medium from 7.0 to 7.5 at the start of the eumelanin production phase. A total of 6 g/L of L-tyrosine was added to the culture medium as eumelanin precursor. Under these conditions, a 100% conversion yield of L-tyrosine to eumelanin was observed with a final titer of 6 g/L (**Table 1**) (Lagunas-Muñoz et al., 2006). These results highlight the importance of culture conditions optimization as a factor for reaching the maximum yield and productivity with a recombinant melanogenic strain.

In a bioprospecting study, microorganisms with the capacity of producing melanin were isolated from soil samples in China. One of such microbes was identified as *Streptomyces kathirae* SC-1, it displayed the highest capacity for melanin production among all isolates. A surface response method was employed to optimize medium and growth conditions, allowing the production of 13.7 g/L of melanin (Guo et al., 2014). It is important to point out that the culture medium employed in this study included yeast extract, which provided a mixture of melanin precursors. Therefore, the resulting polymer should be characterized to determine its chemical composition to define the type of melanin produced. To better understand melanogenesis in this organism, a novel tyrosinase was purified to homogeneity. This is a 30-kDa enzyme, displaying K_m for L-DOPA and L-tyrosine of 0.42 and 0.25 mM, respectively. The partial amino acid sequence of this tyrosinase was employed to design primers that allowed the amplification of the encoding *melC* gene and its promoter region. Sequence analysis of the promoter region identified two putative promoters: P_{skmel} and P_{135}. The gene *melC* was cloned under the transcriptional control of either putative promoter and the constitutive promoter *Perm*E* in the replicative plasmid pIJ86 and the resulting constructs transformed in *S. lividans* and *S. kathirae*. The recombinant strains of *S. lividans* were characterized, and it was determined that P_{skmel} is the functional promoter for *melC*. The recombinant strains of *S. kathirae* were cultured under melanin production conditions. It was determined that strains expressing *melC* from *Perm*E* or P_{skmel} produced 24.9 and 28.8 g/L of melanin, respectively (**Table 1**) (Guo et al., 2015). It should be noted that these are the highest melanin titers reported to date, highlighting the potential of applying genetic engineering techniques to further enhance the production capacity of a melanogenic organism (**Table 1**). This production system has the potential for further optimization, in particular regarding culture medium composition. The medium contains a relatively high amount of yeast extract (37 g/L), which is a costly component. Yeast extract could complicate melanin purification procedures and some of its components can react with melanin precursors, yielding a polymer not composed entirely of the L-tyrosine precursor. For these reasons, the search for a culture medium containing only salts and a simple carbon source should be a future research objective to improve the current production scheme.

The phenolic aldehydes are compounds having applications in the chemical and food industries. The microbial production of this class of chemicals in *E. coli* involves the expression of heterologous genes and other modifications to the metabolic network. As part of a study to generate an *E. coli* strain for the synthesis of phenolic aldehydes, this organism was modified to produce caffeic acid from L-tyrosine. This involves the expression of tyrosine ammonia-lyase (TAL) to transform L-tyrosine to coumaric acid and *p*-coumarate 3-hydroxylase (C3H) to produce caffeic acid (**Figure 3**). In these experiments, a dark pigment was observed, having the characteristics of melanin. This caffeic acid melanin is likely produced by oxidation of the catechol moiety by some of the oxidases encoded in the genome of *E. coli*. It was also observed that protocatechualdehyde added to the culture medium and incubated with *E. coli* yielded a melanin pigment with a brown color, whereas caffeic acid melanin was black. As part of this work, the genes encoding feruloyl-CoA synthetase (FCS) and enoyl-CoA hydratase/aldolase (ECH) from *Burkholderia glumae* BGR1 were expressed in *E. coli* (**Figure 3**). The recombinant strain acquired the capacity to convert caffeic acid to protocatechualdehyde. As part of this study, it was observed that in the presence of 5 mM caffeic acid, wild type *E. coli* BL21(DE3) produced 0.15 g/L of melanin (**Table 1**). When the same amount of caffeic acid was added to a culture with a recombinant strain expressing *fcs* and *ech*, melanin was produced at a faster rate, reaching a titer of 0.2 g/L (Jang et al., 2018). This melanin product was not chemically characterized, it is

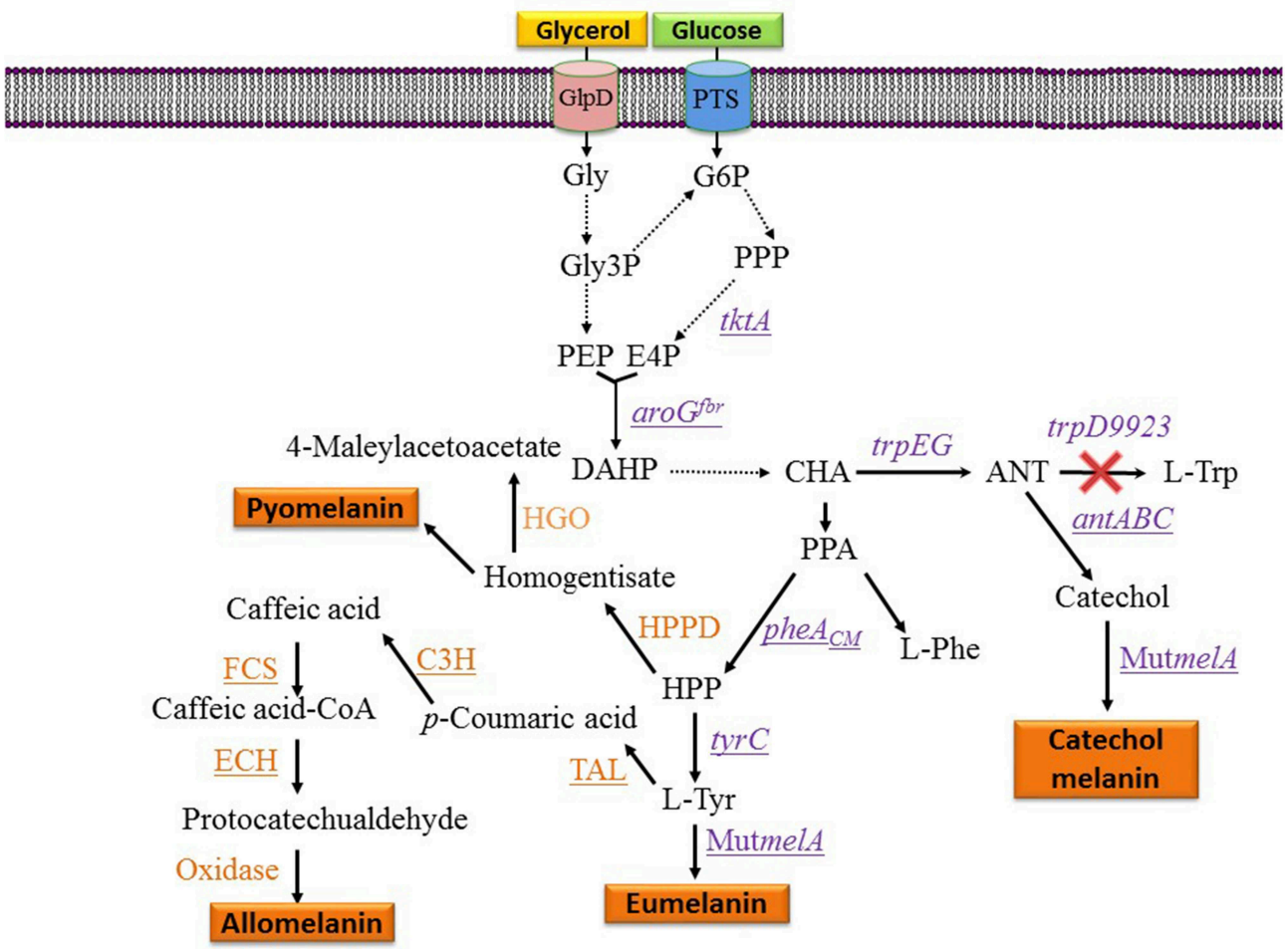

FIGURE 3 | Metabolic pathways and expressed genes related to the synthesis of melanins with engineered microorganisms. Dashed arrows indicate two or more enzyme reactions. Underlined genes were overexpressed from plasmids. PTS, phosphotransferase system glucose transport protein; Gly, glycerol; Gly3P, glycerol-3-phosphate; G6P, glucose-6-phosphate; E4P, D-erythrose 4-phosphate; PEP, phosphoenolpyruvate; DAHP, 3-deoxy-D-*arabino*-heptulosonate 7-phosphate; HPP, 4-hydroxyphenylpyruvate; CHA, chorismate; ANT, anthranilate; PPA, phenylpyruvate; HPPD, hydroxyphenylpyruvate dehydrogenase; HGO, homogentisate 1,2-dioxygenase; L-Tyr, L-tyrosine; L-Phe, L-phenylalanine; L-Trp, L-tryptophan; *tktA*, gene encoding transketolase; $aroG^{fbr}$, gene encoding feedback inhibition resistant DAHP synthase; *trpEG,* genes encoding anthranilate synthase component I; *trpD9923* is a mutant version of *trpD* causing the loss of anthranilate phosphoribosyl transferase activity and retaining anthranilate synthase activity; *tyrC*, gene encoding cyclohexadienyl dehydrogenase; C3H, gene encoding *p*-coumarate 3-hydroxylase; TAL, gene encoding tyrosine ammonia-lyase; FCS, gene encoding feruloyl-CoA synthetase form *B. glumae* BGR1; ECH, gene encoding enoyl-CoA hydratase/aldolase from *B. glumae* BGR1; *antABC,* encodes the terminal oxygenase and the reductase components of anthranilate 1,2-dioxygenase from *P. aeruginosa* PAO1; $pheA_{CM}$, gene encoding chorismate mutase domain from chorismate mutase-prephenate dehydratase; Mut*melA*, gene encoding a mutant version of the tyrosinase from *R. etli*.

likely a polymer composed of a mixture of caffeic acid and protocatechualdehyde moieties. These results demonstrate the production of caffeic acid and protocatechualdehyde melanins with recombinant *E. coli*. It evident that FCS and ECH activities have an influence on the synthesis of melanin and/or melanin precursors in this strain, however, the mechanisms for the observed results are not yet completely understood. The chemical characterization of the produced melanin should provide further insight into the chemical precursors involved in its formation. It should also be of interest to identify the native enzyme from *E. coli* that is involved in the oxidation of caffeic acid and protocatechualdehyde, leading to their polymerization into melanin. The cloning and overexpression of the gene encoding this yet unidentified oxidase should enable improvement of melanin-producing strains. In a subsequent report, it was demonstrated that the protocatechualdehyde-based melanin could be employed to dye soft contact lenses (Ahn et al., 2019). The antibacterial and antioxidant activity of melanins should be advantageous in such an application when compared to chemically synthesized dyes.

RANDOM MUTAGENESIS FOR THE SELECTION OF A MELANOGENIC STRAIN

Strain F6 of the soil bacterium *Pseudomonas putida* was found to display the capacity of producing melanin when grown in

media containing L-tyrosine. To gain insight into the role of genes involved in melanogenesis, transposon mutagenesis was performed. This process yielded two mutants with increased melanin production capacity. One of such mutants (F6-HDO) produced 0.35 g/L of melanin, which corresponds to a 6-fold increase when compared to *P. putida* F6 (**Table 1**). Interestingly, this mutant displayed higher resistance to UV light and H_2O_2 when compared to the wild type. Genetic analysis indicated that transposon mutagenesis disrupted a gene encoding HGA 1,2-dioxygenase (HGO). This enzyme converts HGA into 4-maleylacetoacetate as part of a degradation pathway. Therefore, this mutation is expected to reduce HGA consumption by HGO. This result indicates that HGA is the allomelanin precursor in this mutant strain (**Figure 3**) (Nikodinovic-Runic et al., 2009). The synthesis of HGA originates from the L-tyrosine biosynthetic pathway. The intermediate 4-hydroxyphenylpyruvate (HPP) is transformed into HGA by enzyme hydroxyphenylpyruvate dehydrogenase (HPPD) (**Figure 3**). This is an example where random mutagenesis was employed to isolate mutants with improved melanogenesis. An important advantage of working with melanogenic organisms is the simplicity in the process for identifying mutants since they can be detected visually. Studies, such as this one are essential for identifying novel genes involved in the melanogenesis process. Once the melanogenic pathways are identified, a rational strategy can be applied to enhance the native melanogenic capacity or transfer it to another organism.

Random mutagenesis is a relatively simple method for strain improvement but it is limited to organisms that already have a native melanin production capacity. Usually, the site and type of mutation in the improved melanogenic organism are not known, thus limiting the use of rational strategies for further strain improvement. In addition, the genetic changes produced by random mutagenenis can be unstable so the strain could revert to a low producer phenotype. A solution to these issues can be based on genome sequencing of the improved strain, yielding information about the type of mutation as well as the genes and pathways involved in the observed phenotype. This information can be employed to "reverse-engineer" the melanogenic organism by employing genetic engineering techniques to reintroduce the identified mutations. This strategy can be employed to separate the genetic changes that are related to the improved phenotype from those that could be deleterious or resulting from genetic instability.

The previous examples described recombinant strains and processes for the conversion of diverse aromatic compounds into melanins. By adding various melanin precursors into the culture medium, they can be employed by tyrosinases as substrates to generate specific pigments (**Table 1**). Such processes have the potential for displaying high productivity. Furthermore, by employing diverse aromatic precursors, various types of melanins can be produced. In spite of these advantages, a few drawbacks can be considered. One of them is the relatively high cost of employing pure melanin precursors. However, another problem is created when non-pure and relatively inexpensive melanin precursors are employed, such as yeast extract or protein hydrolysates. The use of complex media can result in variability in the composition of produced melanins, since these culture media can contain diverse and variable amounts of compounds that can be substrates of tyrosinases or that can react with melanin precursor molecules. Furthermore, the use of non-defined media makes melanin purification processes more difficult and expensive.

The genetic modifications employed to generate the previously described production strains are mostly based on the cloning of the genes encoding a tyrosinase on a multicopy expression plasmid (**Table 1**). This approach proved to be effective for achieving titers in the scale of grams in several examples. However, it remains to be determined if the chromosomal expression of these genes could lead to efficient production strains, having the advantage of not requiring the use of antibiotics for plasmid selection. It should be noted that *E. coli* has been chosen frequently as a production host for melanins. This is likely a result of the extensive set of genetic and metabolic engineering tools available for this organism (**Table 1**). However, potential advantages of engineering natural melanogenic organisms should be taken into consideration. The highest melanin titer reported to date was generated in a process with a recombinant strain of *S. kathirae*. It could be expected that melanogenic organisms have physiological traits that make them more suitable as production strains. For example, specialized metabolic pathways for the generation of melanin precursors, enhanced transport processes for the internalization of tyrosinase substrates or for the excretion of melanin.

METABOLIC ENGINEERING APPLIED FOR THE PRODUCTION OF MELANINS FROM SIMPLE CARBON SOURCES BY INCREASING PRECURSOR SUPPLY

One potential solution to the issues mentioned above involves the generation of microbial strains for the total synthesis of melanins from simple carbon sources. This approach is based on applying metabolic engineering strategies to increase flux into the shikimate pathway which provides the precursors for the aromatic amino acids. In one example, metabolic engineering methods were applied to generate an *E. coli* strain with the capacity of producing the eumelanin precursor L-tyrosine from glucose (Chávez-Béjar et al., 2008). This strain was modified to increase carbon flow to the L-tyrosine biosynthetic pathway by overexpressing the genes encoding a feedback-insensitive version of the enzyme 3-deoxy-D-*arabino*-heptulosonate 7-phosphate (DAHP) synthase ($aroG^{fbr}$), cyclohexadienyl dehydrogenase (TyrC) from *Zymomonas mobilis* and the chorismate mutase domain from the native enzyme chorismate mutase-prephenate dehydratase. In addition, this strain expressed the gene Mut*melA* encoding the tyrosinase MutMelA (**Figure 3**). This strain had the potential for synthesizing eumelanin from glucose. However, it was determined that MutMelA activity depleted the L-tyrosine pool, causing a defect in cell growth. The enzyme tyrosinase requires Cu as a cofactor for activity. Therefore, this element was left out of the medium during the first half of the culture to avoid L-tyrosine depletion by MutMelA. The eumelanin production phase was started by adding $CuSO_4$ to

the medium, causing the activation of tyrosinase. This strategy was employed in bioreactor cultures with medium containing 60 g/L of glucose as the sole carbon source. In 120 h, 3.2 g/L of eumelanin were produced (**Table 1**) (Chávez-Béjar et al., 2013). These results were the first example where metabolic engineering was applied to generate a strain for the total synthesis of eumelanin. This study provided useful information regarding the potential negative consequences in cell physiology resulting from the high-level expression of tyrosinase. This problem was alleviated by adopting a delayed activation of the heterologous enzyme. An alternate solution might be based on fine control of gene induction at a specific phase in the production culture.

During the characterization of enzyme MutMelA it was determined that in addition to L-tyrosine, it can also employ catechol as a substrate. Thus, this enzyme could be employed for the synthesis of catechol melanin. To test this idea, a bioconversion process was developed with an *E. coli* strain expressing MutMelA and growing in medium containing glycerol 40 g/L as the carbon source and catechol 0.85 g/L as tyrosinase substrate. After 54 h, 0.29 g/L of catechol melanin were produced. To further improve this process, metabolic engineering was evaluated to generate a strain with the capacity of generating catechol melanin from a simple carbon source. The strategy that was followed is based on employing an engineered *E. coli* strain that can produce catechol from a simple carbon source (Balderas-Hernández et al., 2014). Strain *E. coli* W3110 *trpD9923* is a mutant in the L-tryptophan biosynthetic pathway that overproduces the intermediate anthranilate (Yanofsky et al., 1971). This strain was modified to increase carbon flow to anthranilate by overexpressing genes $aroG^{fbr}$ and *tktA*, encoding a feedback-insensitive version of DAHP synthase and transketolase, respectively (**Figure 3**). These modifications caused a 2-fold increase in anthranilate titer in flask cultures (Balderas-Hernández et al., 2009). This strain was further modified by the expression of the genes *antABC* encoding anthranilate 1,2-dioxygenase from *Pseudomonas aeruginosa* PAO1. This enzyme catalyzes the conversion of anthranilate to catechol (**Figure 3**). In the final step of strain construction, the gene Mut*melA* was integrated into the chromosome at the site of the *lacZ* gene. The resulting strain was evaluated in bioreactor cultures at 1-liter scale. The culture media contained glycerol 40 g/L as the carbon source. Glycerol was chosen over glucose as the carbon source since the former does not consume aromatics precursor PEP during its internalization and phosphorylation. In addition, glycerol is a relatively inexpensive, abundant and renewable carbon and energy source that is obtained mainly as a byproduct of biodiesel and soap production (Tan et al., 2013). Culture media also contained 2 g/L yeast extract since the strain is an L-tryptophan auxotroph. Under these conditions, the engineered strain displayed growth for 17 h then it entered the stationary phase that ended after 72 h of total culture time. The accumulation of catechol melanin was observed to begin at 18 h, very close to the start of the stationary phase. At the end of the culture, 1.21 g/L of catechol melanin were recuperated from the culture medium (**Table 1**) (Mejía-Caballero et al., 2016). The accumulation of 0.73 g/L of catechol was observed at the end of the culture. This result indicates that the rate of synthesis of this precursor surpasses the capacity of MutMelA to consume it. Therefore, in this case, increasing the activity of the tyrosinase should be a target to improve strain performance.

Metabolic engineering efforts to increase melanin production have so far focused on *E. coli*. This is the result of the accumulated knowledge related to the engineering of central metabolism and the shikimate pathway in this organism. For the yeast *Saccharomyces cerevisiae*, there is also a large body of work related to the rational modification of metabolic pathways for the production of aromatic compounds. Some of these modifications have been directed to increase the supply of L-DOPA since this compound is an early intermediate for the synthesis of benzylisoquinoline alkaloids (BIAs). In one report, with the aim of improving an *S. cerevisiae* strain for the production of BIAs, a strategy based on the use of an enzyme-coupled biosensor and mutagenesis was employed. The cytochrome P450 L-DOPA oxidase CYP76AD1 from the sugar beet *Beta vulgaris* was found to display tyrosine hydroxylase activity, leading to the synthesis of L-DOPA. To improve this activity, error-prone PCR was employed to generate a mutant library of CYP76AD1. The identification of mutants with higher activity was based on the visual detection of colonies displaying the highest fluorescence since the cells express an enzyme that converts L-DOPA to betaxanthin. In a second step, DNA shuffling was employed with the genes of the six isolated improved variants of CYP76AD1 to combine the mutations. This procedure allowed the isolation of a mutant version of CYP76AD1 that displayed a 2.8-fold increase in L-DOPA titer when compared to wild type enzyme (DeLoache et al., 2015). In another example, *S. cerevisiae* strains were engineered for the synthesis of natural and novel BIAs. The simultaneous deletion of *zwf1*, encoding glucose-6-phosphate dehydrogenase, upregulation of *TKL1*, encoding transketolase and the expression of $ARO4^{Q166K}$, encoding a feedback-inhibition-resistant mutant version of the tyrosine-inhibited DAHP synthase, improved the endogenous supply of L-tyrosine, leading to a 60-fold increase in the synthesis of the benzylisoquinoline scaffold. In an effort to generate a strain for the production of norcoclaurine, further modifications were introduced to enable the synthesis of L-DOPA. The BH_4-dependent tyrosine hydroxylase from *Rattus norvegicus* was chosen. Codon-optimized genes encoding enzymes involved in BH_4 biosynthesis and tyrosine-hydroxylase were expressed, resulting in the synthesis of 94.5 ug/L of L-DOPA.

It should be noted that these efforts were not aimed exclusively at generating *S. cerevisiae* strains for L-tyrosine or L-DOPA production. Thus, further performance improvement should be possible. It is expected that expression of an enzyme with tyrosinase activity in these strains should yield eumelanin producers. It is interesting to note the similarities and differences regarding metabolic engineering targets when comparing *E. coli* and *S. cerevisiae* L-tyrosine or L-DOPA-production strains. One clear similarity is the need to express feedback-inhibition-resistant mutant versions of enzymes in key points of the aromatic biosynthetic pathways.

CONCLUSIONS AND PERSPECTIVES

The melanins are a class of natural products that can be considered functional polymers with multiple potential applications in industry. Obtaining these products at a large scale, with a chemically defined composition, and at a relatively low cost is a major technical challenge. As discussed in this review, one approach in this direction can be based on the isolation and use of natural melanogenic microorganisms. This scheme has some advantages, such as the possibility of developing a production process in a relatively short time. However, the use of natural melanogenic organisms can have some drawbacks, such as the frequent requirement to use complex media, which is required to induce melanin production. The use of complex media complicates purification procedures and also can result in the synthesis of melanin with non-desired chemical components. One solution to these problems has been based on the use of genetic engineering to modify the expression of native genes involved in melanogenesis, as well as the generation of novel melanogenic organisms. The accumulated knowledge on the biochemistry and genetics of melanin production in various organisms has enabled the possibility of directly manipulating components in this pathway. By employing genetic and metabolic engineering techniques, it has become possible to enhance the synthetic capacity of natural melanogenic organisms. Furthermore, novel melanogenic organisms have been generated with the capacity of synthesizing melanins from simple carbon sources. These efforts have resulted in the generation of strains and processes for obtaining these polymers at the scale of grams (**Table 1**).

The main genetic modification employed to generate or improve melanogenic organisms involves the overexpression of genes encoding tyrosinases. This is frequently based on placing the tyrosinase gene under control of an inducible promoter in a replicative plasmid vector. This strategy enables the precise control of the magnitude and time of gene expression by the addition of inducers, thus allowing production process optimization. However, the use of expression plasmids like those employed in the examples reviewed here requires the addition of antibiotics as a selective pressure to avoid the growth of plasmid-less cells. Another drawback is the requirement for the inclusion of a chemical inducer in culture media. The use of antibiotics and inducers increase production costs and complicates purification procedures. These issues can be avoided by the use of alternative plasmid selection methods that are not based on antibiotics, as well as gene induction methods not dependent on the addition of chemicals (Vidal et al., 2008).

It can be observed in several of the reports reviewed here, that melanin titers and volumetric productivities are lower in processes where the production strain was modified by metabolic engineering to convert the carbon sources to melanins when compared to the strains that transform melanin precursors provided in the culture medium (**Table 1**). The reported titers and productivities for eumelanin fall short of those observed for the production of its precursor L-tyrosine (Santos et al., 2012). This suggests that there is still a potential margin for strain and production process improvement. Further development of the engineered strains will be required to make them more competitive.

The application of synthetic biology, adaptive laboratory evolution (ALE) and mutagenesis strategies should be evaluated for improving the current melanin production strains (Bassalo et al., 2016). The use of ALE can allow the engineering of complex phenotypes. In one report, a synthetic biosensor module that responds to aromatic amino acids intracellular concentration was combined with ALE to allow the generation of an improved *S. cerevisiae* strain for muconic acid production (Leavitt et al., 2017). This strain displays enhanced flux in the common aromatic amino acid pathway, thus, it could be modified to increase L-tyrosine synthesis by following established methods. With such modification, the *S. cerevisiae* strain developed in this study could be a suitable platform for eumelanin synthesis. In another report, a high-throughput screen for L-tyrosine production was developed by coupling the synthesis of this amino acid to the production of melanin in an *E. coli* strain expressing the MelA tyrosinase from *R. etli* (Santos and Stephanopoulos, 2008). This method was applied to identify *E. coli* strains with improved L-tyrosine production capacity. In this study, *E. coli* was engineered by applying rational metabolic engineering strategies that cause L-tyrosine overproduction. To further improve L-tyrosine synthesis capacity, this strain was subjected to global transcription machinery engineering (gTME) (Alper et al., 2006). This method was implemented in *E. coli* by expressing in the engineered strain two separate gTME libraries of the RNA polymerase *rpoA* and *rpoD* subunits. Improved L-tyrosine producers from these two libraries were identified in agar plates based on colony melanin pigmentation. Three mutant isolates were characterized, showing a 2-fold increase in L-tyrosine titer when compared to the engineered parent strain (Santos et al., 2012). It should be noted that in this case, these strains could be employed directly in a process for melanin production from glucose.

As part of the characterization of strains modified to synthesize melanin from a simple carbon source, it has been determined that tyrosinase activity is a factor limiting productivity (Chávez-Béjar et al., 2013; Mejía-Caballero et al., 2016). It is possible that tyrosinase activity could also be limiting melanin production in other engineered strains. It is, therefore, of importance, to evaluate tyrosinase enzymes from diverse biological sources, to identify those with desired properties for biotechnological application. The vast genome and metagenome data that is currently available should provide a large number of genes encoding putative tyrosinases that can be evaluated experimentally. In addition, the application of protein engineering is a viable option to improve this class of enzymes. This methodology has not yet been applied as part of a strategy to improve a melanin production strain. One important advantage of working with tyrosinases is the simple activity assay based on melanin production, which allows high-throughput selection methods (Santos and Stephanopoulos, 2008).

In spite of the technical advances regarding the development of strains and processes for melanin production, many basic questions still remain to be answered. One important issue is related to the dynamics of melanin polymerization. It is assumed that melanin precursors are synthesized in the cytosol, these molecules then exit the cell and start to polymerize in the culture medium. The polymer progressively increases in size, generating a large diversity of melanin molecules. It is interesting that melanin isolated at different times in production cultures, display diverse colors ranging from yellow to black (Chávez-Béjar et al., 2013). It can be expected that these macromolecules will also have distinct physicochemical properties. Performing studies on the dynamics of melanin polymerization in production cultures and the properties of polymers of particular sizes is of great importance since they could yield useful information leading to the isolation of products with defined characteristics.

To be used as a biotechnological product, melanins must be extracted from culture media and purified. A general method for extracting and partially purifying these products is based on the low solubility displayed by these polymers at low pH values. The extraction method followed by most authors starts by removing cells from the culture medium by centrifugation and then precipitation of melanin by adjusting pH to 2.0–3.0 with HCl for 4–16 h at 4–25°C. Precipitated melanin is centrifuged and it can be either dried in an oven at 45–70°C for 24 h or freeze-dried and stored at 4°C. Alternatively, the precipitated melanin can be re-dissolved in water at pH 8.0–9.0 and the cycle of precipitation and re-dissolving is repeated several times with drying as a final step. Liquid chromatography by Pharmacia Sephadex LH-20 has been reported as an additional purification step for eumelanin (Lin et al., 2005). These extraction and purification methods are expected to yield melanins with varying degrees of purity. It is likely that melanin obtained with the previously mentioned procedures could contain varying amounts of protein and other cellular components. However, there is still not a general standard to define melanin purity for specific applications.

As it is evident from the manuscripts reviewed here, most of the published works on microbial melanin production have focused on eumelanin. This is understandable since this polymer has been characterized extensively and it is the most common type of melanin found in humans. Therefore, eumelanin availability could lead to applications in the cosmetic and health industries as well as other technological areas. However, it should be noted that melanins comprise a chemically-diverse group of polymers. So far, only a small fraction of this chemical diversity has been explored. In addition to eumelanin, production processes for catechol, caffeic acid, and protocatechualdehyde melanins have been reported. For specific applications, it can be assumed that different types of melanins would display distinct performances. Indeed, in a recent study, it was shown that protocatechualdehyde-based melanin displayed a better performance as a dye in soft contact lenses, when compared to eumelanin or caffeic acid melanin (Ahn et al., 2019). It should also be noted that non-natural melanins can be generated by employing synthetic non-natural amino acids and other compounds that can be employed as substrates by tyrosinases (della-Cioppa et al., 1990). Therefore, the expected diversity of this type of polymers is very large. The development of strains and processes for generating novel natural and synthetic melanins should vastly increase the number of applications with these aromatic polymers.

AUTHOR CONTRIBUTIONS

LM, AM, and GG participated in the search and analysis of information for this review as well as in writing and critical review of the manuscript.

REFERENCES

Ahn, S. Y., Choi, M., Jeong, D. W., Park, S., Park, H., Jang, K. S., et al. (2019). Synthesis and chemical composition analysis of protocatechualdehyde-based novel melanin dye by 15T FT-ICR: high dyeing performance on soft contact lens. *Dyes and Pigments* 160, 546–554. doi: 10.1016/j.dyepig.2018.08.058

Alper, H., Moxley, J., Nevoigt, E., Fink, G. R., and Stephanopoulos, G. (2006). Engineering yeast transcription machinery for improved ethanol tolerance and production. *Science* 314, 1565–1568. doi: 10.1126/science.1131969

Ambrico, M., Vecchia, N. F. D., Ambrico, P. F., Cardone, A., Cicco, S. R., Ligonzo, T., et al. (2014). A photoresponsive red-hair-inspired polydopamine-based copolymer for hybrid photocapacitive sensors. *Adv. Funct. Mater.* 24, 7161–7172. doi: 10.1002/adfm.201401377

Apte, M., Girme, G., Bankar, A., RaviKumar, A., and Zinjarde, S. (2013). 3, 4-dihydroxy-L-phenylalanine-derived melanin from *Yarrowia lipolytica* mediates the synthesis of silver and gold nanostructures. *J. Nanobiotechnology* 11:2. doi: 10.1186/1477-3155-11-2

Balderas-Hernández, V. E., Sabido-Ramos, A., Silva, P., Cabrera-Valladares, N., Hernández-Chávez, G., Báez-Viveros, J. L., et al. (2009). Metabolic engineering for improving anthranilate synthesis from glucose in *Escherichia coli*. *Microb. Cell Fact.* 8:19. doi: 10.1186/1475-2859-8-19

Balderas-Hernández, V. E., Treviño-Quintanilla, L. G., Hernández-Chávez, G., Martinez, A., Bolívar, F., and Gosset, G. (2014). Catechol biosynthesis from glucose in *Escherichia coli* anthranilate-overproducer strains by heterologous expression of anthranilate 1, 2-dioxygenase from *Pseudomonas aeruginosa* PAO1. *Microb. Cell Fact.* 13:136. doi: 10.1186/s12934-014-0136-x

Bassalo, M. C., Liu, R., and Gill, R. T. (2016). Directed evolution and synthetic biology applications to microbial systems. *Curr. Opin. Biotechnol.* 39, 126–133. doi: 10.1016/j.copbio.2016.03.016

Bothma, J. P., de Boor, J., Divakar, U., Schwenn, P. E., and Meredith, P. (2008). Device-quality electrically conducting melanin thin films. *Adv. Mater.* 20, 3539–3542. doi: 10.1002/adma.200703141

Cabrera-Valladares, N., Martínez, A., Pinero, S., Lagunas-Munoz, V. H., Tinoco, R., De Anda, R., et al. (2006). Expression of the *melA* gene from *Rhizobium etli* CFN42 in *Escherichia coli* and characterization of the encoded tyrosinase. *Enzyme Microb. Technol.* 38, 772–779. doi: 10.1016/j.enzmictec.2005.08.004

Chávez-Béjar, M. I., Balderas-Hernandez, V. E., Gutiérrez-Alejandre, A., Martinez, A., Bolívar, F., and Gosset, G. (2013). Metabolic engineering of *Escherichia coli* to optimize melanin synthesis from glucose. *Microb. Cell Fact.* 12:108. doi: 10.1186/1475-2859-12-108

Chávez-Béjar, M. I., Lara, A. R., López, H., Hernández-Chávez, G., Martinez, A., Ramírez, O. T., et al. (2008). Metabolic engineering of *Escherichia coli* for L-tyrosine production by expression of genes coding for the chorismate mutase domain of the native chorismate mutase-prephenate dehydratase and a cyclohexadienyl dehydrogenase from *Zymomonas mobilis*. *Appl. Environ. Microbiol.* 74, 3284–3290. doi: 10.1128/AEM.02456-07

Clusella-Trullas, S., van Wyk, J. H., and Spotila, J. R. (2007). Thermal melanism in ectotherms. *J. Thermal Biol.* 32, 235–245. doi: 10.1016/j.jtherbio.2007.01.013

Coelho, S. G., Zhou, Y., Bushar, H. F., Miller, S. A., Zmudzka, B. Z., Hearing, V. J., et al. (2009). Long-lasting pigmentation (LLP) of human skin, a new look at an overlooked response to UV. *Pigment Cell Melanoma Res.* 22:238–241. doi: 10.1111/j.1755-148X.2009.00550.x

Cordero, R. J., and Casadevall, A. (2017). Functions of fungal melanin beyond virulence. *Fungal Biol. Rev.* 31, 99–112. doi: 10.1016/j.fbr.2016.12.003

Dadachova, E., Bryan, R. A., Huang, X., Moadel, T., Schweitzer, A. D., Aisen, P., et al. (2007). Ionizing radiation changes the electronic properties of melanin and enhances the growth of melanized fungi. *PLoS ONE* 2:e457. doi: 10.1371/journal.pone.0000457

della-Cioppa, G., Garger, S. J., Sverlow, G. G., Turpen, T. H., and Grill, L. K. (1990). Melanin production in *Escherichia coli* from a cloned tyrosinase gene. *Biotechnology* 8, 634–638. doi: 10.1038/nbt0790-634

DeLoache, W. C., Russ, Z. N., Narcross, L., Gonzales, A. M., Martin, V. J., and Dueber, J. E. (2015). An enzyme-coupled biosensor enables (S)-reticuline production in yeast from glucose. *Nat. Chem. Biol.* 11:465–471. doi: 10.1038/nchembio.1816

d'Ischia, M., Wakamatsu, K., Cicoira, F., Di Mauro, E., Garcia-Borron, J. C., Commo, S., et al. (2015). Melanins and melanogenesis: from pigment cells to human health and technological applications. *Pigment Cell Melanoma Res.* 28, 520–544. doi: 10.1111/pcmr.12393

Fairhead, M., and Thöny-Meyer, L. (2012). Bacterial tyrosinases: old enzymes with new relevance to biotechnology. *N. Biotechnol.* 29, 183–191. doi: 10.1016/j.nbt.2011.05.007

Fogarty, R. V., and Tobin, J. M. (1996). Fungal melanins and their interactions with metals. *Enzyme Microb. Technol.* 19, 311–317. doi: 10.1016/0141-0229(96)00002-6

Ganesh Kumar, C., Sahu, N., Narender Reddy, G., Prasad, R. B. N., Nagesh, N., and Kamal, A. (2013). Production of melanin pigment from *Pseudomonas stutzeri* isolated from red seaweed *Hypnea musciformis*. *Lett. Appl. Microbiol.* 57, 295–302. doi: 10.1111/lam.12111

Garcia-Molina, F., Munoz, J. L., Varon, R., Rodriguez-Lopez, J. N., Garcia-Canovas, F., and Tudela, J. (2007). A review on spectrophotometric methods for measuring the monophenolase and diphenolase activities of tyrosinase. *J. Agric. Food Chem.* 55, 9739–9749. doi: 10.1021/jf0712301

Gibello, A., Ferrer, E., Sanz, J., and Martin, M. (1995). Polymer production by *Klebsiella pneumoniae* 4-hydroxyphenylacetic acid hydroxylase genes cloned in *Escherichia coli*. *Appl. Environ. Microbiol.* 61, 4167–4171.

Glass, K., Ito, S., Wilby, P. R., Sota, T., Nakamura, A., Bowers, C. R., et al. (2012). Direct chemical evidence for eumelanin pigment from the Jurassic period. *Proc. Natl. Acad. Sci. U.S.A.* 109, 10218–10223. doi: 10.1073/pnas.1118448109

González, V., Bustos, P., Ramírez-Romero, M. A., Medrano-Soto, A., Salgado, H., Hernández-González, I., et al. (2003). The mosaic structure of the symbiotic plasmid of *Rhizobium etli* CFN42 and its relation to other symbiotic genome compartments. *Genome Biol.* 4:R36. doi: 10.1186/gb-2003-4-6-r36

Guo, J., Rao, Z., Yang, T., Man, Z., Xu, M., and Zhang, X. (2014). High-level production of melanin by a novel isolate of *Streptomyces kathirae*. *FEMS Microbiol. Lett.* 357, 85–91. doi: 10.1111/1574-6968.12497

Guo, J., Rao, Z., Yang, T., Man, Z., Xu, M., Zhang, X., et al. (2015). Cloning and identification of a novel tyrosinase and its overexpression in *Streptomyces kathirae* SC-1 for enhancing melanin production. *FEMS Microbiol. Lett.* 362:fnv041. doi: 10.1093/femsle/fnv041

Hill, H. Z. (1992). The function of melanin or six blind people examine an elephant. *Bioessays* 14, 49–56. doi: 10.1002/bies.950140111

Horneck, G., Klaus, D. M., and Mancinelli, R. L. (2010). Space microbiology. *Microbiol. Mol. Biol. Rev.* 74, 121–156. doi: 10.1128/MMBR.00016-09

Ito, S. (2003). A chemist's view of melanogenesis. *Pigment Cell Res.* 16, 230–236. doi: 10.1034/j.1600-0749.2003.00037.x

Jalmi, P., Bodke, P., Wahidullah, S., and Raghukumar, S. (2012). The fungus *Gliocephalotrichum simplex* as a source of abundant, extracellular melanin for biotechnological applications. *World J. Microbiol. Biotechnol.* 28, 505–512. doi: 10.1007/s11274-011-0841-0

Jang, S., Gang, H., Kim, B. G., and Choi, K. Y. (2018). FCS and ECH dependent production of phenolic aldehyde and melanin pigment from l-tyrosine in *Escherichia coli*. *Enzyme Microb. Technol.* 112, 59–64. doi: 10.1016/j.enzmictec.2017.10.011

Kim, Y. J., Wu, W., Chun, S. E., Whitacre, J. F., and Bettinger, C. J. (2013). Biologically derived melanin electrodes in aqueous sodium-ion energy storage devices. *Proc. Natl. Acad. Sci. U.S.A.* 110, 20912–20917. doi: 10.1073/pnas.1314345110

Koike, K., and Ebato, A. (2013). *One-Pack Hair Dye Compositions Containing Indole Compounds*. Jpn Tokkyo Koho 2013, JP5363703B220131211.

Krol, E. S., and Liebler, D. C. (1998). Photoprotective actions of natural and synthetic melanins. *Chem. Res. Toxicol.* 11, 1434–1440. doi: 10.1021/tx980114c

Lagunas-Muñoz, V. H., Cabrera-Valladares, N., Bolívar, F., Gosset, G., and Martinez, A. (2006). Optimum melanin production using recombinant *Escherichia coli*. *J. Appl. Microbiol.* 101, 1002–1008. doi: 10.1111/j.1365-2672.2006.03013.x

Leavitt, J. M., Wagner, J. M., Tu, C. C., Tong, A., Liu, Y., and Alper, H. S. (2017). Biosensor-enabled directed evolution to improve muconic acid production in *Saccharomyces cerevisiae*. *Biotechnol. J.* 12:1600687. doi: 10.1002/biot.201600687

Lin, W. P., Lai, H. L., Liu, Y. L., Chiung, Y. M., Shiau, C. Y., Han, J. M., et al. (2005). Effect of melanin produced by a recombinant *Escherichia coli* on antibacterial activity of antibiotics. *J. Microbiol. Immunol. Infect.* 38, 320–326.

Lindgren, J., Moyer, A., Schweitzer, M. H., Sjövall, P., Uvdal, P., Nilsson, D. E., et al. (2015). Interpreting melanin-based coloration through deep time: a critical review. *Proc. R. Soc. B Biol. Sci.* 282:20150614. doi: 10.1098/rspb.2015.0614

Liu, Y. C., Chen, S. M., Liu, J. H., Hsu, H. W., Lin, H. Y., and Chen, S. Y. (2015). Mechanical and photo-fragmentation processes for nanonization of melanin to improve its efficacy in protecting cells from reactive oxygen species stress. *J. Appl. Phys.* 117:064701. doi: 10.1063/1.4907997

López-Serrano, D., Solano, F., and Sanchez-Amat, A. (2004). Identification of an operon involved in tyrosinase activity and melanin synthesis in *Marinomonas mediterranea*. *Gene* 342, 179–187. doi: 10.1016/j.gene.2004.08.003

Madhusudhan, D. N., Mazhari, B. B. Z., Dastager, S. G., and Agsar, D. (2014). Production and cytotoxicity of extracellular insoluble and droplets of soluble melanin by *Streptomyces lusitanus* DMZ-3. *Biomed Res. Int.* 2014:306895. doi: 10.1155/2014/306895

Manivasagan, P., Venkatesan, J., Sivakumar, K., and Kim, S. K. (2013). Actinobacterial melanins: current status and perspective for the future. *World J. Microbiol. Biotechnol.* 29, 1737–1750. doi: 10.1007/s11274-013-1352-y

McGraw, K. J. (2008). An update on the honesty of melanin-based color signals in birds. *Pigment Cell Melanoma Res.* 21, 133–138. doi: 10.1111/j.1755-148X.2008.00454.x

Mejía-Caballero, A., de Anda, R., Hernández-Chávez, G., Rogg, S., Martinez, A., Bolívar, F., et al. (2016). Biosynthesis of catechol melanin from glycerol employing metabolically engineered *Escherichia coli*. *Microb. Cell Fact.* 15:161. doi: 10.1186/s12934-016-0561-0

Meredith, P., and Sarna, T. (2006). The physical and chemical properties of eumelanin. *Pigment Cell Res.* 19, 572–594. doi: 10.1111/j.1600-0749.2006.00345.x

Montefiori, D. C., and Zhou, J. (1991). Selective antiviral activity of synthetic soluble L-tyrosine and L-dopa melanins against human immunodeficiency virus *in vitro*. *Antiviral Res.* 15, 11–25. doi: 10.1016/0166-3542(91)90037-R

Nikodinovic-Runic, J., Martin, L. B., Babu, R., Blau, W., and O'Connor, K. E. (2009). Characterization of melanin-overproducing transposon mutants of *Pseudomonas putida* F6. *FEMS Microbiol. Lett.* 298, 174–183. doi: 10.1111/j.1574-6968.2009.01716.x

Nofsinger, J. B., Liu, Y., and Simon, J. D. (2002). Aggregation of eumelanin mitigates photogeneration of reactive oxygen species. *Free Radic. Biol. Med.* 32, 720–730. doi: 10.1016/S0891-5849(02)00763-3

Palumbo, A. (2003). Melanogenesis in the ink gland of *Sepia officinalis*. *Pigment Cell Res.* 16, 517–522. doi: 10.1034/j.1600-0749.2003.00080.x

Paproski, R. J., Li, Y., Barber, Q., Lewis, J. D., Campbell, R. E., and Zemp, R. (2015). Validating tyrosinase homologue melA as a photoacoustic reporter gene for imaging *Escherichia coli*. *J. Biomed. Opt.* 20:106008. doi: 10.1117/1.JBO.20.10.106008

Patel, K. R., Wyman, J. A., Patel, K. A., and Burden, B. J. (1996). A mutant of *Bacillus thuringiensis* producing a dark-brown pigment with increased UV resistance and insecticidal activity. *J. Invertebr. Pathol.* 67, 120–124. doi: 10.1006/jipa.1996.0018

Patil, S., Sistla, S., Bapat, V., and Jadhav, J. (2018). Melanin-mediated synthesis of silver nanoparticles and their affinity towards tyrosinase. *Appl. Biochem. Microbiol.* 54, 163–172. doi: 10.1134/S0003683818020096

Piñero, S., Rivera, J., Romero, D., Cevallos, M. A., Martínez, A., Bolívar, F., et al. (2007). Tyrosinase from *Rhizobium etli* is involved in nodulation efficiency and symbiosis-associated stress resistance. *J. Mol. Microbiol. Biotechnol.* 13, 35–44. doi: 10.1159/000103595

Prieto, M. A., Perez-Aranda, A., and Garcia, J. L. (1993). Characterization of an *Escherichia coli* aromatic hydroxylase with a broad substrate range. *J. Bacteriol.* 175, 2162–2167. doi: 10.1128/jb.175.7.2162-2167.1993

Raman, N. M., Shah, P. H., Mohan, M., and Ramasamy, S. (2015). Improved production of melanin from *Aspergillus fumigatus* AFGRD105 by optimization of media factors. *AMB Express* 5:72. doi: 10.1186/s13568-015-0161-0

Rózanowska, M., Sarna, T., Land, E. J., and Truscott, T. G. (1999). Free radical scavenging properties of melanin: interaction of eu-and pheo-melanin models with reducing and oxidising radicals. *Free Radic. Biol. Med.* 26, 518–525. doi: 10.1016/S0891-5849(98)00234-2

Ruan, L., He, W., He, J., Sun, M., and Yu, Z. (2005). Cloning and expression of *mel* gene from *Bacillus thuringiensis* in *Escherichia coli*. *Antonie Van Leeuwenhoek* 87, 283–288. doi: 10.1007/s10482-004-4775-5

Ruan, L., Yu, Z., Fang, B., He, W., Wang, Y., and Shen, P. (2004). Melanin pigment formation and increased UV resistance in *Bacillus thuringiensis* following high temperature induction. *Syst. Appl. Microbiol.* 27, 286–289. doi: 10.1078/0723-2020-00265

Saini, A. S., and Melo, J. S. (2013). Biosorption of uranium by melanin: kinetic, equilibrium and thermodynamic studies. *Bioresour. Technol.* 149, 155–162. doi: 10.1016/j.biortech.2013.09.034

Saini, A. S., and Melo, J. S. (2015). One-pot green synthesis of eumelanin: process optimization and its characterization. *RSC Adv.* 5, 47671–47680. doi: 10.1039/C5RA01962A

Santos, C. N. S., and Stephanopoulos, G. (2008). Melanin-based high-throughput screen for L-tyrosine production in *Escherichia coli*. *Appl. Environ. Microbiol.* 74, 1190–1197. doi: 10.1128/AEM.02448-07

Santos, C. N. S., Xiao, W., and Stephanopoulos, G. (2012). Rational, combinatorial, and genomic approaches for engineering L-tyrosine production in *Escherichia coli*. *Proc. Natl. Acad. Sci. U.S.A.* 109, 13538–13543. doi: 10.1073/pnas.1206346109

Sarna, T., Hyde, J. S., and Swartz, H. M. (1976). Ion-exchange in melanin: an electron spin resonance study with lanthanide probes. *Science* 192, 1132–1134. doi: 10.1126/science.179142

Shanmuganathan, K., Cho, J. H., Iyer, P., Baranowitz, S., and Ellison, C. J. (2011). Thermooxidative stabilization of polymers using natural and synthetic melanins. *Macromolecules* 44, 9499–9507. doi: 10.1021/ma202170n

Surwase, S. N., Jadhav, S. B., Phugare, S. S., and Jadhav, J. P. (2013). Optimization of melanin production by *Brevundimonas* sp. SGJ using response surface methodology. *3 Biotech* 3, 187–194. doi: 10.1007/s13205-012-0082-4

Tan, H. W., Aziz, A. A., and Aroua, M. K. (2013). Glycerol production and its applications as a raw material: a review. *Renew. Sustain. Energy Rev.* 27, 118–127. doi: 10.1016/j.rser.2013.06.035

Tarangini, K., and Mishra, S. (2014). Production of melanin by soil microbial isolate on fruit waste extract: two step optimization of key parameters. *Biotechnol. Rep.* 4, 139–146. doi: 10.1016/j.btre.2014.10.001

Trias, J., Viñas, M., Guinea, J., and Lorèn, J. G. (1989). Brown pigmentation in *Serratia marcescens* cultures associated with tyrosine metabolism. *Can. J. Microbiol.* 35, 1037–1042. doi: 10.1139/m89-172

Valderrama, B., Oliver, P., Medrano-Soto, A., and Vazquez-Duhalt, R. (2003). Evolutionary and structural diversity of fungal laccases. *Antonie Van Leeuwenhoek* 84, 289–299. doi: 10.1023/A:1026070122451

Vavricka, C. J., Han, Q., Mehere, P., Ding, H., Christensen, B. M., and Li, J. (2014). Tyrosine metabolic enzymes from insects and mammals: a comparative perspective. *Insect Sci.* 21, 13–19. doi: 10.1111/1744-7917.12038

Vidal, L., Pinsach, J., Striedner, G., Caminal, G., and Ferrer, P. (2008). Development of an antibiotic-free plasmid selection system based on glycine auxotrophy for recombinant protein overproduction in *Escherichia coli*. *J. Biotechnol.* 134, 127–136. doi: 10.1016/j.jbiotec.2008.01.011

Westerhof, W. (2006). The discovery of the human melanocyte. *Pigment Cell Res.* 19, 183–193. doi: 10.1111/j.1600-0749.2006.00313.x

Williams, R. F. (1994). *Melanin-based Agents For Image Enhancement*. U.S. Patent No. 5,310,539.

Wogelius, R. A., Manning, P. L., Barden, H. E., Edwards, N. P., Webb, S. M., Sellers, W. I., et al. (2011). Trace metals as biomarkers for eumelanin pigment in the fossil record. *Science* 333, 1622–1626. doi: 10.1126/science.1205748

Yanofsky, C., Horn, V., Bonner, M., and Stasiowski, S. (1971). Polarity and enzyme functions in mutants of the first three genes of the tryptophan operon of *Escherichia coli*. *Genetics* 69, 409.

Zhang, F., Kearns, S. L., Orr, P. J., Benton, M. J., Zhou, Z., Johnson, D., et al. (2010). Fossilized melanosomes and the colour of Cretaceous dinosaurs and birds. *Nature* 463, 1075–1078. doi: 10.1038/nature08740

Zhao, S. H., and Tong-Suo, M. A. (2012). High yield of melanin production by the strain *Rhizobium* sp. R 593 in liquid state fermentation. *Asian J. Chem.* 24, 335–338.

Conflict of Interest: The authors declare that the research was conducted in the absence of any commercial or financial relationships that could be construed as a potential conflict of interest.

frontiers in Bioengineering and Biotechnology

REVIEW
published: 20 February 2020
doi: 10.3389/fbioe.2020.00096

Bioprocess Optimization for the Production of Aromatic Compounds With Metabolically Engineered Hosts: Recent Developments and Future Challenges

Adelaide Braga and Nuno Faria*

Centre of Biological Engineering, University of Minho, Braga, Portugal

The most common route to produce aromatic chemicals – organic compounds containing at least one benzene ring in their structure – is chemical synthesis. These processes, usually starting from an extracted fossil oil molecule such as benzene, toluene, or xylene, are highly environmentally unfriendly due to the use of non-renewable raw materials, high energy consumption and the usual production of toxic by-products. An alternative way to produce aromatic compounds is extraction from plants. These extractions typically have a low yield and a high purification cost. This motivates the search for alternative platforms to produce aromatic compounds through low-cost and environmentally friendly processes. Microorganisms are able to synthesize aromatic amino acids through the shikimate pathway. The construction of microbial cell factories able to produce the desired molecule from renewable feedstock becomes a promising alternative. This review article focuses on the recent advances in microbial production of aromatic products, with a special emphasis on metabolic engineering strategies, as well as bioprocess optimization. The recent combination of these two techniques has resulted in the development of several alternative processes to produce phenylpropanoids, aromatic alcohols, phenolic aldehydes, and others. Chemical species that were unavailable for human consumption due to the high cost and/or high environmental impact of their production, have now become accessible.

Keywords: aromatic compounds, metabolic engineering, microorganisms, process optimization, synthetic biology, shikimate pathway

OPEN ACCESS

Edited by:
Nils Jonathan Helmuth Averesch, Stanford University, United States

Reviewed by:
Nicolai Kallscheuer, Radboud University, Netherlands
Xiangzhao Mao, Ocean University of China, China
Mattijs K. Julsing, Wageningen University and Research, Netherlands

****Correspondence:***
Adelaide Braga
abraga@deb.uminho.pt

Specialty section:
This article was submitted to Bioprocess Engineering, a section of the journal Frontiers in Bioengineering and Biotechnology

Received: *25 June 2019*
Accepted: *03 February 2020*
Published: *20 February 2020*

Citation:
Braga A and Faria N (2020) Bioprocess Optimization for the Production of Aromatic Compounds With Metabolically Engineered Hosts: Recent Developments and Future Challenges. Front. Bioeng. Biotechnol. 8:96. doi: 10.3389/fbioe.2020.00096

INTRODUCTION

The increasing demand for "natural" labeled products, the adoption of a healthy life style associated with growing concerns about global warming and limited supplies of fossil fuels, promote the development of alternative ways for producing fuels and commodity chemicals using renewable feedstocks in eco-friendly processes. In this scenario, the use of biotechnological platforms for their production is becoming a promising alternative (Sun et al., 2015; Braga et al., 2018a; Milke et al., 2018; Park et al., 2018).

An important class of petrochemical compounds that have been considered as promising targets for biotechnological production are aromatic compounds (Knaggs, 2003; Lee and Wendisch, 2017; Noda and Kondo, 2017). They are typically produced employing fossil feedstocks as raw materials and have a wide range of industrial and commercial applications as building blocks for the synthesis of polymer materials like functional plastics and fibers, food and feed additives, nutraceuticals and pharmaceuticals (Krömer et al., 2013; Averesch and Krömer, 2018). The economic importance of these compounds is quite significant; in 2017 their global market size was USD185.9 billion and it is expected that, in 2025, their global production volume will reach 168,733.35 thousand tons (Averesch and Kayser, 2014), with the demand for aromatic compounds for gasoline, pharmaceuticals and detergents as main driving force.

In the last decades, microorganisms have emerged as attractive platforms for producing former petroleum-derived compounds from renewable starting materials (Borodina and Nielsen, 2014; Krivoruchko and Nielsen, 2015; Noda and Kondo, 2017). Until now, several derivatives of BTX (benzene, toluene, and the three isomers of xylene), such as styrene, hydroxystyrene, phenol and vanillin, have been produced using microbial hosts by direct bioconversion of precursors or via *de novo* synthesis (Wierckx et al., 2005; Vannelli et al., 2007; Mckenna and Nielsen, 2011; Ni et al., 2015). However, only a few compounds, such as vanillin and resveratrol, have reached bio-based production at commercial scale (Nakamura and Whited, 2003; Yim et al., 2011; Paddon et al., 2013; Van Dien, 2013). Nevertheless, despite the efforts that have been made until now, the production of benzene, toluene or xylene in a renewable way has not been reported.

Microorganisms can grow with high growth rates and achieve high biomass yields, in scalable cultivation and production processes. They are also able to grow in diverse media, from abundant and inexpensive feedstocks. However, they do not naturally (over-)produce these compounds or, if they do, the yields are very low. In order to enable production, it is necessary to functionally integrate heterologous pathways or genetically modify the microbial hosts (Rodrigues et al., 2015; Chouhan et al., 2017; Gottardi et al., 2017; Milke et al., 2018; Wang J. et al., 2018). Aromatic compounds are produced by microbial hosts via the shikimate pathway, which leads to the production of aromatic amino acids as well as other aromatic precursors (Herrmann, 1995; Maeda and Dudareva, 2012; Averesch and Krömer, 2018). This can be achieved by the functional reconstruction of naturally occurring pathways or by *de novo* pathway engineering (Dhamankar and Prather, 2011; Wu et al., 2018). *Escherichia coli* and *Saccharomyces cerevisiae* are the most commonly employed microorganisms for aromatic compound production. However, more recently, other hosts have also been explored due to their peculiarities, such as *Corynebacterium glutamicum, Lactococcus lactis, Pseudomonas putida,* and *Streptomyces lividans* (Sachan et al., 2006; Gosset, 2009; Verhoef et al., 2009; Gaspar et al., 2016; Kallscheuer et al., 2016, 2019; Dudnik et al., 2017, 2018; Braga et al., 2018a; Tilburg et al., 2019).

This review presents an overview of recent advances in microbial production of the most relevant aromatic compounds, including vanillin, salicylic acid, *p*-hydroxybenzoic acid and others strategies for strain design are compared with an emphasis on the development of biosynthetic pathways, the application of protein engineering, carbon flux redirection, use of alternative substrates, engineering substrate uptake and optimization of culture conditions. We present and explain some of the current challenges and gaps that in our knowledge, must be overcome in order to render the biotechnological production of aromatic compounds, in an attractive and feasible way for the commercial scale. **Table 1** presents a summary of the recent reports (last 4 years) regarding the production of aromatic compounds in engineered microbial hosts, comparing the used carbon source, organism and strain, (over-)expressed and/or knocked out genes.

THE SHIKIMATE PATHWAY: A PATH FOR AROMATIC COMPOUNDS PRODUCTION

In microorganisms, the production of aromatic compounds is almost always obtained via the shikimate (SKM) pathway. This route leads to the biosynthesis of aromatic amino acids, L-tyrosine (L-Tyr), L-tryptophan (L-Trp) and L-phenylalanine (L-Phe), and a wide range of aromatic precursors (Knaggs, 2003; Noda et al., 2016; Lai et al., 2017). The first reaction in the shikimate pathway is the condensation of the central carbon metabolism intermediates, phosphoenolpyruvate (PEP) and erythrose-4-phosphate (E4P), to yield 3-deoxy-D-arabino-heptulosonate-7-phosphate (DAHP). After that, six successive enzymatic reactions lead to the production of chorismate (CHO), the end product of the SKM pathway (**Figure 1**) and the starter unit for the production of aromatic amino acids as well as different aromatic compounds (phenylpropanoids, salicylic acid, *p*-hydroxybenzoic acid, aromatic alcohols, vanillin, among others) (Noda et al., 2016).

The first step for L-Phe and L-Tyr production is catalyzed by chorismate mutase (CM), which converts CHO to prephenate (PHA). After that, PHA undergoes decarboxylation and dehydration yielding phenylpyruvate (PPY) or is oxidatively decarboxylated to 4-hydroxyphenylpyruvate (4-HPP). The reactions are catalyzed by prephenate dehydratase (PDT) and prephenate dehydrogenase (PDH), respectively. The last step comprises the transamination of PPY to L-Phe and of 4-HPP to L-Tyr that is catalyzed by an aminotransferase (AT) (Tzin et al., 2001; **Figure 1**). The pathway for L-Trp production from CHO requires six steps. The first one is catalyzed by anthranilate synthase (AS) that converts CHO to anthranilate (ANTH), which is further converted to phosphoribosylanthranilate (PA) by anthranilate phosphoribosyl transferase (PAT). The third step in this pathway leads to the production of l-(*O*-carboxyphenylamino)-l-deoxyribulose-5–phosphate (CDRP) by phosphoribosylanthranilate isomerase (PAI). The fourth enzyme of L-Trp biosynthesis is indole-3-glycerol phosphate synthase (IGPS), which catalyzes the conversion of CDRP to indole-3-glycerol phosphate (IGP). In the last two steps, IGP is cleaved by tryptophan synthase (TS) into indole (ID) that is ligated to L-serine to yield L-Trp (**Figure 1**; Priya et al., 2014).

One of the main bottlenecks in the microbial production of aromatic compounds is the availability of the precursors PEP

TABLE 1 | Summary of the literature on the production titer of some aromatic compounds obtained through metabolic engineering in microorganisms, in the last 4 years.

Compound	Microorganism	Heterologous enzymes (source)	Substrate/precursor	Titer (mg L^{-1})	References
Salicylic acid	*Escherichia coli*	*pykF*, *pykA pheA*, *tyrA* deleted *menF* (*E. coli)* *pchB* (*Pseudomonas aeruginosa*)	Glucose	11500	Noda et al., 2016
p-Hydroxybenzoate	*Corynebacterium glutamicum*	*xylA*, *xylB*, bglF, bglA, aroA, aroD, *aroE*, *aroCKB*, *araBAD*, *araE*, *tkt*, *tal* overexpressed *aroG* (*E. coli*) *ubiC* (*Providencia rustigianii*) *ldhA*, *qsuB*, *qsuD*, *pobA*, *poxF*, *pyk*, *hd*pA deleted	Glucose	36600	Kitade et al., 2018
	Pseudomonas putida	*UbiC* (*E. coli*) *aroG*^{fbr} *pobA*, *phA*, *trpE*, *hexR* deleted	Glucose	1730	Krömer, 2016
	S. cerevisiae	Overexpression *ARO4*^{K229L} *aroL*, *ubiC* (*E. coli*) *ARO4*^{fbr} *ARO7*, *TRP3* deleted	Glucose	2900	Averesch et al., 2017
	P. taiwanensis VLB120	*pobA* and *hpd* deleted *fcs*, *ech* and *vhd* (*P. putida* S12) PAL (*Rhodosporidium toruloides*) *aroG*^{fbr} and *try*^{fbr} overexpression *ppsA* and *pgi*	Glycerol	9900	Lenzen et al., 2019
p-Coumaric acid	*E. coli*	C4H (*Lycoris aurea*) PAL (*Arabidopsis thaliana*) overexpression *pntAB*	Glucose	25.6	Li et al., 2018
	S. cerevisiae	*Aro10*, *pdc5* deleted TAL (*Flavobacterium johnsoniaeu*) *Aro7*^{fbr} *and Aro4*^{fbr} *aroL* (*E. coli*)	Xylose	242	Borja et al., 2019
	E. coli BL21 (DE3)	TAL (*Saccharothrix espanaensis)* *tyrR* and *pheA* deleted *aroG*^{fbr} and *tyrA*^{fbr}	Glucose	100.1	Gyuun et al., 2016
	S. cerevisiae	*Aro10*, *pdc5* deleted TAL (*Flavobacterium johnsoniaeu*) *Aro7*^{G141} *and Aro4*^{K229} *aroL* (*E. coli*)	Glucose	2400	Rodriguez et al., 2017
Caffeic acid	*E. coli BL21 (DE3)*	*tyrR* and *tyrA* deleted TAL (*Saccharothrix espanaensis)* *aroG*^{fbr} and *tyrA*^{fbr} *sam5* (*S. espanaensis)*	Glucose	138.2	Gyuun et al., 2016
	S. cerevisiae	Codon optimized *hpaB* (*P. aeruginosa*) Codon optimized *hpaC* (*Salmonella entérica*) TAL (*Rhodosporidium toruloides*)	L-Tyr	289.4	Liu et al., 2019a
	E. coli	*tryR* deleted *tyrA*^{fbr} *aroG*^{fbr} *tktA* and *ppsA* overexpressed *hpaBC* (*P. aeruginosa*) fe*vV* (*Streptomyces* sp. WK-5344)	Kraft pulp	233	Kawaguchi et al., 2017
2-Phenylethanol	*E. coli*	*aroG*^{fbr} and *pheA*^{fbr} *kdc* (*S. cerevisiae)* overexpression *yigB* *Aro8* (*S. cerevisiae)*	Glucose	1016	Liu et al., 2018
	S. cerevisiae YS58	*ARO8* and *ARO10* overexpressed	L-Phe	3200	Wang et al., 2017
	E. coli	*aroG*^{fbr} and *pheA*^{fbr} *kdc* (*S. cerevisiae* YPH499) *yigB* overexpressed *aro8* (*S. cerevisiae)*	Glucose	1000	Guo et al., 2018
	S. cerevisiae	*Gap1*, *ARO8*, *ARO10*, *Adh2*, *Gdh2* overexpressed	Glucose	6300	Wang Z. et al., 2018
Vanillin	*E. coli top 10*	*fcs* and *ech* (*Amycolatopsis* sp. HR)	Ferulic acid	68	Chakraborty et al., 2016
	E. coli	*fcs* and *ech* (*P. fluorescens* BF13)	Ferulic acid	4258.8	Luziatelli et al., 2019

frb, feedback-resistant; TAL, tyrosine ammonia lyase; PAL, phenylalanine ammonia lyase.

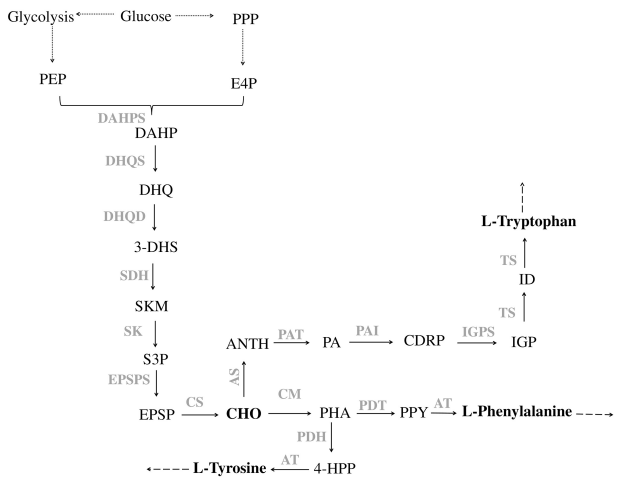

FIGURE 1 | Pathway of aromatic amino acid biosynthesis. PPP, pentose phosphate pathway; E4P, erythrose 4-phosphate; PEP, phosphoenolpyruvate; DAHPS, DAHP synthase; DAHP, 3-Deoxy-D-arabinoheptulosonate 7-phosphate; DHQS, 3-dehydroquinate synthase; DHQ, 3-dehydroquinate; DHQD, 3-dehydroquinate dehydratase; 3-DHS, 3-dehydroshikimate; SDH, shikimate 5-dehydrogenase; SKM, shikimate; SK, shikimate kinase; S3P, shikimate 3-phosphate; EPSPS, 5-enolpyruvylshikimate 3-phosphate synthase; EPSP, 5-enolpyruvylshikimate-3-phosphate; CS, chorismate synthase; CHO, chorismate; CM, chorismate mutase; PHA, prephenate; PDH, prephenate dehydrogenase; 4-HPP, 4-hydroxyphenylpyruvate; AT, aminotransferase; PDT, prephenate dehydratase; PPY, phenylpyruvate; AS, anthranilate synthase; ANTH, anthranilate; PAT, phosphoribosylanthranilate transferase; PA, phosphoribosylanthranilate; PAI, phosphoribosylanthranilate isomerase; CDRP, 1-(*O*-carboxyphenylamino)-1-deoxyribulose-5-phosphate; IGPS, indole-3-glycerol phosphate synthase; IGP, indole-3-glycerol phosphate; TS, tryptophan synthase; ID, indole. Solid lines indicate a single step; dotted lines indicate multiple steps.

(produced during glycolysis) and E4P (derived from the pentose phosphate pathway – PPP) (Suástegui et al., 2016; Noda and Kondo, 2017; Averesch and Krömer, 2018; Wu et al., 2018). Different strategies have been described in order to engineer the central carbon metabolism into this direction (Leonard et al., 2005; Papagianni, 2012; Nielsen and Keasling, 2016). In fact, the available fluxes of both precursors differ considerably. Suástegui et al. (2016) studied the E4P and PEP flux in *S. cerevisiae* using metabolic flux analysis and observed that E4P was clearly the limiting precursor. Therefore, establishing a balance between the ratio of both precursors and increasing their availability appeared to be the two main strategies to follow in order to increase aromatic compounds production.

E4P can be produced from PPP or from sedoheptulose-1,7-bisphosphate in a reaction that is probably favored when the intracellular levels of sedoheptulose-7-phosphate (S7P)are high (Nagy and Haschemi, 2013). S7P is an intermediate in non-oxidative part of PPP, that is produced from xylulose 5-phosphate and ribose 5-phosphate by transketolase. The most common approaches to increase E4P production are the overexpression of transaldolase and transketolase genes, to promote the conversion of S7P and glyceraldehyde-3-phosphate (G3P) to E4P and fructose 6-phosphate (F6P) (Bongaerts et al., 2001; Noda and Kondo, 2017; Averesch and Krömer, 2018) and to enhance the supply of E4P (Lütke-Eversloh and Stephanopoulos, 2007; Bulter et al., 2003). Following this strategy, Knop et al. (2001) observed an increase in the shikimic acid titer, an intermediate of the SMK pathway, from 38 to 52 g L^{-1}, after overexpression of transketolase gene (*tktA*) in *E. coli*. The role of transaldolase for the production of the PPP was analyzed by Lu and Liao (1997) and Sprenger et al. (1998). They observed that the overexpression of *talB* increases the production of DAHP from glucose. Moreover, Lu and Liao (1997) concluded that transketolase is more effective in directing the carbon flux to the aromatic pathway than transaldolase. In fact, the overexpression of the transaldolase gene in strains which already overexpress the transketolase gene did not show a further increase in production of aromatic compounds. This result may be related with the saturation of E4P supply when *tktA* was overexpressed (Lu and Liao, 1997). Nevertheless, the overexpression of the transketolase gene proved to have a limited impact in the E4P poll which can be correlated with the preference of this enzyme for catalyzing the E4P consuming reaction (Curran et al., 2013). Other efforts to increase the carbon flux in the PPP include the overexpression of the gene coding for glucose-6-phosphate dehydrogenase, that has been shown to increase the availability of ribulose-5-phosphate (R5P) and E4P (Yakandawala et al., 2008; Rodriguez et al., 2013) or the deletion of genes that encode the phosphoglucose isomerase, that forces the cell to metabolize the substrate completely via PPP (Mascarenhas et al., 1991). However, the later approach blocks the oxidative shunt of the PPP, which is the main source of the redox cofactor NADPH, required by the shikimate dehydrogenase as well as by many enzymes in downstream pathways (Zhang J. et al., 2015). The use of other carbon sources that have different transporters, such as hexoses (as sucrose and gluconate), pentoses (xylose and arabinose) and glycerol (Kai Li and Frost, 1999; Ahn et al., 2008; Martínez et al., 2008; Chen et al., 2012), is also an alternative way to increase the E4P poll. In the last year, Liu et al. (2019b) proposed a different strategy to increase the scarcity of E4P in *S. cerevisiae*. They investigated a heterologous phosphoketolase (PHK) pathway, including a phosphoketolase from *Bifidobacterium breve* (*Bbxfpk*) and a phosphotransacetylase from *Clostridium kluyveri* (*Ckpta*). Phosphoketolase is able to split fructose-6-phosphate into E4P and acetyl-phosphate, and the introduction of this pathway could, theoretically, divert part of the carbon flux from glycolysis directly toward E4P. The authors observed a 5.4-fold enhance in E4P concentration in the *BbXfpk*-expressing strain. When compared with the overexpression of the transketolase-encoding gene, this approach resulted in a lower E4P availability (Liu et al., 2019b). However, none of these strategies were able to efficiently divert carbon flux from glycolysis toward E4P, to provide sufficient levels for the biosynthesis of aromatic compounds.

The availability of the other precursor, PEP, is also an important factor that needs to be considered when designing a strategy to construct a strain able to produce aromatic compounds (Rodriguez et al., 2013; Noda and Kondo, 2017). PEP is required for the simultaneous uptake and phosphorylation of glucose (PEP:glucose phosphotransferase system – PTS)

and it is also involved in reactions catalyzed by the enzymes phosphoenolpyruvate carboxylase and pyruvate kinase that catalyzes the ATP-producing conversion of PEP to pyruvate. The glucose transport by PTS is the main PEP consuming activity and for this reason the construction of PTS-deficient strains is one of the most common approaches to increase PEP availability and therefore, aromatic compounds yield from glucose (Gu et al., 2012, 2013). However, the main problem of this strategy is the low cellular growth rate. The use of a non-PTS system which does not consume PEP is an alternative way to allow high PEP availability (Sprenger et al., 1998; Chandran et al., 2003). For example, glucose can be transported by galactose permease (encoded by *galP*) and further phosphorylated by glucokinase (encoded by *glk*) (Yi et al., 2003; Balderas-hernández et al., 2009). Additionally, Yi et al. (2003) described the utilization of a glucose facilitator from *Zymomonas mobilis* (encoded by *glf*), that transports glucose by facilitated diffusion, in combination with plasmid-localized *Z. mobilis glk* (encoded glucokinase), attaining a 3-dehydroshikimic acid (a key intermediate for aromatic compounds production) production of 60 g L^{-1}, in *E. coli*. In 2011, Ikeda et al. (2011) identified a new non-PTS system, a *myo*-inositol-induced transporter (encoded by *iolT1*) in *C. glutamicum*. Furthermore, an increase in the PEP availability has been achieved by modulation of the carbon flux from PEP to the tricarboxylic acid cycle (TCA) by inactivation of pyruvate kinase genes (Gosset et al., 1996; Chandran et al., 2003; Escalante et al., 2010) and PEP carboxylase (Tan et al., 2013). On the other hand, the overexpression of the genes that encode PEP synthetase which catalyzes the conversion of pyruvate into PEP, enhanced its level (Patnaik and Liao, 1994; Tatarko and Romeo, 2001). PEP carboxykinase catalyzes the formation of PEP from oxaloacetate. The overexpression of the gene that encodes it – *pckA* – has also been proposed as a strategy to increase the yield of aromatic amino acids (Gulevich et al., 2006). An interesting approach to enhance the PEP availability is the attenuation of CsrA, a protein that regulates transcription of genes involved in carbon metabolism and energy metabolism (Wang et al., 2013). It was found that the absence of CsrA could enhance the metabolic flow of gluconeogenesis, contributing to the accumulation of PEP. Tatarko and Romeo (2001) knocked out the *csraA* gene and observed an increase in the PEP concentration. The overexpression of *csrB*, a small untranslated RNA from the carbon storage regulator, also improves the availability of PEP in *E. coli* (Yakandawala et al., 2008).

Notwithstanding the progress achieved, the industrial application of these strategies still poses some problems. The redirection of the carbon flux into a desired pathway usually results in a reduced cell growth rate and/or production of unwanted by-products (Patnaik et al., 1992) which usually ruins the economic viability of an eventual industrial process as will be further discussed (section "Discussion").

After the establishment of an adequate supply of precursors it is essential to redirect this carbon toward the SKM pathway and remove limiting steps to increase the production of target compounds. The SKM pathway is highly complex. It is mainly regulated at the transcription and enzymatic activity level. As previously described, the first step of the SKM pathway is the DAHP production, catalyzed by DAHP synthases. This is one of the most strictly regulated steps in this route (**Figure 1**). In fact, DAHP synthase activity is regulated by the concentration of the downstream reaction products of the SKM pathway, the aromatic amino acids. This mechanism is a clever way for cells to make just the right amount of product. When the concentration of aromatic amino acids is high, they will block the DAHP synthase activity, preventing its production until the existing supply has been used up (Bongaerts et al., 2001; Gosset, 2009; Gottardi et al., 2017). In *S. cerevisiae*, two DAHP synthase isozymes (encoded by *ARO3* and *ARO4* genes) are feedback inhibited by L-Phe and L-Tyr, respectively (Paravicini et al., 1989). *E. coli* has three different DAHP synthase isozymes (encoded by *aroF, aroG, aroH*), and each one is vulnerable to inhibition by an aromatic amino acids: L-Phe, L-Tyr and L-Trp, respectively (Hu et al., 2003; Gu et al., 2012). In addition to the allosteric inhibition, it is also necessary to take into account the transcriptional repression mediated by the protein TyrR (tyrosine repressor). This can repress *aroF* and *aroG,* whereas the transcription of *aroH* is controlled by the protein TrpP (tryptophan repressor) (Pittard et al., 2005; Keseler et al., 2013). In *C. glutamicum*, the DAHP synthase isozymes are encoded by *aroG* and *aroF. AroG* is feedback inhibited by L-Phe, chorismate and prephenate, whereas *aroF* is feedback inhibited by L-Tyr and L-Trp (Lee et al., 2009).

To overcome this natural limitation, different strategies have been described, such as the use of DAHP synthase which is not sensitive to feedback-inhibition (feedback-resistant – fbr) (Frost and Draths, 1995). Shumilin et al. (1999) determined a 3D structure of DAHP synthase co-crystallized with PEP, demonstrating the possible nine binding sites of L-Phe for feedback-inhibition. Random or directed mutagenesis at these specific amino acids residues, such as Asp146Asn, and Pro150Leu (Kikuchi et al., 1997), is the most common approach used to generate feedback-resistant variants of DAHP synthase. Hartmann et al. (2003) determined the crystal structure of Aro4p and demonstrated that with a single lysine-to-leucine substitution at position 229, the protein is L-Phe and L-Tyr insensitive. In combination with the deletion of *ARO3,* this strategy led to a 4-fold increase in the flux through the aromatic amino acid-forming pathway (Luttik et al., 2008). Similarly, the introduction of a tyrosine-insensitive *ARO4* allele ($ARO4^{G226S}$) was also reported by Schnappauf et al. (1998). In *E. coli* a similar approach was also described with the introduction of feedback-resistant derivatives of $aroF^{fbr}$ and $aroG^{fbr}$, using either plasmids or chromosomal integration for expression of the modified encoding genes (Ger et al., 1994; Jossek et al., 2001). In this context, the reactions catalyzed by 3-dehydroquinate synthase, shikimate kinase and shikimate 5-dehydrogenase are also considered rate-limiting (Dell and Frost, 1993; Kramer et al., 2003; Oldiges et al., 2004; Juminaga et al., 2012). Different strategies have been applied to overcome these limitations, such as: the overexpression of the genes that encode these enzymes by plasmid-cloned genes, their chromosomal integration, promoter engineering by chromosomal evolution, or co-expression of the genes in a modular operon under control of diverse promoters (Chandran et al., 2003; Lütke-Eversloh and Stephanopoulos, 2005; Escalante et al., 2010; Rodriguez et al., 2013; Cui et al., 2014).

Another regulatory point is present at the chorismate branch, at which the chorismate mutase and prephenate dehydratase are feedback regulated by the end products, L-Phe and L-Try (Lütke-Eversloh and Stephanopoulos, 2005; Reifenrath et al., 2018). The most common strategies to overcome this bottleneck are the application of mutations that confer feedback resistance to chorismate mutase-prephenate dehydratase or the utilization of evolved genes (*pheA*^{ev}) (Báez-Viveros et al., 2004; Lütke-Eversloh and Stephanopoulos, 2005; Ikeda, 2006; Sprenger, 2007; Luttik et al., 2008). Backman et al. (1990) used a recombinant *E. coli* strain carrying *pheA*^{fbr} and *aroF*^{fbr} for L-Phe production and achieved a titer of 50 g L^{-1} with a yield of 0.25 (mol L-Phe mol glucose^{-1}) after 36 h. This is the highest titer reported so far. Furthermore, Báez-Viveros et al. (2004) observed that the overexpression of evolved genes (*pheA*^{ev}) had a positive and significant impact on L-Phe production in *E. coli*, showing a 3–4-fold improvement, when compared with equivalent strains expressing *pheA*^{fbr}. The use of L-Tyr- or L-Phe-overproducing strains for the production of some aromatic compounds, derived from aromatic amino acids, has been reported by many authors. For their construction, the most common approaches include overexpression of *aroG*^{fbr} and *tyrA*^{fbr} and in some cases *ppsA, tktA* and the deletion of *tyrR* (Kang et al., 2012; Lin and Yan, 2012; Santos et al., 2012; Huang et al., 2013), achieving L-Phe and L-Try titers of 50 and 55 g L^{-1}, respectively (Patnaik and Liao, 1994; Ikeda, 2006; Sprenger, 2007). However, most of the studies that have been performed, reported the expression and/or regulation of key genes, under the control of constitutively expressed or inducible promoters in plasmid-cloned operons. Nevertheless, this approach has several drawbacks, ranging from structural and segregational instability to metabolic burden of plasmid replication (Noack et al., 1981; Bentley et al., 1990). To overcome these drawbacks, Cui et al. (2014) developed a plasmid free methodology for shikimic acid production, an important intermediate of the SKM pathway, in *E. coli*. *AroG*^{fbr}, *aroB, aroE,* and *tktA* genes were chromosomally integrated by tuning the copy number and expression using chemically induced chromosomal evolution with triclosan. They also overexpressed the *ppsA* and *csrB* genes to enhance the PEP/pyruvate pool. Finally, *pntAB* or *nadK* genes were also chromosomally overexpressed in order to increase the NADPH pull. The final strain was able to produce 3.12 g L^{-1} of shikimic acid with a glucose yield of 0.33 mol mol^{-1}. They also demonstrated that the overexpression of *pntAB* or *nadK* genes increase the NADPH availability. This is the first report of an engineered shikimic acid producing strain of *E. coli* that lacks both a plasmid and an antibiotic marker.

Despite the efforts that have been made, it is also important to study different strategies to minimize carbon loss to competing pathways. Gu et al. (2012) reported an increase in L-Trp concentration after a knock out in the gene *tnaA*, which codes for a tryptophanase to avoid product degradation. On the other hand, the modification of aromatic compounds transport system, as the inactivation of permease genes *aroP*, *mtr* and *tnaB* to avoid product re-internalization, or the overexpression of genes that encodes exporter proteins (e.g., *yddG*), can also be used as interesting approaches to increase its production (Liu et al., 2012; Wang et al., 2013). Rodriguez et al. (2013) demonstrated that the inactivation of *ydiB* (coding for shikimate dehydrogenase/quinate dehydrogenase) leads to a decrease in byproduct formation, improving the carbon flux toward the desired aromatic compound production.

STRATEGIES FOR PRODUCTION OF AROMATIC COMPOUNDS

In the last decade, several attempts to implement the production of aromatic compounds in cells have been reported (Bongaerts et al., 2001; Dias et al., 2017; Lee and Wendisch, 2017; Beata et al., 2019). The first studies focused on the identification of the microorganisms that are able to produce, natively, aromatic compounds, such as 2-phenylethanol, and/or metabolites that are biosynthetic precursors or derivatives of aromatic compounds, such as SKM, chorismate (CHO), and aromatic amino acids (L-Phe, L-Tyr and Trp), with high efficiency. Then, engineered strains were developed and the production processes optimized in order to raise the product titer to g L^{-1}-scale. Nowadays, microbial hosts are able to produce a large spectrum of target products, including chemicals they do not naturally produce (Pandey et al., 2016; Wang et al., 2016).

In this section, we will focus on illustrating the current strategies described for producing aromatic compounds, beginning with the products that are considered industrial building blocks, as salicylic acid, *p*-hydroxybenzoic acid, *p*-coumaric acid, cinnamic acid, ferulic acid and 2-phenylethanol. A brief overview of some relevant aromatic compounds that are widely used as fine chemicals, such as vanillin, will be further presented.

Salicylic acid (SLA) (2-hydroxybenzoic acid) is a valuable aromatic compound that can be obtained from CHO (Lin et al., 2014; Jiang and Zhang, 2016). SLA is an important drug precursor mainly used to produce acetylsalicylic acid, widely applied as a non-steroidal anti-inflammatory drug, in the treatment of fever, pain, aches and inflammations (Vane and Botting, 2003). Isochorismate synthase (ICS) converts CHO to isochorismate and then isochorismate pyruvate lyase (IPL) converts isochorismate into SLA (Serino et al., 1997; **Figure 2**). Lin et al. (2013) attained an SLA titer of 158 mg L^{-1} in *E. coli* after the expression of *entC* from *E. coli* (ICS step) and *pfpchB* from *P. fluorescens* (IPL step), as an operon. Lin et al. (2014) further improved the metabolic flux toward SLA using a medium copy number plasmid, pCA-APTA, to express *aroL*, *ppsA*, *tktA* and *aroG*^{fbr}, under the control of an IPTG-inducible promoter ($P_L$lacO1), attaining an SLA titer of 1.2 g L^{-1}, using glycerol as carbon source. Noda et al. (2016) reported the highest SLA titer to the date, 11.5 g L^{-1} (**Table 1**), with a yield of 41.1 % from glucose, after enhancing the availability of PEP in *E. coli*. They removed the endogenous PEP consuming PTS, that was replaced by GalP/Glk system, as well as the genes responsible for the conversion of PEP to pyruvate (*pykF* and *pykA*). Finally, the strain was further modified by the introduction of *menF* from *E. coli* (ICS step) and *pchB* from *P. aeruginosa* (IPL step). In that report, an 8-fold increase in SLA

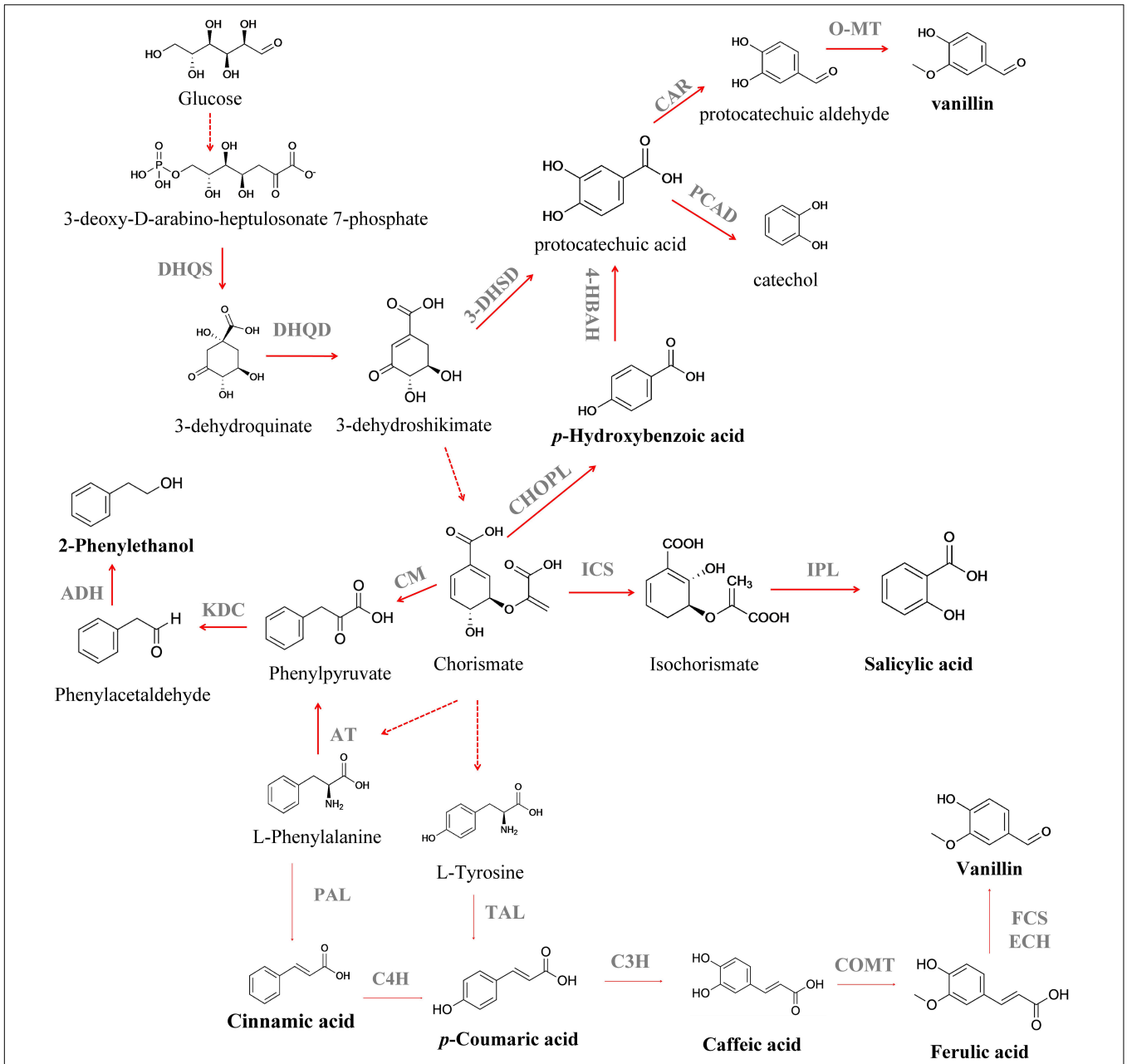

FIGURE 2 | Biosynthesis of different aromatic compounds derived from the extended shikimate pathway. DHQS, 3-dehydroquinate synthase; DHQD, 3-dehydroquinate dehydratase; 3-DHSD, 3-dehydroshikimate dehydratase; CAR, carboxylic acid reductase; PCAD, protocatechuic acid decarboxylase; O-MT, *O*-methyltransferase; ICS, isochorismate synthase; CHOPL, chorismate pyruvate lyase; IPL, isochorismate pyruvate lyase; 4-HBAH, 4-hydroxybenzoic acid hydroxylase; CM, chorismate mutase; KDC, phenylpyruvate decarboxylase; ADH, alcohol dehydrogenase; PAL, phenylalanine ammonia lyase; C4H, cinnamate 4-hydroxylase; TAL, tyrosine ammonia lyase; FCS, feruloyl-CoA synthetase; ECH, feruloyl-CoA hydratase/lyase; C3H, *p*-coumarate 3-hydroxylase; AT, aminotransaminase. Solid lines indicate a single step; dotted lines indicate multiple steps.

concentration (from 1.4 to 11. 5 g L^{-1}) was attained after the process scale up to 1-L jar fermenter. These findings demonstrate the importance of balancing the plasmid copy number and the impact of deleting the genes from SKM pathway in cell growth and production titers. However, the SA toxicity toward the producing cell remains a challenge, and it is necessary to develop more resistant strains or explore alternative chassis that naturally exhibit high tolerance toward toxic compounds, as *Pseudomonas aeruginosa* (Jiménez et al., 2002; Nikel and de Lorenzo, 2018). The microbial production of *p*-hydroxybenzoic acid (PHBA) can also be achieved from CHO by chorismate pyruvate lyase (**Figure 2**). This aromatic compound is used as a building block for liquid crystal polymers and for antibacterial parabens – a key group of compounds used as food preservatives (Barker and

Frost, 2001), with an estimated market value of $150 million per year (Krömer et al., 2013). Nowadays, PHBA is chemically synthesized from benzene via cumene and phenol (Heinz-Gerhard and Jurgen, 2012). The biotechnological production of PHBA has already been described in plants, like tobacco (*Nicotiana tabacum L.)* and potato (*Solanum tuberosum* L.) (Köhle et al., 2003), in *E. coli* (Barker and Frost, 2001), *Klebsiella pneumoniae* (Müller et al., 1995), *C. glutamicum* (Kallscheuer and Marienhagen, 2018), and *P. putida* (Verhoef et al., 2007), using glucose as carbon source or with complex mixtures such as sugar cane (Mcqualter et al., 2005). Barker and Frost (2001) reported PHBA production in *E. coli* after overexpression of $aroF^{fbr}$ (feedback-inhibition resistant DAHP synthase), as well as the genes involved in the SKM pathway (*tktA*, *aroA*, *aroL*, *aroC*, and *aroB*) and encoding chorismate pyruvate lyase (*ubiC*, that was expressed in a plasmid under the control of a tac promoter). A PHBA yield of 12 g L^{-1} was obtained in a fed-batch fermentation. The application of an *E. coli–E. coli* co-culture system was recently reported by Zhang H. et al. (2015) for PHBA production from glucose and xylose, a sugar mixture that can be derived from lignocellulose. The authors reported a 8.6-fold improvement in PHBA production when its biosynthesis was switched from the monoculture strategy to the co-culture strategy. Finally, a fed-batch bioreactor was used to scale up the PHBA production and under this new condition its titer was improved to 2.3 g L^{-1}. The production of this aromatic compound in yeast was described for the first time by Krömer et al. (2013). The authors reported a PHBA titer of 90 mg L^{-1} in *S. cerevisiae* after overexpression of an *ubiC* from *E. coli* and deletion of *ARO7* and *TRPp3*, avoiding the biosynthesis of aromatic amino acids. To increase the flux to chorismate, they expressed $ARO4^{K229L}$ and *aroL*. This strain was then used and allowed a PHBA formation from CHO, with a titer of 2.9 g L^{-1} and yield of 3.1 mg $g_{glucose}^{-1}$, in a fed-batch process (Averesch et al., 2017). To date, the highest PHBA titer was reported by Kitade et al. (2018) in *C. glutamicum* (**Table 1**). This was achieved by chromosomal integration of *aroG* from *E. coli* and wild-type *aroCKB* from *C. glutamicum*, encoding chorismate synthase, shikimate kinase, and 3-dehydroquinate synthase. In order to convert CHO to HPBA a highly HPBA-resistant chorismate pyruvate lyase (encoded by *ubiC*) from the intestinal bacterium *Providencia rustigianii* was used. In order to increase product formation, the synthesis of by-products was also reduced by deleting *hdpA* and *pyk*. The final strain produced 36.6 g L^{-1} of PHBA from glucose after 24 h, with a glucose yield of 40 % (mol mol^{-1}). Despite the efforts that have been made to increase the production yields and concentration of PHBA, the obtained results still fall behind those benchmarks from an industrial perspective. In fact, PHBA itself could also be toxic to the cells at high concentrations and the application of *in situ* product removal (ISPR) strategies will lead to a continuous PHBA removal from the fermentation broth. An interesting approach was presented by Johnson et al. (2000) that applied an *in situ* product removal technique for PHBA production with *E. coli* using Amberlite IRA-400 as adsorbent, and observed an increase in the PHBA titer from 6 to 22.9 g L^{-1}. In the future, further improvements in the biotechnological process will be necessary, such as the utilization of low-cost substrates, as residues and wastes, as well as the development of a "green" downstream process, to pique the industry interest in these processes.

Hydroxycinnamic acids are an important class of hydroxylated aromatic acids that contain a phenol ring and at least one organic carboxylic acid group. This group of compounds includes *p*-coumaric acid, caffeic acid and ferulic acid, among others. *p*-Coumaric acid is an important platform chemical used as monomer of liquid crystal polymers for electronics (Kaneko et al., 2006), as well as precursor for the synthesis of polyphenols (Rodriguez et al., 2015). The route for their production starts with L-Phe and L-Tyr deamination to further produce the phenylpropanoid cinnamic acid and *p*-coumaric acid, respectively, by the activity of phenylalanine ammonia lyase (PAL) (MacDonald and D'Cunha, 2007) and tyrosine ammonia lyase (TAL) (Nishiyama et al., 2010; **Figure 2**). The enzyme P450 monooxygenase cinnamate 4-hydroxylase (C4H) can further oxidize the cinnamic acid yielding the *p*-coumaric acid (Rasmussen et al., 1999; Achnine et al., 2004). The heterologous expression of TAL and PAL/TAL encoding genes allowed the *p*-coumaric acid production in *E. coli*, *S. cerevisiae*, *Streptomyces lividans* and *P. putida* (**Table 1**; Nijkamp et al., 2007; Trotman et al., 2007; Vannelli et al., 2007; Kawai et al., 2013; Rodriguez et al., 2015; Vargas-Tah and Gosset, 2015). However, due to their low activity, first studies reported its production from culture medium supplemented with L-Phe or L-Tyr (Ro and Douglas, 2004; Hwang et al., 2003; Watts et al., 2004; Jendresen et al., 2015; Mao et al., 2017). Efforts have also been made to find enzymes from different sources with higher PAL or TAL activity (Nijkamp et al., 2005, 2007; Vannelli et al., 2007; Kang et al., 2012; Jendresen et al., 2015). *p*-Coumaric acid production from a simple carbon source, such as glucose, is desirable. In order to achieve this, *S. cerevisiae* was genetically modified (Vannelli et al., 2007). The encoding PAL/TAL gene from *Rhodotorula glutinis* (expressed under the control of the galactose promoter) was used due to its higher affinity toward L-Tyr compared to L-Phe. The heterologous expression of a C4H gene from *Helianthus tuberosus* allowed its production via the PAL route. More recently, Li et al. (2018) proposed the *p*-coumaric acid production from glucose via phenylalanine in *E. coli*. They expressed the C4H-encoding gene from *Lycoris aurea* and PAL1 of *Arabidopsis thaliana*, under a trc promoter induced by IPTG, attaining a titer of 25.6 mg L^{-1} in shake flasks, after the regulation of the intracellular level of NADPH. The authors observed that the level of intracellular NADPH has a strong impact on the conversion of *trans*-cinnamic acid into *p*-coumaric acid and different strategies were tested in order to increase the level of intracellular NADPH. When *pntAB*, that encodes a membrane-bound transhydrogenase that catalyzes the NADH to NADPH conversion, was overexpressed under the control of a T7 constitutive promoter and the synthetic small regulatory RNA (srRNA) anti(SthA) was used to specifically repress the translation of the soluble transhydrogenase SthA, a synergetic positive effect was observed on the *de novo* production of *p*-coumaric acid. To date, the highest *p*-coumaric acid titer, 2.4 g L^{-1}, has been achieved in *S. cerevisiae* after overexpression

of the encoding TAL gene from *Flavobacterium johnsoniae;* overexpression of *aroL* from *E. coli*, under control of the P-TEF promoter; overexpression of $Aro7^{G141S}$ and $Aro4^{K229L}$ from *S. cerevisiae* under control of the promoters P-TEF and P-PGK1, respectively and deletion of *Aro10* and *Pdc5* genes (Rodriguez et al., 2017; **Table 1**). However, it is also important to explore the application of other raw materials derived from biomass as carbon sources – see section "Discussion." Vargas-Tah and Gosset (2015) managed to produce cinnamic acid and *p*-coumaric acid in *E. coli* using lignocellulosic hydrolysates as complex carbon source. However, other strains that grow naturally on complex carbon sources were also used in the production of these hydroxycinnamic acids, such as *Streptomyces lividans* (Noda et al., 2011, 2012; Kawai et al., 2013) with product concentrations ranging from 130 to 736 mg L^{-1}. In the last year, Borja et al. (2019) constructed a *S. cerevisiae* strain that uses xylose as sole carbon source for *p*-coumaric acid production, attaining a titer of 242 mg L^{-1}, that represents a 45-fold increase over their condition with glucose (5.25 mg L^{-1}) (**Table 1**). To construct this strain, they knocked out *Aro10* and *Pdc5* genes, in order to reduce the byproduct formation, and overexpressed the encoding TAL gene from *F. johnsoniae* and *aroL* from *E. coli.* To increase the carbon flux through the aromatic amino acid pathway they overexpress $Aro7^{fbr}$ (feedback-inhibition resistant DAHP synthase) and $Aro4^{fbr}$ (feedback-inhibition resistant chorismite mutase). Another important issue detected in these studies is the toxic effect of *p*-coumaric acid to the producing cells. An alternative strategy was proposed by Huang et al. (2013), that involves pulse feeding to avoid the accumulation of *p*-coumaric acid to a toxic level. The resistance to toxic compounds can also be increased using membrane transport engineering as a method to decrease the intracellular concentration of a toxic compound. In *E. coli*, the overexpression of *aaeXAB* gene, that encodes an efflux pump for several aromatic compounds, resulted in a twofold increase in tolerance to *p*-coumaric acid (Dyk et al., 2004; Sariaslani, 2007). Caffeic acid is another important intermediate of the phenylpropanoid metabolism. It serves as a precursor for the synthesis of caffeoyl alcohol and 3,4-dihydroxystyrene (monomer for plastic synthesis) (Zhang and Stephanopoulos, 2013). Caffeic acid is biosynthesized by hydroxylation of *p*-coumaric acid through *p*-coumarate 3-hydroxylase (C3H) (Berner et al., 2006; **Figure 2**). First studies have reported microbial caffeic acid production with medium supplementation of the precursors such as L-Tyr and *p*-coumaric acid (Sachan et al., 2006; Choi et al., 2011). In order to produce it directly from *p*-coumaric acid, it is necessary to express the genes that encode enzymes with suitable ring 3-hydroxylation activity (Berner et al., 2006; Furuya et al., 2012). In fact, one of the major difficulties in the heterologous expression of genes of the plant phenylpropanoid pathway in *E. coli* is the lack of cytochrome P450 reductase activity making the search for alternative strategies essential. Choi et al. (2011) identified that the *sam5* gene from *Saccharothrix espanaensis* encodes C3H, that is a FAD-dependent enzyme. This enzyme was then used to produce caffeic acid in *E. coli*, demonstrating the feasibility of this two-step pathway to produce caffeic acid using alternative enzymes. It was also demonstrated that a bacterial cytochrome P450 CYP199A2, from *Rhodopseudomonas palustris,* was able to efficiently convert *p*-coumaric acid to caffeic acid (Hernández-Chávez et al., 2019). Some microorganisms, harboring genes encoding the two sub-units of the enzyme 4-hydroxyphenylacetate 3-hydroxylase (4HPA3H), have proved to be able to act on aromatic compounds (Galán et al., 2000). It was also observed that 4HPA3H is able to convert *p*-coumaric acid into caffeic acid. Based on this Furuya and Kino (2014) expressed the 4HPA3H gene from *Pseudomonas aeruginosa* in *E. coli* and a caffeic acid production of 10.2 g L^{-1} was obtained after repeated additions of *p*-coumaric acid (20 mM each pulse), in a medium with glycerol as carbon source. For caffeic acid biosynthesis from L-Tyr an additional step of non-oxidative deamination, catalyzed by TAL (Rodrigues et al., 2015) is needed, and the first approach is the search for alternative enzymes from different sources. TAL from *R. glutinis* proved to be the most active TAL identified (Vannelli et al., 2007; Santos et al., 2011). However, the production of this compound from simple carbon sources is much more desirable and the production of caffeic acid from glucose and xylose was described (Lin and Yan, 2012; Zhang and Stephanopoulos, 2013). The use of renewable feedstocks, such as lignocellulosic biomass, was also evaluated using *E. coli* as producing host (Kawaguchi et al., 2017). A maximum caffeic acid concentration of 233 mg L^{-1} (**Table 1**) was produced from kraft pulp using a tyrosine-overproducing *E. coli* strain harboring the *hpaBC* gene from *P. aeruginosa* and *fevV* gene from *Streptomyces* sp. WK-5344. Ferulic acid is a component of lignocellulose (De Oliveira et al., 2015). This *O*-methylated hydroxycinnamic acid is biosynthesized from caffeic acid by caffeic acid *O*-methyltransferase (COMT) (**Figure 2**). However, there are few reports about the heterologous production of ferulic acid in microbial hosts. Choi et al. (2011) reported the production of ferulic acid in *E. coli* by expression of *sam5,* a TAL gene from *S. espanaensis* and a COMT gene from *A. thaliana*, under the control of a T7 promoter, attaining a titer of 0.1 mg L^{-1} from L-Tyr. Later, Kang et al. (2012) engineered an *E. coli* strain capable of producing 196 mg L^{-1} of ferulic acid from glucose, after introduction of COMT from *A. thaliana* in a caffeic acid-over-producing strain, containing a codon optimized *tal* gene, under the control of a T7 promoter. This aromatic acid can also be used as substrate for vanillin and coniferyl alcohol biosynthesis (Hua et al., 2007; Lee et al., 2009; Chen et al., 2017). Research efforts have been made in order to make the microbial production of hydroxycinnamic acids a competitive process.

Another important class of aromatic compounds is the aromatic flavors class. The two most popular benzenoid flavors are 2-phenylethanol (2-PE) and vanillin. 2-PE is an aromatic alcohol with a delicate fragrance of rose petals widely used in flavor and fragrances industries (Burdock, 2010; Carlquist et al., 2015). It was recently identified as a potent next generation biofuel (Keasling and Chou, 2008). Furthermore, 2-PE can also be used as raw material to produce other flavor compounds (2-phenylethyl acetate and phenylacetaldehyde) and styrene (Etschmann et al., 2002). Microorganisms can naturally produce 2-PE as part of their amino acid metabolism (Etschmann et al., 2002). This benzoid flavor can be produced through the SKM pathway or via Ehrlich pathway from L-Phe

(Albertazzi et al., 1994; Carlquist et al., 2015; **Figure 2**). Through the Ehrlich pathway, L-Phe is firstly converted to phenylpyruvate by transamination, which is then transformed to phenylacetaldehyde by decarboxylation. Then, the derivative aldehyde is reduced to 2-PE by an alcohol dehydrogenase (Etschmann et al., 2002; **Figure 2**). This is the fastest pathway to produce 2-PE, however cheaper precursors than L-Phe should be used to achieve a more competitive process (ÄYräpää, 1965; Kim T.Y. et al., 2014; Zhang et al., 2014). Thus, *de novo* production of 2-PE has been described in different microorganisms: *Kluyveromyces marxianus* (Kim T.Y. et al., 2014), *E. coli* (Guo et al., 2018; Liu et al., 2018), and *Enterobacter* sp. (Zhang et al., 2014; **Table 1**). The 2-PE production from the SKM pathway is achieved from its end product phenylpyruvate, that is decarboxylated to phenylacetaldehyde, followed by a dehydrogenation that leads to 2-PE production (Etschmann et al., 2002; Carlquist et al., 2015; **Figure 2**).

Nonetheless, the *de novo* synthesis is inefficient since glycolysis and PPP are mainly used for cell growth, producing very low 2-PE concentrations. The most common strategies employed for strain constructions focus on increasing phenylpyruvate decarboxylase and alcohol dehydrogenase activities, which are the rate-limiting enzymes in *de novo* synthesis pathway, in combination with feedback-resistant DAHP synthase and chorismate mutase. Kim B. et al. (2014) overexpressed the *Aro*10, that encodes a transaminated amino acid decarboxylase and *Adh*2, encoding an alcohol dehydrogenase, from *S. cerevisiae* in *K. marxianus* BY25569, under the control of the constitutive promoter *Sc*PGK1/*Sc*TEF1. Then, serial subcultures with an L-Phe analog, *p*-fluorophenylalanine, were conducted in order to obtain an evolved strain resistant to the L-Phe analog. Finally, the expression of *aroG*^{fbr} from *Klebsiella pneumoniae*, that encodes a feedback-resistant mutant of DAHP synthase, was also performed. This genetically modified strain was able to produce 1.3 g L^{-1} of 2-PE from glucose without addition of L-Phe. More recently, Liu et al. (2018) constructed a heterologous pathway from *Proteus mirabilis* in *E. coli* and the recombinant strain was able to produce 1.2 g L^{-1} of 2-PE without L-Phe supplementation (**Table 1**).

Another challenge in the biosynthesis of 2-PE is its toxicity. Different strategies were investigated in order to improve the process yield and productivity, being the most common the optimization of medium composition, operational conditions and application of ISPR techniques (Chung et al., 2000; Hua et al., 2010; Cui et al., 2011; Celińska et al., 2013; Mihal' et al., 2014). 2-PE production is highly dependent on media composition and culture conditions (Garavaglia et al., 2007). The utilization of an interesting alternative carbon source was reported by Celińska et al. (2013). They use glycerol as carbon source in bioconversion of L-Phe to 2-PE by *Yarrowia lipolytica* NCYC3825, reaching a 2-PE production of 0.77 g L^{-1} after 54 h. Another recent approach for this flavor production was reported by Martínez-Avila et al. (2018). In the proposed system, *K. marxianus* ATCC10022 used the available nutrients from a residue-substrate (sugarcane bagasse) supplemented with L-Phe, achieving a 2-PE production of 10.21 mg g^{-1} (mass of product per mass of solid) in a fed-batch system. The application of alternative modes of operation, such as fed-batch and continuous, that allow the possible removal or dilution of 2-PE in the medium, are also interesting approaches recently reported. Last year, *de novo* production of 2-PE by *Metschnikowia pulcherrima* NCYC373 reached higher titers in continuous mode operation, than in batch and fed-batch cultures (Chantasuban et al., 2018). In continuous fermentation, 2-PE concentration levels reached 1.5 g L^{-1}, before it became too toxic and caused the flush out (**Table 1**). Even with the efforts to optimize the culture medium and cultivation conditions, and choose the most producing microorganism, product inhibition is still the major problem of 2-PE biosynthesis (Carlquist et al., 2015). Some strategies, such as ISPR techniques, have been developed to reduce the 2-PE toxicity in the fermentation medium, increasing its production (Carlquist et al., 2015). Recently, Chantasuban et al. (2018) reported the application of oleyl alcohol as an extraction phase in the 2-PE production by *M. pulcherrima* NCYC373. The production levels were enhanced with the application of this ISPR technique, achieving a 2-PE concentration of 1.96 g L^{-1} in the aqueous phase and an overall production of 3.13 g L^{-1}. Gao and Daugulis (2009) reported a highly significant enhancement in the 2-PE production, using a solid-liquid two-phase partition bioreactor with polymer beads as the sequestering immiscible phase. The batch mode system reached a final 2-PE concentration of 13.7 g L^{-1} (88.74 g L^{-1} in the polymer phase and 1.2 g L^{-1} in the aqueous phase), whereas the fed-batch achieved an overall titer of 20.4 g L^{-1} (97.0 g L^{-1} in the polymer phase and 1.4 g L^{-1} in the aqueous phase). During the last years, great improvements have been achieved in the bioproduction of 2-PE leaving its industrial application closer. In fact, 2-PE concentrations of 21 g L^{-1} were reached (Mihal' et al., 2014), in an hybrid system that consists of a fed-batch stirred tank bioreactor and a hollow fiber membrane module immersed at the bottom of the bioreactor, where 2-PE is continuously extracted from the fermentation broth using pentane as the organic phase.

Vanillin (4-hydroxy-3-methoxybenzaldehyde), a widely used flavor compound in different industries, is the primary component of the extract of the vanilla bean. The economic importance of this plant natural product is quite significant; it was reported that synthetic vanillin has a price of around US$ 11 kg^{-1}, while biotech vanillin is sold for a price of around US$ 1000 kg^{-1} (Schrader et al., 2004). Over the last years, vanillin production through biotransformation of ferulic acid, isoeugenol, lignin, was reported, with vanillin titers that range from 0.13 to 32.5 g L^{-1} (Huang et al., 1993; Priefert et al., 2001; Zhao et al., 2005; Kaur and Chakraborty, 2013). Furuya et al. (2015) reported a vanillin concentration of 7.8 g L^{-1} from ferulic acid in a two-stage process with an *E. coli* carrying two expression plasmids harboring *fdc* from *Bacillus pumilus* and *cso2* from *Caulobacter segnis*. However, the vanillin production through these pathways has several bottlenecks that include the price of precursors, the formation of undesired side-products and the cytotoxicity of the precursors (Gallage and Møller, 2015). Based on this, its production by *de novo* biosynthesis from cheap and more available carbon sources is much more attractive.

In the pathway from 3-dehydroshikimate (3-DHS) to vanillin, the first step is the dehydration of 3-DHS to protocatechuic acid, catalyzed by 3-dehydroshikimate dehydratase, that is further converted to protocatechuic aldehyde, by carboxylic acid reductase; and, the final step is catalyzed by an *O*-methyltransferase leading to vanillin (Hansen et al., 2009; **Figure 2**). Li and Frost (1998) were the first to report an engineered pathway for vanillin production in *E. coli*. Here, protocatechuic acid was converted to vanillic acid by catechol-*O*-methyltransferase, and further reduced to vanillin by an aryl aldehyde dehydrogenase. Hansen et al. (2009) explored for the first time the vanillin production in the yeasts *Schizosaccharomyces pombe* and *S. cerevisiae*. The authors introduced a DHS dehydratase (3DSD) from *Podospora pausiceta*, an aromatic carboxylic acid reductase (ACAR) from *Nocardia* sp., a phosphopantetheinyl transferase (PPTase) from *C. glutamicum* to activate ACAR, and an *O*-methyl transferase (OMT) from *Homo sapiens*, allowing a vanillin production of 45 mg L^{-1}. More recently, Kunjapur et al. (2014) used an *E. coli* strain with decreased aromatic aldehyde reduction activity as a host for the biosynthesis of vanillin. A vanillin titer of 119 mg L^{-1} was achieved using an *E. coli* strain expressing a *Bacillus thuringiensis* 3-dehydroshikimate dehydrogenase gene (*asbF*), a *H. sapiens O*-methyltransferase gene (*Hs-S-COMT)* and *Nocardia iowensis* carboxylic acid reductase gene (*car*), that are codon optimized and expressed in a plasmid. They also introduced a feedback-resistant DAHP synthase (encoded by *aroG*) and a phosphopantetheinyl transferase (encoded by *sfp*) from *B. subtilis*, which have been shown to activate CAR.

However, *de novo* vanillin production in recombinant bacteria and yeasts still has challenges that are not only related with product formation itself but also the product toxicity. The major hurdle in the biotechnological production of vanillin is the strong inhibitory effect that this flavor has on microorganism growth (Gallage et al., 2014; Ma and Daugulis, 2014). An interesting approach was proposed by Brochado et al. (2010), in which the natural pathway for vanillin production in plants was mimicked and assembled in *S. cerevisiae*. To overcome the toxicity of vanillin, a gene encoding an uridine diphosphate–glucose glycosyltransferase (UGT) from *Arabidopsis thaliana* was expressed in *S. cerevisiae.* This UGT catalyzes the glycosylation of vanillin and produces a less toxic final product, vanillin-β-d-glucoside (VG). The same strategy was implemented by Ni et al. (2015) allowing a VG production of 500 mg L^{-1}, with a yield of 32 mg $g_{glucose}{}^{-1}$, that is 5-fold higher than the 45 mg L^{-1} reported by Hansen et al. (2009). A different strategy was presented by Yoon et al. (2007) for vanillin production from ferulic acid using an *E. coli* strain harboring a plasmid with *fcs* (feruloyl-CoA synthase) and *ech* (enoyl-CoA hydratase/aldolase) genes from *Amycolatopsis* sp. strain. To reduce the vanillin toxicity, they improved the vanillin-resistance of this strain using NTG mutagenesis as well as a XAD-2 resin to remove the vanillin from the medium. When 50 % (w/v) of XAD-2 resin was used with 10 g L^{-1} of ferulic acid, the vanillin production with the NTG-VR1 mutant strain was 2.9 g L^{-1}, which was 2-fold higher than that obtained without resin. Recently, Luziatelli et al. (2019) reported, for the first time, the vanillin production from ferulic acid using a plasmid free *E. coli* strain, after chromosomal integration of *fcs* and e*ch* genes from *Pseudomonas*. In addition, they also performed an optimization of the bioconversion conditions (namely stirring speed and initial substrate concentration) using a response surface methodology. At the same time, the authors used a two-phase (solid-liquid) system where the substrate was incorporated in a gel matrix (agarose-gel) in order to perform a fixed volume fed-batch approach, for controlled release of ferulic acid. Using this two-phase system, a vanillin titer of 4.3 g L^{-1} was attained in the liquid phase – one of the highest found in the literature for recombinant *E. coli* strains (**Table 1**).

DISCUSSION

The production of aromatic compounds through plant extraction or chemical synthesis is a profitable business that's been in place for quite a few years, now. In order to replace these industrial processes by fermentation based biotechnological processes, these must have clear economic, environmental and/or product wise advantages. From an economic point of view, the advantages have to be significant enough to justify the investment on new industrial equipment.

In general, these processes have a lower environment impact and are able to produce high quality final products when compared to their plant extraction and/or chemical synthesis counterparts (Thompson et al., 2015; Dudnik et al., 2017; Kallscheuer et al., 2019).

One of the advantages of fermentation based processes is the low-cost and abundance of the raw materials – low added value sugars. However, in order to achieve this advantage, the processes must not consider the supply of expensive precursors, antibiotics, inducers, etc... The optimization of the microorganisms in order to produce the desired aromatic compound directly form the substrate is usually a requirement to achieve economic feasibility. This is supported by Li et al. (2018) and Liu et al. (2018) studies – among other examples previously presented (**Table 1**) – showing that the strain engineering toward deregulation of the aromatic amino acids metabolism and an optimal connection of the heterologous pathways to the host metabolism enable aromatic compounds production starting from glucose without any need for supplementation of precursor metabolites.

In recent years, some research effort has been put into replacing the hydrocarbon source for these fermentation processes by residues and waste materials (Vargas-Tah and Gosset, 2015; Martínez-Avila et al., 2018; Borja et al., 2019). Sugars like glucose are abundant low-cost raw materials. On the other the use of waste materials in large scale industrial processes implies assuring a reliable constant supply and usually a pre-treatment step that may add a significant cost to the process. Nevertheless, whenever there is a need to process these wastes in order avoid their environmental impact, a fermentation process that converts them to higher added value products is an alternative worth considering.

Another possible bottleneck for the industrialization of these processes is the cost of the purification step. Microorganisms tend

to produce a mixture of by-products where the compound of interest may be in higher or lower concentration. Although the amount of research put into this field is not always as significant as one would expect, the search for higher titers and the use of ISPR techniques has direct impact on the economic sustainability of these processes (Van Hecke et al., 2014). Moreover, it will also be interesting to study the synergetic application of engineered strains, able to use wastes and residues as substrates, in systems using ISPR techniques, as well as the product recovery and purification (Braga et al., 2018b; Kallscheuer et al., 2019).

Different microorganisms have been used to produce aromatic compounds. The most commonly used hosts are *E. coli*, *S. cerevisiae* and *C. glutamicum*. However, tolerant and thermotolerant microorganisms, as well as a broad spectrum of bacteria were also employed as aromatic compound producers (**Table 1**). The choice of the microorganism employed is always a determinant factor for the outcome of any research project in this field. The exploitation of well established platform organisms, for which metabolic engineering tools are available, is the most common approach. However, it is also important to explore non-model organisms that can naturally produce the desired compounds, even though the available genetic tools are still scarce. For example, the metabolic versatility of *Pseudomonas* as well as it inherent tolerance to toxic compounds, offers an excellent starting point for suppressing the hurdles of using and producing toxic compounds of natural or heterogeneous origin (Krömer, 2016; Lenzen et al., 2019; **Table 1**).

Some aromatic compounds are toxic for the producing host. In order to tackle this obstacle, several alternative strategies have been proposed such as: starting the fermentation with a lower substrate concentration and further additions following its consumption rate (step-wise fed-batch); the use of *in situ* product removal strategies and the application of adaptive evolution to obtain strains with enhanced resistance to toxic products. Aiming at industrial scale operation, the reduction of the production costs is always crucial. In order to reduce the medium cost, chromosomal integration of heterologous genes avoid the use of expensive antibiotics and inducers for plasmid maintenance and inducible expression (Cui et al., 2014).

Nowadays, the microbial production of aromatic compounds is already implemented at industrial scale in economically viable process. Evolva, for instance, has launched a process for vanillin production from glucose with a genetically modified *Schizosaccharomyces pombe* (Vanilla, 2014). Similarly, Solvay has a process for vanillin production with *Streptomyces setonii* from ferulic acid (Muheim et al., 2001). In these cases, the product titers attained are in the order of a hundred g *per* L, and the methodologies for product separation and purification are well established. However, despite the efforts that have been made to increase the production titers with microbial hosts, the concentrations obtained for more complex compounds are still too low (mg and μg *per* L) for an industrial process (**Table 1**), and these molecules are still produced by extraction from natural sources or by chemical synthesis. In fact, it has been predicted that the market value of a bulk chemical is less than \$10 kg^{-1}. On the other hand, fine chemicals are produced in limited volumes (<1000 tons per year) but at relatively high prices (>\$10kg^{-1}) (Joshi and Ranade, 2016). Based on this, at least for now, the commercialization of fine aromatic compounds will emerge with more successes (Cao et al., 2019). The current challenges that still need to be addressed are the metabolic imbalances in the producer strain, the availability of the metabolites required for biomass formation and the product extraction and purification. In a near future it can be expected that with the application of novel synthetic biology approaches, such as CRISPR/Cas9, rational strain engineering, adaptive laboratory evolution and high-throughput screening approaches, it will be possible to render the microbial production of additional aromatic compounds and its derivatives economically viable.

FINAL REMARKS

Production cost is, by far, the main obstacle to overcome in order to industrialize the production of aromatic compounds through fermentation. This explains the two main research goals mentioned throughout this review: the maximization of product titers and the removal of expensive fermentation media ingredients.

The main challenges to address are still the low availability of precursor molecules by the microbial metabolism, the elimination of complex pathway regulations, disruption of competing pathways and the low activity of heterologous enzymes in the microbial hosts. It is expected that with recent technological innovations the engineering of microbial host strains will be faster providing more precursor molecules to increase aromatic compound synthesis. Identification of the most suitable enzymes and their further improvement will also be an important step toward the production of different aromatic chemicals, avoiding the accumulation of undesired intermediates that can be toxic to the microbial host and leading to an increase in the final product titer. Metabolic engineering, system and synthetic biology tools for strain design, together with process engineering strategies have been and will continue to be the main resources applied. In addition, the identification of novel enzymes that catalyze non-natural reactions, or novel synthetic pathways not found in nature, allow the production of the desired molecule with a high yield or a non-natural compound with possibly superior or new therapeutic properties.

Overall, the paradigm moves toward the development of better microbial chassis and new metabolic pathways that allow the shift from producing aromatic compounds from fossil resources to a bio-based production. The authors consider that now, the biotechnological production of aromatics is not a question of whether or not it is theoretically possible, but of when will it become technically and economically feasible.

AUTHOR CONTRIBUTIONS

AB and NF contributed to the conception and design of the study. AB reviewed the literature, extracted the data, and drafted the manuscript. NF edited the manuscript. Both authors read and approved the submitted version.

REFERENCES

Achnine, L., Blancaflor, E. B., Rasmussen, S., Dixon, R. A., Division, P. B., Roberts, S., et al. (2004). Colocalization of L -Phenylalanine ammonia-lyase and cinnamate 4-Hydroxylase for metabolic channeling in Phenylpropanoid biosynthesis. *Plant Cell* 16, 3098–3109. doi: 10.1105/tpc.104.024406.pathways

Ahn, J. O., Lee, H. W., Saha, R., Park, M. S., Jung, J. K., and Lee, D. Y. (2008). Exploring the effects of carbon sources on the metabolic capacity for shikimic acid production in *Escherichia coli* using in silico metabolic predictions. *J. Microbiol. Biotechnol.* 18, 1773–1784. doi: 10.4014/jmb.0700.705

Albertazzi, E., Cardillo, R., Servi, S., and Zucchi, G. (1994). Biogeneration of 2-phenylethanol and 2-phenylethylacetate important aroma components. *Biotechnol. Lett.* 16, 491–496. doi: 10.1007/BF01023331

Averesch, N. J. H., and Kayser, O. (2014). Assessing heterologous E xpression of Hyoscyamine 6-β-Hydroxylase - a feasibility study. *Proc. Chem.* 13, 69–78. doi: 10.1016/j.proche.2014.12.008

Averesch, N. J. H., and Krömer, J. O. (2018). Metabolic engineering of the shikimate pathway for production of aromatics and derived compounds—present and future strain construction strategies. *Front. Bioeng. Biotechnol.* 6:32. doi: 10.3389/fbioe.2018.00032

Averesch, N. J. H., Prima, A., and Kro, J. O. (2017). Enhanced production of para -hydroxybenzoic acid by genetically engineered *Saccharomyces cerevisiae*. *Bioprocess Biosyst. Eng.* 40, 1283–1289. doi: 10.1007/s00449-017-1785-z

ÄYräpää, T. (1965). Tthe formation of phenethyl alcohol from 14C-labelled Phenylalanine. *J. Inst. Brew.* 71, 341–347. doi: 10.1002/j.2050-0416.1965.tb02068.x

Backman, K., Oconnor, M. J., Maruya, A., Rudd, E., McKay, D., Balakrishnan, R., et al. (1990). Genetic engineering of metabolic pathways applied to the production of phenylalanine. *Ann. N. Y. Acad. Sci.* 589, 16–24. doi: 10.1111/j.1749-6632.1990.tb24231.x

Báez-Viveros, J., Osuna, J., Hernández-Chávez, G., Soberón, X., Bolívar, F., and Gosset, G. (2004). Metabolic engineering and protein directed evolution increase the yield of L-phenylalanine synthesized from glucose in *Escherichia coli*. *Biotechnol. Bioeng.* 87, 516–524. doi: 10.1002/bit.20159

Balderas-hernández, V. E., Sabido-ramos, A., Silva, P., Cabrera-valladares, N., Hernández-chávez, G., Báez-, J. L., et al. (2009). Metabolic engineering for improving anthranilate synthesis from glucose in *Escherichia coli*. *Microb. Cell Fact.* 12, 1–12. doi: 10.1186/1475-2859-8-19

Barker, J. L., and Frost, J. W. (2001). Microbial synthesis of p-hydroxybenzoic acid from glucose. *Biotechnol. Bioeng.* 76, 376–339.

Beata, Ż, Niemczyk, E., and Lipok, J. (2019). Metabolic relation of cyanobacteria to aromatic compounds. *Appl. Microbiol. Biotechnol.* 103, 1167–1178. doi: 10.1007/s00253-018-9568-2

Bentley, W. E., Mirjalili, N., Andersen, D. C., Davis, R. H., and Kompala, D. S. (1990). Plasmid-encoded protein: the principal factor in the "metabolic burden" associated with recombinant bacteria. *Biotechnol. Bioeng.* 35, 668–681. doi: 10.1002/bit.260350704

Berner, M., Krug, D., Bihlmaier, C., Vente, A., Mu, R., and Bechthold, A. (2006). Genes and enzymes involved in Caffeic acid biosynthesis in the actinomycete *Saccharothrix espanaensis*. *J. Bacteriol.* 188, 2666–2673. doi: 10.1128/JB.188.7.2666

Bongaerts, J., Krämer, M., Müller, U., Raeven, L., and Wubbolts, M. (2001). Metabolic engineering for microbial production of aromatic amino acids and derived compounds. *Metab. Eng.* 3, 289–300. doi: 10.1006/mben.2001.0196

Borja, G. M., Rodriguez, A., Campbell, K., Borodina, I., Chen, Y., and Nielsen, J. (2019). Metabolic engineering and transcriptomic analysis of *Saccharomyces cerevisiae* producing p-coumaric acid from xylose. *Microb. Cell Fact.* 18, 1–14. doi: 10.1186/s12934-019-1244-1244

Borodina, I., and Nielsen, J. (2014). Advances in metabolic engineering of yeast *Saccharomyces cerevisiae* for production of chemicals. *Biotechnol. J.* 9, 609–620. doi: 10.1002/biot.201300445

Braga, A., Ferreira, P., Oliveira, J., Rocha, I., and Faria, N. (2018a). Heterologous production of resveratrol in bacterial hosts: current status and perspectives. *World J. Microbiol. Biotechnol.* 34:122. doi: 10.1007/s11274-018-2506-2508

Braga, A., Silva, M., Oliveira, J., Silva, A. R., Ferreira, P., Ottens, M., et al. (2018b). An adsorptive bioprocess for production and recovery of resveratrol with *Corynebacterium glutamicum*. *J. Chem. Technol. Biotechnol.* 93, 1661–1668. doi: 10.1002/jctb.5538

Brochado, A., Matos, C., Møller, B. L., Hansen, J., Mortensen, U. H., and Patil, K. (2010). Improved vanillin production in baker's yeast through in silico design. *Microb. Cell Fact.* 9:84. doi: 10.1186/1475-2859-9-84

Bulter, T., Bernstein, J. R., and Liao, J. C. (2003). A perspective of metabolic engineering strategies: moving up the systems hierarchy. *Biotechnol. Bioeng.* 84, 815–821. doi: 10.1002/bit.10845

Burdock, G. A. (2010). *Flavor Ingredients*, 6th Edn. Boca Raton, FL: Fenaroli's Handbook CRC Press.

Cao, M., Gao, M., Suastegui, M., Mei, Y., and Shao, Z. (2019). Building microbial factories for the production of aromatic amino acid pathway derivatives: from commodity chemicals to plant-sourced natural products. *Metab. Eng.* doi: 10.1016/j.ymben.2019.08.008 [Epub ahead of print],

Carlquist, M., Gibson, B., Yuceer, Y. K., Paraskevopoulou, A., Sandell, M., Angelov, A. I., et al. (2015). Process engineering for bioflavour production with metabolically active yeasts – a mini-review. *Yeast* 32, 123–143. doi: 10.1002/yea.3058

Celińska, E., Kubiak, P., Białas, W., Dziadas, M., and Grajek, W. (2013). Yarrowia lipolytica: the novel and promising 2-phenylethanol producer. *J. Ind. Microbiol. Biotechnol.* 40, 389–392. doi: 10.1007/s10295-013-1240-1243

Chakraborty, D., Gupta, G., and Kaur, B. (2016). Metabolic engineering of *E. coli* top 10 for production of vanillin through FA catabolic pathway and bioprocess optimization using RSM. *Protein Expr. Purif.* 128, 123–133. doi: 10.1016/j.pep.2016.08.015

Chandran, S., Yi, J., Draths, K., Von Daeniken, R., Weber, W., Frost, J. W., et al. (2003). Phosphoenolpyruvate availability and the biosynthesis of Shikimic acid. *Biotechnol. Prog.* 19, 808–814. doi: 10.1021/bp025769p

Chantasuban, T., Santomauro, F., Gore-lloyd, D., Parsons, S., Henk, D., Scott, J., et al. (2018). Elevated production of the aromatic fragrance molecule, 2-phenylethanol, using *Metschnikowia pulcherrima* through both de novo and ex novo conversion in batch and continuous modes. *J. Chem. Technol. Biotechnol.* 93, 2118–2130. doi: 10.1002/jctb.5597

Chen, K., Dou, J., Tang, S., Yang, Y., Wang, H., Fang, H., et al. (2012). Deletion of the aroK gene is essential for high shikimic acid accumulation through the shikimate pathway in *E. coli*. *Bioresour. Technol.* 119, 141–147. doi: 10.1016/j.biortech.2012.05.100

Chen, Z., Sun, X., Li, Y., Yan, Y., and Yuan, Q. (2017). Metabolic engineering of *Escherichia coli* for microbial synthesis of monolignols. *Metab. Eng.* 39, 102–109. doi: 10.1016/j.ymben.2016.10.021

Choi, O., Wu, C.-Z., Kang, S. Y., Ahn, J. S., Uhm, T.-B., and Hong, Y.-S. (2011). Biosynthesis of plant-specific phenylpropanoids by construction of an artificial biosynthetic pathway in *Escherichia coli*. *J. Ind. Microbiol. Biotechnol.* 38, 1657–1665. doi: 10.1007/s10295-011-0954-953

Chouhan, S., Sharma, K., Zha, J., Guleria, S., and Koffas, M. A. G. (2017). Recent advances in the recombinant biosynthesis of polyphenols. *Front. Microbiol.* 8:2259. doi: 10.3389/fmicb.2017.02259

Chung, H., Lee, S. L., and Chou, C. C. (2000). Production and molar yield of 2-phenylethanol by Pichia fermentans L-5 as affected by some medium components. *J. Biosci. Bioeng.* 90, 142–147. doi: 10.1016/S1389-1723(00)80101-80102

Cui, Y., Ling, C., Zhang, Y., Huang, J., and Liu, J. (2014). Production of shikimic acid from *Escherichia coli* through chemically inducible chromosomal evolution and cofactor metabolic engineering. *Microb. Cell Fact.* 13, 1–11. doi: 10.1186/1475-2859-13-21

Cui, Z., Yang, X., Shen, Q., Wang, K., and Zhu, T. (2011). Optimisation of biotransformation conditions for production of 2-phenylethanol by a *Saccharomyces cerevisiae* CWY132 mutant. *Nat. Prod. Res.* 25, 754–759. doi: 10.1080/14786419.2010.529441

Curran, K. A., Leavitt, J. M., Karim, A. S., and Alper, H. S. (2013). Metabolic engineering of muconic acid production in *Saccharomyces cerevisiae*. *Metab. Eng.* 15, 55–66. doi: 10.1016/j.ymben.2012.10.003

De Oliveira, D. M., Finger-teixeira, A., Mota, T. R., Salvador, V. H., Moreira-vilar, C., Bruno, H., et al. (2015). Ferulic acid: a key component in grass lignocellulose recalcitrance to hydrolysis. *Plant Biotechnol. J.* 13, 1224–1232. doi: 10.1111/pbi.12292

Dell, K. A., and Frost, J. W. (1993). Identification and removal of impediments to biocatalytic synthesis of aromatics from D-Glucose: rate-limiting enzymes in the common pathway of aromatic amino acid biosynthesis. *J. Am. Chem. Soc.* 115, 11581–11589. doi: 10.1021/ja00077a065

Dhamankar, H., and Prather, K. L. J. (2011). Microbial chemical factories: recent advances in pathway engineering for synthesis of value added chemicals. *Curr. Opin. Struct. Biol.* 21, 488–494. doi: 10.1016/j.sbi.2011.05.001

Dias, F. M. S., Gomez, J. G. C., and Silva, L. F. (2017). Exploring the microbial production of aromatic fine chemicals to overcome the barriers of traditional methods. *Adv. Appl. Sci. Res.* 8, 94–109. doi: 10.1038/nmeth.1297

Dudnik, A., Almeida, A. F., Andrade, R., Avila, B., Bañados, P., Barbay, D., et al. (2017). BacHBerry: BACterial Hosts for production of Bioactive phenolics from bERRY fruits. *Phytochem. Rev.* 17, 291–326. doi: 10.1007/s11101-017-9532-9532

Dudnik, A., Gaspar, P., Neves, A. R., and Forster, J. (2018). Engineering of microbial cell factories for the production of plant polyphenols with health-beneficial properties. *Curr. Pharm. Des.* 24, 2208–2225. doi: 10.2174/1381612824666180515152049

Dyk, T. K., Van Templeton, L. J., Cantera, K. A., Sharpe, P. L., and Sariaslan, F. S. (2004). Characterization of the *Escherichia coli* AaeAB efflux pump: a metabolic relief valve? *J. Bacteriol.* 186, 7196–7204. doi: 10.1128/JB.186.21.7196

Escalante, A., Calderón, R., Valdivia, A., de Anda, R., Hernández, G., Ramírez, O. T., et al. (2010). Metabolic engineering for the production of shikimic acid in an evolved *Escherichia coli* strain lacking the phosphoenolpyruvate: carbohydrate phosphotransferase system. *Microb. Cell Fact.* 9, 1–12. doi: 10.1186/1475-2859-9-21

Etschmann, M., Bluemke, W., Sell, D., and Schrader, J. (2002). Biotechnological production of 2-phenylethanol. *Appl. Microbiol. Biotechnol.* 59, 1–8. doi: 10.1007/s00253-002-0992-x

Frost, J. W., and Draths, K. M. (1995). Biocatalytic syntheses of aromatics from D-glucose: renewable microbial sources of aromatic compounds. *Annu. Rev. Microbiol.* 49, 557–579. doi: 10.1146/annurev.mi.49.100195.003013

Furuya, T., Arai, Y., and Kino, K. (2012). Biotechnological production of caffeic acid by bacterial cytochrome. *Appl. Environ. Microbiol.* 78, 6087–6094. doi: 10.1128/AEM.01103-1112

Furuya, T., and Kino, K. (2014). Catalytic activity of the two-component flavin-dependent monooxygenase from *Pseudomonas aeruginosa* toward cinnamic acid derivatives. *Appl. Microbiol. Biotechnol.* 98, 1145–1154. doi: 10.1007/s00253-013-4958-y

Furuya, T., Miura, M., Kuroiwa, M., and Kino, K. (2015). High-yield production of vanillin from ferulic acid by a coenzyme-independent decarboxylase/oxygenase two-stage process. *N. Biotechnol.* 32, 335–339. doi: 10.1016/j.nbt.2015.03.002

Galán, B., Díaz, E., Prieto, M. A., and García, J. L. (2000). Functional analysis of the small component of the 4-Hydroxyphenylacetate 3-Monooxygenase of *Escherichia coli* W: a prototype of a new flavin: NAD (P)H reductase subfamily. *J. Bacteriol.* 182, 627–636. doi: 10.1128/jb.182.3.627-636.2000

Gallage, N. J., Hansen, E. H., Kannangara, R., Olsen, C. E., Motawia, M. S., Jørgensen, K., et al. (2014). Vanillin formation from ferulic acid in Vanilla planifolia is catalysed by a single enzyme. *Nat. Commun.* 5:5037. doi: 10.1038/ncomms5037

Gallage, N. J., and Møller, B. L. (2015). Vanillin-bioconversion and bioengineering of the most popular plant flavor and its de novo biosynthesis in the vanilla orchid. *Mol. Plant* 8, 40–57. doi: 10.1016/j.molp.2014.11.008

Gao, F., and Daugulis, A. J. (2009). Bioproduction of the aroma compound 2-phenylethanol in a solid-liquid two-phase partitioning bioreactor system by *Kluyveromyces marxianus*. *Biotechnol. Bioeng.* 104, 332–339. doi: 10.1002/bit.22387

Garavaglia, J., Flôres, S. H., Pizzolato, T. M., Peralba, M. D. C., and Ayub, M. A. Z. (2007). Bioconversion of L-phenylalanine into 2-phenylethanol by Kluyveromyces marxianus in grape must cultures. *World J. Microbiol. Biotechnol.* 23, 1273–1279. doi: 10.1007/s11274-007-9361-9363

Gaspar, P., Dudnik, A., Neves, A. R., and Föster, J. (2016). "Engineering Lactococcus lactis for stilbene production," in *Proceedings of the Abstract from 28th International Conference on Polyphenols 2016*, Vienna.

Ger, Y. M., Chen, S. L., Chiang, H. J., and Shiuan, D. (1994). A single ser-180 mutation desensitizes feedback inhibition of the phenylalanine-sensitive 3-deoxy-D-arabino-heptulosonate 7-phosphate (DAHP) synthetase in *Escherichia coli*. *J. Biochem.* 116, 986–990. doi: 10.1093/oxfordjournals.jbchem.a124657

Gosset, G. (2009). Production of aromatic compounds in bacteria. *Curr. Opin. Biotechnol.* 20, 651–658. doi: 10.1016/j.copbio.2009.09.012

Gosset, G., Yong-Xiao, J., and Berry, A. (1996). A direct comparison of approaches for increasing carbon flow to aromatic biosynthesis in *Escherichia coli*. *J. Ind. Microbiol.* 17, 47–52. doi: 10.1007/BF01570148

Gottardi, M., Reifenrath, M., Boles, E., and Tripp, J. (2017). Pathway engineering for the production of heterologous aromatic chemicals and their derivatives in *Saccharomyces cerevisiae*: bioconversion from glucose. *FEMS Yeast Res.* 17:fox035. doi: 10.1093/femsyr/fox035

Gu, P., Kang, J., Yang, F., and Wang, Q. (2013). The improved L -tryptophan production in recombinant *Escherichia coli* by expressing the polyhydroxybutyrate synthesis pathway. *Appl. Microbiol. Biotechnol.* 97, 4121–4127. doi: 10.1007/s00253-012-4665-4660

Gu, P., Yang, F., Kang, J., Wang, Q., and Qi, Q. (2012). One-step of tryptophan attenuator inactivation and promoter swapping to improve the production of L-tryptophan in *Escherichia coli*. *Microb. Cell Fact.* 11, 1–9. doi: 10.1186/1475-2859-11-30

Gulevich, A., Biryukova, I., Zimenkov, D., Skorokhodova, A., Kivero, A., Belareva, A., et al. (2006). *Method for Producing An L-amino Acid Using A Bacterium Having Enhanced Expression of the pckA Gene*. United States Patent Application 20060035348.

Guo, D., Zhang, L., Kong, S., Liu, Z., Li, X., and Pan, H. (2018). Metabolic engineering of *Escherichia coli* for production of 2-Phenylethanol and 2-Phenylethyl acetate from glucose. *J. Agric. Food Chem.* 66, 5886–5891. doi: 10.1021/acs.jafc.8b01594

Gyuun, D., Mi, A., Cha, N., and Prabhu, S. (2016). Bacterial synthesis of four hydroxycinnamic acids. *Appl. Biol. Chem.* 59, 173–179. doi: 10.1007/s13765-015-0137-134

Hansen, E. H., Møller, B. L., Kock, G. R., Bünner, C. M., Kristensen, C., Jensen, O. R., et al. (2009). De novo biosynthesis of Vanillin in fission yeast (schizosaccharomyces pombe) and baker's yeast (*Saccharomyces cerevisiae*). *Appl. Environ. Microbiol.* 75, 2765–2774. doi: 10.1128/AEM.02681-2688

Hartmann, M., Schneider, T. R., Pfeil, A., Heinrich, G., Lipscomb, W. N., and Braus, G. H. (2003). Evolution of feedback-inhibited/barrel isoenzymes by gene duplication and a single mutation. *Proc. Natl. Acad. Sci. U.S.A.* 100, 862–867. doi: 10.1073/pnas.0337566100

Heinz-Gerhard, F., and Jurgen, S. (2012). *Industrial Aromatic Chemistry: Raw Materials· Processes· Products*. Berlin: Springer Science & Business Media.

Hernández-Chávez, G., Martinez, A., and Gosset, G. (2019). Metabolic engineering strategies for caffeic acid production in *Escherichia coli*. *Electr. J. Biotechnol.* 38, 19–26. doi: 10.1016/j.ejbt.2018.12.004

Herrmann, K. M. (1995). The Shikimate pathway: early steps in the biosynthesis of aromatic compounds. *Plant Cell* 7:907. doi: 10.2307/3870046

Hu, C., Jiang, P., Xu, J., Wu, Y., and Huang, W. (2003). Mutation analysis of the feedback inhibition site of phenylalanine- sensitive 3-deoxy-D-arabino-heptulosonate 7-phosphate synthase of *Escherichia coli*. *J. Basic Microbiol.* 43, 399–406. doi: 10.1002/jobm.200310244

Hua, D., Lin, S., Li, Y., Chen, H., Zhang, Z., Du, Y., et al. (2010). Enhanced 2-phenylethanol production from L-phenylalanine via in situ product adsorption. *Biocatal. Biotrans.* 28, 259–266. doi: 10.3109/10242422.2010.500724

Hua, D., Ma, C., Song, L., Lin, S., Zhang, Z., Deng, Z., et al. (2007). Enhanced vanillin production from ferulic acid using adsorbent resin. *Appl. Microbiol. Biotechnol.* 74, 783–790. doi: 10.1007/s00253-006-0735-735

Huang, Q., Lin, Y., and Yan, Y. (2013). Caffeic acid production enhancement by engineering a phenylalanine over-producing *Escherichia coli* strain. *Biotechnol. Bioeng.* 110, 3188–3196. doi: 10.1002/bit.24988

Huang, Z., Dostal, L., and Rosazza, J. P. N. (1993). Microbial transformations of ferulic acid by *Saccharomyces cerevisiae* and *Pseudomonas fluorescens*. *Appl. Environ. Microbiol.* 59, 2244–2250. doi: 10.1128/aem.59.7.2244-2250.1993

Hwang, E. Il, Hwang, E. Il, Ohnishi, Y., Ohnishi, Y., Horinouchi, S., and Horinouchi, S. (2003). Production of plant-specific flavanones by *Escherichia coli* containing an artificial gene cluster. *Appl. Environ. Microbiol.* 69, 2699–2706. doi: 10.1128/AEM.69.5.2699

Ikeda, M. (2006). Towards bacterial strains overproducing L -tryptophan and other aromatics by metabolic engineering. *Appl. Microbiol. Biotechnol.* 69, 615–626. doi: 10.1007/s00253-005-0252-y

Ikeda, M., Mizuno, Y., and Awane, S. (2011). Identification and application of a different glucose uptake system that functions as an alternative to the phosphotransferase system in *Corynebacterium glutamicum*. *Appl. Microbiol. Biotechnol.* 90, 1443–1451. doi: 10.1007/s00253-011-3210-x

Jendresen, C. B., Stahlhut, S. G., Li, M., Gaspar, P., Siedler, S., Förster, J., et al. (2015). Highly active and specific tyrosine ammonia-lyases from diverse origins enable enhanced production of aromatic compounds in bacteria and *Saccharomyces cerevisiae*. *Appl. Environ. Microbiol.* 81, 4458–4476. doi: 10.1128/AEM.00405-415

Jiang, M., and Zhang, H. (2016). Engineering the shikimate pathway for biosynthesis of molecules with pharmaceutical activities in *E. coli*. *Curr. Opin. Biotechnol.* 42, 1–6. doi: 10.1016/j.copbio.2016.01.016

Jiménez, J. I., Miñambres, B., García, J. L., and Díaz, E. (2002). Genomic analysis of the aromatic catabolic pathways from *Pseudomonas putida* KT2440. *Environ. Microbiol.* 4, 824–841. doi: 10.1046/j.1462-2920.2002.00370.x

Johnson, B., Amaratunga, M., and Lobos, J. H. (2000). *Method for Increasing Total Production of 4-Hydroxybenzoic Acid by Biofermentation*. US patent application US 0 129.

Joshi, S. S., and Ranade, V. V. (2016). *Industrial Catalytic Processes for Fine and Specialty Chemicals*. Amsterdem: Elsevier.

Jossek, R., Bongaerts, J., and Sprenger, G. A. (2001). Characterization of a new feedback-resistant 3-deoxy-D-arabino-heptulosonate 7-phosphate synthase AroF of *Escherichia coli*. *FEMS Microbiol. Lett.* 202, 145–148. doi: 10.1016/S0378-1097(01)00311-311

Juminaga, D., Baidoo, E. E. K., Redding-Johanson, A. M., Batth, T. S., Burd, H., Mukhopadhyay, A., et al. (2012). Modular engineering of L-tyrosine production in *Escherichia coli*. *Appl. Environ. Microbiol.* 78, 89–98. doi: 10.1128/AEM.06017-6011

Kallscheuer, N., and Marienhagen, J. (2018). *Corynebacterium glutamicum* as platform for the production of hydroxybenzoic acids. *Microb. Cell Fact.* 17:70. doi: 10.1186/s12934-018-0923-x

Kallscheuer, N., Menezes, R., Foito, A., Henriques da Silva, M. D., Braga, A., Dekker, W., et al. (2019). Identification and microbial production of the raspberry phenol salidroside that is active against Huntingtons disease. *Plant Physiol.* 179, 969–985. doi: 10.1104/pp.18.01074

Kallscheuer, N., Vogt, M., Stenzel, A., Gätgens, J., Bott, M., and Marienhagen, J. (2016). Construction of a *Corynebacterium glutamicum* platform strain for the production of stilbenes and (2S)-flavanones. *Metab. Eng.* 38, 47–55. doi: 10.1016/j.ymben.2016.06.003

Kaneko, T., Thi, T. H., Shi, D. J., and Akashi, M. (2006). Environmentally degradable, high-performance thermoplastics from phenolic phytomonomers. *Nat. Mater.* 5, 966–970. doi: 10.1038/nmat1778

Kang, S., Choi, O., Lee, J. K., Hwang, B. Y., and Uhm, T. (2012). Artificial biosynthesis of phenylpropanoic acids in a tyrosine overproducing *Escherichia coli* strain. *Microb. Cell Fact.* 11:153. doi: 10.1186/1475-2859-11-153

Kaur, B., and Chakraborty, D. (2013). Biotechnological and molecular approaches for vanillin production: a review. *Appl. Biochem. Biotechnol.* 169, 1353–1372. doi: 10.1007/s12010-012-0066-61

Kawaguchi, H., Katsuyama, Y., Danyao, D., Kahar, P., Yoshihara, K., Minami, H., et al. (2017). Caffeic acid production by simultaneous saccharification and fermentation of kraft pulp using recombinant *Escherichia coli*. *Appl. Microbiol. Biotechnol.* 101, 5279–5290. doi: 10.1007/s00253-017-8270-8270

Kawai, Y., Noda, S., Ogino, C., Takeshima, Y., Okai, N., and Tanaka, T. (2013). p -Hydroxycinnamic acid production directly from cellulose using endoglucanase- and tyrosine ammonia lyase-expressing Streptomyces lividans. *Microb. Cell Fact.* 12:45. doi: 10.1186/1475-2859-12-45

Keasling, J. D., and Chou, H. (2008). Metabolic engineering delivers next-generation biofuels Tiny tiles, tiny targets. *Nat. Biotechnol.* 26, 298–299. doi: 10.1038/ng.85

Keseler, I. M., Mackie, A., Peralta-gil, M., Santos-zavaleta, A., Kothari, A., Krummenacker, M., et al. (2013). EcoCyc: fusing model organism databases with systems biology. *Nucleic Acids Res.* 41, 605–612. doi: 10.1093/nar/gks1027

Kikuchi, Y., Tsujimoto, K., and Kurahashi, O. (1997). Mutational analysis of the feedback sites of phenylalanine-sensitive synthase of *Escherichia coli*. *Appl. Environ. Microbiol.* 63, 761–762. doi: 10.1128/aem.63.2.761-762.1997

Kim, B., Cho, B. R., and Hahn, J. S. (2014). Metabolic engineering of *Saccharomyces cerevisiae* for the production of 2-phenylethanol via Ehrlich pathway. *Biotechnol. Bioeng.* 111, 115–124. doi: 10.1002/bit.24993

Kim, T. Y., Lee, S. W., and Oh, M. K. (2014). Biosynthesis of 2-phenylethanol from glucose with genetically engineered *Kluyveromyces marxianus*. *Enzyme Microb. Technol.* 6, 44–47. doi: 10.1016/j.enzmictec.2014.04.011

Kitade, Y., Hashimoto, R., Suda, M., Hiraga, K., and Inuia, M. (2018). Production of 4-Hydroxybenzoic acid by an aerobic growth- arrested bioprocess using metabolically engineered *Corynebacterium glutamicum*. *Appl. Environ. Microbiol.* 84, 1–12. doi: 10.1128/AEM.02587-17

Knaggs, A. R. (2003). The biosynthesis of shikimate metabolites. *Nat. Prod. Rep.* 20, 119–136. doi: 10.1039/b100399m

Knop, D. R., Draths, K. M., Chandran, S. S., Barker, J. L., Daeniken, R., Von Weber, W., et al. (2001). Hydroaromatic equilibration during biosynthesis of shikimic acid. *J Am. Chem. Soc.* 123, 10173–10182. doi: 10.1021/ja0109444

Köhle, A., Sommer, S., Li, S., Schilde-rentschler, L., Ninnemann, H., and Heide, L. (2003). Secondary metabolites in transgenic tobacco and potato: high accumulation of 4-hydroxybenzoic acid glucosides results from high expression of the bacterial gene ubi C. *Mol. Breed.* 11, 15–24.

Kramer, M., Bongaerts, ÃJ., Bovenberg, R., Kremer, S., Mu, U., Orf, S., et al. (2003). Metabolic engineering for microbial production of shikimic acid. *Metab. Eng.* 5, 277–283. doi: 10.1016/j.ymben.2003.09.001

Krivoruchko, A., and Nielsen, J. (2015). Production of natural products through metabolic engineering of *Saccharomyces cerevisiae*. *Curr. Opin. Biotechnol.* 35, 7–15. doi: 10.1016/j.copbio.2014.12.004

Krömer, J. O. (2016). Metabolic engineering of *Pseudomonas putida* KT2440 for the production of para -hydroxy benzoic acid. *Front. Bioeng. Biotechnol.* 4:90. doi: 10.3389/fbioe.2016.00090

Krömer, J. O., Nunez-Bernal, D., Averesch, N. J. H., Hampe, J., Varela, J., and Varela, C. (2013). Production of aromatics in *Saccharomyces cerevisiae*-A feasibility study. *J. Biotechnol.* 163, 184–193. doi: 10.1016/j.jbiotec.2012.04.014

Kunjapur, A. M., Tarasova, Y., and Prather, K. L. J. (2014). Synthesis and accumulation of aromatic aldehydes in an engineered strain of *Escherichia coli*. *J. Am. Chem. Soc.* 136, 11644–11654. doi: 10.1021/ja506664a

Lai, B., Plan, M. R., Averesch, N. J. H., Yu, S., Kracke, F., Lekieffre, N., et al. (2017). Quantitative analysis of aromatics for synthetic biology using liquid chromatography. *Biotechnol. J.* 12:1600269. doi: 10.1002/biot.201600269

Lee, E., Yoon, S., Das, A., Lee, S., Li, C., Kim, J., et al. (2009). Directing vanillin production from ferulic acid by increased acetyl-CoA consumption in recombinant *Escherichia coli*. *Biotechnol. Bioeng.* 102, 200–208. doi: 10.1002/bit.22040

Lee, J., and Wendisch, V. (2017). Biotechnological production of aromatic compounds of the extended shikimate pathway from renewable biomass. *J. Biotechnol.* 257, 211–221. doi: 10.1016/j.jbiotec.2016.11.016

Lenzen, C., Wynands, B., Otto, M., Bolzenius, J., Mennicken, P., Blank, L. M., et al. (2019). High-Yield production of 4-Hydroxybenzoate from glucose or glycerol by an engineered *Pseudomonas taiwanensis* VLB120. *Front. Bioeng. Biotechnol.* 7:130. doi: 10.3389/fbioe.2019.00130

Leonard, E., Yan, Y., Lim, K. H., Koffas, M. A. G., Al, L. E. T., and Icrobiol, A. P. P. L. E. N. M. (2005). Investigation of two distinct flavone synthases for plant-specific flavone biosynthesis in *Saccharomyces cerevisiae*. *Appl. Environ. Microbiol* 71, 8241–8248. doi: 10.1128/AEM.71.12.8241

Li, K., and Frost, J. W. (1998). Synthesis of vanillin from glucose [2]. *J. Am. Chem. Soc.* 120, 10545–10546. doi: 10.1021/ja9817747

Li, K., and Frost, J. W. (1999). Microbial synthesis of 3-dehydroshikimic acid: a comparative analysis of D-xylose, L-arabinose, and D-glucose carbon sources. *Biotechnol. Prog.* 15, 876–883. doi: 10.1021/bp990095c

Li, Y., Li, J., Qian, B., Cheng, L., Xu, S., and Wang, R. (2018). De Novo Biosynthesis of p-Coumaric Acid in *E. coli* with a trans-Cinnamic Acid 4-Hydroxylase from the Amaryllidaceae Plant *Lycoris aurea*. *Molecules* 23:3185. doi: 10.1007/s00253-005-0197-191

Lin, Y., Shen, X., Yuan, Q., and Yan, Y. (2013). Microbial biosynthesis of the anticoagulant precursor 4-hydroxycoumarin. *Nat. Commun.* 4:3603. doi: 10.1038/ncomms3603

Lin, Y., Sun, X., Yuan, Q., and Yan, Y. (2014). Extending shikimate pathway for the production of muconic acid and its precursor salicylic acid in *Escherichia coli*. *Metab. Eng.* 23, 62–69. doi: 10.1016/j.ymben.2014.02.009

Lin, Y., and Yan, Y. (2012). Biosynthesis of caffeic acid in *Escherichia coli* using its endogenous hydroxylase complex. *Microb. Cell Fact.* 11, 3–11. doi: 10.1186/1475-2859-11-42

Liu, C., Zhang, K., Cao, W., Zhang, G., Chen, G., Yang, H., et al. (2018). Genome mining of 2 - phenylethanol biosynthetic genes from *Enterobacter* sp . CGMCC

5087 and heterologous overproduction in *Escherichia coli*. *Biotechnol. Biofuels* 11:305. doi: 10.1186/s13068-018-1297-1293

Liu, L., Liu, H., Zhang, W., Yao, M., Li, B., Liu, D., et al. (2019a). Engineering the biosynthesis of caffeic acid in *Saccharomyces cerevisiae* with heterologous enzyme combinations. *Engineering* 5, 287–295. doi: 10.1016/j.eng.2018.11.029

Liu, Q., Yu, T., Li, X., Chen, Y., Campbell, K., Nielsen, J., et al. (2019b). Rewiring carbon metabolism in yeast for high level production of aromatic chemicals. *Nat. Commun.* 10, 1–13. doi: 10.1038/s41467-019-12961-12965

Liu, Q., Cheng, Y., Xie, X., Xu, Q., and Chen, N. (2012). Modification of tryptophan transport system and its impact on production of L -tryptophan in *Escherichia coli*. *Bioresour. Technol.* 114, 549–554. doi: 10.1016/j.biortech.2012.02.088

Lu, J. L., and Liao, J. C. (1997). Metabolic engineering and control analysis for production of aromatics: role of transaldolase. *Biotechnol. Bioeng.* 53, 132–138.

Lütke-Eversloh, T., and Stephanopoulos, G. (2005). Feedback inhibition of Chorismate Mutase / Prephenate Dehydrogenase (TyrA) of *Escherichia coli*: generation and characterization of Tyrosine-Insensitive mutants. *Appl Env. Microbiol.* 71, 7224–7228. doi: 10.1128/AEM.71.11.7224

Lütke-Eversloh, T., and Stephanopoulos, G. (2007). L-Tyrosine production by deregulated strains of *Escherichia coli*. *Appl. Microbiol. Biotechnol.* 75, 103–110. doi: 10.1007/s00253-006-0792-799

Luttik, M. A. H., Vuralhan, Z., Suir, E., Braus, G. H., Pronk, J. T., and Daran, J. M. (2008). Alleviation of feedback inhibition in *Saccharomyces cerevisiae* aromatic amino acid biosynthesis: quantification of metabolic impact. *Metab. Eng.* 10, 141–153. doi: 10.1016/j.ymben.2008.02.002

Luziatelli, F., Brunetti, L., Ficca, A. G., and Ruzzi, M. (2019). Maximizing the efficiency of vanillin production by biocatalyst enhancement and process optimization. *Front. Bioeng. Biotechnol.* 7:279. doi: 10.3389/fbioe.2019.00279

Ma, X. K., and Daugulis, A. J. (2014). Transformation of ferulic acid to vanillin using a fed-batch solid-liquid two-phase partitioning bioreactor. *Biotechnol. Prog.* 30, 207–214. doi: 10.1002/btpr.1830

MacDonald, M. J., and D'Cunha, G. B. (2007). A modern view of phenylalanine ammonia lyase. *Biochem. Cell Biol.* 85, 273–282. doi: 10.1139/O07-018

Maeda, H., and Dudareva, N. (2012). The Shikimate pathway and aromatic amino acid biosynthesis in plants. *Annu. Rev. Plant Biol.* 63, 73–105. doi: 10.1146/annurev-arplant-042811-105439

Mao, J., Liu, Q., Song, X., Wang, H., Feng, H., Xu, H., et al. (2017). Combinatorial analysis of enzymatic bottlenecks of l-tyrosine pathway by p-coumaric acid production in *Saccharomyces cerevisiae*. *Biotechnol. Lett.* 39, 977–982. doi: 10.1007/s10529-017-2322-2325

Martínez, K., de Anda, R., Hernández, G., Escalante, A., Gosset, G., Ramírez, O. T., et al. (2008). Co-utilization of glucose and glycerol enhances the production of aromatic compounds in an *Escherichia coli* strain lacking the phosphoenolpyruvate: carbohydrate phosphotransferase system. *Microb. Cell Fact.* 7:1. doi: 10.1186/1475-2859-7-1

Martínez-Avila, O., Sánchez, A., and Font, X. (2018). Bioproduction of 2-phenylethanol and 2-phenethyl acetate by *Kluyveromyces marxianus* through the solid-state fermentation of sugarcane bagasse. *Appl. Microbiol. Biotechnol.* 102, 4703–4716. doi: 10.1007/s00253-018-8964-y

Mascarenhas, D., Ashworth, D. J., and Chen, C. S. (1991). Deletion of pgi alters tryptophan biosynthesis in a genetically engineered strain of *Escherichia coli*. *Appl. Environ. Microbiol.* 57, 2995–2999. doi: 10.1177/1077546315573916

Mckenna, R., and Nielsen, D. R. (2011). Styrene biosynthesis from glucose by engineered *E. coli*. *Metab. Eng.* 13, 544–554. doi: 10.1016/j.ymben.2011.06.005

Mcqualter, R. B., Chong, B. F., Meyer, K., Dyk, D. E., Van Shea, M. G. O., Walton, N. J., et al. (2005). Initial evaluation of sugarcane as a production platform for p -hydroxybenzoic acid. *Plant Biotechnol. J.* 31, 29–41. doi: 10.1111/j.1467-7652.2004.00095.x

Mihal', M., Goncalves, R. F., and Markoš, J. (2014). Intensive 2-phenylethanol production in a hybrid system combined of a stirred tank reactor and an immersed extraction membrane module. *Chem. Pap.* 68, 1656–1666. doi: 10.2478/s11696-014-0575-571

Milke, L., Aschenbrenner, J., Marienhagen, J., and Kallscheuer, N. (2018). Production of plant-derived polyphenols in microorganisms: current state and perspectives. *Appl. Microbiol. Biotechnol.* 102, 1575–1585. doi: 10.1007/s00253-018-8747-8745

Muheim, A., Müller, B., Münch, T., and Wetli, M. (2001). *Microbiological Process for Producing Vanillin*. Karnataka: GIVAUDAN-ROURE.

Müller, R., Wagener, A., Schmidt, K., and Leistner, E. (1995). Microbial production of specifically ring-13C-labelled 4-hydroxybenzoic acid. *Appl. Microbiol. Biotechnol.* 43, 985–988. doi: 10.1007/bf00166913

Nagy, C., and Haschemi, A. (2013). Sedoheptulose kinase regulates cellular carbohydrate metabolism by sedoheptulose 7-phosphate supply. *Biochem. Soc. Trans.* 41, 674–680. doi: 10.1042/BST20120354

Nakamura, C. E., and Whited, G. M. (2003). Metabolic engineering for the microbial production of 1,3-propanediol. *Curr. Opin. Biotechnol.* 14, 454–459. doi: 10.1016/j.copbio.2003.08.005

Ni, J., Tao, F., Du, H., and Xu, P. (2015). Mimicking a natural pathway for de novo biosynthesis: natural vanillin production from accessible carbon sources. *Sci. Rep.* 5:13670. doi: 10.1038/srep13670

Nielsen, J., and Keasling, J. D. (2016). Engineering cellular metabolism. *Cell* 164, 1185–1197. doi: 10.1016/j.cell.2016.02.004

Nijkamp, K., Van Luijk, N., De Bont, J. A. M., and Jan, W. (2005). The solvent-tolerant *Pseudomonas putida* S12 as host for the production of cinnamic acid from glucose. *Appl. Microbiol. Biotechnol.* 69, 170–177. doi: 10.1007/s00253-005-1973-1977

Nijkamp, K., Westerhof, R. G. M., Ballerstedt, H., Bont, J. A. M., and De Wery, J. (2007). Optimization of the solvent-tolerant *Pseudomonas putida* S12 as host for the production of p -coumarate from glucose. *Appl. Microbiol. Biotechnol.* 74, 617–624. doi: 10.1007/s00253-006-0703-700

Nikel, P. I., and de Lorenzo, V. (2018). *Pseudomonas* putida as a functional chassis for industrial biocatalysis: From native biochemistry to trans-metabolism. *Metab. Eng.* 50, 142–155. doi: 10.1016/j.ymben.2018.05.005

Nishiyama, Y., Yun, C. S., Matsuda, F., Sasaki, T., Saito, K., and Tozawa, Y. (2010). Expression of bacterial tyrosine ammonia-lyase creates a novel p-coumaric acid pathway in the biosynthesis of phenylpropanoids in *Arabidopsis*. *Planta* 232, 209–218. doi: 10.1007/s00425-010-1166-1161

Noack, D., Roth, M., Geuther, R., Müller, G., Undisz, K., Hoffmeier, C., et al. (1981). Maintenance and genetic stability of vector plasmids pBR322 and pBR325 in *Escherichia coli* K12 strains grown in a chemostat. *MGG Mol. Gen. Genet.* 184, 121–124. doi: 10.1007/BF00271207

Noda, S., and Kondo, A. (2017). Recent advances in microbial production of aromatic chemicals and derivatives. *Trends Biotechnol.* 35, 785–796. doi: 10.1016/j.tibtech.2017.05.006

Noda, S., Miyazaki, T., and Miyoshi, T. (2011). Cinnamic acid production using Streptomyces lividans expressing phenylalanine ammonia lyase. *J. Ind. Microbiol. Biotechnol.* 38, 643–648. doi: 10.1007/s10295-011-0955-952

Noda, S., Miyazaki, T., Tanaka, T., Ogino, C., and Kondo, A. (2012). Production of Streptoverticillium cinnamoneum transglutaminase and cinnamic acid by recombinant Streptomyces lividans cultured on biomass-derived carbon sources. *Bioresour. Technol.* 104, 648–651. doi: 10.1016/j.biortech.2011.10.045

Noda, S., Shirai, T., Oyama, S., and Kondo, A. (2016). Metabolic design of a platform *Escherichia coli* strain producing various chorismate derivatives. *Metab. Eng.* 33, 119–129. doi: 10.1016/j.ymben.2015.11.007

Oldiges, M., Kunze, M., Degenring, D., Sprenger, G. A., and Takors, R. (2004). Stimulation, monitoring, and analysis of pathway dynamics by metabolic profiling in the aromatic amino acid pathway. *Biotechnol. Prog.* 20, 1623–1622.

Paddon, C. J., Westfall, P. J., Pitera, D. J., Benjamin, K., Fisher, K., McPhee, D., et al. (2013). High-level semi-synthetic production of the potent antimalarial artemisinin. *Nature* 496:528. doi: 10.1038/nature12051

Pandey, R. P., Parajuli, P., Koffas, M. A. G., and Sohng, J. K. (2016). Microbial production of natural and non-natural flavonoids: pathway engineering, directed evolution and systems/synthetic biology. *Biotechnol. Adv.* 34, 634–662. doi: 10.1016/j.biotechadv.2016.02.012

Papagianni, M. (2012). Recent advances in engineering the central carbon metabolism of industrially important bacteria. *Microb. Cell Fact.* 11, 1–13. doi: 10.1186/1475-2859-11-50

Paravicini, G., Mosch, H., Schmidheini, T., and Braus, G. (1989). The general control activator protein GCN4 is essential for a basal level of AR03 gene expression in *Saccharomyces cerevisiae*. *Mol. Cell. Biol.* 9, 144–151. doi: 10.1128/mcb.9.1.144

Park, S. Y., Yang, D., Ha, S. H., and Lee, S. Y. (2018). Metabolic engineering of microorganisms for the production of natural compounds. *Adv. Biosyst.* 2:1700190. doi: 10.1002/adbi.201700190

Patnaik, R., and Liao, J. C. (1994). Engineering of *Escherichia coli* central metabolism for aromatic metabolite production with near theoretical yield. *Appl. Environ. Microbiol.* 60, 3903–3908. doi: 10.7550/rmb.31286

Patnaik, R., Roof, W. D., Young, R. F., and Liao, J. C. (1992). Stimulation of glucose catabolism in *Escherichia coli* by a potential futile cycle. *J. Bacteriol.* 174, 7527–7532. doi: 10.1128/jb.174.23.7527-7532.1992

Pittard, J., Camakaris, H., and Yang, J. (2005). The TyrR regulon. *Mol. Microbiol.* 55, 16–26. doi: 10.1111/j.1365-2958.2004.04385.x

Priefert, H., Rabenhorst, J., and Steinbüchel, A. (2001). Biotechnological production of vanillin. *Appl. Microbiol. Biotechnol.* 56, 296–314. doi: 10.1007/s002530100687

Priya, V. K., Sarkar, S., and Sinha, S. (2014). Evolution of tryptophan biosynthetic pathway in microbial genomes: a comparative genetic study. *Syst. Synth. Biol.* 8, 59–72. doi: 10.1007/s11693-013-9127-9121

Rasmussen, S., Dixon, R. A., Division, P. B., Roberts, S., Foundation, N., and Parkway, S. N. (1999). Transgene-mediated and Elicitor-induced perturbation of metabolic channeling at the entry point into the phenylpropanoid pathway. *Plant Cell* 11, 1537–1551. doi: 10.1105/tpc.11.8.1537

Reifenrath, M., Bauer, M., Oreb, M., and Boles, E. (2018). Bacterial bifunctional chorismate mutase-prephenate dehydratase PheA increases flux into the yeast phenylalanine pathway and improves mandelic acid production. *Metab. Eng. Commun.* 7, 1–9. doi: 10.1016/j.mec.2018.e00079

Ro, D., and Douglas, C. J. (2004). Reconstitution of the entry point of plant phenylpropanoid metabolism in yeast (*Saccharomyces cerevisiae*). *J. Biol. Chem.* 279, 2600–2607. doi: 10.1074/jbc.M309951200

Rodrigues, J. L., Prather, K. L. J., Kluskens, L. D., and Rodrigues, L. R. (2015). Heterologous production of curcuminoids. *Microbiol. Mol. Biol. Rev.* 79, 39–60. doi: 10.1128/MMBR.00031-14

Rodriguez, A., Chen, Y., Khoomrung, S., Özdemir, E., and Borodina, I. (2017). Comparison of the metabolic response to over-production of p -coumaric acid in two yeast strains. *Metab. Eng.* 44, 265–272. doi: 10.1016/j.ymben.2017.10.013

Rodriguez, A., Kildegaard, K. R., Li, M., Borodina, I., and Nielsen, J. (2015). Establishment of a yeast platform strain for production of p- coumaric acid through metabolic engineering of aromatic amino acid biosynthesis. *Metab. Eng.* 31, 181–188. doi: 10.1016/j.ymben.2015.08.003

Rodriguez, A., Martínez, J. A., Báez-Viveros, J. L., Flores, N., Hernández-Chávez, G., Ramírez, O. T., et al. (2013). Constitutive expression of selected genes from the pentose phosphate and aromatic pathways increases the shikimic acid yield in high-glucose batch cultures of an *Escherichia coli* strain lacking PTS and pykF. *Microb. Cell Fact.* 12:86. doi: 10.1186/1475-2859-12-86

Sachan, A., Ghosh, S., Sen, S. K., and Mitra, A. (2006). Co-production of caffeic acid and p-hydroxybenzoic acid from p-coumaric acid by Streptomyces caeruleus MTCC 6638. *Appl. Microbiol. Biotechnol.* 71, 720–727. doi: 10.3390/molecules23123185

Santos, C. N. S., Koffas, M., and Stephanopoulos, G. (2011). Optimization of a heterologous pathway for the production of flavonoids from glucose. *Metab. Eng.* 13, 392–400. doi: 10.1016/j.ymben.2011.02.002

Santos, C. N. S., Xiao, W., and Stephanopoulos, G. (2012). Rational, combinatorial, and genomic approaches for engineering L-tyrosine production in *Escherichia coli*. *Proc. Natl. Acad. Sci. U.S.A.* 109, 13538–13543. doi: 10.1073/pnas.1206346109

Sariaslani, F. S. (2007). Development of a combined biological and chemical process for production of industrial aromatics from renewable resources. *Annu. Rev. Microbiol.* 61, 51–69. doi: 10.1146/annurev.micro.61.080706.093248

Schnappauf, G., Hartmann, M., Künzler, M., and Braus, G. H. (1998). The two 3-deoxy-D-arabino-heptulosonate-7-phosphate synthase isoenzymes from *Saccharomyces cerevisiae* show different kinetic modes of inhibition. *Arch. Microbiol.* 169, 517–524. doi: 10.1007/s002030050605

Schrader, J., Etschmann, M. M. W., Sell, D., Hilmer, J., and Rabenhorst, J. (2004). Applied biocatalysis for the synthesis of natural flavour compounds. *Biotechnol. Lett.* 26, 463–472. doi: 10.1023/b:bile.0000019576.80594.0e

Serino, L., Reimmann, C., Visca, P., Beyeler, M., Chiesa, V. D., Haas, D., et al. (1997). Biosynthesis of pyochelin and Dihydroaeruginoic acid requires the iron-regulated pchDCBA operon in *Pseudomonas aeruginosa*. *J. Bacteriol.* 179, 248–257. doi: 10.1128/jb.179.1.248-257.1997

Shumilin, I. A., Kretsinger, R. H., and Bauerle, R. H. (1999). Crystal structure of phenylalanine-regulated 3-deoxy- D - arabino - heptulosonate-7-phosphate synthase from *Escherichia coli*. *Structure* 7, 865–875. doi: 10.1016/S0969-2126(99)80109-80109

Sprenger, G., Siewe, R., Martin, K., and Sonke, T. (1998). *Microbial Preparation of Substances from Aromatic Metabolism*. Patent No.US6316232B1 United States.

Sprenger, G. A. (2007). From scratch to value: engineering *Escherichia coli* wild type cells to the production of L-phenylalanine and other fine chemicals derived from chorismate. *Appl. Microbiol. Biotechnol.* 75, 739–749. doi: 10.1007/s00253-007-0931-y

Suástegui, M., Guo, W., Feng, X., and Shao, Z. (2016). Investigating strain dependency in the production of aromatic compounds in *Saccharomyces cerevisiae*. *Biotechnol. Bioeng.* 113, 2676–2685. doi: 10.1002/bit.26037

Sun, X., Shen, X., Jain, R., Lin, Y., Wang, J., Sun, J., et al. (2015). Synthesis of chemicals by metabolic engineering of microbes. *Chem. Soc. Rev.* 44, 3760–3785. doi: 10.1039/c5cs00159e

Tan, Z., Zhu, X., Chen, J., and Li, Q. (2013). Activating phosphoenolpyruvate carboxylase and phosphoenolpyruvate carboxykinase in combination for improvement of succinate production. *Appl. Environ. Microbiol.* 79, 4838–4844. doi: 10.1128/AEM.00826-813

Tatarko, M., and Romeo, T. (2001). Disruption of a global regulatory gene to enhance central carbon flux into phenylalanine biosynthesis in *Escherichia coli*. *Curr. Microbiol.* 43, 26–31. doi: 10.1007/s002840010255

Thompson, B., Machas, M., and Nielsen, D. R. (2015). Creating pathways towards aromatic building blocks and fine chemicals. *Curr. Opin. Biotechnol.* 36, 1–7. doi: 10.1016/j.copbio.2015.07.004

Tilburg, A. Y., Van Cao, H., Meulen, S. B., and Van Der Kuipers, O. P. (2019). Metabolic engineering and synthetic biology employing Lactococcus lactis and Bacillus subtilis cell factories. *Curr. Opin. Biotechnol.* 59, 1–7. doi: 10.1016/j.copbio.2019.01.007

Trotman, R. J., Camp, C. E., Ben-bassat, A., Dicosimo, R., Huang, L., Crum, G. A., et al. (2007). Calcium alginate bead immobilization of cells containing tyrosine ammonia lyase activity for use in the production of p -hydroxycinnamic acid. *Biotechnol. Prog.* 23, 638–644. doi: 10.1021/bp060379e

Tzin, V., Galili, G., and Ahroni, A. (2001). Shikimate pathway and aromatic amino acid biosynthesis. *eLS* 1–10. doi: 10.1002/9780470015902.a0001315.pub2

Van Dien, S. (2013). From the first drop to the first truckload: commercialization of microbial processes for renewable chemicals. *Curr. Opin. Biotechnol.* 24, 1061–1068. doi: 10.1016/j.copbio.2013.03.002

Van Hecke, W., Kaur, G., and De Wever, H. (2014). Advances in in-situ product recovery (ISPR) in whole cell biotechnology during the last decade. *Biotechnol. Adv.* 32, 1245–1255. doi: 10.1016/j.biotechadv.2014.07.003

Vane, J. R., and Botting, R. M. (2003). The mechanism of action of aspirin. *Thromb. Res.* 110, 255–258. doi: 10.1016/S0049-3848(03)00379-377

Vanilla (2014). *A Sustainable Production Route. Evolva A/S*. Available at: https://www.evolva.com/vanillin/ (accessed April 26, 2019).

Vannelli, T., Qi, W. W., Sweigard, J., Gatenby, A. A., and Sariaslani, F. S. (2007). Production of p-hydroxycinnamic acid from glucose in *Saccharomyces cerevisiae* and *Escherichia coli* by expression of heterologous genes from plants and fungi. *Metab. Eng.* 9, 142–151. doi: 10.1016/j.ymben.2006.11.001

Vargas-Tah, A., and Gosset, G. (2015). Production of cinnamic and p-hydroxycinnamic acids in engineered microbes. *Front. Bioeng. Biotechnol.* 3:116. doi: 10.3389/fbioe.2015.00116

Verhoef, S., Ruijssenaars, H. J., Bont, J. A. M., and De Wery, J. (2007). Bioproduction of p -hydroxybenzoate from renewable feedstock by solvent-tolerant *Pseudomonas putida* S12. *J. Biotechnol.* 132, 49–56. doi: 10.1016/j.jbiotec.2007.08.031

Verhoef, S., Wierckx, N., Westerhof, R. G. M., Winde, J. H., and De Ruijssenaars, H. J. (2009). Bioproduction of p -hydroxystyrene from glucose by the solvent-tolerant bacterium *Pseudomonas putida* S12 in a two-phase water-decanol fermentation. *Appl. Microbiol. Biotechnol.* 75, 931–936. doi: 10.1128/AEM.02186-2188

Wang, J., Cheng, L., Wang, J., and Liu, Q. (2013). Genetic engineering of *Escherichia coli* to enhance production of L -tryptophan. *Appl. Microbiol. Biotechnol.* 97, 7587–7596. doi: 10.1007/s00253-013-5026-5023

Wang, J., Guleria, S., Koffas, M. A. G., and Yan, Y. (2016). Microbial production of value-added nutraceuticals. *Curr. Opin. Biotechnol.* 37, 97–104. doi: 10.1016/j.copbio.2015.11.003

Wang, J., Yang, Y., and Yan, Y. (2018). "Bioproduction of Resveratrol," in *Biotechnology of Natural Products*, eds W. Schwab, B. M. Lange, and M. Wüst,

(Cham: Springer International Publishing), 61–79. doi: 10.1007/978-3-319-67903-7_3

Wang, Z., Jiang, M., Guo, X., Liu, Z., and He, X. (2018). Reconstruction of metabolic module with improved promoter strength increases the productivity of 2 - phenylethanol in *Saccharomyces cerevisiae*. *Microb. Cell Fact.* 17:60. doi: 10.1186/s12934-018-0907-x

Wang, Z., Bai, X., Guo, X., and He, X. (2017). Regulation of crucial enzymes and transcription factors on 2-phenylethanol biosynthesis via Ehrlich pathway in *Saccharomyces cerevisiae*. *J. Ind. Microbiol. Biotechnol.* 44, 129–139. doi: 10.1007/s10295-016-1852-1855

Watts, K. T., Lee, P. C., and Schmidt-dannert, C. (2004). Exploring recombinant flavonoid biosynthesis in metabolically engineered *Escherichia coli*. *ChemBioChem* 5, 500–507. doi: 10.1002/cbic.200300783

Wierckx, N. J. P., Ballerstedt, H., Bont, J. A. M., and De Wery, J. (2005). Engineering of solvent-tolerant *Pseudomonas putida* S12 for bioproduction of phenol from glucose. *Appl. Env. Microbiol.* 71, 8221–8227. doi: 10.1128/AEM.71.12.8221

Wu, F., Cao, P., Song, G., Chen, W., and Wang, Q. (2018). Expanding the repertoire of aromatic chemicals by microbial production. *J. Chem. Technol. Biotechnol.* 93, 2804–2816. doi: 10.1002/jctb.5690

Yakandawala, N., Romeo, T., Friesen, A. D., and Madhyastha, S. (2008). Metabolic engineering of *Escherichia coli* to enhance phenylalanine production. *Appl. Microbiol. Biotechnol.* 78, 283–291. doi: 10.1007/s00253-007-1307-z

Yi, J., Draths, K. M., Li, K., and Frost, J. W. (2003). Altered Glucose Transport and Shikimate Pathway Product Yields in *E. coli*. *Biotechnol. Prog.* 19, 1450–1459. doi: 10.1021/bp0340584

Yim, H., Haselbeck, R., Niu, W., Pujol-baxley, C., Burgard, A., Boldt, J., et al. (2011). Metabolic engineering of *Escherichia coli* for direct production of 1,4-butanediol. *Nat. Chem. Biol.* 7, 444–445. doi: 10.1038/nchembio.580

Yoon, S. H., Lee, E. G., Das, A., Lee, S. H., Li, C., Ryu, H. K., et al. (2007). Enhanced vanillin production from recombinant *E. coli* using NTG mutagenesis and adsorbent resin. *Biotechnol. Prog.* 23, 1143–1148. doi: 10.1021/bp070153r

Zhang, H., Cao, M., Jiang, X., Zou, H., Wang, C., Xu, X., et al. (2014). De-novo synthesis of 2-phenylethanol by *Enterobacter* sp. CGMCC 5087. *BMC Biotechnol.* 14:30. doi: 10.1186/1472-6750-14-30

Zhang, H., Pereira, B., Li, Z., and Stephanopoulos, G. (2015). Engineering *Escherichia coli* coculture systems for the production of biochemical products. *Proc. Natl. Acad. Sci. U.S.A.* 112, 8266–8271. doi: 10.1073/pnas.1506781112

Zhang, J., Pierick, A. Ten, Van Rossum, H. M., Maleki Seifar, R., Ras, C., Daran, J. M., et al. (2015). Determination of the cytosolic NADPH/NADP ratio in *Saccharomyces cerevisiae* using shikimate dehydrogenase as sensor reaction. *Sci. Rep.* 5, 12846. doi: 10.1038/srep12846

Zhang, H., and Stephanopoulos, G. (2013). Engineering *E. coli* for caffeic acid biosynthesis from renewable sugars. *Appl. Microbiol. Biotechnol.* 97, 3333–3341. doi: 10.1007/s00253-012-4544-4548

Zhao, L.-Q., Sun, Z.-H., Zheng, P., and Zhu, L.-L. (2005). Biotransformation of isoeugenol to vanillin by a novel strain of *Bacillus fusiformis*. *Biotechnol. Lett.* 27, 1505–1509. doi: 10.1007/s10529-005-1466-x

Conflict of Interest: The authors declare that the research was conducted in the absence of any commercial or financial relationships that could be construed as a potential conflict of interest.

frontiers in Bioengineering and Biotechnology

ORIGINAL RESEARCH
published: 13 May 2020
doi: 10.3389/fbioe.2020.00403

Economic Process Evaluation and Environmental Life-Cycle Assessment of Bio-Aromatics Production

Jens O. Krömer[1], Rafael G. Ferreira[2], Demetri Petrides[3] and Norbert Kohlheb[4]*

[1] Systems Biotechnology, Department of Solar Materials, Helmholtz Centre for Environmental Research – UFZ, Leipzig, Germany, [2] Intelligen Brazil, São Paulo, Brazil, [3] Intelligen Inc., Scotch Plains, NJ, United States, [4] Department Environmental and Biotechnology Centre, Helmholtz Centre for Environmental Research – UFZ, Leipzig, Germany

The bio-based production of aromatics is experiencing a renaissance with systems and synthetic biology approaches promising to deliver bio-catalysts that will reach yields, rates, and titers comparable to already existing bulk bio-processes for the production of amino acids for instance. However, aromatic building blocks derived from petrochemical routes have a huge economic advantage, they are cheap, and very cheap in fact. In this article, we are trying to shed light on an important aspect of biocatalyst development that is frequently overlooked when working on strain development: economic and environmental impact of the production process. We estimate the production cost and environmental impact of a microbial fermentation process depending on culture pH, carbon source and process scale. As a model molecule we use *para*-hydroxybenzoic acid (pHBA), but the results are readily transferrable to other shikimate derived aromatics with similar carbon yields and production rates.

Keywords: life-cycle assessment, process development, aromatics, fermentation, pHBA

OPEN ACCESS

Edited by:
Nils Jonathan Helmuth Averesch, Stanford University, United States

Reviewed by:
Till Tiso, RWTH Aachen University, Germany
Massimo Merighi, Ginkgo BioWorks, United States

****Correspondence:***
Jens O. Krömer
jens.kroemer@ufz.de

Specialty section:
This article was submitted to Bioprocess Engineering, a section of the journal Frontiers in Bioengineering and Biotechnology

Received: *08 November 2019*
Accepted: *09 April 2020*
Published: *13 May 2020*

Citation:
Krömer JO, Ferreira RG, Petrides D and Kohlheb N (2020) Economic Process Evaluation and Environmental Life-Cycle Assessment of Bio-Aromatics Production. Front. Bioeng. Biotechnol. 8:403. doi: 10.3389/fbioe.2020.00403

INTRODUCTION

Aromatic chemicals are very important building blocks for the fiber, coating, resin, and packaging industries as well as precursors for the pharmaceutical and cosmetic industries (Krömer et al., 2013; Averesch and Krömer, 2018). Currently aromatics are almost exclusively derived from fossil fuels, despite the fact that biology potentially offers greener and more sustainable alternatives (Averesch and Krömer, 2018).

Despite initial work on the metabolic engineering of microbes for the production of aromatics starting in the mid 1990s (Barker and Frost, 2001), bio-production of aromatics has not yet been commercialized to the best of our knowledge. However, in recent years the interest in strain development for aromatics production has surged for a large variety of molecules (Averesch and Krömer, 2018) and one can only assume that this is also driven by revived commercial interest. The scope of molecules currently in focus can be clearly distinguished into high-value low-volume and low-value high-volume applications. A common assumption is that competitive production of lower volume higher price chemicals is easier to accomplish biotechnologically. This ignores the fact that a higher price also benefits the chemical synthesis for such molecules and in the end biotechnology always has to compete on production costs, no matter how expensive the molecule is.

In addition, the unit production costs (UPC) will also sharply increase as the production volume decreases. So margins could be limited. A high price may not only be a reflection of the production cost but also a question of supply and demand. In general, only for molecules that cannot be chemically synthesized due to their complexity (monoclonal antibodies, proteins, and antibiotics, etc.) do biotechnological processes find a niche, without chemical competition, and here usually very high prices can be achieved. But for most aromatics chemical competition has to be faced with the low end of the price range probably covered by purified terephthalic acid (PTA) that has an estimated market volume of over 60 million metric tons globally and a price of around 0.65 $ per kg (09/2019).

Another common assumption is that a biotechnological process is greener and more sustainable (Mojsov, 2015), because the carbon sources are usually considered renewable (Harding, 2008). This assumption has to be carefully evaluated, since the production of renewable carbon sources for biotech processes has an ecological footprint as well. In addition, the biotechnological production of chemicals usually happens in very dilute aqueous solutions requiring energy, and/or resource intensive downstream processing, which quite often produces considerable waste streams (Stottmeister et al., 2005).

When looking at the biotechnological production of aromatics, the key metabolic pathway is the shikimate pathway (Averesch and Krömer, 2018), which is responsible in bacteria, fungi and plants for providing the precursors for the synthesis of aromatic amino acids, folate, and quinones. But, as demonstrated in the articles of this special issue, this pathway is a central step toward many interesting compounds such as cinnamic acid, dehydroshikimate, melanin, vanillin, and para-hydroxy benzoic acid (pHBA). The latter can be considered a mid-range molecule, which currently has an estimated world market of 50,000 t p.a. at a price of around 2,600 US$/t. pHBA is an essential component in liquid crystal polymers which find widespread use in electronics. pHBA is also a precursor for parabens, a class of preservatives in the pharma (Ma et al., 2016) and cosmetics industries (Matwiejczuk et al., 2020). For our early-stage process and sustainability assessment, we use pHBA as a model molecule. This molecule has been produced in lab scale in microbial systems from sugars, achieving titers (T) of 37 g/L, productivities (R) of over 1.5 g/l/h, and carbon yields (Y) of 66% (Kitade et al., 2018). While this is still too low for commercialization, the necessary TRY parameters could be achieved with further strain and process optimization.

In principle, higher value aromatics can also be derived from chemical synthesis and unless a cost benefit compared to the existing technology can be realized with a biological route, the bio-process cannot be implemented. The problem at this point is two-fold: On the one hand, researchers usually do not know the true production costs of existing processes and in the case of specialty molecules also do not easily get access to real market prices. On the other hand, researchers also lack information about the anticipated production costs of a newly developed bio-based building block and the impact on market price, if additional (bio-based) product volume is added to the market.

To the best of our knowledge, the bio-production of pHBA has not been realized commercially at large scale, and hence the presented model rests on a range of assumptions. Nevertheless, we hope to provide a starting point for researchers and bio-process developers placing their research agenda for developing bio-based aromatics on a firmer footing. At the same time, we strive to define some cost boundaries for the production of one of the simplest bio-based aromatics molecule and also provide an environmental impact assessment. We compare this to a reference scenario, which is the Kolbe–Schmitt carboxylation of potassium phenolate to pHBA. The model should be transferrable to other aromatic building blocks derived from the microbial shikimate pathway when adjusting to the respective theoretical carbon yields and assuming similar downstream processing.

PROCESS MODELING

We established a fermentation process in SuperPro Designer v10 (Intelligen Inc., Scotch Plains, NJ, United States). Due to the absence of a current commercial operation for pHBA bio-production, we developed the model under the core assumption that comparable production rates, yields, and downstream processing options that have been described for amino acids and organic acids could be achieved in the future (explained in detail below). The environmental impact assessment was done using the material and energy streams from SuperPro Designer as inputs into the life-cycle assessment (LCA) model. The SuperPro Designer models can be found online under "Resources"[1]. All inputs and detailed results are provided in the **Supplementary Material**.

Our LCA model is based on the ISO 14040:2006 standard (Finnveden et al., 2009; Guinee et al., 2011; Gargalo et al., 2016), and applies a cradle-to-gate LCA approach to capture the input material and energy flows from the cultivation and down-stream process. The production of 1 kg pHBA was determined to be the functional unit, and all necessary inputs were referenced to it. Using the CML2001–January 2016 characterization model, all the environmental impacts in this model were considered. The calculation was made using the LCA software, GaBi8© with GaBi Professional, GaBi Construction Materials, GaBi Food and Feed, and Ecoinvent databases.

We gained the economic indicator of UPC from the SuperPro Designer model which was calculated for all scenarios.

As the final step, the environmental and economic results were aggregated. Since the indicators fall into different categories, their aggregation is only possible when they are converted to the same dimension. In our case, we used a ratio scale approach; the simple internal normalization method where the highest number of categories was used as the normalization factor (Tugnoli et al., 2008; Patel et al., 2012). Then, the normalized value of the three sustainability dimensions is totaled and the alternatives ranked according to their overall value. The alternative with the lowest overall value is the most sustainable option relative to all other options.

[1]https://www.ufz.de/index.php?en=42204

In order to perform the simulations, a range of assumptions had to be made:

Substrates

The carbon source assessed in this example is sucrose, which is a readily available carbon source that can be obtained at various purities, which helps with down-stream processing. For our environmental analysis we used two possible sources of sugar: from sugar beet and from sugar cane. This way we could capture the differences of the two production lines. Adapting the model to other carbon sources could be easily done. For the economic evaluation we assumed the average May 2019 spot price for white sugar of about 0.12 US$ per lb or 0.264 US$ per kg.[2] For all other required media components and process chemicals we assume the prices given in the **Supplementary Material**. We sourced the prices from US-import statistics.[3] These prices indicate the dutiable value on the US border prior to applying tariffs and in our opinion reflect the bulk prices for chemicals robustly. We assume that a mineral medium is based on a previously published yeast-based process (Averesch et al., 2017). For the bacterial process, it is assumed that sucrose metabolism is as active as glucose metabolism, which was previously demonstrated for certain strains of *Escherichia coli* (Arifin et al., 2014), for instance.

Biocatalysts

For this simulation we assume a production either with a recombinant strain of baker's yeast as described previously (Averesch et al., 2017) or an optimized strain of *Corynebacterium glutamicum* (Kitade et al., 2018). The yeast-based process could be run in an acidic pH range and potentially under anaerobic conditions, while the bacterial process needs to be controlled around pH 7.0 with sufficient aeration. The reported yields, rates, and titers are still sub-optimal (especially for the yeast scenario), therefore we assumed that we can achieve 90% of the theoretical maximum carbon yield as predicted with elementary flux mode analysis previously (Krömer et al., 2013). Another essential assumption is a minimum productivity of 4 gg_{CDW}^{-1} h^{-1}. The productivity will determine the fermentation time, which directly determines the number of batches per year and hence the required fermentation vessels for a given annual production. It will also determine running costs (energy etc.) per kg product produced. This assumed productivity is realistic, as it has been demonstrated for example for lysine production in *C. glutamicum* (Becker et al., 2011). Since the shikimate pathway also provides the essential amino acids Phenylalanine, Tyrosine, and Tryptophan and their combined anabolic demand exceeds the demand for Lysine (Stephanopoulos et al., 1998), it is a reasonable assumption that at least a comparable flux capacity exists in both the lysine and the shikimate pathways.

Fermentation Section

The Fermentation section encompasses the mixing and sterilization of media components, seed fermentation steps to generate a sizable inoculum, and the main fermentation process that actually produces pHBA. Solutions of sucrose (50% w/w), sodium di-hydrogen phosphate (34.3 g/L), di-ammonium sulfate (3.14 g/L), and ammonium chloride (129.9 g/L) are prepared, heat-sterilized and stored in separate tanks. Each tank feeds the corresponding nutrient to the seed fermenters and to the main fermenter. The seed train is composed of three seed fermenters of increasing size: 40 L, 1 m^3, and 10 m^3; the latter is connected to the main fermenter, of 196 m^3. In the first seed reactor biomass was expanded to 50 g/L, while we assumed that the subsequent larger reactors would reach 30 g/L of biomass. The whole broth was transferred as inoculum to the next stage. The seed fermenters operate in batch mode; the microbial growth in each one of them is represented by the following stoichiometric equation:

$$0.05\ (NH_4)_2O_4 + 1.99\ NH_4Cl + 0.54\ NaH_2PO_4 + 17.42\ \text{Sucrose} \rightarrow 7.84\ \text{Biomass} + 12.16 CO_2$$

Note that these coefficients are mass-based.

The main fermenter operates in fed-batch mode, in order to obtain a high level of pHBA. The cells first go through a growth phase, reaching a biomass concentration of 30 g/L, followed by a production phase which is triggered by the feed of carbon source under nitrogen limitation. The biosynthesis of pHBA is modeled by the following equation:

$$250.86\ (NH_4)_2SO_4 + 9951.81\ NH_4Cl + 2695.02\ NaH_2PO_4 + 204172.62\ \text{Sucrose} \rightarrow 22912.16\ \text{Biomass} + 114158.15\ CO_2 + 80000\ \text{pHBA (aq)}$$

Again, these coefficients are mass-based. It is worth noting that the solubility of pHBA in pure water is rather low, equal to 5.79 g/L at 25°C (Nordstrom and Rasmuson, 2006). However, buffering pH around 7 will allow for higher concentrations of the deprotonated (anionic) form of pHBA in the solution; in fact, this is likely the reason why titers of over 36 g/L pHBA in *C. glutamicum* cultivation have been reported (Kitade et al., 2018). For this reason, in the bacterial case, calcium hydroxide is continuously added to the broth, in order to neutralize pHBA and therefore stabilize the pH. In the yeast case, however, no base is added; instead, an *in situ* product crystallization system was implemented. This strategy is described in further detail in the next section. Moreover, in both cases we assumed that a final titer of 100 g/L of pHBA, or the equivalent of pHBA calcium salt, could be achieved.

Downstream Section

In the bacterial scenario, we assumed that cells are first separated by microfiltration, and then the broth is concentrated threefold by ultrafiltration. Next, the pHBA salt is converted into the acid (uncharged) form by neutralization with nitric acid (70%), and the resulting product, which is highly insoluble in water, is isolated by crystallization at 5°C in an appropriate vessel. After that, the pHBA crystals are separated from the mother liquor with the aid of a basket centrifuge. Finally, the crystals are dried in a fluid-bed dryer with air in order to obtain a pHBA product with

[2] https://www.isosugar.org

[3] dataweb.usitc.gov

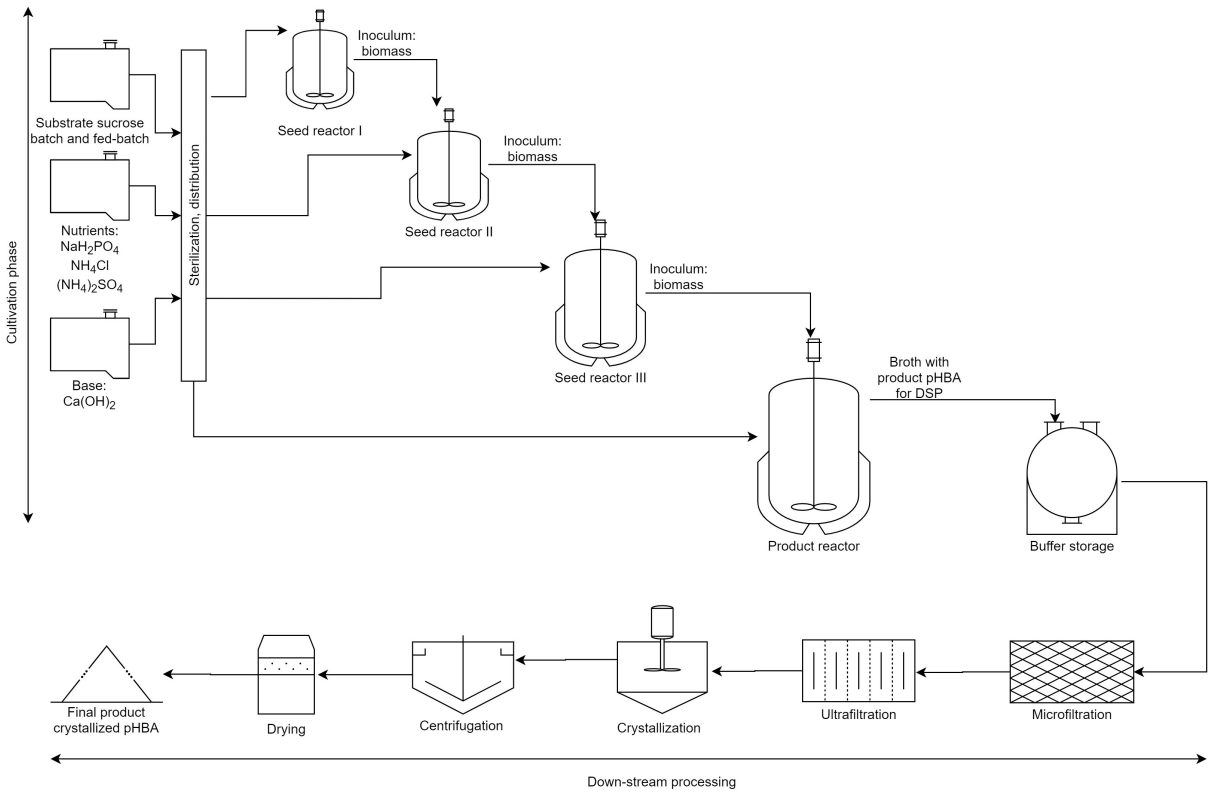

FIGURE 1 | Simplified bacterial bioprocess where pH regulation is included (note that aeration is not detailed). The first part of the process contains the cultivation phase, where the biomass is produced in consecutive three seed reactors and then the fermentation is done. The second part presents the DSP with filtrations, crystallization, and centrifugation and drying. In the DSP of the yeast-based alternative no microfiltration is made.

a purity of 99.5%. The complete bacterial process is schematically presented in **Figure 1**.

In the yeast scenario, on the other hand, we assume an *in situ* product removal system as described by Buque-Taboada et al. (2006). In this system, the broth is continuously removed from the fermenter; firstly, it passes through an ultrafilter that separates the cells and large contaminants from the pHBA solution, and those are recycled to the fermenter (approximately 15% in volume). Then, the clarified solution is cooled to 5°C in a crystallizer, and the resulting pHBA crystals are separated from the mother liquor using a basket centrifuge, similarly to the bacterial case. However, in the yeast case the liquid phase from the basket centrifuge is returned to the fermenter, while the pHBA crystals are dried in a fluid-bed dryer to 99.5% purity.

Scenarios

In total we have considered 17 scenarios: As a reference chemical scenario (i) we use the LCA model for potassium phenolate production followed by the Kolbe–Schmitt carboxylation (5 atm CO_2, 220; Markovic et al., 2006; Elvers, 2014). We assume a total conversion yield of 50% for the phenolate (Iijima and Yamaguchi, 2007; Elvers, 2014). The ratio of ortho-hydroxy benzoic acid to pHBA is at best 1:2.3 meaning that around a third of the product is salicylic acid (Markovic et al., 2006; Iijima and Yamaguchi, 2007), but for simplicity reasons we here assume that pHBA is exclusively made. Due to the lack of knowledge about the chemical downstream processing, we assume the same energy, and environmental footprint as we have for the biotech system.

The base scenarios are the aforementioned bacterial process (ii) and the yeast process (viii), based on sucrose derived from sugar beet. For the bacterial case we then developed scenarios in which it would be possible to recycle 90% of the water (iv) or to recycle 75% of the biomass as active catalyst (iii). In an optimized scenario both recycling strategies are combined and the sucrose is sourced from cane sugar (v). With this best case scenario of the bacterial process, the impact of scale-up was investigated. In the case of scale-up the plant produced 50,000 t p.a. instead of 10,000 t p.a. Both production with cane sugar (vi) and beet sugar (vii) was analyzed for the bacterial case. In the case of cane sugar based scenarios, labor costs were also adjusted to the average in Brazil (about 20% of the salaries assumed in SuperPro for US-based production). Finally, the respective scaled-up processes with cane and beet sugar were also analyzed for the yeast case (ix and x, respectively). While the recycling of biomass as active catalyst might be questionable in the real world, this provided an easy way to explore the economic impact of such a process. In reality maybe cell extracts could be recycled back into the seed reactors, but here many additional assumptions would have to be taken, especially around the problems in DSP arising from feeding bacterial or yeast extracts in the seed reactors.

Based on published titers, rates, and yields (TRY) in *C. glutamicum* (Kitade et al., 2018) one needs to achieve approximate improvements of 2.7, 43.6, and 1.3 fold, respectively, showing that production rate is still the most limiting factor amongst TRY parameters. We therefore performed a sensitivity analysis by also developing additional scenarios with longer fermentation durations. Fermentation time is determined by the time we need to achieve the target concentration and hence extended time equals a decreased production rate. All time dependent costs in the process will scale accordingly. We assumed a fermentation time of 54 and 72 h, equaling production rates of 2.67 gg_{CDW}^{-1} h^{-1} and 2 gg_{CDW}^{-1} h^{-1}, respectively. To analyze the impact of fermentation duration and with this the impacts of productivity we developed 7 scenarios in addition. For the bacterial process this was a base case with 54 h (xi) and two best cases with cane sugar lasting for 54 and 72 h (xii and xiii, respectively). For the yeast process two base cases with 54 and 72 h duration (xiv and xv) and two best cases with cane sugar for 54 and 72 h (xvi and xvii) were developed. Inventory tables for scenarios are given in the **Supplementary Material**.

The environmental impact of electricity generation in our analysis assumes the current electricity mix in the US for the sugar beet cases and the electricity mix of Brazil for the cane sugar cases.

RESULTS

Generating a process model and then performing a LCA allowed us to study the largest drivers in price and environmental impact of a sugar based bio-production for aromatics.

Economic Impact

The production cost for pHBA was assessed for our 17 scenarios (for details please refer to the **Supplementary Information**). This includes operating costs (incl. depreciation over 10 years)

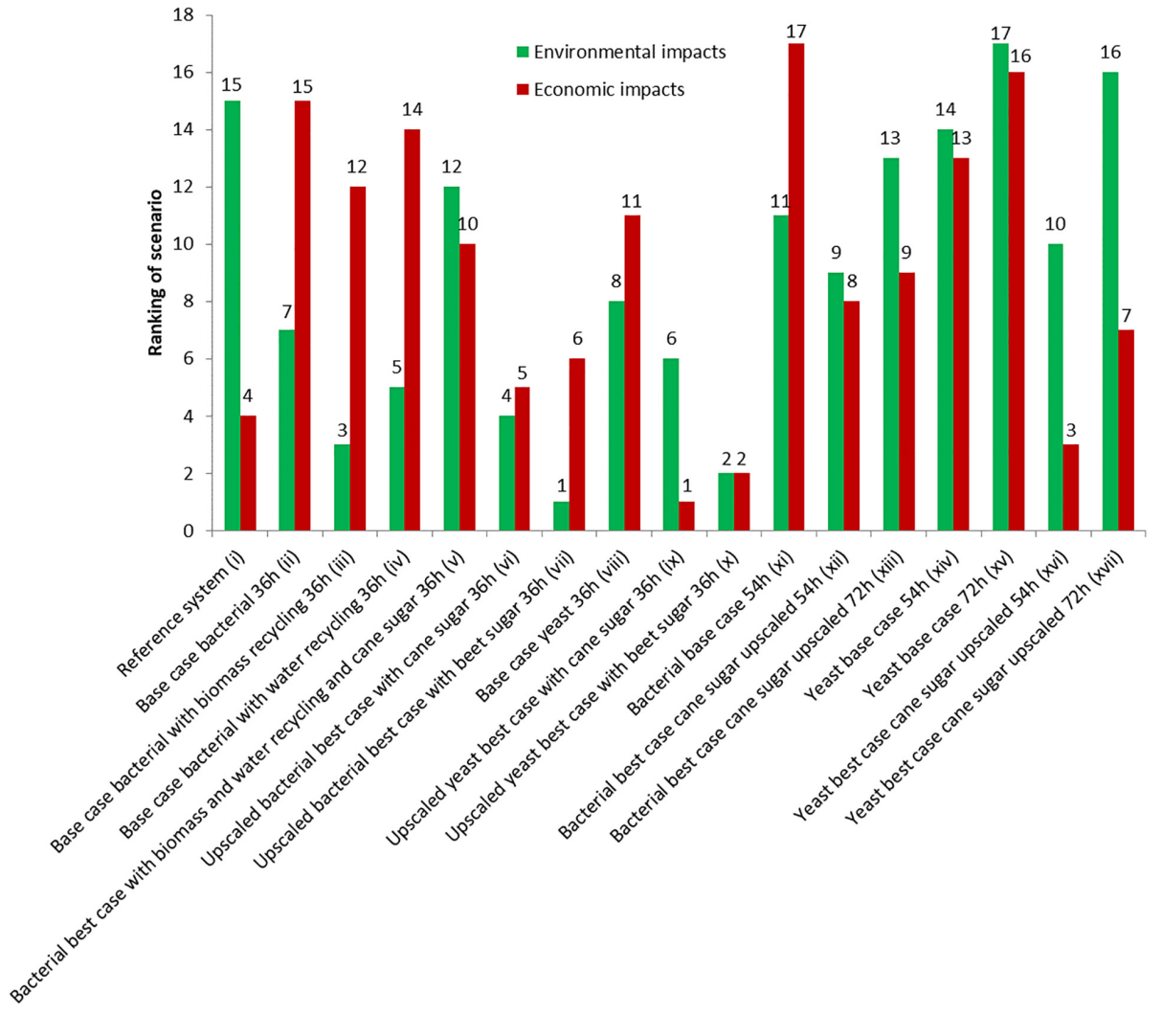

FIGURE 2 | Overall ranking of the different scenarios based on their economic and environmental impacts.

and investment costs (payback-time of around 6 years). For the reference case of petrochemical production (scenario i), we assume 2 $/kg. The implemented bio-process models predicted prices of between 1.61 and 3.59 $/kg, which is well above current world prices and most likely due to weak assumptions around the used equipment, rather than the raw material streams, and which are defined through the stoichiometry. The bio-production in the bacterial (ii) and the yeast base (viii) scenarios differed significantly, with 3.25 $/kg, and 2.65 $/kg. The reasons for this difference are the lower material costs, for the yeast case, since pH regulation is not required and the downstream processing is simpler. However, the yeast case employed downstream processing steps, which involved more labor dampening the impact on product cost. In both cases we assume a production scale of 10,000 t p.a., which is a significant share (20%) of the current world market. One of the largest by-products is biomass and the most important process stream besides sugar is water. In scenarios iii and iv we therefore explored the impact of the theoretical possibilities of recycling 75% of the biomass as active catalyst and of recycling 90% of the water. We found that water recycling only had a minor impact on cost (3.24 $/kg) while biomass recycling caused a drop to 3.07 $/kg. In a best-case scenario for the bacterial process (scenario v), we combined both recycling loops, and moved production to Brazil. Here the raw material would be sucrose from cane [same raw sugar price, but different environmental impact, and compared to sugar beet (scenario vii)] and labor costs would be significantly lower (∼20% of the default US labor costs assigned in SuperPro Designer). This lowered the production cost to 2.55 $/kg in the bacterial case and when upscaling this plant to 50,000 t p.a., which would be feasible under the parameters assumed for the bioprocess, the cost will drop to 2.01 $/kg. Making the same assumptions for the yeast process (scenario ix) will reduce the production cost even further to 1.61 $/kg. Ranking the first ten scenarios in terms of economic impact showed that based on our assumption a production based on yeast in large scale would be price competitive with the current chemical process (**Figure 2**).

Among the seven additional scenarios with different fermentation durations base cases for bacterial (xi–3.59 $/kg) and yeast (xv–3.4 $/kg) are obviously worse than their more effective counterparts (ii and viii). On the other hand it is important to underline that changes in fermentation duration have only minor effect on the economic performance, in this case, however, more main fermenters are needed which will drive investment costs up. Much more important are scale and substrate which are able to outperform the adverse effects of longer durations. For example in scenarios xvi and xvii, where upscaling, and switching to cane sugar considerably dropped the costs to 1.94 and 2.14 $/kg, respectively.

Environmental Impact

Overall, the scenarios were also ranked based on their total environmental impact (**Figure 2**). Biomass recycling had a much

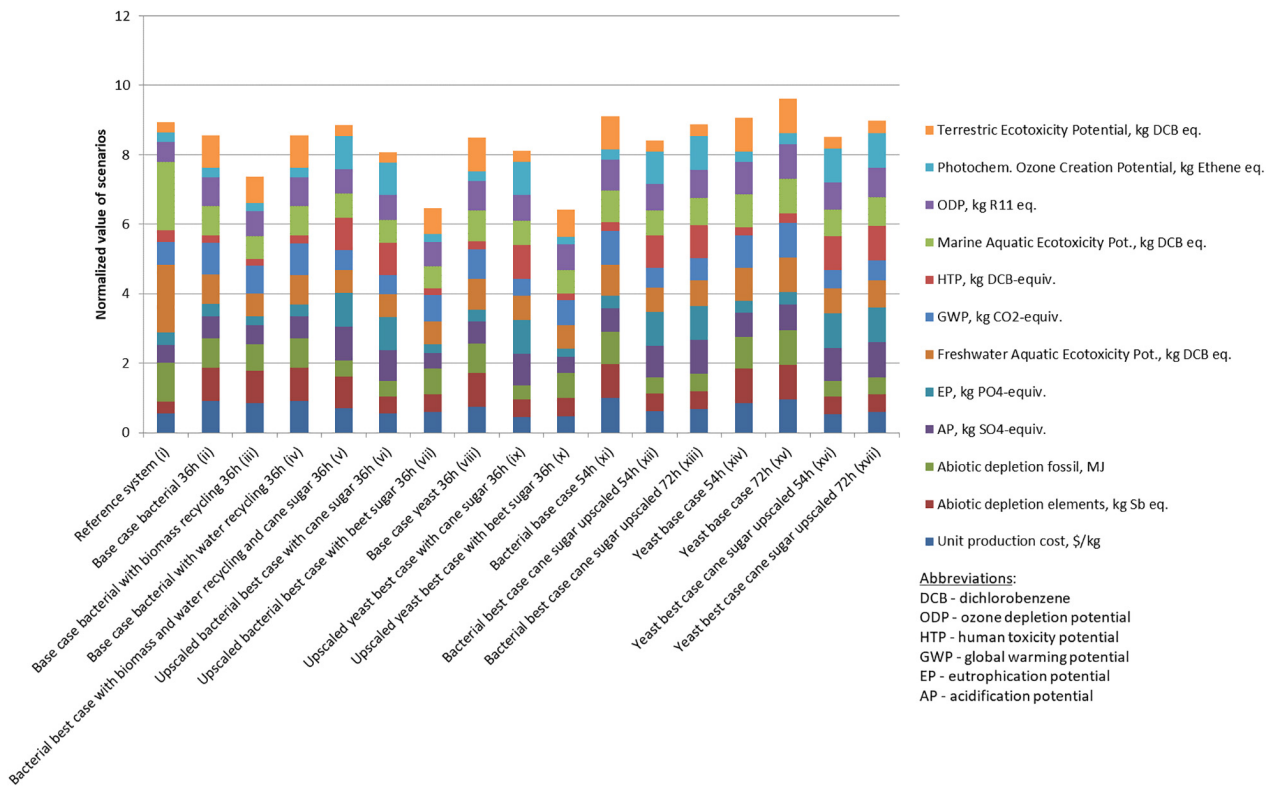

FIGURE 3 | Contribution of different impact factors to the total impact of the different scenarios.

higher impact than the impact of water recycling (scenarios ii, iii, and iv). However, the highest impact was induced by switching the substrates (scenarios vi, vii, ix, and x): the overall trend for the bio-tech scenarios was that the cane-sugar based scenarios had a worse environmental impact than the processes based on sugar beet. In addition, upscaling induced some further environmental improvements. Consequently, a large scale production based on bacteria, and sugar from beets being the overall best process. When analyzing the patterns within the eleven different ecological criteria, a more complex pattern emerged (**Figure 3**). The processes based on sugar cane were in fact better than the scenarios based on sugar beet in the observed global warming potential (GWP) expressed as CO_2 equivalents per kg product, ecotoxicology potential, and the fossil abiotic depletion potential, while the sugar-beet processes achieved similar or better values in the remaining criteria. Interestingly, the yeast and bacterial base cases were almost identical (e.g., scenarios ii and viii in **Figure 3**), highlighting that the alternative down-stream processing has minor impact on the ecology, but more on the economy.

The chemical production as our reference case (scenario i) here showed an overall comparable performance to the biotechnological processes, but it ranked only 15th in the overall ranking (**Figure 2**). Individual criteria are worse in the chemical case, while others are surprisingly good (e.g., abiotic depletion potential, acidification, and eutrophication potential, GWP) given in **Figure 3**. This is because the bioprocesses use chemicals such as nitric acid and sodium hydroxide that have a high GWP. In addition, the estimated electricity demand of the reference scenario is an order of magnitude less than of the bioprocesses

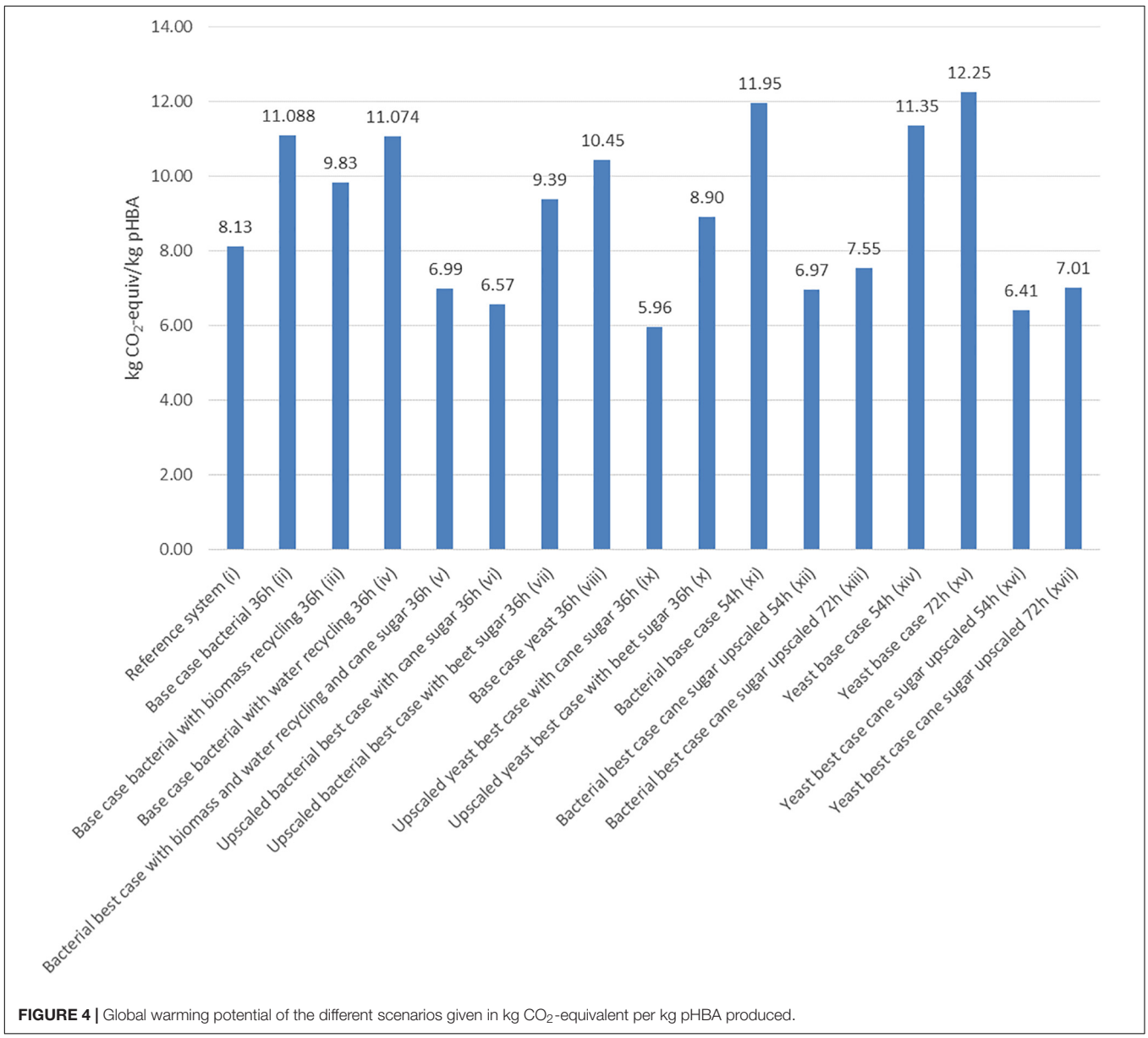

FIGURE 4 | Global warming potential of the different scenarios given in kg CO_2-equivalent per kg pHBA produced.

which is the third most important factor producing greenhouse gases in the bioprocess.

When looking at GWP only, the petrochemical route is actually amongst the better options (**Figure 4**). When comparing the ii–x biological scenarios amongst themselves, the two up-scaled processes (scenario vi and ix) lead to a reduction of GWP. In addition, shifting from sugar beets to sugar cane as substrate is highly beneficial (scenarios vi–vii and ix–x) as sugar cane has a much better yield per hectare and invested materials and hence has a smaller environmental footprint than sugar beet. In GWP the acidic yeast process slightly outcompetes the bacterial process. This is because increasing batch time raised GWP, e.g., for scenarios ii and viii, but again, differences are rather minor compared to changes in substrate.

An increase of fermentation time from 36 h to 54 h and 72 h obviously deteriorates environmental performance shown by scenarios xi–xvii in **Figures 2**, **3**. Interestingly, up-scaled scenarios with fermentation time of 54 h (xii and xvi) are still better than the reference scenario (i), however, scenarios with longer fermentation time (xiii and xvii) are worse or equal (**Figure 3**).

DISCUSSION

The economic analysis clearly shows that the bio-based production of aromatics could be competitive with the current petrochemical route. As with most processes, the scale will have a dramatic impact on price and similar to the production of other weak acids, such as lactic acid for instance (Miller et al., 2017), a production at acidic pH is also a key target for pHBA production. It is obvious that producing 50,000 t p.a. of pHBA in a single fermentation facility would supply the entire current world demand in one location and this seems as such not a viable option from a market perspective. But the advantage of the bio-process would be that the same large-scale facility could sequentially produce different aromatic molecules for different markets, as long as the down-stream processing could be adapted. Upstream processes, such as inoculum preparation and substrate supply would be easily adjusted for the production of different aromatics with different strains of the same organism. That way, the beneficial economy of scale can be achieved, without flooding the market.

We assume here that the production cost in the petrochemical route is around the 2 $/kg mark. Obviously, this is an estimate, but considering the current market price of 2.6 $/kg, and the interest of a pHBA manufacturer (personal communication) in bio-based production around the benchmark of 1.5 $/kg suggests that this is a reasonable guess. This means that production of bio-based aromatics is within reach from a commercial perspective, if the titers, rates, and yields assumed above can be achieved.

From an environmental perspective it is clear that the chemical reference process does not seem to be generally performing worse than bio-based production. One has to weigh up the different criteria which will also depend on the location of a production facility and the available resources. It is obvious that the source for the sugar has a major impact. Here beet sugar or cane sugar have different advantages and disadvantages. Depending on the location, these impacts would weigh in differently. For instance, cane sugar will be better from resource depletion and global warming perspective, while beet-sugar is much better in terms of eutrophication, acidification, and toxicity potentials. A careful analysis for the respective location of the plant is needed. The choice of production host and hence DSP seems to be first of all an economic decision. Overall the production in yeast with beet sugar seems to perform best (scenario x – second both in economic and environmental terms). Finally, moving to biotechnology might become more of an economic than an environmental decision, especially when a reduction in oil production due to decarbonization of the energy markets might lead to increased barrel prices and hence an increase in chemical prices, long before we actually run out of oil.

DATA AVAILABILITY STATEMENT

All datasets generated for this study are included in the article/**Supplementary Material**.

AUTHOR CONTRIBUTIONS

NK and RF implemented the SuperPro Designer models. NK implemented the LCA models and conducted the assessment. DP provided expertise on bioprocess synthesis and cost analysis. JK designed the study and drafted the manuscript. All authors edited and approved the final manuscript.

SUPPLEMENTARY MATERIAL

The Supplementary Material for this article can be found online at: https://www.frontiersin.org/articles/10.3389/fbioe.2020.00403/full#supplementary-material

REFERENCES

Arifin, Y., Archer, C., Lim, S., Quek, L. E., Sugiarto, H., Marcellin, E., et al. (2014). *Escherichia coli* W shows fast, highly oxidative sucrose metabolism and low acetate formation. *Appl. Microbiol. Biotechnol.* 98, 9033–9044 doi: 10.1007/s00253-014-5956-4

Averesch, N. J. H., and Krömer, J. O. (2018). Metabolic engineering of the shikimate pathway for production of aromatics and derived compounds-present and future strain construction strategies. *Front. Bioeng Biotechnol.* 6:32. doi: 10.3389/fbioe.2018.00032

Averesch, N. J. H., Prima, A., and Krömer, J. O. (2017). Enhanced production of para-hydroxybenzoic acid by genetically engineered *Saccharomyces cerevisiae*. *Bioprocess. Biosyst. Eng.* 40, 1283–1289. doi: 10.1007/s00449-017-1785-z

Barker, J. L., and Frost, J. W. (2001). Microbial synthesis of *p*-hydroxybenzoic acid from glucose. *Biotechnol. Bioeng* 76, 376–390. doi: 10.1002/bit.10160

Becker, J., Zelder, O., Häfner, S., Schröder, H., and Wittmann, C. (2011). From zero to hero–design-based systems metabolic engineering of *Corynebacterium glutamicum* for L-lysine production. *Metab. Eng.* 13, 159–168. doi: 10.1016/j.ymben.2011.01.003

Buque-Taboada, E. M., Straathof, A. J. J., Heijnen, J. J., and van der Wielen, L. A. M. (2006). In situ product recovery (ISPR) by crystallization. basic principles, design, and potential applications in whole-cell biocatalysis. *Appl. Microbiol. Biotechnol.* 71, 1–12. doi: 10.1007/s00253-006-0378-6

Elvers, B. (2014). *Ullmann's Fine Chemicals*. Weinheim: Wiley-VCH Verlag GmbH & Co: KGaA.

Finnveden, G., Hauschild, M. Z., Ekvall, T., Guinee, J., Heijungs, R., Hellweg, S., et al. (2009). Recent developments in life cycle assessment. *J. Environ. Manage.* 91, 1–21. doi: 10.1016/j.jenvman.2009.06.018

Gargalo, C. L., Cheali, P., Posada, J. A., Carvalho, A., Gernaey, K. V., Sin, G., et al. (2016). Assessing the environmental sustainability of early stage design for bioprocesses under uncertainties. An analysis of glycerol bioconversion. *J. Clean Prod.* 139, 1245–1260. doi: 10.1016/j.jclepro.2016.08.156

Guinee, J. B., Heijungs, R., Huppes, G., Zamagni, A., Masoni, P., Buonamici, R., et al. (2011). Life cycle assessment. past, present, and futures. *Environ. Sci. Technol.* 45, 90–96. doi: 10.1021/es101316v

Harding, K. (2008). *A Generic Approach To Environmental Assessment Of Microbial Bioprocesses Through Life Cycle Assessment (LCA)*. PhD Thesis, University of Cape Town, Cape Town

Iijima, T., and Yamaguchi, T. (2007). The improved Kolbe-Schmitt reaction using supercritical carbon dioxide. *Tetrahedron. Lett.* 48, 5309–5311. doi: 10.1016/j.tetlet.2007.05.132

Kitade, Y., Hashimoto, R., Suda, M., Hiraga, K., and Inui, M. (2018). Production of 4-Hydroxybenzoic acid by an aerobic growth-arrested bioprocess using metabolically engineered corynebacterium glutamicum. *Appl. Environ. Microbiol.* 84:e02587-17. doi: 10.1128/AEM.02587-17

Krömer, J. O., Nunez-Bernal, D., Averesch, N. J., Hampe, J., Varela, J., Varela, C., et al. (2013). Production of aromatics in Saccharomyces cerevisiae–a feasibility study. *J. Biotechnol.* 163, 184-193. doi: 10.1016/j.jbiotec.2012.04.014

Ma, W. L., Zhao, X., Lin, Z. Y., Mohammed, M. O., Zhang, Z. F., Liu, L. Y., et al. (2016). A survey of parabens in commercial pharmaceuticals from China and its implications for human exposure. *Environ. Int.* 95, 30–35. doi: 10.1016/j.envint.2016.07.013

Markovic, Z., Markovic, S., and Begovic, N. (2006). Influence of alkali metal cations upon the Kolbe-Schmitt reaction mechanism. *J. Chem. Inf Model* 46, 1957–1964. doi: 10.1021/ci0600556

Matwiejczuk, N., Galicka, A., and Brzoska, M. M. (2020). Review of the safety of application of cosmetic products containing parabens. *J. Appl. Toxicol.* 40 176–210. doi: 10.1002/jat.3917

Miller, A., Fosmer, A., Rush, B., McMullin, T., Beacom, D., Suominen P., et al. (2017). "Industrial production of lactic acid," in. *Comprehensive Biotechnology*. ed M. Moo-Young. (Amsterdam: Elsevier).

Mojsov, K. (2015). Comparison between conventional chemical processes and bioprocesses in cotton fabrics. *Tekstilna Industrija* 6, 21–25.

Nordstrom, F. L., and Rasmuson, A. C. (2006). Phase equilibria and thermodynamics of p-hydroxybenzoic acid. *J. Pharm. Sci.* 95, 748–760. doi: 10.1002/jps.20569

Patel, A. D., Meesters, K., den Uil, H., de Jong, E., Blok, K., Patel, M. K., et al. (2012). Sustainability assessment of novel chemical processes at early stage. application to biobased processes. *Energ. Environ. Sci.* 5, 8430–8444. doi: 10.1039/c2ee21581k

Stephanopoulos, G., Aristidou, A. A., and Nielsen, J. H. (1998). *Metabolic engineering . Principles and Methodologies*. San Diego, CA: Academic Press.

Stottmeister, U., Aurich, A., Wilde, H., Andersch, J., Schmidt, S., Sicker, D., et al. (2005). White biotechnology for green chemistry. fermentative 2-oxocarboxylic acids as novel building blocks for subsequent chemical syntheses. *J. Ind. Microbiol Biotechnol.* 32, 651–664. doi: 10.1007/s10295-005-0254-x

Tugnoli, A., Santarelli, F., and Cozzani, V. (2008). An approach to quantitative sustainability assessment in the early stages of process design. *Environ. Sci. Technol.* 42, 4555–4562. doi: 10.1021/es702441r

Conflict of Interest: RF and DP are employed by Intelligen Inc., the company that develops and markets SuperPro Designer, the process simulator used for the analysis of the various scenarios presented in this article.

The remaining authors declare that the research was conducted in the absence of any commercial or financial relationships that could be construed as a potential conflict of interest.

The handling Editor declared a past collaboration with one of the authors, JK.

Advantages of publishing in Frontiers

OPEN ACCESS
Articles are free to read for greatest visibility and readership

FAST PUBLICATION
Around 90 days from submission to decision

HIGH QUALITY PEER-REVIEW
Rigorous, collaborative, and constructive peer-review

TRANSPARENT PEER-REVIEW
Editors and reviewers acknowledged by name on published articles

Frontiers
Avenue du Tribunal-Fédéral 34
1005 Lausanne | Switzerland

Visit us: www.frontiersin.org
Contact us: info@frontiersin.org | +41 21 510 17 00

REPRODUCIBILITY OF RESEARCH
Support open data and methods to enhance research reproducibility

DIGITAL PUBLISHING
Articles designed for optimal readership across devices

FOLLOW US
@frontiersin

IMPACT METRICS
Advanced article metrics track visibility across digital media

EXTENSIVE PROMOTION
Marketing and promotion of impactful research

LOOP RESEARCH NETWORK
Our network increases your article's readership